

**The stress-protectants and chemical
chaperones ectoine and hydroxyectoine:
enzymes, importer, exporter and
transcriptional regulation**

DISSERTATION

**zur Erlangung des akademischen Grades
Doktor der Naturwissenschaften
(Dr. rer. nat.)**

**dem Fachbereich Biologie der
Philipps-Universität Marburg
vorgelegt
(Hochschulkennziffer 1180)**

**von
Laura Czech
(Master of Science)
aus Weilmünster**

Marburg (Lahn), Oktober 2019

Die Untersuchungen zur vorliegenden Arbeit wurden von Oktober 2014 bis August 2019 am Fachbereich 17 Biologie im Laboratorium für Molekulare Mikrobiologie der Philipps-Universität Marburg unter der Leitung von Prof. Dr. Erhard Bremer durchgeführt.

Vom Fachbereich Biologie
der Philipps-Universität Marburg (Hochschulkennziffer 1180)
als Dissertation am _____ angenommen

Erstgutachter: Prof. Dr. Erhard Bremer (Fachbereich Biologie, Philipps-Universität Marburg)

Zweitgutachter: Prof. Dr. Gert Bange (Fachbereich Chemie, Philipps-Universität Marburg)

Weitere Mitglieder der Prüfungskommission:

Prof. Dr. Uwe Maier (Fachbereich Biologie, Philipps-Universität Marburg)

Prof. Dr. Ulrich Mösch (Fachbereich Biologie, Philipps-Universität Marburg)

Tag der Disputation: _____

Declaration of authorship

I hereby declare that this submission „**The stress-protectants and chemical chaperones ectoine and hydroxyectoine: enzymes, importer, exporter and transcriptional regulation**“ is entirely of my own and to the best of my knowledge has not been submitted, either in part or whole, for a degree at this or any other educational institution except where acknowledgement is made in this work. Quotes and paraphrased material are clearly acknowledged and all sources are referenced.

Laura Czech Marburg, October 1st, 2019

Erklärung

Hiermit versichere ich, dass ich die vorliegende Dissertation mit dem Titel:

„**The stress-protectants and chemical chaperones ectoine and hydroxyectoine: enzymes, importer, exporter and transcriptional regulation**“ eigenständig verfasst und keine anderen als die im Text angegebenen Hilfsmittel verwendet habe. Sämtliche Textstellen, die im Wortlaut oder dem Sinn nach anderen Werken entnommen wurden, sind mit der entsprechenden Quellenangabe kenntlich gemacht.

Die Dissertation wurde weder in der jetzigen, noch einer ähnlichen Form bei einer anderen Hochschule eingereicht und hat noch keinen anderen Prüfungszwecken gedient.

Laura Czech Marburg, 1. Oktober 2019

Das Schönste, was wir erleben können, ist das Geheimnisvolle.

Albert Einstein

Man sieht nur mit dem Herzen gut.

Das Wesentliche ist für die Augen unsichtbar.

Antoine de Saint-Exupéry

Meiner Familie

1. List of publications

In association with my thesis, the following review articles, original publications, or submitted and draft manuscripts have been put together. Asterisks (*) indicate co-authorship.

Original paper with peer-review process (published)

- (1) **Widderich N*, Czech L*, Elling FJ, Könneke M, Stöveken N, Pittelkow M, Riclea R, Dickschat JS, Heider J, Bremer E.** Strangers in the archaeal world: osmostress-responsive biosynthesis of ectoine and hydroxyectoine by the marine thaumarchaeon *Nitrosopumilus maritimus*. *Environ Microbiol* 2016;18(4):1227–1248.
- (2) **Czech L, Stöveken N, Bremer E.** EctD-mediated biotransformation of the chemical chaperone ectoine into hydroxyectoine and its mechanosensitive channel-independent excretion. *Microb Cell Fact* 2016;15(126): doi: 10.1186/s12934-016-0525-4.
- (3) **Czech L, Poehl S, Hub P, Stöveken N, Bremer E.** Tinkering with osmotically controlled transcription allows enhanced production and excretion of ectoine and hydroxyectoine from a microbial cell factory. *Appl Environ Microbiol* 2018;84(2): e01772-17. doi: 10.1128/AEM.01772-17.
- (4) **Czech L*, Höppner A*, Kobus S, Seubert A, Riclea R, Dickschat JS, Heider H, Smits SHJ, Bremer E.** Illuminating the catalytic core of ectoine synthase through structural and biochemical analysis. *Sci Rep* 2019;9(364): doi: 10.1038/s41598-018-36247-w.

Original paper with peer-review process (submitted)

- (1) **Czech L, Wilcken S, Czech O, Linne U, Brauner J, Smits SHJ, Galinski EA, Bremer E.** Exploiting substrate promiscuity of ectoine hydroxylase for regio- and stereoselective modification of homoectoine. *submitted to Front Microbiol*.

Draft manuscripts

- (1) **Czech L, Smits SHJ, Bremer E.** In depth analysis of importers, exporters and mechanosensitive channels associated with ectoine biosynthetic gene clusters. *manuscript prepared for submission*.
- (2) **Czech L, Höppner A, Kobus S, Smits SHJ, Bremer E.** Crystal structure and *in vitro* analysis of the MarR-type regulator EctR involved in ectoine biosynthesis. *draft manuscript*.

Manuscripts or publications with minor contribution (not included in this work)

- (1) Richter AA, Mais CN, Czech L, Geyer K, Erb TJ, Smits SHJ, Bange G, Bremer E. Biosynthesis of the stress-protectant and chemical chaperon ectoine: biochemistry of the transaminase EctB. *under revision at Front Microbiol.*
- (2) Richter AA, Kobus S, Czech L, Höppner A, Zarzycki J, Erb TJ, Lauterbach L, Dickschat JS, Bremer E, Smits SHJ. Making the versatile stress-protectant and chemical chaperone ectoine: architecture of the EctA diaminobutyrate acetyltransferase active site. *submitted to J Biol Chem.*

Review articles with peer-review process

- (1) Czech L, Hermann L, Stöveken N, Richter AA, Höppner A, Smits SHJ, Heider H, Bremer E. Role of the extremolytes ectoine and hydroxyectoine as stress protectants and nutrients: genetics, phylogenomics, biochemistry, and structural analysis. *Genes (Basel)* 2018;9(177): doi: 10.3390/genes9040177.
- (2) Czech L, Bremer E. With a pinch of extra salt - Did predatory protists steal genes from their food? *PLOS Biol* 2018;16(2): e20:1–12. doi: 10.1371/journal.pbio.2005163.

2. Zusammenfassung

Fluktuationen des extrazellulären osmotischen Potentials zählen zu den häufigsten Stressfaktoren für Mikroorganismen. Nicht nur zahlreiche Organismen der Domäne *Bacteria*, sondern auch einige *Archeen* und wenige einzellige, halophile *Eukaryoten* besitzen die genetische Information zur Synthese der kompatiblen Solute und chemischen Chaperone, Ectoin und 5-Hydroxyectoin. Unter hochosmolaren Bedingungen werden diese Substanzen innerhalb des Zytoplasmas angehäuft, um den Ausstrom des Wassers entlang des Konzentrationsgradienten zu verhindern und somit, den essentiellen Turgordruck innerhalb der Zelle aufrecht zu erhalten. Ectoine erfüllen nicht nur wichtige Schutzfunktion für Mikroorganismen, sie besitzen darüber hinaus nützliche physikalisch-chemische und funktions-erhaltende Eigenschaften. Diese Attribute führten zur industriellen Produktion und kommerziellen Verwendung von Ectoinen. Die drei Enzyme EctB (L-2,4-Diaminobutyrat Aminotransferase), EctA (L-2,4-Diaminobutyrat Acetyltransferase) und das Schlüsselenzym EctC (Ectoin Synthase) sind für die Biosynthese von Ectoin aus dem Vorläufer L-Aspartat- β -Semialdehyd verantwortlich. Zusätzlich kann durch die Ectoin Hydroxylase (EctD) eine Hydroxylgruppe eingeführt werden, was zur Entstehung von 5-Hydroxyectoin führt. Die Gene des Ectoin-Biosynthesewegs sind meist in einem Operon kodiert [*ectABC(D)*], das durch einen osmotisch-induzierbaren Promotor gesteuert wird. Neben der *de novo* Synthese von Ectoinen, besitzen die meisten Mikroorganismen spezielle Osmolyttransporter, die deren Aufnahme aus der Umwelt ermöglichen.

Im Rahmen dieser Dissertation wurden folgende Bereiche untersucht und Ergebnisse erhalten:

- **Bioinformatische Analysen zur phylogenetischen Verbreitung** von Ectoin-Biosynthesegenen und Untersuchung der Genomumgebungen von *ect* Clustern
- **Strukturelle und funktionelle Analyse von Enzymen des Ectoin-Biosynthese-Wegs**
 - Kristallographische, biochemische und funktionelle Analyse des Schlüsselenzyms EctC führten zur Postulierung des Reaktionsmechanismus
 - Die Substratpromiskuität der Ectoin-Hydroxylase (EctD) ermöglichte die stereo- und regio-selektive Hydroxylierung des synthetischen Ectoin-Derivats Homoectoin
- **Etablierung von Ectoin/5-Hydroxyectoin-produzierenden Zellfabriken**
 - Die Sekretion der Produkte erfolgt unabhängig von mechanosensitiven Kanälen und den Aufnahmesystemen für Ectoine im heterologen Produzenten *E. coli*
- **Regulation der Ectoine-Biosynthese-Gene**
 - Detaillierte molekulare und funktionelle Analyse des *ect* Promotor aus *P. stutzeri* A1501 identifizierten einen untypischen Sigma-70-abhängigen Promotor und lieferte neue Einblicke in die Determinanten für die osmotische Regulation der *ect* Gene
 - Bioinformatische, kristallographische und funktionelle Analyse des MarR-typ Regulators EctR aus *Novosphingobium*

- **Untersuchung von Transportern in der Genomumgebung von Ectoin-Biosynthese-Clustern**
 - Co-Transkription neuer Transporter und mechanosensitiver Kanäle
 - Charakterisierung zwei neuer Ectoin-Transportern mit breitem Substratspektrum (EctI) und hoher Spezifität für Ectoine (EctU)
 - Funktionelle Analyse von mechanosensitiven Kanälen, die in *ect* Genclustern kodiert sind
 - Identifizierung und Charakterisierung eines spezifischen Exporters für Ectoine (EctE)

3. Summary

Changes within the external osmotic potential belong to the most ubiquitous stress factors that microbial cells encounter. A large group of *Bacteria*, but also a few *Archaea* and unicellular halophilic *Eukarya* possess the genetic information to produce the compatible solutes and chemical chaperones ectoine and its derivative 5-hydroxyectoine. These compounds are consequently amassed within the cytoplasm to counteract the reduction in turgor pressure resulting from the outflow of water during high extracellular osmolarity. Ectoines are not only major stress protective compounds for microorganisms but their physicochemical attributes and function-preserving features also entailed their industrial production and use in the fields of biotechnology, medicine and cosmetics. Ectoine biosynthesis from the precursor L-aspartate- β -semialdehyde is achieved in a three step enzymatic reaction involving the enzymes: EctB (L-2,4-diaminobutyrate aminotransferase), EctA (L-2,4-diaminobutyrate acetyltransferase) and the key enzyme EctC (ectoine synthase). Furthermore, a hydroxyl group can be attached to the ectoine molecule by the ectoine hydroxylase (EctD) yielding 5-hydroxyectoine. The underlying biosynthetic genes are mostly encoded in a gene cluster [*ectABC(D)*] that is controlled by an osmotically responsive promoter. Besides *de novo* synthesis of the stress protective compounds, they can also be imported from environmental resources through specific osmotically controlled uptake systems.

In the following paragraph the research subjects and major results of my PhD thesis will be briefly summarized:

- **Bioinformatical analysis focusing on the phylogenetic distribution** of the genes for ectoine biosynthesis and investigation of their gene neighborhoods
- **Structural and functional analysis of ectoine/5-hydroxyectoine biosynthetic enzymes**
 - Crystallographic, biochemical and functional analysis of the key enzyme for ectoine biosynthesis EctC led to the postulation of the performed reaction mechanism
 - Substrate ambiguity of the ectoine hydroxylase (EctD) was exploited for the stereo- and regioselective hydroxylation of the synthetic ectoine derivative homoectoine
- **Establishment of ectoine/5-hydroxyectoine-producing cell factories**
 - Secretion of the products is independent of the mechanosensitive channels and ectoine import systems in the heterologous producer *E. coli*
- **Regulation of the expression of ectoine biosynthetic genes**
 - Detailed molecular and functional analysis of the *ect* promoter from *P. stutzeri* A1501 led to the identification of an unusual sigma-70-type promoter and insights into the determinants involved in osmotic regulation of the *ect* genes
 - Bioinformatical, crystallographic and functional analysis of the MarR-type regulator EctR from *Novosphingobium*

- **Analysis and characterization of transporters present in the gene neighborhood of ectoine biosynthetic gene clusters**
 - Co-transcription of novel transporters and mechanosensitive channels
 - Functional characterization of two novel ectoine transporters with a broad substrate spectrum (EctI) and specificity for ectoines (EctU)
 - Functional analysis of mechanosensitive channels, that are encoded within *ect* gene clusters
 - Identification and characterization of an ectoine/5-hydroxyectoine specific exporter (EctE)

Table of content

1.	List of publications	11
2.	Zusammenfassung.....	15
3.	Summary	17
4.	Introduction	23
4.1.	Osmotic stress.....	23
4.1.1.	The <i>salt-in</i> and <i>salt-out</i> strategies in osmotic stress response.....	24
4.1.2.	Compatible solutes	25
4.2.	Ectoine and 5-hydroxyectoine	26
4.2.1.	Discovery of ectoines and their biosynthetic pathway	26
4.2.2.	Ectoine biosynthesis - Genes and Enzymes	27
4.2.2.1.	L-2,4-diaminobutyrate (DABA) aminotransferase EctB.....	28
4.2.2.2.	L-2,4-diaminobutyrate acetyltransferase EctA.....	29
4.2.2.3.	Ectoine synthase EctC.....	30
4.2.2.4.	Ectoine hydroxylase EctD	31
4.2.2.5.	Specialized aspartokinase Ask_ect	32
4.2.3.	Regulation of <i>ect</i> gene expression and other osmstress responsive genes	32
4.2.3.1.	The MarR-type regulator EctR and other regulatory proteins involved compatible solute accumulation.....	35
4.2.4.	Properties of ectoines.....	36
4.2.5.	Biotechnological production of ectoines.....	37
4.2.5.1.	Aims to develop natural and synthetic ectoine cell factories	37
4.2.5.2.	Industrial and medical applications of ectoines.....	40
4.2.6.	The use of ectoines as nutrients	41
4.2.7.	Transport of ectoines	45
4.2.8.	Ectoines as stress protectants in Eukarya.....	48
4.3.	Imposing low external salinity - mechanosensitive channels as emergency release valves	49
5.	Peer-reviewed publications.....	53
5.1.	Review articles	53
5.1.1.	Role of the extremolytes ectoine and hydroxyectoine as stress protectants and nutrients: genetics, phylogenomics, biochemistry, and structural analysis	53
5.1.1.1.	Original publication.....	55
5.1.2.	With a pinch of extra salt - Did predatory protists steal genes from their food?	111
5.1.2.1.	Original publication.....	113
5.2.	Research papers	125
5.2.1.	Strangers in the archaeal world: osmstress-responsive biosynthesis of ectoine and hydroxyectoine by the marine thaumarchaeon <i>Nitrosopumilus maritimus</i>	125
5.2.1.1.	Original publication.....	127
5.2.2.	EctD-mediated biotransformation of the chemical chaperone ectoine into hydroxyectoine and its mechanosensitive channel-independent excretion	149
5.2.2.1.	Original publication.....	151
5.2.3.	Tinkering with osmotically controlled transcription allows enhanced production and excretion of ectoine and hydroxyectoine from a microbial cell factory	167
5.2.3.1.	Original publication.....	169
5.2.4.	Illuminating the catalytic core of ectoine synthase through structural and biochemical analysis.....	199

5.2.4.1.	Original publication.....	201
5.2.5.	Exploiting substrate promiscuity of ectoine hydroxylase to produce the synthetic osmoprotectant hydroxy-homoectoine.....	223
5.2.5.1.	Original publication.....	225
5.2.6.	<i>Draft manuscript</i> In depth analysis of importers, exporters and mechanosensitive channels associated with ectoine biosynthetic gene clusters	291
5.2.7.	<i>Draft manuscript</i> The MarR-type regulator from <i>Novosphingobium</i> sp. LH128	331
6.	Discussion and Perspectives	363
6.1.	Phylogenomic distribution of ectoine biosynthetic genes and horizontal gene transfer	363
6.2.	New insights into the key enzymes for ectoine and 5-hydroxyectoine production.....	366
6.3.	Ectoine biosynthesis - a structural view	368
6.4.	Production of ectoine and 5-hydroxyectoine in microbial cell factories and their biotechnological use	369
6.5.	Regulation of ectoine biosynthesis - a dark spot	371
6.6.	Novel insights into ectoine transport	374
7.	References.....	379
8.	Scientific CV	393
9.	Danksagung.....	395

4. Introduction

4.1. Osmotic stress

The most striking advantage of microbial cells is their enormous ability to rapidly adapt to changing environmental situations and stress conditions. Within their natural habitats all microorganisms are exposed to a multitude of different stress factors such as extremes in temperature, water activity, or nutrient limitations. One of the most ubiquitous stressful cues is the fluctuation of the osmotic potential within their direct environment [1–4]. Increases or decreases in the water activity directly result in a change of the osmotic gradient that consequently provokes the in- or outflow of water across the semipermeable membrane [1, 5, 6]. This semipermeable membrane is an essential feature of microbial cells as it provides a secured space for the replication and transcription of genetic information, for the reactions of biochemical pathways and the generation of energy required for growth and division. High concentrations of proteins, metabolites and nucleic acids within the cytoplasm cause the influx of water and thereby the generation of intracellular turgor [7, 8]. As this turgor is essential for growth, cells aim to constantly balance this hydrostatic pressure when it is threatened by fluctuations in the external osmolarity/salinity [1, 7, 9, 10]. When bacterial cells face high external osmotic concentrations, for example after long desiccation periods or during their transition from rivers to marine habitats, the surrounding environment possesses a higher ionic strength than the cytoplasm. This results in an outflow of water along the osmotic gradient and consequently causes a drop in turgor pressure. This dehydration of the cytoplasm endangers survival of the cells as they rely on the intracellular turgor pressure for growth and division [2, 4, 11, 12]. In contrast, a sudden drop in the external salinity e. g. due to rainfall or when cells transit to low salinity environments, causes the flow of water into the cell. This event leads to an increased intracellular pressure, which might ultimately result in bursting of the bacterial cells [6].

While the presence of aquaporins in bacterial membranes allow the passive flux of water via diffusion, no bacterial cell possesses membrane proteins that can actively pump water into or out of the cell to outbalance the concentration gradients [13]. To counteract the harmful consequences of these osmotic changes, bacterial cells have developed a variety of emergency mechanisms to ensure not only persistence and survival but also growth and proliferation. As the key mechanism, they indirectly influence the amount and direction of water flow by the active amassment or release of organic compounds and ions [1, 3, 14]. Under high osmolarity conditions microorganisms accumulate either specific ions (e. g. K^+ ; Cl^-), if they are *salt-in* strategists, or organic compounds, so called compatible solutes, when they employ the *salt-out* strategy (see 4.1.1) [11, 12, 15–17]. In the opposite case - under low osmolarity conditions - bacterial cells harbor emergency release valves, namely mechanosensitive channels, to rapidly and unspecifically expel ions and other solutes from the cytoplasm (Figure 1) (see chapter 4.3) [6, 18, 19].

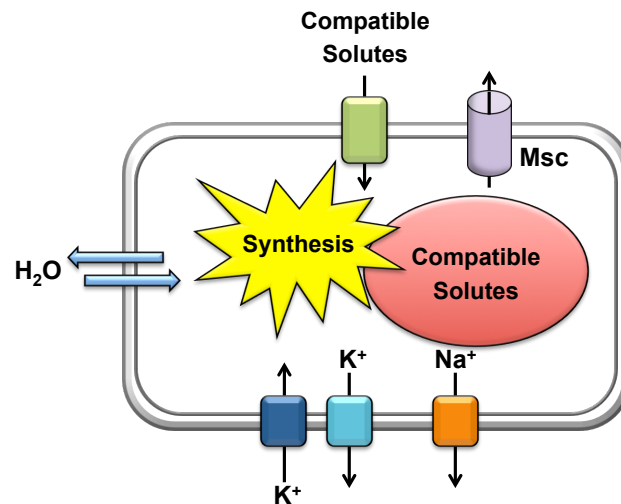


Figure 1 Schematic illustration of the salt-out adjustment strategy of a microbial cell to hyper- and hypoosmotic challenges. taken from Czech & Bremer (2018) *PLoS Biology* (16) e2005163. doi: 10.1371/journal.pbio.2005163.

4.1.1. The *salt-in* and *salt-out* strategies in osmotic stress response

Halophilic bacteria and archaea (*Haloarchaea*) that mostly inhabit permanently high saline environments accumulate K^+ and Cl^- ions from environmental resources and at the same time expel cytotoxic Na^+ ions from the cells to outbalance the effects of high external salt concentrations [11, 12, 16]. On the long-term, this *salt-in* strategy resulted in the evolution of a so-called acidic proteome [11, 16]. In order to maintain their function and solubility, the proteins adapted to the high intracellular ionic strength by the enrichment of negatively charged amino acids on the protein surfaces and the narrow distribution of isoelectric points. This amassment of ions and permanent adaptation of the proteome is on the one hand less energy demanding than the accumulation of organic solutes (*salt-out*), but on the other hand it provides less flexibility for the cells [20, 21]. In contrast, most microorganisms inhabiting fluctuating environments rely on a more flexible adjustment mechanism - the *salt-out* strategy [1, 14]. As the first emergency reaction, the cells import K^+ ions (Figure 1) [1–3]. Since these cations interfere at high concentrations with the cellular metabolism, they are subsequently replaced by organic osmolytes, so-called compatible solutes (see 4.1.2). These solutes are either imported or synthesized *de novo* to counteract the osmotically instigated outflow of water (Figure 1) [1–3].

It was long thought, that different microorganisms exclusively employ either the *salt-in* or the *salt-out* strategy - a view that is challenged by recent discoveries. Some halophilic Archaea (*Halobacteriales*) were found to combine the accumulation of K^+ ions and the compatible solutes trehalose and 2-sulfotrehalose upon high osmolarity stress [22, 23]. Moreover for *Halobacterium salinarum* it was demonstrated, to chemotactically approach the compatible solutes glycine betaine, carnitine and choline [24]. Furthermore, the ability to import compatible solutes seems to be more frequent in halophilic Archaea than expected [24]. These recent observations lead to the conclusion that even more organisms might combine the *salt-in* and *salt-out* strategy under certain environmental circumstances and that the long-held view of strict *salt-in* and *salt-out* dependent bacteria might be further challenged by future investigations.

4.1.2. Compatible solutes

Compatible solutes play a key role for the osmotic stress response in organisms originating from all three domains of life [4, 14, 25]. Their low-molecular weight, high solubility and often zwitter-ionic state enable their accumulation up to molar concentrations without interfering with vital cellular processes [26, 27]. Compatible solutes are also described as cytoprotectants since they do not only effectively protect the cells against high osmolarity but also against extremes in temperature, freezing, drying, hydrostatic pressure and radiation [1, 3, 14, 28–40]. Bacterial compatible solutes can be classified into different groups according to their chemical origin: (I) quaternary amines (e.g., glycine betaine, arsenobetaine, L-carnitine, proline-betaine, tri-methylammoniumoxide) and their sulfonium analogues (dimethylsulfoniopropionate [DMSP], taurine); (II) amino acids and their derivatives (L-proline, L-glutamate, ectoines); (III) sugars (e.g., trehalose, sucrose); (IV) polyols (glycerol; *myo*-inositol) (V) heterosides (composed of a polyol and sugar moiety, such glycosyl-glycerol or galactosyl-glycerol); (VI) small peptides (*N*-acetyl-glutaminyl-glutamine amide); and (VII) sulfate esters (e.g., choline-*O*-sulfate) [1, 3, 4, 14, 27, 41–44].

While some of these are only rarely used by subgroups of microorganism, others are highly abundant and even used by all three domains of life [45]. One of these examples is the most widely used compatible solute glycine betaine (Figure 2) as many *Bacteria*, *Archaea*, *Fungi*, plants, and animals are able to synthesize this stress-relieving compound [45]. Yet another very important compatible solute, DMSP, functions a major component of the global carbon- and sulfur-cycle and is produced in millions of tons within marine habitats by phytoplankton and macroalgae. Furthermore, its volatile degradation product dimethylsulfide (DMS) acts as a highly relevant climate gas [46].

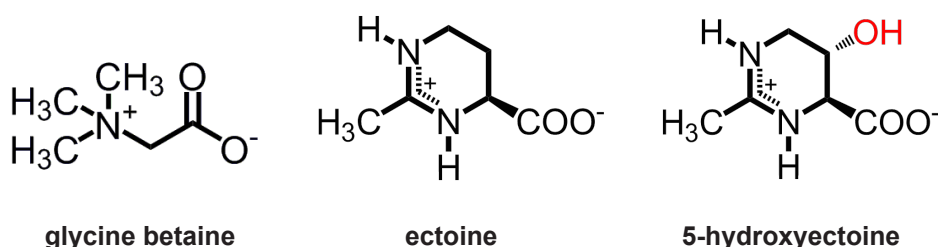


Figure 2 Chemical structures of glycine betaine, ectoine and 5-hydroxyectoine.

In many cases, archaeal compatible solutes resemble their bacterial counterparts in structure, with the difference that a large number carries a negative charge [4, 47]. Frequently occurring compatible solutes in *Archaea* are for example trehalose, 2-sulfo-trehalose, diglycerol phosphate (DGP), glucosylglycerate, di-*myo*-inositol phosphate (DIP), β -glutamate or mannosylglycerate [4, 47]. Many cyanobacteria accumulate glucosylglycerol or glycerol in response to elevated external osmolarity [4, 44, 48–50]. This latter compound also functions as an osmstress protectant in many Eukarya, such as the yeast *Saccharomyces cerevisiae* [51]. Interestingly, in the case of bacteria, glycerol can freely diffuse across their cellular membranes [52]. Other commonly used eukaryotic osmolytes are (as mentioned before) glycine betaine

(Figure 2) [27], *myo*-inositol, polyols such as sorbitol, or mannitol, or sugars and amino acids, like proline, valine, arginine, glucose, trehalose or fructose [51].

One of the most important features of compatible solutes is their preferential exclusion from the direct hydration shell of the proteins - an effect that has entailed their designation as *chemical chaperones* [53, 54]. This mechanism generates a thermodynamic force that stabilizes proteins in their compact and native fold [53, 55, 56]. Furthermore, compatible solutes thereby protect protein complexes, as well as protein-DNA complexes and even whole cells [1, 57].

Within the framework of my PhD thesis, I focused on two of the probably most abundant compatible solutes in bacteria, ectoine and 5-hydroxyectoine (Figure 2) (see 4.2) [58], which are biotechnologically used and produced due to their superior function-preserving properties (see chapter 4.2.3 and 4.2.5) [57, 59–61].

4.2. Ectoine and 5-hydroxyectoine

4.2.1. Discovery of ectoines and their biosynthetic pathway

When Galinski and co-workers discovered the amino acid derivative ectoine in 1985 [(4*S*)-2-methyl-1,4,5,6-tetrahydropyrimidine-4-carboxylic acid] in the halophilic bacterium *Ectothiorhodospira halochloris*, it was expected to be a rarely occurring stress protectant (Figure 2) [58]. Only a few years later its hydroxylated derivative 5-hydroxyectoine [(4*S*,5*S*)-2-methyl-5-hydroxy-1,4,5,6-tetrahydropyrimidine-4-carboxylic acid] was identified in *Streptomyces parvulus* by Inbar & Lapidot (Figure 2) [62]. Both compounds are heterocyclic amino acids that possess a partially hydrogenated pyrimidine ring (Figure 2) [63]. 5-hydroxyectoine harbors an additional hydroxyl group at the C5-position of the pyrimidine ring compared to ectoine (Figure 2) [62, 64]. Detailed screening procedures using different HPLC and NMR techniques together with the discovery of the underlying genes for the biosynthetic enzymes revealed their wide spread occurrence mainly in the domain of the *Bacteria* [36, 59, 64–67]. Especially the determination of the ectoine (*ectABC*) [64, 68] and 5-hydroxyectoine biosynthetic genes (*ectD*) [64, 69, 70] opened up new analytical possibilities as it enabled *in silico* genome mining within the ever increasing number of sequenced microbial genomes (Figure 3A) (see 5.1.1) [59, 67, 71]. First bioinformatical approaches reported by Widderich *et al.* led to the discovery of ectoine biosynthetic genes in ten bacterial phyla, and even in a restricted number of Archaea (belonging to two different phyla) (see 5.2.1), while recent investigations on the osmotic stress response of halophilic protists also surprisingly revealed their synthesis in these unicellular eukaryotes (see 4.2.8, 5.1.2 and 5.2.1) [59, 72–76]. In sum, ectoines play a major role in the osmoprotection of a large group of organisms and moreover their abundance and useful physico-chemical attributes have prompted the development of an dedicated ectoine-specific research field.

4.2.2. Ectoine biosynthesis - Genes and Enzymes

As stated in briefly above, detailed biochemical and crystallographic studies on the enzymes involved in the biosynthesis of ectoines have been conducted within the past years. Ectoine is produced in a

4.2.2. Ectoine biosynthesis - Genes and Enzymes

As stated in briefly above, detailed biochemical and crystallographic studies on the enzymes involved in the biosynthesis of ectoines have been conducted within the past years. Ectoine is produced in a sequential three-step enzymatic reaction involving the L-2,4-diaminobutyrate (DABA) aminotransferase EctB (EC 2.6.1.76), the L-2,4-diaminobutyrate acetyltransferase EctA (EC 2.3.1.178), and the ectoine synthase EctC (EC 4.2.1.108) from the precursor and central molecule of the amino acid metabolism, L-aspartate- β -semialdehyde (Figure 3) [59, 77]. A subgroup of ectoine producers additionally encodes the enzyme for the ectoine hydroxylase EctD (EC 1.14.11.55), that stereo- and regio-selectively attaches an OH-group to the C5-atom of the ectoines pyrimidine ring (Figure 3) [59, 64, 67, 78]. Moreover, some ectoine/5-hydroxyectoine producers possess a specialized feedback-resistant aspartokinase Ask_Ect (Figure 3) [59, 79].

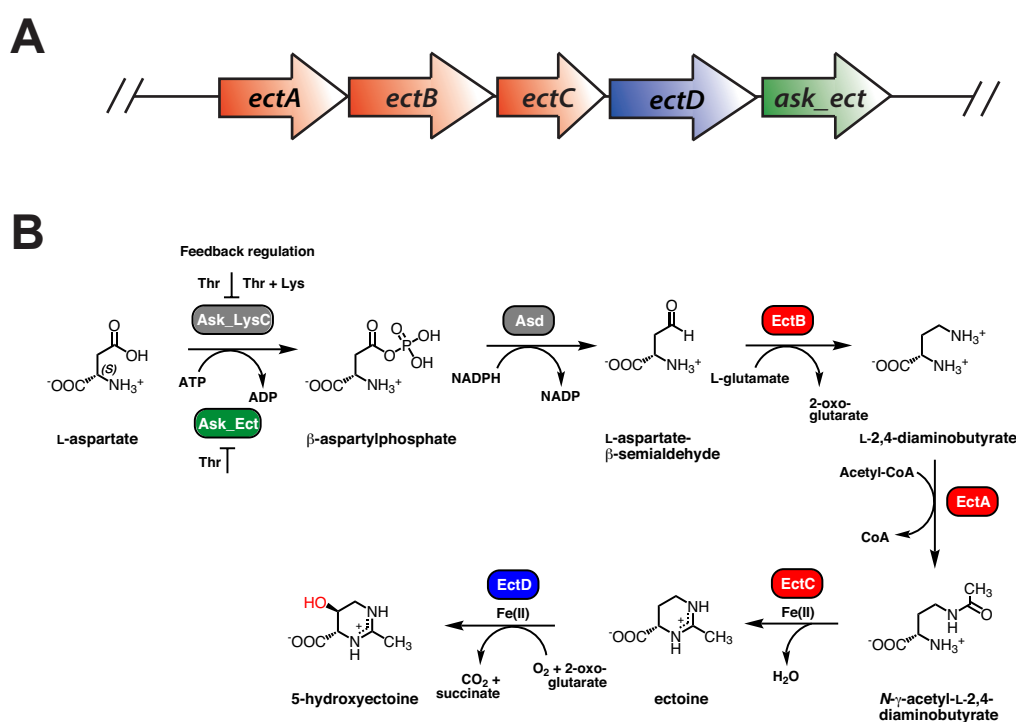


Figure 3 Ectoine/5-hydroxyectoine biosynthetic genes and synthesis route. **A** Scheme of a classical ectoine gene cluster. **B** Ectoine biosynthesis pathway, depicting the involved enzymes, intermediates, co-substrates and side products. Ask: aspartokinase; Asd: L-aspartate- β -semialdehyde dehydrogenase; EctB: L-2,4-diaminobutyrate aminotransferase; EctA: L-2,4-diaminobutyrate acetyltransferase; EctC: ectoine synthase; EctD: ectoine hydroxylase. Adapted from Czech *et al.* (2018) *Genes* (9) doi: 10.3390/genes9040177.

Peters *et al.* first described the ectoine biosynthetic pathway in 1990 using *E. halochloris* and *Halomonas elongata* as model organisms [80]. Nine years later Murooka and co-workers purified the ectoine biosynthetic enzymes from *H. elongata* and thereby opened the field for the biochemical characterization of the EctABC proteins [77]. Later, Reshetnikov *et al.* published biochemical data on the ectoine enzymes

from methylotrophic bacteria and furthermore, the ectoine biosynthetic enzyme from a variety of bacteria and also one archaeum were studied (see 5.2.1) [81].

The underlying ectoine biosynthetic genes (*ectABC*) were first described by Louis and Galinski in 1997 in *Marinococcus halophilus* [68] and followed by the investigations on the ectoine and 5-hydroxyectoine biosynthetic genes of *Streptomyces cryomallus* in 2004 (Figure 3A) [69]. These two publications provided the basis for a molecular analysis and later on enabled the database-wide genome mining using the amino acid sequence of the signature enzyme for ectoine production EctC as the search template [59, 67, 72]. These analyses revealed that the co-localization of the genes *ectA*, *ectB* and *ectC* together with their highly conserved genetic succession is a widespread signature of the *ect* operon [59, 67]. Moreover, studies on *Chromohalobacter salexigens* and *Sphingopyxis salexigens* revealed that the gene for ectoine hydroxylase *ectD* can either be part of the *ectABC(D)* gene cluster or can be encoded elsewhere in the genome [59, 64, 67, 70, 78, 82]. This is also the case in *H. elongata* and furthermore *C. salexigens* was shown to harbor two *ectD*-type genes [59, 70]. In some rare cases the genes required for ectoine biosynthesis are separated and encoded at different locations in the genome. A studied example is the halophilic organism *Spiribacter salinus*, where the functionality of the separated ectoine biosynthetic genes has been proven (see also 6.1) [83].

Within the following sections, the knowledge gained about the different ectoine biosynthetic enzymes will be summarized.

4.2.2.1. L-2,4-diaminobutyrate (DABA) aminotransferase EctB

The first enzyme involved in the pathway of ectoine biosynthesis is the L-2,4-diaminobutyrate (DABA) aminotransferase, called EctB since it is the second gene in the sequence of a *classical* ectoine gene cluster. As other aminotransferases, EctB contains a PLP-cofactor that is required during enzyme activity [84]. During the catalyzed transamination reaction an amino-group from the donor molecule L-glutamate is transferred to L-aspartate- β -semialdehyde resulting in the formation of L-2,4-diaminobutyrate and 2-oxoglutarate - a molecule that could be subsequently used as co-substrate for the ectoine hydroxylase (Figure 3) (see section 4.2.2.4) [64, 78, 85]. Biochemical characterizations of EctB enzymes from *H. elongata* and *Methylobacterium alcaliphilum* have been published and both enzymes were shown to be homo-hexamers, to require K^+ for their catalytic activity and to perform the reverse reaction as well [77, 81]. The EctB protein from *H. elongata* possessed a K_m value of 9.1 mM for L-glutamate and 4.5 mM for L-aspartate- β -semialdehyde [77]. Recently, the EctB enzyme from the thermo-tolerant bacterium *Paenibacillus lautus* (*Pt*) has been studied on a biochemical and functional level (Richter *et al.*, *submitted manuscript*). Modeling studies, combined with biochemical, functional and mutational analyses revealed that (*Pt*)EctB is mechanistically identical to other PLP-dependent γ -aminobutyrate aminotransferases but possesses differences in respect to substrate binding (Richter *et al.*, *submitted manuscript*).

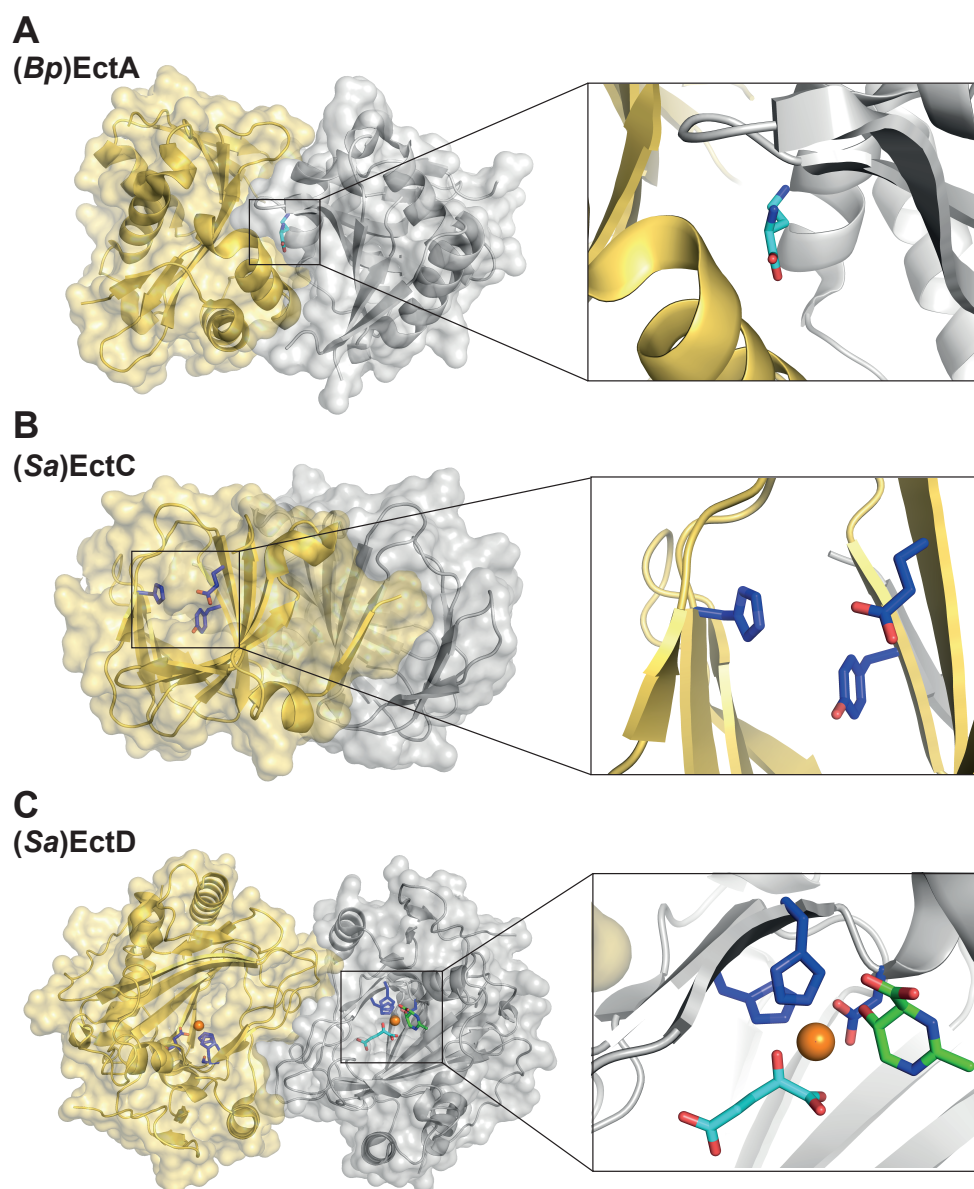


Figure 4 Crystal structure of enzymes involved in ectoine/5-hydroxyectoine biosynthesis. **A** Dimer of L-2,4-diaminobutyrate acetyltransferase EctA from *Bordatella parapertussis* and zoom of the L-2,4-diaminobutyrate (DABA) found at the dimer interface (PDB: 3D3S); **B** Dimer of the ectoine synthase EctC from *Spingopyxis alaskensis* and zoom into the proposed iron binding site (blue sticks) (PDB: 5BY5) [86] **C** Dimer of the ectoine hydroxylase EctD from *S. alaskensis* in complex with iron (orange), 5-hydroxyectoine (green) and 2-oxoglutarate (blue) and zoom into its active site (PDB: 4Q5O) [78].

4.2.2.2. L-2,4-diaminobutyrate acetyltransferase EctA

The reaction of DABA to *N*- γ -acetyl-2,4-diaminobutyrate (*N*- γ -ADABA) is performed by the L-2,4-diaminobutyrate acetyltransferase EctA and requires the co-substrate acetyl-coenzyme A (acetyl-CoA) (Figure 3) [87]. Like other enzymes of the GCN5-related-*N*-acetyltransferase-family (GNAT), EctA transfers an acetyl-group from the acetyl-CoA to the primary amine of the acceptor molecule [77, 87]. EctA from *H. elongata* and three different methylotrophs were described as homo-dimers and

biochemically characterized [77, 81]. A crystal structure of the EctA protein from *Bordatella parapertussis* (PDB: 3D3S) was deposited at the database without the publication of an associated research study. The enzyme was crystallized as a homo-dimer with the substrate DABA bound within the dimeric interface (Figure 4A). Since biochemical and experimental data of this enzyme is missing, it is unclear if this represents the actual substrate binding side. Recent crystallographic data argue against the relevance of this crystal structure with respect to the DABA binding pocket (Richter *et al.*, *submitted manuscript*). In this study, the EctA enzyme from *P. lautus* was crystallized in the apo-form, and in complexes with with CoA alone, DABA alone, CoA and DABA, and in the presence of *N*- γ -ADABA (Richter *et al.*, *submitted manuscript*). This comprehensive set of crystal structures in combination with biochemical and mutational data enabled a detailed description of the structure-function relationship of (*P*)EctA (Richter *et al.*, *submitted manuscript*). The essential residues involved in substrate binding were determined and a reaction mechanism was proposed (Richter *et al.*, *submitted manuscript*).

4.2.2.3. Ectoine synthase EctC

The key step in ectoine biosynthesis is the ring-closure of the substrate *N*- γ -ADABA to form ectoine involving the elimination of a water molecule (Figure 3B) [71]. This reaction is performed by the ectoine synthase EctC, a member of the cupin superfamily [71, 86]. As a carbon-oxygen hydrolyase, it eliminates a water molecule from the carbonyl C=O-bond and thereby generates an intramolecular imino bond (Figure 3B) [88–90]. Again the EctC enzyme from *H. elongata* has been biochemically characterized and possessed a K_m value of 11 mM under low salt concentration (0.05 M NaCl), and a decreased K_m of 8.4 mM in presence of elevated salt concentrations (0.77 M NaCl) [77]. Furthermore, the ectoine synthases from *Sphingopyxis alaskensis* [86], *Acidiphilum cryptum* [91] and the archaeon *Cand. Nitrosopumilus maritimus* [72] have been biochemically studied. Moreover, in case of the *S. alaskensis* EctC also mutant and structural studies were conducted [86]. While EctC from *H. elongata* and *S. alaskensis* were demonstrated to be highly salt tolerant or even dependent on NaCl addition, the corresponding enzyme from *A. cryptum* was rather inhibited in the presence of salt and seemed to be pH-dependent [77, 86, 91]. Moreover, the archaeal EctC protein was more restricted to a narrow range of salt concentrations [72]. The K_m and V_{max} values of the EctC enzymes from *S. alaskensis* were 25.4 mM and 24.6 U mg⁻¹ [86], while the *N. maritimus* EctC possessed a K_m of 7 mM and V_{max} of 13 U mg⁻¹ [72].

As stated above, the crystal structure of the EctC enzyme from *S. alaskensis* was obtained at 1.2 Å in the apo- and iron-bound form (PDB: 5BXX; 5BY5) revealing the presence of an iron catalyst within the cupin barrel [88] that is tightly coordinated by three conserved amino acid residues (Glu-57, Tyr-85 and His-93) (Figure 4B) [86]. The importance and conservation of these amino acid residues was supported by the analysis of site-specific mutants and bioinformatics. The crystallographic study revealed a head-to-tail arrangement of the EctC dimer [86].

During my PhD thesis I contributed to the investigations on the ectoine synthase from the thermophilic bacterium *P. lautus*. Together with our co-workers A. Höppner, S. Smits and J. Heider, a

research study on the crystallographic, mutational and phylogenomic analysis allowing the postulation of a detailed reaction mechanism was published in Scientific Reports (see 5.2.4) [71].

4.2.2.4. Ectoine hydroxylase EctD

Approximately fifty percent of the putative ectoine producers also possess the ectoine hydroxylase EctD to synthesize 5-hydroxyectoine that is often endowed with superior function-preserving attributes (see 4.2.3 and 5.1.1) [59, 64, 67, 78]. The ectoine hydroxylase was shown to be strictly dependent on molecular oxygen and attaches a hydroxyl-group in a highly regio- and stereo-selective manner to the C5-atom of the ectoine ring resulting in *trans*- or (4*S*,5*S*)-configured hydroxyectoine (Figure 3B) [64]. During this reaction the co-substrate 2-oxoglutarate is decarboxylated and the side products CO₂ and succinate are formed (Figure 3B) [64, 67, 78, 92]. The enzyme is a member of the non-heme Fe(II)-containing and 2-oxoglutarate-dependent dioxygenase-family and was first studied by Bursy *et al.* in *Virgibacillus salexigens* and *Streptomyces coelicolor* [36, 64] followed by a first crystallographic analysis [85]. Later in a comparative approach, the ectoine hydroxylases from *V. salexigens*, *S. coelicolor*, *S. alaskensis*, *P. lautus*, *Pseudomonas stutzeri*, *Alkalilimnicola ehrlichii*, *A. cryptum*, *H. elongata* and the archaeon *Cand. N. maritimus* have been studied biochemically and revealed kinetic parameters (*K_m* values) that ranged between 6 and 10 mM for the substrate ectoine and between 3 and 5 mM for the co-substrate 2-oxoglutarate [67, 72, 78]. Moreover, the crystal structures of the EctD proteins from *S. alaskensis* and *V. salexigens* have been obtained in the apo-form (PDB: 4MHR; 4NMI) and in complex with Fe(II) (PDB: 3EMR; 4MHU). In case of *S. alaskensis* the structure has also been solved in complex with Fe(II), 5-hydroxyectoine and 2-oxoglutarate (Figure 4C) (PDB: 4Q5O) [78, 85, 92]. Both studied enzymes form homo-dimers and detailed mutational and bioinformatical analyses revealed the amino acids involved in the coordination of the iron, co-substrate and reaction product. Moreover, a highly conserved signature sequence of 17 amino acids (F-x-W-H-S-D-F-E-T-W-H-x-E-D-G-M/L-P) was identified that is present in all *bona fide* EctD proteins [78]. This signature amino acid sequence is highly important from a structural point of view, as it forms one side of the cupin barrel [78]. Moreover, it is also critical for enzyme function as it harbors five residues involved in the binding of the iron catalyst, the co-substrate 2-oxoglutarate, and the reaction-product 5-hydroxyectoine [78]. However, it is important to notice, that ectoine hydroxylases are often miss-annotated in genome sequences as either proline- or phytanoyl-hydroxylases and that *bona fide* EctD-type enzyme can be distinguished from related 2-oxoglutarate-dependent dioxygenases through the presence of the above mentioned signature sequence.

During my PhD thesis the enzyme promiscuity of the ectoine hydroxylase was exploited for the stereo- and regio-selective *in vivo* and *in vitro* hydroxylation of the synthetic compound homoectoine (see 5.2.5). In another part of my thesis, the EctD enzyme was employed for the construction of a whole cell catalyst producing pure 5-hydroxyectoine (see 5.2.2). The first described research project was partially conducted by S. Wilcken, a master student that I have supervised and has been submitted to Frontiers in Microbiology. The second investigation was published in Microbial Cell Factories [93].

4.2.2.5. Specialized aspartokinase Ask_ect

L-aspartate- β -semialdehyde not only serves as the precursor molecule for ectoine biosynthesis, it also functions as a central metabolite of bacterial amino acid metabolism and cell wall synthesis [77, 79, 94–96]. The metabolic flux into the direction of ectoine production must therefore be tightly controlled to avoid inappropriate accumulation of ectoine and the waste of precursor molecules and energy [97–99]. On the other hand, precursor delivery must be secured under osmotic stress conditions to allow enhanced ectoine production and thereby confer effective stress protection. Approximately one third of putative ectoine producing microorganisms harbor the gene for a specialized aspartokinase within the transcriptional unit of the ectoine biosynthetic gene cluster (see 4.2.2 and 5.1.1) [59, 79]. The corresponding enzyme is called Ask_Ect since it differs from other aspartokinases in respect to its allosteric control [79].

First, the amino acid L-aspartate is converted to L-4-aspartyl- β -phosphate through an ATP-dependent phosphorylation by an aspartokinase (Figure 3B). In the next step, this intermediate is reduced by the ubiquitous (housekeeping) NADPH-dependent L-aspartate- β -semialdehyde-dehydrogenase (Asd) to L-aspartate- β -semialdehyde (Figure 3B). When the Ask_Ect enzyme was biochemically compared to Ask_LysC, both originating from *P. stutzeri* A1501, it became apparent that both enzymes possessed approximately the same kinetic parameter, but Ask_Ect was more feedback resistant [79]. While Ask_LysC was inhibited in presence of L-lysine and L-threonine, the activity of Ask_Ect was only affected by L-threonine and only to a minor degree. Furthermore, expression of the *P. stutzeri* *ectABCD* genes in *Escherichia coli* host cells led to increased ectoine/5-hydroxyectoine production, when the corresponding *ask_ect* gene was co-expressed [79]. Hence, this enzyme allows the bacterial cells to rapidly direct the flux into the ectoine biosynthetic pathway under osmotically unfavorable conditions. It remains unclear how this is achieved by the majority of ectoine producers as these lack such a specialized Ask_Ect enzyme.

4.2.3. Regulation of *ect* gene expression and other osmotic stress responsive genes

A fundamental aspect of compatible solute production was pointed out by A. Oren in his review on the *Bioenergetics of Halophilism* [20]. He calculated the energy demand in ATP equivalents that is needed to produce one molecule of ectoine or other compatible solutes. Approximately 40 ATP molecules are needed in a heterotrophic bacterium growing on glucose to produce one ectoine molecule, while the production in an autotrophic bacterium growing on CO₂ is estimated to even cost 15 ATP more (55 ATP in total) [20]. In contrast the import of an ectoine molecule via e. g. an ATP-fueled ABC-transporter only requires the hydrolysis of two ATP molecules (see 4.2.7). It becomes immediately apparent from these numbers that the production of compatible solutes must be tightly controlled in order to avoid the waste of energy.

Various studies on the regulation of osmotically responsive gene expression and the control of ectoine biosynthetic gene expression in different organisms have been published within the past decade. Notably, there seems to be different ways to control the expression of stress responsive genes: (I) through the

activity of one or more regulators [100–108], (II) through deviations in the promoter regions from consensus sequences [109–111], (III) through the changing concentrations of cyclic small messenger molecules [e.g. c-di-AMP (cyclic di-adenosine monophosphate)] [112–116], probably by the modulation of DNA superhelicity [117–121] and through yet unknown signaling mechanisms triggered by increased external salinities (Figure 5) [100, 109, 122]. Moreover, analysis of the transcriptional control of the *proU* operon encoding an osmoprotectant uptake system in *E. coli* revealed an effect of potassium glutamate, which is accumulated in the cells during the initial phase of their adaptation to high osmolarity [122–124]. It was also postulated that during the initial phase of osmotic stress response high levels of potassium glutamate might trigger a global switch in gene expression by acting differentially on RNA polymerase at promoters, which differ in their response to salt stress (Figure 5) [123].

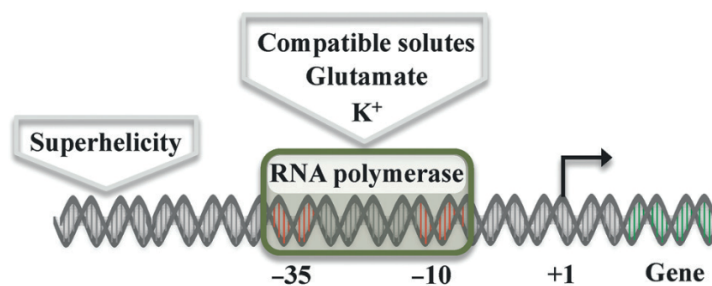


Figure 5 Schematic drawing of factors potentially influencing gene expression under high salinity stress conditions. taken from Hoffmann & Bremer (2016) *Stress and Environmental Regulation of Gene Expression and Adaptation in Bacteria* (398) 193-214.

Interestingly for various osmotically regulated genes, different expression and thereby regulatory patterns have been observed. Genes involved in the synthesis and acquisition of compatible solutes such as the *ect* genes in *P. stutzeri* A1501 [79], *proU* from *E. coli* [125], or the *opuE* gene and the *proHI* gene cluster from *Bacillus subtilis* [111, 126] often show a linear response to the externally applied degree of salinity. In contrast, the *yqiHIK* gene cluster in *B. subtilis*, that encodes enzymes involved in the remodeling of the cell wall during high osmolarity conditions, only exhibits a linear induction of expression when the external salt concentrations higher than 0.6 M NaCl are imposed [110]. While other osmotically responsive genes such as the *opuA* gene, encoding the OpuA ABC transport system for glycine betaine in *B. subtilis*, reaches a plateau in its expression level once the external osmotic stress is larger than 0.6 M NaCl [127]. This observation indicates the interplay of different regulatory mechanisms acting on diverse salt-responsive genes present in the same organism (e. g. *B. subtilis*). The cells are able to transform the same environmental information into an individual transcriptional pattern depending on their physiological importance or function [128]. Notably, different studies in *B. subtilis* revealed, that many osmotically regulated genes possess two promoters that are recognized by different sigma factors. Gene expression is thereby often jointly controlled by the house-keeping factor sigma-A (sigma-70 in *E. coli*) and sigma-B-regulon, the alternative sigma factor of the general stress response system [128]. Activation of sigma-B itself and its subsequent influence on global gene expression in response to a wide range of stress

and starvation stimuli have been best studied in *B. subtilis* [129]. The activity of sigma-B leads to the dramatic induction of about 150 sigma-B-dependent genes in *B. subtilis* and it is regulated by a complex signaling transduction cascade with at least three main pathways [129]. It involves a partner switching mechanism, in which interactions between alternative binding partners are controlled by serine and threonine phosphorylation [129–132]. In more detail, the activation is facilitated via a large protein complex called the *stressosome* [133]. Different members of the RsbR (Rbs = regulator of sigma-B) co-antagonist family and the RsbS antagonist build this 1.8 MDa multi-protein complex [133]. The formed icosahedral core sequesters the RsbT serine-threonine kinase, while the phosphorylation of the described core by RsbT is associated with RsbT release, which in turn activates downstream signaling [129–133]. In unstressed cells sigma-B is held inactive by the RsbW anti-sigma factor, which also acts as a serine kinase to phosphorylate and inactivate the RsbV anti-anti-sigma [130]. Following stress, one or another of the signaling phosphatases removes this modification from RsbV, allowing it to bind the RsbW anti-sigma [130]. Thus dephosphorylation of RsbV is the key event forcing RsbW to switch partners and release sigma-B, which can in turn function as an alternative sigma factor and activate target gene expression [129–133].

In terms of regulation of the ectoine biosynthetic genes, their osmotic control was studied through reporter gene fusions, Northern Blot analysis, qRT-PCR and RNA sequencing analysis in different Gram-positive and -negative organisms, such as *H. elongata*, *C. salexigens*, *Virgibacillus panthotenticus*, *S. salinus*, *Vibrio cholera*, *M. halophilus*, *P. stutzeri*, *M. alcaliphilum*, *Streptomyces rimosus* and *Methylophaga thalassica*, and also in the Archaeon *Cand. N. maritimus* [68, 72, 79, 83, 100–102, 134–139]. Some bacteria, such as *M. alcaliphilum* or *M. thalassica* harbor the MarR-type regulator EctR in the vicinity of the ectoine biosynthetic genes [100, 101] (see 4.2.3.1 and 5.2.7), while many other microorganisms do not possess this transcriptional regulator and must thereby rely on other regulatory mechanisms. However, in both cases it has not been understood yet, which stimulus the cells sense when they face salinity stress and how this environmental signal is processed and transduced to a transcriptional response activating for example *ect* gene expression. In studies using *V. salexigens* the ectoine biosynthetic genes were found to increase in a linear relationship to the degree of the externally imposed osmotic stress and *ect* gene expression was directed from a classical sigma-A-type promoter, which is the housekeeping sigma factor of *Bacilli* [64]. This expression pattern was resembled by the transcription profile of the gene encoding the ectoine/5-hydroxyectoine transporter EctT in *V. panthotenticus*. Interestingly, the *ectT* gene was driven by a sigma-B-type promoter [37]. To which stimulus these sigma factors respond and how this signal is then transduced remains still unknown.

More attempts towards the identification of promoters driving *ect* gene expression have been made in *M. halophilus* [68, 140], *H. elongata* [97] and *C. salexigens* [134, 139, 141]. However, in these studies many findings miss the appropriate controls and the observations stated in some publications are inconsistent. Their often sweeping conclusions are insufficiently corroborated by experimental data. Taken together, only little is known about detailed mechanisms responsible for the regulation of ectoine biosynthetic

genes, as well as the exact stimuli to which the cells respond and how this signal is then transferred to yet unidentified regulatory elements, different sigma factors or promoter regions.

Within a research project of my PhD thesis I worked on the detailed molecular autopsy of the *ect* promoter from *P. stutzeri* A1501 and its regulatory determinants (see 5.2.3). The findings were published in Applied and Environmental Microbiology [109] and my bachelor students P. Hub and B. Pöhl participated in this study.

4.2.3.1. The MarR-type regulator EctR and other regulatory proteins involved compatible solute accumulation

Various regulators from different organisms have been identified to be involved in the regulation of osmopress responsive genes. As mentioned above, Trotsenko and co-workers studied the MarR-type regulator EctR (MarR = Multiple antibiotic resistance regulator) in different methylotrophs [100, 101, 142]. *M. alcaliphilum* is a highly salt tolerant microorganism, that mainly accumulates ectoine as osmotic stress protectant [143, 144]. It possesses an *ectABC-ask_ect* operon, that is transcribed from two sigma-70 type promoters (*ectAp₁*, *ectAp₂*) located upstream of *ectA* [145]. The *ectR1* gene is encoded divergently and upstream of the *ect* gene cluster. Size exclusion chromatography and DNaseI footprint analysis revealed that EctR1 forms a homodimer that binds to an imperfect inverted repeat upstream of the *ectA* gene in a region that overlaps the -10 box of the *ectAp₁* promoter [100]. Thereby, EctR1 functions as repressor for the *ect* genes [100]. The transcription of the *ect* gene cluster is osmotically induced, but surprisingly the external addition of ectoine or glycine betaine did not reduce the activity of L-2,4-diaminobutyrate acetyltransferase (EctA), which was used as an indicator for the induction of the ectoine biosynthesis pathway [100]. Interestingly, a *M. alcaliphilum* mutant strain, in which *ectR* was genetically inactivated, did not show any growth defect under different osmotic conditions [100]. Moreover, the *ect* genes in this mutant showed higher transcription levels under low salt conditions but were still osmotically induced in the presence of moderate or high salt stress [100]. It is still unclear how salt induction of the ectoine biosynthetic genes is regulated in *M. alcaliphilum* as EctR1 does not seem to be the only regulatory player involved in this process. Furthermore it is not known to which cellular cue or stimulus EctR1 responds and how it senses the imposed osmotic stress.

A study in *V. cholera* has shed light on the regulation of the *ectABC* gene cluster by the MarR-type regulator CosR, which is related to the above described EctR regulator (51% sequence identity) [102]. Shikuma *et al.* showed that this regulator negatively controls gene expression of the *ect* genes and the gene encoding the compatible solute transporter OpuD [102]. The *cosR* gene is located upstream and divergent of the *opuD* gene and *cosR* expression increases linearly to the externally applied salinity. Furthermore CosR represses genes important for motility and induces genes involved in biofilm formation [102]. Therefore, this regulator connects osmotic stress protection and biofilm formation. Under high salinity conditions, both *cosR* and the genes for the synthesis and uptake of compatible solutes show increased expression levels [102]. An observation leading to the conclusion, that CosR is involved in a negative autoregulatory circuit and hence allows a rapid adaption to fluctuating environmental conditions.

Interestingly, CosR does not sense osmolarity but might react to ionic strength [102]. This phenomenon has also been reported for the GntR-type regulator BusR from *Lactococcus lactis* [103, 104, 146]. BusR functions as a transcriptional repressor for the glycine betaine uptake system BusA. Interestingly, its C-terminus is highly similar to a component of the K⁺/H⁺-symporter Trk from *E. coli* and is able to bind the small second messenger molecule, c-di-AMP [103, 147].

Another regulator, controlling ectoine biosynthetic genes has been described in *S. coelicolor* - GlnR, the global regulator for nitrogen metabolism in actinomycetes [148]. This protein functions as a negative regulator for the transcription of ectoine/hydroxyectoine biosynthetic genes and the physiological role of this transcriptional repression by GlnR is proposed to protect the intracellular glutamate pool, which acts as a key nitrogen donor for both the nitrogen metabolism and the ectoine/hydroxyectoine biosynthesis [149]. As it has been observed for EctR1, the ectoine biosynthetic genes in an *S. coelicolor* mutant strain lacking *glnR* were still osmotically controlled, but their overall expression under each tested osmolarity increased [149].

In one unpublished part of my PhD thesis I have studied the EctR-type regulator from *Novosphingobium* sp. LH128 (see 5.2.7). Together with our collaboration partners S. Smits, A. Höppner, and S. Kobus (University of Düsseldorf) we obtained a crystal structure of EctR at a resolution of 2.2 Å. Furthermore, I studied the binding of EctR upstream of the *ect* gene cluster and in front of the *ectR* coding region itself and performed first experiments with an *ectR* deletion mutant (see 5.2.7).

4.2.4. Properties of ectoines

As most compatible solutes, ectoines can be accumulated by stressed cells up to molar concentrations because of their low-molecular mass, zwitter-ionic state and very high solubility in water [57, 60, 150, 151]. The underlying mechanisms that equip ectoines with superior protective capacities have been studied by biophysical approaches and molecular dynamics simulations [151–160]. As described above for the activity of *chemical chaperones*, ectoines are excluded from the monolayer of water around proteins as well as the hydration layer between membranes and the surrounding liquid [151, 153]. Both compounds are able to enhance the properties of hydrogen bonds resulting in a stabilizing effect for macromolecules [161–163]. Furthermore, the zwitter-ionic nature of ectoines influences their interaction with water leading to a strong influence on the local water structure [151, 156, 157, 164, 165]. Simulation approaches demonstrated that ectoine and 5-hydroxyectoine are strong water binders and that this water-coordinating behavior is not altered at high salt concentrations [157, 166]. Taken together, these physico-chemical features endow ectoines with major stress-relieving and cyto-protective properties. In a recent publication by Galinski and co-workers the molecular basis of ectoine as a scavenger for hydroxyl radicals was illuminated [167]. The authors report that ectoine is converted into two major products during its reaction with hydroxyl radicals: *N*-acetimide aspartate and *N*-acetimide-β-alanine [167]. Moreover, they propose a reaction mechanism in which the heterocycle of ectoine is cleaved and this cleaved product is further oxidized at the C-terminus [167]. Hence, the radical scavenging ability of ectoine was proven for the first

time and forms the basis to explain the observed anti-inflammatory effects of ectoine, when it is applied to ameliorate skin, lung and bowel diseases [167].

Bacterial cells are somehow able to sense the externally applied strength of osmotic stress, and consequently transform this information to a cellular signal that then effectuates the production and accumulation of the used compatible solute e. g. ectoines [66, 109, 139]. Yet microorganisms not only accumulate ectoines in response to high extracellular osmolarity, some bacteria also use them as thermoprotectants against heat or cold stress [36, 37, 40, 70, 137, 168]. The accumulation under unfavorable temperatures occurs through synthesis and often via uptake from environmental resources [36, 37, 168]. However, until now it is not known, how ectoines function as thermolytes.

Organisms, that produce both ectoine and 5-hydroxyectoine, often accumulate a mixture of both protectants even though the ratio can vary between species [57, 79, 82, 93]. Moreover, some organisms accumulate higher amounts of 5-hydroxyectoine when they enter the stationary growth phase pointing to superior stress-relieving properties on 5-hydroxyectoine under these growth conditions [82, 169–171]. In addition, some other bacteria switch between different osmolytes. This strategy has been first studied in the moderately halophilic, chloride-dependent bacterium *Halobacillus halophilus*. It switches its osmolyte strategy with the salinity in its environment as it only accumulates ectoine only at very high osmolarities and contingent on its growth phase [171–174]. Osmolyte switching has also been studied in *V. parvotonicus*, which accumulates proline in response to moderate osmotic stress, but activates the production of ectoine under enhanced NaCl stress conditions [137]. Especially 5-hydroxyectoine seems to possess different and superior physical and protective properties compared to ectoine. One example is its enhanced ability to form glasses, which results from stronger intermolecular hydrogen bonds with the OH-group [175]. In addition, 5-hydroxyectoine acts as a potent desiccation protectant due to its increased glass transition temperature [175] and it was even found to protect *C. salexigens* against oxidative stress [141].

4.2.5. Biotechnological production of ectoines

The above-described extraordinary functional attributes of ectoine and 5-hydroxyectoine led to large biotechnological interests and the development of industrial, biotechnological, medical and cosmetical applications [57, 60, 61]. The increasing demand on ectoine therefor effectuated the establishment of industrial production mechanisms and the research on natural and synthetic cell factories [57, 60, 61].

4.2.5.1. Aims to develop natural and synthetic ectoine cell factories

Industrial scale production of ectoine started approximately in 1998 when Sauer and Galinski developed the method of *bacterial milking* [176]. The natural ectoine producer *H. elongata* is highly salt-tolerant and produces large amounts of ectoine in response to the applied osmotic stress. During the former bacterial milking procedure, the natural producer strain was cultivated to high cell densities (40 g l⁻¹) in a fermentation process in the presence of 15% NaCl to promote ectoine production. After reaching a

cell density of 40 g l⁻¹ the culture was filtered to 20% of the total volume and the bioreactor was refilled with distilled water resulting in an severe osmotic down-shock from 15% to 3% NaCl, that enforces the opening of the mechanosensitive channels to prevent rupture of the hypoosmotically stressed *H. elongata* cells [6, 176]. As a result, the produced ectoine together with other low-molecular weight solutes and ions are unspecifically released via mechanosensitive channels to ensure survival of the bacteria (see 4.3) [6]. This allows on the one hand the purification of ectoine from the cells supernatant, and on the other hand the recultivation of the bacterial biomass in high salinity medium for another round of ectoine production. In downstream processes ectoine is purified through acidic protein precipitation, cation exchange chromatography, cross-filtering, and evaporation/crystallization [176]. Since this procedure is rather complex and time-demanding, further attempts in strain development have been made, that resulted in an engineered *H. elongata* mutant strain by Kunte and co-workers, which permanently secretes the produced ectoine into the medium [60]. This secretion was achieved by the genetic deletion of the ectoine specific uptake system TeaABC hindering the reimport of ectoine (see 4.2.7) [177, 178], while the exact mechanism or involved efflux system remains unidentified. Furthermore, blocking of the ectoine catabolic pathway through the deletion of the gene *doeA*, which encodes the ectoine hydrolase, the first enzyme involved in ectoine degradation, additionally increased ectoine production (see 4.2.6) [60, 97]. The resulting engineered *H. elongata* strain is now used by the company bitop (bitop AG, Witten, Germany) to produce ectoine on an industrial scale. While the companies do not disclose their ectoine production yields, the world wide annual production is estimated to reach 15000 tons with a price of at least 900 € per kg [179]. With more concrete numbers, for example, the chemical company Sigma-Aldrich (distribution: Merck KGaA, Darmstadt, Germany) sells ectoine in different qualities ranging from 552 to 1300 € per 100 g. However, although the producer companies do not disclose exact numbers, it becomes apparent, that ectoine is a high value and important natural product and that it possesses the greatest potential for commercial use compared to other known compatible solutes [180].

This industrial interest has promoted both, the research on and development of other natural and synthetic ectoine cell factories. Comprehensive reviews published by Pastor *et al.*, Lentzen & Schwarz and Kunte *et al.* summarize the efforts made on the biotechnological production and use of ectoines [57, 60, 61]. I'll now describe some of the attempts in brief.

In addition to *H. elongata*, ectoine production through fed-batch or batch cultivation of natural producers has been studied in *Brevibacterium epidermis* DSM 20659 [181], *Brevibacterium* sp. JCM 6894 [182], *Marinococcus* sp. M52 [169, 183], *C. salexigens* DSM 3043 [184], *Halomonas boliviensis* DSM 15516 [185] and *Halomonas salina* DSM5928 [186] leading to production yields ranging between 70 and 540 mg per mg dry weight [57]. Moreover, different media compositions in terms of variations in the addition of yeast extract or sodium glutamate to yield ectoines have been studied for example in *Marinococcus* sp. ECT1 [187], *H. salina* BRCR17875 [188, 189] or *Halomonas hydrothermalis* [190]. In a report by Lang *et al.* *H. salina* DSM5928 facilitated ectoine production in a combined process consisting of batch-fermentation of growing cells and ectoine production and excretion in phosphate-limited resting cells [191]. Furthermore, natural ectoine producers were exploited to synthesize ectoines growing on cheap and renewable resources.

Tanimura *et al.* aimed the production of ectoine from lignocellulose biomass-derived sugar mixtures and Cantera *et al.* published several attempts to use methanotrophs growing on the second most important climate gas methane as natural ectoine producing cell factories [192–196]. Moreover, several studies have been published, in which ectoine production was increased through the genetic engineering of the natural producer strain, such as the overexpression of sugar transporters in *H. elongata* [197], the deletion of *ectD* in *H. hydrothermalis* Y2 [190] or flux balance analysis in *C. salexigens* [98].

Nevertheless, it must be clarified that often mixtures of ectoine and hydroxyectoine or even ectoines and other solutes such as proline [198], glutamate [183] or the biopolyester poly(3-hydroxybutyrate) (PHB) [185] are accumulated by natural ectoine producers, which might entail further costly and difficult purification steps. Furthermore, a range of different techniques was used for the extraction of the produced ectoines, including the previously described hypoosmotic shock or permanent excretion, ethanolic or methanolic extraction and thermal permeabilization of the producer cells, while its secretion represents the cheapest and most time-saving way [57].

In terms of synthetic cell factories, mainly different *E. coli* wild type strains, such as BL21, DH5 α or W3110, were employed as host strains for ectoine biosynthetic genes originating from different organisms [199–201]. Naturally, the enterobacterium *E. coli* neither possesses the ability to produce nor degrade ectoines. The employed *E. coli* strains served as chassis cells for the ectoine biosynthetic pathways originating from various organisms, such as *H. elongata* [200–204], *M. halophilus* [68, 96], *C. salexigens* DSM 3043 [134, 199], *Bacillus halodurans* [205], *A. cryptum* [91] or different *P. stutzeri* strains [109, 170]. Also the industrial work horse *Corynebacterium glutamicum* was employed for heterologous ectoine production carrying the genes from *P. stutzeri* A1501 [94, 179], or from *C. salexigens* [206]. In these studies, *C. glutamicum* was further genetically engineered to increase ectoine yield, for example through the de-repression of the glucose metabolism by deletion of the regulatory gene *sugR* and avoiding L-lactate formation by inactivation of the lactate dehydrogenase gene *ldhA* [206] or the implementation of a mutant aspartokinase enzyme to ensure efficient supply of the precursor L-aspartate- β -semialdehyde [94]. Furthermore, *B. subtilis* was employed as a host for the ectoine biosynthetic genes of *Bacillus pasteurii* [66], *C. salexigens* for those originating from *Streptomyces cryomallum* [69] and even the tobacco plant *Nicotiana tabacum* for the expression of bacterial *ect* genes from *M. halophilus* [207]. Moreover, the yeast *Hansenula polymorpha* harboring the *ectABCD* gene cluster from *H. elongata* produced and secreted almost exclusively hydroxyectoine when it was grown in media with pH 5 [208]. Most of these cell factories contained the *ect* genes encoded on a plasmid differing in their copy numbers and promoters, as they were either the natural ones or synthetic promoters that were constitutively transcribed or activated by an inducer molecule [91, 94, 96, 109, 196, 203, 205, 206, 209]. Only *B. subtilis* harbored the ectoine biosynthetic genes of *B. pasteurii* in its genome [66].

With few exceptions, most microorganism that possess the ectoine hydroxylase EctD produce a mixture of ectoine and 5-hydroxyectoine [59, 93, 169, 183, 208]. One of these exceptions is *Marinococcus* M52 that was shown to produce up to 96.4% 5-hydroxyectoine when it is cultivated for 48h in fish peptone medium. Interestingly the amount of 5-hydroxyectoine increased by 25% when the cells entered

the stationary growth phase. An observation, that might be explained by the superior protective effects of 5-hydroxyectoine (see above), a slower turn-over rate, or higher stability of the EctD enzyme [169]. Similar observations were reported for the production of ectoine and 5-hydroxyectoine when the *ect* genes from *P. stutzeri* DSM5190 were heterologously expressed in *E. coli* DH5 α [170].

In context of this PhD thesis several synthetic cell factories have been investigated, in brief: (I) an EctD-overexpressing *E. coli* cell factory aiming the production and secretion of pure 5-hydroxyectoine via whole cell catalysis (see chapter 5.2.2), (II) promoter engineering and improvement of heterologous expression of the *ect* gene originating from *P. stutzeri* A1501 in an *E. coli* mutant lacking the osmoprotectant uptake systems ProP and ProU as well as the trehalose biosynthetic enzyme OtsA (see chapter 5.2.3); and (III) the cell-factory-based hydroxylation of the synthetic ectoine derivative homoectoine (see chapter 5.2.5). The work of part II was supported by two bachelor and part III by one master student that I have supervised and the first two parts led to a publication in a peer-reviewed journal. The manuscript about the regio- and stereoselective hydroxylation of homoectoine has been submitted to *Frontiers in Microbiology*.

4.2.5.2. Industrial and medical applications of ectoines

Over the last decades, more and more biotechnological, medical and skin care applications for ectoines have been studied and a considerable number of ectoine-containing products have been commercially launched (<https://www.bitop.de/de/products>) [57, 60, 61, 165, 180, 210]. Most of them rely on hygroscopic properties of ectoines [151, 157, 166], and their ability to stabilize macromolecular complexes, proteins or entire cells by its coordinated water layer. Applications of ectoines can be grouped into three categories: (I) protection of biological macromolecules, (II) protection of cells, and (III) protection of skin and mucosa - all fields contain therapeutic uses of ectoines [57, 60, 61, 165]. Examples for applications of ectoines in the field of macromolecules are their ability to effectively protect antibodies from proteolytic cleavage [61] and immunotoxins from the stress during freezing and thawing [211]. Furthermore their stabilizing effect on proteins was demonstrated in case of misfolding, unfolding, degradation, aggregation, freezing, thermostability, drying, oxidative damage, melting temperature and treatment with urea [57, 60, 211–215]. Ectoine was even shown to function as a stabilizer of transcriptional complexes (DNA-protein-complexes) involving the regulatory proteins Lrp (Leucine-Responsive regulatory Protein) and H-NS (Heat-stable Nucleoid-Structuring protein) [216]. This observation was followed by the discovery that both ectoines influence the structure of the DNA and protect it against UV and ionization radiation [158, 159, 217]. Ectoine and 5-hydroxyectoine have furthermore been shown to alter and improve the quality of DNA microarrays and the efficiency of PCRs [218, 219]. In the latter case also synthetic ectoine derivatives have been studied, showing that homoectoine, a seven-membered ring-analogue of ectoine, acts as the most potent PCR enhancer [218]. Within human biology ectoines were further studied in respect to their anti-inflammatory effect [165, 220–226], their ability to reduce apoptotic cell death [220, 226] and to inhibit the aggregation and neurotoxicity

of Alzheimer's β -amyloid [152, 210, 227, 228]. Furthermore, a beneficial role of hydroxyectoine-modified Histidine-Tryptophan-Ketoglutarate (HTK) solution has been observed in a study on the preservation of deceased after cardiac death donor (DCD) livers used for organ transplantations [229].

With respect to the ability to stabilize entire cells, hydroxyectoine has been shown to protect *Pseudomonas putida* and *E. coli* against desiccation and plastic encapsulation [38, 230]. In *E. coli* strains ectoines preserved the respiratory activity [231], induce thermotolerance [40] and protect the cells against the effects of drying and storing [39]. Furthermore, a promoting effect on ethanol fermentation has been observed in *Zymomonas mobilis* [232] and in the detoxification of phenol in *Halomonas* sp. EF11 [233]. In addition to its osmoprotective effect on many bacteria, ectoine has been shown to enhance salt-tolerance of tobacco and tomato plants, when the *ect* genes of *H. elongata* were introduced into the plants [234, 235]. In medical trials, ectoine was described to protect human skin and membranes [57, 61, 144, 153, 165, 221, 236, 237] and the mitochondrial DNA in human dermal fibroblasts [57, 237]. The synthetic compound homoectoine was further found to protect mice against colitis by preventing a claudin switch in epithelial tight junctions [238].

As a consequence, an interesting market for ectoines is their application in skin care and medical products [61, 165]. Furthermore, new applications for ectoines are continuously developed, e.g. their use in dietary supplements (<https://www.bitop.de/en/products/health-and-wellbeing/food-supplements>) or animal health care (<https://www.bitop.de/en/products/animal-health>). In the field of skin care products, ectoine has been shown to protect the skin barrier against water loss and drying out [165, 221], furthermore, to contribute to the protection of skin immune cells against UV radiation [57] and the reduction of UV-induced sunburn cells [57, 165, 239, 240]. Moreover ectoine was demonstrated to prevent UVA-induced photoaging [239] and conferred cytoprotection to keratinocytes [237, 241]. To date, several pharmaceutical products containing ectoine have been launched, especially in the fields of allergy treatment e. g. nasal sprays, eye drops and inhalants, mouth and throat spray, or cough drops and the therapy of different skin diseases. For example, it is mixed into creams against eczema and inflammatory skin problems (<https://www.bitop.de/en/products/health-and-wellbeing/otc-self-medication>).

4.2.6. The use of ectoines as nutrients

Ectoine and 5-hydroxyectoine are nitrogen-rich compounds (Figure 2) that can not only be produced and accumulate by a large group of microorganisms in response to different environmental stresses, but can also be utilized as nutrients either by the producer cell itself or by other microorganisms living in the same habitat [59, 242]. Ectoine catabolism has been studied to detail in *S. meliloti*, *Ruegeria pomeroyi* DSS-3, *H. elongata* and *C. salexigens* within the last decades [136, 230, 242–245]. The underlying proteins important for ectoine uptake and catabolism in *S. meliloti* have been detected by Jebbar *et al.* through a proteomic analysis of cells grown in the presence or absence of ectoines [243]. The proteins of eight ectoine-induced genes have been identified and their coding regions are co-located in the same gene cluster present on the pSymB mega-plasmid of *S. meliloti*. The ectoine catabolic operon (*eutABCDE*) in *S. meliloti* also harbors the genes encoding the ectoine-specific ABC-transporter EhuABCD (Figure 6A) (see chapter 4.2.7).

Furthermore, a gene encoding the GntR-type transcriptional regulator, EnuR, is located down-stream of this operon and the coding region of an AsnC/Lrp-type regulator is positioned up-stream of the ectoine catabolic gene cluster. Transcriptional analysis of the *ehuABCD-entABCDE* operon in *S. meliloti* showed that the expression is substrate-inducible and thereby confirmed the proteomics data [243]. After the initial description of the ectoine utilization genes in *S. meliloti*, the import and catabolic gene cluster for ectoines were identified and studied in *H. elongata* [97], *R. pomeroyi* [242] and *C. salexigens* [35, 246]. In comparison to the highly conserved organization of the ectoine biosynthetic gene clusters, the identified ectoine catabolic gene clusters differ largely in their gene content and genomic organization (Figure 6A). One major difference is the presence of ectoine uptake systems: while the ABC transporter EhuABCD is present in *S. meliloti*, *R. pomeroyi* harbors a TRAP transporter (UehABC) [242, 243, 247, 248] (Figure 6A and Figure 7) (see section 4.2.7). None of these transporters is co-located with the ectoine catabolic genes in the closely related organisms *H. elongata* and *C. salexigens* (Figure 6A), but they both harbor an osmotically inducible ectoine-specific uptake system (TeaABC) belonging to the TRAP family at a different position in their genomes [177, 178, 242, 249]. However, since the Tea-transport systems are osmotically regulated, it is yet unclear if these transporters are also involved in the import of ectoines for their use as nutrients.

The identification of the proteins involved in ectoine degradation led to a first proposal of the underlying biochemical pathway in *H. elongata* by Schwibbert *et al.* [97]. According to this proposal, ectoine degradation starts with the enzymatic activity of the ectoine hydrolase, DoeA/EutD, that opens the pyrimidine ring of the ectoine molecule and thereby forms *N*- α -acetyl-2,4-diaminobutyrate (*N*- α -ADABA) (Figure 6B). Heterologous expression of the *H. elongata doeA* gene in *E. coli* resulted in the hydrolysis of ectoine to *N*- α -ADABA and *N*- γ -ADABA in a 2:1-ratio [97]. An interesting observation, since *N*- γ -ADABA is the main substrate for ectoine formation by the ectoine synthase EctC and it is still unclear how the cells avoid the "re-formation" of ectoine through the enzymatic activity of EctC. Hypothetically, a possible mechanism could be substrate channeling between the ectoine degradation enzyme EutD and EutE.

In the proposed ectoine degradation route, the resulting *N*- α -ADABA is converted to DABA and acetate through the enzymatic activity of the *N*- α -acetyl-2,4-diaminobutyrate deacetylase (DoeB/EutE), followed by the formation of L-aspartate- β -semialdehyde and L-glutamate through the transamination of DABA by the DoeD/Atf enzyme (Figure 6B). L-aspartate- β -semialdehyde is then oxidized to L-aspartate by DoeC/Ssd, a protein related to succinate semialdehyde dehydrogenases (Figure 6B). In a study of Schulz *et al.* on ectoine/5-hydroxyectoine degradation in *R. pomeroyi* DSS-3, the proposed biochemical route was expanded by a suggestion for the conversion of 5-hydroxyectoine to ectoine. This conversion was assigned to the potential activity of the EutABC proteins that might be involved in the removal of the hydroxyl group from the ectoine ring (Figure 6B) [242]. It is apparent from these proposals that the ectoine degradation pathway mainly traces the ectoine biosynthetic route backwards using the activity of different enzymes. However, it has to be pointed out that the pathways proposed by Schwibbert *et al.* [97] and Schulz *et al.* [242] are not build on biochemical and experimental evidences, and thus require further

intensive functional studies in the future. Especially the suggested pathway for the conversion of 5-hydroxyectoine to ectoine is very speculative and it might in reality differ substantially from the proposal. Particularly, since the EutB enzyme (dehydratase), which was suggested to eliminate the hydroxyl-group from the hydroxyectoine molecule, is a PLP-dependent enzyme (Figure 6). However, at this indicated step no free amino group is present that is required for the formation of a Schiff base. Hence, it can be assumed that the EutB enzyme is rather involved in a later step of the ectoine/5-hydroxyectoine degradation pathway, once the pyrimidine ring has been opened.

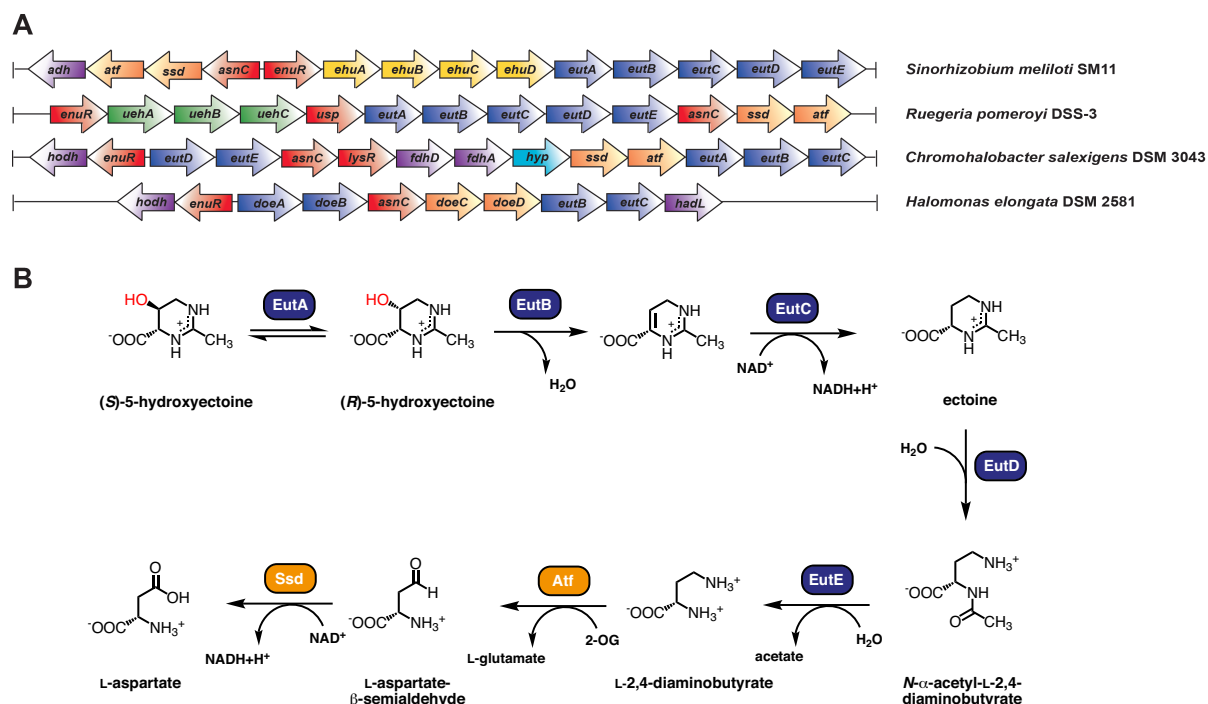


Figure 6 Genetic organization of ectoine catabolic genes and ectoine/5-hydroxyectoine degradation pathway. **A** Schematic illustration of the ectoine catabolic gene clusters from *S. meliloti* [243, 250], *R. pomeroyi* [242, 249], *C. salexigens*, and *H. elongata* [97]. **B** Proposed ectoine/5-hydroxyectoine degradation pathway. EutA: racemase; EutB: dehydratase; EutC: ectoine dehydrogenase; DoeA/EutD: ectoine hydrolase; DoeB/EutE: N-α-acetyl-L-2,4-diaminobutyrate deacetylase; DoeD/Atf: aminotransferase; DoeC/Ssd: dehydrogenase [97, 242, 249]. Taken from Czech *et al.* (2018) *Genes* (9) doi: 10.3390/genes9040177.

Based on these biochemical hypothesis and the first experiments by Schwibbert *et al.* [97], the ectoine hydrolase (EutD) can be described as the key enzyme involved in ectoine utilization [97, 242]. In a comprehensive bioinformatical analysis by Schulz *et al.* [242] 539 EutD orthologs were detected in all bacterial and archaeal genomes that were present in the IMG database at that time. Interesting all of the identified ectoine degrading organisms belonged to the phylum of *Proteobacteria* [251], while *ect* biosynthetic genes are found in ten different bacterial phyla [59, 67].

In terms of genetic regulation, an intricate regulatory network for the ectoine catabolic genes was identified in *R. pomeroyi* DSS-3 [249]. The *uehABC-usp-eutABCDE-asnC-ssd-atf* gene cluster (Figure 6A) of this marine bacterium is also induced in presence of ectoine and 5-hydroxyectoine, but none of the two

compounds serves as the true inducer molecule. In depth biochemical and physiological analysis showed that the intermediates of the ectoine degradation pathway, *N*- α -ADABA and, to a minor extent, DABA function as the internal inducers of the ectoine catabolic genes in *R. pomeroyi* DSS-3. This regulation involves the transcriptional regulator EnuR, and the corresponding *enuR* gene is located upstream of the ectoine catabolism operon in *R. pomeroyi*. The EnuR regulator belongs to the MocR/GabR sub-group of the GntR superfamily of regulators and bioinformatic analysis revealed its presence in the gene neighborhood of 456 (from 539 gene clusters in total; 85%) potential ectoine/5-hydroxyectoine catabolic gene clusters [249]. Members of the GntR regulator superfamily consist of two domains: a N-terminal DNA binding domain and a C-terminal dimerization domain that is structurally related to aminotransferases [146, 252, 253]. The EnuR is highly similar to the well-known GabR regulator from *B. subtilis* that controls the expression of genes involved in γ -aminobutyrate metabolism [254]. Like other members of the MocR/GabR sub-group of the GntR superfamily, EnuR harbors a PLP co-factor that is covalently bound to a Lys-residue (Lys-302) within the C-terminal aminotransferase domain via a Schiff base forming an internal aldimine [146, 249, 252, 253]. Mutational analysis revealed that this Lys residue is indispensable for its regulatory function. The regulatory mechanism is described as follows: ectoine/5-hydroxyectoine enter the cells through the import system EhuABCD, low basal transcription of the ectoine catabolic genes results in the presence of the ectoine degradation enzymes that enzymatically catalyze the formation of *N*- α -ADABA and DABA. Since these two molecules possess a primary amino-group, they can bind to the PLP-cofactor that was previously bound in the aminotransferase domain of the EnuR regulator. This *N*- α -ADABA-/DABA-PLP complex forms an external aldimine and results in an EnuR with a free Lys-residue. As a consequence, this probably triggers conformational changes within the EnuR regulator and thereby modulates its DNA binding properties. Biochemical experiments with the purified EnuR protein revealed a very high affinity for *N*- α -ADABA ($K_d = 1.7 \mu\text{M}$), while DABA is only bound with highly reduced affinity ($K_d = 457 \mu\text{M}$); *N*- α -ADABA therefor serves as the main inducer for the EnuR regulator. Furthermore, mutant analysis disrupting the *enuR* gene in *R. pomeroyi* and *S. meliloti* highlighted the function of EnuR as a repressor for the ectoine uptake and catabolic genes [249, 250].

Besides the EnuR regulator, Schulz *et al.* identified two other systems involved in the regulatory network of the ectoine degradation genes in *R. pomeroyi* DSS-3: the AsnC regulator and the two-component system NtrYX [249]. The AsnC protein is co-localized with the ectoine catabolic genes in 494 of the 539 potential ectoine degraders (92%), a frequency that highlights the importance of this regulator for ectoine catabolism. Mutant analysis in *R. pomeroyi* identified the AsnC regulator as an essential activator for the transcription of the ectoine degradation genes [249]. The same regulatory influence was observed for the two-component system (TCS) NtrYX - deletion of this regulatory element prevented the use of ectoines as the sole carbon source in *R. pomeroyi* [249]. However, it requires further investigations to which environmental cue or signal these two regulators respond. Interestingly, variations in the regulatory mechanisms and interplay of the regulators for the ectoine catabolic genes must be assumed, since only 45% of the predicted ectoine consumers possess all three regulatory systems [249]. While EnuR and AsnC are present in different sub-phyla of the *Proteobacteria*, the TCS NtrYX was only found in members of the

Alphaproteobacteria [249]. The interplay of these regulators and the dissimilarities in gene content between differently equipped microbial ectoine degraders will be an interesting research field in the future.

4.2.7. Transport of ectoines

Import of ectoines from environmental resources is an energetically cheap and flexible way to accumulate osmotic stress protectants when microbial cells are confronted with unfavorable, high external salt concentration or to take up ectoines for their use as nutrients [20, 242, 243]. As stated above the production of one ectoine molecule costs between 40 and 55 ATP, while the uptake through e. g. an ATP-consuming ABC-transporter requires only two ATP [20]. Compatible solutes are present in the natural habitats of microorganisms [255–259], since producer cells that can either be other bacteria, or higher organisms, such as diatoms or flagellates, secrete them [59, 76, 260]. They can be released through the transient opening of mechanosensitive channels during osmotic down-shocks (see 4.3) [6], through their active secretion, by rotting plant material, or from lysed bacterial cells attacked by phages or toxins, or through the predatory activity of microorganisms and eukaryotic cells [46]. Uptake systems for compatible solutes are therefor found ubiquitously in microorganisms inhabiting different ecosystems and either allow their import in response to elevated osmotic stress or for their use as nutrients [1, 7, 8, 14, 177, 243, 247, 261, 262].

In the case of osmolyte transporters, their transport activity and transcriptional response is commonly osmotically regulated [1, 263, 264]. Their almost instantaneous activation and their subsequent elevated production allow a rapid adjustment to an extracellular osmotic upshift. Hence, uptake systems for compatible solutes and their precursors play a crucial role in the osmotic stress response of microorganism [1, 105, 116, 265]. In many cases microbial cells possess various import systems for osmotic stress protectants, which differ in their substrate profiles and affinities, and also their transport mechanism [1, 7, 116, 266–268].

Osmotically induced uptake systems for ectoine and 5-hydroxyectoine have been described in numerous Gram-negative and Gram-positive bacterial species and these transporters belong to four different families: (I) ATP-binding cassette (ABC)-transporters that are dependent on a substrate binding protein and energized by the hydrolysis of ATP - representatives of this group are the ProU system from *E. coli*, the OusB transporter from *Erwinia chrysanthemi*, the OpuC system from *B. subtilis* and the ProU transporter from *Vibrio anguillarum* [168, 268–270]; (II) Major Facilitator Superfamily (MFS) transporters that depend on the proton motif force such as ProP from *E. coli* and OusA from *E. chrysanthemi* [268, 271]; (III) members of the Betaine-Choline-Carnitine Transporter (BCCT) family that are either fueled by sodium or proton gradients - examples are OpuD from *B. subtilis*, EctT from *V. pantothenicus*, EctM from *M. halophilus*, or EctP and LcoP from *C. glutamicum* [37, 261, 269, 272–275]; and (IV) members of the tripartite ATP independent periplasmic (TRAP) transporter family, which are dependent on proton or sodium gradients, such as TeaABC from *H. elongata* [177, 178]. Most of these transporters possess a broad

substrate spectrum, while others such as the Tea-system from *H. elongata* or EctT from *V. pantothenticus* are highly specialized transporters for ectoines [37, 116, 125, 177, 276].

From the described transport systems involved in the bacterial adaptation to osmotic stress, high-resolution crystal structures of the TeaA periplasmatic ligand-binding protein have been solved in complex with ectoine (PDB: 2VPN) (Figure 7A) and hydroxyectoine (PDB: 2VPO) (Figure 7A) [178]. This binding protein is highly specific for ectoines and possesses K_d values of 0.2 μ M for ectoine and 3.8 μ M for 5-hydroxyectoine, respectively [178]. Moreover, the crystal structure of OpuCC, the substrate binding protein from the *B. subtilis* OpuC transporter, has been obtained with a bound ectoine molecule even though this uptake system has only a weak affinity for ectoine ($K_i = 1.56$ mM) (PDB: 3PPR) (Figure 7B) [116, 269, 277].

In contrast to these osmotically regulated uptake systems for compatible solutes, transporters importing osmolytes for their utilization as nutrients are mostly substrate-induced [243, 247]. Since cell-free compatible solutes are scarce, bacterial cells employ high affinity uptake system for their acquisition as carbon-, nitrogen- and energy source [255–259, 278]. Such uptake systems for the use of ectoines as nutrients have been studied in the plant-root-associated bacterium *S. meliloti*, that employs the ABC transporter EhuABCD, and in *R. pomeroyi* DSS-3, that harbors the TRAP transporter UehABC to scavenge ectoines for nutritional purposes [243, 247, 248]. Both transporters are dependent on a substrate binding protein that binds ectoines in the periplasm and attaches to the membrane-standing parts of the transporters for the translocation of the substrates into the cytoplasm of the bacterial cells. Their ligand binding proteins, EhuB and UehA, have been studied on a biochemical and structural basis and possess a very high affinity in the low micro molar range for the substrates ectoine and 5-hydroxyectoine (Figure 7C and Figure 7D) [247, 248]. The crystallographic analysis of UehA (PDB: 3FXB) (Figure 7D) and EhuB (PDB: 2Q88; 2Q89) (Figure 7C) in complex with ectoines combined with the analysis of site-directed mutations allowed detailed insights into architecture of the active site and the mode of ligand binding [247, 248].

The TRAP transport system UehABC is highly similar to the above-mentioned TeaABC transporter that has been studied in respect of osmotic stress-mediated uptake of ectoines in *H. elongata*. Comparison of the obtained crystal structures of the binding protein TeaA [PDB: 2VPN (ectoine); 2VPO (hydroxyectoine)] (Figure 7A) to its counterpart from *R. pomeroyi* EhuB (Figure 7C) reveals that the substrate-binding sites are superimposable although the transporters are involved in two different physiological tasks, nutrient acquisition vs. osmotic stress protection [178, 247]. Furthermore, deletion studies with the TeaABC transporter in *H. elongata* underlined its involvement in the recapturing of newly synthesized ectoines that are leaked or actively excreted from the *H. elongata* producer cells [177]. However the underlying molecular mechanism that facilitates the release of ectoine from *H. elongata* has not been identified.

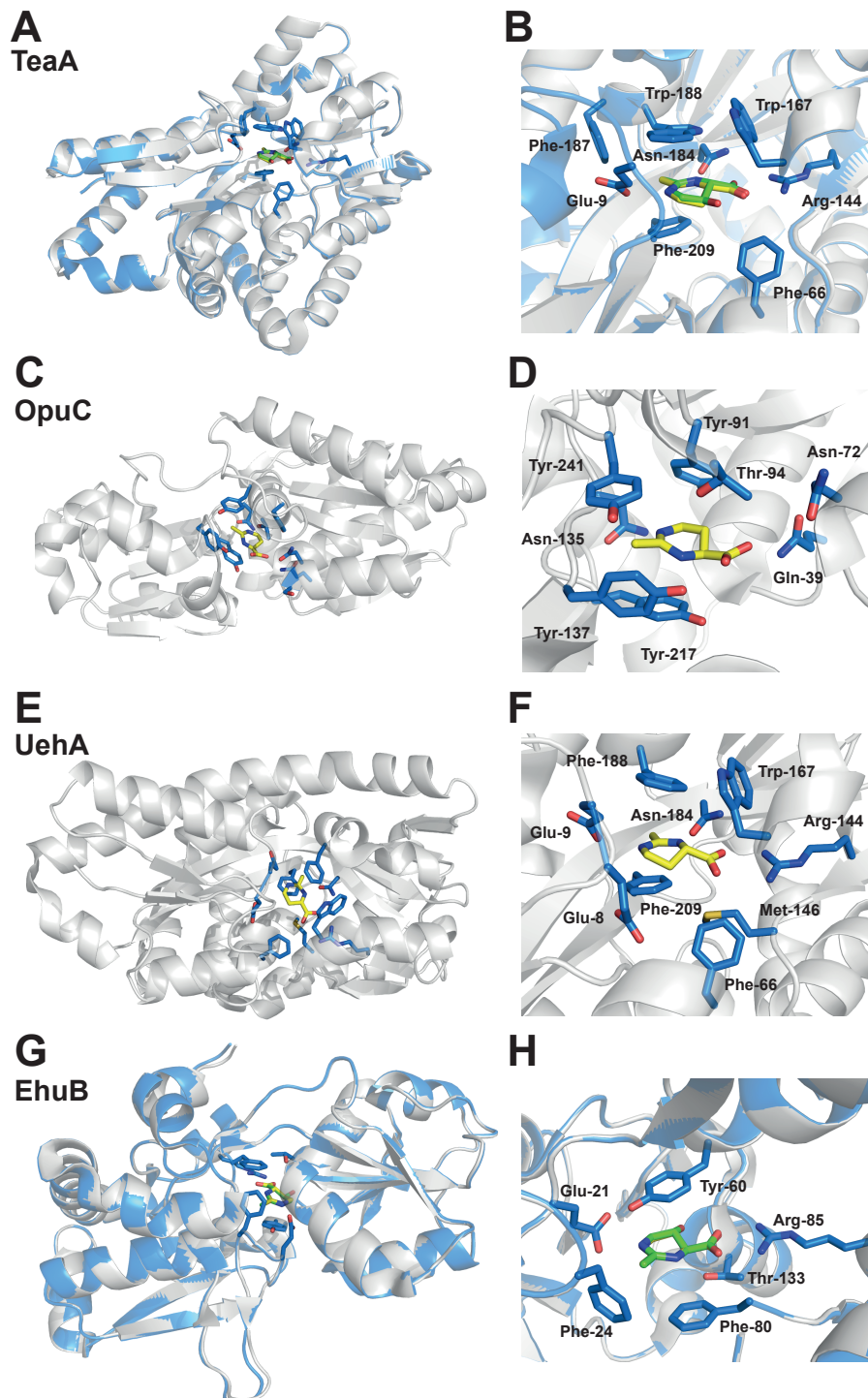


Figure 7 Crystal structures of substrate binding proteins from ectoine/5-hydroxyectoine uptake systems. **A, B** Overlay of the TeaA substrate binding protein of the TeaABC transporter from *H. elongata* in complex with ectoine (yellow; PDB: 2VPN) and 5-hydroxyectoine (green; 2VPO). The overall fold is shown in panel **A**, panel **B** depicts a zoom into the substrate binding site [178]. **C** Overall fold of the substrate binding protein of the OpuC transporter from *B. subtilis* with ectoine (yellow; PDB: 3PPR) bound in its substrate binding pocket (**D**) [277]. **E** Overall fold of the substrate binding protein UehA from the UehABC transporter from *R. pomeroyi* in complex with ectoine (yellow; PDB: 3FXB) (**F**) [247]. **G, H** Overlay of the ligand binding protein EhuB from the EhuABCD transporter from *S. meliloti* in complex with ectoine (yellow; PDB: 2Q88) and 5-hydroxyectoine (green; PDB 2Q89). **H** The position of the substrates within ligand binding pocket is superimposable [248]. All residues involved in ectoine/5-hydroxyectoine are depicted as blue sticks.

During my PhD thesis I studied three novel transporters (EctI, EctU and EctE) that are involved in ectoine import and export, and which are genetically encoded in the ectoine gene clusters of two *Alphaproteobacteria*, *Novosphingobium* sp. LH128 and *Hyphomonas neptunium*. The first exploratory experiments with one of these newly found transporters (EctI) were conducted during my master thesis and the project was followed up and expanded during my time as a PhD student. The physiological data was supported with an in depth database-wide genomic analysis on ectoine gene clusters from all fully sequenced bacteria and archaea that additionally contained different potential ectoine import or export system (see chapter 5.2.6).

4.2.8. Ectoines as stress protectants in Eukarya

For decades, ectoines were assumed to be rarely occurring osmotic stress protectants and moreover they were thought to be restricted to the kingdom of *Bacteria* [57, 60]. This thought was first challenged, when their occurrence in a restricted group of *Archaea* was discovered (reported as a result in this thesis) and it can be assumed that these archaeal ectoine biosynthetic gene clusters were obtained via horizontal gene transfer (see 5.1.1 and 5.2.1) [67, 72, 279]. Recent investigation on the osmstress response of halophilic protists now changed this long-held view, since the presence of ectoine biosynthetic genes was detected in the bacterivorous nanoflagellat *Halocafeteria seosinensis* by Harding *et al.* [73, 280–282], followed by the observation of osmstress-responsive ectoine production in the ciliate *Schmidingerothrix salinarum* [75, 283] and four other ciliates [74].

H. seosinensis and *S. salinarum* are bacterivorous, halophilic, unicellular *Eukarya* that use bacteria as their food source [282, 283]. In *H. seosinensis* *ectABCD* and *ask_ect* genes were found to be salt-induced and possessed spliceosomal introns as well as mitochondrial target sequences verifying their eukaryotic origin and excluding the contamination by bacterial DNA during genome sequence assembly [73, 280, 281]. Additional database analysis revealed the presence of *ectA*- and *ectC*- related sequences in the transcriptomic data of other *Eukarya*, such as the lancelet *Branchiostoma floridae* and the marine invertebrate *Saccoglossus kowalevskii* [73]. These findings were strengthened by a study from Weinisch *et al.* The authors showed for the first time the production and accumulation of ectoines and glycine betaine in an *Eukaryote*, the protist *S. salinarum* [75]. Furthermore, they also found that externally supplied ectoine and glycine betaine can be taken up by *S. salinarum* and accumulate in the cytoplasm, thereby functioning as the main osmstress protectants [75]. In a recent publication four other halophilic heterotrophic ciliates (*Cyclidium glaucoma*, *Euplotes* sp., *Fabrea salina*, and *Pseudocohnilembus persalinus*) were in addition described to produce and accumulate ectoine and glycine betaine in response to elevated external osmolality [74].

Physiologically and taxonomically diverse bacteria, archaea and also eukaryotes such as halophilic protists collectively inhabit marine and hypersaline environments [284]. It can therefor be hypothesized that unicellular eukaryotes also acquired the ectoine biosynthetic genes through horizontal gene transfer and adjusted the transcriptional composition to their eukaryotic machinery and functional principles. It

will be highly interesting if future work can unravel the origin and distribution of ectoine biosynthesis in *Eukarya*.

When Filker and co-workers published their findings on ectoine synthesis and uptake in the halophilic protist *S. salinarum* [75], E. Bremer and I were invited to write a *Primer* for PLoS Biology [76]. This short review on osmotic stress response and ectoines was published in PLoS Biology after a peer-review process (see section 5.1.2).

4.3. Imposing low external salinity - mechanosensitive channels as emergency release valves

Mechanosensitive channels fulfill an essential role in the protection of microorganisms against rapid decreases in the surrounding osmolarity [6, 285, 286]. When cells are confronted with an osmotic down shock e. g. as a result of extensive rainfalls or when marine organisms are flushed out into brackish or fresh water systems, such as rivers, the intracellular solute concentrations are higher than the concentrations in the surrounding environment. In numbers, the transition from seawater (1000 mOsm) to fresh water (10-100 mOsm) results in a change in turgor pressure of around 22 atm for a marine bacterium [6, 287]. But not only marine microorganism are threatened by osmotic down shocks, also bacteria living in other habitats face these harsh environmental changes: soil bacteria during rainfall, intestinal microbes when they are excreted or host-dependent microorganism during their transition to a new host [287]. The semipermeable nature of bacterial membranes allows the free diffusion of water along the osmotic gradient and results in a water flux into the cells when they possess a cytoplasm with an increased osmotic potential. Consequently the intracellular turgor pressure rises and the cells are threatened to burst. During such hypoosmotic shocks mechanosensitive channels function as *emergency release valves*, since intracellular solutes are released through their transient opening (Figure 1) [6, 287, 288]. Gating of these channels is a consequence of the increased tension of the lateral plain of the cytoplasmic membrane that results from an increased turgor pressure [6, 286]. This opening happens within milliseconds [6] and the cells non-specifically expel low-molecular-weight solutes (ions and organic compounds). After reduction of the osmotic potential of the cytoplasm, the channels close again [19, 286, 287, 289, 290].

The existence of mechanosensitive channels was first assumed in the 1960s, but their molecular discovery was only reported in 1987 by Martinac *et al.* [294, 295]. Mechanosensitive channels are ubiquitously found in nature as they are present in the kingdom of *Bacteria*, *Archaea*, and *Eukarya*, such as plants, fungi and also higher animals [288, 296, 297]. Many organisms possess several copies of mechanosensitive channels, and their functions and activities often overlap and can even be redundant [287, 298]. To date, mechanosensitive channels of various classes have been detected in bacteria and their collective interplay and roles during osmoadaptation have been studied to detail. The channels are grouped according to their pore size, gating behavior or substrate/ion dependence: MscL (large conductance) [299], MscS (small conductance), MscM (mini conductance), MscK (K⁺ dependent). Some experts describe MscM and MscK channels as a subgroup of MscS-type channels (Figure 1) [286, 287].

Moreover, in *C. glutamicum* even a specialized mechanosensitive channel (MscCG) that possess specificity for the release of newly synthesized glutamate has been reported [300–303]. The differences in their gating behaviors result from the imposed tension/pressure that these channels respond to [6, 304]. While small mechanosensitive channels gate during small osmotic changes, large mechanosensitive channel open during harsh hypoosmotic shocks and thereby represent the last survival mechanism for osmotically shocked cells. This coaction allows a graded response to the severity of the change in osmotic potential [6, 19, 287, 293, 299].

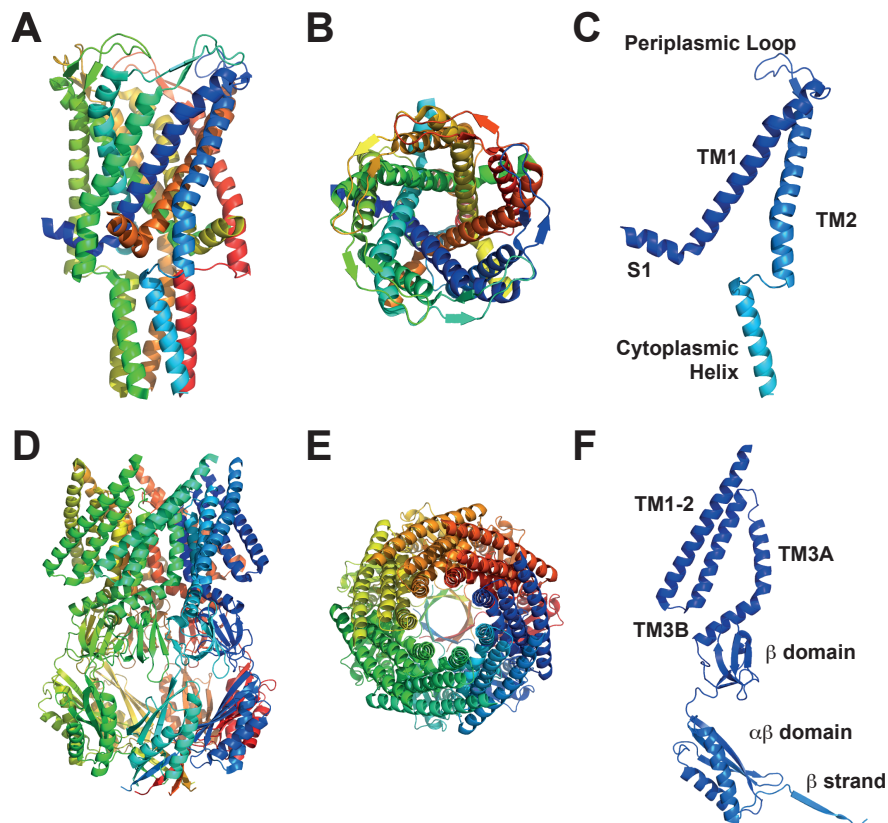


Figure 8 Crystal structures of an MscL- and MscS-type mechanosensitive channel. **A-C** Structure of the (*Mt*)MscL channel from *Mycobacterium tuberculosis* (PDB: 2OAR) [287, 291, 292]. A pentamer of (*Mt*)MscL viewed from the side is depicted in panel **A** and from the top/periplasm in panel **B**. **C** A single subunit of the homopentamer is colored in blue and each structural element is labeled. **D-F** Structure of the open form of (*Ec*)MscS (PDB: 2VV5) [287, 293]. Heptameric (*Ec*)MscS viewed from the side (**D**) and from the top/periplasm (**E**). **F** A single subunit of the homoheptamer is colored in blue. Each distinct structural element is labeled.



To date various crystal structures and detailed biochemical, physiological and simulation studies of MscS- and MscL-like mechanosensitive channel have been determined and their function and roles have been best studied in the enterobacterium *E. coli* (Figure 8) [287, 291, 293, 298, 305]. Both channels possess a very high conductivity - the MscL channel has a conductance of 3.8 nS and represents the largest known mechanosensitive channel with a calculated pore length and a channel diameter of 34 to 46 Å (Figure 8A)

[306], while the open pore of the MscS channel [307] has a conductance of 1 nS and an estimated pore size of 14-16 Å (Figure 8B) [287, 308]. Interestingly, the calculated size of the open pore of the *E. coli* MscL channel [309] is approximately three times as large as the diameter of the permanently open porins, OmpC and OmpF (Outer membrane protein) responsible for non-specific passive diffusion of hydrophilic substances across the outer membrane [310]. MscS and MscL belong to two different protein families. MscL channels are highly conserved and most microorganisms harbor only one copy of the corresponding gene. In contrast, MscS-type channels are very diverse and many bacteria possess multiple copies of these channels, whereas each MscS-like channel might play an important role under a different environmental condition [287, 288, 311–313]. *E. coli* possess for example one large conductance MscL-type channel and 6 channels that can be assigned to MscS-type channels, including MscM and MscK channels [288, 307, 313]. The MscS channel from *E. coli* is a heptamer with each monomer consisting of three N-terminal transmembrane helices (TM1-3) and a large C-terminal cytoplasmic soluble domain [288] (Figure 8B). MscS channels can vary in their protein length and thereby size, and the third transmembrane helice (TM3) consisting of TM3a and TM3b (Figure 8C) always exhibits the highest sequence identities [288]. The central pore of the MscS channel is formed by the TM2 helices and the soluble C-terminal domain forms a central cage in the cytoplasm (Figure 8B, C) [288, 293, 314]. This cage consists of seven TM3a helices and seven compactly folded α - and β -domains (Figure 8B, C) [288, 293]. This structural arrangement led to the hypothesis, that the cytoplasmic cage functions as a portal/strainer allowing the inflow of ions and small solutes, which can then pass through the membrane via the open pore formed by the transmembrane parts of the channel [288]. Importantly, mechanosensitive channels are only essential when bacterial cells are confronted with a hypoosmotic shock but are not active during growth under any steady state osmotic condition.

Three parts of my PhD thesis addressed the role of mechanosensitive channels: (I) ectoine secretion from heterologous hosts occurs independent from its mechanosensitive channels (see 5.2.2 and 5.2.5) (II) the ectoine gene clusters of *Cand. N. maritimus* and *Novosphingobium* sp. LH128 harbour functional mechanosensitive channels (see 5.2.1 and 5.2.6).

Review

Role of the Extremolytes Ectoine and Hydroxyectoine as Stress Protectants and Nutrients: Genetics, Phylogenomics, Biochemistry, and Structural Analysis

Laura Czech ¹, Lucas Hermann ¹, Nadine Stöveken ^{1,2}, Alexandra A. Richter ¹, Astrid Höppner ³ , Sander H. J. Smits ^{3,4}, Johann Heider ^{1,2} and Erhard Bremer ^{1,2,*} 

5. Peer-reviewed publications

5.1. Review articles

5.1.1. Role of the extremolytes ectoine and hydroxyectoine as stress protectants and nutrients: genetics, phylogenomics, biochemistry, and structural analysis

Czech L, Hermann L, Stöveken N, Richter AA, Höppner A, Smits SHJ, Heider J and Bremer E. Role of the extremolytes ectoine and hydroxyectoine as stress protectants and nutrients: genetics, phylogenomics, biochemistry, and structural analysis. *Genes (Basel)* 2018;9:177 doi: 10.3390/genes9040177.

In the following chapter, the published review article "Role of the extremolytes ectoine and hydroxyectoine as stress protectants and nutrients: genetics, phylogenomics, biochemistry, and structural analysis" is attached. The article was published in the journal *Genes* after a peer-reviewing process. Prof. E. Bremer and I wrote this article with input from L. Hermann, N. Stöveken, and J. Heider. A. A. Richter, A. Höppner, and S. H. J. Smits commented on the manuscript. I performed detailed bioinformatical analysis on the phylogenomics of ectoine biosynthesis and analyzed the gene neighborhood of the putative *ect* gene clusters. I prepared all figures included in the publication, while L. Hermann helped during figure preparation of the ectoine catabolism part.

5.1.1.1. Original publication



Review

Role of the Extremolytes Ectoine and Hydroxyectoine as Stress Protectants and Nutrients: Genetics, Phylogenomics, Biochemistry, and Structural Analysis

Laura Czech ¹, Lucas Hermann ¹, Nadine Stöveken ^{1,2}, Alexandra A. Richter ¹, Astrid Höppner ³, Sander H. J. Smits ^{3,4}, Johann Heider ^{1,2} and Erhard Bremer ^{1,2,*}

¹ Laboratory for Microbiology, Department of Biology, Philipps-University Marburg, Karl-von-Frisch Str. 8, D-35043 Marburg, Germany; lauraczeh@hotmail.de (L.C.); lucas.hermann@biologie.uni-marburg.de (L.H.); nadine@stoeveken.com (N.S.); alexandra.richter@biologie.uni-marburg.de (A.A.R.); heider@staff.uni-marburg.de (J.H.)

² LOEWE—Center for Synthetic Microbiology, Philipps-University Marburg, Hans-Meerwein Str. 6, D-35043 Marburg, Germany

³ Center for Structural Studies, Heinrich-Heine University Düsseldorf, Universitäts Str. 1, D-40225 Düsseldorf, Germany; astrid.hoepfner@uni-duesseldorf.de (A.H.); sander.smits@hhu.de (S.H.J.S.)

⁴ Institute of Biochemistry, Heinrich-Heine University Düsseldorf, Universitäts Str. 1, D-40225 Düsseldorf, Germany

* Correspondence: bremer@staff.uni-marburg.de; Tel.: (+49)-6421-2821529

Received: 10 February 2018; Accepted: 15 March 2018; Published: 22 March 2018

Abstract: Fluctuations in environmental osmolarity are ubiquitous stress factors in many natural habitats of microorganisms, as they inevitably trigger osmotically instigated fluxes of water across the semi-permeable cytoplasmic membrane. Under hyperosmotic conditions, many microorganisms fend off the detrimental effects of water efflux and the ensuing dehydration of the cytoplasm and drop in turgor through the accumulation of a restricted class of organic osmolytes, the compatible solutes. Ectoine and its derivative 5-hydroxyectoine are prominent members of these compounds and are synthesized widely by members of the Bacteria and a few Archaea and Eukarya in response to high salinity/osmolarity and/or growth temperature extremes. Ectoines have excellent function-preserving properties, attributes that have led to their description as chemical chaperones and fostered the development of an industrial-scale biotechnological production process for their exploitation in biotechnology, skin care, and medicine. We review, here, the current knowledge on the biochemistry of the ectoine/hydroxyectoine biosynthetic enzymes and the available crystal structures of some of them, explore the genetics of the underlying biosynthetic genes and their transcriptional regulation, and present an extensive phylogenomic analysis of the ectoine/hydroxyectoine biosynthetic genes. In addition, we address the biochemistry, phylogenomics, and genetic regulation for the alternative use of ectoines as nutrients.

Keywords: osmotic stress; high salinity; growth temperature extremes; enzymes; crystal structures; gene expression; genomics; chemical chaperones; biotechnology

1. Introduction

Microorganisms face myriad stressful conditions and nutrient limitations in their natural habitats; challenging circumstances to which they must react in a timely manner to ensure survival, persistence, and growth. An important parameter that affects essentially all microorganisms is the

osmolarity/salinity of their surroundings [1–6], as increases or decreases in the environmental water activity will inevitably trigger water fluxes across the cytoplasmic membrane.

Water is the active matrix of life [7,8], and the invention of the semi-permeable cytoplasmic membrane was a key event in the evolution of primordial cells. This membrane provided a confined space for the faithful copying of the genetic material, a reaction vessel for biochemical transformations and for the generation of energy to fuel growth. The cytoplasm of microorganisms is a highly crowded compartment caused by large concentrations of nucleic acids, proteins, and metabolites [9]. Together, these compounds generate a considerable osmotic potential [10] and thereby instigate osmotically driven water influx, a process that in turn causes the build-up of a hydrostatic pressure in walled cells, the turgor [2,10–14]. Turgor is considered essential for cell growth in many bacteria [15]. As microbial cells seem to strive to attain crowding homeostasis [9], they maintain turgor within physiologically acceptable boundaries through the accumulation and expulsion of ions and organic solutes [1–6], and they accomplish this even when faced with sudden fluctuations in the external osmolarity, or when they are exposed to persistent high or low osmolarity surroundings.

The development of the cytoplasmic membrane was a prerequisite for the evolution of microbial cells as we know them today; however, its semi-permeable nature makes cells vulnerable to osmotic fluctuations in their surroundings [2,6,10,11]. In extreme cases, the integrity of the cell is threatened by excessive water influx and a concomitant build-up of turgor to non-sustainable levels (under hypo-osmotic conditions) [16–20], or the ability of the cell to perform vital physiological tasks is impaired by the dehydration of the cytoplasm and the ensuing reduction/collapse of turgor when water exits the cell (under hyperosmotic conditions) [2,10]. It is apparent that coordinated cellular stress responses are needed to prevent such catastrophic effects.

Despite the existence of aquaporins in microorganisms that mediate diffusion-driven accelerated water fluxes across the cytoplasmic membrane [21,22], no microorganism can actively pump water (by means of an energy consuming process) into or out of the cell to compensate for water fluxes through this membrane that are instigated by changes in the external osmolarity. Microorganisms can, however, actively influence the direction and scale of water fluxes into or out of the cell by dynamically modulating the osmotic potential of the cytoplasm through the accumulation or expulsion of ions and organic compounds [2,5,10,11,20]. These combined activities allow microbial cells to cope dynamically with increases and decreases in the external osmolarity and are also crucial for their ability to colonize habitats with permanently high salinities/osmolarities [23,24].

When exposed to high-osmolarity environments, microorganisms amass ions and organic osmolytes to increase the osmotic potential of their cytoplasm (Figure 1A). This curbs water efflux and promotes water influx, thereby balancing the vital osmotic gradient across the cytoplasmic membrane under osmotically unfavorable environmental circumstances [4,5,24,25]. An increase in the osmotic potential of the cytoplasm can be accomplished by one of two cellular adjustment strategies. These are to accumulate high levels of either selected salt ions (primarily K^+ and Cl^-) (the *salt-in* strategy) or of physiologically compliant organic osmolytes, the compatible solutes (the *salt-out* strategy) [1,5,25].

While the accumulation of ions and/or organic osmolytes ensures survival and growth of microorganisms under high osmolarity/salinity conditions (Figure 1A), the high intracellular pools of the very same compounds threatens the integrity of the cell when it is suddenly exposed to a drop in the external osmolarity [11,16–18,20]. Such conditions occur, for instance, for soil-dwelling bacteria upon rainfall and by washout into freshwater sources, for microorganisms living in brackish ecosystems, and for enteric bacteria when they exit the intestine of their host. The ensuing osmotic down-shocks require a very rapid cellular adjustment response in order to avoid bursting [11,20,26,27]. For instance, turgor pressure in *Escherichia coli* has been estimated to lie between 0.3 atm and 3 atm [13,14], values that increase practically instantaneously to about 20 atm upon a sudden and severe osmotic down-shift [11]. Such a drastic increase in turgor cannot be restrained by the stress-bearing peptidoglycan sacculus [28,29] of the cell wall alone, and consequently, the cell would burst [11,16–19].

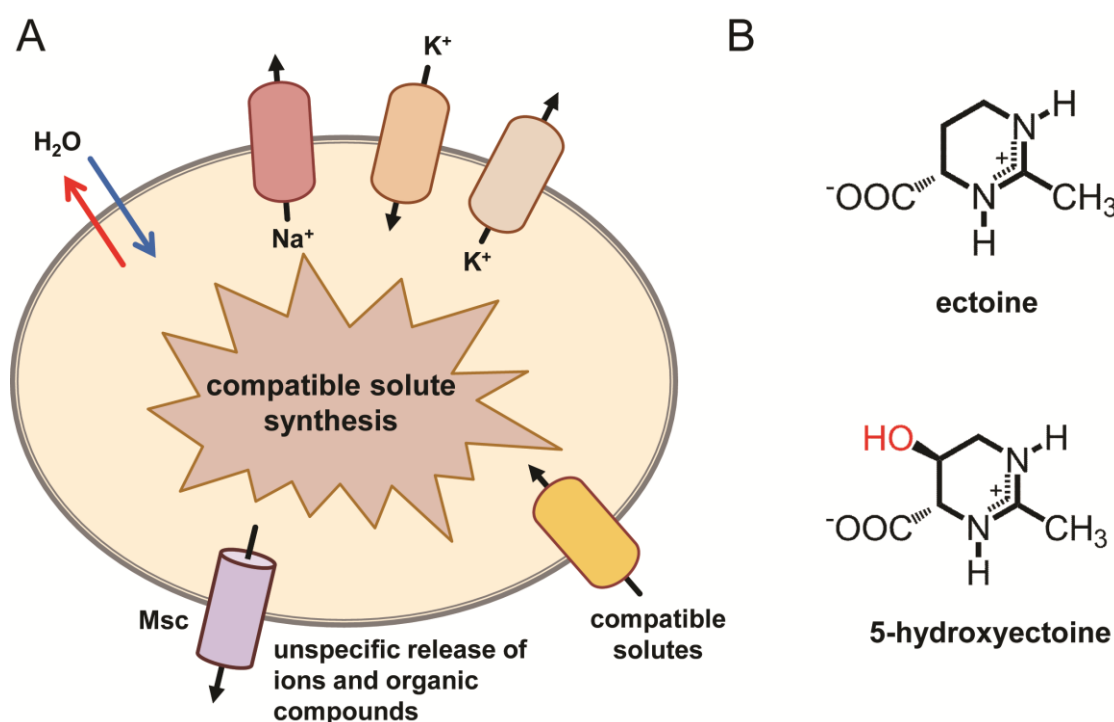


Figure 1. (A) General overview of the microbial *salt-out* osmostress adaptation strategy. The components, ion fluxes, and compatible solute pools generated via import and synthesis under hyperosmotic conditions [1,2], and the non-specific release of ions and low molecular weight organic compounds via mechanosensitive channels (Msc) under suddenly imposed hypo-osmotic circumstances are depicted [11,20]. (B) Chemical structures of the compatible solutes ectoine and 5-hydroxyectoine.

To avoid rupture under suddenly imposed hypo-osmotic condition, bacteria engage safety valves embedded in the cytoplasmic membrane, the mechanosensitive channels (Figure 1A). An immediate consequence of the osmotically driven water influx upon down-shock is the gating of these channels, a process caused by the increase in the tension of the lateral plain of the cytoplasmic membrane as the consequence of increased turgor. Often, multiple types of mechanosensitive channels [MscM (mini), MscS (small), MscL (large)] are present in a given microbial cell and they possess different pore sizes and gating behaviors [11,20,26,27,30–32]. Their transient opening allows a rapid, non-specific jettison of low-molecular-weight solutes (both ions and organic compounds), whereupon the mechanosensitive channels close again as a result of the reduction in the osmotic potential of the cytoplasm and the ensuing decrease in turgor. Consequently, by relying on the turgor-driven opening and closing of mechanosensitive channels (Figure 1A), the cell can mount a timely and graded response to the severity of the suddenly imposed osmotic imbalance [11,20,30,32]. Mechanosensitive channels are essential for cellular survival under severe osmotic down-shock conditions [11,16–18], but not during steady-state growth at either high or low osmolarity [16,17].

2. The Salt-In and Salt-Out Strategies for Coping with High Osmolarity Environments

The *salt-in* strategy relies on the massive accumulation of K⁺ and Cl[−] ions from environmental sources through transport and the active extrusion of cytotoxic Na⁺ ions from the cell [24,25]. As a consequence of the permanently high ion content of the cytoplasm, the biochemical properties and the compositions of all proteins have to be adjusted to keep them soluble and functional. On an evolutionary time scale, this has left an acidic signature on the proteome with a narrow distribution of isoelectric points as the consequence of reduced hydrophobicity of proteins and a strong increase in negatively charged amino acids exposed on protein surfaces [33–35]. The *salt-in* strategy is energetically favorable [36,37], and is thus particularly effective in habitats with sustained very high

salinity [23–25], but seems less useful in environments in which the salinity/osmolarity fluctuates more often [1,3–5].

A more flexible adjustment to high-osmolarity environments is provided by the *salt-out* strategy, which is therefore used widely in the microbial world [1,5]. This strategy also entails a rapid uptake of potassium ions as an emergency reaction to a sudden challenge by high osmolarity, but part of the initially amassed K^+ pool is subsequently replaced by the cells through types of organic osmolytes that are highly compliant with cellular functions, the compatible solutes (Figure 1A) [1–4]. In this way, the cell attains a level of hydration of the cytoplasm that is appropriate for biochemical processes and simultaneously upholds turgor without concurrently raising the intracellular ionic strength, as this would greatly impair most physiological activities of the cell [2,10]. As an added benefit, the *salt-out* strategy does not require an evolutionary adjustment in the proteome profile. However, the amassing of compatible solutes, either through uptake or synthesis [1,2], is energetically substantially more demanding than the *salt-in* strategy [36,37].

It was thought that the *salt-in* and *salt-out* strategies were mutually exclusive, and that the observation of an acidic proteome was predictive for the use of the *salt-in* strategy. While this is probably correct in general, recent findings require a modification of this long-held view [38,39]. For instance, a group of *Halobacteriales*, halophilic Archaea, was found to combine a high K^+ cytoplasm with the accumulation of the compatible solutes trehalose and 2-sulfotrehalose [38]. Notably, in the extreme halophilic archaeon *Halobacterium salinarum*, even chemotaxis towards the osmoprotectants glycine betaine, carnitine, and choline has been detected [40]. While pathways for the synthesis of compatible solutes in extremely halophilic Archaea seem to be rare, those for the uptake of compatible solutes are prevalent [41]. These observations indicate that some haloarchaea, at least under certain environmental conditions, might combine the *salt-in* and *salt-out* strategies to combat the detrimental effects of high salinity on cellular physiology. It is also noteworthy that in several phylogenetically closely related members of the genus *Halorhodospira*, different osmoprotection adaptation strategies can be found. For instance, in *Halorhodospira halophila*, a highly acidic proteome is combined with a high K^+/Cl^- pool, while in *Halorhodospira halochloris* this is not the case; instead, this halo-alkaliphilic microorganism is a producer of compatible solutes [24,39,42]. Finally, it was thought that obligate protein halophilicity was the price evolution had to pay for the *salt-in* strategy, but *H. halophila* can substantially reduce its K^+ content from about 2.1 M in cells grown at high salinity to a level (0.4 M) comparable to that of *E. coli* when it is cultivated in media with more moderate salt concentrations (0.21 M) [39]. As stated by A. Oren in his insightful review on intracellular K^+ and acid proteomes [24], the previously clear-cut picture of a correlation between phylogenetic affiliation and mode of salt adaptation, and the correlation between acidic proteomes, accumulation of high K^+ content, and the use of compatible solutes needs a careful re-evaluation. The findings that some microorganisms combine an acidic proteome with the accumulation of compatible solutes [24,38,41,43], and that a substantial reduction in K^+ content can be accomplished in *salt-in* adopters under more moderate salt-stress conditions [39], prompts the exploration of new avenues of research and raises intriguing questions about the role played by protein halophilicity in the evolution of microbial osmoprotection responses.

3. Compatible Solutes

Stress-Relieving Cytoprotectants Used in All Three Domains of Life

One of the main physiological roles played by compatible solutes in Archaea, Bacteria and Eukarya is to counteract the negative effects of high external osmolarity on cellular hydration and volume [1,5,44–47]. They are therefore amassed by microbial cells with pool sizes that increase in accordance with the degree of the imposed osmotic stress. Compatible solutes are operationally defined as organic osmolytes that can be accumulated by cells to exceedingly high levels without disturbing vital cellular functions [48]. They are also addressed as counteracting [44] or compensatory [49] organic solutes to highlight their cytoprotective effects against challenges in addition to those posed by high osmolarity/salinity; for example, low and high temperate extremes, hydrostatic

pressure, freezing, desiccation, and the denaturation of macromolecules by ions and urea. These types of solutes have physico-chemical properties that distinguish them from other types of organic compounds, and similar types of low-molecular weight compounds have been selected during the course of evolution in all three domains of life to fulfill cellular functions as cytoprotectants [1,5,45–47,50]. One of the most widely distributed compatible solutes on Earth is glycine betaine. This compound, and many other compatible solutes as well, is not only employed as an effective osmoprotectant, but also provides cytoprotection against challenges posed by extremes in growth temperature and hydrostatic pressure, attributes that lead to the description of particular compatible solutes as thermolytes and piezolytes, respectively [50–58].

A hallmark of compatible solutes is their preferential exclusion from the immediate hydration shell of proteins [59], an effect largely caused by unfavorable interactions between these solutes and the protein backbone [60–62]. This preferential exclusion [59] leads to an uneven distribution of compatible solutes in the cell water and therefore generates a thermodynamic driving force that acts against the denatured and aggregated state of proteins. Hence, proteins are forced to adopt a compact and well-folded state under intracellular unfavorable osmotic and ionic conditions to minimize the number of excluded compatible solute molecules from surfaces [61,62]. Consequently, the accumulation of compatible solutes not only has beneficial effects on cellular hydration and maintenance of turgor, but also promotes the functionality of macromolecules (e.g., in particular, proteins and membranes, and protein:DNA interactions) under otherwise activity-inhibiting conditions [54,63–69].

The function-preserving property of compatible solutes has attracted considerable biotechnological interest, and the term “chemical chaperones” was coined in the literature [54,70,71] to reflect the beneficial effects of these compounds as protein stabilizers and protectants for entire cells [72–75]. The function of compatible solutes as chemical chaperones will certainly contribute to their role as protectants against extremes in either high or low temperatures for microorganisms [51–54,76–81], an underappreciated physiologically important attribute of these types of solutes. For instance, the hyperthermophile *Archaeoglobus fulgidus* cannot grow at 90 °C in a chemically fully defined minimal medium [82], despite the fact that this archaeon synthesizes the extremolyte diglycerol phosphate in response to heat stress, an excellent stabilizer of protein function at high temperature [56,83]. However, the addition of 1 mM glycine betaine to the growth medium and its import via the heat stress inducible ProU ABC transporter efficiently rescued growth of *A. fulgidus* at the extreme temperature of 90 °C [82]. In other words, glycine betaine can act as an effective thermoprotectant for a hyperthermophile. Similarly, a defect in the molecular chaperone DnaK that causes thermo-sensitivity of *E. coli* at 42 °C, can be functionally rescued by an external supply of the compatible solutes L-proline, glycine betaine and by the glycine betaine biosynthetic precursor choline [53,76]. Furthermore, a broad spectrum of compatible solutes serves as thermoprotectants at the cutting upper (about 52 °C) and lower (about 13 °C) temperature boundaries for growth of *Bacillus subtilis* in a chemically defined minimal medium [51,52,84,85].

Although originally coined for unusual compatible solutes produced by microorganisms that live in habitats with extreme temperature, salt and pH profiles [86], the term extremolyte can be applied to these types of solutes in general [5,55,57,86,87]. This is exemplified by the above-cited example of the impressive thermoprotection of *A. fulgidus* by the “ordinary” compatible solute glycine betaine. Within the domain of the Bacteria, important representatives of compatible solutes are the amino acid L-proline, the trimethylammonium compound glycine betaine and its analogue arsenobetaine, proline-betaine, the sugar trehalose, the heteroside glucosylglycerol, the sulfur-containing dimethylsulfoniopropionate (DMSP), and the tetrahydropyrimidines ectoine and 5-hydroxyectoine. We refer readers to several excellent overviews that address the diversity of compatible solutes produced and imported by Bacteria and Archaea [4,5,55,57,87].

Here we focus on the synthesis and import of the compatible solute ectoine and its derivative 5-hydroxyectoine (Figure 1B), their stress-relieving properties, and their alternative function as versatile microbial nutrients.

4. Ectoine and Hydroxyectoine

4.1. Discovery

Ectoine [(4S)-2-methyl-1,4,5,6-tetrahydropyrimidine-4-carboxylic acid] (Figure 1B) was originally discovered in the extremely halophilic phototrophic purple sulfur bacterium *Ectothiorhodospira halochloris* (now taxonomically re-classified as *H. halochloris*) by Galinski et al. in 1985 [88]. This seminal discovery was followed by the detection of a hydroxylated derivative of ectoine, 5-hydroxyectoine [(4S,5S)-2-methyl-5-hydroxy-1,4,5,6-tetrahydropyrimidine-4-carboxylic acid] by Inbar and Lapidot in 1988 in the Gram-positive soil bacterium *Streptomyces parvulus* [89], a compound that the authors initially referred to as THP (A) [2-methyl-4-carboxy-5-hydroxy-3,4,5,6-tetrahydropyrimidine]. Ectoine and 5-hydroxyectoine (Figure 1B) can chemically be classified as either heterocyclic amino acids or as partially hydrogenated pyrimidine derivatives [88–90]. Both ectoine and 5-hydroxyectoine were initially viewed as rare naturally occurring compatible solutes (e.g., in comparison with the almost universally distributed glycine betaine molecule). However, improved screening procedures using HPLC analysis and, in particular, ¹³C-natural abundance NMR spectroscopy revealed their widespread synthesis in bacteria in response to high salinity [25,55]. Ectoine producers can be found within a physiologically and taxonomically diverse set of microbial species [91–94]. Today, ectoines are known to be one of the most ubiquitously distributed compatible solutes in the microbial world.

The identification of ectoine biosynthetic genes (*ectABC*) [95] and of the gene coding for the ectoine hydroxylase (*ectD*) [96–98] proved to be a major step forward for an in silico assessment of the distribution of ectoine/5-hydroxyectoine biosynthesis in microorganisms, an approach made possible by the rapid and unabated growth in the number of available genome sequences of Bacteria and Archaea [92,93]. Producers of ectoines are primarily found among members of the domain of the Bacteria [91,93,99] and in a rather restricted number of the Archaea [92]. Surprisingly, ectoine/5-hydroxyectoine biosynthetic genes and production of ectoine have recently also been detected in some bacteriovorous unicellular Eukarya [100–102] that live in permanently high-salinity ecosystems [103]; these protists probably acquired the ectoine/5-hydroxyectoine biosynthetic genes through lateral gene transfer from their food bacteria [100,104].

4.2. Physico-Chemical Attributes

Like other compatible solutes [61,62], ectoine and 5-hydroxyectoine (Figure 1B) are low-molecular mass compounds that are highly soluble in water (about 4 M at 20 °C) [105], thereby allowing the amassing of these compounds to near molar concentrations in severely osmotically stressed microbial cells [91,94,106]. A variety of biophysical techniques have been used to study the effects of ectoine on the hydration of proteins and cell membranes and on interactions mediated via hydrogen bonding. Collectively, these data showed that ectoine is excluded from the monolayer of dense hydration water around soluble proteins and from the immediate hydration layer at the membrane/liquid interface [66,105]. Ectoine enhances the properties of hydrogen bonds in aqueous solutions and thereby contributes to the dynamics and stabilization of macromolecular structures. Ectoine possesses a negatively charged carboxylate group attached to a ring structure that contains a delocalized positive charge (Figure 1B). The resulting interplay between hydrophilic and hydrophobic forces influences water-water and water-solute interactions [107] and thereby exerts strong effects on the hydration of ectoine itself, the binding of ions and the influence on the local water structure [108–111].

Molecular dynamics simulations have indicated that ectoine and 5-hydroxyectoine are strong water-binders and are able to accumulate seven and nine water molecules, respectively, around them at a distance smaller than 0.6 nm [67]. This results in the formation of a large number of hydrogen bonds at specific functional groups of molecules. Furthermore, these studies indicated that the water-binding behavior of ectoines is not abrogated or perturbed at high salt concentrations [67]. The influence of ectoines on the local water structure also exerts pronounced effects on protein-DNA interactions [109,112–114], a crucial effect that might alter the transcriptional profile of salt-stressed

cells on a genome-wide scale [68]. Collectively, the physico-chemical attributes of ectoines allow a physiologically adequate hydration of the cytoplasm upon their osmostress-responsive accumulation, afford effects on the local water structure, and also exert a major protective influence on the stability of proteins and the functionality of macromolecules [72,73,105,114,115].

4.3. Stress-Protective Properties

Ectoine and 5-hydroxyectoine are produced by microorganisms in response to true osmotic stress, and not just in response to increases in the external salinity [116]. In cases where the build-up of ectoine/5-hydroxyectoine pools has been studied in more detail, there is often a linear relationship between the cellular content of these solutes and the external salinity/osmolarity [116–118]. This finding implies that bacterial cells can perceive incremental increases in the degree of the environmentally imposed osmotic stress, can process this information genetically/physiologically, and can then set its ectoine/5-hydroxyectoine biosynthetic capacity in a finely tuned fashion to relieve the constraints imposed by high-osmolarity on cellular hydration, physiology, and growth [1–4]. As described in greater detail in Section 5.2., high-osmolarity-dictated increases in the cellular ectoine pools are largely accomplished through osmotically-responsive increases in the transcription of the ectoine/5-hydroxyectoine biosynthetic genes, although there might be post-transcriptional effects as well. Attesting to the role of ectoine as a potent osmostress protectant is the finding that the disruption of the *ectABC* biosynthetic genes (see Section 5.1) causes osmotic sensitivity [119,120] and the genetic disruption of the gene (*ectD*) for the ectoine hydroxylase in *Chromohalobacter salexigens* impairs the ability to cope effectively with high growth temperature extremes [97].

In addition, environmental challenges other than high osmolarity also trigger enhanced production of ectoines in some microorganisms, in particular, extremes in either high or low growth temperatures [77,81,97]. Furthermore, the function of ectoines as thermolytes is also manifested when microbial cells acquire these solutes from environmental sources through transport processes [78,79,121]. Although the term chemical chaperone is suggestive of a description of the function-preserving attributes of compatible solutes, it is not truly clear how the thermoprotective effects of ectoines are achieved on a biochemical and molecular level. We find it also important to note in this context that the mechanisms underlying the cytoprotective effects of ectoines at high and low temperature do not necessarily need to be the same. In addition, both processes might be, in their core, different from the cytoprotective effects exerted by ectoines when they act as osmostress protectants.

In microorganisms that are capable of synthesizing both ectoine and 5-hydroxyectoine, a mixture of these two solutes is frequently found. Interestingly, such a 1:1 mixture (0.5 mM each) provided the best salt and heat stress protection to *Streptomyces coelicolor* when it was added to the growth medium [79]. However, there are also microorganisms that seem to produce almost exclusively 5-hydroxyectoine during osmotic stress and different growth phases of the culture [122,123].

An interesting phenomenon that has been dubbed osmolyte switching [124,125], plays an important role in the temporal dynamics of ectoine production in some microorganisms. For instance, *Halobacillus halophilus*, which uses a hybrid osmostress adjustment strategy of Cl^- and compatible solute accumulation [125], initially uses L-glutamate as its primary organic osmolyte and then switches to the synthesis of L-proline when the external salinity is further increased. A second switch in the preferred compatible solute then occurs from L-proline to ectoine at the transition from exponential to stationary phase [124,125]. Similarly, *Virgibacillus pantothenicus* initially relies on the synthesis of L-proline when it is osmotically challenged by moderate increases in the external salinity, and then triggers enhanced ectoine production once the salinity of the growth medium is increased above 0.6 M NaCl [77]. Hence, in microorganisms that produce several organic osmolytes, there seems to be, at least in certain cases, a temporal hierarchy in the type(s) of the dominantly synthesized compatible solute(s). Apparently, when the environmental and cellular circumstances get particularly tough, ectoine is preferentially produced. This notion fits nicely with the results of a study in which the dominantly produced compatible solute(s) in a substantial number of Bacilli were assessed by natural abundance

^{13}C -NMR-spectroscopy [98,117]. Three groups were detected: (i) those that synthesize exclusively L-glutamate, (ii) those that synthesize L-glutamate and L-proline, and (iii) those that synthesize both L-glutamate and ectoine. Some members of this latter group also produce 5-hydroxyectoine. Although not studied in detail, there seems to be a correlation between the type of compatible solute synthesized and the degree of the attained osmotic stress resistance, with ectoine/5-hydroxyectoine producers being the most salt-stress tolerant Bacilli [98,117]. Presumably, this phenomenon is related to the different physico-chemical attributes of L-glutamate, L-proline, and ectoine and the ensuing effectiveness by which they can then serve as compatible solutes [107,126–128].

As mentioned above, a substantial increase in 5-hydroxyectoine content occurs not only in response to osmotic challenges in some microorganisms, but also when cells enter stationary phase [121,129]. This observation implies that the hydroxylated derivative of ectoine possesses stress-relieving properties that will allow the cell to better cope with the multitude of challenges imposed by stationary phase [130,131]. This attribute might stem from the frequently observed superior function-preserving properties of 5-hydroxyectoine when tested either in vivo [79,97] or in vitro [72–75,114,132–134]. Fourier transform infrared and electron spin resonance studies revealed that 5-hydroxyectoine has a substantially greater glass-forming propensity than ectoine, a trait that stems from stronger intermolecular hydrogen-bonds with the OH group of 5-hydroxyectoine (Figure 1B) [132]. As a consequence of the strongly increased glass transition temperature (87 °C for 5-hydroxyectoine versus 47 °C for ectoine), 5-hydroxyectoine is an excellent desiccation protectant, a characteristic that not only allows the stabilization of individual biomolecules, but the protection of entire cells from anhydrobiotic-induced damage [74,75]. Biosynthesis and external application of 5-hydroxyectoine can thus be exploited for synthetic anhydrobiotic engineering [84,85,132]. In *C. salexigens*, 5-hydroxyectoine has also been found to be a better protectant than ectoine against oxidative stress caused by an excess supply of iron in the growth medium [135].

In *Alcalivorans borkumensis* SK2, a member of a widely distributed genus dominating oil spills worldwide, ectoine has been suggested to function as a piezolyte by protecting the cell against excess hydrostatic pressure [136]. However, a previous study found no evidence for such a function for ectoine by comparing the pressure survival of the piezo-sensitive *E. coli* cell (non-ectoine producer) with that of *C. salexigens* (an ectoine producer) [137]. Ectoines also have pronounced effects on the melting temperature of DNA, but ectoine and 5-hydroxyectoine differ in this regard. While ectoine lowers the melting temperature, 5-hydroxyectoine increases it [114]. Furthermore, ectoine protects DNA against the induction of single-strand breaks by ionizing radiation and serves as a scavenger for hydroxyl radicals [138–140]. Ectoine is also a potent protectant against UV-induced cellular stress [141,142]. Interesting stress-protective and function-preserving properties might also be derived from synthetic ectoines with reduced or expanded ring sizes [143] or by chemical modifications that provide a hydrophobic anchor (e.g., lauryl-ectoine) to the otherwise highly water-soluble ectoine molecule [144].

4.4. Biotechnological Production and Practical Applications of Ectoines

The excellent function-preserving attributes of ectoines have attracted considerable attention to their exploitation in the fields of biotechnology, skin care, and medicine [86,91,94,145–147]. This demand for ectoines for practical purposes has led to an industrial-scale production process that exploits *Halomonas elongata* as a natural and engineered cell factory, delivering ectoines on the scale of tons [86,91,94]. Data reported in the literature [148,149] estimate a worldwide production level of ectoines of about 15,000 tons per annum, which putatively have an estimated sales value of approximately 1000 US Dollars kg^{-1} . However, another study reports a price for ectoine at between about 14,000 and 18,000 Euro kg^{-1} [150]. We are not certain what these numbers are actually based upon, since details pertinent to their calculations are not given in these publications [148–150]. However, there can be no doubt that ectoines are high-value natural products. By consulting catalog prices listed by vendors of laboratory chemicals (and not by the major industrial producer of ectoine; bitop AG, Dortmund, Germany; <https://www.bitop.de/>), the purchasing costs for one kg of ectoines ranges between 9000 Euro (Acadchem, Hong Kong, China) and 17,000 Euro (AppliChem,

Darmstadt, Germany) kg⁻¹ for ectoine, and the sale price for 1 kg of 5-hydroxyectoine is about 17,000 Euro (Merck, Darmstadt, Germany).

Of the extremolytes currently considered for practical applications [146], ectoine and 5-hydroxyectoine certainly have the greatest potential for sustained commercial exploitation [86,91,94,145,147]. It is outside the scope of this overview to address in depth the biotechnological production of ectoines in natural and synthetic microbial cell factories, or to describe in detail the varied practical applications for these compounds. Insightful reviews covering these topics have been published [86,91,94,145], and recent reports have summarized the current status of efforts to improve the productivity of natural and synthetic microbial cell factories for ectoines [116,123,151–157].

Briefly, the industrial-scale production scheme for ectoine relies on the highly salt-tolerant gammaproteobacterium *H. elongata* as a natural cell factory [86,158]. It exploits the massive production of ectoines under high-salinity growth conditions by this bacterium [158] and their non-specific release from the producer cells via the transient opening of mechanosensitive channels upon a severe osmotic down-shock [91,94,159]. Since the gating of mechanosensitive channels prevents cell rupture [11,20,32], the biomass formed during the originally high-cell density fermentation of *H. elongata* under osmotic stress conditions can be re-introduced into the fermentation vessel for a new round of ectoine production and release [91,94,159]. This innovative production process has been fashionably dubbed bacterial milking [159]. During subsequent strain development, the production process was amended by the use of *H. elongata* mutants that lack the TeaABC system, a TRAP-type [160] ectoine/5-hydroxyectoine-specific transporter that can serve as a recycling system for newly synthesized ectoines released, or actively excreted, from the *H. elongata* producer cells [161]. Use of *tea* mutants in the industrial production strain leads to the continuous accumulation of ectoines in the growth medium [94,161]. Ectoines jettisoned during osmotic downshifts of *H. elongata* cells, or released into the growth medium by the *tea* mutant strain, can be recovered from the fermentation medium with high yield and purity by down-stream processes via protein precipitation through acidification, cation exchange chromatography, and evaporation/crystallization [86,91,94,145–147].

A number of commercial applications for ectoines have been developed that rely, in their core, on the ability of ectoine and 5-hydroxyectoine to serve as water-attracting and water-structure-forming compounds [109–111], to stabilize macromolecules and entire cells through their chaperon and glass-forming effects [66,67,86,91,94,105,132,145], to protect DNA from ionizing radiation [138,140], and to prevent UV-induced cell damage of skin cells [141,142,145]. These latter two properties and the moisturizing effects of ectoines have fostered the development of a wide range of products for skin care and cosmetics [145]. Ectoines are used to stabilize enzyme activity in vitro, for promoting protein folding in vivo, for protecting molecules and cells against cycles of freezing and thawing, for promoting their desiccation resistance, for enhancing the resistance of cells and DNA against ionizing radiation and damage elicited by UV, as oxidative and temperature stress protectants, for preventing the impairment of cell membrane functions, for cytoprotection of eukaryotic cells and organs, and they have even been evaluated as protectants against neurodegenerative diseases [86,91,94,145,147].

Compatible solutes have also been explored as beneficial additives to biological waste and wastewater treatment systems to counteract osmotic and other types of environmental stresses [150]. In addition to glycine betaine and trehalose, the effects of ectoine have also been evaluated in this regard. A denitrifying microbial consortium has been used to study the effect of ectoine on denitrification at increased salinity. The addition of ectoine (1 mM) accelerated the de-nitrification process, promoted the almost complete removal of nitrates and nitrites relative to that of control samples in a shorter time frame, and enhanced the activity of key degradative enzymes [162]. The addition of ectoine also stimulated the Anammox process (by about 40%) under conditions of increased salinity [163]. While these pilot studies demonstrate the use of compatible solutes in general, and that of ectoine in particular, for these types of applications [150], it is unlikely that ectoine can ever be used in large-scale biological waste and wastewater treatment systems unless the production costs for ectoine would drop precipitously and become competitive with the bulk-chemical glycine betaine (196 Euro kg⁻¹) (Merck, Darmstadt, Germany).

5. Ectoine/5-Hydroxyectoine Biosynthetic Routes and Crystal Structures of Selected Enzymes

5.1. Biosynthetic Pathway: An Overview

Three enzymes are involved in ectoine synthesis: L-2,4-diaminobutyrate (DABA) transaminase (EctB; EC 2.6.1.76), L-2,4-diaminobutyrate acetyltransferase (EctA; EC 2.3.1.178), and ectoine synthase (EctC; EC 4.2.1.108). 5-hydroxyectoine is formed in a subgroup of ectoine producers through a position- and stereo-specific hydroxylation of ectoine, an enzymatic reaction catalyzed by the ectoine hydroxylase (EctD; EC 1.14.11.55) (Figure 2).

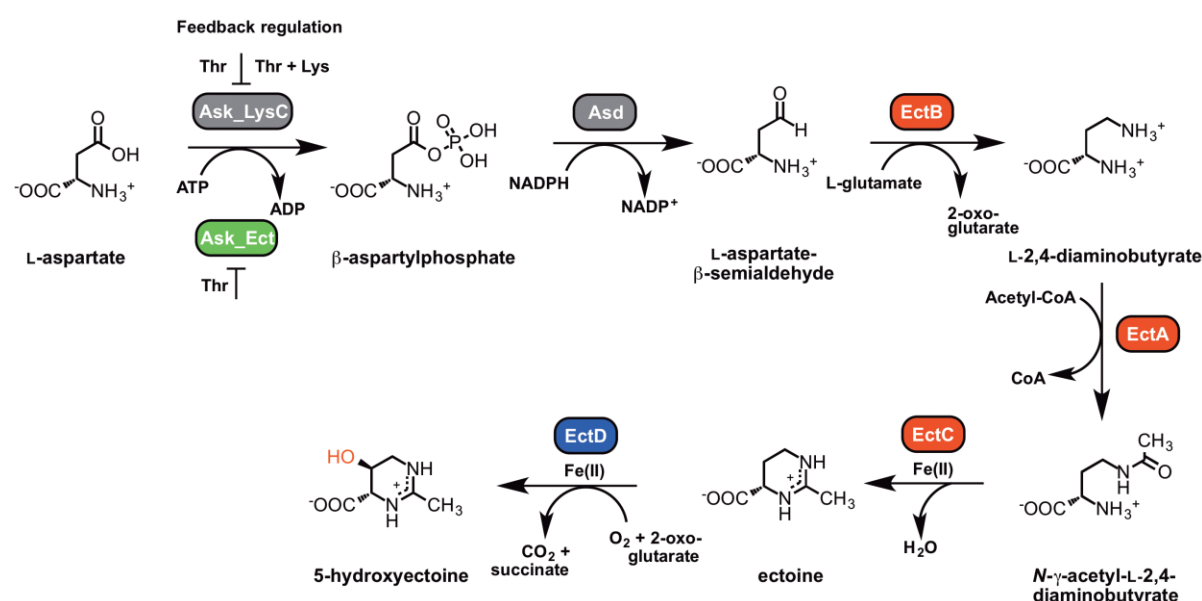


Figure 2. Routes for ectoine and 5-hydroxyectoine biosynthesis.

The ectoine biosynthetic route was originally elucidated by Peters et al. [164] through an analysis of enzyme activities present in cell-free extracts of *E. halochloris* and *H. elongata*. Ono et al. [165] subsequently made major contributions to an understanding of the biochemistry of the ectoine biosynthetic enzymes; these authors used purified EctABC proteins from *H. elongata* to study their enzymatic properties. In addition, biochemical procedures to study these enzymes from various methylotrophic bacteria were summarized by Reshetnikov et al. [166]. The biochemical properties of ectoine hydroxylase from *Salibacillus salexigens* were first determined by Bursy et al. [79,98], and Widderich et al. [92,93] subsequently studied this enzyme from a substantial number of Bacteria and from a single archaeon. Ectoine is synthesized from the precursor L-aspartate-β-semialdehyde (Figure 2), a central intermediate of microbial amino acid metabolism and cell wall and antibiotic synthesis [167]. In a sub-group of ectoine/5-hydroxyectoine producers, the ectoine/5-hydroxyectoine biosynthetic gene cluster contains a gene (*ask_ect*) for a specialized aspartokinase [93,168]. Its biochemical properties were studied by Stöveken et al. [122] using the Ask_Ect enzyme from *Pseudomonas stutzeri* A1501 and by Reshetnikov et al. [166] using the corresponding enzyme from *Methylobacterium extorquens* AM1.

In comparison with the energetic demands to sustain the *salt-in* osmopressure adjustment strategy through the import of ions, implementation of the *salt-out* strategy through the production of massive amounts of compatible solutes is energetically very costly for microorganisms [36,37]. This is, of course, also true for the synthesis of ectoine. As calculated by A. Oren, the energy requirements (expressed in ATP equivalents) for the synthesis of a single ectoine molecule by an aerobic heterotroph growing on glucose corresponds to about 40 ATP equivalents and increases to approximately 55 ATP equivalents when ectoine is synthesized by an autotroph from CO₂ [37]. These values closely resemble those calculated for the synthesis of the compatible solute glycine betaine under these two growth conditions [37] when it is produced either via the sequential methylation of

glycine [169] or the through oxidation of choline [170–172]. From an energetic point of view, synthesis of ectoine and glycine betaine are considerable less expensive than that of the compatible solute trehalose, whose production by an aerobic heterotroph growing on glucose requires the expenditure of about 79 ATP equivalents, an energetic cost that rises to about 109 molecules of ATP when this disaccharide is produced by an autotroph from CO₂ [37].

5.2. Characteristics of the Ectoine/5-Hydroxyectoine Biosynthetic Enzymes

5.2.1. L-2,4-Diaminobutyrate Transaminase EctB

Ectoine synthesis starts with the transamination of the precursor L-aspartate- β -semialdehyde, a reaction catalyzed by the L-2,4-diaminobutyrate-2-oxoglutarate transaminase EctB. EctB might be a pyridoxal-5'-phosphate (PLP)-dependent enzyme [173] similar to other aminotransferases, and requires K⁺ for its activity and stability [165]. The EctB enzyme accepts L-aspartate- β -semialdehyde as its substrate and catalyzes the reversible transfer of an amino group from L-glutamate to the aldehyde group of the substrate, thereby forming L-2,4-diaminobutyrate (DABA) and 2-oxoglutarate (Figure 2). Biochemical characterization of EctB was reported for the orthologous enzymes from *H. elongata* [165] and *Methylobacterium alcaliphilum* [99]. Both enzymes are homo-hexameric proteins and have a strong requirement of K⁺ for their enzymatic activity and stability. The preferred amino group donors are L-glutamate for the forward reaction (forming DABA) and DABA or 4-aminobutyrate for the reverse reaction (forming glutamate). Optimal catalytic activities were recorded for the enzyme from *H. elongata* at temperatures of 25 °C, a slightly alkaline pH of 8.6, and KCl concentrations of 0.5 M. Addition of NaCl (0.05–0.5 M) also enhanced the enzyme activity, but the enhancing effect of KCl in the range of 0.01–0.5 M on enzyme activity was much stronger. The apparent *K_m* values are 9.1 mM for the amino group donor L-glutamate and 4.5 mM for the amino group acceptor L-aspartate- β -semialdehyde [165].

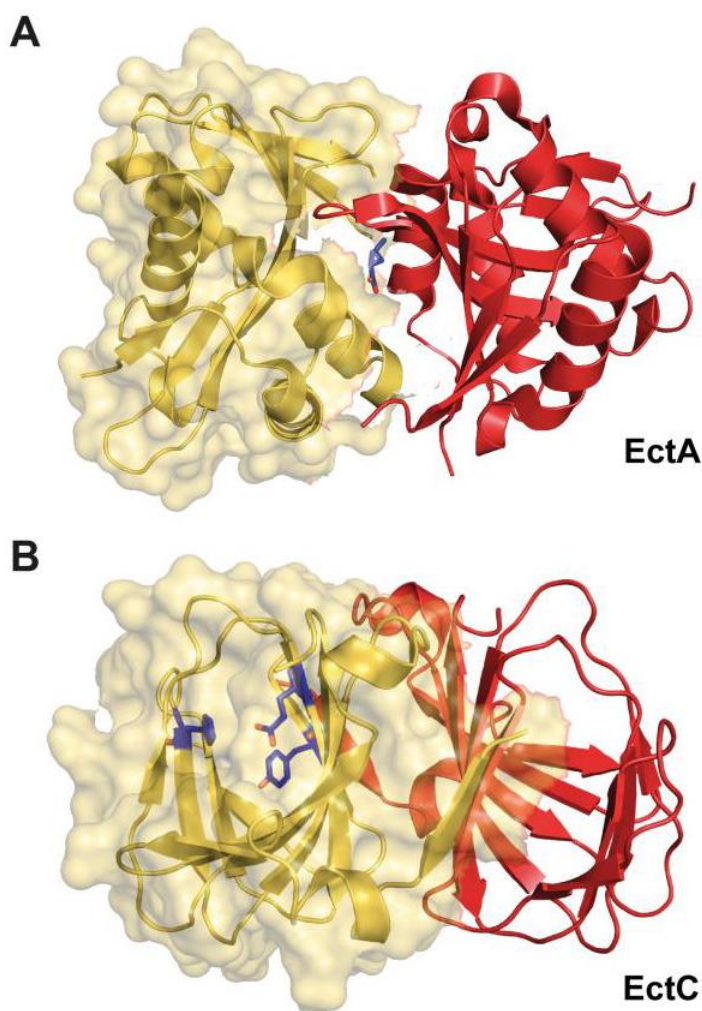
An innovative approach was taken by Chen et al. [156] to identify variants of the *H. elongata* EctB enzyme with substantially enhanced catalytic activity. These authors re-engineered the AraC transcription factor from *E. coli* so that it would preferentially respond in its DNA-binding activity to the *ara* promoter (P_{BAD}) to the cellular ectoine pool, instead of to its natural effector molecule L-arabinose. They then combined the synthetic AraC^{Ect} regulatory protein with a P_{BAD}-ECFP fluorescent reporter system in a strain simultaneously expressing the *H. elongata* *ectABC* gene cluster on a plasmid. In this way, they were able to identify variants of the *ectABC* gene cluster, generating higher cellular ectoine pools. These strains carried amino acid substitutions in EctB, the enzyme that controls the flux of the precursor L-aspartate- β -semialdehyde into the ectoine biosynthetic route (Figure 2) [165,166]. One of the recovered *ectB* mutants simultaneously carried three mutations, leading to amino acid substitutions D180V/F320Y/Q325R. The encoded mutant EctB enzyme exhibited a notably improved (by about 4.1-fold) catalytic efficiency (*K_{cat}*/*K_m*), and thereby concomitantly increased cellular ectoine titers in the heterologous *E. coli* host by about 3.3-fold relative to a strain possessing the wild-type EctB protein [156]. The bio-sensing metabolic engineering approach used by Chen et al. [156] should be generally applicable for improving the biotechnological production of ectoines for practical purposes, both in natural and in synthetic cell factories and might, as evidenced by EctB, yield interesting variants of the ectoine biosynthetic enzymes.

5.2.2. L-2,4-Diaminobutyrate Acetyltransferase EctA

The transformation of DABA and the co-substrate acetyl-coenzyme A into *N*- γ -acetyl-2,4-diaminobutyrate (*N*- γ -ADABA) and CoA is catalyzed by the L-2,4-diaminobutyrate acetyltransferase EctA. This enzyme belongs to the large superfamily of GCN5-related-*N*-acetyltransferases (GNAT) that catalyze the transfer of an acetyl-group from acetyl-coenzyme A as donor to a primary amine as acceptor molecule [174]. Ono et al. [165] were the first to report on the enzymatic properties of an EctA ortholog isolated from *H. elongata*. The partially purified enzyme showed its highest activities at pH 8.2, at temperatures of about 20 °C, and in the presence of 0.4 M NaCl. Gel filtration experiments revealed a native molecular mass of about 45 kDa, which represents a homodimer of the EctA

subunit. Three further EctA orthologs from methanotrophic or methylotrophic bacteria (*M. alcaliphilum*, *Methylophaga thalassica*, and *Methylophaga alcalica*) were subsequently biochemically characterized by Trotsenko and co-workers [99,168,175]. Their properties reflect the different physiologies of the host species from which they were isolated. The highest enzyme activities were recorded at a slightly alkaline pH of 8.5 for the enzyme derived from the neutrophilic *M. thalassica* and at a more alkaline pH of 9.5 for the enzymes obtained from the alcaliphiles *M. alcalica* and *M. alcaliphilum*. Interestingly, the activities of the EctA enzymes from the two methylotrophic *Methylophaga* species were inhibited by addition of NaCl or KCl, while the orthologous protein of the methanotrophic *M. alcaliphilum* was activated by these salts with an optimum of salt concentration of about 0.2 M NaCl or 0.25 M KCl [99].

A crystal structure of the homo-dimeric EctA protein from the human pathogen *Bordetella parapertussis* has been solved [Protein Data Bank (PDB) accession code 3D3S]. In this structure, a single molecule of the substrate DABA is bound within the dimer interface (Figure 3A). However, the experimental details of this particular EctA crystal structure or the biochemistry of the enzyme have not been formally published. Hence, nothing is known about the enzymatic properties of the *B. parapertussis* EctA enzyme and whether the unusual position of the substrate within the dimer assembly was experimentally verified through site-directed mutagenesis of residues within the supposed active site.



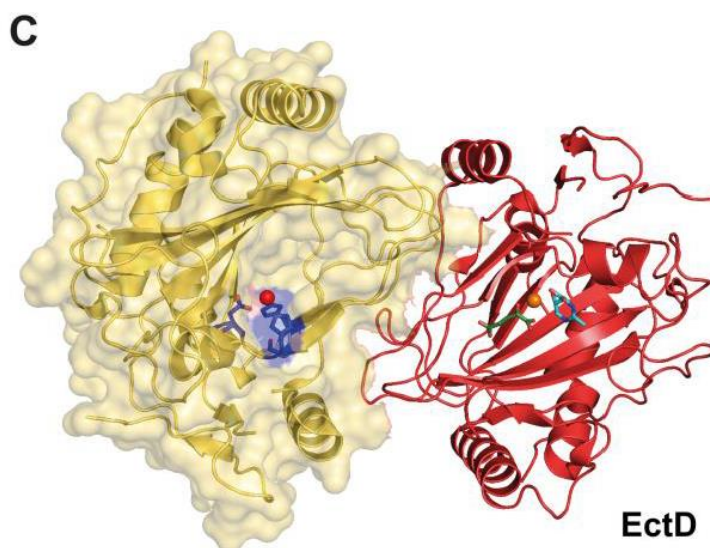


Figure 3. Crystal structures of the EctA and EctC ectoine biosynthetic enzymes and that of the ectoine hydroxylase EctD. Dimers of the L-2,4-diaminobutyrate acetyltransferase (EctA), ectoine synthase (EctC), and ectoine hydroxylase (EctD) are depicted. (A) In the crystal structure of the EctA protein from *Bordetella parapertussis* [Protein Data Bank (PDB) accession code 3D3S] a single molecule of the substrate DABA is bound at the dimer interface. (B) Crystal structure of the EctC protein from *Sphingopyxis alaskensis* (PDB accession code 5BXX). In one of the dimers, the putative metal-binding residues (Glu⁵⁷, Tyr⁸⁵, His⁹³) are highlighted; these protrude into the lumen of the cupin barrel, where the predicted active site of the enzyme is located [176]. (C) Crystal structure of the EctD protein from *S. alaskensis* (PDB accession code 4Q5O). In the left monomer of the dimer assembly, the three residues (His¹⁴⁴, Asp¹⁴⁶, His²⁴⁵) coordinating the catalytically important iron (shown as an orange sphere) are highlighted. In the right monomer of the dimer assembly, the position of the co-substrate for the EctD enzyme, 2-oxoglutarate, and the ectoine-derived product 5-hydroxyectoine are depicted relative to that of the iron catalyst [177].

5.2.3. Ectoine Synthase EctC

The last step in ectoine biosynthesis, the ring closure to form the end product ectoine, consists of an intramolecular condensation reaction catalyzed by the ectoine synthase EctC (EC 4.2.1.108) (Figure 2). As a member of the carbon-oxygen hydro-lyases (EC 4.2.1), EctC catalyzes the ring enclosure of ectoine by the elimination of a water molecule from a carbonyl C=O-bond in the substrate *N*- γ -ADABA and the generation of an intramolecular imino bond.

The ectoine synthase of *H. elongata* [165] shows its highest enzymatic activity at a pH of 8.5–9.0, a temperature of 15 °C, and in the presence of 0.5 M NaCl. The purified enzyme appears to be stabilized in vitro by the presence of high NaCl concentrations since the optimal temperature for the enzyme reaction can be shifted from 15 °C to 30 °C by raising the NaCl concentration from 0.77 M to 3 M. The NaCl concentration also affects the kinetic properties of EctC. The K_m value of the EctC enzyme for its substrate *N*- γ -ADABA is about 11 mM under low salt concentration (0.05 M NaCl), but decreases to 8.4 mM upon addition of 0.77 M NaCl. The studied EctC enzyme from *H. elongata* showed high substrate specificity towards *N*- γ -ADABA, and Ono et al. [165] found no evidence for a reverse hydrolyzing activity of EctC that would convert the cyclic ectoine molecule into the linear *N*- γ -ADABA. *N*- γ -ADABA (Figure 2) can provide osmoprotection to a degree similar to that afforded by ectoine when it is accumulated in an ectoine synthase (EctC)-deficient mutant of *C. salexigens* [120], or when it is externally provided to salt-stressed *Salmonella typhimurium* cells [178]. Since *N*- γ -ADABA can also protect thermolabile proteins from denaturation [179], it possesses properties that are hallmarks of compatible solutes [54,61,62]. It remains to be seen, however, if this intermediate in ectoine biosynthesis is accumulated in ectoine-producing wild-type strains to cellular levels that would be relevant for notable function-preserving effects.

The biochemically and structurally best-characterized ectoine synthase is that of the cold-adapted marine alphaproteobacterium *Sphingopyxis alaskensis* [177]. Like other EctC orthologs, it is a dimer in solution, and also in the crystal structures. It possesses the following kinetic parameters: a K_m of about 5 mM, V_{max} of about 25 U mg⁻¹, a k_{cat} of about 7 s⁻¹. Reflecting the permanently cold habitat of *S. alaskensis*, the temperature optimum of its ectoine synthase is 15 °C, and the enzyme has a pH optimum of 8.5. The optimum salt concentration for the enzyme is around 0.25 M of either KCl or NaCl, but the *S. alaskensis* EctC protein is highly salt-tolerant, as substantial enzyme activity is observed when high concentrations of KCl (up to 1 M) or NaCl (up to 0.5 M) are present in the assay buffer [176].

The biochemical properties of the ectoine synthase from the acidiphilic alphaproteobacterium *Acidiphilium cryptum* have been studied, as well [180]. Interestingly, the best enzymatic activity of the recombinantly produced EctC protein was observed in the absence of salt. This difference in the enzymatic properties of the *A. cryptum* ectoine synthase with reference to the strong salt-dependence of the *H. elongata* enzyme (pI 4.87) [165] prompted Moritz et al. [180] to calculate the theoretical isoelectric point (pI) of 80 EctC-type proteins. In this dataset, the *A. cryptum* enzyme exhibits one of the least acidic calculated pI's (6.03), a feature that might contribute to the salt-independence of this particular ectoine synthase.

Only a few members of the Archaea are capable of ectoine synthesis (see Section 6.3). One of them is the thaumarchaeon *Nitrosopumilus maritimus* SCM1 [92]. Its ectoine synthase was heterologously produced and biochemically characterized. The enzyme is a dimer in solution and possesses the following kinetic parameters for its natural substrate *N*- γ -ADABA: a K_m of about 7 mM, a V_{max} of about 13 U mg⁻¹, a k_{cat} of about 6 s⁻¹, and a k_{cat}/K_m of about 1 s⁻¹ mM⁻¹. Its temperature and pH optima are about 30 °C and 7, respectively [92]. While the kinetic parameters of the archaeal EctC enzyme resemble those of its bacterial counterpart from *H. elongata* [165], their enzyme activity profile in response to salt is strikingly different. As outlined above, the *H. elongata* enzyme is strongly dependent on high salinity, while the activity of the *N. maritimus* SCM1 ectoine synthase is restricted to a narrow range of salt concentrations [92].

The ectoine synthase can also be exploited to produce non-natural compatible solutes. Witt et al. [181] demonstrated that L-glutamine can be used as an alternative substrate to DABA by the *H. elongata* EctC enzyme, albeit with a very low catalytic efficiency. In this reaction, L-glutamine is converted into the cyclic condensation product 5-amino-3,4-dihydro-2H-pyrrole-2-carboxylate (ADPC). ADPC is a synthetic compatible solute as it enhances bacterial growth under salt stress conditions and also stabilizes enzymes against denaturation caused by repeated cycles of freezing and thawing [181]. The EctC-catalyzed formation of ADPC is reversible, with the equilibrium of this reaction lying largely on the site of the hydrolytic product L-glutamine. The *H. elongata* EctC enzyme is also able to hydrolyze the synthetic ectoine analogs [143] homoectoine [(*S*)-4,5,6,7-tetrahydro-2-methyl-1H-(1,3)-diazepine-4-carboxylic acid], and DL-DHMICA [(*RS*)-4,5-dihydro-2-methyl-imidazole-4-carboxylic acid], whereas its hydrolytic activity for ectoine was found to be negligible [181].

The ectoine synthase belongs to the functionally diverse superfamily of cupin proteins [182,183], and it contains a characteristic cupin domain comprising two conserved motifs [176]. Most members of this protein superfamily are metal-dependent enzymes, and highly conserved residues that are derived from both conserved cupin motifs usually anchor and position the metal cofactor in the active site [182]. Like other cupins [182,183], studies with the *S. alaskensis* EctC enzyme revealed that it is promiscuous with respect to the divalent metal used in enzyme catalysis, but Fe²⁺ is the most-likely biochemically relevant cofactor for the EctC-catalyzed enzyme reaction [176].

The crystal structure of the *S. alaskensis* EctC protein (Figure 3B) has been elucidated at a resolution of 1.2 Å (PDB accession codes 5BXX and 5BY5) [176] and exhibits an overall barrel-type fold typical for cupins [182,183]. While the crystal structures of the *S. alaskensis* ectoine synthase are of high resolution, they unfortunately lack the catalytically important metal, and contain neither the substrate *N*- γ -ADABA nor the reaction product ectoine. Bioinformatics and site-directed mutagenesis identified the most likely residues involved in the binding of the catalytically important metal by the *S. alaskensis* ectoine synthase. The corresponding three residues (Glu⁵⁷, Tyr⁸⁵, His⁹³) of

the *S. alaskensis* EctC protein are evolutionarily highly conserved among a large group of EctC-type proteins. Their side chains protrude into the lumen of the cupin barrel (Figure 3B) [176], the location at which the cyclo-condensation of the *N*- γ -ADABA substrate to ectoine will take place [182,183]. The *S. alaskensis* EctC protein is a head-to-tail dimer; the dimer interface is formed by two anti-parallel β -sheets present near the N- and C-termini of each monomer, stabilizing interactions that thus occurs twice within the EctC dimer assembly (Figure 3B).

5.2.4. Ectoine Hydroxylase EctD

A substantial number of the ectoine producers additionally synthesize 5-hydroxyectoine [92,93,98] through a position- and stereo-specific hydroxylation of ectoine (Figure 2). Bursy et al. [79,98] elucidated the biochemical basis for the formation of 5-hydroxyectoine through studies with the purified ectoine hydroxylases (EctD; EC 1.14.11.55) from the moderate halophile *S. salexigens* (taxonomically now reclassified as *Virgibacillus salexigens*) and the soil bacterium *S. coelicolor*. This biochemical analysis and subsequent structural work [177,184] revealed that EctD is a member of the superfamily of non-heme Fe(II)-containing and 2-oxoglutarate-dependent dioxygenases [185]. The O₂-dependent hydroxylation of the substrate ectoine is accompanied by the oxidative decarboxylation of 2-oxoglutarate to form succinate and CO₂, while the iron cofactor acts as a catalyst for the activation of molecular oxygen [186] (Figure 2). Therefore, the catalytic activity of the EctD enzyme is strongly dependent on the presence of molecular oxygen [92,93,177,184]. 5-hydroxyectoine produced in vivo by *S. parvulus* is known to have the (4*S*,5*S*) stereo-chemical configuration [90], and the very same configuration is also found in the reaction product formed in vitro by the purified *V. salexigens* EctD enzyme as analyzed by one-dimensional ¹H-NMR spectroscopy [98].

To date, nine ectoine hydroxylases have been biochemically characterized; eight of these originate from various, mostly extremophilic, bacteria (*V. salexigens*, *S. coelicolor*, *S. alaskensis*, *Paenibacillus lautus*, *P. stutzeri*, *Alkalilimnicola ehrlichii*, *A. cryptum*, *H. elongata*) [93,184], and one of the studied enzymes was derived from the archaeon *N. maritimus* SCM1 [92]. The EctD-containing microorganisms live in ecophysiological rather different habitats, but the biochemical properties of the studied ectoine hydroxylases are all very similar. Their enzyme activities are not strongly dependent on salts, and their pH (between 7.5 and 8) and temperature optima (between 32 and 40 °C) range within narrow windows. The apparent kinetic parameters of these enzymes for the substrate ectoine (*K_m* values between 6 and 10 mM) and the co-substrate 2-oxoglutarate (*K_m* values between 3 and 5 mM) are similar, and their catalytic efficiencies (*k_{cat}*/*K_m*) vary only between 0.12 and 1.5 mM⁻¹ s⁻¹ [92,93,184]. Hence, ectoine hydroxylases possess rather moderate affinities for their substrate ectoine, a property that is potentially connected with the fact that the accumulation of ectoine to a substantial intracellular level via de novo synthesis typically precedes the production of 5-hydroxyectoine [79,98,122,123]. Although all ectoine hydroxylases studied to date possess similar kinetic parameters, it should be noted that the in vivo performance of these enzymes can differ substantially when they are expressed in an *E. coli*-based synthetic cell factory that imports externally provided ectoine via the osmotically induced ProP and ProU osmolyte import systems [187–189], hydroxylates it, and then excretes the newly formed 5-hydroxyectoine almost quantitatively into the growth medium [151]. These differences in performance might stem from differences in the production levels or the stability of the recombinant proteins in the heterologous host, or the properties of the *E. coli* cytoplasm is not optimal for the enzymatic activities of the various EctD proteins. Such differences in the in vivo performance of ectoine hydroxylases with seemingly similar in vitro kinetic parameters need to be carefully considered when such enzymes are used in heterologous microbial cell factories for the biotechnological production of 5-hydroxyectoine [116].

Among the four enzymes involved in ectoine/5-hydroxyectoine biosynthesis [164–166], the ectoine hydroxylase is certainly the best studied [92,93,177,184,186]. A substantial number of EctD enzymes have been biochemically assessed that were derived from physiologically and taxonomically distinct groups of microorganisms [92,93]. Furthermore, the structure/function relationship of this enzyme has been studied by site-directed mutagenesis, by molecular dynamics simulations and finally via crystal structure analysis [93,177,184,186]. Together, these studies have

led to a detailed understanding of the EctD-mediated enzyme reaction [186] and illuminated the architecture of the active site [177]. Crystal structures of *V. salexigens* without any substrates or products [184], and that of *S. alaskensis* with various ligands [177] have been reported.

The ectoine hydroxylase is a dimer in solution and in the crystal structure. The dimer interface of the swapped head-to-tail dimeric structure is primarily formed through interactions by loop areas pointing from one monomer towards the other (Figure 3C). bona fide EctD-type proteins can be distinguished from other members of the broadly distributed non-heme Fe(II)-containing and 2-oxoglutarate-dependent dioxygenases superfamily through an evolutionarily highly conserved signature sequence consisting of a continuous stretch of 17 amino acids (F-x-W-H-S-D-F-E-T-W-H-x-E-D-G-M/L-P) [177,184]. When the signature amino acid sequence is viewed in the context of the EctD crystal structure, this segment of the EctD polypeptide chain is important from a structural point of view, as it forms one side of the cupin barrel (Figure 3C). In addition, it also contains five residues involved in the binding of the iron catalyst, the co-substrate 2-oxoglutarate, and the reaction-product 5-hydroxyectoine [177,184].

In their excellent and widely appreciated overview on ectoines as stress protectants and commercially interesting compounds, Pastor et al. [91] suggest that 5-hydroxyectoine may also be formed by first converting the EctA-formed *N*- γ -acetyl-2,4-diaminobutyrate (Figure 2) into 3-hydroxy-*N*- γ -acetyl-2,4-diaminobutyrate, which is proposed to be subsequently cyclized to 5-hydroxyectoine. In this envisioned pathway, the activity of EctC is circumvented by an unknown enzyme and the existence of an additional unknown enzyme is invoked that would cyclize the linear 3-hydroxy-*N*- γ -acetyl-2,4-diaminobutyrate molecule to 5-hydroxyectoine [80]. This proposal for an alternative route for the formation of 5-hydroxyectoine is primarily based on the properties of a particular *ectC* mutant (*ectC::Tn1732*; strain CHR63) of *C. salexigens* [120] in which, quite surprisingly, both ectoine and 5-hydroxyectoine were still detected [179]. There have been no follow-up studies on this hypothetical 5-hydroxyectoine biosynthetic route since it was originally proposed by Canovas et al. in 1999 [179]. Synthesis of ectoine and 5-hydroxyectoine in the *ectC* mutant may be a particular feature of the studied *C. salexigens* genetic background [120,179], or the fact that *C. salexigens* is also able to catabolize ectoines [80,190] and may thus use some of the degradative enzymes (see Section 7) to partially restore ectoine/5-hydroxyectoine production.

We suggest that the envisioned EctC- and EctD-independent route for the synthesis of 5-hydroxyectoine [91] is of no physiological relevance in natural settings of osmotically stressed wild-type 5-hydroxyectoine-producing microorganisms. To avoid confusion, this hypothetical pathway should, in our view, not be presented in the literature [80,91] as a true alternative to the biochemically and structurally buttressed direct and stereo-specific hydroxylation of ectoine by the ectoine hydroxylase EctD [92,93,98,177] until it is further substantiated by molecular and biochemical evidence.

5.2.5. Specialized Aspartokinase Ask_Ect

The precursor for ectoine synthesis (Figure 2), L-aspartate- β -semialdehyde, is a central metabolic hub in microorganisms from which a branched network of various biosynthetic pathways diverges [167]. L-aspartate- β -semialdehyde is synthesized through the sequential enzymatic reactions of an aspartokinase (Ask; EC 2.7.2.4) and a L-aspartate-semialdehyde-dehydrogenase (Asd; EC 1.2.1.11). Ask synthesizes L-4-aspartyl- β -phosphate via an ATP-dependent phosphorylation of L-aspartate, which is then in turn reduced to L-aspartate- β -semialdehyde by the Asd enzyme in an NADPH-dependent reaction (Figure 2). To avoid a wasteful production of the energy-rich intermediate L-4-aspartyl- β -phosphate, the enzymatic activities of aspartokinases are usually regulated by feedback inhibition and the expression of the corresponding *ask* gene is also often subjected to sophisticated transcriptional regulation [167]. Since major production routes of biotechnologically interesting antibiotics and commercially used amino acids (e.g., L-lysine) branch off from L-aspartate- β -semialdehyde as the initial metabolite, aspartokinases are often targeted in genetic engineering approaches to relieve their feedback inhibition. This leads to an increased cellular L-aspartate- β -semialdehyde pool and thereby fosters the flow of this precursor into biosynthetic pathways of

interest [152,191]. When applied to the heterologous production of ectoine in *E. coli*, a bacterium that does not naturally synthesize ectoine [187], the yield was indeed improved by co-expressing a feedback-resistant aspartokinase (LysC) derived from *Corynebacterium glutamicum* together with the ectoine biosynthetic genes obtained from *Marinococcus halophilus* [191]. Such feedback-resistant aspartokinases have also been employed in the design of engineered synthetic microbial cell factories, thereby resulting in enhanced production of ectoines [152,153,155].

Because the feedback-control of Ask enzyme activity could potentially lead to a bottleneck in ectoine biosynthesis [191], the report of Reshetnikow et al. [168] that the osmotically inducible ectoine biosynthetic gene cluster of *M. alcaliphilum* was co-transcribed with a gene encoding an aspartokinase was of considerable interest. This finding indicated that the enzyme encoded by this particular *ask* gene could play a specialized role in ectoine biosynthesis. Indeed, it was observed in subsequent studies [93] that a considerable number of ectoine/5-hydroxyectoine biosynthetic gene clusters include an additional paralogous *ask* gene (referred to in the following as *ask_ect*) [122] (see Section 5.3).

A comprehensive cohesion group analysis of aspartokinases revealed that the Ask_Ect enzymes form a distinct sub-cluster among the large aspartokinase enzyme family, and that those residues implicated in participating in the feedback control of various Ask enzymes are not conserved in the Ask_Ect group [167]. Stöveken et al. [122] purified such an Ask_Ect enzyme from the ectoine/5-hydroxyectoine-producing plant-root-associated bacterium *P. stutzeri* A1501 and benchmarked its biochemical properties against those of the biosynthetic standard aspartokinase (Ask_LysC) present in this bacterium as well. Both enzymes possess similar kinetic parameters, but exhibit significant differences with regard to the allosteric control by biosynthetic products derived from L-aspartate. Ask_LysC was inhibited by L-threonine alone and in a concerted fashion by L-threonine and L-lysine, whereas Ask_Ect showed inhibition only by L-threonine. Moreover, the inhibiting effect by L-threonine on the latter enzyme was significantly reduced when the enzyme activity assay was carried out in presence of 650 mM NaCl or KCl [122].

An *E. coli* strain carrying the plasmid-based *ectABCD-ask_ect* gene cluster from *P. stutzeri* A1501 produced substantially more (about 5-fold) ectoine/5-hydroxyectoine than a strain expressing the same gene cluster without the *ask_ect* gene [122]. Taken together, these findings suggest that the *ask_ect* gene encodes an aspartokinase with a specialized role for the biosynthesis of ectoine and 5-hydroxyectoine. The frequent co-expression of this gene with osmotically inducible *ect* gene clusters [93,122,168] (Figure 4 and Section 6.3) will ensure an optimal supply of the precursor L-aspartate- β -semialdehyde under osmotic stress conditions. However, it should be noted that the majority of ectoine/5-hydroxyectoine-producing bacteria do not contain such a specialized Ask_Ect enzyme (Figure 5), indicating that they may use different strategies to maintain their L-aspartate- β -semialdehyde pools at high enough cellular levels to support their large-scale ectoine/5-hydroxyectoine biosynthetic activities under high-salinity growth conditions.

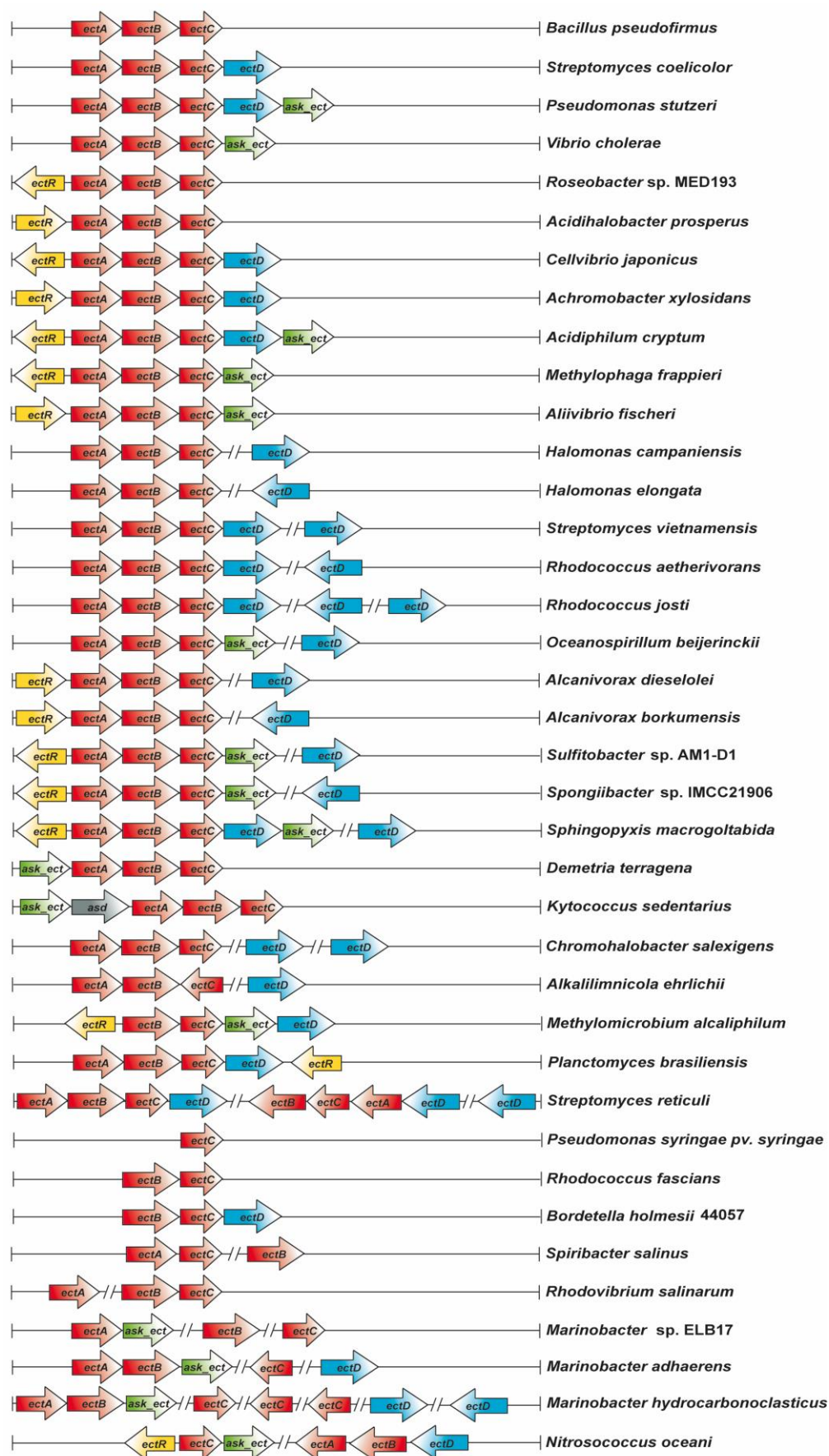


Figure 4. Diversity of the genetic organization of ectoine and 5-hydroxyectoine biosynthetic gene clusters in microbial genomes.

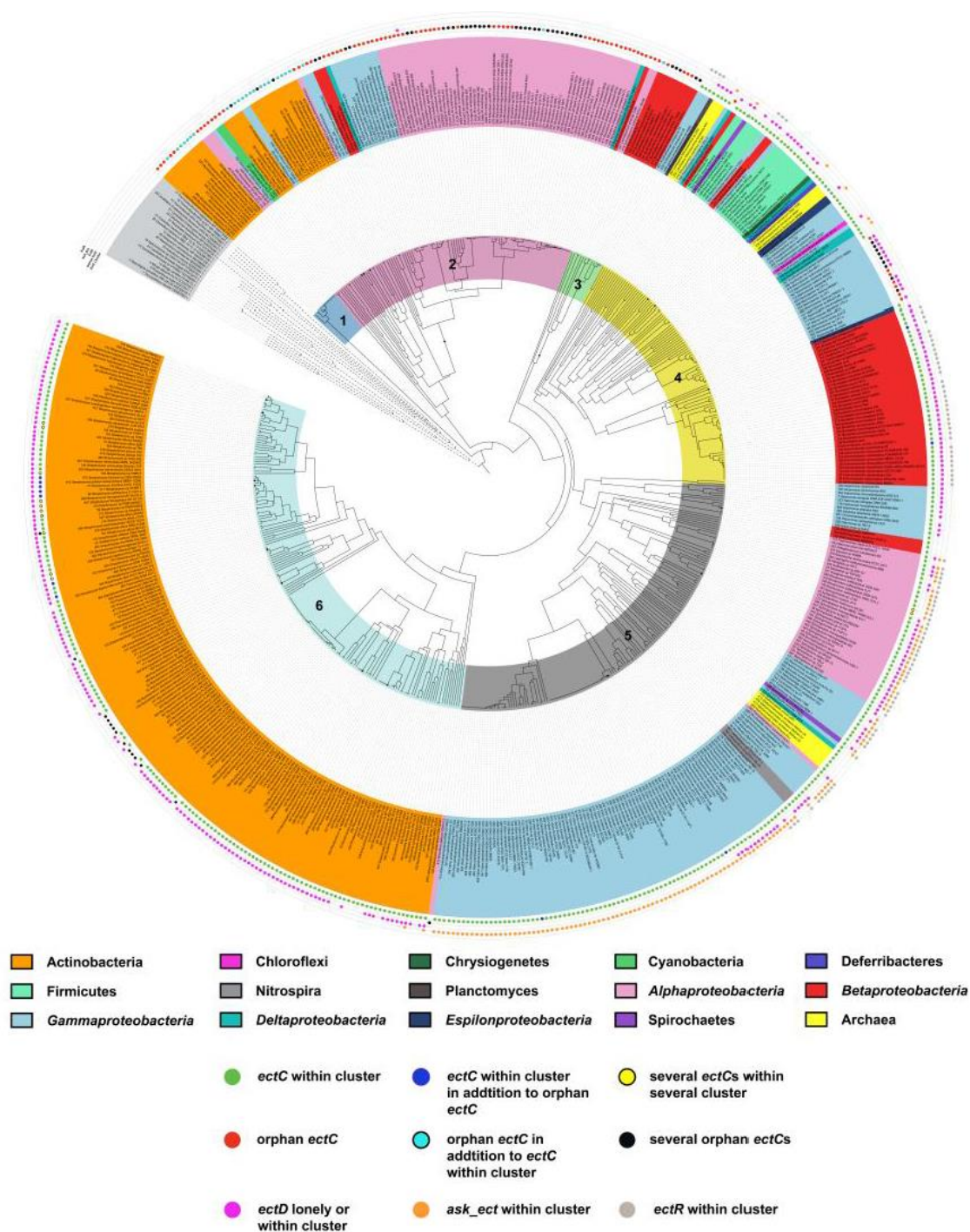


Figure 5. Phylogenomics of the ectoine synthase. The amino acid sequences of 582 EctC-type proteins were retrieved from microorganisms with fully sequenced genomes, aligned with MAFFT [192] and then used for a clade analysis using the iTOL software [193]. The tree was rooted with a number of microbial cupin-type proteins, a superfamily of proteins [182,183] to which the EctC protein also belongs [176]. The phylogenetic affiliation of the various EctC proteins is depicted in different colors shown in the outer ring, and the color code is explained in the figure. Different groups (1 to 6) in which the EctC-type proteins can be clustered are depicted in the inner colored circle. The dots in the outmost 5 rings depict (from the inside to the outside) if the EctC protein is encoded within an *ect* biosynthetic gene cluster, if the EctC protein is an orphan, if the pertinent EctC-containing microorganism also possesses the ectoine hydroxylase EctD, if the specialized aspartokinases Ask_Ect is part of the *ect* cluster, or if the *ect* gene cluster is affiliated with a gene encoding the EctR regulatory protein.

5.2.6. Adjusting Central Carbon Metabolism to the Drain Exerted by Ectoine Biosynthesis

Under osmotic stress conditions, ectoines can be accumulated through synthesis to exceedingly high intracellular concentrations [91,94], and the degree of the imposed osmotic stress dictates their pool size. There seems to be a linear relationship between the external osmolarity/salinity and the amounts of the produced ectoines [116–118]. As a consequence, the microbial cell has to sensitively adjust its metabolism to constraints imposed by high-level synthesis of the nitrogen-rich ectoine/5-hydroxyectoine molecules (Figure 1B), which will impose a serious drain of available carbon- and nitrogen-sources. Hence, it is necessary to understand the interplay of the carbon and nitrogen supplies for the production of ectoines in greater detail [194]. Their synthesis burdens the assimilation of nitrogen via the glutamine synthetase pathway and central metabolic routes by recruiting TCA-cycle intermediates—in particular, oxaloacetate and acetyl-CoA [195–197]. Consequently, anaplerotic routes have to be engaged to replenish the TCA cycle for routine central carbon metabolism and at the same time an increased flux of metabolites into the ectoine/5-hydroxyectoine biosynthetic pathway has to be ensured. Genome-scale modeling and integrative systems biology approaches have recently provided insights into how this is accomplished by *C. salexigens* [196] and *H. elongata* [197]. These studies paint a complex picture of the involved metabolic changes and highlight the considerable metabolic and energetic burden [24,37,106] that osmotically stressed cells face when they try to alleviate osmotically imposed constraints on growth through the synthesis of stress-relieving ectoines [194–197]. This aspect is not only important for a full understanding of the cells' behavior under osmotic stress conditions, but is also a pre-requisite to further improvement of the high-yield production of ectoines by natural and synthetic microbial cell factories.

6. Genetics and Phylogenomics of Ectoine and 5-Hydroxyectoine Biosynthetic Genes

6.1. Genetic Organization of the Ectoine/5-Hydroxyectoine Biosynthetic Gene Clusters

The description of the *ectABC* genes in *M. halophilus* [95], along with that of the *ectABCD* locus in *Streptomyces chrysomallus* [96], provided the primers for a molecular analysis of the ectoine/5-hydroxyectoine biosynthetic genes. Studies on *C. salexigens* [97] and *S. salexigens* [98] subsequently demonstrated that the *ectD* gene was not necessarily part of the *ectABC* gene cluster but could be encoded somewhere else in the genome, with *C. salexigens* possessing even two *ectD*-type genes [80,97] (Figure 4). Previous genome assessments [91–93,99], and our current own comprehensive database searches (see Section 6.3), revealed an evolutionarily rather conserved genetic configuration of the ectoine/5-hydroxyectoine biosynthetic genes in many bacterial and some archaeal genomes. In some notable cases, several copies of complete ectoine/5-hydroxyectoine biosynthetic gene clusters are even present that might have arisen either through gene duplication or lateral gene transfer. *Streptomyces reticuli* is an example where two copies of the *ectABCD* gene clusters are present, and an additional copy of an *ectD*-type can even be found in the genome of this actinobacterium. The occurrence of multiple copies of *ectD*-type genes in the same genome is not unusual (Figure 4).

As highlighted in Figure 4, the *ectABC* and *ectABCD* gene clusters build a conserved backbone in most ectoine/5-hydroxyectoine producers that can additionally be genetically configured with the gene (*ask_ect*) for the specialized aspartokinases and/or the gene (*ectR*) for a MarR-type regulator, EctR (see Section 5.2) [91–93,99,122,168,198]. In practically all ectoine/5-hydroxyectoine gene clusters inspected by us, we found that the gene for the second enzyme (L-aspartate- β -semialdehyde-dehydrogenase, Asd) involved in providing the ectoine biosynthetic precursor L-aspartate- β -semialdehyde is absent (Figures 2 and 4). The notable exception to this rule is the *ect* gene cluster from the marine actinobacterium and opportunistic pathogen *Kytococcus sedentarius* where *ask_ect* and *asd* are encoded up-stream of the *ectABC* operon (Figure 4).

In addition to the evolutionarily conserved *ectABC/ectD* gene arrangement, substantially re-arranged configurations of the *ect* genes can be found in a sizable number of microorganisms (Figure 4). There can be a re-arrangement of individual genes within the *ect* cluster, but there are also cases where individual *ect* genes have been separated from each other, or where multiple copies of the same gene (e.g., *ectC*) are present at various locations within the genome (Figure 4).

Many representatives with re-arranged or disentangled *ect* biosynthetic genes live in marine ecosystems [199]. Given the re-arrangement of the canonical *ect* gene configuration in these bacteria, one wonders if they are capable of ectoine/5-hydroxyectoine production. One representative of this group of microorganisms is the gammaproteobacterium *Spiribacter salinus*, an ecophysiologicaly successful and abundant inhabitant of hypersaline ecosystems [200]. In its genome, *ectAB* and a separate *ectC* gene can be found (Figure 4); despite this non-canonical arrangement of the *ect* biosynthetic genes, a recent study demonstrated the production of ectoine in *S. salinus* in response to increases in the external salinity [199].

6.2. Regulation of *ect* Gene Expression

It is fitting from the main physiological function of ectoines as osmoprotectants that the transcription of the corresponding biosynthetic genes is under osmotic control. Indeed, studies with reporter gene fusions and Northern-blot analysis have demonstrated that this is the case in both Gram-negative and Gram-positive bacteria. However, the way osmotic stress is sensed by the bacterial cell and the way the gleaned information is processed to trigger enhanced *ect* transcription is far from understood. As a matter of fact, the literature pertinent to this topic is plagued with a considerable over-interpretation of preliminary findings.

Northern-blot analysis of osmotically stressed *V. (Salibacillus) salexigens* cells proved that transcription of the *ectABC* genes, and of the separately encoded *ectD* gene, is strongly enhanced in high-salinity growth media. Primer extension analysis pinpointed a single *ectABC* promoter that resembles in its sequence typical SigA-type promoters [98], the housekeeping sigma factor of Bacilli [201]. Transcription of the *ectABC* genes from *V. pantothenticus* was found to be responsive both to increases in osmolarity and to decreases (but not to increases) in growth temperature [77]. In this Gram-positive bacterium, transcription of the gene for the ectoine/5-hydroxyectoine transporter EctT followed the same pattern of gene expression, and primer extension analysis demonstrated that this response is mediated by a single SigB-type promoter [78]; SigB is the general stress-responsive alternative sigma factor in Bacilli [202] and salt and temperature stress are major inducers of the SigB-regulon in *B. subtilis* [203]. The dependence of the *V. pantothenticus* *ectT* gene on SigB was verified in a *sigB* mutant of *B. subtilis* [78], but the implicated dependence of *ectABC* transcription on SigB activity in *V. pantothenticus* was not experimentally tested [77].

When the DNA sequence of the first ever cloned *ectABC* gene cluster was reported by Louis and Galinski [95], these authors proposed that its expression was mediated by a single SigB-dependent promoter positioned upstream of *ectA*. Because *M. halophilus* is a Gram-positive bacterium, this was a reasonable assumption, but no experimental evidence for the involvement of SigB was provided in this study [95]. However, in view of the fact that *E. coli* does not possess SigB and that SigB-dependent promoters differ substantially from the consensus sequence of promoters recognized by the housekeeping sigma factor RpoD or the general stress alternative sigma factor RpoS of *E. coli* [204,205], it was rather surprising that the introduction of the *M. halophilus* recombinant *ect* genes into this Gram-negative host bacterium led to an osmoprotectant-responsive production of ectoine [95]. Bestvater and Galinski [206] subsequently rationalized this finding by invoking the fortuitous existence of stationary-phase/general stress-type RpoS-dependent promoters in front of the *M. halophilus* *ectABC* genes. If these types of promoters exist, they certainly cannot have any physiological relevance in the authentic *M. halophilus* host because Gram-positive bacteria do not possess RpoS-type alternative sigma factors [205]. Hence, the dependence of the *M. halophilus* *ectABC* gene cluster on SigB awaits experimental verification.

In *H. elongata*, the industrially used bacterium for the production of ectoines [86,91,94], two promoters preceding the *ectABC* genes and an additional promoter present in front of *ectC* were mapped by RACE-PCR [158]. Based upon DNA-sequence inspection, Schwibbert et al. [158] suggested that the promoter exclusively driving *ectC* transcription was recognized by the alternative transcription factor Sig-54, a sigma factor that is frequently involved in regulating the expression of genes involved in physiological processes connected to nitrogen metabolism. However, it is not obvious to us what the function of this internal promoter within the *H. elongata* *ect* gene cluster might

be; its implicated dependence on Sig-54 activity was not verified experimentally [158]. One of the two promoters present in front of *ectA* was described by Schwibbert et al. [158] as a promoter recognized by the housekeeping sigma factor RpoD (Sig-70); the distal located promoter was deemed to be dependent on the stationary-phase/general stress sigma factor RpoS (Sig-38). While the putative RpoS-dependent promoter of the *H. elongata ect* gene cluster exhibited features found in some other osmotically regulated RpoS-dependent promoters from *E. coli* [207,208], the *H. elongata* promoter nevertheless deviates considerably (in particular in the spacing of the -10 and -35 regions) from typical RpoS-type promoters [130,131,205]. Osmoregulation of either the proposed RpoD- or RpoS-dependent *H. elongata ect* promoters was not studied in any detail, nor was the involvement of RpoS in *ect* gene expression verified by mutant analysis [158].

The importance of a careful genetic analysis is exemplified by data reported on the apparent complex transcriptional control of the *ectABC* genes from *C. salexigens*, a salt-tolerant bacterium closely related to *H. elongata* [80,118]. S1 mRNA protection assays suggested the existence of four promoters driving *ectABC* transcription, three of which were deemed by Calderon et al. [118] to be osmotically responsive. When a *ectA-lacZ* reporter fusion expressed from the three promoters mapped in front of *ectA* was introduced into *E. coli*, expression of the reporter fusion was linearly dependent on the osmotic strength of the growth medium and its activity increased strongly in stationary phase. One (*PectA-3*) of the suggested promoters of the *C. salexigens* biosynthetic *ect* gene cluster [118] resembled, with respect to certain features of the -10 and -35 regions, osmoregulated *E. coli* promoters that are dependent on the alternative sigma-factor RpoS [130,131,205,207,208]. Since the activity of above described *ectA-lacZ* reporter fusion carrying all three promoters was reduced by about 50% in an *E. coli rpoS* mutant, Calderon et al. [118] ascribed an important role to this alternative sigma-factor for the direct transcriptional regulation of the *C. salexigens ect* gene cluster in the heterologous *E. coli* host. However, subsequent follow-up studies by the same laboratory showed that the observed effect of RpoS was indirect [209]; in other words, the initially envisioned direct effect of RpoS on the proposed *C. salexigens PectA-3* promoters does not exist.

In studying the interplay between iron homeostasis and the salt stress response of *C. salexigens*, Argandona et al. [135] found that the amount and relative proportion of ectoine and 5-hydroxyectoine was affected by excess iron in the growth medium. These authors ascribed an activator function of the Fur regulatory protein for the transcription of the ectoine biosynthetic genes, and through in silico inspection of the *ect* regulatory region, noted the presence of several potential Fur DNA-binding boxes overlapping two of the putative *ect* promoters. In quantitative RT-PCR experiments, they observed a drastic fall in the *ectA* transcript in a *fur* mutant [135], consistent with previous *ectA-lacZ* transcriptional reporter fusion studies that revealed a down-regulation of *ect* expression in *C. salexigens* wild-type cells grown at high salinity in the presence of excess iron [118]. However, the data reported by Argandona et al. [135] on the suggested direct interaction of the Fur protein with the *ect* regulatory region and the proposed activator function of the Fur regulatory protein are hard to reconcile with the findings of these authors that there was no real difference in ectoine/hydroxyectoine content between the *C. salexigens* wild-type and its isogenic *fur* mutant [135]. Hence, the inferred interaction of Fur with the *ect* promoter region and the role of Fur as an activator of *ect* transcription [135] awaits verification through DNA-binding studies and mutational analysis.

The S1 mRNA protection data reported by Calderon et al. [118] also suggested the existence of a heat-shock (RpoH; Sig-32)-dependent promoter (*PectB*) that is positioned upstream of the *C. salexigens ectB* gene. The physiological rationale for producing a separate *ectB-ectC* transcript under heat-shock conditions is not immediately apparent but reporter gene fusion studies showed enhanced expression of a *PectB-lacZ* reporter fusion at high temperature (40 °C) [118]. However, a molecular analysis that would identify this promoter as a direct target for RNA-polymerase complexed with the alternative sigma factor RpoH was not performed.

We generally consider the assignment of putative *ect* promoters that are in their core exclusively based on DNA-sequence gazing as unreliable, and we caution against the over-interpretation of such suggestions in published reports. In our view, reliable data on the transcriptional regulation of *ect* genes can only be attained through site-directed mutagenesis of the proposed promoter(s) and, if an

alternative sigma factor is invoked in their transcriptional activity, through studies with appropriate mutant strains (if at all possible) in the authentic ectoine/5-hydroxyectoine producer bacterium.

DNA sequence inspection can readily overlook the true osmotically controlled promoter(s) of *ect* biosynthetic genes, as these might deviate considerably from the consensus sequences one might look for. In a recent report, Czech et al. [116] studied the osmostress-responsive transcription of the *ect* biosynthetic genes from the plant-root-associated Gram-negative bacterium *P. stutzeri* A1501 in heterologous *E. coli* host strains. While the *ect* promoter possesses a good match (TTGAGA) to the consensus sequence (TTGACA) of the -35 element of Sig-70-type *E. coli* promoters [204], its highly G/C-rich -10 sequence (TACCCT) [116] deviates strikingly from the A/T-rich consensus sequence (TATAAT) of these types of promoters. Furthermore, the spacing of the -10 and -35 elements of the *ect* promoter with a length of 18 bp was sub-optimal for Sig-70-type *E. coli* promoters [204]. Osmostress-responsive promoters with such G/C-rich -10 elements and sub-optimal spacer length have previously been described both in *E. coli* and *B. subtilis* [84], but no *ect* promoter has been reported with such an unusual configuration in its -10 region. This prompted the study of the salient features of this promoter through *lacZ* reporter gene studies and extensive site-directed mutagenesis experiments [116]. The transcriptional activity of a wild-type *ect-lacZ* reporter fusion, when introduced into *E. coli*, proved to be linearly dependent on the external salinity and responded to true osmotic cues, as both ionic (NaCl, KCl) and non-ionic (sucrose, lactose) osmolytes triggered similar increases in promoter activity [116]. Osmotic induction of the *ect-lacZ* reporter fusion required the establishment of an osmotically active trans-membrane gradient, as high concentration of membrane-permeable glycerol did not trigger enhanced *ect* promoter activity [116].

Site-directed mutagenesis studies proved that the *P. stutzeri ect* promoter was critically dependent for its activity on the function of the *E. coli* house-keeping Sig-70 transcription factor. Furthermore, point mutations rendering its -35 and -10 regions, or that of the spacer length, towards a closer match to the consensus sequence, conferred drastic changes in gene expression. Typically, the activity of the mutant *ect* promoters rose substantially under both non-salt and salt-stress conditions [116]. Studies with *E. coli* mutants with defects in *hns*, *rpoS*, *ompR*, or *cya*, genes that have been implicated in osmoregulation of various *E. coli* genes demonstrated that the *P. stutzeri ect* promoter operates in its osmotic control completely independently of these important transcription factors [116].

None of the 18 variants of the *P. stutzeri ect* promoter constructed by site-directed mutagenesis lost osmotic control altogether; surprisingly, this was even true for an *ect* promoter variant that was synthetically adjusted to the complete consensus sequence of Sig-70 *E. coli* promoters [116]. Hence, one can conclude from this study that (i) the deviations of the *P. stutzeri ect* promoter from the consensus sequence serve to keep promoter activity low when the cell does not have to rely on the synthesis of ectoines, while simultaneously allowing strong osmotic induction of *ect* transcription when the cell physiologically needs these cytoprotectants for its adjustment to the adverse environmental conditions; and that (ii) a determinant for osmotic control must be present outside the particular sequence of the -10 and -35 regions and of the spacer that separates them. Osmotic control of the *P. stutzeri ect* promoter was traced through deletion analysis to a 116-bp DNA fragment [116]. Hence, despite the fact that *E. coli* does not synthesize ectoines naturally [187], the *P. stutzeri ect* promoter retained its exquisitely sensitive osmotic control in the heterologous host bacterium, indicating that osmoregulation of this promoter is an inherent feature of the rather small regulatory region per se. It is not yet clear yet how this can be accomplished mechanistically, but Czech et al. [116] speculated that RNA polymerase alone, perhaps in response to changes in osmotically triggered changes in DNA supercoiling [210], and in combination with changes in the intracellular ion pool (in particular the pair of K⁺ and L-glutamate) [207,208,211] and the size of the compatible solute pool [212,213], might afford osmoregulation of *ect* expression. It is currently difficult to grasp intuitively that the exquisitely sensitive osmotic control of the *ect* promoter and the tuning of its strength via incremental increases in sustained osmotic stress can be explained by this molecular mechanism alone. It will be a challenge to experimentally verify or refute this model through in vivo or in vitro studies.

A highly interesting finding with respect to the genetic control of *ect* genes is the report of Mustakhimov et al. [198], who studied these biosynthetic genes in the halotolerant methanotroph *M. alcaliphilum* 20Z. These authors detected a gene (*ectR*) positioned upstream of the *ectABC-ask_ect-ectD* gene cluster (Figure 4) that encodes a MarR-type regulator, a super-family of widely distributed transcription factors [214]. Primer extension analysis showed that the osmoregulated *ect* genes of *M. alcaliphilum* 20Z are expressed from two closely spaced promoters. Through foot-printing analysis, Mustakhimov et al. [198] found that EctR binds a homodimeric protein to a region overlapping the -10 region of the promoter most distal to the beginning of the *ectA* gene. EctR acts as a repressor of *ect* expression in *M. alcaliphilum* 20Z but notably, salt-stress responsive induction of the *ect* genes still occurred in an *ectR* mutant strain [198]. Hence, EctR is certainly not solely responsible for osmotic induction of the *ect* genes. Interestingly, EctR controls the transcription of its own gene in *M. alcaliphilum* 20Z [198].

In the methanol-utilizing bacterium *M. alcalica*, EctR served as a repressor for the ectoine biosynthetic gene cluster as well [215], and in the methylotroph *Methylophaga thalassica*, the purified EctR protein interacted in DNA-band shift assays with a region carrying the two promoters of the *ect* biosynthetic genes. However, in contrast to the situation in *M. alcaliphilum* 20Z, no auto-regulation of *ectR* transcription was found [99]. In both *M. alcaliphilum* 20Z and *M. thalassica*, the level of the *ectR* transcript increased upon osmotic up-shock and a complex array of three intertwined promoters was found to direct the transcription of the *M. thalassica ectR* gene [215].

All currently available data point to the function of EctR as a repressor of ectoine biosynthesis genes. Unfortunately, the cellular or environmental cues to which this interesting regulatory protein reacts are not known. It seems possible that EctR responds to changes in the ionic/osmotic strength of the cytoplasm. Such a mechanism has been proposed for the BusR regulatory protein, which regulates the expression of an operon (*busAA-busAB*), encoding an ABC-type compatible solute import system in *Lactococcus lactis* [216,217], and for the CosR regulator controlling (among other genes) genes for ectoine biosynthesis and compatible solute import in *Vibrio cholerae* [218]. Our database searches (see Section 6.3) revealed that *ectR*-type genes are found in close proximity to *ect* biosynthetic genes in 19% (97 out of 510) of putative ectoines producers and that all of the *ectR*-harboring microorganisms belong to members of the *Alphaproteobacteria*, *Betaproteobacteria*, and *Gammaproteobacteria* (Figure 5). Previous phylogenetic analysis of EctR-type proteins conducted by Reshetnikov et al. [99] and Mustakhimov et al. [215] showed that they form a specific phylogenetic subgroup within the very large superfamily of MarR-type transcriptional regulators [214]. Like other MarR-type regulatory proteins, EctR is predicted to contain a winged-helix-turn-helix DNA-binding motive, and the EctR operator sequence in *M. alcaliphilum* 20Z, as revealed by DNA-foot-printing analysis, comprises a pseudo-palindromic highly A/T-rich DNA-sequence composed of two eight-bp half-sites separated by two bp [198,215].

In the context of discussions on the genetic control of the ectoine/5-hydroxyectoine biosynthetic genes, it is noteworthy that in *S. coelicolor*, GlnR—a major regulator for nitrogen metabolism—serves as a negative regulator for *ect* gene expression [219]. In our phylogenomic analysis (Figure 5), and in contrast to the distribution of *ectR*, we found no *glnR*- or *cosR*-type regulatory genes in close association with any ectoine/5-hydroxyectoine biosynthetic gene cluster. However, a possible genetic or physiological link of ectoine/5-hydroxyectoine biosynthesis to the overall nitrogen control in microbial cells [194] is an interesting aspect for future studies, given that ectoines are nitrogen-rich compounds (Figure 1B).

The genetic control of *ect* gene expression is embedded in the overall osmopressure adjustment response of cells using the *salt-out* strategy (Figure 1A). Frequently, the size of the ectoine/5-hydroxyectoine pool is substantially reduced when other compatible solutes (e.g., glycine betaine) are imported from the growth medium. This effect can be traced through reporter fusion studies to a dampening influence of the imported solutes on the strength of *ect* transcription [116,118,206]. However, there is also a report in the literature that claims an inducing effect of imported ectoines on the transcription of the *ectABCD* gene cluster from *Streptomyces rimosus* C-2012 under salt stress

conditions [220]. However, such an effect, to the best of our knowledge, has not been observed in any other microorganism in which the regulation of *ect* gene expression has been studied.

The dampening effect of imported compatible solutes on *ect* transcription is not unique to this particular type of promoter(s), as the activity of many osmotic stress responsive promoters is down-regulated when externally provided compatible solutes are accumulated [84,212,213]. Hence, it seems plausible that newly synthesized ectoines will influence *ect* promoter activity when the cellular pools of these compatible solutes rise in response to increased osmotic stress. This regulatory effect might provide the cell with a homeostatic system not to wastefully overproduce ectoines when it has attained osmotic equilibrium and it might be a contributing factor to the striking linear relationship between *ect* expression and the external salinity observed in several microorganisms [116,117]. It is currently not known whether the dampening effects of imported osmotic stress protectants on the strength of *ect* transcription are directly exerted via an influence on the activity of RNA-polymerase or its ability to productively interact with the *ect* promoter, or whether the effects are somehow indirectly caused by the weakened osmotic stress perceived by the microbial cell [84].

6.3. Phylogenomics of *ect* Genes

While the EctA (L-2,4-diaminobutyrate acetyltransferase) and EctB (L-2,4-diaminobutyrate transaminase) enzymes have close paralogs related in their amino acid sequences and function in microbial biosynthetic pathways not related to ectoine biosynthesis, the ectoine synthase (EctC) can be regarded as a diagnostic enzyme for ectoine producers. However, microorganisms have been discovered, which either possess EctC-related proteins but lack the *ectAB* genes or possess solitary *ectC*-type genes in addition to a canonical *ectABC* gene cluster [93,176,221]. Hence, when EctC is used as the search query to assess the phylogenomics of microbial ectoine producers, it is critical to inspect the gene neighborhood of each retrieved *ectC* hit. Likewise, *bona fide* ectoine hydroxylases (EctD) need to be distinguished from related 2-oxoglutarate-dependent dioxygenases with different enzymatic functions, as EctD proteins are often miss-annotated in genome sequences either as proline- or phytanoyl-hydroxylases. True EctD proteins (see Section 5.2.4) can be distinguished from the other members of the non-heme Fe(II)-containing and 2-oxoglutarate-dependent dioxygenase enzyme super-family [182] by a highly conserved consensus sequence motif harboring residues critical for substrate binding and enzyme catalysis [177,184].

We used the Integrated Microbial Genomes and Microbiomes (IMG/M) database of the Joint Genomics Institute (JGI) of the US Department of Energy (<http://img.jgi.doe.gov/cgi-bin/w/main.cgi>) [222] for our new database searches to identify putative producers of ectoines, since the web-tools of this Internet portal allow a simple evaluation of the gene neighborhood of the gene(s) of interest. For our analysis, we used the amino acid sequence of the EctC protein from *V. salexigens* as the search query, since this particular ectoine synthase has been intensively characterized by both enzymatic and structural approaches [93,177]. At the time of our search (13. Nov. 2017) the IMG/M database contained 56,624 bacterial and 1325 archaeal genomes; from this data set we identified 4493 bacterial and 20 archaeal EctC-type proteins. It should be noted that the IMG/M database, like other microbial genome databases, is skewed with respect to the types of microorganisms covered because sequences of certain microbial species/strains are strongly overrepresented. For instance, in the dataset of 4493 bacterial genomes containing *ectC*-type genes, 1215 *Vibrio* species/strains (with 443 *V. cholerae* strains alone) and 511 *Streptomyces* isolates are represented.

When only considering fully sequenced microbial genomes, our final dataset contained 499 bacterial and 11 archaeal species/strains that collectively possessed 582 predicted EctC-type proteins. We inspected these genome sequences for the presence of other ectoine biosynthesis related genes (*ectAB*, *ectD*, *ask_ect*, *ectR*) in the neighborhood of *ectC* or elsewhere. We retrieved the 582 EctC-related protein sequences, aligned them using the MAFFT multiple amino acid sequence alignment server (<https://mafft.cbrc.jp/alignment/server/>) [192], and then conducted a clade analysis of the putative ectoine synthase proteins using bioinformatics resources provided by the Interactive Tree of Life (iTOL software) (<https://itol.embl.de/>) [193] (Figure 5). We have rooted the EctC-protein based tree with out-group sequences of several microbial cupin-type proteins [182,183] not involved in ectoine

biosynthesis, as the EctC synthase belongs to this protein superfamily [176]. In Figure 5, we highlight not only the taxonomic affiliation of the microorganisms from which we retrieved the particular EctC sequence, but also the presence of the ectoine hydroxylase EctD [96–98], that of the specialized aspartokinases Ask_Ect [122,166,168], and that of the regulatory protein EctR [99,198,215]. Data from this analysis of the genetic configuration of ectoine/5-hydroxyectoine biosynthetic genes (*ectABC/ectD*) in 510 completely sequenced bacterial and archaeal genomes of predicted ectoine/5-hydroxyectoine producers and additional genes involved in providing the ectoine biosynthetic precursor L-aspartate- β -semialdehyde (*ask_ect*) or in the transcriptional control of *ect* gene expression (*ectR*) are summarized in Table 1.

Table 1. Analysis of the genetic neighborhood of the 582 EctC-type proteins obtained through genome database analysis.

Gene	<i>ectC</i> (in Total)	<i>ectC</i> (within <i>ect</i> Cluster)	<i>ectC</i> (Solitary)	<i>ectD</i> (within <i>ect</i> Cluster)	<i>ectD</i> (Separated from <i>ect</i> Cluster)	<i>ask_ect</i> (within <i>ect</i> Cluster)	<i>ectR</i>
Abundance	582	437	145	259	68	133	97

EctC-type proteins are phylogenetically associated with ten bacterial (including five subphyla of the *Proteobacteria*) and two archaeal phyla. In this clade analysis, EctC proteins that are encoded within true *ect* gene clusters follow, in general, the taxonomic affiliation of the predicted ectoine-producing microorganism. In those few cases where this is not the case, their position in the EctC-derived protein sequence clade can probably be explained by lateral gene transfer events (Figure 5). The EctC protein tree is dominated by ectoine synthases originating from *Actinobacteria* and from *Alphaproteobacteria*, *Betaproteobacteria*, and *Gammaproteobacteria*, which together make up 91% of our dataset. EctC proteins from members of the other EctC-containing ten bacterial phyla or subphyla (*Firmicutes*, *Delta*- and *Epsilonproteobacteria*, *Nitrospirae*, *Planctomycetes*, *Chrysiogenetes*, *Deferribacteres*, *Chloroflexi*, *Cyanobacteria*, and *Spirochaetes*) are only scarcely represented (Figure 5). Because of the existing bias of available genome sequences in databases, it is too early to conclude how much of the apparent incidence of ectoine synthesis actually differs between these phyla or arises from insufficient representation of some phyla in the IMG/M database.

Lateral gene transfer is a major driver of microbial evolution [223,224] and has in particular shaped the genome of Archaea that acquired many genes from bacterial donors [225]. This is also evident for the rare cases where EctC-type proteins have been detected in Archaea [92]. In our dataset, 11 archaeal EctC protein sequences cluster in three different locations in the tree. These genomes represent members of two archaeal phyla, the *Thaumarchaeota* and *Euryarchaeota* (Figure 5). All 11 archaeal representatives in our dataset possess a complete *ectABC* gene cluster. The EctC proteins of the three marine representatives of the *Thaumarchaeota* (all strains of *Nitrosopumilus* sp.) cluster with that of the marine bacterium *Planctomyces brasiliensis* (Figure 5). In contrast to the joint clustering of the EctC proteins from the three *Thaumarchaeota*, the eight EctC proteins from the *Euryarchaeota* are present in two different segments of the phylogenomic EctC protein tree. Three EctC proteins from various *Methanobacterium formicicum* strains are part of a cluster of EctC proteins present in strictly anaerobic members of rather heterogeneous bacterial taxa that comprise representatives of the phyla *Chrysiogenetes*, *Deferribacteres*, and *Deltaproteobacteria* (Figure 5).

In our dataset, 437 microbial genomes contained the *ectC* gene in the immediate vicinity of other *ect* genes; 76 genomes contained only *ectC* (e.g., *Pseudomonas fluorescens* L228, *Burkholderia multivorans* CEPA 002), and in 11 genomes, a complete set of ectoine biosynthetic genes was present, in addition to a single orphan *ectC* (e.g., *Rhizobium gallicum*, *Mycobacterium abscessus* FLAC 0046). Another subgroup of the inspected genomes contained several orphan *ectC* genes but no complete *ect* gene cluster (31 genomes) (e.g., *Pseudomonas syringae* pv. *syringae* B301D, *Burkholderia cepacia*). Interestingly, some bacteria contained several complete *ect* biosynthetic gene clusters (e.g., *S. reticuli*, *Streptomyces flavogriseus*, *Rhodovulum sulfidophilum* DSM 1374). From this extended phylogenomic analysis, it is apparent that the vast majority (75%) of *ectC*-containing genomes contain a complete set of ectoine biosynthetic genes. Most orphan *ectC* gene products cluster close to the root of the tree,

possibly indicating early evolutionary states (Figure 5). In a notable number of instances, microorganisms carrying both solitary *ectC* genes and additional *ect* gene clusters, or even several copies of complete *ect* gene clusters were detected. This leaves 76 genomes in our dataset, which contain exclusively solitary *ectC* genes.

Solitary *ectC* genes were first discovered in the context of a genome-driven investigation of compatible solute synthesis in the plant pathogen *Pseudomonas syringae* pv. *syringae* B728a [221]. This bacterium does not produce ectoine naturally under laboratory conditions, as it lacks the *ectAB* genes. However, when surface-sterilized leaves of its host plant *Syringa vulgaris* were added to high-salinity grown cultures, ectoine production was observed, indicating that the plant provides the substrate (*N*- γ -ADABA) (Figure 2) for the EctC ectoine synthase, and that the solitary EctC-type protein *P. syringae* pv. *syringae* B728a was functional [221]. Indeed, heterologous expression of the solitary *ectC* gene from *P. syringae* pv. *syringae* B728a in an *ectC* mutant of *H. elongata*, led to ectoine production. However, while externally provided *N*- γ -ADABA was readily imported by *P. syringae* pv. *syringae* B728a, the expected ectoine formation was not observed [221]. Hence, this dataset is, in its core, not yet conclusive. Previous database searches have already indicated that the existence of solitary EctC-type proteins is not an isolated incident in *P. syringae* pv. *syringae* B728a [92,176]; we detected their presence in 13% out of the studied 457 genomes (Table 1).

EctC-type proteins can be assigned to six major clusters of sequence similarity. The three most basal of these clusters contain most of the proteins from orphan *ectC* genes, while the three others contain all EctC proteins encoded by *ect* gene clusters and only a few by isolated genes (Figure 5). The most basal major cluster (group 1) exclusively represents EctC-like proteins from various strains of *M. abscessus*, which may not be true ectoine synthases because the same strains also contain paralogs of more conventional EctC proteins. The next two major clusters (groups 2 and 3) correspond to most other organisms containing orphan *ectC* genes and comprise mostly members of the *Alphaproteobacteria*, notable groups of *Actinobacteria*, *Betaproteobacteria* and *Gammaproteobacteria*, together with two strains affiliated with the *Cyanobacteria* and two with the *Deltaproteobacteria* (Figure 5). It is currently not clear whether the solitary EctC proteins are remnants of a previously intact ectoine biosynthetic route, whether they were recruited by the EctAB proteins to form the ectoine biosynthetic pathway as we know it today (Figure 2), or whether they have evolved a new enzymatic function that nevertheless might allow in a side-reaction the cyclization of the *N*- γ -ADABA molecule to ectoine. However, the placement of the orphan EctC protein from *P. syringae* [221] in group 2 (Figure 5) suggests that these proteins might represent catalytically competent ectoine synthases. Still, careful genetic and biochemical analysis will be required in the future to establish the true function of these solitary EctC-type proteins.

The major group 4 contains mainly EctC proteins from *Firmicutes*, marine *Gamma*- and *Betaproteobacteria*, together with rare orthologs from the *Planctomycetes*, *Spirochaetes*, *Delta*- and *Epsilonproteobacteria*, *Chrysiogenetes*, *Chloroflexi*, *Deferribacteres* and two archaeal groups comprising the *Nitrosopumilus* and *Methanobacterium* strains. Group 5 contains the proteins from mostly marine *Alphaproteobacteria*, *Betaproteobacteria* and *Gammaproteobacteria*, including many members of the *Roseobacteriales*, *Halomonadales* and *Vibrionales*, together with one spirochaete, one sulfate-reducing *Deltaproteobacterium*, three *Leptospirillum* strains affiliated to the *Nitrospirae* and the remaining *ect* gene clusters containing archaeal species representing five members of the *Methanosarcinales*. Finally, group 6 represents exclusively terrestrial *Actinobacteria*, with the exception of one basal EctC sequence from a strain of the alphaproteobacterium *R. gallicum* (Figure 5).

The formation of 5-hydroxyectoine depends on the prior synthesis of ectoine and is catalyzed in a position- and stereo-specific reaction by the ectoine hydroxylase (EctD) [98,177]. The *ectD* gene can be found in one of two different genetic contexts: (i) it either can be present in the vicinity of other *ect* biosynthetic genes, or (ii) it can be encoded somewhere else in the genome of a predicted ectoine producer [96–98]. In our dataset of 510 predicted ectoine producers, 314 (62%) possess an *ectD* gene; in 259 genomes, *ectD* is part of the biosynthetic gene cluster, and 68 *ectD* genes are found outside of the *ect* gene cluster (Figures 4 and 5). Some organisms (20 genome sequences) possess an external *ectD* gene, in addition to the *ectD* gene encoded in the *ect* gene cluster. Since the EctD enzyme is a

member of the non-heme-containing, iron(II)- and 2-oxoglutarate-dependent dioxygenase enzyme superfamily [177,185], all predicted 5-hydroxyectoine producers are either aerobic or, at least, oxygen-tolerant microorganisms. This can be nicely observed in those Archaea that are predicted to synthesize ectoine either alone or in combination with 5-hydroxyectoine. In the strictly anaerobic methanogenic Archaea belonging to the genera *Methanosaeta* and *Metanobacterium*, only an *ectABC* cluster can be found, while in the oxygen-dependent nitrifying Archaea of the genus *Nitrosopumilus*, *ectABCD* gene clusters are present [92] (Figure 5).

As outlined above, some *ectABC(D)* gene clusters are associated with a gene (*ask_ect*) encoding a specialized aspartokinase [122,166–168]. We assessed the phylogenetic occurrence of the Ask_Ect (Figure 5) and the genetic organization of its structural gene within the context of the *ect* biosynthetic genes (Figure 4). In our dataset of 510 putative producers of ectoines, 133 ectoine/5-hydroxyectoine biosynthetic gene clusters contained the gene for the specialized aspartokinase. These gene clusters are primarily found in *Alphaproteobacteria* and *Gammaproteobacteria* (Figure 5).

Ectoine producers can populate ecological niches with rather different attributes. This is actually not surprising, because microorganisms will experience increases in the environmental osmolarity not only in marine and high-saline surroundings (e.g., open ocean waters, marine sediments, salterns, brines), but also, for instance, when the soil slowly dries out. If one views the putative ectoine/5-hydroxyectoine producers in an ecophysiological context, many marine and terrestrial microorganisms are represented, as are some bacteria that live associated with plants or animals. Among the latter group of microbes, bacteria are found that are beneficial to plant growth (e.g., many *Rhizobium*, *Sinorhizobium* or *Bradyrhizobium* strains), others are formidable plant pathogens (e.g., many *Pseudomonas syringae* pathovars). Likewise, some of the putative ectoine/5-hydroxyectoine producers are human or animal pathogens (e.g., *V. cholerae*, *M. abscessus*, *B. cepacia*, *B. paraptentis*, or *Bordetella bronchiseptica*). Some ectoine producers are also found among microorganisms that live in rather specialized habitats. A striking example is the gammaproteobacterium *Teredinibacter turnerae*, an intracellular endosymbiont in the gills of *Lyrodus pedicellatus*, commonly known as shipworms. This mollusk digests wood immersed in salt water, a catabolic process that relies on cellulases produced by *T. turnerae* [226]. Interestingly, ectoine/5-hydroxyectoine producers are also found in a few representatives of the phylogenetically deep-branching phylum *Planctomycetes*, microorganisms with highly interesting cell biology that are widely distributed in marine and terrestrial habitats. Physiological studies with slight halophilic representative of the genus *Planctomyces*, *P. brasiliensis* (recently re-classified as *Rubinisphaera brasiliensis*) and *Planctomyces maris* (recently re-classified as *Gimesia maris*) showed that ectoine and 5-hydroxyectoine play major roles in osmotic stress adaptation [227]. Attesting to the metabolic flexibility of these microorganisms under severe osmotic stress conditions, non-nitrogen-containing compatible solutes (e.g., sucrose and glucosylglycerate) are produced when nitrogen becomes limiting [227].

Ectoine/5-hydroxyectoine producers are also found in ecosystems whose salinity is not particularly high; one example is *A. cryptum*, a heterotrophic alphaproteobacterium that thrives in acidic, metal-rich environments, but which is not known to tolerate high concentrations of salt [180]. One also needs to keep in mind that taxonomically closely related microorganisms can rely, as far as the accumulation of ectoines is concerned, on the accumulation of different types of compatible solutes. This is exemplified by studies with the marine predatory heterotrophic myxobacteria *Enhygromyxa salina* SWB007 and *Plesiocystis pacifica* SIR-1 [228]. While *P. pacifica* SIR-1 relied on the accumulation of amino acids for its osmotic stress adjustment process, *E. salina* SWB007 employed, besides glycine betaine, 5-hydroxyectoine as its dominant compatible solute under high-salinity growth conditions. Accordingly, no ectoine/5-hydroxyectoine biosynthetic genes were found in the genome sequence of *P. pacifica* SIR-1, while an *ect_ask-ectABCD* gene cluster was present in the genome sequence of *E. salina* SWB007. This ectoine/5-hydroxyectoine biosynthetic gene cluster is also associated with a copy of the *ectR* regulatory gene [228].

While the *ect* genes are widely distributed in ecophysiological different types of microorganisms, there is evidence in certain groups of ectoine/5-hydroxyectoine producers for ecotype diversification. For instance, ectoine/5-hydroxyectoine biosynthetic genes were found not

only in the archaeon *N. maritimus* strain SCM1 [92] but are also present in the draft genomes of halotolerant *Nitrosopumilus* species populating brine-seawater interfaces, whereas they are not present in genomes of *Nitrosopumilus* species enriched from low-salinity estuary and coastal environments [229]. The clearest evidence reported to date for an association of ectoine biosynthesis with microbial niche diversification stems from a comprehensive phylogenomic analysis of *Rhodobacteraceae* [230]. These *Alphaproteobacteria* are metabolically highly versatile and are key players in global biogeochemical cycling [231,232]. Based upon the analysis of 106 genome sequences, Simon et al. [230] found that during the evolution of this group of microorganisms several shifts between marine and non-marine habitats occurred and signature changes in genomic content reflect the different ecosystem populated by members of the *Rhodobacteraceae*. During this process, marine *Rhodobacteraceae* gained the genes for ectoine synthesis and that for the production of the compatible solute carnitine, and they also acquired the ability to import this latter osmoprotectant [230]. In a study addressing the phylogeny of the ectoine biosynthetic genes in aerobic, moderate halophilic methylotrophic bacteria, Reshetnikov et al. [99] found that the amino acid sequence relationship of the ectoine biosynthetic proteins did not strictly correlate with the phylogenetic affiliation of the studied methylotrophic species and strains, thereby suggesting that the ability to synthesize ectoine most likely results from lateral gene transfer events. Such gene transfer events are clearly manifested when one views the position of the EctC proteins from Archaea within the clade analysis of ectoine synthases present in Bacteria (Figure 5) [92].

7. Scavenging Ectoines as Stress Protectants from Environmental Sources

Ectoines are produced and accumulated in high-osmolarity-stressed microorganisms to exceedingly high cellular levels [91,94]. They are released from these producers through the transient opening of mechanosensitive channels during osmotic down-shocks, through secretion, by decomposing microbial cells attacked by phages or toxins, or through the predatory activity of microorganisms and eukaryotic cells [233]. Hence, it is not surprising that environmentally compatible solutes, including ectoines, have been detected in different ecosystems [234–239]. As a result, the presence of cell-free ectoines provides new opportunities for microorganisms living in the same habitat as the ectoine producers by allowing them to ameliorate osmotic or temperature stress through import of these compatible solutes.

Transport systems for compatible solutes are ubiquitous in microorganisms, and these are typically osmotically regulated both at the level of transport activity and in the transcriptional response of their structural genes [2,6,10,240–242]. The activity regulation of osmolyte transporters provides the cell with a practically instantaneous adjustment response to osmotic up-shift [240,242–246] that, depending on the severity, can strongly impair growth [247]. The transcriptional induction of the transporter genes will then provide enhanced transport capacity for osmoprotectants to permit growth under sustained osmotically unfavorable conditions [2,84,85]. Hence, uptake systems for compatible solutes [1–3,241], or for their biosynthetic precursors (e.g., choline for the synthesis of glycine betaine) [171,248], are integral parts of the overall osmoprotectant adjustment strategy of many microbial cells (Figure 1A). They typically possess K_m values in the low μM range, thereby allowing the recovery of stress protective solutes from scarce environmental sources. Often, a given microbial cell possesses several osmoprotectant uptake systems, which frequently differ in their substrate profile and mode in which the transport process is energized [10,84,85,240,249], thereby providing additional flexibility to the osmotically challenged cell.

Ectoine/5-hydroxyectoine transport systems involved in alleviating osmotic or temperature stress have been characterized in various Gram-negative and Gram-positive bacteria. These importers belong to four different transporter families: (i) binding protein-dependent ABC transporters [250,251] that use ATP to fuel substrate translocation across the cytoplasmic membrane (e.g., the ProU system from *E. coli*, the OusB system from *Erwinia chrysanthemi*, the OpuC transporter from *B. subtilis* and the ProU system from *Vibrio anguillarum*) [121,187,252,253], (ii) members of the Major Facilitator Family (MFS) [254] that are dependent on the proton motive force (e.g., the ProP and OusA system from *E. coli* and *E. chrysanthemi*, respectively) [243,255], (iii) members of the Betaine-

Choline-Carnitine Transporters (BCCT) [241] that are energized either by proton or sodium gradients (e.g., the OpuD transporter from *B. subtilis*, EctT from *V. parvithenticus*, EctM from *M. halophilus*, EctP and LcoP from *C. glutamicum*) [78,256–259], and (iv) members of the periplasmic binding protein-dependent tripartite ATP independent periplasmic transporter family (TRAP-T) [160] that are energized by proton or sodium gradients (e.g., the TeaABC system from *H. elongata*) [161]. Often, transporters used for the import of ectoines exhibit broad substrate specificity (e.g., the ProU and ProP systems from *E. coli* and the OpuC transporter from *B. subtilis*) [84,85,188,189], but dedicated importers for these compounds are also known (e.g., the TeaABC system from *H. elongata* and the EctT transporter from *V. parvithenticus*) [78,161].

In the context of osmotic stress-responsive transporters for ectoine/5-hydroxyectoine, it is important to note that some compatible solute transporters (e.g., BCCT- and TRAP-types) import substantial amounts of Na⁺ into the cell, along with the stress-relieving substrate. For instance, the glycine betaine transporter BetP from *C. glutamicum*, the biochemically and structurally best-studied transporter of the BCCT family [241], to which the ectoine/5-hydroxyectoine transporter EctT, EctM, EctP, and LcoP also belong [78,257–259], has a stoichiometry of two Na⁺ ions per imported glycine betaine molecule [241,245,246,260]. Since substantial compatible solute pools are generated through transport, effective export systems for the co-transported cytotoxic Na⁺ ions are key players in the overall osmotic stress adjustment strategy of microorganisms using the *salt-out* strategy (Figure 1A).

High-resolution crystal structures of the TeaA periplasmic ligand-binding protein, in complex with either ectoine (PDB accession code 2VPN) or 5-hydroxyectoine (PDB accession code 2VPO), have been determined [261]. The crystal structure of another ectoine-binding protein (OpuCC) (PDB accession code 3PPR) has also been reported [262]. OpuCC is the extracellular solute receptor of the promiscuous, osmotically inducible OpuC ABC transporter from *B. subtilis* [84,85]. In contrast to the high affinity TeaABC system [261], OpuC imports ectoine only in a side reaction (the *K_i* of ectoine import via OpuC is about 1.5 mM) [252] and thus will not play a decisive role for ectoine import in natural settings of *B. subtilis* where ectoines will only be present in very low concentrations [234–237].

8. Ectoines as Nutrients

8.1. Physiology

A hallmark of microorganisms is their enormous metabolic potential. There is essentially no compound synthesized by microorganisms that cannot be catabolized, either by the producer cell itself or by other microorganisms living in the same habitat. This is also true for the nitrogen-rich ectoine/5-hydroxyectoine molecules (Figure 1B); their use as sole carbon, nitrogen and energy sources has been demonstrated for different microbial species [74,158,190,263–266]. Environmental ectoines have been detected in various ecosystems [234–237,239], and their presence provides new opportunities for microbial ectoine consumers living in habitats that are also populated by ectoine producers. Ectoine-catabolizing microorganisms can scavenge these valuable compounds from the environment through high-affinity, substrate-induced transport systems such as the ABC-system EhuABCD or the TRAP transporter UehABC [263,265,267,268]. Since ectoines are unlikely to be continuously present in a given habitat, it makes physiologically sense for nutrient-limited microorganisms to exert a tight transcriptional control over ectoine/5-hydroxyectoine importer and catabolic genes. We will address below the taxonomic affiliation of ectoine consumers, the catabolic route for ectoines, transport systems for their acquisition, and the genetics underlying the transcriptional control of ectoine/5-hydroxyectoine import and degradation gene clusters.

8.2. Genetics and Phylogenomics of Ectoine Catabolic Genes

While the use of ectoines as nutrients has been known about for quite some time [74,190,263–266], inroads into a molecular and biochemical understanding of ectoine/5-hydroxyectoine catabolism have only been made recently. In a pioneering study, Jebbar et al. [265] used a proteomics approach to identify proteins induced in cells of the symbiotic plant-root-associated soil bacterium *Sinorhizobium meliloti* grown in the presence of ectoine. The protein products of eight ectoine-induced

genes were identified by mass-spectrometry, and their genes co-localized in the same gene cluster together with several other genes whose products had not been detected by proteomics (Figure 6A) [265]. This gene cluster is carried by the pSymB mega-plasmid of *S. meliloti*. Four of the nine ectoine-inducible genes encode the components of a binding-protein-dependent ABC-transporter (EhuABCD; *ehu*: ectoine-hydroxyectoine-uptake) and form an operon with five additional genes (*eutABCDE*; *eut*: ectoine utilization) predicted to encode enzymes for ectoine/5-hydroxyectoine catabolism. The entire *ehuABCD-eutABCDE* gene cluster is preceded by a gene encoding a member of the GntR superfamily of transcriptional regulators [269] (Figure 6A), a regulatory gene that is now known as *enuR* (ectoine nutrient regulator) [270]. Divergently oriented from the *S. meliloti* *ehuABCD-eutABCDE* operon was an additional regulatory gene (*asnC*) encoding a member of the AsnC/Lrp family of the feast-and-famine DNA-binding proteins [271–273] and three ectoine-inducible genes functionally annotated as an aminotransferase, an oxidoreductase, and a succinate semialdehyde dehydrogenase (Figure 6A) [265]. Using an *ehuAB-uidA* transcriptional reporter system, enhanced expression of the reporter fusion was observed when either ectoine or 5-hydroxyectoine was present in the growth medium, but neither glycine betaine nor high salinity triggered enhanced gene expression [265]. Hence, the *ehuABCD-eutABCDE* operon is substrate inducible, as expected for a catabolic system. Building on these findings in *S. meliloti* [265], related ectoine/5-hydroxyectoine import and catabolic gene clusters were identified and experimentally studied in *H. elongata* [158] and the marine bacterium *Ruegeria pomeroyi* DSS-3 [263]. For *H. elongata* [158], a genetic nomenclature different from those used for the annotation of the ectoine/5-hydroxyectoine catabolic genes in *S. meliloti* and *R. pomeroyi* was used; in Figure 6A we have compared the corresponding gene organization in these three organisms to minimize confusion that can be caused by the different annotation of the *H. elongata* genes.

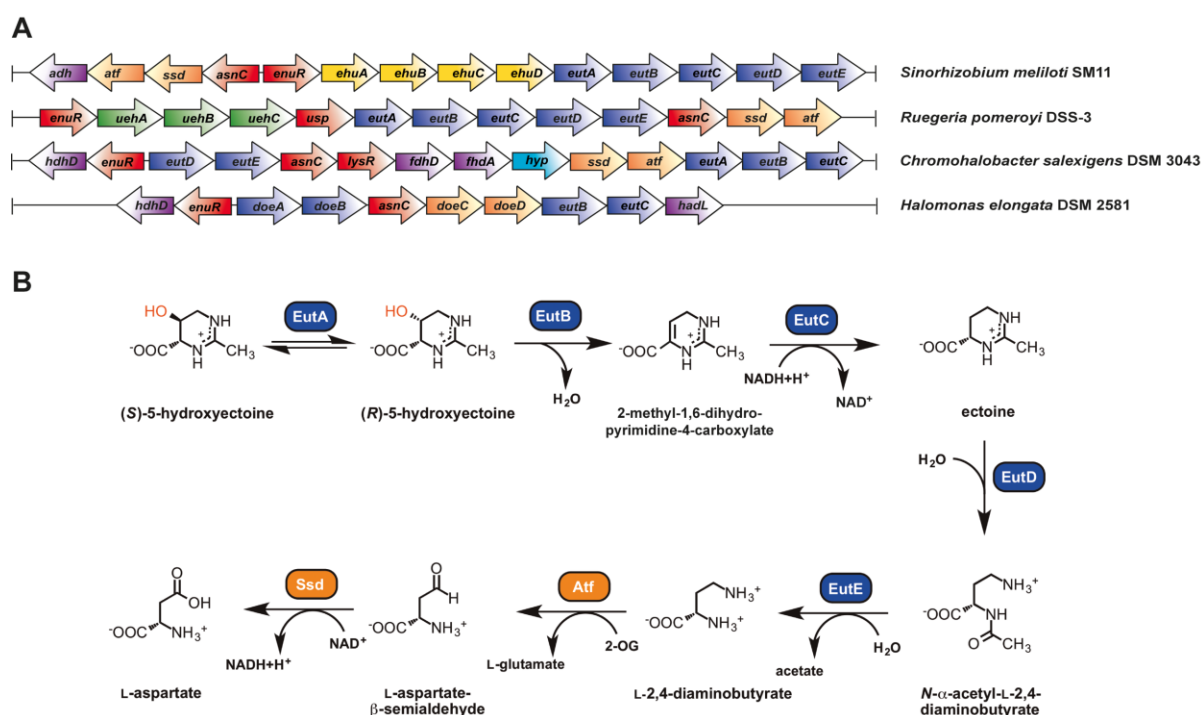


Figure 6. Genetics and catabolic pathways for the utilization of ectoine and 5-hydroxyectoine as nutrients. (A) Genetic organization of the ectoine/5-hydroxyectoine-catabolic gene cluster in *Sinorhizobium meliloti* SM11 [265], *Ruegeria pomeroyi* DSS-3 [263,270], *Halomonas elongata* DSM 258 [158] and *Chromohalobacter salexigens* DSM 3043 (predicted from the genome sequence) [274]. In addition to the transporter and catabolic genes discussed in the main text, some of these gene clusters contain genes with yet undefined roles in ectoine catabolism. Their gene products have bioinformatically predicted functions as alcohol dehydrogenase (*adh*), hydroxyacid dehydrogenase (*hdhD*), formate dehydrogenases (*fdhD*, *fdhA*), haloacid dehalogenase (*hadL*), transcriptional regulator (*lysR*) and a hypothetical protein (*hyp*). (B) Predicted pathway for the catabolism of ectoine and its derivative 5-

hydroxyectoine in *R. pomeroyi* DSS-3. The EutABC-enzymes are predicted to convert 5-hydroxyectoine in a three-step reaction into ectoine. The ectoine ring is subsequently hydrolyzed by the EutD enzyme, resulting in the production of *N*- α -ADABA, an intermediate, which is then further catabolized to L-aspartate by the EutE, Atf and Ssd enzymes. These data were compiled from the literature [158,263,270]. The ectoine-derived metabolites *N*- α -ADABA and L-2,4-diaminobutyrate (DABA) serve as inducers for the transcriptional control of the ectoine/5-hydroxyectoine import and catabolic gene clusters by the EnuR regulatory protein [270].

In this figure, we have also included the genetic organization of the ectoine catabolic genes from *C. salexigens*, a gammaproteobacterium taxonomically closely related to *H. elongata*, in which ectoine/5-hydroxyectoine synthesis has been studied in quite some detail [80,194] and in which catabolism of these compounds has also been physiologically assessed [266]. An inspection of the ectoine/5-hydroxyectoine catabolic and importer gene clusters from these four organisms reveals a considerable variation in genetic organization and gene content (Figure 6A). For instance, while the *S. meliloti* gene cluster encodes an ABC import system (EhuABCD) for ectoines [265,267], that of *R. pomeroyi* DSS-3 possesses a TRAP transporter (UehABC) for their uptake [263,268]. In contrast, the *H. elongata* and *C. salexigens* catabolic gene clusters lack genes for an import system for ectoines altogether (Figure 6A), but they both possess genes for UehABC-related ectoine/5-hydroxyectoine-specific import systems (TeaABC) [161,261] somewhere else in their genomes [263,270]. It is, however, not clear whether the TeaABC transporter serves for the acquisition of ectoines as nutrients since the transcription of the *teaABC* operon is osmotically inducible in *H. elongata* [161].

Using the ectoine hydrolase (EutD), a key enzyme of ectoine catabolism (Figure 6B) [158,263], as a search query for the analysis of 32,523 bacterial and 654 archaeal genomes, 539 EutD orthologues were found [263]. Inspection of the *eutD* gene neighborhoods then revealed a diverse genetic organization and gene content of the ectoine/5-hydroxyectoine import and catabolic gene clusters on a broad scale [158,263]. This stands in contrast to the rather stable and evolutionarily conserved genetic organization of the ectoine/5-hydroxyectoine biosynthetic genes as an *ectABC/ectD*-type operon (Figure 4A). Strikingly, while microbial ectoine/5-hydroxyectoine producers can be found in ten bacterial and two archaeal phyla (Figure 5), ectoine consumers are taxonomically restricted to the phylum of *Proteobacteria* [263]. In the particular dataset of the 539 *eutD*-containing microbial genomes inspected by Schulz et al. [263], 58% belong to the *Alphaproteobacteria*, 15% were from *Betaproteobacteria*, 27% were from *Gammaproteobacteria*, and there was only a single representative (*Desulfovibrio bastinii* DSM 16055) from the *Deltaproteobacteria*.

Interestingly, among the 539 predicted ectoine/5-hydroxyectoine consumers, 100 microorganisms are predicted to synthesize ectoines as well [263]. The simultaneous presence of ectoine/5-hydroxyectoine biosynthetic and catabolic genes in a given microorganism will require a careful genetic and physiological wiring of these physiologically and biochemically conflicting processes (see Section 7.5) in order to avoid a futile cycle (see Section 7.5). One of the organisms capable of ectoine synthesis and degradation is *H. elongata*, and in the context of its genome annotation and analysis of ectoine synthesis and catabolism, Schwibbert et al. [158] suggested that the ability to both synthesize and degrade ectoines might aid the *H. elongata* cell to physiologically navigate osmotic downshifts. If this hypothesis holds true, then it can only apply to situations where the environmental osmolarity is decreased rather slowly, since mechanosensitive channels (genes for these safety-valves are present in *H. elongata*) (Figure 1A) will otherwise open within milliseconds during harsh osmotic downshifts to reduce the ectoine pool rapidly [11]. Furthermore, Schwibbert et al. [158] calculated that a futile cycle of simultaneous synthesis and degradation of ectoine would saddle the metabolism of *H. elongata* under already energetically and physiologically challenging osmotic conditions [37,106,197] with the expenditure of two additional ATP molecules per turn of ectoine synthesis. Microorganisms capable of both ectoine synthesis and catabolism are quite prevalent in nature; in the dataset of Schulz et al. [263], about 19% of ectoine/5-hydroxyectoine producers were also able to degrade these compounds. It will thus be of considerable interest to learn in future studies how these types of microbes can avoid wasteful futile cycles under steady-state high osmolarity growth conditions.

8.3. Transporters for the Scavenging of Ectoines for Their Use as Nutrients

Ectoines present in the environment occur at very low concentrations [234–239]; hence, high-affinity transporters are required for their recovery and use as nutrients. The EhuABCD ABC transporter from *S. meliloti* and the UehABC TRAP transporter from *R. pomeroyi* are uptake systems whose main function is the scavenging of ectoines for nutritional purposes [263,265,267,268]. The transcription of the underlying structural genes is substrate inducible, but they are not osmotically induced. Although the Ehu and Ueh systems belong to different transporter families (ABC and TRAP transporters, respectively) [160,250,251], they are both dependent on a periplasmic substrate-binding protein (EhuB and UehA, respectively) [267,268]. These binding proteins trap ectoines that have passed the outer membrane via passive diffusion (probably via general porins) with high affinity in the periplasm and deliver them to the core components of the Ehu and Ueh transporters present in the inner membrane for energy-dependent translocation into the cytoplasm. Ligand-binding studies with the purified EhuB and UehA proteins revealed their high affinity for ectoine and 5-hydroxyectoine; EhuB has apparent K_d values of 1.6 μM for ectoine and 0.5 μM for 5-hydroxyectoine [265,267], while UehA exhibits apparent K_d values of 1.4 μM for ectoine and 1.1 μM for 5-hydroxyectoine [268]. Crystallographic studies of the EhuB (PDB accession codes 2Q88 and 2Q89) [267] and UehA (PDB accession code 3FXB) [268] proteins in complex with ectoines revealed the details of the architecture of a ligand-binding site for these compatible solutes, thereby providing further insights into the structural principles of substrate recognition and binding of organic osmolytes that are preferentially excluded from protein surfaces [60–62].

Similar design principles for trapping the ectoine ligand were observed in the crystal structure of the binding protein (TeaA) of the TeaABC TRAP transporter from *H. elongata* [261], a system that primarily serves for the acquisition of ectoines when they are used as osmoprotectants and as a recovery system for newly synthesized ectoines that are leaked or actively excreted from the *H. elongata* producer cell [161]. Crystal structures of the TeaA protein in complex with either ectoine (PDB accession code 2VPN) or 5-hydroxyectoine (PDB accession code 2VPO) have been determined [261]. This protein has K_d values of 0.2 μM for ectoine and 3.8 μM for 5-hydroxyectoine, respectively [261]. Interestingly, the crystal structures of the UehA and TeaA ligand-binding sites are virtually superimposable [261,268], despite the fact that the TeaABC and UehABC TRAP-type transporters serve different physiological functions. Hence, nature has taken a proven transporter module for the import of ectoines and endowed the transcription of the underlying structural genes with regulatory patterns that allow the transporter either to serve in osmoprotection (TeaABC) [161], or to enable the feeding on ectoines (UehABC) [263,270].

As indicated above, the TeaABC-type transporter might not only serve in osmoprotection, but might also function in the acquisition of ectoines as nutrients. While genes for Ehu-type (370 genomes out of a dataset of 539 ectoine degraders) and Ueh-type (48 genomes out of a dataset of 539 ectoine degraders) transporters are widely affiliated with the corresponding catabolic gene clusters, there is a substantial group of ectoine consumers (122 representatives) that lack transporter genes in the immediate vicinity of the catabolic gene cluster [263]. Since ectoines need to be imported before they can be consumed, it is obvious that transporter genes for these compounds must be encoded somewhere else in the genomes. Perhaps additional transporters for the acquisition of ectoines as nutrients might await discovery. Notably, a sub-group (23 representatives) of predicted ectoine consumers lacking genes for transporters in the vicinity of the catabolic genes possesses genes for TeaABC-type transporters somewhere else in their genome sequence [263], and *H. elongata* is a representative of this group [158,161]. Because mutants with inactivated *ectABC* and *teaABC* genes are available [94,158,161], *H. elongata* would be well-suited to testing the idea [263] that the osmoregulated TeaABC-type transporter might also be involved in the uptake of ectoines when these are consumed.

8.4. Biochemistry of Ectoine/5-Hydroxyectoine Catabolism

Building on the data reported by Jebbar et al. [265] on the identification of ectoine-inducible proteins in *S. meliloti*, Schwibbert et al. [158] made the first concrete proposal for the degradation pathway of ectoine using the blueprint of the *H. elongata* genome sequence. According to this

proposal, ectoine degradation begins with the enzymatic opening of the ectoine ring by the ectoine hydrolase (DoeA/EutD; EC 3.5.4.44) to form *N*- α -acetyl-L-2,4-diaminobutyrate (*N*- α -ADABA) as a key intermediate which is further catabolized by the *N*- α -acetyl-L-2,4-diaminobutyrate deacetylase (DoeB/EutE; EC 3.5.1.125) to acetate and DABA. The DoeD/Atf enzyme then converts DABA to L-aspartate- β -semialdehyde and L-glutamate by a transamination reaction; this enzyme belongs to the family of acetyl ornithine aminotransferases. The DoeC/Ssd enzyme then further oxidizes the L-aspartate- β -semialdehyde formed by the DoeD/Atf enzyme to L-aspartate, an important intermediate in central metabolism; the DoeC/Ssd protein is an enzyme related to known succinate semialdehyde dehydrogenases (Figure 6B). Notably, this proposal for ectoine catabolism [158,263] traces the ectoine biosynthetic route (Figure 2) backwards but the types of enzymes involved in the anabolic and catabolic routes are obviously different.

Heterologous expression of the *H. elongata* ectoine hydrolase (DoeA/EutD) in *E. coli* showed that it converts ectoine into both the α - and γ -isomers of ADABA in a 2:1 ratio [158], with *N*- γ -ADABA being the main substrate for the ectoine synthase EctC (Figure 2). Since *N*- γ -ADABA does not seem to be a substrate for the DoeB/EutE enzyme (Figure 6B) [158], it is currently not clear if the formation of *N*- α -ADABA and *N*- γ -ADABA by the ectoine hydrolase (DoeA/EutD) is a specific feature of those microorganisms capable of both synthesizing and catabolizing ectoine (note that *H. elongata* possesses both pathways [158]). Otherwise the formation of *N*- γ -ADABA by the ectoine hydrolase could be rather wasteful, unless the EutE enzyme (Figure 6B) is able to transform both *N*- α -ADABA and *N*- γ -ADABA into DABA.

Examining the ectoine/5-hydroxyectoine catabolic pathway in *R. pomeroyi* DSS-3, Schulz et al. [263] concurred with the proposal by Schwibbert et al. [158] with respect to the degradation route of ectoine to L-aspartate, but they additionally made a proposal for the conversion of 5-hydroxyectoine into ectoine. The removal of the 5-hydroxyl group from the ectoine ring is envisioned as a three-step enzymatic process that involves the EutABC proteins (Figure 6B). The first step in this reaction is the steric inversion of the hydroxy group by the racemase EutA, converting the native (*S*)-5-hydroxyectoine conformation to the (*R*)-5-hydroxyectoine enantiomer to fit the stereochemical requirements of the next enzyme, EutB (Figure 6B). The EutB enzyme belongs to the family of threonine dehydratases and might be a pyridoxal-5'-phosphate (PLP) dependent enzyme which eliminates a water molecule from the 5-(*R*)-hydroxyectoine enantiomer. The predicted reaction product of EutB is 2-methyl-1,6-dihydropyrimidine-4-carboxylate, which is proposed to be reduced to ectoine by the EutC enzyme, a protein that is thought to serve in a NADH-dependent reduction as an ectoine dehydrogenase (Figure 6B) [263].

We stress here that the envisioned conversion of 5-hydroxyectoine to ectoine and its further catabolism to L-aspartate as suggested by Schwibbert et al. [158] and Schulz et al. [263] have not been biochemically evaluated, with the exception of the preliminary assessment of the opening of the ectoine ring by the ectoine hydrolase from *H. elongata* in cells of a heterologous host bacterium [158]. Furthermore, the rather varied gene content of ectoine/5-hydroxyectoine catabolic gene clusters (Figure 6A) [158,263] suggests that variations of the 5-hydroxyectoine to ectoine to L-aspartate catabolic route are likely to exist in microorganisms. In particular, many of these gene clusters lack a homolog of the *eutA* gene. It is also possible that some microorganisms can catabolize ectoine, but cannot use 5-hydroxyectoine as a nutrient, as suggested by the inspection of the gene content of a substantial number of ectoine catabolic gene clusters [263].

8.5. Genetic Regulation of Ectoine/5-Hydroxyectoine Catabolism

As expected for a catabolic system, the ectoine/5-hydroxyectoine import and catabolic gene clusters of *S. meliloti* and of *R. pomeroyi* DSS-3 are substrate inducible [263,265,268,270]. Detailed genetic studies with this system in *R. pomeroyi* DSS-3 revealed that an external supply of either ectoine or 5-hydroxyectoine triggers enhanced import of these compounds and strongly increases the transcription of the *uehABC-usp-eutABCDE-asnC-ssd-atf* gene cluster, forming a 13.5 Kbp polycistronic mRNA [268,270]. However, neither ectoine nor 5-hydroxyectoine serve as the true inducers for the de-repression of the transcription of this operon; instead two intermediates in ectoine

catabolism, *N*- α -ADABA and DABA (Figure 6B), serve as the physiologically relevant inducers [270]. These compounds are recognized by EnuR, a member of the MocR/GabR sub-group of the large GntR superfamily of transcriptional regulators [275,276]. The *enuR* structural gene (*enuR*: ectoine nutrient utilization regulator) is positioned upstream of the *uehABC-usp-eutABCDE-asnC-ssd-atf* gene cluster (Figure 6A) and is expressed from a separate non-ectoine responsive promoter in *R. pomeroyi* DSS-3 [270]. This situation is apparently different from that observed in *S. meliloti* where substrate induction of *enuR* transcription was reported [277]. The EnuR protein appears to play an important role in controlling the transcription of ectoine/5-hydroxyectoine import and catabolic gene clusters in many microorganisms. In the dataset of 539 putative microbial ectoine consumers analyzed by Schulz et al. [270], 456 ectoine/5-hydroxyectoine catabolic gene clusters were associated with an *enuR* gene.

MocR/GabR-type transcriptional regulators are widely distributed in microorganisms [275,276], but are clearly an understudied sub-group of the GntR super-family [269]. The best-studied representative of the MocR/GabR group is the GabR regulator from *B. subtilis* that serves to control genes involved in the metabolism of γ -aminobutyrate (GABA) [278]. The GabR protein is a head-to-tail swapped dimer with an N-terminal DNA reading head containing a winged helix-turn-helix DNA binding motif that is connected via a long flexible linker region to a large carboxy-terminal effector binding/dimerization domain [279]. This latter domain, structurally related to aminotransferases of type-1 fold, contains a covalently bound PLP molecule. However, the C-terminal domain of GabR does not perform a full aminotransferase reaction; instead, a partial aminotransferase reaction occurs [279–283]. In this chemical sequence of events, the co-factor PLP binds to the side-chain of a particular Lys residue of GabR, yielding a Schiff base and thereby resulting in the formation of an internal aldimine [173]. Subsequently, the system-specific low-molecular mass effector molecule GABA binds to the PLP molecule, which then leads to the detachment of the PLP molecule from the Lys residue of GabR and the formation of an PLP:GABA complex, the external aldimine [173,279–282]. This sequence of events triggers a conformational change of the GabR dimer [279,282], which in turn dictates the DNA-binding activity of the regulatory protein to function either as an activator of the *gabTD* metabolic operon, or as a repressor of its own structural gene (*gabR*) [278].

A homology model of the EnuR dimer based on the crystal structure from the *B. subtilis* GabR regulatory protein [279] is shown in Figure 7A. The EnuR protein from *R. pomeroyi* DSS-3, as heterologously produced (in *E. coli*) and purified by affinity chromatography, has a striking yellow color [263] and possesses spectroscopic properties resembling those of PLP-containing enzymes [173,284,285]. Modeling studies identified Lys³⁰² in the EnuR aminotransferase domain as the PLP-binding residue. Its substitution by a His residue (EnuR*) via site-directed mutagenesis leads to loss of the yellow color exhibited by the EnuR wild-type protein in solution and alters its authentic spectroscopic properties. When the *enuR** gene was expressed in a *R. pomeroyi* DSS-3 wild-type strain (*enuR*⁺), the EnuR* protein conferred a dominant negative phenotype. In other words: the EnuR* protein abrogated the ability of *R. pomeroyi* DSS-3 to use ectoines as nutrients, since its DNA-binding to the cognate operator sequence cannot be relieved in vivo [270]. These combined genetic and biochemical data unambiguously show that the PLP molecule covalently attached to Lys³⁰² is critical for the regulatory function of EnuR. EnuR acts as a repressor for the ectoine/5-hydroxyectoine uptake and catabolic genes of *R. pomeroyi* DSS-3 and *S. meliloti* since an *enuR* gene disruption mutation leads to de-repression of the corresponding gene clusters [270,277]. However, since some MocR/GabR-type transcriptional regulators can act both as repressors and activators [278], it remains to be seen in future studies if EnuR possesses these two types of regulatory attributes as well. Operator sequences for EnuR-type proteins have been deduced through bioinformatics in many microorganisms [276] and DNA fragments of *R. pomeroyi* DSS-3 and *S. meliloti* containing these in silico predicted sequences are recognized and stably bound by purified EnuR proteins from the corresponding bacteria [270,277]. In DNA-band-shift assays with the EnuR protein from *R. pomeroyi* DSS-3, specific DNA:EnuR complexes began to form at concentrations of EnuR as low as 75 nM [270].

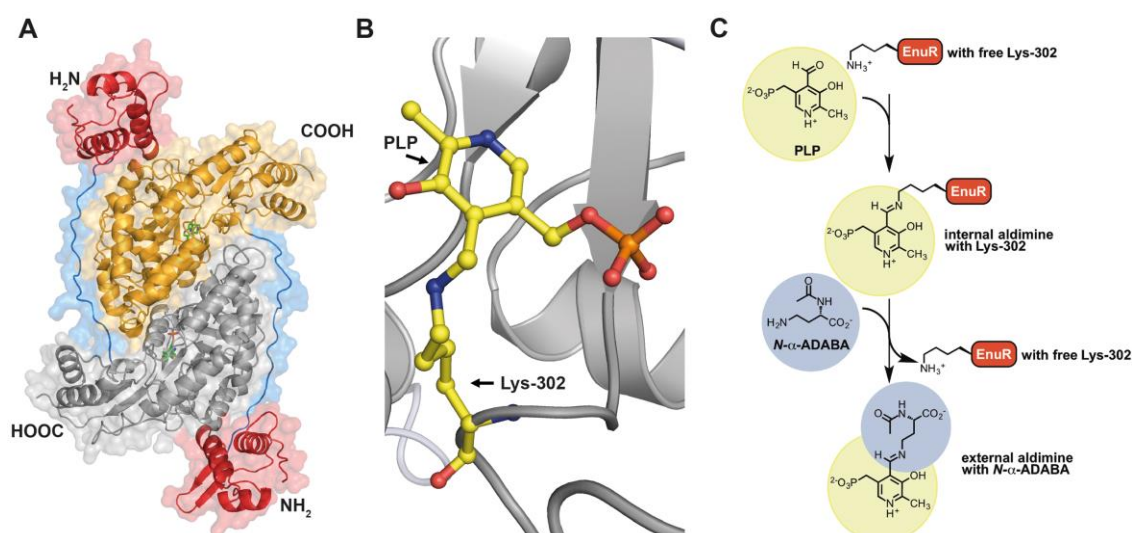


Figure 7. EnuR, a PLP-containing transcriptional regulator of ectoine/5-hydroxyectoine gene clusters. (A) in silico model of the predicted *Ruegeria pomeroyi* DSS-3 EnuR dimer that was derived from the crystallographic structure of the *Bacillus subtilis* GabR (PDB accession code 4N0B) [279]. The EnuR model was built with the SWISS-MODEL web server (<https://swissmodel.expasy.org/>) [286] and visualized using the PyMOL Molecular Graphics System suit (<https://pymol.org/2/>) [287]. The C-terminal aminotransferase-domains of the EnuR dimer are shown in grey/yellow, the N-terminal DNA-binding domains are represented in red and the flexible linkers connecting these domains are depicted in blue. Each monomer contains a PLP molecule covalently bound via an Schiff base to Lys³⁰² in the aminotransferase domain [263,270]. This internal aldimine [173] is depicted in (B) in a close-up view. (C) Model for the chemistry underlying binding and release of the inducer *N*-α-ADABA to the PLP-cofactor bound to Lys³⁰² of the EnuR regulator. In the first step, PLP is covalently bound by the side-chain of Lys³⁰² and thus forms an internal aldimine [173]. Upon binding of the inducer *N*-α-ADABA to PLP, PLP is released from Lys³⁰² and an external aldimine [173] is formed. This sequence of events is envisioned to trigger a conformational change in EnuR, thereby altering its DNA-binding properties. This scheme for inducer binding by EnuR is based upon detailed biochemical and structural analysis of the *B. subtilis* GabR regulator that uses GABA as its inducer [279–283].

The chemistry underlying the reaction between the Lys-bound PLP cofactor in MocR/GabR-type regulators and the system-specific inducer requires a primary amino group [278,279,282,283]. Although an external supply of ectoine or 5-hydroxyectoine induces the transcription of the ectoine/5-hydroxyectoine uptake and catabolic gene cluster [263,270], neither of these compounds possesses such a primary amino group (Figure 1B). Consequently, the purified and PLP-containing EnuR protein from *R. pomeroyi* DSS-3 did not bind these two ectoines [270].

It seemed logical that the system-specific inducer molecule that will interact with the Lys³⁰² bound PLP co-factor is generated through the metabolism of ectoines. Indeed, several ectoine-derived metabolites possess primary amino groups (Figure 6B). Microscale thermophoresis (MST) experiments revealed that *N*-α-ADABA serves as the primary system-specific inducer for EnuR; it is bound by the EnuR-PLP protein with a *K_d* value of about 1.7 μM. In Figure 7C we provide a scheme for the binding of the PLP molecule to EnuR/Lys³⁰² to form the internal aldimine, the subsequent reaction of the inducer *N*-α-ADABA with the covalently bound PLP molecule and the subsequent formation of the PLP:*N*-α-ADABA complex, the external aldimine [270]. Additional binding studies showed that DABA also interacts with the purified EnuR protein in a Lys³⁰²- and PLP-dependent fashion, but the binding constant (*K_d* about 457 μM) for this reaction is about 270-fold reduced in comparison with the *K_d* value of *N*-α-ADABA [270]. As a consequence, substantial DABA concentrations (30 mM) were required to displace in vitro the EnuR protein (also referred to in the literature as EhuR or EutR [276,277]) in DNA band-shift assays from its DNA target sequence at the ectoine/5-hydroxyectoine gene cluster of *S. meliloti* [277].

Apart from the high affinity of EnuR for *N*- α -ADABA, this compound has the additional advantage of being an ectoine-catabolism-specific metabolite (Figure 6B), whereas DABA also occurs as an intermediate in other metabolic and biosynthetic processes in microorganisms, including the biosynthesis of ectoine (Figure 2). Taken together, the pairing of the EnuR repressor with its covalently attached PLP co-factor and ectoine-derived metabolites (*N*- α -ADABA and DABA) establishes a sensitive intracellular trigger to relieve EnuR-mediated repression of the ectoine/5-hydroxyectoine catabolic gene cluster [270]. The finding that the isomer of the inducer *N*- α -ADABA, *N*- γ -ADABA, the main substrate for the ectoine synthase (Figure 2), is not recognized by the PLP-bound EnuR regulatory protein [270] is a physiologically highly relevant result. It is of critical importance for the group of microorganisms that are capable of both ectoine synthesis and catabolism in order to avoid a wasteful futile cycle. However, the report by Schwibbert et al. [158] that the ectoine hydrolase of *H. elongata* can generate both *N*- α - and *N*- γ -ADABA molecules raises questions about the ability of microorganisms to establish a strict genetic separation of ectoine synthesis and catabolic pathways.

Many ectoine/5-hydroxyectoine uptake and catabolic gene clusters (494 representatives from a dataset of 539 ectoine consumers [263,270]) contain an *asnC* gene. It encodes a member of the broadly distributed AsnC/Lrp-family of transcriptional regulators that can wrap DNA into nucleosome-like structures and frequently respond in their DNA-binding properties to low-molecular mass effector molecules generated through metabolism (e.g., amino acids) [271,272,288]. In many cases, these proteins respond to feast-and-famine situations, and thereby permit the efficient exploitation of sudden burst in the supply of nutrients. Studies with *asnC* mutants from the ectoine/5-hydroxyectoine uptake and catabolic gene cluster of *R. pomeroyi* DSS-3 revealed a clear activating influence on the transcription of this operon and the ability of *R. pomeroyi* DSS-3 to use ectoine as sole carbon source was abolished in the *asnC* mutant strain [270]. It is currently unclear as to which metabolite or cellular cue AsnC responds, but given the reported data for the effector molecules of EnuR (*N*- α -ADABA and DABA) [270]), we would not be surprised if this regulator uses intermediates or end-products of ectoine degradation (Figure 6B) to alter its DNA-binding activity. Preliminary DNA-binding studies with the AsnC homolog (referred to as DoeX) from *H. elongata* showed that it binds to DNA segments in the proposed regulatory region of the ectoine catabolic gene cluster [158]. Relevant for an understanding of the role played by AsnC is the fact that feast-and-famine type DNA-binding proteins can work in concert with other regulatory proteins [289], a facet in gene regulation that is probably highly relevant for the large group of microbial ectoine consumers that possess both EnuR and AsnC (85% of the 539 predicted ectoine consumers in the dataset of Schulz et al. [263,270]).

Two-component regulatory systems (TCS) are major sensor devices through which microbial cells monitor either extra- or intracellular changes [290]. Most TCS consist of a cytoplasmic membrane-embedded histidine kinase and a cytoplasmic response regulator. Upon detection of a specific signal, the histidine kinase auto-phosphorylates using ATP as phosphor donor; it then transfers the phosphoryl group to the response regulator, which will communicate with the transcriptional apparatus of the cell to alter, in many cases, gene expression [290]. Transposon mutagenesis of *R. pomeroyi* DSS-3 revealed the involvement of such a system, NtrYX [291], in the genetic control of its ectoine/5-hydroxyectoine catabolic gene cluster [270]. The NtrX response regulator is an unusual member of the NtrC-family and its cognate sensor kinase NtrY is a protein with four predicted transmembrane regions and a large, 161-amino-acids-long, extra-cytoplasmic domain. The NtrYX TCS has been implicated in a variety of cellular functions in various microorganisms, including the control of catabolic genes for nitrogen-containing compounds [291–293]. Genetic inactivation of *R. pomeroyi* DSS-3 *ntrYX* genes renders this bacterium unable to use ectoine as the sole carbon source [270]. Hence, the NtrYX TCS functions as a positive regulatory device for ectoine catabolism. However, it is currently unknown whether the NtrY sensor kinase recognizes externally provided ectoine directly and what the target sequences for the NtrX response regulator in the large *uehABC-usp-eutABCDE-asnC-ssd-atf* operon are. While *enuR* and *asnC* genes are widely distributed among all branches of ectoine degrading *Proteobacteria*, the *ntrYX* genes are only found in ectoine-consuming members of the *Alphaproteobacteria* [263,270].

Genetic studies addressing the transcriptional regulation of ectoine/5-hydroxyectoine uptake and catabolism in the marine proteobacterium *R. pomeroyi* DSS-3 have significantly advanced the understanding of the genetic wiring of this process [270]. In the dataset reported by Schulz et al. [263,270], 45% of the 539 inspected genome sequences of predicted ectoine consumers possess all three regulatory systems (EnuR, AsnC, NtrYX) that we have described in some detail in this overview. Hence, it is highly likely that their intricate interplay will set the genetic regulation of ectoine/5-hydroxyectoine catabolism in many different microbial species and strains. On the other hand, the report by Schulz et al. [270] also revealed considerable variations in terms of the presence of the *enuR*, *asnC*, and *ntrYX* genes in a given bacterium, suggesting that variants of the regulatory circuit discovered in *R. pomeroyi* DSS-3 exist.

While these studies already paint a rather complex picture of the genetic control of microbial ectoine/5-hydroxyectoine catabolism [270], the recent discovery of a regulatory small trans-acting RNA controlling ectoine catabolic genes in the *S. meliloti* strain Sm2B3001 [294] already adds a new dimension to this process. Transcription of the gene for this small non-coding RNA (NfeR1; Nodule formation efficiency RNA) is stimulated by high osmolarity, and lack of the NfeR1 RNA altered the expression of an array of salt-responsive genes in this symbiotic bacterium. Notably, under high-salinity growth conditions, the level of the *eutAED* mRNA is down-regulated in a NfeR1 RNA-dependent fashion [294]. However, the details of this interesting regulatory circuit, its physiological consequences, and its possible wider occurrence in ectoine-consuming microorganisms need to be further explored.

9. Ectoines in Eukarya: A Recent Discovery

Ectoines have so far been considered as compatible solutes exclusively synthesized and used as stress protectants by members of the Bacteria, and by a few Archaea [91–94]. Recent studies with halophilic protists now change this picture substantially [104], since ectoine/5-hydroxyectoine biosynthetic genes have been detected in *Halocafeteria seosinensis* [100,101] and ectoine production has been directly observed in *Schmidingerothrix salinarum* [102]. *H. seosinensis* is a heterotrophic, borderline extreme halophilic nano-flagellate that actively ingests bacteria as its food source; 18S rRNA-based phylogenetic analysis placed this protist into the stramenophile lineage, and it was taxonomically positioned into the order *Bicosoecida* [295]. *S. salinarum* is a bacteriovorous heterotroph as well; it is a halotolerant ciliate and a member of the order *Stichotrichia* [296].

Marine and hypersaline habitats are populated not only by a physiologically and taxonomically diverse group of Bacteria and Archaea [23,297] but halophilic protists are also ecophysiologically critical inhabitants of these challenging ecosystems [103]. These unicellular eukaryotes serve crucial roles as primary producers and decomposers in these habitats, and some of them exert a major influence on the abundance of microorganisms and the release of bacteria-derived metabolites into the environment through their bacterivorous activity. However, their salt-stress adaptation strategy has largely been neglected [103].

In their studies on the genome sequence of *H. seosinensis* and its salt-stress-responsive transcriptional profile, Harding et al. [100,101] discovered the presence and the salt-stress responsive induction of ectoine/5-hydroxyectoine biosynthetic and *ask_ect* genes. Since *H. seosinensis* is a heterotroph feeding on microorganisms living in its habitat, the detection of DNA sequences related to microbial genes is at least initially of some concern. The misinterpretation of these sequences as being of eukaryotic origin can seriously compromise assembly into DNA scaffolds of the eukaryotic genome sequence and the interpretation of biological findings [298]. In the case of *H. seosinensis*, at least for the *ectABCD* and *ask_ect* genes, one can exclude this complication, since each of these genes harbors spliceosomal introns [100,101], genetic elements that are not found in Bacteria and Archaea [299]. The *H. seosinensis* ectoine/5-hydroxyectoine biosynthetic enzymes possess N-terminal mitochondrial targeting signals, while their bacterial and archaeal counterparts are all cytoplasmic enzymes [165]. This observation suggests that the production of these compatible solutes might occur in the mitochondria of the protists, cell compartments in which the biosynthetic precursors (Glu and Asp) of ectoines are synthesized using intermediates of the Krebs cycle [101].

In extended database searches of eukaryotic genomes, Harding et al. [101] discovered *ectA*- and *ectC*-related sequences in previously reported transcriptional profiles of other protists and in various other Eukarya. This includes even the deuterostome animals *Branchiostoma floridae* and *Saccoglossus kowalevskii*. *B. floridae* is a lancelet, modern survivors of an ancient chordate lineage [300], while *S. kowalevskii* belongs to the hemicordate phylum, marine invertebrates that are taxonomically classified together with the Chordata as Deuterostomia [301]. Experimental proof that the protist *H. seosinensis*, or for that matter any other *ect* gene-containing eukaryote, actually produces ectoines is missing in the interesting report of Harding et al. [101]. This important gap has now been closed by a comprehensive study conducted by Weinisch et al. [102], in which the salt-stress-dependent synthesis of ectoine was directly demonstrated by ¹H-NMR spectroscopy in the halophilic heterotrophic ciliate *S. salinarum*. Since no genome sequence of *S. salinarum* is currently publicly available, the genetic organization of the ectoine biosynthetic genes remains to be determined. Interestingly, *S. salinarum* is also able to import ectoine and can derive osmoprotection from this process [102].

Detailed phylogenetic considerations reported by Harding et al. [100,101] on the *H. seosinensis* *ectABC-ectD* genes lead to the conclusion that they might have been acquired via lateral gene transfer from a prokaryote and were subsequently genetically adjusted to the transcriptional and translational apparatus of the new eukaryotic host. Considering that both *H. seosinensis* and *S. salinarum* are predatory protists [103], this is a plausible evolutionary scenario, particularly since many microbial ectoine/5-hydroxyectoine producers are inhabitants of high-saline ecosystems (Figure 5) [91–94]. It is well established that Eukarya can acquire novel metabolic traits and stress resistance determinants by stealing pre-formed gene clusters from microorganisms [302]. Since ectoines are potent protectants against osmotic, desiccation, and temperature stress, it is highly likely that the acquisition of *ect* genes by *H. seosinensis* and *S. salinarum* from their microbial food prey [100,101,104] will provide a distinct growth and survival advantage to these eukaryotic cells in their physiologically challenging high-salinity habitats [103].

Another interesting finding related to the synthesis of ectoines by Eukarya stems from a recent study by Landa et al. [303], in which the remodeling of the transcriptional profile of *R. pomeroyi* DSS-3 co-cultured with the diatom *Thalassiosira pseudonana* was assessed. The observed gene expression pattern indicates that, in addition to dihydroxypropanesulfonate, xylose, and glycolate, ectoine also fueled carbon and energy metabolism of the heterotroph *R. pomeroyi*. In view of the findings on the substrate-induction of the ectoine/5-hydroxyectoine uptake and catabolic genes [263,265,270], the report by Landa et al. [303] implies that the diatom produces and releases ectoine/5-hydroxyectoine that are then detected by the prokaryotic partner and exploited as a nutrient [263,270]. This interpretation rests on the assumption that the culture of *T. pseudonana* used in this study [303] is truly axenic. The finding of Landa et al. [303] and the genetic data on the transcriptional induction of the ectoine/5-hydroxyectoine uptake and catabolic gene cluster by intermediates in ectoine degradation (Figures 6 and 7) [263,270] have broader implications. Members of the metabolically and ecophysiologically versatile *Roseobacter* clade are not only found as widespread free-living members of marine habitats, but also associate closely with the cells of diverse phytoplankton groups in the ocean [230,232]. Hence ectoines could play an important role in establishing and maintaining ecophysiological relevant food webs in various ecological niches.

10. Conclusions and Perspectives

The data presented here provide the most comprehensive study to date on the phylogenomics of the ectoine (*ectABC*) and 5-hydroxyectoine (*ectD*) biosynthetic gene clusters, and the genes functionally associated with them, with respect to the production (*ask_ect*) of their biosynthetic precursor or the transcriptional regulation (*ectR*) of their structural genes (Figure 5). This data set can therefore serve as a reference point for the distribution of the *ect* genes in future studies, as new genome sequences of Bacteria and Archaea are determined at an ever-increasing pace. Despite the existing bias of the available genome sequences in databases, one can conclude from our phylogenomic analysis that the taxonomic affiliation of presumed ectoine/5-hydroxyectoine producers is dominated by representatives of the *Actinobacteria* and members from the

Alphaproteobacteria, *Betaproteobacteria*, and *Gammaproteobacteria*, which together make up 91% of our dataset. Although some ectoine/5-hydroxyectoine producers are found among members of the Archaea, we conclude that the synthesis of ectoines is primarily a bacterial trait, since available evidence (Figure 5) points to the transmission of the *ectABC/ectD* genes via lateral gene transfer into the genomes of a restricted number of Archaea from members of the Bacteria [92]. This evolutionarily important process [223–225,302] is in all likelihood also responsible for the acquisition of *ect* biosynthetic genes by unicellular Eukarya that live in high-saline habitats [100–102]. This recent finding opens new avenues of research, and follow-up studies might hold surprising discoveries. Our overview on the phylogenomics of *ectABC* and *ectD* biosynthetic genes can also aid the further development and biotechnological exploitation of natural and synthetic microbial cell factories for ectoines, commercially high-value natural products [86,91,94,145,146,148], since there are many microorganisms with different life-styles to choose from (Figure 5).

The accumulation of ectoines by high-osmolarity/salinity stressed cells through synthesis and import [1] has a major influence on the hydration status of the cytoplasm, and hence on cell volume and turgor [2,10,108–111] and their function-preserving attributes [91,94,105,145–147] will also likely contribute to the ability of the cell to strive under osmotically challenging growth conditions. An understanding of the role of ectoines as highly effective microbial osmoprotectants therefore seems rather straightforward. However, it is not clear yet how the thermoprotective effects of ectoines [77–79,97,121] are achieved on a biochemical and molecular level. While the portrayal of ectoines as chemical chaperones is suggestive, the molecular mechanisms underpinning the function-preserving characteristics of these compounds do not necessarily need to be the same at high and low growth temperatures. From the perspective of basic science, and with respect to practical applications, studies addressing the function of ectoines as thermolytes might prove to be highly rewarding.

The core of the ectoine/5-hydroxyectoine biosynthetic route and the properties of the involved enzymes (Figure 2) are now reasonably well understood, but nevertheless require further focused efforts to attain a detailed structure/function description of each of the involved biocatalysts. This has already been accomplished in quite some detail for the ectoine hydroxylase (EctD) through biochemical, structural, site-directed mutagenesis, and modeling approaches [93,177,186]. Ectoine/5-hydroxyectoine producers live in ecophysiological varied and often stressful habitats that might require evolutionary adaptation of the underlying biosynthetic enzymes. The phylogenomic data (Figure 5) might therefore serve as a guide to choosing those ectoine biosynthetic enzymes that are best suited for structural approaches. Our extended overview of the genetic context of *ectC* genes underscored recent reports on the widespread occurrence of solitary EctC-type proteins [92,93]. Their biochemical properties and potential physiological function [221] are so far unresolved and certainly should be a topic for future studies.

From the view of basic science, the understanding of the genetic and physiological regulatory circuits controlling *ect* gene expression in response to environmental and cellular cues is a pressing issue. There is no consistent picture of how this is accomplished, and the literature on this topic is plagued with claims that are not sufficiently substantiated by experimental data. In the bacteria studied so far, transcription of the ectoine/5-hydroxyectoine biosynthetic genes is under osmotic control, fully consistent with the major physiological function of these potent osmoprotectants. However, the underlying genetic regulatory mechanisms might differ in different microbial species and might entail promoters that operate independently of specific regulatory proteins [116], while others might be dependent on such transcription factors (e.g., RpoS; SigB) [77,78]. Most interesting is the association of the *ect* genes in many *Proteobacteria* with a gene (*ectR*) that encodes a member of the MarR super-family of transcriptional regulators (Figure 5). So far, EctR has only been functionally studied in a few aerobic, moderately halophilic methylotrophic bacteria (*M. alcaliphilum* 20Z, *M. alcalica*, *M. thalassica*), where it serves as a repressor of *ect* gene expression [99,198,215], but does not seem to be critical for their osmoprotectant-responsive transcription [198]. The environmental or cellular cues to which EctR responds in its DNA-binding activity are unknown and hence our understanding of the role of this intriguing regulatory protein in controlling *ect* gene expression is rather incomplete.

The widespread occurrence of ectoine/5-hydroxyectoine producers in terrestrial and marine habitats (Figure 5) also leads to the presence of cell-free ectoines in natural ecosystems when these cells are osmotically down-shocked or when they lyse [233]. The recovery of ectoines by microorganisms from environmental sources via high affinity transport systems will aid these bacteria in their attempts to withstand osmotic and temperature extremes. These transporters are of ecophysiological importance not only for the acquisition of ectoines, where they act as stress protectants, but they also seem to serve as recycling systems for newly synthesized ectoines that are either leaked or actively excreted from the producer cells [161,304]. Continued efforts are required to understand the physiological relevance and molecular underpinning of this latter process [161,304,305], and to further enhance our understanding of the structure/function relationship of ectoine/5-hydroxyectoine importers [241,261,267,268]. Furthermore, new selection or screening procedures might lead to the identification of additional members (and perhaps also novel types) of transporters for ectoines.

Ectoine/5-hydroxyectoine import systems (e.g., EhuABCD, UehABC) also play a crucial role in scavenging these compounds from scarce environmental sources, where these nitrogen-rich molecules (Figure 1B) are used as nutrients. Consistent with their important contribution to ectoine/5-hydroxyectoine catabolism, the transcription of the *ehu* and *ueh* structural genes is substrate-inducible but is not subjected to osmotic control [265,267,268,270]. In contrast to the already rather well studied ectoine/5-hydroxyectoine biosynthetic genes, an understanding of the biochemistry of the catabolic enzymes is in its infancy. Although experimentally testable proposals for the catabolism of 5-hydroxyectoine and ectoine have been made (Figure 6B) [158,263], the inspection of the corresponding gene clusters not only revealed a considerable variation in their genetic organization but also in their gene content (Figure 6A) [158,263,270]. This variation suggests that alternatives (or additions) to the proposed catabolic pathways might exist in microorganisms.

Recent studies on the genetics of the transcriptional control of ectoine/5-hydroxyectoine utilization genes paint a rather complex picture of this process [270], but they have already uncovered a central role of the MocR/GabR-type EnuR regulator and its ectoine-derived inducers *N*- α -ADABA and DABA [270,277]. Nevertheless, further in-depth studies are required to elucidate the complete regulatory circuit controlling import and catabolism of ectoines and to illuminate the role played by the feast-and-famine regulator AsnC and the NtrYX two-component regulatory system [270]. Although about 45% of the genomes of the 539 predicted ectoine/5-hydroxyectoine consumers simultaneously possess the EnuR, AsnC, and NtrYX regulatory systems implicated in controlling ectoine/5-hydroxyectoine catabolic genes [270], there is again a considerable variation in their phylogenetic distribution, suggesting that differently configured regulatory circuits control the catabolism of ectoines in different microorganisms.

The recent discovery of ectoine/5-hydroxyectoine biosynthetic genes in the halophilic protist *H. seosinensis* [100,101] and the salt-stress-responsive production and import of ectoine in *S. salinarum* [102] came at a considerable surprise for scholars of microbial osmostress response systems [104]. The data reported by Harding et al. [100,101] suggest the presence of ectoine/5-hydroxyectoine biosynthetic genes in Eukarya other than *H. seosinensis* and *S. salinarum*. As a case in point, the re-programming and induction of ectoine/5-hydroxyectoine uptake and catabolic genes in the marine bacterium *R. pomeroyi* in a co-culture with the diatom *T. pseudonana* [303] strongly suggest that this eukaryote produces and releases ectoines, because enhanced expression of these genes by *R. pomeroyi* DSS-3 is strictly dependent on ectoine-derived metabolites [270,277]. Taken together, these findings underscore the importance of ectoines not only as effective stress- and cytoprotectants but also suggest an important function of these nitrogen-rich compounds as mediators of ecophysologically important food webs. Ectoines will remain a fascinating research topic for many years to come, both from the perspective of basic science and applied approaches.

Acknowledgments: We greatly appreciate the expert help of Vickie Koogler in the language editing of our manuscript. Work in the laboratory of E.B. at the University of Marburg on the synthesis and degradation of compatible solutes is supported by the Deutsche Forschungsgemeinschaft (DFG) through the SFB 987 and by the LOEWE-Center for Synthetic Microbiology. We thank Stefanie Kobus of the Center of Structural Studies

(CSS) at the Heinrich-Heine University of Düsseldorf (Germany) for her focused efforts and expert help in the determination of crystal structures of ectoine/5-hydroxyectoine biosynthetic enzymes and components of ectoine transporters. E.B. thanks Joeren Dickschat (University of Bonn, Germany) for fruitful collaborations on the synthesis and catabolism of ectoines. L.C. is a member of the International Max Planck Research School on Environmental, Cellular and Molecular Microbiology (IMPRS-Mic Marburg) and gratefully acknowledges its financial support.

Author Contributions: L.C. and E.B. wrote the manuscript with input from the other authors.

Conflict of Interests: The authors declare no conflict of interest.

References

1. Kempf, B.; Bremer, E. Uptake and synthesis of compatible solutes as microbial stress responses to high osmolality environments. *Arch. Microbiol.* **1998**, *170*, 319–330.
2. Bremer, E.; Krämer, R. Coping with osmotic challenges: Osmoregulation through accumulation and release of compatible solutes. In *Bacterial Stress Responses*; Storz, G., Hengge-Aronis, R., Eds.; ASM Press: Washington, DC, USA, 2000; pp. 79–97.
3. Wood, J.M.; Bremer, E.; Csonka, L.N.; Krämer, R.; Poolman, B.; van der Heide, T.; Smith, L.T. Osmosensing and osmoregulatory compatible solute accumulation by bacteria. *Comp. Biochem. Physiol. A Mol. Integr. Physiol.* **2001**, *130*, 437–460.
4. Csonka, L.N. Physiological and genetic responses of bacteria to osmotic stress. *Microbiol. Rev.* **1989**, *53*, 121–147.
5. Roesser, M.; Müller, V. Osmoadaptation in bacteria and archaea: Common principles and differences. *Environ. Microbiol.* **2001**, *3*, 743–754.
6. Wood, J.M. Osmosensing by bacteria: Signals and membrane-based sensors. *Microbiol. Mol. Biol. Rev.* **1999**, *63*, 230–262.
7. Ball, P. Water is an active matrix of life for cell and molecular biology. *Proc. Natl. Acad. Sci. USA* **2017**, *114*, 13327–13335.
8. De Lima Alves, F.; Stevenson, A.; Baxter, E.; Gillion, J.L.; Hejazi, F.; Hayes, S.; Morrison, I.E.; Prior, B.A.; McGenity, T.J.; Rangel, D.E.; et al. Concomitant osmotic and chaotropicity-induced stresses in *Aspergillus wentii*: Compatible solutes determine the biotic window. *Curr. Genet.* **2015**, *61*, 457–477.
9. van den Berg, J.; Boersma, A.J.; Poolman, B. Microorganisms maintain crowding homeostasis. *Nat. Rev. Microbiol.* **2017**, *15*, 309–318.
10. Wood, J.M. Bacterial osmoregulation: A paradigm for the study of cellular homeostasis. *Annu. Rev. Microbiol.* **2011**, *65*, 215–238.
11. Booth, I.R. Bacterial mechanosensitive channels: Progress towards an understanding of their roles in cell physiology. *Curr. Opin. Microbiol.* **2014**, *18*, 16–22.
12. Whatmore, A.M.; Reed, R.H. Determination of turgor pressure in *Bacillus subtilis*: A possible role for K⁺ in turgor regulation. *J. Gen. Microbiol.* **1990**, *136*, 2521–2526.
13. Deng, Y.; Sun, M.; Shaevitz, J.W. Direct measurement of cell wall stress stiffening and turgor pressure in live bacterial cells. *Phys. Rev. Lett.* **2011**, *107*, 158101.
14. Cayley, D.S.; Guttman, H.J.; Record, M.T., Jr. Biophysical characterization of changes in amounts and activity of *Escherichia coli* cell and compartment water and turgor pressure in response to osmotic stress. *Biophys. J.* **2000**, *78*, 1748–1764.
15. Rojas, E.R.; Huang, K.C. Regulation of microbial growth by turgor pressure. *Curr. Opin. Microbiol.* **2017**, *42*, 62–70.
16. Levina, N.; Totemeyer, S.; Stokes, N.R.; Louis, P.; Jones, M.A.; Booth, I.R. Protection of *Escherichia coli* cells against extreme turgor by activation of MscS and MscL mechanosensitive channels: Identification of genes required for mscs activity. *Embo J.* **1999**, *18*, 1730–1737.
17. Hoffmann, T.; Boiangiu, C.; Moses, S.; Bremer, E. Responses of *Bacillus subtilis* to hypotonic challenges: Physiological contributions of mechanosensitive channels to cellular survival. *Appl. Environ. Microbiol.* **2008**, *74*, 2454–2460.
18. Cetiner, U.; Rowe, I.; Schams, A.; Mayhew, C.; Rubin, D.; Anishkin, A.; Sukharev, S. Tension-activated channels in the mechanism of osmotic fitness in *Pseudomonas aeruginosa*. *J. Gen. Physiol.* **2017**, *149*, 595–609.
19. Reuter, M.; Hayward, N.J.; Black, S.S.; Miller, S.; Dryden, D.T.; Booth, I.R. Mechanosensitive channels and bacterial cell wall integrity: Does life end with a bang or a whimper? *J. R. Soc. Interface* **2014**, *11*, 20130850.
20. Cox, C.D.; Bavi, N.; Martinac, B. Bacterial mechanosensors. *Annu. Rev. Physiol.* **2018**, *80*, 71–93.

21. Calamita, G. The *Escherichia coli* aquaporin-Z water channel. *Mol. Microbiol.* **2000**, *37*, 254–262.
22. Jiang, J.; Daniels, B.V.; Fu, D. Crystal structure of AqpZ tetramer reveals two distinct Arg-189 conformations associated with water permeation through the narrowest constriction of the water-conducting channel. *J. Biol. Chem.* **2006**, *281*, 454–460.
23. Ventosa, A.; Nieto, J.J.; Oren, A. Biology of moderately halophilic aerobic bacteria. *Microbiol. Mol. Biol. Rev.* **1998**, *62*, 504–544.
24. Oren, A. Life at high salt concentrations, intracellular KCl concentrations, and acidic proteomes. *Front. Microbiol.* **2013**, *4*, 315.
25. Galinski, E.A.; Trüper, H.G. Microbial behaviour in salt-stressed ecosystems. *FEMS Microbiol. Rev.* **1994**, *15*, 95–108.
26. Buda, R.; Liu, Y.; Yang, J.; Hegde, S.; Stevenson, K.; Bai, F.; Pilizota, T. Dynamics of *Escherichia coli*'s passive response to a sudden decrease in external osmolarity. *Proc. Natl. Acad. Sci. USA* **2016**, *113*, E5838–E5846.
27. Bialecka-Fornal, M.; Lee, H.J.; Phillips, R. The rate of osmotic downshock determines the survival probability of bacterial mechanosensitive channel mutants. *J. Bacteriol.* **2015**, *197*, 231–237.
28. Egan, A.J.; Cleverley, R.M.; Peters, K.; Lewis, R.J.; Vollmer, W. Regulation of bacterial cell wall growth. *FEBS J.* **2017**, *284*, 851–867.
29. Typas, A.; Banzhaf, M.; Gross, C.A.; Vollmer, W. From the regulation of peptidoglycan synthesis to bacterial growth and morphology. *Nat. Rev. Microbiol.* **2012**, *10*, 123–136.
30. Rasmussen, T. How do mechanosensitive channels sense membrane tension? *Biochem. Soc. Trans.* **2016**, *44*, 1019–1025.
31. Booth, I.R.; Blount, P. The MscS and MscL families of mechanosensitive channels act as microbial emergency release valves. *J. Bacteriol.* **2012**, *194*, 4802–4809.
32. Pliotas, C.; Naismith, J.H. Spectator no more, the role of the membrane in regulating ion channel function. *Curr. Opin. Struct. Biol.* **2017**, *45*, 59–66.
33. Coquelle, N.; Talon, R.; Juers, D.H.; Girard, E.; Kahn, R.; Madern, D. Gradual adaptive changes of a protein facing high salt concentrations. *J. Mol. Biol.* **2010**, *404*, 493–505.
34. Talon, R.; Coquelle, N.; Madern, D.; Girard, E. An experimental point of view on hydration/solvation in halophilic proteins. *Front. Microbiol.* **2014**, *5*, 66.
35. Tadeo, X.; Lopez-Mendez, B.; Trigueros, T.; Lain, A.; Castano, D.; Millet, O. Structural basis for the amino acid composition of proteins from halophilic archaea. *PLoS Biol.* **2009**, *7*, e1000257.
36. Oren, A. Thermodynamic limits to microbial life at high salt concentrations. *Environ. Microbiol.* **2011**, *13*, 1908–1923.
37. Oren, A. Bioenergetic aspects of halophilism. *Microbiol. Mol. Biol. Rev.* **1999**, *63*, 334–348.
38. Youssef, N.H.; Savage-Ashlock, K.N.; McCully, A.L.; Luedtke, B.; Shaw, E.I.; Hoff, W.D.; Elshahed, M.S. Trehalose/2-sulfotrehalose biosynthesis and glycine-betaine uptake are widely spread mechanisms for osmoadaptation in the *Halobacteriales*. *ISME J.* **2014**, *8*, 636–649.
39. Deole, R.; Challacombe, J.; Raiford, D.W.; Hoff, W.D. An extremely halophilic proteobacterium combines a highly acidic proteome with a low cytoplasmic potassium content. *J. Biol. Chem.* **2013**, *288*, 581–588.
40. Kokoeva, M.V.; Storch, K.F.; Klein, C.; Oesterhelt, D. A novel mode of sensory transduction in archaea: Binding protein-mediated chemotaxis towards osmoprotectants and amino acids. *EMBO J.* **2002**, *21*, 2312–2322.
41. Becker, E.A.; Seitzer, P.M.; Tritt, A.; Larsen, D.; Krusor, M.; Yao, A.I.; Wu, D.; Madern, D.; Eisen, J.A.; Darling, A.E.; et al. Phylogenetically driven sequencing of extremely halophilic archaea reveals strategies for static and dynamic osmo-response. *PLoS Genet.* **2014**, *10*, e1004784.
42. Lippert, K.; Galinski, E.A.; Truper, H.G. Biosynthesis and function of trehalose in *Ectothiorhodospira halochloris*. *Antonie Leeuwenhoek* **1993**, *63*, 85–91.
43. Vaidya, S.; Dev, K.; Sourirajan, A. Distinct osmoadaptation strategies in the strict halophilic and halotolerant bacteria isolated from Lunsu salt water body of North West Himalayas. *Curr. Microbiol.* **2018**, doi:10.1007/s00284-018-1462-8.
44. Yancey, P.H.; Clark, M.E.; Hand, S.C.; Bowlus, R.D.; Somero, G.N. Living with water stress: Evolution of osmolyte systems. *Science* **1982**, *217*, 1214–1222.
45. Burg, M.B.; Ferraris, J.D. Intracellular organic osmolytes: Function and regulation. *J. Biol. Chem.* **2008**, *283*, 7309–7313.
46. Gunde-Cimerman, N.; Plemenitas, A.; Oren, A. Strategies of adaptation of microorganisms of the three domains of life to high-salt concentrations. *FEMS Microbiol. Rev.* **2018**, in press.

47. Le Rudulier, D.; Strom, A.R.; Dandekar, A.M.; Smith, L.T.; Valentine, R.C. Molecular biology of osmoregulation. *Science* **1984**, *224*, 1064–1068.
48. Brown, A.D. Microbial water stress. *Bacteriol. Rev.* **1976**, *40*, 803–846.
49. Gilles, R. “Compensatory” organic osmolytes in high osmolarity and dehydration stresses: History and perspectives. *Comp. Biochem. Physiol. A Physiol.* **1997**, *117*, 279–290.
50. Yancey, P.H. Organic osmolytes as compatible, metabolic and counteracting cytoprotectants in high osmolarity and other stresses. *J. Exp. Biol.* **2005**, *208*, 2819–2830.
51. Holtmann, G.; Bremer, E. Thermoprotection of *Bacillus subtilis* by exogenously provided glycine betaine and structurally related compatible solutes: Involvement of opu transporters. *J. Bacteriol.* **2004**, *186*, 1683–1693.
52. Hoffmann, T.; Bremer, E. Protection of *Bacillus subtilis* against cold stress via compatible-solute acquisition. *J. Bacteriol.* **2011**, *193*, 1552–1562.
53. Caldas, T.; Demont-Caulet, N.; Ghazi, A.; Richarme, G. Thermoprotection by glycine betaine and choline. *Microbiology* **1999**, *145*, 2543–2548.
54. Diamant, S.; Eliahu, N.; Rosenthal, D.; Goloubinoff, P. Chemical chaperones regulate molecular chaperones in vitro and in cells under combined salt and heat stresses. *J. Biol. Chem.* **2001**, *276*, 39586–39591.
55. Da Costa, M.S.; Santos, H.; Galinski, E.A. An overview of the role and diversity of compatible solutes in *Bacteria* and *Archaea*. *Adv. Biochem. Eng. Biotechnol.* **1998**, *61*, 117–153.
56. Martins, L.O.; Huber, R.; Huber, H.; Stetter, K.O.; da Costa, M.S.; Santos, H. Organic solutes in hyperthermophilic archaea. *Appl. Environ. Microbiol.* **1997**, *63*, 896–902.
57. Santos, H.; da Costa, M.S. Compatible solutes of organisms that live in hot saline environments. *Environ. Microbiol.* **2002**, *4*, 501–509.
58. Yancey, P.H. Compatible and counteracting solutes: Protecting cells from the Dead Sea to the deep sea. *Sci. Prog.* **2004**, *87*, 1–24.
59. Arakawa, T.; Timasheff, S.N. The stabilization of proteins by osmolytes. *Biophys. J.* **1985**, *47*, 411–414.
60. Auton, M.; Rösgen, J.; Sinev, M.; Holthauzen, L.M.; Bolen, D.W. Osmolyte effects on protein stability and solubility: A balancing act between backbone and side-chains. *Biophys. Chem.* **2011**, *159*, 90–99.
61. Bolen, D.W.; Baskakov, I.V. The osmophobic effect: Natural selection of a thermodynamic force in protein folding. *J. Mol. Biol.* **2001**, *310*, 955–963.
62. Street, T.O.; Bolen, D.W.; Rose, G.D. A molecular mechanism for osmolyte-induced protein stability. *Proc. Natl. Acad. Sci. USA* **2006**, *103*, 13997–14002.
63. Bourot, S.; Sire, O.; Trautwetter, A.; Touze, T.; Wu, L.F.; Blanco, C.; Bernard, T. Glycine betaine-assisted protein folding in a *lysA* mutant of *Escherichia coli*. *J. Biol. Chem.* **2000**, *275*, 1050–1056.
64. Ignatova, Z.; Gierasch, L.M. Inhibition of protein aggregation in vitro and in vivo by a natural osmoprotectant. *Proc. Natl. Acad. Sci. USA* **2006**, *103*, 13357–13361.
65. Stadtmiller, S.S.; Gorenssek-Benitez, A.H.; Guseman, A.J.; Pielak, G.J. Osmotic shock induced protein destabilization in living cells and its reversal by glycine betaine. *J. Mol. Biol.* **2017**, *429*, 1155–1161.
66. Harishchandra, R.K.; Wulff, S.; Lentzen, G.; Neuhaus, T.; Galla, H.J. The effect of compatible solute ectoines on the structural organization of lipid monolayer and bilayer membranes. *Biophys. Chem.* **2010**, *150*, 37–46.
67. Smiatek, J.; Harishchandra, R.K.; Galla, H.J.; Heuer, A. Low concentrated hydroxyectoine solutions in presence of DPPC lipid bilayers: A computer simulation study. *Biophys. Chem.* **2013**, *180–181*, 102–109.
68. Record, M.T., Jr.; Courtenay, E.S.; Cayley, S.; Guttman, H.J. Biophysical compensation mechanisms buffering *E. coli* protein-nucleic acid interactions against changing environments. *Trends Biochem. Sci.* **1998**, *23*, 190–194.
69. Record, M.T., Jr.; Courtenay, E.S.; Cayley, D.S.; Guttman, H.J. Responses of *E. coli* to osmotic stress: Large changes in amounts of cytoplasmic solutes and water. *Trends Biochem. Sci.* **1998**, *23*, 143–148.
70. Tatzelt, J.; Prusiner, S.B.; Welch, W.J. Chemical chaperones interfere with the formation of scrapie prion protein. *EMBO J.* **1996**, *15*, 6363–6373.
71. Kolp, S.; Pietsch, M.; Galinski, E.A.; Gutschow, M. Compatible solutes as protectants for zymogens against proteolysis. *Biochim. Biophys. Acta* **2006**, *1764*, 1234–1242.
72. Lippert, K.; Galinski, E.A. Enzyme stabilization by ectoine-type compatible solutes: Protection against heating, freezing and drying. *Appl. Micro Biotechnol.* **1992**, *37*, 61–65.
73. Knapp, S.; Ladenstein, R.; Galinski, E.A. Extrinsic protein stabilization by the naturally occurring osmolytes beta-hydroxyectoine and betaine. *Extremophiles* **1999**, *3*, 191–198.

74. Manzanera, M.; Garcia de Castro, A.; Tondervik, A.; Rayner-Brandes, M.; Strom, A.R.; Tunnacliffe, A. Hydroxyectoine is superior to trehalose for anhydrobiotic engineering of *Pseudomonas putida* KT2440. *Appl. Environ. Microbiol.* **2002**, *68*, 4328–4333.
75. Manzanera, M.; Vilchez, S.; Tunnacliffe, A. High survival and stability rates of *Escherichia coli* dried in hydroxyectoine. *FEMS Microbiol. Lett.* **2004**, *233*, 347–352.
76. Chattopadhyay, M.K.; Kern, R.; Mistou, M.Y.; Dandekar, A.M.; Uratsu, S.L.; Richarme, G. The chemical chaperone proline relieves the thermosensitivity of a *dnaK* deletion mutant at 42 °C. *J. Bacteriol.* **2004**, *186*, 8149–8152.
77. Kuhlmann, A.U.; Bursy, J.; Gimpel, S.; Hoffmann, T.; Bremer, E. Synthesis of the compatible solute ectoine in *Virgibacillus pantothenicus* is triggered by high salinity and low growth temperature. *Appl. Environ. Microbiol.* **2008**, *74*, 4560–4563.
78. Kuhlmann, A.U.; Hoffmann, T.; Bursy, J.; Jebbar, M.; Bremer, E. Ectoine and hydroxyectoine as protectants against osmotic and cold stress: Uptake through the SigB-controlled betaine-choline- carnitine transporter-type carrier EctT from *Virgibacillus pantothenicus*. *J. Bacteriol.* **2011**, *193*, 4699–4708.
79. Bursy, J.; Kuhlmann, A.U.; Pittelkow, M.; Hartmann, H.; Jebbar, M.; Pierik, A.J.; Bremer, E. Synthesis and uptake of the compatible solutes ectoine and 5-hydroxyectoine by *Streptomyces coelicolor* A3(2) in response to salt and heat stresses. *Appl. Environ. Microbiol.* **2008**, *74*, 7286–7296.
80. Vargas, C.; Argandona, M.; Reina-Bueno, M.; Rodriguez-Moya, J.; Fernandez-Aunion, C.; Nieto, J.J. Unravelling the adaptation responses to osmotic and temperature stress in *Chromohalobacter salexigens*, a bacterium with broad salinity tolerance. *Saline Syst.* **2008**, *4*, 14.
81. Malin, G.; Lapidot, A. Induction of synthesis of tetrahydropyrimidine derivatives in *Streptomyces* strains and their effect on *Escherichia coli* in response to osmotic and heat stress. *J. Bacteriol.* **1996**, *178*, 385–395.
82. Tschapek, B.; Pittelkow, M.; Sohn-Bosser, L.; Holtmann, G.; Smits, S.H.; Gohlke, H.; Bremer, E.; Schmitt, L. Arg149 is involved in switching the low affinity, open state of the binding protein A₁ProX into its high affinity, closed state. *J. Mol. Biol.* **2011**, *411*, 36–52.
83. Lamosa, P.; Burke, A.; Peist, R.; Huber, R.; Liu, M.Y.; Silva, G.; Rodrigues-Pousada, C.; LeGall, J.; Maycock, C.; Santos, H. Thermostabilization of proteins by diglycerol phosphate, a new compatible solute from the hyperthermophile *Archaeoglobus fulgidus*. *Appl. Environ. Microbiol.* **2000**, *66*, 1974–1979.
84. Hoffmann, T.; Bremer, E. Management of osmotic stress by *Bacillus subtilis*: Genetics and physiology. In *Stress and Environmental Regulation of Gene Expression and Adaptation in Bacteria*; de Bruijn, F.J., Ed.; Wiley-Blackwell Publishers: Hoboken, NJ, USA, 2016; Volume 1, pp. 657–676.
85. Hoffmann, T.; Bremer, E. Guardians in a stressful world: The Opu family of compatible solute transporters from *Bacillus subtilis*. *Biol. Chem.* **2017**, *398*, 193–214.
86. Lentzen, G.; Schwarz, T. Extremolytes: Natural compounds from extremophiles for versatile applications. *Appl. Microbiol. Biotechnol.* **2006**, *72*, 623–634.
87. Roberts, M.F. Osmoadaptation and osmoregulation in archaea: Update 2004. *Front. BioSci.* **2004**, *9*, 1999–2019.
88. Galinski, E.A.; Pfeiffer, H.P.; Trüper, H.G. 1,4,5,6-tetrahydro-2-methyl-4-pyrimidinecarboxylic acid. A novel cyclic amino acid from halophilic phototrophic bacteria of the genus *Ectothiorhodospira*. *Eur. J. Biochem.* **1985**, *149*, 135–139.
89. Inbar, L.; Lapidot, A. The structure and biosynthesis of new tetrahydropyrimidine derivatives in actinomycin D producer *Streptomyces parvulus*. Use of ¹³C- and ¹⁵N-labeled L-glutamate and ¹³C and ¹⁵N NMR spectroscopy. *J. Biol. Chem.* **1988**, *263*, 16014–16022.
90. Inbar, L.; Frolow, F.; Lapidot, A. The conformation of new tetrahydropyrimidine derivatives in solution and in the crystal. *Eur. J. Biochem.* **1993**, *214*, 897–906.
91. Pastor, J.M.; Salvador, M.; Argandona, M.; Bernal, V.; Reina-Bueno, M.; Csonka, L.N.; Iborra, J.L.; Vargas, C.; Nieto, J.J.; Canovas, M. Ectoines in cell stress protection: Uses and biotechnological production. *Biotechnol. Adv.* **2010**, *28*, 782–801.
92. Widderich, N.; Czech, L.; Elling, F.J.; Köneke, M.; Stöveken, N.; Pittelkow, M.; Ridea, R.; Dickschat, J.S.; Heider, J.; Bremer, E. Strangers in the archaeal world: Osmostress-responsive biosynthesis of ectoine and hydroxyectoine by the marine thaumarchaeon *Nitrosopumilus maritimus*. *Environ. Microbiol.* **2016**, *18*, 1227–1248.
93. Widderich, N.; Höppner, A.; Pittelkow, M.; Heider, J.; Smits, S.H.; Bremer, E. Biochemical properties of ectoine hydroxylases from extremophiles and their wider taxonomic distribution among microorganisms. *PLoS ONE* **2014**, *9*, e93809.

94. Kunte, H.J.; Lentzen, G.; Galinski, E. Industrial production of the cell protectant ectoine: Protection, mechanisms, processes, and products. *Curr. Biotechnol.* **2014**, *3*, 10–25.
95. Louis, P.; Galinski, E.A. Characterization of genes for the biosynthesis of the compatible solute ectoine from *Marinococcus halophilus* and osmoregulated expression in *Escherichia coli*. *Microbiology* **1997**, *143*, 1141–1149.
96. Prabhu, J.; Schauwecker, F.; Grammel, N.; Keller, U.; Bernhard, M. Functional expression of the ectoine hydroxylase gene (*thpD*) from *Streptomyces chrysomallus* in *Halomonas elongata*. *Appl. Environ. Microbiol.* **2004**, *70*, 3130–3132.
97. Garcia-Esteva, R.; Argandona, M.; Reina-Bueno, M.; Capote, N.; Iglesias-Guerra, F.; Nieto, J.J.; Vargas, C. The *ectD* gene, which is involved in the synthesis of the compatible solute hydroxyectoine, is essential for thermoprotection of the halophilic bacterium *Chromohalobacter salexigens*. *J. Bacteriol.* **2006**, *188*, 3774–3784.
98. Bursy, J.; Pierik, A.J.; Pica, N.; Bremer, E. Osmotically induced synthesis of the compatible solute hydroxyectoine is mediated by an evolutionarily conserved ectoine hydroxylase. *J. Biol. Chem.* **2007**, *282*, 31147–31155.
99. Reshetnikov, A.S.; Khmelenina, V.N.; Mustakhimov, I.; Kalyuzhnaya, M.; Lidstrom, M.; Trotsenko, Y.A. Diversity and phylogeny of the ectoine biosynthesis genes in aerobic, moderately halophilic methylotrophic bacteria. *Extremophiles* **2011**, *15*, 653–663.
100. Harding, T.; Roger, A.J.; Simpson, A.G.B. Adaptations to high salt in a halophilic protist: Differential expression and gene acquisitions through duplications and gene transfers. *Front. Microbiol.* **2017**, *8*, 944.
101. Harding, T.; Brown, M.W.; Simpson, A.G.; Roger, A.J. Osmoadaptative strategy and its molecular signature in obligately halophilic heterotrophic protists. *Genome Biol. Evol.* **2016**, *8*, 2241–2258.
102. Weinisch, L.; Kuhner, S.; Roth, R.; Grimm, M.; Roth, T.; Netz, D.J.A.; Pierik, A.J.; Filker, S. Identification of osmoadaptive strategies in the halophile, heterotrophic ciliate *Schmidingerothrix salinarum*. *PLoS Biol.* **2018**, *16*, e2003892.
103. Harding, T.; Simpson, A.G.B. Recent advances in halophilic protozoa research. *J. Eukaryot. Microbiol.* **2018**, doi:10.1111/jeu.12495.
104. Czech, L.; Bremer, E. With a pinch of extra salt—Did predatory protists steal genes from their food? *PLoS Biol.* **2018**, *16*, e2005163.
105. Zaccai, G.; Bagyan, I.; Combet, J.; Cuello, G.J.; Deme, B.; Fichou, Y.; Gallat, F.X.; Galvan Josa, V.M.; von Gronau, S.; Haertlein, M.; et al. Neutrons describe ectoine effects on water H-bonding and hydration around a soluble protein and a cell membrane. *Sci. Rep.* **2016**, *6*, 31434.
106. Dötsch, A.; Severin, J.; Alt, W.; Galinski, E.A.; Kreft, J.U. A mathematical model for growth and osmoregulation in halophilic bacteria. *Microbiology* **2008**, *154*, 2956–2969.
107. Held, C.; Neuhaus, T.; Sadowski, G. Compatible solutes: Thermodynamic properties and biological impact of ectoines and prolines. *Biophys. Chem.* **2010**, *152*, 28–39.
108. Eiberweiser, A.; Nazet, A.; Kruchinin, S.E.; Fedotova, M.V.; Buchner, R. Hydration and ion binding of the osmolyte ectoine. *J. Phys. Chem. B* **2015**, *119*, 15203–15211.
109. Hahn, M.B.; Solomun, T.; Wellhausen, R.; Hermann, S.; Seitz, H.; Meyer, S.; Kunte, H.J.; Zeman, J.; Uhlig, F.; Smiatek, J.; et al. Influence of the compatible solute ectoine on the local water structure: Implications for the binding of the protein G5P to DNA. *J. Phys. Chem. B* **2015**, *119*, 15212–15220.
110. Smiatek, J. Osmolyte effects: Impact on the aqueous solution around charged and neutral spheres. *J. Phys. Chem. B* **2014**, *118*, 771–782.
111. Smiatek, J.; Harishchandra, R.K.; Rubner, O.; Galla, H.J.; Heuer, A. Properties of compatible solutes in aqueous solution. *Biophys. Chem.* **2012**, *160*, 62–68.
112. Malin, G.; Iakobashvili, R.; Lapidot, A. Effect of tetrahydropyrimidine derivatives on protein-nucleic acids interaction. Type II restriction endonucleases as a model system. *J. Biol. Chem.* **1999**, *274*, 6920–6929.
113. Lapidot, A.; Ben-Asher, E.; Eisenstein, M. Tetrahydropyrimidine derivatives inhibit binding of a Tat-like, arginine-containing peptide, to HIV TAR RNA in vitro. *FEBS Lett.* **1995**, *367*, 33–38.
114. Kurz, M. Compatible solute influence on nucleic acids: Many questions but few answers. *Saline Syst.* **2008**, *4*, 6.
115. Barth, S.; Huhn, M.; Matthey, B.; Klimka, A.; Galinski, E.A.; Engert, A. Compatible-solute-supported periplasmic expression of functional recombinant proteins under stress conditions. *Appl. Environ. Microbiol.* **2000**, *66*, 1572–1579.

116. Czech, L.; Poehl, S.; Hub, P.; Stoeveken, N.; Bremer, E. Tinkering with osmotically controlled transcription allows enhanced production and excretion of ectoine and hydroxyectoine from a microbial cell factory. *Appl. Environ. Microbiol.* **2108**, 84, e01772–e01717.
117. Kuhlmann, A.U.; Bremer, E. Osmotically regulated synthesis of the compatible solute ectoine in *Bacillus pasteurii* and related *Bacillus* spp. *Appl. Environ. Microbiol.* **2002**, 68, 772–783.
118. Calderon, M.I.; Vargas, C.; Rojo, F.; Iglesias-Guerra, F.; Csonka, L.N.; Ventosa, A.; Nieto, J.J. Complex regulation of the synthesis of the compatible solute ectoine in the halophilic bacterium *Chromohalobacter salexigens* DSM 3043T. *Microbiology* **2004**, 150, 3051–3063.
119. Göller, K.; Ofer, A.; Galinski, E.A. Construction and characterization of an NaCl sensitive mutant of *Halomonas elongata* impaired in ectoine biosynthesis. *FEMS Microbiol. Lett.* **1998**, 161, 293–300.
120. Canovas, D.; Vargas, C.; Iglesias-Guerra, F.; Csonka, L.N.; Rhodes, D.; Ventosa, A.; Nieto, J.J. Isolation and characterization of salt-sensitive mutants of the moderate halophile *Halomonas elongata* and cloning of the ectoine synthesis genes. *J. Biol. Chem.* **1997**, 272, 25794–25801.
121. Ma, Y.; Wang, Q.; Xu, W.; Liu, X.; Gao, X.; Zhang, Y. Stationary phase-dependent accumulation of ectoine is an efficient adaptation strategy in *Vibrio anguillarum* against cold stress. *Microbiol. Res.* **2017**, 205, 8–18.
122. Stöveken, N.; Pittelkow, M.; Sinner, T.; Jensen, R.A.; Heider, J.; Bremer, E. A specialized aspartokinase enhances the biosynthesis of the osmoprotectants ectoine and hydroxyectoine in *Pseudomonas stutzeri* A1501. *J. Bacteriol.* **2011**, 193, 4456–4468.
123. Seip, B.; Galinski, E.A.; Kurz, M. Natural and engineered hydroxyectoine production based on the *Pseudomonas stutzeri* ectABCD-ask gene cluster. *Appl. Environ. Microbiol.* **2011**, 77, 1368–1374.
124. Saum, S.H.; Müller, V. Salinity-dependent switching of osmolyte strategies in a moderately halophilic bacterium: Glutamate induces proline biosynthesis in *Halobacillus halophilus*. *J. Bacteriol.* **2007**, 189, 6968–6975.
125. Saum, S.H.; Müller, V. Regulation of osmoadaptation in the moderate halophile *Halobacillus halophilus*: Chloride, glutamate and switching osmolyte strategies. *Saline Syst.* **2008**, 4, 4.
126. Cheng, X.; Guinn, E.J.; Buechel, E.; Wong, R.; Sengupta, R.; Shkel, I.A.; Record, M.T. Basis of protein stabilization by K glutamate: Unfavorable interactions with carbon, oxygen groups. *Biophys. J.* **2016**, 111, 1854–1865.
127. Diehl, R.C.; Guinn, E.J.; Capp, M.W.; Tsodikov, O.V.; Record, M.T., Jr. Quantifying additive interactions of the osmolyte proline with individual functional groups of proteins: Comparisons with urea and glycine betaine, interpretation of *m*-values. *Biochemistry* **2013**, 52, 5997–6010.
128. Cayley, S.; Lewis, B.A.; Record, M.T., Jr. Origins of the osmoprotective properties of betaine and proline in *Escherichia coli* K-12. *J. Bacteriol.* **1992**, 174, 1586–1595.
129. Tao, P.; Li, H.; Yu, Y.; Gu, J.; Liu, Y. Ectoine and 5-hydroxyectoine accumulation in the halophile *Virgibacillus halodenitrificans* PDB-F2 in response to salt stress. *Appl. Microbiol. Biotechnol.* **2016**, 100, 6779–6789.
130. Klauck, E.; Typas, A.; Hengge, R. The sigmaS subunit of RNA polymerase as a signal integrator and network master regulator in the general stress response in *Escherichia coli*. *Sci. Prog.* **2007**, 90, 103–127.
131. Hengge-Aronis, R. Back to log phase: Sigma S as a global regulator in the osmotic control of gene expression in *Escherichia coli*. *Mol. Microbiol.* **1996**, 21, 887–893.
132. Tanne, C.; Golovina, E.A.; Hoekstra, F.A.; Meffert, A.; Galinski, E.A. Glass-forming property of hydroxyectoine is the cause of its superior function as a desiccation protectant. *Front. Microbiol.* **2014**, 5, 150.
133. Borges, N.; Ramos, A.; Raven, N.D.; Sharp, R.J.; Santos, H. Comparative study of the thermostabilizing properties of mannosylglycerate and other compatible solutes on model enzymes. *Extremophiles* **2002**, 6, 209–216.
134. Van-Thuoc, D.; Hashim, S.O.; Hatti-Kaul, R.; Mamo, G. Ectoine-mediated protection of enzyme from the effect of pH and temperature stress: A study using *Bacillus halodurans* xylanase as a model. *Appl. Microbiol. Biotechnol.* **2013**, 97, 6271–6278.
135. Argandona, M.; Nieto, J.J.; Iglesias-Guerra, F.; Calderon, M.I.; Garcia-Esteva, R.; Vargas, C. Interplay between iron homeostasis and the osmotic stress response in the halophilic bacterium *Chromohalobacter salexigens*. *Appl. Environ. Microbiol.* **2010**, 76, 3575–3589.
136. Scoma, A.; Boon, N. Osmotic stress confers enhanced cell integrity to hydrostatic pressure but impairs growth in *Alcanivorax borkumensis* SK2. *Front. Microbiol.* **2016**, 7, 729.
137. Kish, A.; Griffin, P.L.; Rogers, K.L.; Fogel, M.L.; Hemley, R.J.; Steele, A. High-pressure tolerance in *Halobacterium salinarum* NCR-1 and other non-piezophilic prokaryotes. *Extremophiles* **2012**, 16, 355–361.
138. Schröter, M.A.; Meyer, S.; Hahn, M.B.; Solomun, T.; Sturm, H.; Kunte, H.J. Ectoine protects DNA from damage by ionizing radiation. *Sci. Rep.* **2017**, 7, 15272.

139. Hahn, M.B.; Meyer, S.; Schröter, M.A.; Kunte, H.J.; Solomun, T.; Sturm, H. DNA protection by ectoine from ionizing radiation: Molecular mechanisms. *Phys. Chem. Chem. Phys.* **2017**, *19*, 25717–25722.
140. Meyer, S.; Schröter, M.A.; Hahn, M.B.; Solomun, T.; Sturm, H.; Kunte, H.J. Ectoine can enhance structural changes in DNA in vitro. *Sci. Rep.* **2017**, *7*, 7170.
141. Buenger, J.; Driller, H. Ectoine: An effective natural substance to prevent UVA-induced premature photoaging. *Skin Pharmacol. Physiol.* **2004**, *17*, 232–237.
142. Bünger, J.; Degwert, J.; Driller, H. The protective function of compatible solute ectoine on skin cells and its biomolecules with respect to uv-radiation, immunosuppression and membrane damage. *IFSCC Mag.* **2001**, *4*, 1–6.
143. Schnoor, M.; Voss, P.; Cullen, P.; Boking, T.; Galla, H.J.; Galinski, E.A.; Lorkowski, S. Characterization of the synthetic compatible solute homoectoine as a potent PCR enhancer. *Biochem. Biophys. Res. Commun.* **2004**, *322*, 867–872.
144. Wedeking, A.; Hagen-Euteneuer, N.; Gurgui, M.; Broere, R.; Lentzen, G.; Tolba, R.H.; Galinski, E.; van Echten-Deckert, G. A lipid anchor improves the protective effect of ectoine in inflammation. *Curr. Med. Chem.* **2014**, *21*, 2565–2572.
145. Graf, R.; Anzali, S.; Buenger, J.; Pfluecker, F.; Driller, H. The multifunctional role of ectoine as a natural cell protectant. *Clin. Dermatol.* **2008**, *26*, 326–333.
146. Jorge, C.D.; Borges, N.; Bagyan, I.; Bilstein, A.; Santos, H. Potential applications of stress solutes from extremophiles in protein folding diseases and healthcare. *Extremophiles* **2016**, *20*, 251–259.
147. Bownik, A.; Stepniewska, Z. Ectoine as a promising protective agent in humans and animals. *Arch. Ind. Hig. Toksikol.* **2016**, *67*, 260–265.
148. Strong, P.J.; Kalyuzhnaya, M.; Silverman, J.; Clarke, W.P. A methanotroph-based biorefinery: Potential scenarios for generating multiple products from a single fermentation. *Bioresour. Technol.* **2016**, *215*, 314–323.
149. Cantera, S.; Munoz, R.; Lebrero, R.; Lopez, J.C.; Rodriguez, Y.; Garcia-Encina, P.A. Technologies for the bioconversion of methane into more valuable products. *Curr. Opin. Biotechnol.* **2018**, *50*, 128–135.
150. Vyrides, I.; Stuckey, D.C. Compatible solute addition to biological systems treating waste/wastewater to counteract osmotic and other environmental stresses: A review. *Crit. Rev. Biotechnol.* **2017**, *37*, 865–879.
151. Czech, L.; Stöveken, N.; Bremer, E. EctD-mediated biotransformation of the chemical chaperone ectoine into hydroxyectoine and its mechanosensitive channel-independent excretion. *Microb. Cell Fact.* **2016**, *15*, 126.
152. Becker, J.; Schafer, R.; Kohlstedt, M.; Harder, B.J.; Borchert, N.S.; Stöveken, N.; Bremer, E.; Wittmann, C. Systems metabolic engineering of *Corynebacterium glutamicum* for production of the chemical chaperone ectoine. *Microb. Cell Fact.* **2013**, *12*, 110.
153. Ning, Y.; Wu, X.; Zhang, C.; Xu, Q.; Chen, N.; Xie, X. Pathway construction and metabolic engineering for fermentative production of ectoine in *Escherichia coli*. *Metabol. Eng.* **2016**, *36*, 10–18.
154. Rodriguez-Moya, J.; Argandona, M.; Iglesias-Guerra, F.; Nieto, J.J.; Vargas, C. Temperature- and salinity-decoupled overproduction of hydroxyectoine by *Chromohalobacter salexigens*. *Appl. Environ. Microbiol.* **2013**, *79*, 1018–1023.
155. Perez-Garcia, F.; Ziert, C.; Risse, J.M.; Wendisch, V.F. Improved fermentative production of the compatible solute ectoine by *Corynebacterium glutamicum* from glucose and alternative carbon sources. *J. Biotechnol.* **2017**, *258*, 59–69.
156. Chen, W.; Zhang, S.; Jiang, P.X.; Yao, J.; He, Y.Z.; Chen, L.C.; Gui, X.W.; Dong, Z.Y.; Tang, S.Y. Design of an ectoine-responsive arac mutant and its application in metabolic engineering of ectoine biosynthesis. *Metabol. Eng.* **2015**, *30*, 149–155.
157. Chen, W.C.; Hsu, C.C.; Lan, J.C.; Chang, Y.K.; Wang, L.F.; Wei, Y.H. Production and characterization of ectoine using a moderately halophilic strain *Halomonas salina* BCRC17875. *J. BioSci. Bioeng.* **2018**, doi:10.1016/j.biosc.2017.12.011.
158. Schwibbert, K.; Marin-Sanguino, A.; Bagyan, I.; Heidrich, G.; Lentzen, G.; Seitz, H.; Rampp, M.; Schuster, S.C.; Klenk, H.P.; Pfeiffer, F.; et al. A blueprint of ectoine metabolism from the genome of the industrial producer *Halomonas elongata* DSM 2581T. *Environ. Microbiol.* **2011**, *13*, 1973–1994.
159. Sauer, T.; Galinski, E.A. Bacterial milking: A novel bioprocess for production of compatible solutes. *Biotechnol. Bioengineer* **1998**, *57*, 306–313.
160. Rosa, L.T.; Bianconi, M.E.; Thomas, G.H.; Kelly, D.J. Tripartite ATP-independent periplasmic (TRAP) transporters and tripartite tricarboxylate transporters (TTT): From uptake to pathogenicity. *Front. Cell. Infect. Microbiol.* **2018**, *8*, 33.

161. Grammann, K.; Volke, A.; Kunte, H.J. New type of osmoregulated solute transporter identified in halophilic members of the bacteria domain: TRAP transporter TeaABC mediates uptake of ectoine and hydroxyectoine in *Halomonas elongata* DSM 2581(T). *J. Bacteriol.* **2002**, *184*, 3078–3085.
162. Cyplik, P.; Piotrowska-Cyplik, A.; Marecik, R.; Czarny, J.; Drozdzyńska, A.; Chrzanowski, L. Biological denitrification of brine: The effect of compatible solutes on enzyme activities and fatty acid degradation. *Biodegradation* **2012**, *23*, 663–672.
163. Liu, M.; Peng, Y.; Wang, S.; Liu, T.; Xiao, H. Enhancement of anammox activity by addition of compatible solutes at high salinity conditions. *Bioresour. Technol.* **2014**, *167*, 560–563.
164. Peters, P.; Galinski, E.A.; Trüper, H.G. The biosynthesis of ectoine. *FEMS Microbiol. Lett.* **1990**, *71*, 157–162.
165. Ono, H.; Sawada, K.; Khunajakr, N.; Tao, T.; Yamamoto, M.; Hiramoto, M.; Shinmyo, A.; Takano, M.; Murooka, Y. Characterization of biosynthetic enzymes for ectoine as a compatible solute in a moderately halophilic eubacterium, *Halomonas elongata*. *J. Bacteriol.* **1999**, *181*, 91–99.
166. Reshetnikov, A.S.; Khmelenina, V.N.; Mustakhimov, I.; Trotsenko, Y.A. Genes and enzymes of ectoine biosynthesis in halotolerant methanotrophs. *Methods Enzymol.* **2011**, *495*, 15–30.
167. Lo, C.C.; Bonner, C.A.; Xie, G.; D'Souza, M.; Jensen, R.A. Cohesion group approach for evolutionary analysis of aspartokinase, an enzyme that feeds a branched network of many biochemical pathways. *Microbiol. Mol. Biol. Rev.* **2009**, *73*, 594–651.
168. Reshetnikov, A.S.; Khmelenina, V.N.; Trotsenko, Y.A. Characterization of the ectoine biosynthesis genes of haloalkalotolerant obligate methanotroph “*Methylobacterium alcaliphilum* 20z”. *Arch. Microbiol.* **2006**, *184*, 286–297.
169. Nyssölä, A.; Kerovuo, J.; Kaukinen, P.; von Weymarn, N.; Reinikainen, T. Extreme halophiles synthesize betaine from glycine by methylation. *J. Biol. Chem.* **2000**, *275*, 22196–22201.
170. Boch, J.; Kempf, B.; Schmid, R.; Bremer, E. Synthesis of the osmoprotectant glycine betaine in *Bacillus subtilis*: Characterization of the *gbsAB* genes. *J. Bacteriol.* **1996**, *178*, 5121–5129.
171. Lamark, T.; Kaasen, I.; Eshoo, M.W.; Falkenberg, P.; McDougall, J.; Strom, A.R. DNA sequence and analysis of the *bet* genes encoding the osmoregulatory choline-glycine betaine pathway of *Escherichia coli*. *Mol. Microbiol.* **1991**, *5*, 1049–1064.
172. Salvi, F.; Wang, Y.F.; Weber, I.T.; Gadda, G. Structure of choline oxidase in complex with the reaction product glycine betaine. *Acta Crystallogr. D Biol. Crystallogr.* **2014**, *70*, 405–413.
173. Oliveira, E.F.; Cerqueira, N.M.; Fernandes, P.A.; Ramos, M.J. Mechanism of formation of the internal aldimine in pyridoxal 5'-phosphate-dependent enzymes. *J. Am. Chem. Soc.* **2011**, *133*, 15496–15505.
174. Vetting, M.W.; LP, S.d.C.; Yu, M.; Hegde, S.S.; Magnet, S.; Roderick, S.L.; Blanchard, J.S. Structure and functions of the GNAT superfamily of acetyltransferases. *Arch. Biochem. Biophys.* **2005**, *433*, 212–226.
175. Mustakhimov, I.; Rozova, O.N.; Reshetnikov, A.S.; Khmelenina, V.N.; Murrell, J.C.; Trotsenko, Y.A. Characterization of the recombinant diaminobutyric acid acetyltransferase from *Methylophaga thalassica* and *Methylophaga alcalica*. *FEMS Microbiol. Lett.* **2008**, *283*, 91–96.
176. Widderich, N.; Kobus, S.; Höppner, A.; Ricela, R.; Seubert, A.; Dickschat, J.S.; Heider, J.; Smits, S.H.J.; Bremer, E. Biochemistry and crystal structure of the ectoine synthase: A metal-containing member of the cupin superfamily. *PLoS ONE* **2016**, *11*, e0151285.
177. Höppner, A.; Widderich, N.; Lenders, M.; Bremer, E.; Smits, S.H.J. Crystal structure of the ectoine hydroxylase, a snapshot of the active site. *J. Biol. Chem.* **2014**, *289*, 29570–29583.
178. Garcia-Esteva, R.; Canovas, D.; Iglesias-Guerra, F.; Ventosa, A.; Csonka, L.N.; Nieto, J.J.; Vargas, C. Osmoprotection of *Salmonella enterica* serovar Typhimurium by *N*- γ -acetyldiaminobutyrate, the precursor of the compatible solute ectoine. *Syst. Appl. Microbiol.* **2006**, *29*, 626–633.
179. Canovas, D.; Borges, N.; Vargas, C.; Ventosa, A.; Nieto, J.J.; Santos, H. Role of *N*- γ -acetyldiaminobutyrate as an enzyme stabilizer and an intermediate in the biosynthesis of hydroxyectoine. *Appl. Environ. Microbiol.* **1999**, *65*, 3774–3779.
180. Moritz, K.D.; Amendt, B.; Witt, E.M.H.J.; Galinski, E.A. The hydroxyectoine gene cluster of the non-halophilic acidophile *Acidiphilium cryptum*. *Extremophiles* **2015**, *19*, 87–99.
181. Witt, E.M.; Davies, N.W.; Galinski, E.A. Unexpected property of ectoine synthase and its application for synthesis of the engineered compatible solute ADPC. *Appl. Microbiol. Biotechnol.* **2011**, *91*, 113–122.
182. Dunwell, J.M.; Purvis, A.; Khuri, S. Cupins: The most functionally diverse protein superfamily? *Phytochemistry* **2004**, *65*, 7–17.

183. Dunwell, J.M.; Culham, A.; Carter, C.E.; Sosa-Aguirre, C.R.; Goodenough, P.W. Evolution of functional diversity in the cupin superfamily. *Trends Biochem. Sci.* **2001**, *26*, 740–746.
184. Reuter, K.; Pittelkow, M.; Bursy, J.; Heine, A.; Craan, T.; Bremer, E. Synthesis of 5-hydroxyectoine from ectoine: Crystal structure of the non-heme iron(II) and 2-oxoglutarate-dependent dioxygenase EctD. *PLoS ONE* **2010**, *5*, e10647.
185. Clifton, I.J.; McDonough, M.A.; Ehrismann, D.; Kershaw, N.J.; Granatino, N.; Schofield, C.J. Structural studies on 2-oxoglutarate oxygenases and related double-stranded beta-helix fold proteins. *J. Inorg. Biochem.* **2006**, *100*, 644–669.
186. Widderich, N.; Pittelkow, M.; Hoppner, A.; Mulnaes, D.; Buckel, W.; Gohlke, H.; Smits, S.H.; Bremer, E. Molecular dynamics simulations and structure-guided mutagenesis provide insight into the architecture of the catalytic core of the ectoine hydroxylase. *J. Mol. Biol.* **2014**, *426*, 586–600.
187. Jebbar, M.; Talibart, R.; Gloux, K.; Bernard, T.; Blanco, C. Osmoprotection of *Escherichia coli* by ectoine: Uptake and accumulation characteristics. *J. Bacteriol.* **1992**, *174*, 5027–5035.
188. Lucht, J.M.; Bremer, E. Adaptation of *Escherichia coli* to high osmolarity environments: Osmoregulation of the high-affinity glycine betaine transport system ProU. *FEMS Microbiol. Rev.* **1994**, *14*, 3–20.
189. MacMillan, S.V.; Alexander, D.A.; Culham, D.E.; Kunte, H.J.; Marshall, E.V.; Rochon, D.; Wood, J.M. The ion coupling and organic substrate specificities of osmoregulatory transporter ProP in *Escherichia coli*. *Biochim. Biophys. Acta* **1999**, *1420*, 30–44.
190. Rodriguez-Moya, J.; Argandona, M.; Reina-Bueno, M.; Nieto, J.J.; Iglesias-Guerra, F.; Jebbar, M.; Vargas, C. Involvement of EupR, a response regulator of the NarL/FixJ family, in the control of the uptake of the compatible solutes ectoines by the halophilic bacterium *Chromohalobacter salexigens*. *BMC Microbiol.* **2010**, *10*, 256.
191. Bestvater, T.; Louis, P.; Galinski, E.A. Heterologous ectoine production in *Escherichia coli*: By-passing the metabolic bottle-neck. *Saline Syst.* **2008**, *4*, 12.
192. Kuraku, S.; Zmasek, C.M.; Nishimura, O.; Katoh, K. aLeaves facilitates on-demand exploration of metazoan gene family trees on MAFFT sequence alignment server with enhanced interactivity. *Nucleic Acids Res.* **2013**, *41*, W22–W28.
193. Letunic, I.; Bork, P. Interactive tree of life (iTOL) v3: An online tool for the display and annotation of phylogenetic and other trees. *Nucleic Acids Res.* **2016**, *44*, W242–W245.
194. Salar-Garcia, M.J.; Bernal, V.; Pastor, J.M.; Salvador, M.; Argandona, M.; Nieto, J.J.; Vargas, C.; Canovas, M. Understanding the interplay of carbon and nitrogen supply for ectoines production and metabolic overflow in high density cultures of *Chromohalobacter salexigens*. *Microb. Cell Fact.* **2017**, *16*, 23.
195. Pastor, J.M.; Bernal, V.; Salvador, M.; Argandona, M.; Vargas, C.; Csonka, L.; Sevilla, A.; Iborra, J.L.; Nieto, J.J.; Canovas, M. Role of central metabolism in the osmoadaptation of the halophilic bacterium *Chromohalobacter salexigens*. *J. Biol. Chem.* **2013**, *288*, 17769–17781.
196. Piubeli, F.; Salvador, M.; Argandona, M.; Nieto, J.J.; Bernal, V.; Pastor, J.M.; Canovas, M.; Vargas, C. Insights into metabolic osmoadaptation of the ectoines-producer bacterium *Chromohalobacter salexigens* through a high-quality genome scale metabolic model. *Microb. Cell Fact.* **2018**, *17*, 2.
197. Kindzierski, V.; Raschke, S.; Knabe, N.; Siedler, F.; Scheffer, B.; Pfluger-Grau, K.; Pfeiffer, F.; Oesterheld, D.; Marin-Sanguino, A.; Kunte, H.J. Osmoregulation in the halophilic bacterium *Halomonas elongata*: A case study for integrative systems biology. *PLoS ONE* **2017**, *12*, e0168818.
198. Mustakhimov, I.; Reshetnikov, A.S.; Glukhov, A.S.; Khmelenina, V.N.; Kalyuzhnaya, M.G.; Trotsenko, Y.A. Identification and characterization of EctR1, a new transcriptional regulator of the ectoine biosynthesis genes in the halotolerant methanotroph *Methylobacterium alcaliphilum* 20Z. *J. Bacteriol.* **2010**, *192*, 410–417.
199. Leon, M.J.; Hoffmann, T.; Sanchez-Porro, C.; Heider, J.; Ventosa, A.; Bremer, E. Compatible solute synthesis and import by the moderate halophile *Spiribacter salinus*: Physiology and genomics. *Front. Microbiol.* **2018**, *9*, 108.
200. León, M.J.; Fernandez, A.B.; Ghai, R.; Sanchez-Porro, C.; Rodriguez-Valera, F.; Ventosa, A. From metagenomics to pure culture: Isolation and characterization of the moderately halophilic bacterium *Spiribacter salinus* gen. nov., sp. nov. *Appl. Environ. Microbiol.* **2014**, *80*, 3850–3857.
201. Haldenwang, W.G. The sigma factors of *Bacillus subtilis*. *Microbiol. Rev.* **1995**, *59*, 1–30.
202. Hecker, M.; Pane-Farre, J.; Völker, U. SigB-dependent general stress response in *Bacillus subtilis* and related gram-positive bacteria. *Annu. Rev. Microbiol.* **2007**, *61*, 215–236.
203. Nannapaneni, P.; Hertwig, F.; Depke, M.; Hecker, M.; Mäder, U.; Völker, U.; Steil, L.; van Hijum, S.A. Defining the structure of the general stress regulon of *Bacillus subtilis* using targeted microarray analysis and random forest classification. *Microbiology* **2012**, *158*, 696–707.

204. Feklistov, A.; Sharon, B.D.; Darst, S.A.; Gross, C.A. Bacterial sigma factors: A historical, structural, and genomic perspective. *Annu. Rev. Microbiol.* **2014**, *68*, 357–376.
205. Typas, A.; Becker, G.; Hengge, R. The molecular basis of selective promoter activation by the sigmaS subunit of RNA polymerase. *Mol. Microbiol.* **2007**, *63*, 1296–1306.
206. Bestvater, T.; Galinski, E.A. Investigation into a stress-inducible promoter region from *Marinococcus halophilus* using green fluorescent protein. *Extremophiles* **2002**, *6*, 15–20.
207. Gralla, J.D.; Huo, Y.X. Remodeling and activation of *Escherichia coli* RNA polymerase by osmolytes. *Biochemistry* **2008**, *47*, 13189–13196.
208. Gralla, J.D.; Vargas, D.R. Potassium glutamate as a transcriptional inhibitor during bacterial osmoregulation. *EMBO J.* **2006**, *25*, 1515–1521.
209. Salvador, M.; Argandona, M.; Pastor, J.M.; Bernal, V.; Canovas, M.; Csonka, L.N.; Nieto, J.J.; Vargas, C. Contribution of RpoS to metabolic efficiency and ectoines synthesis during the osmo- and heat-stress response in the halophilic bacterium *Chromohalobacter salexigens*. *Environ. Microbiol. Rep.* **2015**, *7*, 301–311.
210. Higgins, C.F.; Dorman, C.J.; Stirling, D.A.; Waddell, L.; Booth, I.R.; May, G.; Bremer, E. A physiological role for DNA supercoiling in the osmotic regulation of gene expression in *S. typhimurium* and *E. coli*. *Cell* **1988**, *52*, 569–584.
211. Booth, I.R.; Higgins, C.F. Enteric bacteria and osmotic stress: Intracellular potassium glutamate as a secondary signal of osmotic stress? *FEMS Microbiol. Rev.* **1990**, *6*, 239–246.
212. Hoffmann, T.; Wensing, A.; Brosius, M.; Steil, L.; Völker, U.; Bremer, E. Osmotic control of *opuA* expression in *Bacillus subtilis* and its modulation in response to intracellular glycine betaine and proline pools. *J. Bacteriol.* **2013**, *195*, 510–522.
213. Hoffmann, T.; Bleisteiner, M.; Sappa, P.K.; Steil, L.; Mader, U.; Volker, U.; Bremer, E. Synthesis of the compatible solute proline by *Bacillus subtilis*: Point mutations rendering the osmotically controlled *proHJ* promoter hyperactive. *Environ. Microbiol.* **2017**, *19*, 3700–3720.
214. Deochand, D.K.; Grove, A. MarR family transcription factors: Dynamic variations on a common scaffold. *Crit. Rev. Biochem. Mol. Biol.* **2017**, *52*, 595–613.
215. Mustakhimov, I.; Reshetnikov, A.S.; Fedorov, D.N.; Khmelenina, V.N.; Trotsenko, Y.A. Role of RctR as transcriptional regulator of ectoine biosynthesis genes in *Methylophaga thalassica*. *Biochem. Biokhimiia* **2012**, *77*, 857–863.
216. Romeo, Y.; Bouvier, J.; Gutierrez, C. Osmotic regulation of transcription in *Lactococcus lactis*: Ionic strength-dependent binding of the BusR repressor to the *busA* promoter. *FEBS Lett.* **2007**, *581*, 3387–3390.
217. Romeo, Y.; Obis, D.; Bouvier, J.; Guillot, A.; Fourcans, A.; Bouvier, I.; Gutierrez, C.; Mistou, M.Y. Osmoregulation in *Lactococcus lactis*: BusR, a transcriptional repressor of the glycine betaine uptake system BusA. *Mol. Microbiol.* **2003**, *47*, 1135–1147.
218. Shikuma, N.J.; Davis, K.R.; Fong, J.N.C.; Yildiz, F.H. The transcriptional regulator, CosR, controls compatible solute biosynthesis and transport, motility and biofilm formation in *Vibrio cholerae*. *Environ. Microbiol.* **2013**, *15*, 1387–1399.
219. Shao, Z.; Deng, W.; Li, S.; He, J.; Ren, S.; Huang, W.; Lu, Y.; Zhao, G.; Cai, Z.; Wang, J. GlnR-mediated regulation of *ectABCD* transcription expands the role of the GlnR regulon to osmotic stress management. *J. Bacteriol.* **2015**, *197*, 3041–3307.
220. Sadeghi, A.; Soltani, B.M.; Nekouei, M.K.; Jouzani, G.S.; Mirzaei, H.H.; Sadeghizadeh, M. Diversity of the ectoines biosynthesis genes in the salt tolerant *Streptomyces* and evidence for inductive effect of ectoines on their accumulation. *Microbiol. Res.* **2014**, *169*, 699–708.
221. Kurz, M.; Burch, A.Y.; Seip, B.; Lindow, S.E.; Gross, H. Genome-driven investigation of compatible solute biosynthesis pathways of *Pseudomonas syringae* pv. *syringae* and their contribution to water stress tolerance. *Appl. Environ. Microbiol.* **2010**, *76*, 5452–5462.
222. Chen, I.A.; Markowitz, V.M.; Chu, K.; Palaniappan, K.; Szeto, E.; Pillay, M.; Ratner, A.; Huang, J.; Andersen, E.; Huntemann, M.; et al. IMG/M: Integrated genome and metagenome comparative data analysis system. *Nucleic Acids Res.* **2017**, *45*, D507–D516.
223. Soucy, S.M.; Huang, J.; Gogarten, J.P. Horizontal gene transfer: Building the web of life. *Nat. Rev. Genet.* **2015**, *16*, 472–482.
224. Treangen, T.J.; Rocha, E.P.C. Horizontal transfer, not duplication, drives the expansion of protein families in prokaryotes. *PLoS Genet.* **2011**, *7*, e1001284.

225. Wagner, A.; Whitaker, R.J.; Krause, D.J.; Heilers, J.H.; van Wolferen, M.; van der Does, C.; Albers, S.V. Mechanisms of gene flow in archaea. *Nat. Rev. Microbiol.* **2017**, *15*, 492–501.
226. Yang, J.C.; Madupu, R.; Durkin, A.S.; Ekborg, N.A.; Pedomallu, C.S.; Hostetler, J.B.; Radune, D.; Toms, B.S.; Henrissat, B.; Coutinho, P.M.; et al. The complete genome of *Teredinibacter turnerae* T7901: An intracellular endosymbiont of marine wood-boring bivalves (shipworms). *PLoS ONE* **2009**, *4*, e6085.
227. Ferreira, C.; Soares, A.R.; Lamosa, P.; Santos, M.A.; da Costa, M.S. Comparison of the compatible solute pool of two slightly halophilic planctomycetes species, *Gimesia maris* and *Rubinisphaera brasiliensis*. *Extremophiles* **2016**, *20*, 811–820.
228. Amiri Moghaddam, J.; Boehringer, N.; Burdziak, A.; Kunte, H.J.; Galinski, E.A.; Schäberle, T.F. Different strategies of osmoadaptation in the closely related marine myxobacteria *Enhygromyxa salina* SWB007 and *Plesiocystis pacifica* SIR-1. *Microbiology* **2016**, *162*, 641–661.
229. Qin, W.; Heal, K.R.; Ramdasi, R.; Kobelt, J.N.; Martens-Habben, W.; Bertagnolli, A.D.; Amin, S.A.; Walker, C.B.; Urakawa, H.; Konneke, M.; et al. *Nitrosopumilus maritimus* gen. nov., sp. nov., *Nitrosopumilus cobalaminigenes* sp. nov., *Nitrosopumilus oxycinae* sp. nov., and *Nitrosopumilus ureiphilus* sp. nov., four marine ammonia-oxidizing archaea of the phylum thaumarchaeota. *Int. J. Syst. Evol. Microbiol.* **2017**, *67*, 5067–5079.
230. Simon, M.; Scheuner, C.; Meier-Kolthoff, J.P.; Brinkhoff, T.; Wagner-Döbler, I.; Ulbrich, M.; Klenk, H.P.; Schomburg, D.; Petersen, J.; Göker, M. Phylogenomics of *Rhodobacteraceae* reveals evolutionary adaptation to marine and non-marine habitats. *ISME J.* **2017**, *11*, 1483–1499.
231. Wagner-Döbler, I.; Biebl, H. Environmental biology of the marine *Roseobacter* lineage. *Annu. Rev. Microbiol.* **2006**, *60*, 255–280.
232. Luo, H.; Moran, M.A. Evolutionary ecology of the marine *Roseobacter* clade. *Microbiol. Mol. Biol. Rev.* **2014**, *78*, 573–587.
233. Welsh, D.T. Ecological significance of compatible solute accumulation by micro-organisms: From single cells to global climate. *FEMS Microbiol. Rev.* **2000**, *24*, 263–290.
234. Warren, C. Do microbial osmolytes or extracellular depolymerization products accumulate as soil dries? *Soil Biol. Biochem.* **2016**, *98*, 54–63.
235. Warren, C.R. Quaternary ammonium compounds can be abundant in some soils and are taken up as intact molecules by plants. *New Phytol.* **2013**, *198*, 476–485.
236. Warren, C.R. Response of osmolytes in soil to drying and rewetting. *Soil Biol. Biochem.* **2014**, *70*, 22–32.
237. Bouskill, N.J.; Wood, T.E.; Baran, R.; Hao, Z.; Ye, Z.; Bowen, B.P.; Lim, H.C.; Nico, P.S.; Holman, H.Y.; Gilbert, B.; et al. Belowground response to drought in a tropical forest soil. II. Change in microbial function impacts carbon composition. *Front. Microbiol.* **2016**, *7*, 323.
238. Bouskill, N.J.; Wood, T.E.; Baran, R.; Ye, Z.; Bowen, B.P.; Lim, H.; Zhou, J.; Nostrand, J.D.; Nico, P.; Northen, T.R.; et al. Belowground response to drought in a tropical forest soil. I. Changes in microbial functional potential and metabolism. *Front. Microbiol.* **2016**, *7*, 525.
239. Mosier, A.C.; Justice, N.B.; Bowen, B.P.; Baran, R.; Thomas, B.C.; Northen, T.R.; Banfield, J.F. Metabolites associated with adaptation of microorganisms to an acidophilic, metal-rich environment identified by stable-isotope-enabled metabolomics. *mBio* **2013**, *4*, e00484–e00412.
240. Poolman, B.; Spitzer, J.J.; Wood, J.M. Bacterial osmosensing: Roles of membrane structure and electrostatics in lipid-protein and protein-protein interactions. *Biochim. Biophys. Acta* **2004**, *1666*, 88–104.
241. Ziegler, C.; Bremer, E.; Krämer, R. The BCCT family of carriers: From physiology to crystal structure. *Mol. Microbiol.* **2010**, *78*, 13–34.
242. Krämer, R. Bacterial stimulus perception and signal transduction: Response to osmotic stress. *Chem. Rec* **2010**, *10*, 217–229.
243. Culham, D.E.; Shkel, I.A.; Record, M.T., Jr.; Wood, J.M. Contributions of coulombic and Hofmeister effects to the osmotic activation of *Escherichia coli* transporter ProP. *Biochemistry* **2016**, *55*, 1301–1313.
244. Gul, N.; Schuurman-Wolters, G.; Karasawa, A.; Poolman, B. Functional characterization of amphipathic alpha-helix in the osmoregulatory ABC transporter OpuA. *Biochemistry* **2012**, *51*, 5142–5152.
245. Perez, C.; Faust, B.; Mehdipour, A.R.; Francesconi, K.A.; Forrest, L.R.; Ziegler, C. Substrate-bound outward-open state of the betaine transporter BetP provides insights into Na⁺ coupling. *Nat. Commun.* **2014**, *5*, 4231.
246. Perez, C.; Koshy, C.; Yildiz, O.; Ziegler, C. Alternating-access mechanism in conformationally asymmetric trimers of the betaine transporter BetP. *Nature* **2012**, *490*, 126–130.

247. Hahne, H.; Mäder, U.; Otto, A.; Bonn, F.; Steil, L.; Bremer, E.; Hecker, M.; Becher, D. A comprehensive proteomics and transcriptomics analysis of *Bacillus subtilis* salt stress adaptation. *J. Bacteriol.* **2010**, *192*, 870–882.
248. Kappes, R.M.; Kempf, B.; Kneip, S.; Boch, J.; Gade, J.; Meier-Wagner, J.; Bremer, E. Two evolutionarily closely related ABC transporters mediate the uptake of choline for synthesis of the osmoprotectant glycine betaine in *Bacillus subtilis*. *Mol. Microbiol.* **1999**, *32*, 203–216.
249. Morbach, S.; Krämer, R. Body shaping under water stress: Osmosensing and osmoregulation of solute transport in bacteria. *ChemBiochem* **2002**, *3*, 384–397.
250. Rice, A.J.; Park, A.; Pinkett, H.W. Diversity in ABC transporters: Type I, II and III importers. *Crit. Rev. Biochem. Mol. Biol.* **2014**, *49*, 426–437.
251. Ter Beek, J.; Guskov, A.; Slotboom, D.J. Structural diversity of ABC transporters. *J. Gen. Physiol.* **2014**, *143*, 419–435.
252. Jebbar, M.; von Blohn, C.; Bremer, E. Ectoine functions as an osmoprotectant in *Bacillus subtilis* and is accumulated via the ABC-transport system OpuC. *FEMS Microbiol. Lett.* **1997**, *154*, 325–330.
253. Choquet, G.; Jehan, N.; Pissavin, C.; Blanco, C.; Jebbar, M. OusB, a broad-specificity ABC-type transporter from *Erwinia chrysanthemi*, mediates uptake of glycine betaine and choline with a high affinity. *Appl. Environ. Microbiol.* **2005**, *71*, 3389–3398.
254. Yan, N. Structural biology of the major facilitator superfamily transporters. *Annu. Rev. Biophys.* **2015**, *44*, 257–283.
255. Gloux, K.; Touze, T.; Pagot, Y.; Jouan, B.; Blanco, C. Mutations of *ousA* alter the virulence of *Erwinia chrysanthemi*. *Mol. Plant. Microbe Interact.* **2005**, *18*, 150–157.
256. Kappes, R.M.; Kempf, B.; Bremer, E. Three transport systems for the osmoprotectant glycine betaine operate in *Bacillus subtilis*: Characterization of OpuD. *J. Bacteriol.* **1996**, *178*, 5071–5079.
257. Vermeulen, V.; Kunte, H.J. *Marinococcus halophilus* DSM 20408T encodes two transporters for compatible solutes belonging to the betaine-carnitine-choline transporter family: Identification and characterization of ectoine transporter EctM and glycine betaine transporter BetM. *Extremophiles* **2004**, *8*, 175–184.
258. Steger, R.; Weinand, M.; Krämer, R.; Morbach, S. LcoP, an osmoregulated betaine/ectoine uptake system from *Corynebacterium glutamicum*. *FEBS Lett.* **2004**, *573*, 155–160.
259. Peter, H.; Weil, B.; Burkovski, A.; Kramer, R.; Morbach, S. *Corynebacterium glutamicum* is equipped with four secondary carriers for compatible solutes: Identification, sequencing, and characterization of the proline/ectoine uptake system, ProP, and the ectoine/proline/glycine betaine carrier, EctP. *J. Bacteriol.* **1998**, *180*, 6005–6012.
260. Perez, C.; Koshy, C.; Ressler, S.; Nicklisch, S.; Krämer, R.; Ziegler, C. Substrate specificity and ion coupling in the Na⁺/betaine symporter BetP. *EMBO J.* **2011**, *30*, 1221–1229.
261. Kuhlmann, S.I.; Terwisscha van Scheltinga, A.C.; Bienert, R.; Kunte, H.J.; Ziegler, C. 1.55 Å structure of the ectoine binding protein TeaA of the osmoregulated TRAP-transporter TeaABC from *Halomonas elongata*. *Biochemistry* **2008**, *47*, 9475–9485.
262. Du, Y.; Shi, W.W.; He, Y.X.; Yang, Y.H.; Zhou, C.Z.; Chen, Y. Structures of the substrate-binding protein provide insights into the multiple compatible solute binding specificities of the *Bacillus subtilis* ABC transporter OpuC. *Biochem. J.* **2011**, *436*, 283–289.
263. Schulz, A.; Stöveken, N.; Binzen, I.M.; Hoffmann, T.; Heider, J.; Bremer, E. Feeding on compatible solutes: A substrate-induced pathway for uptake and catabolism of ectoines and its genetic control by EnuR. *Environ. Microbiol.* **2017**, *19*, 926–946.
264. Galinski, E.A.; Herzog, R.M. The role of trehalose as a substitute for nitrogen-containing compatible solutes (*Ectothiorhodospira halochloris*). *Arch. Microbiol.* **1990**, *153*, 607–613.
265. Jebbar, M.; Sohn-Bosser, L.; Bremer, E.; Bernard, T.; Blanco, C. Ectoine-induced proteins in *Sinorhizobium meliloti* include an ectoine ABC-type transporter involved in osmoprotection and ectoine catabolism. *J. Bacteriol.* **2005**, *187*, 1293–1304.
266. Vargas, C.; Jebbar, M.; Carrasco, R.; Blanco, C.; Calderon, M.I.; Iglesias-Guerra, F.; Nieto, J.J. Ectoines as compatible solutes and carbon and energy sources for the halophilic bacterium *Chromohalobacter salexigens*. *J. Appl. Microbiol.* **2006**, *100*, 98–107.
267. Hanekop, N.; Höing, M.; Sohn-Böscher, L.; Jebbar, M.; Schmitt, L.; Bremer, E. Crystal structure of the ligand-binding protein EhuB from *Sinorhizobium meliloti* reveals substrate recognition of the compatible solutes ectoine and hydroxyectoine. *J. Mol. Biol.* **2007**, *374*, 1237–1250.

268. Lecher, J.; Pittelkow, M.; Zobel, S.; Bursy, J.; Bonig, T.; Smits, S.H.; Schmitt, L.; Bremer, E. The crystal structure of UehA in complex with ectoine—A comparison with other TRAP-T binding proteins. *J. Mol. Biol.* **2009**, *389*, 58–73.
269. Rigali, S.; Derouaux, A.; Giannotta, F.; Dusart, J. Subdivision of the helix-turn-helix GntR family of bacterial regulators in the FadR, HutC, MocR, and YtrA subfamilies. *J. Biol. Chem.* **2002**, *277*, 12507–12515.
270. Schulz, A.; Hermann, L.; Freibert, S.-A.; Bönig, T.; Hoffmann, T.; Riclea, R.; Dickschat, J.S.; Heider, J.; Bremer, E. Transcriptional regulation of ectoine catabolism in response to multiple metabolic and environmental cues. *Environ. Microbiol.* **2017**, *19*, 4599–4619.
271. Kumarevel, T.; Nakano, N.; Ponnuraj, K.; Gopinath, S.C.; Sakamoto, K.; Shinkai, A.; Kumar, P.K.; Yokoyama, S. Crystal structure of glutamine receptor protein from *Sulfolobus tokodaii* strain 7 in complex with its effector L-glutamine: Implications of effector binding in molecular association and DNA binding. *Nucleic Acids Res.* **2008**, *36*, 4808–4820.
272. Shrivastava, T.; Ramachandran, R. Mechanistic insights from the crystal structures of a feast/famine regulatory protein from *Mycobacterium tuberculosis* h37rv. *Nucleic Acids Res.* **2007**, *35*, 7324–7335.
273. Yokoyama, K.; Ishijima, S.A.; Clowney, L.; Koike, H.; Aramaki, H.; Tanaka, C.; Makino, K.; Suzuki, M. Feast/famine regulatory proteins (FFRPs): *Escherichia coli* LRP, AsnC and related archaeal transcription factors. *FEMS Microbiol. Rev.* **2006**, *30*, 89–108.
274. Copeland, A.; O'Connor, K.; Lucas, S.; Lapidus, A.; Berry, K.W.; Detter, J.C.; Del Rio, T.G.; Hammon, N.; Dalin, E.; Tice, H.; et al. Complete genome sequence of the halophilic and highly halotolerant *Chromohalobacter salexigens* type strain (1H11^T). *Stand. Genom. Sci.* **2011**, *5*, 379–388.
275. Bramucci, E.; Milano, T.; Pascarella, S. Genomic distribution and heterogeneity of MocR-like transcriptional factors containing a domain belonging to the superfamily of the pyridoxal-5'-phosphate dependent enzymes of fold type I. *Biochem. Biophys. Res. Commun.* **2011**, *415*, 88–93.
276. Suvorova, I.; Rodionov, D. Comparative genomics of pyridoxal 5'-phosphate-dependent transcription factor regulons in *Bacteria*. *MGen* **2016**, *2*, e000047.
277. Yu, Q.; Cai, H.; Zhang, Y.; He, Y.; Chen, L.; Merritt, J.; Zhang, S.; Dong, Z. Negative regulation of ectoine uptake and catabolism in *Sinorhizobium meliloti*: Characterization of the EhuR gene. *J. Bacteriol.* **2017**, *199*, e00119–e00116.
278. Belitsky, B.R. *Bacillus subtilis* GabR, a protein with DNA-binding and aminotransferase domains, is a PLP-dependent transcriptional regulator. *J. Mol. Biol.* **2004**, *340*, 655–664.
279. Edayathumangalam, R.; Wu, R.; Garcia, R.; Wang, Y.; Wang, W.; Kreinbring, C.A.; Bach, A.; Liao, J.; Stone, T.A.; Terwilliger, T.C.; et al. Crystal structure of *Bacillus subtilis* GabR, an autorepressor and transcriptional activator of *gabT*. *Proc. Natl. Acad. Sci. USA* **2013**, *110*, 17820–17825.
280. Okuda, K.; Ito, T.; Goto, M.; Takenaka, T.; Hemmi, H.; Yoshimura, T. Domain characterization of *Bacillus subtilis* GabR, a pyridoxal 5'-phosphate-dependent transcriptional regulator. *J. Biochem.* **2015**, *158*, 225–234.
281. Okuda, K.; Kato, S.; Ito, T.; Shiraki, S.; Kawase, Y.; Goto, M.; Kawashima, S.; Hemmi, H.; Fukada, H.; Yoshimura, T. Role of the aminotransferase domain in *Bacillus subtilis* GabR, a pyridoxal 5'-phosphate-dependent transcriptional regulator. *Mol. Microbiol.* **2015**, *95*, 245–257.
282. Park, S.A.; Park, Y.S.; Lee, K.S. Crystal structure of the C-terminal domain of *Bacillus subtilis* GabR reveals a closed conformation by gamma-aminobutyric acid binding, inducing transcriptional activation. *Biochem. Biophys. Res. Commun.* **2017**, *487*, 287–291.
283. Wu, R.; Sanishvili, R.; Belitsky, B.R.; Juncosa, J.I.; Le, H.V.; Lehrer, H.J.; Farley, M.; Silverman, R.B.; Petsko, G.A.; Ringe, D.; et al. Plp and GABA trigger GabR-mediated transcription regulation in *Bacillus subtilis* via external aldimine formation. *Proc. Natl. Acad. Sci. USA* **2017**, *114*, 3891–3896.
284. Steffen-Munsberg, F.; Vickers, C.; Kohls, H.; Land, H.; Mallin, H.; Nobili, A.; Skalden, L.; van den Bergh, T.; Joosten, H.J.; Berglund, P.; et al. Bioinformatic analysis of a PLP-dependent enzyme superfamily suitable for biocatalytic applications. *Biotechnol. Adv.* **2015**, *33*, 566–604.
285. Phillips, R.S. Chemistry and diversity of pyridoxal-5'-phosphate dependent enzymes. *Biochim. Biophys. Acta* **2015**, *1854*, 1167–1174.
286. Biasini, M.; Bienert, S.; Waterhouse, A.; Arnold, K.; Studer, G.; Schmidt, T.; Kiefer, F.; Cassarino, T.G.; Bertoni, M.; Bordoli, L.; et al. SWISS-MODEL: Modelling protein tertiary and quaternary structure using evolutionary information. *Nucleic Acids Res.* **2014**, *42*, W252–W258.
287. Delano, W.L. *The PyMol Molecular Graphics System*; Delano Scientific: San Carlos, CA, USA, 2002.

288. Dey, A.; Shree, S.; Pandey, S.K.; Tripathi, R.P.; Ramachandran, R. Crystal structure of *Mycobacterium tuberculosis* H37Rv AldR (Rv2779c), a regulator of the *ald* gene: DNA-binding, and identification of small-molecule inhibitors. *J. Biol. Chem.* **2016**, *291*, 11967–11980.
289. Kamensek, S.; Browning, D.F.; Podlessek, Z.; Busby, S.J.; Zgur-Bertok, D.; Butala, M. Silencing of DNase colicin e8 gene expression by a complex nucleoprotein assembly ensures timely colicin induction. *PLoS Genet.* **2015**, *11*, e1005354.
290. Zschiedrich, C.P.; Keidel, V.; Szurmant, H. Molecular mechanisms of two-component signal transduction. *J. Mol. Biol.* **2016**, *428*, 3752–3775.
291. Fernandez, I.; Cornaciu, I.; Carrica, M.D.; Uchikawa, E.; Hoffmann, G.; Sieira, R.; Marquez, J.A.; Goldbaum, F.A. Three-dimensional structure of full-length NtrX, an unusual member of the NtrC family of response regulators. *J. Mol. Biol.* **2017**, *429*, 1192–1212.
292. Bonato, P.; Alves, L.R.; Osaki, J.H.; Rigo, L.U.; Pedrosa, F.O.; Souza, E.M.; Zhang, N.; Schumacher, J.; Buck, M.; Wassem, R.; et al. The NtrY-NtrX two-component system is involved in controlling nitrate assimilation in *Herbaspirillum seropedicae* strain SmR1. *FEBS J.* **2016**, *283*, 3919–3930.
293. Calatrava-Morales, N.; Nogales, J.; Amezttoy, K.; van Steenberg, B.; Soto, M.J. The NtrY/NtrX system of *Sinorhizobium meliloti* GR4 regulates motility, EPS I production and nitrogen metabolism but is dispensable for symbiotic nitrogen fixation. *Mol. Plant. Microbe Interact.* **2017**, *30*, 566–577.
294. Robledo, M.; Peregrina, A.; Millan, V.; Garcia-Tomsig, N.I.; Torres-Quesada, O.; Mateos, P.F.; Becker, A.; Jimenez-Zurdo, J.I. A conserved alpha-proteobacterial small RNA contributes to osmoadaptation and symbiotic efficiency of rhizobia on legume roots. *Environ. Microbiol.* **2017**, *19*, 2661–2680.
295. Park, J.S.; Cho, B.C.; Simpson, A.G.B. *Halocafeteria seosinensis* gen. et. sp. nov. (bicosoecida), a halophilic bacterivorous nanoflagellate isolated from a solar saltern. *Extremophiles* **2006**, *10*, 493–504.
296. Foissner, W.; Filker, S.; Stoeck, T. *Schmidingerothrix salinarum* nov spec. is the molecular sister of the large oxytrichid clade (ciliophora, hypotricha). *J. Eukary Microbiol.* **2014**, *61*, 61–74.
297. Ventosa, A.; de la Haba, R.R.; Sanchez-Porro, C.; Papke, R.T. Microbial diversity of hypersaline environments: A metagenomic approach. *Curr. Opin. Microbiol.* **2015**, *25*, 80–87.
298. Moreira, D.; Lopez-Garcia, P. Protist evolution: Stealing genes to gut it out. *Curr. Biol.* **2017**, *27*, R223–R225.
299. Rogozin, I.B.; Carmel, L.; Csuros, M.; Koonin, E.V. Origin and evolution of spliceosomal introns. *Biol. Direct* **2012**, *7*, 11.
300. Putnam, N.H.; Butts, T.; Ferrier, D.E.K.; Furlong, R.F.; Hellsten, U.; Kawashima, T.; Robinson-Rechavi, M.; Shoguchi, E.; Terry, A.; Yu, J.K.; et al. The amphioxus genome and the evolution of the chordate karyotype. *Nature* **2008**, *453*, 1064–1071.
301. Simakov, O.; Kawashima, T.; Marletaz, F.; Jenkins, J.; Koyanagi, R.; Mitros, T.; Hisata, K.; Bredeson, J.; Shoguchi, E.; Gyoja, F.; et al. Hemichordate genomes and deuterostome origins. *Nature* **2015**, *527*, 459–465.
302. Husnik, F.; McCutcheon, J.P. Functional horizontal gene transfer from bacteria to eukaryotes. *Nat. Rev. Microbiol.* **2018**, *16*, 67–79.
303. Landa, M.; Burns, A.S.; Roth, S.J.; Moran, M.A. Bacterial transcriptome remodeling during sequential co-culture with a marine dinoflagellate and diatom. *ISMEJ* **2017**, *11*, 2677–2690.
304. Hoffmann, T.; von Blohn, C.; Stanek, A.; Moses, S.; Barzantny, S.; Bremer, E. Synthesis, release, and recapture of the compatible solute proline by osmotically stressed *Bacillus subtilis* cells. *Appl. Environ. Microbiol.* **2012**, *78*, 5753–5762.
305. Börngen, K.; Battle, A.R.; Möker, N.; Morbach, S.; Marin, K.; Martinac, B.; Krämer, R. The properties and contribution of the *Corynebacterium glutamicum* MscS variant to fine-tuning of osmotic adaptation. *Biochim. Biophys. Acta* **2010**, *1798*, 2141–2149.



PRIMER

With a pinch of extra salt—Did predatory protists steal genes from their food?

Laura Czech¹, Erhard Bremer^{1,2*}

1 Department of Biology, Laboratory for Molecular Microbiology, Philipps-University Marburg, Marburg, Germany, **2** LOEWE-Center for Synthetic Microbiology, Philipps-University Marburg, Marburg, Germany

* bremer@staff.uni-marburg.de

5.1.2. With a pinch of extra salt - Did predatory protists steal genes from their food?

Czech L, Bremer E. With a pinch of extra salt - Did predatory protists steal genes from their food? *PLoS Biol* 2018;16:e2005163. doi: 10.1371/journal.pbio.2005163.

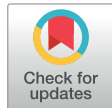
The following mini review "With a pinch of extra salt - Did predatory protists steal genes from their food?" was published as a *Primer* in *PLoS Biology* accompanying the research paper by Weinisch *et al.* on ectoine production in the halophilic ciliate *S. salinarum* [75]. When this seminal discovery was accepted by *PLoS Biology*, Prof. E. Bremer and I were invited to write a short review about ectoines as stress protectants in *Bacteria* and *Archaea*. E. Bremer and I wrote the manuscript together and I prepared all figures that are part of this publication. The mini review was then published after a peer-review process.

5.1.2.1. Original publication



PRIMER

With a pinch of extra salt—Did predatory protists steal genes from their food?

Laura Czech¹, Erhard Bremer^{1,2*}¹ Department of Biology, Laboratory for Molecular Microbiology, Philipps-University Marburg, Marburg, Germany, ² LOEWE-Center for Synthetic Microbiology, Philipps-University Marburg, Marburg, Germany* bremer@staff.uni-marburg.de

OPEN ACCESS

Citation: Czech L, Bremer E (2018) With a pinch of extra salt—Did predatory protists steal genes from their food? PLoS Biol 16(2): e2005163. <https://doi.org/10.1371/journal.pbio.2005163>

Published: February 2, 2018

Copyright: © 2018 Czech, Bremer. This is an open access article distributed under the terms of the [Creative Commons Attribution License](https://creativecommons.org/licenses/by/4.0/), which permits unrestricted use, distribution, and reproduction in any medium, provided the original author and source are credited.

Funding: Deutsche Forschungsgemeinschaft (DFG) (grant number Collaborative Research Center SFB 987). The funder had no role in study design, data collection and analysis, decision to publish, or preparation of the manuscript.

Competing interests: The authors have declared that no competing interests exist.

Abbreviations: DMS, dimethylsulfide; DMSP, dimethylsulfoniopropionate; MscL, mechanosensitive channel large; MscM, mechanosensitive channel mini; MscS, mechanosensitive channel small; SAM, S-adenosylmethionine.

Provenance: Commissioned; externally peer reviewed

Abstract

The cellular adjustment of Bacteria and Archaea to high-salinity habitats is well studied and has generally been classified into one of two strategies. These are to accumulate high levels either of ions (the “salt-in” strategy) or of physiologically compliant organic osmolytes, the compatible solutes (the “salt-out” strategy). Halophilic protists are ecophysiological important inhabitants of salt-stressed ecosystems because they are not only very abundant but also represent the majority of eukaryotic lineages in nature. However, their cellular osmotic stress responses have been largely neglected. Recent reports have now shed new light on this issue using the geographically widely distributed halophilic heterotrophic protists *Halo-caferia seosinensis*, *Pharyngomonas kirbyi*, and *Schmidingerothrix salinarum* as model systems. Different approaches led to the joint conclusion that these unicellular Eukarya use the salt-out strategy to cope successfully with the persistent high salinity in their habitat. They accumulate various compatible solutes, e.g., glycine betaine, myo-inositol, and ectoines. The finding of intron-containing biosynthetic genes for ectoine and hydroxyectoine, their salt stress-responsive transcription in *H. seosinensis*, and the production of ectoine and its import by *S. salinarum* come as a considerable surprise because ectoines have thus far been considered exclusive prokaryotic compatible solutes. Phylogenetic considerations of the ectoine/hydroxyectoine biosynthetic genes of *H. seosinensis* suggest that they have been acquired via lateral gene transfer by these bacterivorous Eukarya from ectoine/hydroxyectoine-producing food bacteria that populate the same habitat.

Introduction

The invention of a semipermeable cytoplasmic membrane was a key event in the development of primordial cells because it provided a privileged space for the faithful copying of the genetic material, a reaction vessel for biochemical transformations, and for energy generation to fuel growth. The cytoplasm of microorganisms is a highly crowded compartment caused by large concentrations of nucleic acids, proteins, and metabolites [1,2]. Together, these compounds generate a considerable osmotic potential and thereby instigate osmotically driven water influx, a process that, in turn, causes the buildup of a hydrostatic pressure, the turgor [2–4], in walled microbial cells. Decreases and increases in the external osmolarity are ubiquitous environmental cues and stressors that affect growth and survival of many organisms [5]. Cellular

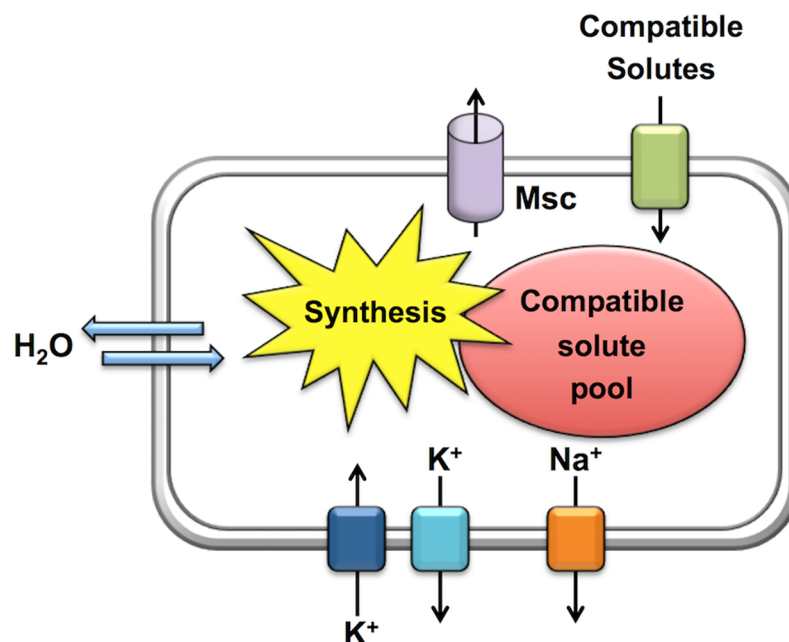


Fig 1. Schematic illustration of the salt-out adjustment strategy of a microbial cell to hyper- and hypoosmotic challenges. Msc, mechanosensitive channels.

<https://doi.org/10.1371/journal.pbio.2005163.g001>

response to fluctuations in external osmolarity have been particularly intensively studied in bacteria (Fig 1) [2,6,7], and these studies also provided a basic framework for an understanding of key osmotic stress adaptation strategies employed by eukaryotic cells [8–11].

Maintenance of turgor is considered critical for the growth of microorganisms [1–4,12], but the semipermeable cytoplasmic membrane makes cells vulnerable to fluctuations in the external osmolarity and salinity, as cells seem to strive to attain crowding homeostasis and thus turgor within physiologically acceptable boundaries [1]. Hyperosmotic conditions result in water efflux, plasmolysis, and reduction in vital turgor [5]. Conversely, hypoosmotic circumstances trigger water influx and thereby cause an undue rise in turgor that can lead in extreme cases to the rupture of the cell [3]. In some organisms, dedicated water channels, the aquaporins, allow accelerated water fluxes across the cytoplasmic membrane in response to external osmotic changes [13], but their potential physiological role in the adaptation of microorganisms to fluctuations in the external osmolarity is not truly understood [14].

Because no cell can actively (e.g., through expenditure of energy) pump water across the cytoplasmic membrane in a directed fashion, adjustment in the proper hydration of the cytoplasm has to rely on indirect measures to direct water fluxes [1–3,5]. To accomplish this under hyperosmotic conditions, microbial cells accumulate ions through transport and synthesize or import physiologically compliant organic osmolytes [15], the compatible solutes (Box 1), to promote water retention and influx (Fig 1) [2,6,7]. Conversely, under hypoosmotic conditions, the cell rapidly expels these compounds through the transient opening of mechanosensitive channels (Msc) (Fig 1) to curb excessive water influx and to prevent a potentially unsustainable increase in turgor [3,16].

Msc: Emergency relief valves

The opening and closing of Msc occurs within milliseconds and is a passive cellular response that is triggered by increased tension in the lateral plain of the cytoplasmic membrane upon

Box 1. Biological function, molecular mechanism, and diversity of compatible solutes

Compatible solutes are operationally defined as organic osmolytes that can be amassed to exceedingly high cellular concentrations without disturbing vital biochemical and physiological processes [17]. They are therefore widely used by Bacteria, Archaea, and Eukarya to counteract the high-salinity-and/or high-osmolarity-instigated water efflux from the cytoplasm [6–8,18]. The physicochemical attributes of compatible solutes make them highly compliant with the functionality of macromolecules and cellular components. With respect to proteins, compatible solutes operate against their denatured state and thereby promote proper hydration, folding, and stability [15,19,20], effects that led to their description as chemical chaperones. Studies into the mechanism(s) through which these stabilizing organic osmolytes act revealed that they are strong water structure formers and are preferentially excluded from the immediate hydration shell of the protein backbone [15]. For thermodynamic reasons, the uneven distribution of these solutes in the cell water generates driving forces acting against protein denaturation and aggregation [19, 20] and thereby favours the well-folded functional state of macromolecules [15, 21].

Compatible solutes synthesized by members of the Bacteria are chemically diverse but are all low-molecular weight uncharged or zwitterionic organic compounds and are highly water soluble [6,7,18]. They can be grouped into the following different chemical classes: (i) sugars (e.g., trehalose, sucrose), (ii) polyols (glycerol, myo-inositol, glycosyl-glycerol), (iii) amino acids and their derivatives (L-proline, L-glutamate, ectoines), (iv) quaternary amines (e.g., glycine betaine, arsenobetaine, L-carnitine, proline-betaine, trimethylammoniumoxide) and their sulfonium analogues (dimethylsulfoniopropionate [DMSP], taurine), (v) sulfate esters (e.g., choline-O-sulfate), and (vi) small peptides (*N*-acetyl-glutaminy-glutamine amide) [22]. Some of these compatible solutes occur rarely in microorganisms, while others are very abundant in nature [5–7,18,22]. An example of the latter group is DMSP, a sulfur-containing compound that is produced in millions of tons in marine habitats by phytoplankton and macroalgae as an osmoprotectant and whose volatile metabolite dimethylsulfide (DMS) is a highly relevant climate gas [23].

Compatible solutes not only serve as effective stress protectants [6–8,18,22] but they are also widely used as nutrients by microorganisms [24]. They are released into the environment as a consequence of sudden osmotic down-shifts through the transient opening of Msc [3]; after the attack and ensuing cell lysis of microorganisms by phages or toxins; through the grazing activities of protozoa on their microbial prey; and through root exudates, decomposing plant material, and urine of mammals [24]. The release of these compounds from the producer cells provides new opportunities for organisms living in the same ecosystem because they can be acquired through high-affinity transport systems either for their reuse as stress protectants [5, 7] or as valuable nutrients [24].

osmotically instigated water influx [3, 16]. Often, multiple types (Msc mini [MscM], Msc small [MscS], Msc large [MscL]) of these safety valves are found in a given microbial cell. They possess different pore sizes and gating behaviour, thereby providing the cell with a finely graded

adjustment response to the severity of the imposed osmotic down-shift [3,16]. Msc are essential under severe osmotic down-shock conditions but not under steady-state growth of microorganisms at high osmolarity [3]. This finding indicates that the stress-bearing peptidoglycan sacculus of gram-positive and gram-negative bacteria [25] is by itself insufficient to restrain the practically instantaneous increase in turgor that occurs during a rapid transition from high to low external osmolarity [3, 16].

The salt-in and salt-out strategy

To cope with sudden or sustained increases in the environmental osmolarity and/or salinity, microorganisms have developed two strategies that are generally referred to as the salt-in and salt-out response [5–7]. In contrast to the passive release of solutes from osmotically down-shocked cells via the transient opening of Msc, adjustment to high-osmolarity surroundings requires active countermeasures to maintain a properly hydrated cytoplasm and a physiologically adequate level of turgor [1,2,6,7]. A restricted number of Bacteria and Archaea that primarily live in permanently high-saline ecosystems use the salt-in strategy and amass molar concentrations of K^+ and Cl^- ions on a permanent basis to balance the osmotic gradient across their cytoplasmic membrane [26]. While energetically favourable [27], the ensuing high-ionic strength cytoplasm forced adjustments of the entire proteome in order to maintain the biological functionality of all extra- and intracellular components [26,28,29]. On an evolutionary timescale, this has left an acidic signature on the proteome with a narrow distribution of isoelectric points as the consequence of reduced hydrophobicity of proteins and a strong increase in negatively charged amino acids exposed on protein surfaces. In a cytoplasm highly enriched in K^+/Cl^- ions, these modifications increase protein hydration, solubility, stability, and functionality and were thought to be coupled with obligate protein halophilicity [26,28,29].

The identification of an acidic proteome was considered as predictive for the use of the salt-in osmoadaptation strategy. While this is probably correct in general, recent findings led to modifications of this long-held view [26] because a considerable number of Halobacteriales, a group of halophilic Archaea, were discovered that combine a high- K^+ cytoplasm with the accumulation of the compatible solutes glycine betaine (Fig 2) and trehalose/2-sulfotrehalose [30]. Furthermore, a highly acidic proteome of the photosynthetic anaerobic proteobacterium *Halorhodospira halophila*, one of the most halophilic microorganisms known, was observed, and the cytoplasmic K^+ content of the cells was strongly regulated by the salinity of the growth medium. The K^+ content of the cells (molar concentration) was very high at high salinity (35%) but rather moderate (mM concentration; at the level of that observed for the non-halophile *Escherichia coli*) at modest external salinities (5%) [31]. Consequently, this finding challenges the traditional view that obligate protein halophilicity is the price evolution has to pay for the salt-in osmoadaptive strategy and prompts the exploration of new avenues of research into the evolution of microbial cellular adjustment strategies to high-salinity environments and the physiological consequences of a highly acidic proteome [26,31].

Microorganisms that employ the salt-out strategy also import large amounts of K^+ ions as an initial, rapid osmoadaptation response, but they avoid their long-term accumulation under sustained osmotic stress conditions [5,7]. Export of cytotoxic Na^+ that can enter the cell through various processes (e.g., via Na^+ -coupled transporters for compatible solutes [5]) is also a very important attribute for maintaining a low-ionic strength cytoplasm (Fig 1) [2,7]. Hence, instead of ions, microbial salt-out adopters balance the osmotic gradient across their cytoplasmic membrane primarily through the high-level accumulation of various types of compatible solutes (Box 1) [2,6,7,15]. This allows them to subsequently reduce the K^+ pool through export (Fig 1) without compromising the level of the osmotic potential of the cytoplasm

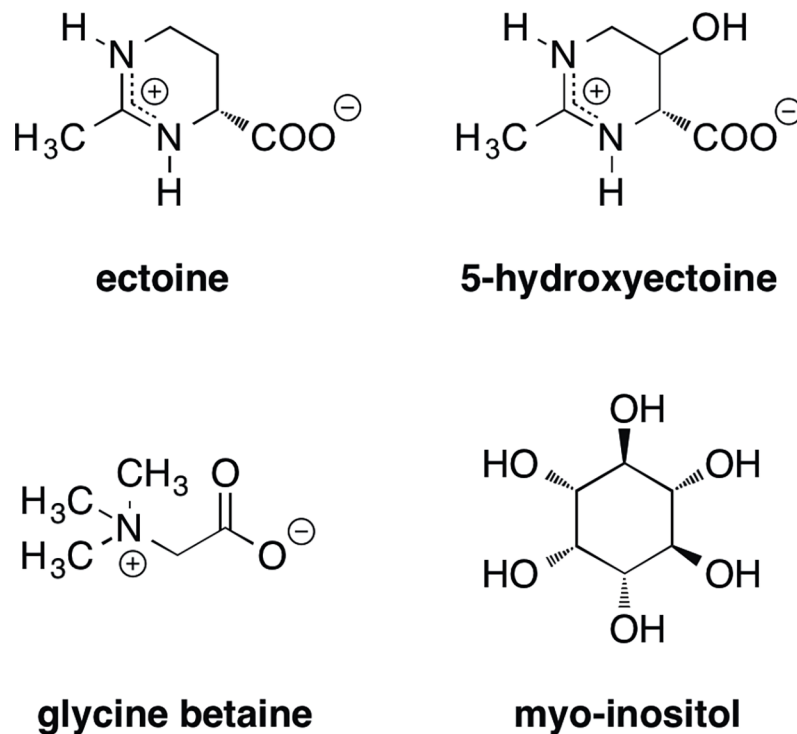


Fig 2. Chemical structures of selected compatible solutes.

<https://doi.org/10.1371/journal.pbio.2005163.g002>

required for growth and maintenance of turgor [1,2,4,12]. The accumulation of compatible solutes also counteracts protein misfolding and aggregation that will occur upon the imposition of osmotic stress (Box 1) [15,19,20]. The amassing of compatible solutes can be accomplished either via osmotically stimulated synthesis or through uptake from environmental sources via osmotically controlled transport systems [2,6,7]. Although synthesis and import of compatible solutes is, from an energetic point of view, far more demanding than the salt-in mechanism [26], it provides a considerable degree of flexibility to salt-out adopters because it does not tie them ecophysiologically to permanently high saline and/or osmolarity habitats. Collectively, these microorganisms adapt to both sudden and sustained increases in environmental osmolarity through coordinated changes in their genome-wide transcriptional profile, through the osmotic stress-responsive induction of genes for compatible solute importers, and modulation of the activity of these transport systems [2,5–7].

Relief from osmotic stress through synthesis of the compatible solutes glycine betaine and ectoine

The trimethylammonium compound glycine betaine (Fig 2) is probably the most widely used compatible solute on Earth because both Pro- and Eukarya employ it as a highly effective protectant against osmotic and other types of stresses (Box 1) [18]. It can be synthesized under aerobic conditions through the oxidation of choline, with glycine betaine aldehyde as the intermediate. Bacteria, Archaea, Fungi, plants, and animals are able to synthesize it from this precursor, and a combination (or types) of various enzymes can be used. In microorganisms, choline typically needs to be imported because most of them lack the ability to synthesize this molecule *de novo*. Some Bacteria and Archaea can also produce glycine betaine through the sequential methylation of glycine [32], but this is not the preferred route for synthesis because

of the high energy demand to regenerate the cofactor [S-adenosylmethionine (SAM)] needed for the activity of the two enzymes that catalyze the methylation of glycine [32]. Both the choline to glycine betaine oxidation pathway and the de novo synthesis route from glycine confer a considerable degree of osmotic stress resistance to microbial cells [5,7,32].

In contrast to the widely distributed glycine betaine molecule in Pro- and Eukarya, the compatible solute ectoine and its derivative 5-hydroxyectoine (Fig 2) were initially perceived as rather specialized microbial osmotic stress protectants. However, the discovery of their biosynthetic genes [33] and subsequent extensive database searches revealed their wide distribution in genomes of members of the Bacteria [34]. Lateral gene transfer, a major driver of microbial evolution [35], is probably responsible for the introduction of the *ect* biosynthetic genes into selected members of the archaeal genera *Nitrosopumilus*, *Methanothrix*, and *Methanobacterium* [36].

Synthesis of ectoine proceeds from L-aspartate-beta-semialdehyde and involves the transformation of this central metabolite by the sequential enzyme activities of diaminobutyrate-2-oxoglutarate aminotransferase (EctB; EC 2.6.1.76), diaminobutyrate acetyltransferase (EctA; EC 2.3.1.178), and ectoine synthase (EctC; EC 4.2.1.108) [33]. A subgroup of ectoine producers also synthesize the ectoine derivative 5-hydroxyectoine (Fig 2), an effective compatible solute in its own right that is often endowed in vivo and in vitro with additional or enhanced stress protective properties in direct comparison with ectoine [33, 34]. All 5-hydroxyectoine producers are aerobic, or at least O₂ tolerant, microorganisms because the ectoine hydroxylase (EctD; EC 1.14.11.55) is an oxygen-dependent enzyme [34, 36]. The ectoine biosynthetic genes (*ectABC*) are typically organized as an osmotically inducible operon [37] that may also contain the gene (*ectD*) for the ectoine hydroxylase and a specialized aspartokinase (Ask_Ect) involved in synthesizing the ectoine precursor L-aspartate-beta-semialdehyde [34,36]. Effective osmotic stress protection can also be accomplished through the import of ectoines, and several types of osmotically induced ectoine/5-hydroxyectoine import systems have been identified in microorganisms (for an example see [38] and additional references therein).

Halophilic protists—How do they do it?

Marine and hypersaline habitats are populated not only by a physiological and taxonomically diverse group of Bacteria and Archaea [26, 27], but halophilic protists are also ecophysiologically critical inhabitants of these challenging ecosystems [39–41]. They serve crucial roles as primary producers and decomposers, and some of them exert through their bacterivorous activity a major influence on biological diversity and abundance of bacteria in these habitats [41]. While the cellular adjustments to osmotically challenging environments have been intensively studied over the years in Bacteria and Archaea [2,5–7], a thorough understanding of the cellular osmotic stress responses of halophilic unicellular eukaryotes lags far behind [41]. However, an in-depth understanding of these organisms is highly desirable because they are not only very abundant in nature but also represent the majority of eukaryotic lineages [39,41,42]. Studies investigating the osmotic stress adaptation strategies in the green algae *Dunaliella salina* [11], in the baker's yeast *Saccharomyces cerevisiae* [9], and in some halotolerant/halophilic fungi (e.g., *Hortaea werneckii*, *Wallemia ichthyophaga*) [10] have already been conducted in quite some detail.

Three recent publications now lay the groundwork to unravel the physiology and molecular biology of osmotic stress adaptation strategies of halophilic heterotrophic protists [41,43–45] and thus allow a comparison with their halophilic or halotolerant bacterial counterparts. These studies focused on *Halocafeteria seosinensis*, *Pharyngomonas kirbyi*, and *Schmidingerthrix salinarum*, phagotrophic protists that were originally isolated on different continents (Europe,

Northern America, Asia), but their common habitat are hypersaline solar ponds, habitats subjected to evaporation and thus leading to gradual increases in salinity that can range between seawater and saturated brines [41]. The reports by Harding et al. [43,44] and Weinisch et al. [45] do not only allow a glimpse into the basic features of the osmotic stress responses used by these species but also hold several surprises for scholars of microbial osmotic stress adjustment systems.

Studies with *H. seosinensis* and *P. kirbyi* showed that their cytoplasmic proteomes are not particularly highly acidic but possess a more hydrophilic signature than eukaryotic microbes inhabiting marine environments, thereby suggesting that they possess a somewhat higher steady-state salt content than marine protists [43]. Consistent with the finding from proteomic studies are data derived by Weinisch et al. [45] using an ion imaging approach. These experiments showed that the cytoplasmic K⁺ and Na⁺ content of *S. salinarum* do not change significantly in response to increases in the external salinity. The conclusions that the three studied halophilic protists do not use a salt-in approach are also supported by experiments assessing the inhibiting effect of salinity on enzyme activity of the *S. salinarum* malate and isocitrate dehydrogenases [45]. However, the occurrence of taxonomically diverse protists capable of growing in habitats of distinct salinities raises the possibility that various lineages of unicellular Eukarya have evolved different adaptation strategies to high-salinity environments [41].

Studies probing the transcriptional response of *H. seosinensis* to high-salinity challenges revealed the involvement of various stress responses (e.g., chaperones that repair misfolded proteins), genes for neutralizing the detrimental effects of oxidative stress, K⁺ and Na⁺ transporters critical for ion homeostasis, metabolism and transport of lipids (e.g., sterol biosynthesis), carbohydrate and amino acid metabolism, and signal transduction pathways, including G-protein-coupled receptors [44]. The studies by Harding et al. [43,44] focusing on *H. seosinensis* and *P. kirbyi* and that of Weinisch et al. [45] on *S. salinarum* show that the synthesis and import of compatible solutes (Box 1) make major contributions to their salt stress adaptation.

The genome-wide transcriptome analysis of salt-stressed *H. seosinensis* cells yielded the totally unexpected finding that predicted biosynthetic genes for the compatible solutes ectoine/5-hydroxyectoine are present in the chromosome of this halophilic protist and that their transcription is up-regulated in response to salt stress [43, 44]. Ectoines (Fig 2) have so far been considered as compatible solutes exclusively synthesized and used by Bacteria and by a few Archaea [33,34,36]. Because *H. seosinensis* and *S. salinarum* are bacterivorous, the detection of DNA sequences in *H. seosinensis* related to microbial genes is at least initially of some concern because their misinterpretation as of eukaryotic origin can seriously compromise assembly into DNA scaffolds and the interpretation of biological findings [46–48]. However, with respect to the data reported by Harding et al. [43] for *H. seosinensis*, one can rest easy because each of the ectoine (*ectABC*) and hydroxyectoine (*ectD*) biosynthetic genes and the specialized aspartokinase (*ask_ect*) harbor spliceosomal introns, genetic elements that are not found in Bacteria and Archaea [49]. Because microbial ectoine/5-hydroxyectoine producers frequently populate marine and hypersaline habitats [33,34,36], a reasonable hypothesis for the occurrence of ectoine/5-hydroxyectoine biosynthetic genes in *H. seosinensis* is their acquisition via horizontal gene transfer from a prokaryotic donor and their subsequent adaptation to the genomic context and transcriptional profile of a eukaryotic host cell. The detection of predicted N-terminal mitochondrial targeting sequences of the ectoine/5-hydroxyectoine biosynthetic enzymes from *H. seosinensis*, all of which are cytoplasmic enzymes in Prokarya [33], led Harding et al. [43] to speculate that the synthesis of ectoines might occur in these organelles of the protists.

Although the overall evolutionary relevance of horizontal gene transfer events from Pro- to Eukarya is still intensively debated [48], it is nevertheless well established that Eukarya can

acquire novel metabolic traits and stress resistance determinants by stealing preformed gene clusters from either Bacteria or Archaea [46,50,51]. It is likely that the acquisition and salt stress-responsive transcription of ectoine/5-hydroxyectoine biosynthetic genes from its food prey will provide a distinct advantage to *H. seosinensis* in its high-salinity habitat [43] because ectoines are very potent osmoprotectants [33,34,36]. The occurrence of ectoine/5-hydroxyectoine biosynthetic genes in the eukaryote *H. seosinensis* does not seem to represent an isolated incident. In extended database searches of eukaryotic genomes, Harding et al. [43] discovered *ectA*- and *ectC*-related sequences in previously reported transcriptional profiles of at least six other protists and in the genome sequences of a considerable number of other Eukarya as well. This includes even the deuterostome animals *Branchiostoma floridae* and *Saccoglossus kowalevskii*. Interestingly, in a number of cases, fusions of the *ectA* and *ectC* open reading frames have occurred. In the dinoflagellate *Azadinium spinosum*, this fused open reading frame also contains *ectD*, suggesting the production of a potentially trifunctional ectoine/5-hydroxyectoine biosynthetic enzyme [43]. In all these cases, experimental verification of ectoine/5-hydroxyectoine production by the corresponding eukaryotic cells is eagerly awaited.

The phylogenetic relationship and genomic arrangement of the *H. seosinensis* *ectABC-ask_ect* gene cluster not only prompted Harding et al. [43] to advocate that these genes were acquired via lateral gene transfer from Prokarya. Their sporadic presence (or at least remnants of them) in various protists also suggested to these authors that the *ect* biosynthetic genes have spread horizontally between various halophilic unicellular eukaryotes [43]. These authors also recorded a number of cases in which salt-regulated genes unrelated to the synthesis of ectoines were part of gene duplication events, indicating that this process, along with several other lateral gene transfer events that they detected, was involved in creating genetic novelties [44], thereby aiding the adaptation of the bacteriophage *H. seosinensis* to its permanently high-saline habitat [41,52].

While the data provided by Harding et al. [43] are very suggestive of ectoine/5-hydroxyectoine biosynthesis in a selected group of Eukarya, definitive proof that this is actually the case in *H. seosinensis* was missing because these authors did not investigate the production of these solutes directly. The study by Weinisch et al., now published in *PLoS Biology* [45], convincingly fills this gap of knowledge by demonstrating the salt-dependent synthesis of ectoine by the halophilic heterotrophic ciliate *S. salinarum*. Although no genome sequence or transcriptional profile is currently available for *S. salinarum* that would allow the verification of the presence of the *ectABC* genes, data derived from ¹H-NMR-spectroscopy provided unequivocal evidence for the synthesis of ectoine [45]. Interestingly, Weinisch et al. [45] also found through tracer experiments with externally provided radiolabeled choline that *S. salinarum* can synthesize glycine betaine through oxidation of this precursor. Even more surprising than the data on the de novo synthesis of ectoine was the finding by Weinisch et al. that externally provided ectoine, and to a lesser extent glycine betaine, enhanced growth under high-salinity conditions [45]. These observations imply that this protist, like many microorganisms [5,38], possesses transporter(s) for these compatible solutes, thereby allowing osmoprotection [45]. We note in this context that many microbial ectoine/5-hydroxyectoine producers live in high-saline ecosystems [33,34,36], and the active export or release of ectoines from these primary producers will make a major contribution of occurrence of ectoines in these habitats.

Taken together, *S. salinarum* employs a set of different imported or newly synthesized compatible solutes to cope with sustained osmotic stress, an adjustment strategy that is frequently found in Bacteria and Archaea as well (Fig 1) [5–7]. This concept is further buttressed by the finding of Harding et al. [43] that the expression of two predicted transporters for myo-inositol (Fig 2), a well-known compatible solute in Eukarya [8], were up-regulated in response to salt stress in *H. seosinensis*.

Finally, ectoines are not only effective osmoprotectants but they are also valuable nutrients for microorganisms [24]. The physiology and genetics of the catabolism of these nitrogen-rich compounds (Fig 2) have been intensively studied in the marine bacterium *Ruegeria pomeroyi* [53]. A unique ectoine-derived metabolite (N- α -L-acetyl-2,4-diaminobutyric acid), and not ectoine or hydroxyectoine themselves, serves as the inducer for the GabR/MocR-type regulatory protein EnuR that controls the transcription of the ectoine/5-hydroxyectoine import and catabolic gene clusters present in many microorganisms [53]. Interestingly, the cocultivation of *R. pomeroyi* with the diatom *Thalassiosira pseudonana* induces the transcription of this operon [54], implying that the diatom produces ectoine (and perhaps also 5-hydroxyectoine) and releases these osmolytes into the marine environment from which *R. pomeroyi* can then scavenge them as nutrients [53].

Taken together, the recently reported data by Harding et al. [43] and Weinisch et al. [45] on ectoine/5-hydroxyectoine biosynthesis by halophilic protists as osmoprotectants, and the report by Landa et al. [54] on the remodeling of the transcriptional profile of the ectoine/5-hydroxyectoine consumer *R. pomeroyi* through metabolites released by the diatom *T. pseudonana*, break new ground. They highlight the unexpected ecophysiological importance of ectoines as stress protectants in a selected group of halophilic Eukarya. These studies also underscore the role of ectoines as mediators of ecophysiological interactions between Pro- and Eukarya in salt-stressed ecosystems beyond a level that was assumed until recently [33,34,36,53].

Acknowledgments

We are grateful to Vickie Koogler for her expert help in the language editing of our manuscript. L.C. is the recipient of a PhD fellowship from the International Max Planck Research School for Environmental, Cellular and Molecular Microbiology (IMPRS-Mic, Marburg) and gratefully acknowledges this support.

References

1. van den Berg J, Boersma AJ, Poolman B. Microorganisms maintain crowding homeostasis. *Nat Rev Microbiol.* 2017; 15(5):309–18. <https://doi.org/10.1038/nrmicro.2017.17> PMID: 28344349.
2. Wood JM. Bacterial osmoregulation: a paradigm for the study of cellular homeostasis. *Annu Rev Microbiol.* 2011; 65:215–38. <https://doi.org/10.1146/annurev-micro-090110-102815> PMID: 21663439.
3. Booth IR. Bacterial mechanosensitive channels: progress towards an understanding of their roles in cell physiology. *Curr Opin Microbiol.* 2014; 18:16–22. <https://doi.org/10.1016/j.mib.2014.01.005> PMID: 24607989.
4. Rojas ER, Huang KC. Regulation of microbial growth by turgor pressure. *Curr Opin Microbiol.* 2017; 42:62–70. <https://doi.org/10.1016/j.mib.2017.10.015> PMID: 29125939.
5. Bremer E, Krämer R. Coping with osmotic challenges: osmoregulation through accumulation and release of compatible solutes. In: Storz G, Hengge-Aronis R, editors. *Bacterial Stress Responses*. Washington DC, USA: ASM Press; 2000. p. 79–97.
6. Roesser M, Müller V. Osmoadaptation in bacteria and archaea: common principles and differences. *Environ Microbiol.* 2001; 3(12):743–54. Epub 2002/02/16. PMID: 11846768.
7. Kempf B, Bremer E. Uptake and synthesis of compatible solutes as microbial stress responses to high osmolality environments. *Arch Microbiol.* 1998; 170:319–30. PMID: 9818351
8. Burg MB, Ferraris JD. Intracellular organic osmolytes: function and regulation. *J Biol Chem.* 2008; 283(12):7309–13. <https://doi.org/10.1074/jbc.R700042200> PMID: 18256030.
9. Hohmann S. An integrated view on a eukaryotic osmoregulation system. *Curr Genet.* 2015; 61(3):373–82. <https://doi.org/10.1007/s00294-015-0475-0> PMID: 25663258.
10. Plemenitis A, Lenassi M, Konte T, Kejzar A, Zajc J, Gostincar C, et al. Adaptation to high salt concentrations in halotolerant/halophilic fungi: a molecular perspective. *Front Microbiol.* 2014; 5:199. <https://doi.org/10.3389/fmicb.2014.00199> PMID: 24860557.

11. Oren A. The ecology of *Dunaliella* in high-salt environments. *J Biol Res (Thessalon)*. 2014; 21(1):23. <https://doi.org/10.1186/s40709-014-0023-y> PMID: 25984505.
12. Rojas ER, Huang KC, Theriot JA. Homeostatic cell growth is accomplished mechanically through membrane tension inhibition of cell-wall synthesis. *Cell Syst*. 2017; 5(6):578–90. <https://doi.org/10.1016/j.cels.2017.11.005> PMID: 29203279.
13. King LS, Kozono D, Agre P. From structure to disease: the evolving tale of aquaporin biology. *Nat Rev Mol Cell Biol*. 2004; 5(9):687–98. <https://doi.org/10.1038/nrm1469> PMID: 15340377.
14. Tanghe A, Van Dijck P, Thevelein JM. Why do microorganisms have aquaporins? *Trends Microbiol*. 2006; 14(2):78–85. <https://doi.org/10.1016/j.tim.2005.12.001> PMID: 16406529.
15. Street TO, Bolen DW, Rose GD. A molecular mechanism for osmolyte-induced protein stability. *Proc Natl Acad Sci U S A*. 2006; 103(38):13997–4002. doi: 0606236103 <https://doi.org/10.1073/pnas.0606236103> PMID: 16968772.
16. Cetiner U, Rowe I, Schams A, Mayhew C, Rubin D, Anishkin A, et al. Tension-activated channels in the mechanism of osmotic fitness in *Pseudomonas aeruginosa*. *J Gen Physiol*. 2017; 149(5):595–609. <https://doi.org/10.1085/jgp.201611699> PMID: 28424229.
17. Brown AD. Microbial water stress. *Bacteriol Rev*. 1976; 40(4):803–46. PMID: 1008746.
18. Yancey PH. Organic osmolytes as compatible, metabolic and counteracting cytoprotectants in high osmolarity and other stresses. *J Exp Biol*. 2005; 208(15):2819–30. <https://doi.org/10.1242/jeb.01730> PMID: 16043587.
19. Stadtmiller SS, Gorensek-Benitez AH, Guseman AJ, Pielak GJ. Osmotic shock induced protein destabilization in living cells and its reversal by glycine betaine. *J Mol Biol*. 2017; 429(8):1155–61. <https://doi.org/10.1016/j.jmb.2017.03.001> PMID: 28263768.
20. Ignatova Z, Gierasch LM. Inhibition of protein aggregation *in vitro* and *in vivo* by a natural osmoprotectant. *Proc Natl Acad Sci U S A*. 2006; 103(36):13357–61. doi: 060377210310.1073/pnas.0603772103. <https://doi.org/10.1073/pnas.0603772103> PMID: 16899544.
21. Bourot S, Sire O, Trautwetter A, Touze T, Wu LF, Blanco C, et al. Glycine betaine-assisted protein folding in a *lysA* mutant of *Escherichia coli*. *J Biol Chem*. 2000; 275(2):1050–6. PMID: 10625645.
22. Empadinhas N, da Costa MS. Osmoadaptation mechanisms in prokaryotes: distribution of compatible solutes. *Int Microbiol*. 2008; 11(3):151–61. PMID: 18843593.
23. Bullock HA, Luo H, Whitman WB. Evolution of dimethylsulfoniopropionate metabolism in marine phytoplankton and bacteria. *Front Microbiol*. 2017; 8:637. <https://doi.org/10.3389/fmicb.2017.00637> PMID: 28469605.
24. Welsh DT. Ecological significance of compatible solute accumulation by micro-organisms: from single cells to global climate. *FEMS Microbiol Rev*. 2000; 24(3):263–90. Epub 2000/06/08. PMID: 10841973.
25. Vollmer W, Seligman SJ. Architecture of peptidoglycan: more data and more models. *Trends Microbiol*. 2010; 18(2):59–66. doi: S0966-842X(09)00260-1 <https://doi.org/10.1016/j.tim.2009.12.004> PMID: 20060721.
26. Oren A. Life at high salt concentrations, intracellular KCl concentrations, and acidic proteomes. *Front Microbiol*. 2013; 4:315. <https://doi.org/10.3389/fmicb.2013.00315> PMID: 24204364.
27. Oren A. Thermodynamic limits to microbial life at high salt concentrations. *Environ Microbiol*. 2011; 13(8):1908–23. <https://doi.org/10.1111/j.1462-2920.2010.02365.x> PMID: 21054738.
28. Talon R, Coquelle N, Madern D, Girard E. An experimental point of view on hydration/solvation in halophilic proteins. *Front Microbiol*. 2014; 5:66. <https://doi.org/10.3389/fmicb.2014.00066> PMID: 24600446.
29. Becker EA, Seitzer PM, Tritt A, Larsen D, Krusor M, Yao AI, et al. Phylogenetically driven sequencing of extremely halophilic archaea reveals strategies for static and dynamic osmo-response. *PLoS Genet*. 2014; 10(11):e1004784. <https://doi.org/10.1371/journal.pgen.1004784> PMID: 25393412.
30. Youssef NH, Savage-Ashlock KN, McCully AL, Luedtke B, Shaw EI, Hoff WD, et al. Trehalose/2-sulfotrehalose biosynthesis and glycine-betaine uptake are widely spread mechanisms for osmoadaptation in the *Halobacteriales*. *ISME J*. 2014; 8(3):636–49. <https://doi.org/10.1038/ismej.2013.165> PMID: 24048226.
31. Deole R, Challacombe J, Raiford DW, Hoff WD. An extremely halophilic proteobacterium combines a highly acidic proteome with a low cytoplasmic potassium content. *J Biol Chem*. 2013; 288(1):581–8. <https://doi.org/10.1074/jbc.M112.420505> PMID: 23144460.
32. Nyssölä A, Kerovuo J, Kaukinen P, von Weymarn N, Reinikainen T. Extreme halophiles synthesize betaine from glycine by methylation. *J Biol Chem*. 2000; 275(29):22196–201. <https://doi.org/10.1074/jbc.M910111199> PMID: 10896953.

33. Pastor JM, Salvador M, Argandona M, Bernal V, Reina-Bueno M, Csonka LN, et al. Ectoines in cell stress protection: uses and biotechnological production. *Biotechnol Adv.* 2010; 28(6):782–801. <https://doi.org/10.1016/j.biotechadv.2010.06.005> PMID: 20600783.
34. Widderich N, Höppner A, Pittelkow M, Heider J, Smits SH, Bremer E. Biochemical properties of ectoine hydroxylases from extremophiles and their wider taxonomic distribution among microorganisms. *PLoS ONE.* 2014; 9(4):e93809. <https://doi.org/10.1371/journal.pone.0093809> PMID: 24714029.
35. Treangen TJ, Rocha EP. Horizontal transfer, not duplication, drives the expansion of protein families in prokaryotes. *PLoS Genet.* 2011; 7(1):e1001284. <https://doi.org/10.1371/journal.pgen.1001284> PMID: 21298028.
36. Widderich N, Czech L, Elling FJ, Könneke M, Stöveken N, Pittelkow M, et al. Strangers in the archaeal world: osmostress-responsive biosynthesis of ectoine and hydroxyectoine by the marine thaumarchaeon *Nitrosopumilus maritimus*. *Env Microbiol.* 2016; 18:1227–48. <https://doi.org/10.1111/1462-2920.13156> PMID: 26636559
37. Czech L, Poehl S, Hub P, Stöveken N, Bremer E. Tinkering with osmotically controlled transcription allows enhanced production and excretion of ectoine and hydroxyectoine from a microbial cell factory. *Appl Environ Microbiol.* 2018; 84e:01772–17. <https://doi.org/10.1128/AEM.01772-17> PMID: 29101191.
38. Kuhlmann AU, Hoffmann T, Bursy J, Jebbar M, Bremer E. Ectoine and hydroxyectoine as protectants against osmotic and cold stress: uptake through the SigB-controlled betaine-choline-carnitine transporter-type carrier EctT from *Virgibacillus pantothenicus*. *J Bacteriol.* 2011; 193(18):4699–708. <https://doi.org/10.1128/JB.05270-11> PMID: 21764932.
39. Massana R, Gobet A, Audic S, Bass D, Bittner L, Boutte C, et al. Marine protist diversity in European coastal waters and sediments as revealed by high-throughput sequencing. *Environ Microbiol.* 2015; 17(10):4035–49. <https://doi.org/10.1111/1462-2920.12955> PMID: 26119494.
40. Filker S, Forster D, Weinisch L, Mora-Ruiz M, Gonzalez B, Farias ME, et al. Transition boundaries for protistan species turnover in hypersaline waters of different biogeographic regions. *Environ Microbiol.* 2017; 19(8):3186–200. <https://doi.org/10.1111/1462-2920.13805> PMID: 28574222.
41. Harding T, Simpson AGB. Recent advances in halophilic protozoa research. *J Eukaryot Microbiol.* 2017. <https://doi.org/10.1111/jeu.12495> PMID: 29266533.
42. Caron DA, Worden AZ, Countway PD, Demir E, Heidelberg KB. Protists are microbes too: a perspective. *ISME J.* 2009; 3(1):4–12. <https://doi.org/10.1038/ismej.2008.101> PMID: 19005497.
43. Harding T, Brown MW, Simpson AG, Roger AJ. Osmoadaptive strategy and its molecular signature in obligately halophilic heterotrophic protists. *Genome Biol Evol.* 2016; 8(7):2241–58. <https://doi.org/10.1093/gbe/evw152> PMID: 27412608.
44. Harding T, Roger AJ, Simpson AGB. Adaptations to high salt in a halophilic protist: differential expression and gene acquisitions through duplications and gene transfers. *Front Microbiol.* 2017; 8:944. <https://doi.org/10.3389/fmicb.2017.00944> PMID: 28611746.
45. Weinisch L, Kühner S, Rozth R, Roth T, Netz DJA, Pierik A, et al. Identification of osmoadaptive strategies in the halophile, heterotrophic ciliate *Schmidingerothrix salinarum*. *PLoS Biol.* 2018; (accepted). <https://doi.org/10.1371/journal.pbio.2003892>
46. Eme L, Gentekaki E, Curtis B, Archibald JM, Roger AJ. Lateral gene transfer in the adaptation of the anaerobic parasite blastocystis to the gut. *Curr Biol.* 2017; 27(6):807–20. <https://doi.org/10.1016/j.cub.2017.02.003> PMID: 28262486.
47. Koutsovoulos G, Kumar S, Laetsch DR, Stevens L, Daub J, Conlon C, et al. No evidence for extensive horizontal gene transfer in the genome of the tardigrade *Hypsibius dujardini*. *Proc Natl Acad Sci U S A.* 2016; 113(18):5053–8. <https://doi.org/10.1073/pnas.1600338113> PMID: 27035985.
48. Moreira D, Lopez-Garcia P. Protist evolution: stealing genes to gut it out. *Curr Biol.* 2017; 27(6):R223–R5. <https://doi.org/10.1016/j.cub.2017.02.010> PMID: 28324738.
49. Rogozin IB, Carmel L, Csuros M, Koonin EV. Origin and evolution of spliceosomal introns. *Biology Direct.* 2012; 7:11. <https://doi.org/10.1186/1745-6150-7-11> PMID: 22507701.
50. Schönknecht G, Chen WH, Ternes CM, Barbier GG, Shrestha RP, Stanke M, et al. Gene transfer from bacteria and archaea facilitated evolution of an extremophilic eukaryote. *Science.* 2013; 339(6124):1207–310. <https://doi.org/10.1126/science.1231707> PMID: 23471408.
51. Husnik F, McCutcheon JP. Functional horizontal gene transfer from bacteria to eukaryotes. *Nat Rev Microbiol.* 2018; 16(2):67–79. <https://doi.org/10.1038/nrmicro.2017.137> PMID: 29176581.
52. Park JS, Cho BC, Simpson AG. *Halocafeteria seosinensis* gen. et sp. nov. (Bicosoecida), a halophilic bacterivorous nanoflagellate isolated from a solar saltern. *Extremophiles.* 2006; 10(6):493–504. <https://doi.org/10.1007/s00792-006-0001-x> PMID: 16874468.

53. Schulz A, Hermann L, Freibert SA, Bönig T, Hoffmann T, Riclea R, et al. Transcriptional regulation of ectoine catabolism in response to multiple metabolic and environmental cues. *Environ Microbiol.* 2017; 19(11):4599–619. <https://doi.org/10.1111/1462-2920.13924> PMID: 28892254.
54. Landa M, Burns AS, Roth SJ, Moran MA. Bacterial transcriptome remodeling during sequential co-culture with a marine dinoflagellate and diatom. *ISME J.* 2017; 11(12):2677–90. <https://doi.org/10.1038/ismej.2017.117> PMID: 28731474.

Environmental Microbiology (2016) 18(4), 1227–1248

doi:10.1111/1462-2920.13156

Strangers in the archaeal world: osmstress-responsive biosynthesis of ectoine and hydroxyectoine by the marine thaumarchaeon *Nitrosopumilus maritimus*

Nils Widderich,^{1†} Laura Czech,^{1†} Felix J. Elling,²
Martin Könneke,² Nadine Stöveken,^{1,3}
Marco Pittelkow,¹ Ramona Riclea,^{4,5}
Jeroen S. Dickschat,^{4,5} Johann Heider^{1,3} and
Erhard Bremer^{1,3*}

those of their counterparts from *Bacteria*. Transcriptional analysis of osmotically stressed 'Ca. *N. maritimus*' cells demonstrated that they possess an ectoine/hydroxyectoine gene cluster (*hyp-ectABCD-mscS*) different from those recognized previously

5.2. Research papers

5.2.1. Strangers in the archaeal world: osmstress-responsive biosynthesis of ectoine and hydroxyectoine by the marine thaumarchaeon *Nitrosopumilus maritimus*

Widderich N*, Czech L*, Elling FJ, Könneke M, Stöveken N, Pittelkow M, Riclea R, Dickschat JS, Heider J and Bremer E. Strangers in the archaeal world: osmstress-responsive biosynthesis of ectoine and hydroxyectoine by the marine thaumarchaeon *Nitrosopumilus maritimus*. *Environ Microbiol* 2016;18:1227–1248.

In the following, the published manuscript with the title "Strangers in the archaeal world: osmstress-responsive biosynthesis of ectoine and hydroxyectoine by the marine thaumarchaeon *Nitrosopumilus maritimus*" is attached. For this study, I conducted the functional experiments with the mechanosensitive channel from *N. maritimus*. I constructed the expression vector, set up the functional experiments using different *E. coli* strains and evaluated the data. Furthermore, I performed sequence and modeling analysis, conducted bioinformatical studies and prepared the figures for these parts of the publication. F. J. Elling and M. Könneke cultivated Cand. *N. maritimus*. R. Riclea and J. S. Dickschat synthesized and purified the precursor, *N*- γ -ADABA, for the ectoine synthase. N. Widderich performed the biochemical experiments using purified EctC- and EctD-enzymes and conducted transcriptional analysis experiments including RT-PCR for operon mapping and quantitative PCR. M. Pittelkow and N. Stöveken were involved during the exploratory phase of the project. I contributed to writing of the manuscript together with N. Widderich, J. Heider and Prof. E. Bremer.

Supplementary Data can be found at:

<https://onlinelibrary.wiley.com/action/downloadSupplement?doi=10.1111%2F1462-2920.13156&file=emi13156-sup-0001-si.pdf>

5.2.1.1. Original publication

environmental
microbiology

Environmental Microbiology (2016) 18(4), 1227–1248

doi:10.1111/1462-2920.13156

Strangers in the archaeal world: osmstress-responsive biosynthesis of ectoine and hydroxyectoine by the marine thaumarchaeon *Nitrosopumilus maritimus*

Nils Widderich,^{1†} Laura Czech,^{1†} Felix J. Elling,²
Martin Könneke,² Nadine Stöveken,^{1,3}
Marco Pittelkow,¹ Ramona Riclea,^{4,5}
Jeroen S. Dickschat,^{4,5} Johann Heider^{1,3} and
Erhard Bremer^{1,3*}

¹Laboratory for Molecular Microbiology, Department of
Biology, Philipps-University, Karl-von-Frisch Str. 8,
D-35043 Marburg, Germany.

²Organic Geochemistry Group, MARUM – Center for
Marine Environmental Sciences, University of Bremen,
PO Box 330 440, D-28334 Bremen, Germany.

³LOEWE-Center for Synthetic Microbiology,
Philipps-University Marburg, Hans-Meerwein-Str. 6,
D-35043 Marburg, Germany.

⁴Kekulé-Institut für Organische Chemie und Biochemie,
Friedrich-Wilhelms-University Bonn, Gerhard-Domagk
Str. 1, D-53121 Bonn, Germany.

⁵Institute of Organic Chemistry, TU Braunschweig,
Hagenring 30, D-38106 Braunschweig, Germany.

Summary

Ectoine and hydroxyectoine are compatible solutes widely synthesized by members of the *Bacteria* to cope with high osmolarity surroundings. Inspection of 557 archaeal genomes revealed that only 12 strains affiliated with the *Nitrosopumilus*, *Methanohalobium* or *Methanobacterium* genera harbour ectoine/hydroxyectoine gene clusters. Phylogenetic considerations suggest that these *Archaea* have acquired these genes through horizontal gene transfer events. Using the Thaumarchaeon '*Candidatus Nitrosopumilus maritimus*' as an example, we demonstrate that the transcription of its *ectABCD* genes is osmotically induced and functional since it leads to the production of both ectoine and hydroxyectoine. The ectoine synthase and the ectoine hydroxylase were biochemically characterized, and their properties resemble

those of their counterparts from *Bacteria*. Transcriptional analysis of osmotically stressed '*Ca. N. maritimus*' cells demonstrated that they possess an ectoine/hydroxyectoine gene cluster (*hyp-ectABCD-mscS*) different from those recognized previously since it contains a gene for an MscS-type mechanosensitive channel. Complementation experiments with an *Escherichia coli* mutant lacking all known mechanosensitive channel proteins demonstrated that the (*Nm*)MscS protein is functional. Hence, '*Ca. N. maritimus*' cells cope with high salinity not only through enhanced synthesis of osmstress-protective ectoines but they already prepare themselves simultaneously for an eventually occurring osmotic down-shock by enhancing the production of a safety-valve (*Nm*MscS).

Introduction

Microorganisms are masters of change. Their genetically encoded and physiologically mediated adaptive responses allow them to cope with nutrient limitations and a multitude of cellular and environmentally imposed stresses that otherwise would impair growth or threaten their viability (Storz and Hengge-Aronis, 2000). Increases in the external salinity or osmolarity are such types of stress and are encountered by essentially all free-living microorganisms (Csonka, 1989; Bremer and Krämer, 2000; Roesler and Müller, 2001). They trigger the rapid and passive outflow of water from the cell, thereby causing a drop in vital turgor and an increase in molecular crowding of the cytoplasm that in extreme cases causes growth arrest or even death (Record *et al.*, 1998; Wood, 2011). In the course of evolution, microorganisms have developed two different, but not necessarily mutually exclusive (Deole *et al.*, 2013; Oren, 2013; Becker *et al.*, 2014; Youssef *et al.*, 2014), mechanisms to counteract high osmolarity-instigated water efflux, the so-called *salt in* and the *salt out* strategies (Galinski and Trüper, 1994; Kempf and Bremer, 1998). Both are based on an active raising by the bacterial cell of the osmotic potential of its cytoplasm, thereby indirectly creating an osmotic driving

Received 31 July, 2015; revised 19 November, 2015; accepted 27 November, 2015. *For correspondence. E-mail bremer@staff.uni-marburg.de; Tel: (+49) 6421 2821529; Fax: (+49) 6421 2828979.
†These authors contributed equally.

© 2015 Society for Applied Microbiology and John Wiley & Sons Ltd

force to promote water retention and re-entry (Csonka, 1989; Record *et al.*, 1998; Bremer and Krämer, 2000; Roesser and Müller, 2001; Wood, 2011).

Microorganisms using the *salt in* strategy accumulate molar concentrations of K⁺ and Cl⁻ ions through transport processes to balance the osmotic gradient across their cytoplasmic membrane (Galinski and Trüper, 1994; Oren, 2013). This is considered as an energetically favourable strategy for microorganisms to adapt to persistent high-salinity environments (Oren, 2011). However, it comes with a penalty since the entire proteome had to be adjusted in the course of evolution to sustained high ionic strength in order to keep proteins soluble and functional (Coquelle *et al.*, 2010; Deole *et al.*, 2013; Talon *et al.*, 2014). As a consequence, only a limited number of microbial species use the *salt in* strategy since it also often restricts the types of habitats that these microorganisms can populate (Galinski and Trüper, 1994; Oren, 2013).

Microorganisms that use the *salt out* strategy amass, either through synthesis or uptake, a restricted set of organic osmolytes, the compatible solutes (Csonka, 1989; da Costa *et al.*, 1998; Kempf and Bremer, 1998; Roesser and Müller, 2001; Wood *et al.*, 2001). This strategy affords a flexible physiological response to both sustained high-salinity surroundings and to osmotic changes in those ecosystems where the salinity fluctuates more often (Galinski and Trüper, 1994; Bremer and Krämer, 2000). Compatible solutes are operationally defined as small, highly water-soluble organic osmolytes that are fully compliant with cellular biochemistry and physiology (Brown, 1976; Bolen and Baskakov, 2001; Wood, 2011). Their benign nature allows their accumulation to exceedingly high intracellular levels without disturbing cellular physiology and biochemistry. The accumulation of compatible solutes occurs in a fashion that is correlated with the degree of the osmotic stress imposed onto the microbial cell (Kuhlmann and Bremer, 2002; Saum and Müller, 2008; Brill *et al.*, 2011; Hoffmann *et al.*, 2013). Compatible solutes used by members of the *Bacteria* are typically uncharged or zwitterionic (Csonka, 1989; da Costa *et al.*, 1998; Kempf and Bremer, 1998; Klähn and Hagemann, 2011). In contrast, members of the *Archaea* often produce charged derivatives of these types of osmolytes and also synthesize types of compatible solutes that are normally not found in *Bacteria* (da Costa *et al.*, 1998; Roesser and Müller, 2001; Roberts, 2004; Müller *et al.*, 2005; Empadinhas and da Costa, 2011).

Here, we focus on the tetrahydropyrimidine ectoine and its derivative 5-hydroxyectoine (Galinski *et al.*, 1985; Inbar and Lapidot, 1988) (Fig. 1A), widely used compatible solutes in the microbial world (Pastor *et al.*, 2010; Widderich *et al.*, 2014a). High-osmolarity environments trigger enhanced expression of the ectoine (*ectABC*) and hydroxyectoine (*ectD*) biosynthetic genes (Louis and

Galinski, 1997; Prabhu *et al.*, 2004; Garcia-Esteva *et al.*, 2006; Bursy *et al.*, 2007), thereby leading to high-level synthesis of these compounds under osmotically unfavourable conditions (Kuhlmann and Bremer, 2002; Calderon *et al.*, 2004; Bursy *et al.*, 2007; Salvador *et al.*, 2015). Genetic disruption of the ectoine biosynthetic genes causes an osmotic-sensitive growth phenotype, underscoring the physiological role of ectoines as effective microbial osmoprotectants (Canovas *et al.*, 1997; Kol *et al.*, 2010).

Synthesis of ectoine progresses from the precursor L-aspartate- β -semialdehyde, a central intermediate in microbial amino acid metabolism and cell wall synthesis (Lo *et al.*, 2009; Stöveken *et al.*, 2011). It comprises the sequential activities of three enzymes: L-2,4-diaminobutyrate transaminase (EctB; EC 2.6.1.76), L-2,4-diaminobutyrate acetyltransferase (EctA; EC 2.3.1.178) and ectoine synthase (EctC; EC 4.2.1.108) (Louis and Galinski, 1997; Ono *et al.*, 1999b) (Fig. 1A). A considerable number of ectoine producers also synthesize an ectoine derivative, 5-hydroxyectoine, through a stereospecific reaction that is catalysed by the ectoine hydroxylase (EctD) (EC 1.14.11) (Bursy *et al.*, 2007; Höppner *et al.*, 2014; Widderich *et al.*, 2014a,b) (Fig. 1A). Hydroxyectoine exhibits stress-protective properties that are partially different from and sometimes exceed those of ectoine, in particular with respect to temperature and desiccation stress (Manzanera *et al.*, 2002; Garcia-Esteva *et al.*, 2006; Bursy *et al.*, 2008; Tanne *et al.*, 2014).

A recent survey of bacterial and archaeal genome sequences revealed that ectoine and hydroxyectoine biosynthetic genes occur widely in *Bacteria*, are rarely found in *Archaea*, and do not exist in *Eukarya* (Widderich *et al.*, 2014a). In a few isolated incidents, the presence of ectoine/hydroxyectoine biosynthetic genes in *Archaea* has been noted, e.g. in the context of the annotation of the genome sequences of the Thaumarchaeon '*Candidatus* Nitrosopumilus maritimus' SCM1 (Walker *et al.*, 2010) and of the methanogen *Methanobacterium formicicum* BRM9 (Kelly *et al.*, 2014). However, it is unclear whether these genes are functional, whether the properties of the key enzymes for ectoine/hydroxyectoine biosynthesis, the ectoine synthase (EctC) and the ectoine hydroxylase (EctD) (Fig. 1A) are different from those of their bacterial counterparts, and whether the transcription of the archaeal *ect* genes is increased in response to osmotic stress as is observed in members of the *Bacteria* (Kuhlmann and Bremer, 2002; Calderon *et al.*, 2004; Bursy *et al.*, 2007; Kuhlmann *et al.*, 2008; Salvador *et al.*, 2015).

Here, we address these questions by interrogating the rapidly expanding number of archaeal genome sequences through bioinformatics to provide a comprehensive overview on the occurrence of ectoine/

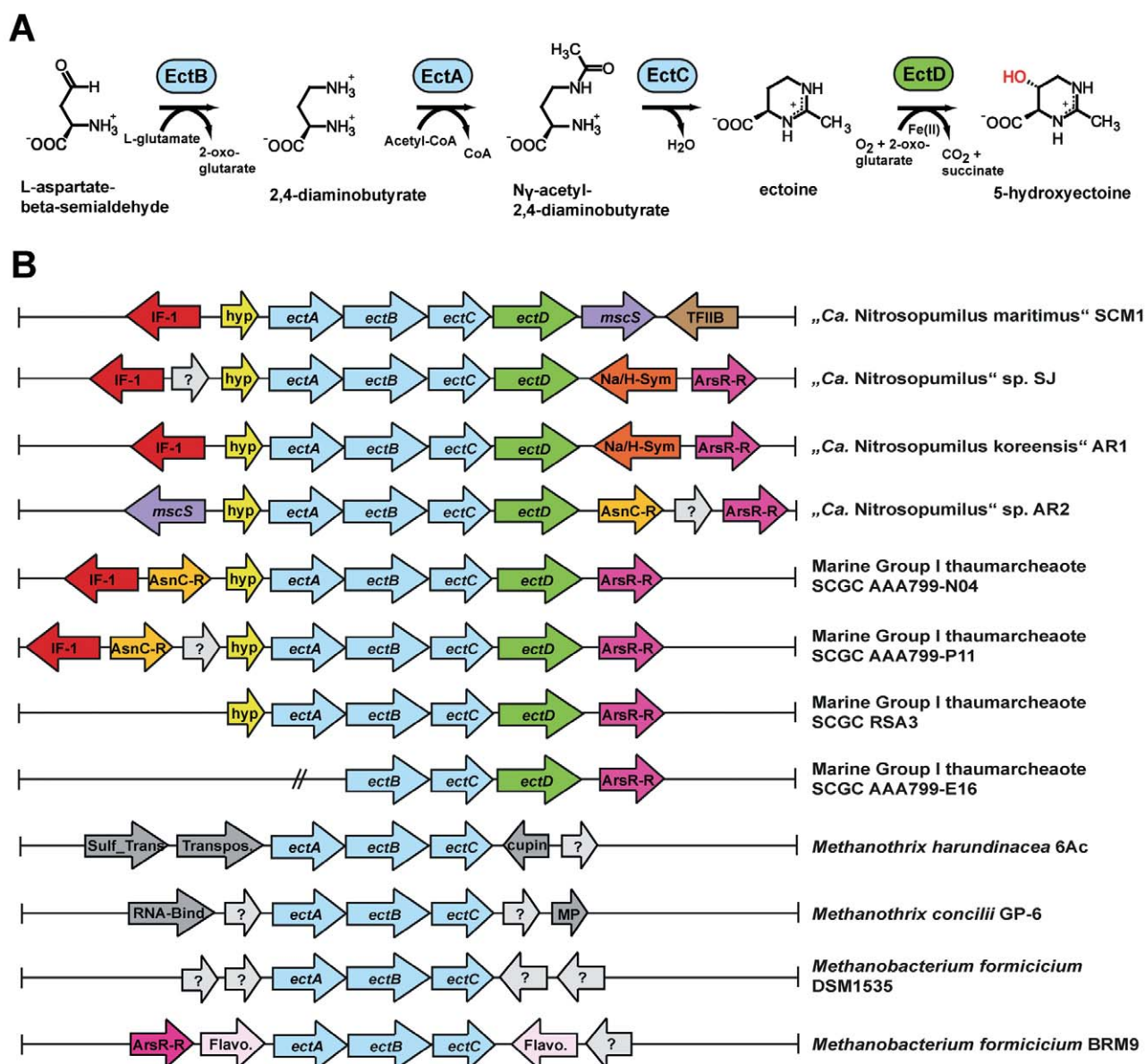


Fig. 1. (A) Biochemical steps required for the biosynthesis of ectoine and 5-hydroxyectoine and (B) genetic organization of *ectABC(D)* gene cluster and their flanking regions in archaeal genomes. In the marine group I thaumarchaeote SCGC AAA799-E16, no *ectA* gene was present; however, this genome sequence was assembled by a metagenomic approach making it likely that this thaumarchaeote also possesses a fully *ectABCD* gene cluster.

hydroxyectoine gene clusters in this domain of life. We used the marine Thaumarchaeon '*Ca. Nitrosopumilus maritimus*' SCM1 (Könneke *et al.*, 2005; Walker *et al.*, 2010), the first cultured representative of the globally abundant ammonia-oxidizing Archaea (AOA) (Stahl and de la Torre, 2012; Offre *et al.*, 2013; Bayer *et al.*, 2015; Gubry-Rangin *et al.*, 2015), as a model system to study ectoine/hydroxyectoine production in detail. We demonstrate for the first time in any archaeon that its *ectABCD* gene cluster is functionally expressed in response to high salinity, and that the biochemical properties of key

enzymes (EctC, EctD) for the synthesis of ectoine and hydroxyectoine resemble those of their bacterial counterparts. Most interestingly, we found that the *ectABCD* genes of '*Ca. N. maritimus*' SCM1 are not only osmotically inducible but that they are also co-transcribed with a gene that encodes a functional mechanosensitive channel of the MscS family. These safety valves are ubiquitously used by both *Bacteria* and *Archaea* to withstand rapid osmotic downshifts (Kloda and Martinac, 2002; Booth and Blount, 2012; Wilson *et al.*, 2013; Booth, 2014). Hence, the osmotically regulated *ectABCD-mscS* transcriptional

unit is a sophisticated genetic device that allows high-salinity challenged '*Ca. N. maritimus*' SCM1 cells to sequentially cope with increases and decreases in the external osmolarity of their marine and estuarine habitat.

Results

Assessing the distribution of ectoine/hydroxyectoine biosynthetic genes in Bacteria and Archaea

To assess the occurrence and taxonomic distribution of ectoine biosynthetic genes, we used the database of the Joint Genome Institute (JGI) of the US Department of Energy (<http://jgi.doe.gov/>) (Nordberg *et al.*, 2013) and the EctC protein from '*Ca. Nitrosopumilus maritimus*' SCM1 (Walker *et al.*, 2010) as the query sequence. While the EctA (2,4-diaminobutyrate acetyltransferase) and EctB (L-2,4-diaminobutyrate transaminase) enzymes have counterparts in microbial biosynthetic pathways not related to ectoine biosynthesis, EctC can be regarded as a diagnostic enzyme for ectoine producers (Widderich *et al.*, 2014a). Of note is that a restricted number of microorganisms exists that possesses *ectC*-type genes but lack the corresponding *ectAB* genes. The functional relevance of these orphan EctC-type proteins for ectoine biosynthesis is currently not fully understood (Kurz *et al.*, 2010; Widderich *et al.*, 2014a).

At the time of the BLAST search (08.07.2015), 27,232 completed and partially completed genome sequences of members of the *Bacteria* were represented in the JGI microbial database and 557 genome sequences of *Archaea* had been deposited. Among these 27,789 microbial genome sequences, 1297 hits to EctC-type proteins were found. After removing redundant entries of closely related strains (e.g. there are 181 genomes of strain of *Vibrio cholerae* represented that each possesses an *ect* gene cluster), the curated data set comprised 723 EctC-type proteins; 711 originate from *Bacteria* and only 12 were derived from *Archaea*. We note in this context that a considerable number of EctC-type proteins are misannotated in the database as L-mannose-6-phosphate isomerases (despite the typical localization of the corresponding genes within *ectABC(D)* gene clusters). Often, they are also referred to as RmlC-type cupins, an error that might originate from the bioinformatics assignment of the EctC protein to the RmlC subgroup of the cupin superfamily (Dunwell *et al.*, 2001). The RmlC enzyme participates in the L-rhamnose biosynthetic pathway, serves as a carbohydrate epimerase (EC 5.1.3.13) (Dong *et al.*, 2007), and therefore catalyses an enzymatic reaction quite different from that of the ectoine synthase EctC (EC 4.2.1.108) (Ono *et al.*, 1999b) (Fig. 1A).

We then focused our further analysis on the genome sequences of those 12 *Archaea* that were identified by our database analysis to harbour *ectC*-type genes (Fig. 1B). In

each of the corresponding genomes, the *ectC* gene is part of either an *ectABC* operon, or is embedded in an *ect* gene cluster that also comprises *ectD*. Eight members affiliated with the genus *Nitrosopumilus* or with Marine Group I.1a Thaumarchaeota (Pester *et al.*, 2011) were represented among the 12 *ect*-containing *Archaea*, and in each of these gene clusters, a copy of the ectoine hydroxylase gene (*ectD*) was also found (Fig. 1B). Two species of the genus *Methanotrix*, *Methanotrix harundinacea* 6Ac and *Methanotrix concilii* GP6 were represented, and two strains of *Methanobacterium* were found as well. In the genome sequence of these four methanogens, a full *ectABC* gene cluster was present, but each of them lacked the ectoine hydroxylase *ectD* gene (Fig. 1B), and such a gene was also not present anywhere else in their genome. The ectoine hydroxylase (EctD) is an oxygen-dependent enzyme (Bursy *et al.*, 2007; Höppner *et al.*, 2014; Widderich *et al.*, 2014b). Since members of the *Methanotrix* and *Methanobacterium* genera are all strict anaerobes, the absence of *ectD* in the genomes of these methanogens is readily understandable. On the other hand, the presence of *ectD* genes in '*Ca. N. maritimus*' SCM1, other members of the *Nitrosopumilus* genus and related Marine Group I Thaumarchaeota (Fig. 1B) is consistent with the lifestyle of these *Archaea* as oxygen-dependent nitrifying microorganisms (Könneke *et al.*, 2005; Pester *et al.*, 2011; Stieglmeier *et al.*, 2014).

'Ca. N. maritimus' SCM1 synthesizes both ectoine and hydroxyectoine in response to osmotic stress

The presence of a particular gene cluster in a microbial genome does not necessarily imply that it is also functional. To study whether any of the detected archaeal *ect* gene clusters were functionally expressed, we chose the Thaumarchaeon '*Ca. N. maritimus*' SCM1 as a model system (Könneke *et al.*, 2005; Walker *et al.*, 2010). '*Candidatus Nitrosopumilus maritimus*' SCM1 was originally isolated from a tropical fish tank of an aquarium in Seattle (USA) and represents the first cultured ammonium oxidizer within the domain *Archaea* (Könneke *et al.*, 2005). '*Ca. N. maritimus*' SCM1 belongs to the phylum Thaumarchaeota (Brochier-Armanet *et al.*, 2008; Stieglmeier *et al.*, 2014), which are among the most abundant microorganisms on Earth. They are ubiquitous in the Ocean (Stahl and de la Torre, 2012), found in estuarine sediments (Zhang *et al.*, 2015) and are also ubiquitous in terrestrial habitats (Gubry-Rangin *et al.*, 2015). Being adapted to extreme oligotrophic conditions (Martens-Habbena *et al.*, 2009; Könneke *et al.*, 2014), ammonia-oxidizing Thaumarchaeota are the predominant nitrifiers in the ocean and contribute significantly to the marine nitrogen cycle (Offre *et al.*, 2013). The predicted EctABCD proteins of '*Ca. N. maritimus*' SCM1

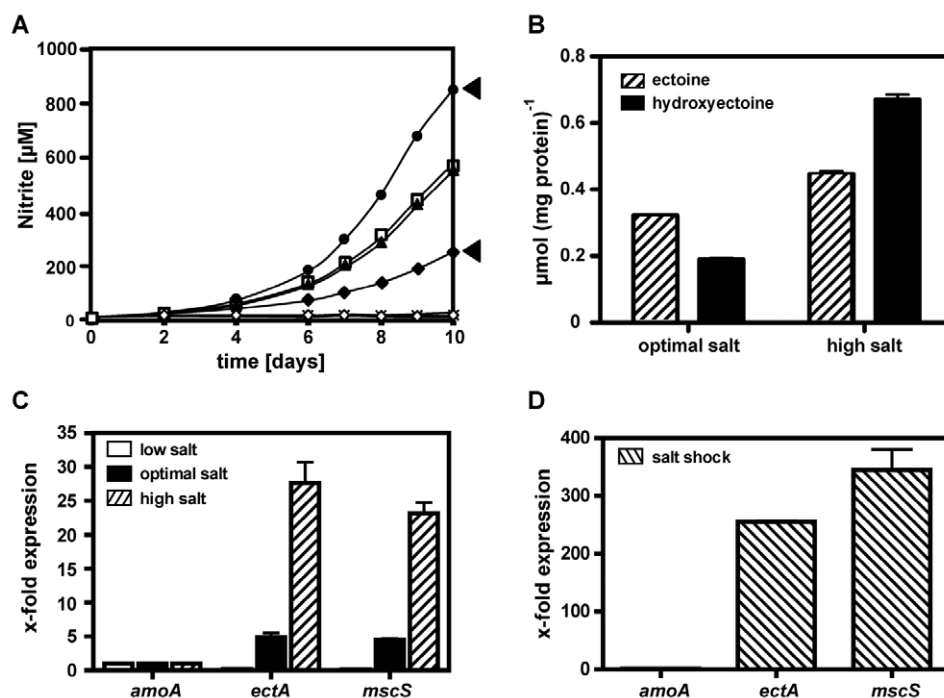


Fig. 2. Growth of 'Ca. N. maritimus' SCM1 in the presence of different NaCl concentrations, its production of ectoines and the expression of its *ect* operon in response to different NaCl concentrations.

A. Growth of 'Ca. N. maritimus' SCM1 cells in the presence of 0 M (closed diamonds), 0.15 M (cross), 0.32 M (open triangles), 0.48 M (closed triangles), 0.63 M (closed circles), 0.79 M (open squares), 0.94 M (closed diamonds) and 1.27 M (open diamonds) NaCl was monitored by nitrite production. Optimal sodium chloride concentration (0.63 M; closed circles) and high salt concentration (0.94 M; closed diamonds) in the growth medium of those cells used for the analysis of their ectoine and hydroxyectoine content are indicated by black arrowheads. B. Intracellular ectoine and hydroxyectoine content per total amount of protein as assessed by HPLC measurements of 'Ca. N. maritimus' SCM1 cells grown under optimal and high salt concentrations. Changes in expression of the 'Ca. N. maritimus' SCM1 *ectA* and *mscS* genes under (C) low, optimal and high salt concentrations and (D) after an osmotic shock as assessed by qRT-PCR are depicted. Relative expression was determined using the *amoA* transcript as a reference.

exhibited a degree of amino acid sequence identity of 41%, 53%, 52% and 47% in comparison with the functionally studied ectoine and hydroxyectoine biosynthetic enzymes of *Halomonas elongata* (Ono *et al.*, 1999b; Widderich *et al.*, 2014a), the natural microbial cell factory for the industrial-scale production of ectoines (Schwibbert *et al.*, 2011; Kunte *et al.*, 2014).

'Ca. N. maritimus' SCM1 can grow over a wide range of salinities (Elling *et al.*, 2015). To assess whether it would synthesize both ectoine and hydroxyectoine in response to salt stress, 'Ca. N. maritimus' SCM1 was grown in a chemically defined medium containing 26 g l⁻¹ NaCl (0.63 M NaCl); this medium has a measured osmolarity of 928 mOsm. To impose additional osmotic stress on 'Ca. N. maritimus' SCM1 cells, we also grew them in the same medium but with increased sodium chloride (NaCl) concentration (48 g l⁻¹) (0.94 M NaCl); this medium had a measured osmolarity of 1.598 mOsm. The increased salinity of the medium had a significant negative impact on the growth of 'Ca. N. maritimus'

SCM1 (Fig. 2A). Under both growth conditions, ectoine and hydroxyectoine were detected by high-performance liquid chromatography (HPLC) analysis, demonstrating that the *ectABCD* gene cluster of 'Ca. N. maritimus' SCM1 was functional. Since 'Ca. N. maritimus' SCM1 is a marine microorganism (Könneke *et al.*, 2005), optimal growth conditions occur only at a substantial osmolarity (26 g NaCl l⁻¹) (0.63 M NaCl). Hence, it was not surprising that we already found ectoine and hydroxyectoine in these cells; their total ectoine and hydroxyectoine content were 0.32 $\mu\text{mol mg protein}^{-1}$ and 0.19 $\mu\text{mol mg protein}^{-1}$ respectively. These values increased to 0.44 $\mu\text{mol mg protein}^{-1}$ of ectoine and 0.67 $\mu\text{mol mg protein}^{-1}$ of hydroxyectoine when the cells were grown under heightened osmotic stress in a medium with a sodium chloride concentration to 48 g l⁻¹ (0.94 M NaCl). Consequently, the level of synthesis of these compatible solutes by 'Ca. N. maritimus' SCM1 is responsive to increased osmotic stress (Fig. 2B).

Biochemical properties of the ectoine synthase and ectoine hydroxylase from 'Ca. N. maritimus' SCM1

EctC and EctD are the key enzymes for ectoine and hydroxyectoine synthesis respectively (Fig. 1A) (Ono *et al.*, 1999b; Bursy *et al.*, 2007; Widderich *et al.*, 2014a). We therefore wondered whether the biochemical properties of the EctC and EctD enzymes derived from *Archaea* possess characteristics similar to their bacterial counterparts, or are different. Consequently, we assessed the properties and kinetics of the EctC and EctD enzymes from the ectoine/hydroxyectoine producer 'Ca. N. maritimus' SCM1. To provide the substantial amounts of proteins required for biochemical studies, we obtained synthetic, codon-optimized versions of the *ectC* and *ectD* genes from 'Ca. N. maritimus' SCM1 (Walker *et al.*, 2010) and inserted them into the pASG-IBA3 expression vector (IBA GmbH, Göttingen, Germany) such that the produced EctC and EctD proteins were attached at their C-termini to a *Strep*-tag II affinity peptide. We refer in the following to these recombinant proteins as (Nm)EctC and (Nm)EctD.

The (Nm)EctC and (Nm)EctD proteins were effectively overproduced in *E. coli* BL21 and could be purified to a high degree of homogeneity by affinity chromatography on a Streptactin matrix (Fig. 3). Size exclusion chromatography demonstrated that preparations of both enzymes were essentially free of protein aggregates (Fig. 3). The molecular masses of the (Nm)EctC-*Strep*-tag II and (Nm)EctD-*Strep*-tag II proteins calculated from their corresponding gene sequences are 15.9 kDa and 35.8 kDa respectively. The two recombinant proteins eluted from the size exclusion columns as species with a calculated molecular mass of 31.9 kDa and 71.4 kDa, respectively, indicating that both the (Nm)EctC and (Nm)EctD enzymes are dimers in solution (Fig. 3). Such a quaternary assembly has previously also been reported for ectoine synthases (Ono *et al.*, 1999a; Kobus *et al.*, 2015) and ectoine hydroxylases (Höppner *et al.*, 2014; Widderich *et al.*, 2014a) from members of the *Bacteria*.

We then determined a set of basic biochemical parameters for the (Nm)EctC and (Nm)EctD enzymes and subsequently used these data to set up optimal enzyme activity assays. The (Nm)EctC and (Nm)EctD enzymes had similar temperature profiles with optima at 30°C and 35°C respectively (Fig. 4A). Both also possessed a similar pH dependency with activity optima of 7.0 and 7.5, for the (Nm)EctC and (Nm)EctD proteins respectively (Fig. 4B). The activity of the ectoine hydroxylase from 'Ca. N. maritimus' SCM1 was only slightly activated by increases in ionic strength (elicited either through the addition of NaCl or KCl to the enzyme assay buffer), whereas the activity of the ectoine synthase was restricted to a narrow concentration range of salts (Fig. 4C and D).

Using optimized enzyme assay conditions, we determined the kinetic parameters of the ectoine synthase and of the ectoine hydroxylase using their natural substrates N-γ-L-2,4-acetyl-diaminobutyrate (Ono *et al.*, 1999b) and ectoine (Bursy *et al.*, 2007; Widderich *et al.*, 2014a) respectively. Both enzymes showed Michaelis–Menten-type kinetics. The apparent kinetic parameters for the ectoine synthase were: $K_m = 6.4 \pm 0.6$ mM; $v_{max} = 12.8 \pm 0.4$ U mg⁻¹, $k_{cat} = 5.7$ s⁻¹, $k_{cat}/K_m = 0.9$ s⁻¹ mM⁻¹ (Fig. 5A). Those for the ectoine hydroxylase were: K_m (ectoine) = 3.8 ± 0.5 mM; K_m (2-oxoglutarate) = 3.1 ± 0.6 mM; $v_{max} = 1.8 \pm 0.1$ U mg⁻¹, $k_{cat} = 1.0$ s⁻¹, $k_{cat}/K_m = 0.3$ s⁻¹ mM⁻¹ (Fig. 5B and C).

The basic biochemical features and kinetic parameters of the 'Ca. N. maritimus' SCM1 ectoine hydroxylase are very similar to those of a considerable number of previously characterized EctD proteins (eight enzymes in total) from members of the *Bacteria* (Bursy *et al.*, 2007; 2008; Widderich *et al.*, 2014a). However, this situation is somewhat different for the ectoine synthase, an enzyme for which only two representatives have been kinetically characterized in some detail so far, namely the enzymes from *H. elongata* and *Acidiphilium cryptum* (Ono *et al.*, 1999a; Moritz *et al.*, 2015). The ectoine synthase from *H. elongata* is a highly salt tolerant enzyme (Ono *et al.*, 1999a), whereas both the EctC proteins from *A. cryptum* JF-1 (Moritz *et al.*, 2015) and 'Ca. N. maritimus' SCM1 (Fig. 4C and D) are sensitive to high salt concentrations. Moritz and colleagues (2015) suggested that these different sensitivities of the EctC enzymes from *H. elongata* and *A. cryptum* JF-1 against high salt concentrations result from their different overall net-negative charge (calculated isoelectric points: 4.87 and 6.03 for the EctC proteins from *H. elongata* and *A. cryptum* respectively). The calculated pI of the 'Ca. N. maritimus' SCM1 EctC protein is 5.65, and hence closer to that of *A. cryptum* JF-1; its salt-sensitive properties (Fig. 4C and D) is thus consistent with the hypothesis put forward by Moritz and colleagues (2015).

The amino acid sequences of key enzymes for ectoine/hydroxyectoine biosynthesis in Archaea cluster with their counterparts from Bacteria

The amino acid sequences of the 723 EctC-type proteins retrieved from the above-described database analysis were aligned and they exhibited, relative to the (Nm)EctC protein, a degree of sequence identity ranging between 79% (EctC from the marine Groupe_I Thaumarchaeota SCGC_AAA799-E16) and 33% (EctC from *Micrococcus luteus*). We then used this amino acid sequence alignment to construct a rooted tree of EctC-type proteins using tools provided via the iTOL web server (Letunic and Bork, 2011), in order to assess the taxonomic distribution

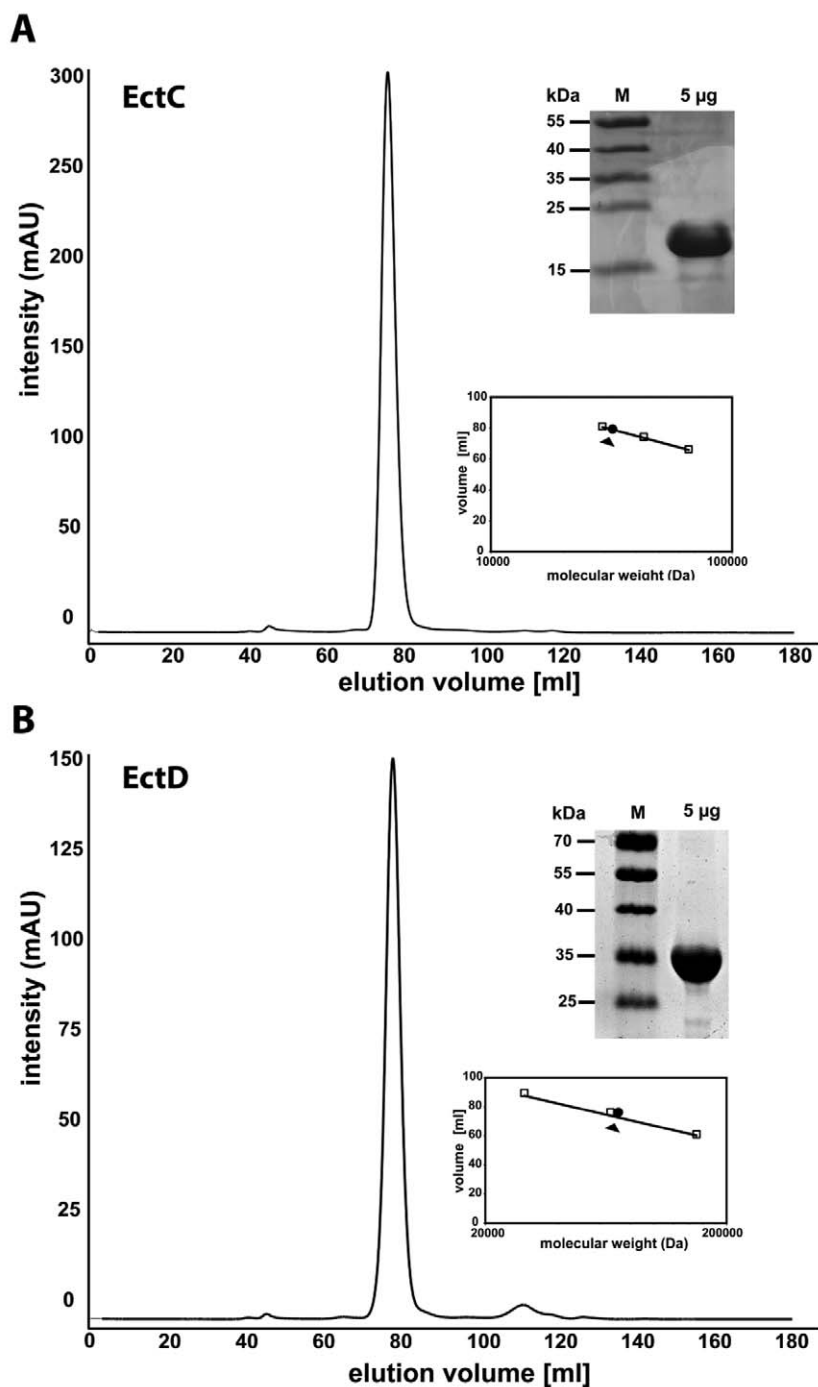


Fig. 3. Assessment of the purity of the (Nm)EctC-Strep-tag II and (Nm)EctD-Strep-tag II proteins and their quaternary assembly. (A) the (Nm)EctC-Strep-tag II and (B) (Nm)EctD-Strep-tag II recombinant proteins were isolated by affinity chromatography on a Streptactin matrix and analysed by SDS-polyacrylamide gel electrophoresis and size exclusion chromatography. (A) (Nm)EctC-Strep-tag II and (B) (Nm)EctD-Strep-tag II. The black arrowhead in the inserts of (A) and (B) indicate the calculated molecular mass of the recombinant proteins relative to that of marker proteins. For the (Nm)EctC-Strep-tag II protein the following marker proteins were used: albumin (66 kDa), ovalbumin (43 kDa), carboanhydrase (29 kDa). For the (Nm)EctD-Strep-tag II protein, the following marker proteins were used: alcohol-dehydrogenase (150 kDa), albumin (66 kDa), carboanhydrase (29 kDa).

of the 12 archaeal proteins and their affiliation with the nearest bacterial orthologues (Fig. 6). Nineteen microbial phyla were represented among those 723 microorganisms that possess EctC-type proteins; 16 of these phyla were derived from *Bacteria*, and three were derived from *Archaea*. The few EctC orthologues from archaeal strains cluster at three locations in the EctC-based phylogenetic tree (Fig. 6) (a phylogenetic tree listing the names of the EctC-possessing microorganisms is provided in Fig. S1),

suggesting that the corresponding *ect* genes were most likely obtained by lateral gene transfer events from bacterial donor strains harbouring closely related orthologues.

In the eight members of the Thaumarchaeota possessing *ect* gene clusters, all EctC orthologues form a monophyletic clade by themselves. EctC proteins of mostly *Halomonas* species and related genera of the *Halomonadaceae*, which are affiliated with the

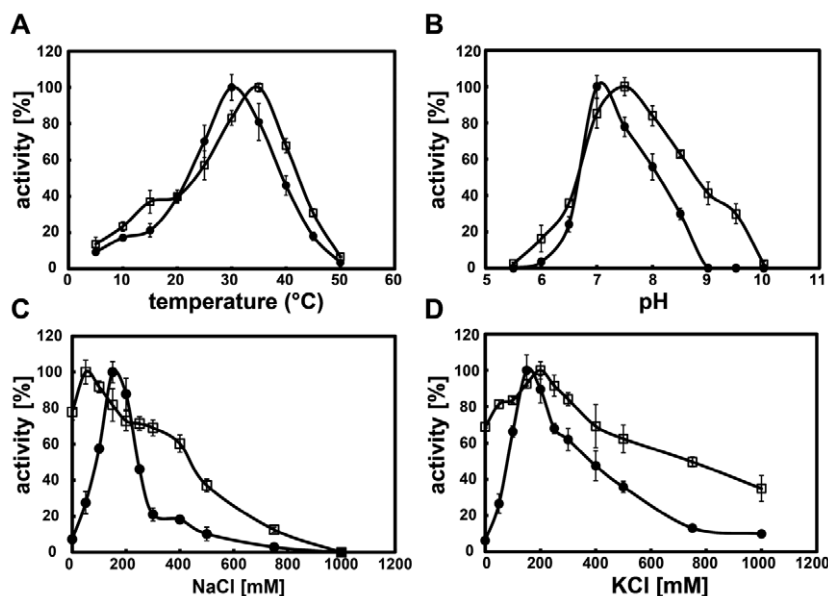


Fig. 4. Biochemical properties of the (Nm)EctC-Strep-tag II and (Nm)EctD-Strep-tag II proteins. Black dots: (Nm)EctC-Strep-tag II; open squares: (Nm)EctD-Strep-tag II.

Gammaproteobacteria, represent the most similar adjacent clade. Because all microorganisms from these two clades populate marine habitats, lateral transfer of the *ect* genes from a member of the *Halomonadaceae* to an ancestral strain of the genus *Nitrosopumilus* is plausible. The presence of some EctC sequences from marine *Alphaproteobacteria* (e.g. genera *Nesiotobacter*, *Zhangella* or *Marinitalea*) within the *Halomonadaceae* clade suggests that lateral gene transfer events have still been ongoing after the *ect* genes were transferred to an ancestor of *Nitrosopumilus*. The acquisition of ectoine/hydroxyectoine biosynthetic genes in the indicated strains by a lateral gene transfer event(s) is further supported by the fact that none of the AOA [*Nitrosopumilus sediminis* AR2, *Nitrosopumilus salaria* BD31, *Nitrosopumilus koreensis* MY1, *Nitrosoarchaeum limnia* (strains SFB1 and BG20), *Nitrosotenuis uzonensis* N4, *Nitrososphaera gargensis* and *Nitrosocaldus* sp.] contain ectoine/hydroxyectoine biosynthetic genes.

The other two clades of archaeal EctC orthologues are present in some members of the methanogenic genera *Methanothrix* and *Methanobacterium*, respectively, but they are not found in all sequenced strains of these genera. In case of *Methanothrix*, the closest relatives are from the strictly anaerobic sulfate-reducing deltaproteobacterial genus *Desulfarculus* and the aerobic alphaproteobacterial genus *Sneathiella*, and they form a common clade. Although very diverse in their taxonomy, all these strains were isolated from freshwater sediments or wastewater treatment plants, creating ample opportunity for lateral gene transfer. From the large phylogenetic distance between *Nitrosopumilus* and *Methanothrix*, it is clear that the respective gene transfer events must have happened independently. Among the seven genome-

sequenced species of the genus *Methanobacterium*, *ect* genes appear only to be present in the species *M. formicicum*. The respective EctC sequences form a common cluster with EctC orthologues from terrestrial and marine *Bacillaceae*, but also some *Betaproteobacteria* and *Gammaproteobacteria*. Therefore, it may be inferred that the *ect* genes in *M. formicicum* have been acquired by a very recent lateral transfer from one of the bacterial species with closely related *ectABC* sequences.

Since it is highly likely that the *ect* gene clusters present in members of the *Archaea* (Fig. 1B) were acquired via lateral gene transfer events, we attempted to identify possible bacterial donors by using the corresponding amino acid sequences of the ectoine/hydroxyectoine biosynthetic enzymes as query sequences in a BLASTP search of microbial genomes (Nordberg *et al.*, 2013) and then recording the top 10 hits. As documented in Table S1 as the results for this type of analysis for the Thaumarchaeota 'Ca. *N. maritimus*' SCM1, 'Ca. *Nitrosopumilus*' sp. SJ, 'Ca. *Nitrosopumilus koreensis*' AR1 and 'Ca. *Nitrosolumilus*' sp. AR2, no clear pattern emerged that would allow to precisely pinpoint possible bacterial donor species for the archaeal *ect* gene clusters.

Taken together, our phylogenetic assessment of EctC-type proteins is consistent with our biochemical and kinetic studies of the 'Ca. *N. maritimus*' SCM1 ectoine synthase (Figs 4 and 5) that ascribe bacterial-like properties to this archaeal protein. In analysing the rooted phylogenetic tree of EctC-type proteins, we noted that all orphan EctC-like proteins (Kurz *et al.*, 2010; Widderich *et al.*, 2014a) cluster together and form a distinct branch close to the root of the tree (Fig. 6). Among the 723 EctC-type proteins analysed, 24 belong to this group, and none was from an archaeon. The taxonomic affiliation

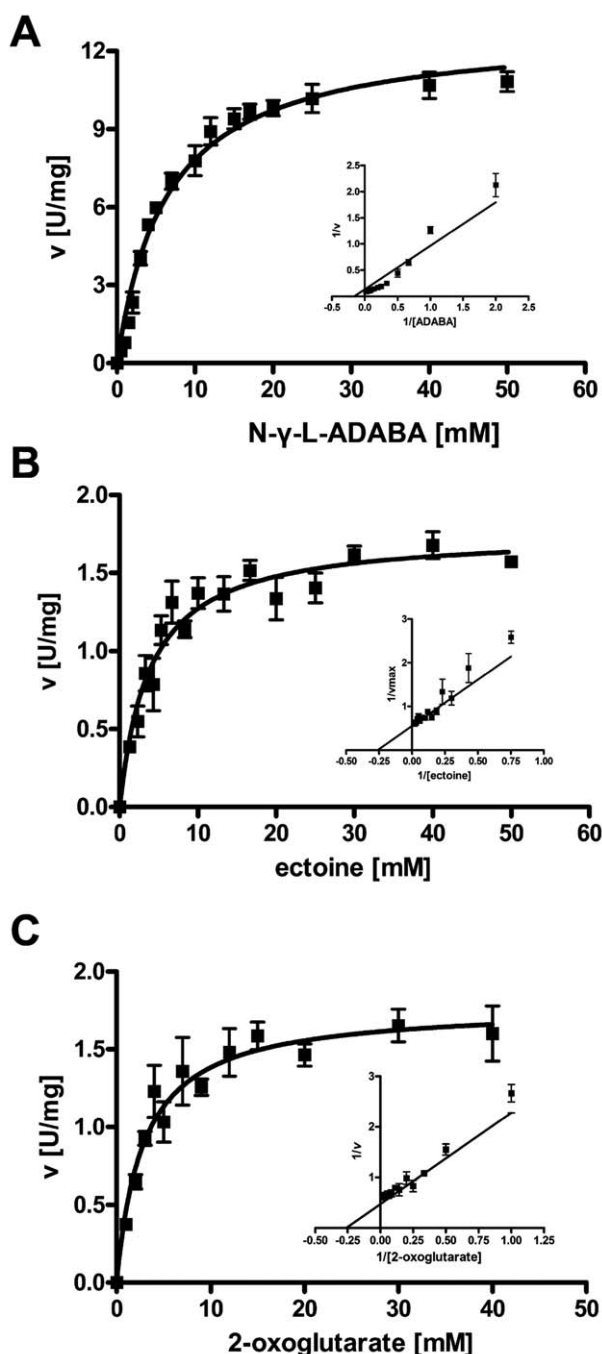


Fig. 5. Kinetic parameters of the (A) EctC for its substrate N γ -ADABA and of the ectoine hydroxylase EctD for its substrate ectoine (B) and its co-substrate 2-oxoglutarate (C).

harbouring these orphan *ectC* genes is rather diverse (Fig. 6).

A novel transcriptional organization of the ect gene cluster in 'Ca. N. maritimus' SCM1

Inspection of the organization of the *ectABCD* gene cluster of 'Ca. N. maritimus' SCM1 and those of other members of

this genus (Fig. 1B) revealed a conserved genetic arrangement that is also found in many members of the *Bacteria* (Widderich *et al.*, 2014a). The distance between the *ectA* and *ectB* genes is three bp, three bp between *ectB* and *ectC*, and the *ectC* and *ectD* coding regions overlap by two bp. These observations suggest that the *ectABCD* gene cluster of 'Ca. N. maritimus' SCM1 is transcribed as part of an operon. While the genetic organization of the 3' region of the *ect* genes is variable (Fig. 1B), they are all preceded in the *Nitrosopumilus* species and other marine *Thaumarchaeota* by an open reading frame (*hyp*) which codes for a hypothetical protein (*Hyp*; 125 amino acids) of unknown function. The coding region of the *hyp* gene and *ectA* in 'Ca. N. maritimus' SCM1 overlaps by three bp, suggesting that the *hyp* gene is co-transcribed with the *ectABCD* gene cluster (Fig. 1B). As a specialty among members the genus *Nitrosopumilus* and other marine *Thaumarchaea* containing *ect* genes, the *ectABCD* genes of 'Ca. N. maritimus' SCM1 are followed by an open reading frame (Fig. 1B) that was originally annotated to code for a protein of unknown function (Walker *et al.*, 2010). Our renewed database searches identified this protein as a member of the *MscS* family (see below), mechanosensitive channels that serve as safety valves against the cell-disrupting consequences of severe osmotic downshifts (Levina *et al.*, 1999). They are ubiquitously found in both *Bacteria* and *Archaea* (Kloda and Martinac, 2002; Booth and Blount, 2012; Naismith and Booth, 2012; Wilson *et al.*, 2013; Booth, 2014; Booth *et al.*, 2015). We refer to this protein in the following as the (*Nm*)*MscS* channel. The distance between the end of the *ectD* gene and the start of the *mscS* gene is 25 bp (Fig. 1B), suggesting that the *mscS* gene might be co-transcribed with the *ectABCD* gene cluster as well. Overall, the tight physical organization of the *hyp-ectABCD-mscS* gene cluster (Gene IDs: Nmar_1347, Nmar_1346, Nmar_1345, Nmar_1344, Nmar_1343, Nmar_1342) suggests that these genes are transcribed as an operon.

To test for a possible co-transcription of the *hyp-ectABCD-mscS* genes (Fig. 7A), we carried out an reverse transcription polymerase chain reaction (RT-PCR) analysis using RNA samples that were isolated from cells of 'Ca. N. maritimus' SCM1 that had been grown under increased osmotic stress conditions (48 g NaCl l⁻¹ which corresponds to 0.94 M NaCl) (Fig. 2A). The data presented in Fig. 7B demonstrate that the *hyp-ectABCD-mscS* gene cluster is indeed expressed as a transcriptional unit. Co-transcription of ectoine/hydroxyectoine biosynthetic genes (Widderich *et al.*, 2014a) has been routinely observed in members of the *Bacteria* (Kuhlmann and Bremer, 2002; Bursy *et al.*, 2007; Kuhlmann *et al.*, 2008). However, there is no report where they are co-transcribed with a gene for a mechanosensitive channel.

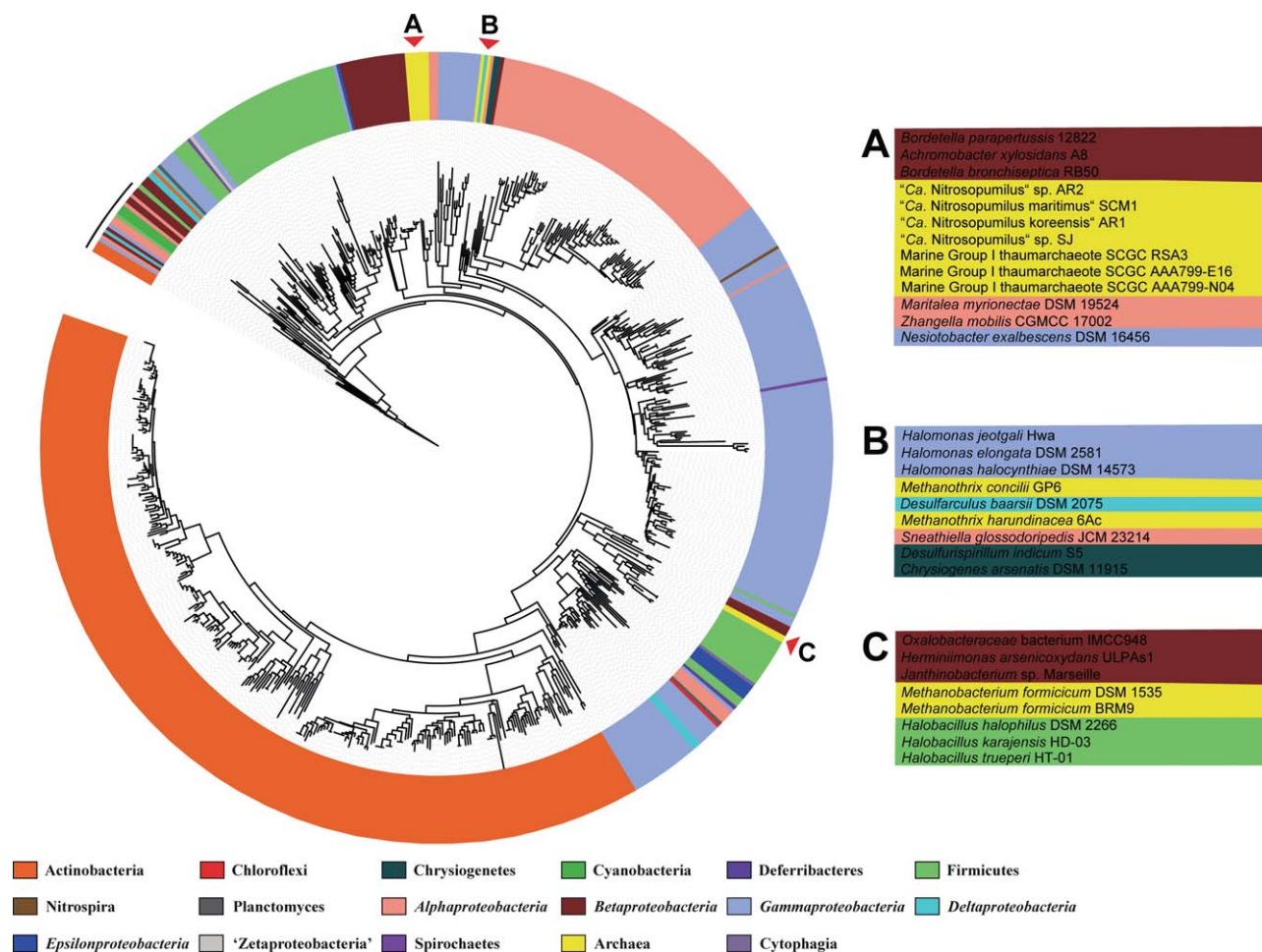


Fig. 6. Phylogenetic analysis of EctC-type proteins. Based on an amino acid sequence alignment of 723 EctC-type proteins, a rooted phylogenetic tree was constructed with the iTOL program (Letunic and Bork, 2011). The different phyla are marked by different colours and, for simplicity, the names of the *ectC*-possessing microorganisms were left out. An expanded version of the tree containing the names of the microorganisms predicted to produce the EctC protein is given in Fig. S1. The three regions in the phylogenetic tree populated by archaeal EctC proteins are highlighted by red arrowheads. An enlarged section of the phylogenetic tree representing the archaeal EctC proteins and their nearest bacterial orthologues are shown in A to C. The position of those 24 EctC-type proteins that originate from bacteria that lack identifiable *ectAB* genes are marked above the phylogenetic tree by a black bar.

The eight *ect* gene clusters present in Thaumarchaeota are all preceded by a gene (*hyp*) (Fig. 1B) that encodes a protein (125 amino acids) of unknown function. These Hyp proteins possess a degree of amino acid sequence identity ranging between 82% to 31%, and such proteins were found through database searches also in the Thaumarchaeota MY2 and N4, both of which do not possess *ect* genes. The Hyp proteins show no significant sequence similarity to annotated proteins in databases, and we can thus neither speculate about their potential function, nor can we comment on the obvious question why the *hyp* gene is co-transcribed with the *ect* gene cluster in various Thaumarchaeota (Fig. 7).

Expression of the *ect* genes in *Bacteria* is typically induced when the cells are exposed either to sustained or suddenly imposed osmotic stress (Kuhlmann and Bremer,

2002; Calderon *et al.*, 2004; Bursy *et al.*, 2007; Kuhlmann *et al.*, 2008; Salvador *et al.*, 2015). We therefore wondered whether this was also the case in the archaeon 'Ca. N. maritimus' SCM 1. We therefore isolated total RNA from cells that had been grown under low, optimal and high salt conditions (Fig. 2A) (13, 25 and 39 g NaCl l⁻¹, respectively) and assayed the transcript levels of a gene positioned either early (*ectA*) or late (*mscS*) in the *hyp-ectABCD-mscS* poly-cistronic messenger (m)RNA via q-RT-PCR. The cells of the cultures grown under different salt-stress conditions were all harvested when they were in the same growth phase to exclude possible effects of this parameter on the quantitative RT-PCR data. We used the transcript of the *amoA* gene (Gene ID: Nmar_1500) of 'Ca. N. maritimus' SCM 1, as a reference (Nakagawa and Stahl, 2013) to benchmark the *ectA* and *mscS* transcript

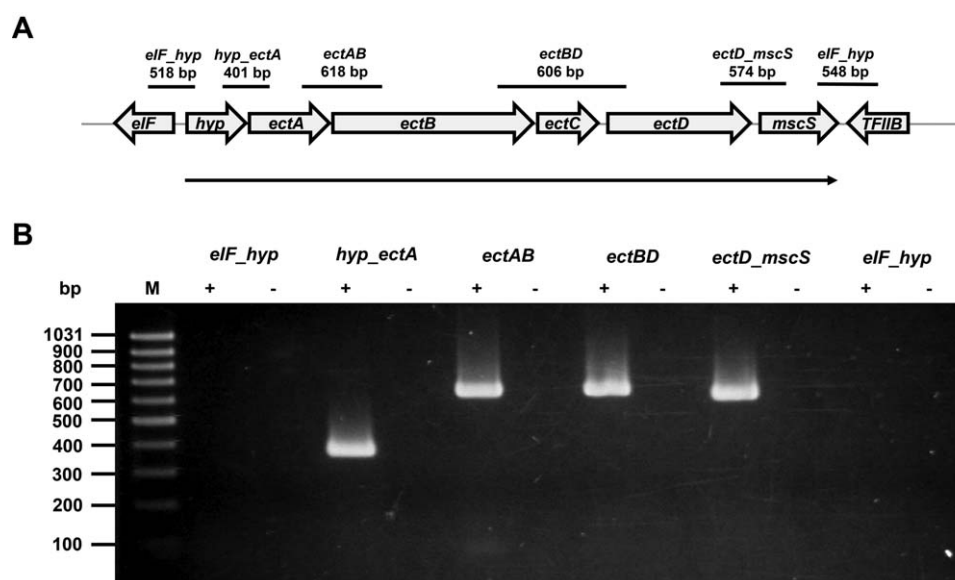


Fig. 7. Analysis of the co-transcription of the *hyp-ectABCD-mscS* gene cluster from 'Ca. N. maritimus' SCM1 by RT-PCR.

A. Genetic organization of the *hyp-ectABCD-mscS* gene cluster and predictions of the size of the PCR fragments made under the assumption that a given set of genes is co-transcribed.

B. Analysis of the sizes of the DNA fragments generated in the RT-PCR experiment by agarose gel electrophoresis. The symbol '+' indicates those samples reacted with reverse transcriptase, and the symbol '-' denotes samples prepared in its absence to ensure that the observed PCR products did not result from DNA contaminations of the RNA samples.

levels. Indeed, the *amoA* transcript turned out to be a suitable reference marker for salt-stressed and non-stressed cells since the level of its mRNA did not vary significantly under the above-described growth conditions (Fig. 2C). In contrast, the level of the *ectA* and of the *mscS* transcripts was strongly upregulated from an already substantial level in response to salt stress; by 5.7-fold and 5.1-fold respectively (Fig. 2C). An even greater enhanced induction of the *ectA* and *mscS* transcript levels was observed when 'Ca. N. maritimus' SCM1 cells that had been grown under optimal salt conditions (Fig. 2A) (26 g NaCl l^{-1}) were subjected to a severe osmotic upshift (by adding 23 g NaCl l^{-1} to the culture). This severe salt shock triggered a 52-fold and 76-fold increase in the *ectA* and *mscS* transcripts from their levels in cells grown under optimal salt conditions (Fig. 2D). Hence, both chronic and acute salt stresses are important environmental cues leading to strongly enhanced transcription of the *hyp-ectABCD-mscS* operon.

(Nm)MscS is a functional mechanosensitive channel

Since there is no report in the literature describing the co-transcription of an *ect* gene cluster with a gene encoding a mechanosensitive channel, we wondered whether the (Nm)MscS channel was functional. To study the functionality of the (Nm)MscS channel, we used a genetic

complementation experiment (Levina *et al.*, 1999) with an *E. coli* mutant strain (MJF641) (also referred to as the $\Delta 7$ strain) that lacks all currently known MscM-, MscS- and MscL-type mechanosensitive channels (Edwards *et al.*, 2012). We obtained a synthetic version of the 'Ca. N. maritimus' SCM 1 *mscS* gene that had been optimized for its expression in *E. coli* and placed it under the transcriptional control of the *lac* promoter present on plasmid pTrc99a (Amann *et al.*, 1988), thereby yielding plasmid pLC18. We then used a test developed by Levina and colleagues (1999) to assess the functionality of mechanosensitive channels *in vivo*. It relies on a rapid down-shock of high osmolarity grown cells lacking or expressing channel-forming proteins and then monitoring cell viability (Levina *et al.*, 1999). The parent (strain Frag1) of the $\Delta 7$ mutant-strain carrying the vector plasmid pTrc99a survived such an osmotic downshift essentially unscathed, whereas only 12.9% ($\pm 5\%$) of the cells of the $\Delta 7$ mutant-strain MJF641 (pTrc99a) survived such a treatment. In contrast, when MJF641 (pLC18; *mscS*⁺) was subjected to such an osmotic down-shock, the (Nm)MscS protein rescued cellular survival to a large extent ($62\% \pm 5\%$ surviving cells) (Fig. 8A). This experiment therefore unambiguously demonstrates that the gene following the *ectABCD* gene cluster (Figs 1B and 7A) in the 'Ca. N. maritimus' SCM1 genome (Walker *et al.*, 2010) encodes a functional mechanosensitive channel.

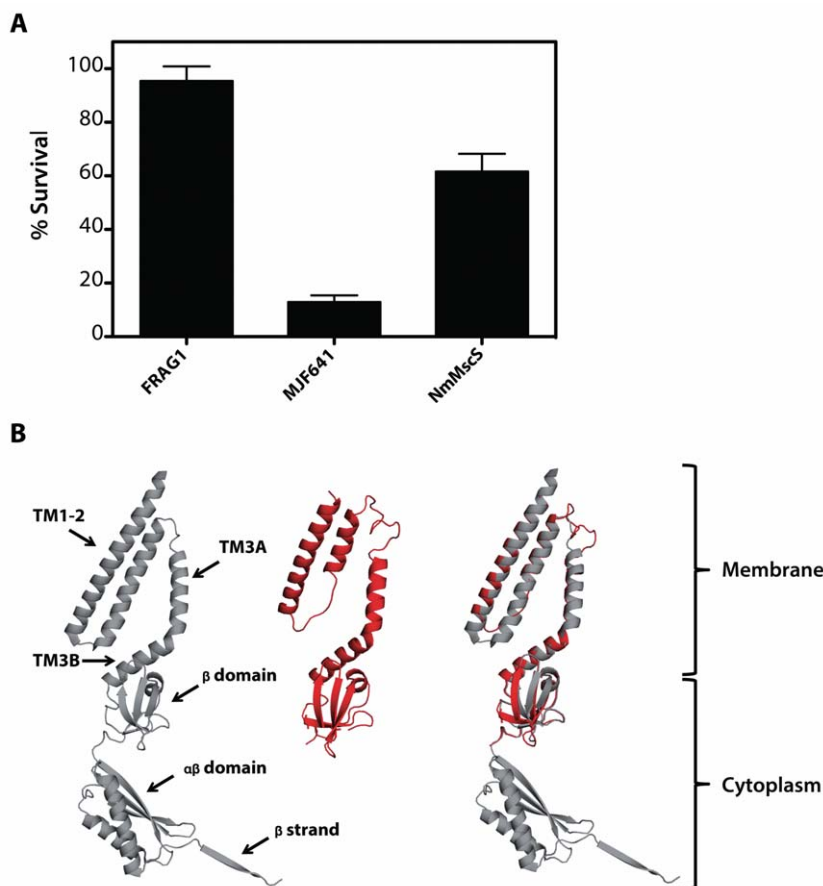


Fig. 8. Functional assessment of the (*Nm*)MscS protein and *in silico* prediction of its structure.

A. Cells of the *E. coli* strain MJF641 which is defective in all currently known MscL-, MscS- and MscM-type channels (also referred to as $\Delta 7$ mutant) (Edwards *et al.*, 2012) and its parent strain Frag1 carrying the empty vector plasmid pTrc99a (Amann *et al.*, 1988) were grown in high-salinity minimal medium (with 0.3 M NaCl) and were then subjected to a rapid osmotic downshift (minimal medium without additional NaCl) (Levina *et al.*, 1999). The same procedure was used with strain MJF641 harbouring a plasmid (pLC18) that contains the '*Ca. N. maritimus*' SCM1 *mscS*⁺ gene expressed under the control of the *lac* promoter present on pTrc99a. The number of cells surviving such rapid osmotic downshifts was determined by spotting them on LB agar plates. The data shown represent the mean and standard deviation of four independently conducted experiments.

B. Crystal structure of a monomer of the *E. coli* MscS protein (left) from the open *E. coli* MscS heptameric channel assembly (protein database accession code: 2VV5) (Wang *et al.*, 2008) was automatically chosen by the SWISS-MODEL web server (Biasini *et al.*, 2014) as the template to generate an *in silico* model (middle) of the (*Nm*)MscS protein. The PYMOL suite (<https://www.pymol.org/>) was used to visualize these structures and overlay them with each other (right).

In silico analysis of the (*Nm*)MscS mechanosensitive channel

Mechanosensitive channels acting as safety valves against osmotic downshifts can be grouped into three types (MscM, MscS, MscL) and provide the microbial cell with a graded stress response to an osmotic challenge through their different threshold levels of opening and their different diameters of the fully open channels (Haswell *et al.*, 2011; Booth and Blount, 2012; Edwards *et al.*, 2012; Booth, 2014). A database search identified the '*Ca. N. maritimus*' SCM1 protein as a member of the MscS family with an overall level of amino acid sequence identity to the *E. coli* MscS protein (Levina *et al.*, 1999) of about 12%. However, in comparison to the *E. coli* protein, (*Nm*)MscS lacks about 100 amino acids at its carboxy-terminus (Fig. S2). When this is taken into consideration, and a stretch of badly aligning 20 amino acids from the N-terminus are removed as well from the comparison of the two proteins, the degree of amino acid sequence identity increases to about 16%. Consistent with this amino acid sequence alignment, the SWISS MODEL server (<http://swissmodel.expasy.org/>) (Biasini *et al.*, 2014) automatically chose a monomer of the homo-heptameric

E. coli MscS channel in its 'open' form (PDB entry 2VV5) (Wang *et al.*, 2008) as its modelling template (Fig. 8B). Like its *E. coli* MscS counterpart (Bass *et al.*, 2002; Wang *et al.*, 2008), the (*Nm*)MscS protein is predicted to contain three membrane-spanning segments and a carboxy-terminus that protrudes into the cytoplasm (Fig. 8B). Inspection of the (*Nm*)MscS *in silico* model revealed an important difference with respect to the *E. coli* MscS protein, as the cytoplasmic $\alpha\beta$ -domain and an adjacent β -sheet is missing (Fig. 8B).

Interestingly, a protein similar to that of (*Nm*)MscS (Fig. S2) is encoded in the genome of '*Ca. Nitrosopumilus*' sp. AR2. However, in contrast to the situation in '*Ca. N. maritimus*' SCM1, the putative *mscS* gene is transcribed divergently from the *hyp-ectABCD* gene cluster (Fig. 1B). Of note is also that the genome sequence of '*Ca. N. maritimus*' SCM1 (Walker *et al.*, 2010) encodes in addition to the (*Nm*)MscS protein (gene ID: Nmar_1342), four other MscS-encoding genes (gene ID: Nmar_1337, Nmar_1773, Nmar_1335, Nmar_0971). These MscS-type proteins vary considerably with respect to the length of their carboxy-termini. '*Ca. Nitrosopumilus maritimus*' SCM1 does not possess a gene for an MscL-type channel.

We also inspected the genome sequences of all other archaeal strains that possess *ect* gene clusters for the presence of *mscS* and *mscL*-type genes. Each of these microorganisms possesses multiple numbers (between one and four) of *mscS*-type genes but only *M. harundinacea* 6Ac and *Methanotrix concilii* GP-6 possess *mscL*-type genes as well (Table S2). Hence, MscS-type mechanosensitive channels (Levina *et al.*, 1999; Wang *et al.*, 2008) seem to be the preferred device to physiologically cope with rapid osmotic downshifts by those *Archaea* whose genome sequences we have inspected.

Discussion

Ectoine and its derivative 5-hydroxyectoine are well-recognized compatible solutes that are synthesized, or taken up, in response to osmotic stress by many microorganisms (Pastor *et al.*, 2010; Widderich *et al.*, 2014a). Their biophysical properties allow them not only to serve as effective stress protectants but also to function as chemical chaperones as they are able to preserve the functionality of proteins, macromolecular complexes, membranes and even entire cells (Lippert and Galinski, 1992; Manzanera *et al.*, 2002; Harishchandra *et al.*, 2010; Pastor *et al.*, 2010; Kunte *et al.*, 2014; Tanne *et al.*, 2014). Our updated database search identified the signature enzyme for ectoine production, the ectoine synthase (Ono *et al.*, 1999b; Widderich *et al.*, 2014a), in about 4.7% of 27.789 microbial genome sequences deposited in the JGI database at the time of the search. Predicted ectoine producers are found in 19 microbial phyla. Only three of these represent *Archaea*, and only 12 archaeal strains belonging to the genera *Nitrosopumilus*, *Methanotrix* and *Methanobacterium* are predicted to engage in ectoine synthesis among the 557 *Archaea* with deposited genome sequences. This data set therefore reinforces our previous conclusion that ectoine is a compatible solute primarily synthesized by members of the *Bacteria* (Widderich *et al.*, 2014a).

It is notable that among the 12 archaeal strains possessing ectoine biosynthetic genes, eight are affiliated with the genus *Nitrosopumilus*. We therefore used 'Ca. *N. maritimus*' SCM1 (Könneke *et al.*, 2005; Walker *et al.*, 2010) as a model system to study ectoine/hydroxyectoine synthesis and the genetic control of its *ect* gene cluster in this physiologically well-characterized and globally abundant member of the domain *Archaea* (Stahl and de la Torre, 2012; Offre *et al.*, 2013). Both the transcription of the ectoine/hydroxyectoine biosynthetic genes and the production of these compatible solutes in 'Ca. *N. maritimus*' SCM1 are responsive to osmotic stress (Fig. 2), thereby strongly suggesting that ectoines serve an osmoprotective function in this Thaumarchaeon, as firmly established in many members of the

Bacteria (Pastor *et al.*, 2010; Kunte *et al.*, 2014). We surmise that the data presented here on these issues for 'Ca. *N. maritimus*' SCM1 are relevant for an understanding of the physiology and genetics of the production of these compatible solutes by other strains and species of the Thaumarchaeota, and we suggest that is also true for those species of the methanogens *Methanotrix* and *Methanobacterium* carrying ectoine biosynthetic genes (Fig. 1B).

A phylogenetic tree derived from an amino acid sequence alignment of 723 unique EctC-type proteins revealed that the 12 archaeal EctC orthologues cluster in three separate locations among their bacterial counterparts (Figs 6 and S1). These data strongly suggest that the *Archaea* harbouring *ectABC(D)* gene clusters have acquired them via horizontal gene transfer events from bacterial donor strains living in the same habitats. This suggestion is also consistent with our finding that the key enzymes for ectoine biosynthesis, the ectoine synthase (EctC) and the ectoine hydroxylase (EctD) from 'Ca. *N. maritimus*' SCM1 possessed biochemical and kinetic properties (Figs 4 and 5) resembling those of their bacterial counterparts (Ono *et al.*, 1999b; Bursy *et al.*, 2007; 2008; Widderich *et al.*, 2014a; Moritz *et al.*, 2015). Since the 12 EctC proteins derived from *Archaea* are found in three different locations in the ectoine synthase-based phylogenetic tree (Figs 6 and S1), it seems likely that the *ectABC(D)* genes were introduced into members of the genera *Nitrosopumilus*, *Methanotrix* and *Methanobacterium* by separate events. However, by comparing the amino acid sequences of the archaeal ectoine/hydroxyectoine biosynthetic enzymes to their nearest orthologues from *Bacteria* (Table S1), we were unable to derive a consistent picture of the potential donor *Bacteria*.

It is well known that horizontal gene transfer is an important driver of microbial evolution helping microorganisms to rapidly obtain new metabolic capabilities and develop new stress management skills so that they can better cope with the situation in their original habitat, or explore new ecosystems (Ochman *et al.*, 2000; Soucy *et al.*, 2015). This process shaped the gene content of archaeal genomes in a major way (Nelson-Sathi *et al.*, 2015). For instance, it was concluded from a metagenomic analysis of deep Mediterranean waters that about 24% of the genes derived from planktonic Thaumarchaeota were of bacterial origin (Deschamps *et al.*, 2014).

While this paper was under review, the genome sequences of two novel *Nitrosopumilus* strains originating from coastal surface waters of the Northern Adriatic Sea became available. We found that neither 'Ca. *Nitrosopumilus* piranensis' D3C, nor 'Ca. *Nitrosopumilus* adriaticus' NF 5 (Bayer *et al.*, 2015) possess ectoine

biosynthetic genes. Remarkably, based upon a 16 S-23S rRNA tree derived from cultivated Thaumarchaeota with sequenced genomes, 'Ca. Nitrosopumilus piranensis' D3C, is the closest relative of 'Ca. N. maritimus' SCM1 and 'Ca. Nitrosopumilus koreensis' AR1 (Bayer *et al.*, 2015), both of which possess ectoine/hydroxyectoine biosynthetic gene clusters (Fig. 1B). Hence, it seems likely that the possession, or lack, of ectoine/hydroxyectoine biosynthetic genes among the AOA reflects specific ecological niche adaptive evolutionary processes (Blainey *et al.*, 2011; Gubry-Rangin *et al.*, 2015).

No genetic system is currently available for 'Ca. N. maritimus' SCM1 (Walker *et al.*, 2010) that would allow the construction of a mutant derivative lacking the *ectABCD* gene cluster. However, the isolation of a taxonomically very close relative, 'Ca. Nitrosopumilus piranensis' D3C, that lacks these genes naturally (Bayer *et al.*, 2015) provides the opportunity to compare the physiology and growth properties of these two Thaumarchaeota to reveal possible benefits of ectoine/hydroxyectoine production.

The function-preserving features of ectoines have triggered considerable biotechnological interest and led to the development of an industrial scale production process that relies on a severe osmotic down-shock to release newly synthesized ectoines from microbial producer cells (Schwibbert *et al.*, 2011; Kunte *et al.*, 2014). This so-called bacterial milking procedure builds on an evolutionarily conserved cellular emergency stress reaction to sudden osmotic down-shocks that relies on the transient opening of MscM-, MscS- and MscL-type mechanosensitive channels to prevent cell rupture (Booth, 2014). These types of safety valves have a deep evolutionary origin and are found both in *Archaea* and *Bacteria* (Kloda and Martinac, 2002; Pivetti *et al.*, 2003).

Most interestingly, we discovered that the *ectABCD* gene cluster of 'Ca. N. maritimus' SCM1 is co-transcribed with the gene for an MscS-type mechanosensitive channel (*hyp-ectABCD-mscS*) (Fig. 7). While nothing can currently be concluded about the role of the *hyp* gene product, the *mscS*-encoded mechanosensitive channel is functional (Fig. 8A). A genetic configuration that entails the co-transcription of a *mscS* gene along with the *ectABC(D)* operon has not been described before in any ectoine/hydroxyectoine-producing microorganism. The *hyp-ectABCD-mscS* operon seems to be a rather sophisticated genetic device to counteract the detrimental effects of osmotic fluctuations on cell physiology. The osmotic induction of its transcription allows 'Ca. N. maritimus' SCM1 to cope with increased salinity through enhanced production of the osmoprotectants ectoine and hydroxyectoine. At the same time, it prepares the high osmolarity stressed cells for an osmotic down-

shift that eventually will occur in narrow transition zones from marine to estuarine ecosystems through enhanced preemptive synthesis of the (*Nm*)MscS (Santoro *et al.*, 2008) mechanosensitive channel. We are aware that in the hyperthermophilic Creanarchaeon *Thermoproteus tenax*, an *mscS*-type gene is co-transcribed with enzymes required for the synthesis of the compatible solute trehalose (Zaparty *et al.*, 2013). However, in contrast to the biological data we provide here for the (*Nm*)MscS protein (Fig. 8A), the functionality of the Msc protein from *T. tenax* has not yet been experimentally assessed.

Both the MscS and the MscL mechanosensitive channels are widely considered as non-specific pores when they are fully opened and they have calculated pore diameters of about 13 Å and 30 Å respectively (Cruickshank *et al.*, 1997; Wang *et al.*, 2008). However, the fact that both in 'Ca. N. maritimus' SCM1 and in *T. tenax*, *mscS*-type genes are co-expressed with genes encoding enzymes for the synthesis of the compatible solutes ectoine/hydroxyectoine and trehalose, respectively, raises the question if the (*Nm*)MscS and (*Tt*)MscS channels are not endowed with a certain degree of substrate specificity. It is of interest to consider in this context the properties of the MscCG mechanosensitive channel of *Corynebacterium glutamicum*. Like (*Nm*)MscS, MscCG is a MscS-type channel and participates in the osmotic stress response of *C. glutamicum* (Börngen *et al.*, 2010). However, it also serves as an export channel for glutamate *in vivo* (Nakamura *et al.*, 2007; Becker and Krämer, 2015). Despite these latter observations, electrophysiological studies did not suggest that the MscCG channel possesses substrate specificity for glutamate (Becker *et al.*, 2013; Nakayama *et al.*, 2013).

Most members of the diverse MscS family are structurally built on a common core architecture in which the monomer possesses three trans-membrane-spanning segments. The membrane-embedded helix one and two form the sensor for membrane tension and part of the broken helix 3 lines the pore of the heptameric channel assembly (Bass *et al.*, 2002; Wang *et al.*, 2008; Naismith and Booth, 2012) (Fig. 8B). This latter helix provides a structural link between the pore domain and the carboxy-terminal part of the MscS monomer that forms an extended funnel-like vestibule inside the cytoplasm in the fully assembled heptameric MscS channel. Solutes and solvents must pass on their way out of the cell through this structurally complex vestibule when the channel opens (Bass *et al.*, 2002; Wang *et al.*, 2008; Naismith and Booth, 2012; Wilson *et al.*, 2013; Booth *et al.*, 2015). Through conformational changes, the cytoplasmic cage probably plays an important role for the opening and closing reactions of the MscS channel as a whole. It might also serve as a sensor for increases in macromolecular crowding of the cytoplasm (Rowe *et al.*, 2014), a process that is

strongly influenced by osmotically instigated water fluxes in or out of the cell (Wood, 2011).

We therefore note with considerable interest that (*Nm*)MscS protein lacks, in comparison with the *E. coli* MscS protein (Bass *et al.*, 2002; Wang *et al.*, 2008), a large part of the carboxy-terminus (Fig. S2). This should lead to a structurally rather different make-up of the cytoplasmic portion of the (*Nm*)MscS channel (Fig. 8B). Mechanosensitive channels open in response to increased tension in the plain of the lipid bilayer of the cytoplasmic membrane that results from an increase in turgor (Naismith and Booth, 2012; Booth, 2014). These types of proteins therefore have to closely interact with lipids to perform their physiological function. The types of lipids that are present in the Thaumarchaeon '*Ca. N. maritimus*' SCM1 are very different from those of *E. coli* (Elling *et al.*, 2014), yet the (*Nm*)MscS protein is physiological active in the surrogate *E. coli* host strain (Fig. 8A). Based on the discussed properties of the (*Nm*)MscS protein, it might be well worthwhile to study its electrophysiological properties, gating behaviour and potential substrate specificity in its own right.

Experimental procedures

Chemicals and synthesis of the substrate of the ectoine synthase

Ectoine and hydroxyectoine were kind gifts from Dr Irina Bagyan (bitop AG, Witten, Germany). Anhydrotetracycline, desthiobiotine and the streptavidin affinity matrix for the purification of *Strep*-tag II-labelled protein were purchased from IBA GmbH (Göttingen, Germany). Alkaline hydrolysis of ectoine was performed as reported previously (Kunte *et al.*, 1993) to obtain the substrate, *N*- γ -acetyl-L-2,4-diaminobutyrate (*N*- γ -ADABA), for the EctC (Peters *et al.*, 1990; Ono *et al.*, 1999b). All chemicals required for this synthetic process were purchased from Sigma Aldrich (Steinheim, Germany) or Acros (Geel, Belgium). Briefly, hydrolysis of ectoine (284 mg, 2.0 mmol) was accomplished in aqueous potassium hydroxide (KOH) (50 ml, 0.1 M) for 20 h at 50°C (Kunte *et al.*, 1993). The reaction mixture was subsequently neutralized with perchloric acid (60% in water, 4 ml), and the precipitated potassium perchlorate was filtered off. The filtrate was concentrated under reduced pressure, and the residue was purified by repeated chromatography on a silica gel column (Merck silica gel 60). Chromatography was performed by using a gradient of ethanol/25% ammonia/water 50:1:2 – 10:1:2 as the eluent to yield *N*- γ -ADABA. We recovered 192 mg (1.20 mmol; 60%) of *N*- γ -ADABA from the starting material (284 mg ectoine, 2.0 mmol). The identity and purity of the isolated *N*- γ -ADABA was unequivocally established both by thin-layer chromatography (TLC) (silica gel 60 F254 TLC plates; Merck) and nuclear magnetic resonance (¹H-NMR and ¹³C-NMR) spectroscopy (Peters *et al.*, 1990; Ono *et al.*, 1998) on a Bruker AVIII-400 or DRX-500 NMR spectrometer. (i) TLC: *R_f* of *N*- γ -ADABA = 0.55 (ethanol/25% ammonia/water 7:1:2); (ii) ¹H-NMR (400 MHz, D₂O): δ = 3.71

(dd, ³J(H,H) = 7.6 Hz, ³J(H,H) = 5.6 Hz, 1H, CH), 3.41 – 3.24 (m, 2H, CH₂), 2.15 – 2.01 (m, 2H, CH₂), 1.99 (s, 3H, CH₃) ppm; (iii) ¹³C-NMR (100 MHz, D₂O): δ = 177.5 (CO), 177.0 (COOH), 55.3 (CH), 38.3 (CH₂), 33.0 (CH₂), 24.6 (CH₃) ppm.

Recombinant DNA procedures and construction of plasmids

The DNA sequences of the *ectC*, *ectD* and *mscS* genes were retrieved from the genome sequence (accession number: NC_010085) (Walker *et al.*, 2010) of '*Ca. N. maritimus*' SCM1 and were used as templates for the synthesis of codon-optimized versions of these genes for their expression in *E. coli*. These synthetic genes were constructed either by GenScript (Piscataway, USA), or by LifeTechnologies (Darmstadt, Germany). Their DNA sequences were deposited in the NCBI database under accession numbers KR002039 (*ectC*), JN019033 (*ectD*) and KT313590 (*mscS*). To allow the overproduction and purification of the '*Ca. N. maritimus*' SCM1 EctC and EctD proteins in *E. coli*, we constructed recombinant versions of the corresponding genes. The *ectC* and *ectD* sequences were retrieved from the plasmids provided by the suppliers of the synthetic constructs, and inserted into the expression vector pASG-IBA3 (IBA GmbH, Göttingen, Germany). The resulting expression vectors [pWN48 (*ectC*⁺) and pMP45 (*ectD*⁺)] permit the effective synthesis of the '*Ca. N. maritimus*' SCM1 recombinant EctC and EctD proteins in *E. coli*. Both proteins are fused at their carboxy-termini with a *Strep*-tag II affinity peptide (NWSHPQFEK). This allows the purification of the (*Nm*)EctC-*Strep*-tag II and (*Nm*)EctD-*Strep*-tag II proteins by affinity chromatography on a streptavidin matrix.

For the heterologous expression of the *mscS* from '*Ca. N. maritimus*' SCM1 in *E. coli*, the codon-optimized synthetic *mscS* gene was amplified from the plasmid obtained from the supplier (LifeTechnologies) by PCR using custom synthesized DNA primers. Short DNA fragments carrying *Nco*I and *Hind*III restriction sites, respectively, were attached either to the 5' or to the 3' prime ends of the PCR product, thereby enabling its directional insertion into the expression vector pTrc99a (Amann *et al.*, 1988). This positioned the transcription of the *mscS* gene under the control of the *lac* promoter carried by the pTrc99a vector and resulted in the isolation of plasmid pLC18. The correct nucleotide sequence of the *mscS* gene carried by pLC18 was ascertained by DNA sequence analysis, which was performed by Eurofins MWG Operon (Ebersberg, Germany).

Bacterial strains

The *E. coli* strain MJF641 which is defective in all currently known MscL-, MscS- and MscM-type channels (*mscL mscS mscK ybdG ybiO yjeP ynaI*) (also referred to as $\Delta 7$) and its parent Frag1 (*thi rha lac gal*) have been described (Edwards *et al.*, 2012) and were a kind gift of Dr Ian Booth and Dr Samanta Miller (University of Aberdeen, Aberdeen, Scotland; UK). The *E. coli* B strain BL21 (Dubendorff and Studier, 1991) served as the host strain for plasmids that were used for the overexpression of recombinant versions of the '*Ca. N. maritimus*' SCM1 *ectC* and *ectD* genes. The '*Ca. N.*

maritimus' strain SCM1 (Könneke *et al.*, 2005) was from stocks of the laboratory of Dr M. Könneke (MARUM, University of Bremen; Germany).

Media and growth conditions

'*Candidatus Nitrosopumilus maritimus*' SCM1 was cultivated at 28°C in 15-l batch cultures using a 4-(2-hydroxyethyl)-1-piperazineethanesulfonate (HEPES)-buffered medium as described previously (Könneke *et al.*, 2005; Martens-Habbenha *et al.*, 2009). Ammonia (1.5 mM NH₄Cl) served as the energy source, and 1 mM sodium bicarbonate was added as the carbon source. For optimal growth conditions, cells of *Ca. N. maritimus* from two batches (a total of 30 l) were grown in media with 26 g l⁻¹ NaCl. This medium has an osmolarity of 928 mOsm. For growth conditions with increased salinity, cells were grown in three batches (a total of 45 l) of media containing 48 g l⁻¹ NaCl. This medium has a measured osmolarity of 1598 mOsm. During incubation, cultures were slightly shaken by hand once a day to provide oxygen. A spectrophotometric assay was used to follow the growth of 'Ca. N. maritimus' SCM1 by measuring the formation of nitrite (Strickland and Parson, 1972). Cells were harvested in the late growth phase (production of 1.1–1.3 mM nitrite) with a cross-flow filtration system equipped with a 0.1 µm pore size filter cassette (Sartocon-Slice Microsart, Sartorius, Göttingen, Germany). For ectoine and hydroxyectoine analysis, concentrated cell suspensions were fixed with 4% formaldehyde (16% formaldehyde solution (w/v) Thermo Scientific, Rockford, USA), and stored refrigerated.

For studying the expression of the *ectA* and *mscS* in 'Ca. N. maritimus' SCM1 at different salt conditions of the growth medium, cells were cultured in 5 L batch cultures at 28°C in HEPES buffered medium (pH 7.6) containing 1.5 mM ammonia as sole energy source as described previously (Könneke *et al.*, 2014). Medium for low, optimal and high salt conditions contained 13, 26 and 39 g NaCl L⁻¹ respectively. Cultures grown at different salinities were harvested in the same growth phase (when about two thirds of the ammonia was converted to nitrite) with a cross-flow filtration system (0.1 µm Sartocon slice Microsart filter, Sartorius Stedim, Göttingen, Germany). Concentrated cells were centrifuged (45 min, 4415 × g), and pellets were stored with RNAlater (SIGMA Life Science, Taufkirchen, Germany) at 4°C following the instructions of the manufacturer. Salt shock conditions were created by addition of 23 g NaCl L⁻¹ into a 15 L batch culture of 'Ca. N. maritimus' SCM1 in mid-growth phase grown at optimal salt conditions (26 g NaCl L⁻¹). After an additional incubation period of 24 h at high-salinity growth conditions, the cells were harvested as described above. Growth in all cultivation experiments of 'Ca. N. maritimus' SCM1 was monitored by following the formation of nitrite. Purity of the cultures was routinely checked by phase contrast microscopy.

Escherichia coli strains were routinely maintained on LB agar plates (Miller, 1972). When strains contained plasmids, ampicillin (100 µg ml⁻¹) was added to the growth medium to select for the presence of the plasmids. For the analysis of cell viability of strains Frag1(pTrc99a), MJF641(pTrc99a) and MJF641(pLC18) subsequent to an osmotic down-shock, we used the growth medium and the procedure described by

Levina and colleagues (1999). Osmotically unstressed cells were grown at 37°C in a 100-ml Erlenmeyer flask filled with 20 ml of medium in a shaking water bath (set to 220 rpm) using a citrate-phosphate buffered chemically defined medium (pH 7.0). It contained per litre: 8.58 g Na₂HPO₄, 0.87 g K₂HPO₄, 1.34 g citric acid, 1.0 g (NH₄SO₄), 0.001 g thiamine, 0.1 g MgSO₄·7H₂O and 0.002 g (NH₄)₂SO₄·FeSO₄·6H₂O, and was supplemented with 0.2% (w/v) glucose as the carbon source (Levina *et al.*, 1999). This medium possesses a measured osmolarity of 235 mOsm. For cells that were grown at high salinity, 0.3 M NaCl were added to the basal medium; it had a measured osmolarity of 730 mOsm. The osmolarity of growth media was determined with an osmometer (Vapor Pressure Osmometer 5500, Wesco, USA).

Functional complementation of the mechano-channel-defective *E. coli* mutant MJF641 by the 'Ca. N. maritimus' SCM1 *mscS* protein

The *E. coli* strains Frag1 and MJF641 (Edwards *et al.*, 2012) harbouring different plasmids were inoculated in 5 ml LB medium containing ampicillin (100 µg ml⁻¹) and were grown for 5 h. Cells were subsequently transferred into the above-described citrate-phosphate medium and incubated overnight at 37°C. Cells were then diluted to an OD₅₇₈ of 0.05 into 20 ml of the above-described minimal medium, or into 20 ml medium that contained 0.3 M NaCl, and the cultures were subsequently grown to an OD₅₇₈ of 0.15. At this point, IPTG was added to the cultures (final concentration 1 mM) to induce the activity of the *lac* promoter present on the backbone of the expression plasmid pTrc99a (Amann *et al.*, 1988), thereby triggering the transcription of the codon-optimized 'Ca. N. maritimus' SCM1 *mscS* gene. Growth of the cells was subsequently continued until they reached an OD₅₇₈ of about 0.35. These cultures were then diluted 20-fold into pre-warmed medium (37°C) containing 1 mM IPTG with (no osmotic down-shock) or without (osmotic down-shock) 0.3 M NaCl; the cells were subsequently incubated at 37°C in a shaking water bath for 30 min. To determine the number of the cells that survived the osmotic down-shock, 50-µl samples were taken after 30 min of incubation from these cultures, serially diluted in four independent sets in media with corresponding osmolarities and four 5 µl samples of the osmotically downshifted cells were then spotted onto Luria-Bertani (LB) agar plates (Miller, 1972). Those from the high osmolarity grown cells were spotted onto LB agar plates with a total NaCl content of 0.3 M NaCl. Colony-forming units were determined after overnight incubation of the LB plates at 37°C.

Overproduction, purification and determination of the quaternary assembly of the ectoine synthase and of the ectoine hydroxylase

Cells of strain BL21, harbouring either the *ectC* expression plasmid pWN48 or the *ectD* expression plasmid pMP45 were grown in a minimal medium, and the overproduction of the (Nm)EctC-Strep-tag II and (Nm)EctD-Strep-tag II proteins was initiated by adding the inducer (anhydrotetracycline) of

the TetR repressor controlled *tet* promoter to the growth medium. Cleared cell extracts of the protein overproducing cultures were prepared and used to purify the (Nm)EctC-*Strep*-tag II and (Nm)EctD-*Strep*-tag II proteins by affinity chromatography on streptactin affinity resin as detailed elsewhere (Hoeppner *et al.*, 2014; Kobus *et al.*, 2015). The purity of the recombinant (Nm)EctC-*Strep*-tag II and (Nm)EctD-*Strep*-tag II proteins was assessed by SDS-polyacrylamide gel electrophoresis (12.5% and 15% respectively); the electrophoretically separated proteins were stained with Coomassie Brilliant Blue. To analyse the quaternary assembly of the ectoine synthase and ectoine hydroxylase, we performed size-exclusion chromatography. For the analysis of the ectoine synthase, a HiLoad 16/600 Superdex 75 pg column (GE Healthcare, München, Germany) was used, and the column was run in a buffer containing 20 mM TES (pH 7.0) and 150 mM NaCl. For the analysis of the ectoine hydroxylase, a HiLoad 16/600 Superdex 200 pg column (GE Healthcare, München, Germany) was used, and the column was run in a buffer containing 20 mM TES (pH 7.5) and 200 mM KCl.

Enzyme assays of the 'Ca. N. maritimus' SCM1 ectoine synthase and of the ectoine hydroxylase

High-performance liquid chromatography-based enzyme assays (Bursy *et al.*, 2007; Widderich *et al.*, 2014a) were used to assess the biochemical and kinetic properties of the affinity-purified (Nm)EctC-*Strep*-tag II and (Nm)EctD-*Strep*-tag II proteins. Single parameters (e.g. the salt concentrations) were changed to determine optimal conditions, and variations of the substrate concentration were used to assess the kinetic parameters of the EctC. The optimized assay buffer contained 20 mM TES (pH 7.0), 150 mM NaCl, 1 mM FeSO₄ and 10 mM N_γ-ADABA and was run for 15 min at 30°C. Similarly, the optimized assay buffer for the EctD contained 20 mM TES (pH 7.5), 200 mM KCl, 1 mM FeSO₄, 10 mM 2-oxoglutarate, and 6 mM ectoine and was run for 15 min at 35°C under vigorous shaking to assure aeration, since EctD is an oxygen-dependent enzyme. To determine the kinetic parameters of the (Nm)EctC and (Nm)EctD enzymes, the substrate concentration was varied for the EctC enzyme between 0 and 50 mM; for EctD, the substrate concentration of ectoine varied between 0 mM and 50 mM while keeping the concentration of the co-substrate 2-oxoglutarate constant at 10 mM. To determine the kinetic parameters for the co-substrate of EctD, the concentration was varied between 0 mM and 40 mM, while the concentration of the ectoine substrate was kept constant at 6 mM. Ectoine synthase and EctD enzyme assays were terminated by adding acetonitrile to a final concentration of 50% to the total enzyme assay solution. Denatured proteins were removed by centrifugation (5 min) in a table-top Eppendorf centrifuge, and portions of the supernatant were then used for HPLC analysis of the formed ectoine or 5-hydroxyectoine respectively.

HPLC analysis of ectoine and hydroxyectoine content

Ectoine and hydroxyectoine were detected by HPLC analysis using an Agilent 1260 Infinity LC system (Agilent, Waldbronn,

Germany), a GROM-SIL Amino 1PR column (GROM, Rottenburg-Hailfingen, Germany) essentially as described (Kuhlmann and Bremer, 2002), with the exception that a 1260 Infinity Diode Array Detector (DAD) (Agilent) was employed, instead of the previously used UV/Vis detection system. The ectoine and hydroxyectoine content of samples was quantified using the OPENLAB software suite (Agilent). When samples of EctC or EctD enzyme activity assays were measured, 5 µl to 10 µl samples were injected into the system. To determine the ectoine and hydroxyectoine content of 'Ca. N. maritimus' SCM1 cells, samples were lysed by re-suspending them in 20% ethanol for 1 h. Cellular debris was then removed by centrifugation (13 000 r.p.m. in a Sorval centrifuge at 4°C) for 20 min, and the supernatant was subsequently lyophilized to complete dryness. The resin was re-suspended in a mixture of water : acetonitrile (50:50 v/v), and samples were then injected into the HPLC system. Since cells of 'Ca. N. maritimus' SCM1 grown at different salinities exhibit different cell sizes, the total protein content of the originally ethanolic extract were used for a protein assay (Pierce Protein Assay Kit; ThermoScientific, Schwerte, Germany), and these values were used to standardize the ectoine/hydroxyectoine content of the cell samples.

Mapping of the transcriptional organization of the ectoine/hydroxyectoine gene cluster

To assess the transcriptional organization of the *ect* operon, cells of 'Ca. N. maritimus' SCM1 grown under enhanced osmotic stress conditions (the medium had an osmolarity of 1598 mOsm) were used to isolate total RNA. Cell lysis was achieved by re-suspension in 20% ethanol, and total RNA was isolated from these cell extracts by using the High Pure RNA Isolation Kit (Roche, Mannheim, Germany) according to the instructions of the user manual. Samples of RNA were further purified using the RNeasy Kit (Qiagen, Hilden, Germany) as described in the user manual and used for one-step RT-PCR assays. To analyse whether the *hyp-ectABCD-mscS* genes are transcribed in a unit, four intergenic regions of the putative operon were amplified from isolated RNA using the Qiagen One Step RT-PCR Kit and custom synthesized DNA primers (MWG, Ebersberg, Germany). As controls, we also amplified DNA regions between genes that were divergently transcribed (Fig. 7A). To ensure that the formed PCR products did not result from DNA contaminations of RNA sample used for the RT-PCR reaction, an assay was performed in which total RNA was added after the reverse transcription step.

Assessment of the transcript levels of the 'Ca. N. maritimus' SCM1 *ectA* and *mscS* genes in response to varying osmolarities

For studying the expression of the ectoine biosynthesis gene cluster in 'Ca. N. maritimus' SCM1 under different osmotic growth conditions, cells that had been cultured either at low (13 g NaCl L⁻¹; 220 mM), optimal (26 g NaCl L⁻¹; 440 mM) or high salt (39 g NaCl L⁻¹; 660 mM) were used. Total RNA was extracted from these cells using the peqGOLD TriFast Kit (VWR International GmbH, Erlangen, Germany) according to

the manufacturer's instructions. The extracted RNA solutions were treated with RNase-free DNase I (Life Technologies GmbH, Darmstadt, Germany) to remove residual chromosomal DNA, again following the manufacturer's instructions. The absence of DNA contamination was ascertained by PCR analysis. The relative abundance of the *hyp-ectABCD-mscS* mRNA to the mRNA of *amoA* (Nmar_1500) was determined by real-time PCR in a CFX96 Touch Real-Time PCR Detection System (Bio-Rad Laboratories GmbH, München, Germany) with the LightCycler RNA Master SYBR green I kit (Roche Diagnostics, Mannheim, Germany). Each reaction of the one-step RT-PCR was conducted in a 20- μ l volume containing 125 ng template RNA, 0.5 μ M of each primer, 3.25 mM Mn(OAc)₂ and 7.5 μ l of LightCycler RNA Master SYBR green I. The following PCR primer sets were used: *ectA_fwd* (5'-TTAGAGAGCCTCGAGTTGATGACGC-3') and *ectA_rev* (5'-GTCAAGAGGCTTGTGTTTTGCACC-3'), *mscS_fwd* (5'-CGCAAAGGAACTATTCTCAAGCTGG-3') and *mscS_rev* (5'-GCGAGAAATTGAAACAAGAACCTCG-3'), and *amoA_fwd* (5'-CCAAGTAGGTAAGTTCTATAA-3') and *amoA_rev* (5'-AAGCGGCCATCCATCTGTA-3') as described previously (Nakagawa and Stahl, 2013). The PCR cycling conditions were used as described in the manufacturer's instructions with denaturation at 95°C for 5 s, annealing at 60°C for 10 s and extension at 72°C for 5 s. The relative expression of each gene under the tested conditions was determined by using the *amoA* transcript level in '*Ca. N. maritimus*' SCM1 cells grown under optimal salt concentrations as the standard. The level of the *amoA* transcript was set to one and those of *ectA* and *mscS* are expressed in relation to this reference transcript.

Database searches and phylogenetic analysis of EctC and EctD-type proteins

The amino acid sequence of the '*Ca. N. maritimus*' SCM1 EctC protein (Walker *et al.*, 2010) was used as the template for BLAST searches of the microbial database of the JGI of the US Department of Energy (<http://jgi.doe.gov/>) (Nordberg *et al.*, 2013). EctC-type amino acid sequences of closely related strains of the same species were removed, and the remaining 723 retrieved amino acid sequences were aligned using the MAFFT multiple amino acid sequence alignment server (<http://mafft.cbrc.jp/alignment/server/>) (Katoh and Standley, 2013). This curated data set was then used to construct a rooted phylogenetic tree of EctC-type sequences by employing the iTOL software suit (<http://itol.embl.de/>) (Letunic and Bork, 2011).

Modelling of three-dimensional protein structures and preparation of figures of crystal structures

The amino acid sequence of the '*Ca. N. maritimus*' SCM1 MscS protein was submitted via the website of the SWISS-Model server (<http://swissmodel.expasy.org/>) (Biasini *et al.*, 2014) to generate an *in silico* model of the three-dimensional structure of this protein. The program automatically chose the monomer of the heptameric *E. coli* MscS open crystal structure (Wang *et al.*, 2008) as the modelling template (PDB accession code: 2VV5). The model of the monomer of the (Nm)MscS protein generated via the SWISS-Model web

server was visualized and compared with the *E. coli* MscS protein using resources provided by the PyMOL suit (<https://www.pymol.org/>).

Acknowledgements

We thank Irina Bagyan for the kind gift of ectoines and Ian Booth and Samata Miller for generously providing bacterial strains. We greatly appreciate the expert technical assistance of Jochen Sohn and Jutta Gade in the course of this project and highly value the kind help of Vickie Koogle in the language editing of our manuscript. We thank Tamara Hoffmann for helpful discussions and critical reading of the manuscript. Funding for this study was provided by the Deutsche Forschungsgemeinschaft (DFG) through the SFB 987 (to E.B. and J.H.) (Marburg), the Transregio SFB 51 (to J.S.D.) (Braunschweig/Oldenburg), The G.W. Leibniz Prize (to K.-U. Hinrichs; MARUM, Bremen) and through the LOEWE Program of the State of Hessen (via the Centre for Synthetic Microbiology; Synmicro; Marburg) (to J.H. and E.B.). N.W. and L.C. are recipients of PhD fellowships from the International Max Planck Research School for Environmental, Cellular and Molecular Microbiology (IMPRS-Mic, Marburg) and gratefully acknowledge its generous support.

References

- Amann, E., Ochs, B., and Abel, K.J. (1988) Tightly regulated tac promoter vectors useful for the expression of unfused and fused proteins in *Escherichia coli*. *Gene* **69**: 301–315.
- Bass, R.B., Strop, P., Barclay, M., and Rees, D.C. (2002) Crystal structure of *Escherichia coli* MscS, a voltage-modulated and mechanosensitive channel. *Science* **298**: 1582–1587.
- Bayer, B., Vojvoda, J., Offre, P., Alves, R.J., Elisabeth, N.H., Garcia, J.A., *et al.* (2015) Physiological and genomic characterization of two novel marine thaumarchaeal strains indicates niche differentiation. *ISME J* in press. doi: 10.1038/ismej.2015.200
- Becker, E.A., Seitzer, P.M., Tritt, A., Larsen, D., Krusor, M., Yao, A.I., *et al.* (2014) Phylogenetically driven sequencing of extremely halophilic archaea reveals strategies for static and dynamic osmo-response. *PLoS Genet* **10**: e1004784.
- Becker, M., and Krämer, R. (2015) MscCG from *Corynebacterium glutamicum*: functional significance of the C-terminal domain. *Eur Biophys J* **44**: 577–588.
- Becker, M., Borngen, K., Nomura, T., Battle, A.R., Marin, K., Martinac, B., and Krämer, R. (2013) Glutamate efflux mediated by *Corynebacterium glutamicum* MscCG, *Escherichia coli* MscS, and their derivatives. *Biochim Biophys Acta* **1828**: 1230–1240.
- Biasini, M., Bienert, S., Waterhouse, A., Arnold, K., Studer, G., Schmidt, T., *et al.* (2014) SWISS-MODEL: modelling protein tertiary and quaternary structure using evolutionary information. *Nucleic Acids Res* **42**: W252–W258.
- Blainey, P.C., Mosier, A.C., Potanina, A., Francis, C.A., and Quake, S.R. (2011) Genome of a low-salinity ammonia-oxidizing archaeon determined by single-cell and metagenomic analysis. *PLoS ONE* **6**: e16626.
- Bolen, D.W., and Baskakov, I.V. (2001) The osmophobic effect: natural selection of a thermodynamic force in protein folding. *J Mol Biol* **310**: 955–963.

- Booth, I.R. (2014) Bacterial mechanosensitive channels: progress towards an understanding of their roles in cell physiology. *Curr Opin Microbiol* **18**: 16–22.
- Booth, I.R., and Blount, P. (2012) The MscS and MscL families of mechanosensitive channels act as microbial emergency release valves. *J Bacteriol* **194**: 4802–4809.
- Booth, I.R., Miller, S., Müller, A., and Lehtovirta-Morley, L. (2015) The evolution of bacterial mechanosensitive channels. *Cell Calcium* **57**: 140–150.
- Börngen, K., Battle, A.R., Möker, N., Morbach, S., Marin, K., Martinac, B., and Krämer, R. (2010) The properties and contribution of the *Corynebacterium glutamicum* MscS variant to fine-tuning of osmotic adaptation. *Biochim Biophys Acta* **1798**: 2141–2149.
- Bremer, E., and Krämer, R. (2000) Coping with osmotic challenges: osmoregulation through accumulation and release of compatible solutes. In *Bacterial Stress Responses*. Storz, G., and Hengge-Aronis, R. (eds). Washington DC, USA: ASM Press, pp. 79–97.
- Brill, J., Hoffmann, T., Bleisteiner, M., and Bremer, E. (2011) Osmotically controlled synthesis of the compatible solute proline is critical for cellular defense of *Bacillus subtilis* against high osmolarity. *J Bacteriol* **193**: 5335–5346.
- Brochier-Armanet, C., Boussau, B., Gribaldo, S., and Forterre, P. (2008) Mesophilic Crenarchaeota: proposal for a third archaeal phylum, the Thaumarchaeota. *Nat Rev Microbiol* **6**: 245–252.
- Brown, A.D. (1976) Microbial water stress. *Bacteriol Rev* **40**: 803–846.
- Bursy, J., Pierik, A.J., Pica, N., and Bremer, E. (2007) Osmotically induced synthesis of the compatible solute hydroxyectoine is mediated by an evolutionarily conserved ectoine hydroxylase. *J Biol Chem* **282**: 31147–31155.
- Bursy, J., Kuhlmann, A.U., Pittelkow, M., Hartmann, H., Jebbar, M., Pierik, A.J., and Bremer, E. (2008) Synthesis and uptake of the compatible solutes ectoine and 5-hydroxyectoine by *Streptomyces coelicolor* A3(2) in response to salt and heat stresses. *Appl Environ Microbiol* **74**: 7286–7296.
- Calderon, M.I., Vargas, C., Rojo, F., Iglesias-Guerra, F., Csonka, L.N., Ventosa, A., and Nieto, J.J. (2004) Complex regulation of the synthesis of the compatible solute ectoine in the halophilic bacterium *Chromohalobacter salexigens* DSM 3043^T. *Microbiology* **150**: 3051–3063.
- Canovas, D., Vargas, C., Iglesias-Guerra, F., Csonka, L.N., Rhodes, D., Ventosa, A., and Nieto, J.J. (1997) Isolation and characterization of salt-sensitive mutants of the moderate halophile *Halomonas elongata* and cloning of the ectoine synthesis genes. *J Biol Chem* **272**: 25794–25801.
- Coquelle, N., Talon, R., Juers, D.H., Girard, E., Kahn, R., and Madern, D. (2010) Gradual adaptive changes of a protein facing high salt concentrations. *J Mol Biol* **404**: 493–505.
- da Costa, M.S., Santos, H., and Galinski, E.A. (1998) An overview of the role and diversity of compatible solutes in Bacteria and Archaea. *Adv Biochem Eng Biotechnol* **61**: 117–153.
- Cruickshank, C.C., Minchin, R.F., Le Dain, A.C., and Martinac, B. (1997) Estimation of the pore size of the large-conductance mechanosensitive ion channel of *Escherichia coli*. *Biophys J* **73**: 1925–1931.
- Csonka, L.N. (1989) Physiological and genetic responses of bacteria to osmotic stress. *Microbiol Rev* **53**: 121–147.
- Deole, R., Challacombe, J., Raiford, D.W., and Hoff, W.D. (2013) An extremely halophilic proteobacterium combines a highly acidic proteome with a low cytoplasmic potassium content. *J Biol Chem* **288**: 581–588.
- Deschamps, P., Zivanovic, Y., Moreira, D., Rodriguez-Valera, F., and Lopez-Garcia, P. (2014) Pangenome evidence for extensive interdomain horizontal transfer affecting lineage core and shell genes in uncultured planktonic thaumarchaeota and euryarchaeota. *Genome Biol Evol* **6**: 1549–1563.
- Dong, C., Major, L.L., Srikannathasan, V., Errey, J.C., Giraud, M.F., Lam, J.S., et al. (2007) RmlC, a C3' and C5' carbohydrate epimerase, appears to operate via an intermediate with an unusual twist boat conformation. *J Mol Biol* **365**: 146–159.
- Dubendorff, J.W., and Studier, F.W. (1991) Controlling basal expression in an inducible T7 expression system by blocking the target T7 promoter with lac repressor. *J Mol Biol* **219**: 45–59.
- Dunwell, J.M., Culham, A., Carter, C.E., Sosa-Aguirre, C.R., and Goodenough, P.W. (2001) Evolution of functional diversity in the cupin superfamily. *Trends Biochem Sci* **26**: 740–746.
- Edwards, M.D., Black, S., Rasmussen, T., Rasmussen, A., Stokes, N.R., Stephen, T.L., et al. (2012) Characterization of three novel mechanosensitive channel activities in *Escherichia coli*. *Channels* **6**: 272–281.
- Elling, F.J., Könneke, M., Lipp, J.S., Becker, K.W., Gagen, E.J., and Hinrichs, K.-U. (2014) Effect of growth phase on the membrane lipid composition of the thaumarchaeon *Nitrosopumilus maritimus* and their implication for archaeal lipid distribution in the marine environment. *Geochim Cosmochim Acta* **141**: 579–597.
- Elling, F.J., Könneke, M., Mußmann, M., Greve, A., and Hinrichs, K.-U. (2015) Influence of temperature, pH, and salinity on membrane lipid composition and Tex86 of marine planktonic thaumarchaeal isolates. *Geochim Cosmochim Acta* in press. doi:10.1016/j.gca.2015.09.004
- Empadinhas, N., and da Costa, M.S. (2011) Diversity, biological roles and biosynthetic pathways for sugar-glycerate containing compatible solutes in bacteria and archaea. *Environ Microbiol* **13**: 2056–2077.
- Galinski, E.A., and Trüper, H.G. (1994) Microbial behaviour in salt-stressed ecosystems. *FEMS Microbiol Rev* **15**: 95–108.
- Galinski, E.A., Pfeiffer, H.P., and Trüper, H.G. (1985) 1,4,5,6-Tetrahydro-2-methyl-4-pyrimidinecarboxylic acid. A novel cyclic amino acid from halophilic phototrophic bacteria of the genus *Ectothiorhodospira*. *Eur J Biochem* **149**: 135–139.
- García-Estépa, R., Argandona, M., Reina-Bueno, M., Capote, N., Iglesias-Guerra, F., Nieto, J.J., and Vargas, C. (2006) The *ectD* gene, which is involved in the synthesis of the compatible solute hydroxyectoine, is essential for thermoprotection of the halophilic bacterium *Chromohalobacter salexigens*. *J Bacteriol* **188**: 3774–3784.
- Gubry-Rangin, C., Kratsch, C., Williams, T.A., McHardy, A.C., Embley, T.M., Prosser, J.I., and Macqueen, D.J. (2015)

- Coupling of diversification and pH adaptation during the evolution of terrestrial Thaumarchaeota. *Proc Natl Acad Sci USA* **112**: 9370–9375.
- Harishchandra, R.K., Wulff, S., Lentzen, G., Neuhaus, T., and Galla, H.J. (2010) The effect of compatible solute ectoines on the structural organization of lipid monolayer and bilayer membranes. *Biophys Chem* **150**: 37–46.
- Haswell, E.S., Phillips, R., and Rees, D.C. (2011) Mechanosensitive channels: What can they do and how do they do it? *Structure* **19**: 1356–1369.
- Hoepfner, A., Widderich, N., Bremer, E., and Smits, S.H.J. (2014) Overexpression, crystallization and preliminary X-ray crystallographic analysis of the ectoine hydroxylase from *Sphingopyxis alaskensis*. *Acta Cryst* **F70**: 493–496.
- Hoffmann, T., Wensing, A., Brosius, M., Steil, L., Völker, U., and Bremer, E. (2013) Osmotic control of *opuA* expression in *Bacillus subtilis* and its modulation in response to intracellular glycine betaine and proline pools. *J Bacteriol* **195**: 510–522.
- Höppner, A., Widderich, N., Lenders, M., Bremer, E., and Smits, S.H.J. (2014) Crystal structure of the ectoine hydroxylase, a snapshot of the active site. *J Biol Chem* **289**: 29570–29583.
- Inbar, L., and Lapidot, A. (1988) The structure and biosynthesis of new tetrahydropyrimidine derivatives in actinomycin D producer *Streptomyces parvulus*. Use of ^{13}C - and ^{15}N -labeled L-glutamate and ^{13}C and ^{15}N NMR spectroscopy. *J Biol Chem* **263**: 16014–16022.
- Katoh, K., and Standley, D.M. (2013) MAFFT multiple sequence alignment software version 7: improvements in performance and usability. *Mol Biol Evol* **30**: 772–780.
- Kelly, W.J., Leahy, S.C., Li, D., Perry, R., Lambie, S.C., Attwood, G.T., and Altermann, E. (2014) The complete genome sequence of the rumen methanogen *Methanobacterium formicicum* BRM9. *Stand Genomic Sci* **9**: 15.
- Kempf, B., and Bremer, E. (1998) Uptake and synthesis of compatible solutes as microbial stress responses to high osmolarity environments. *Arch Microbiol* **170**: 319–330.
- Klähn, S., and Hagemann, M. (2011) Compatible solute biosynthesis in cyanobacteria. *Environ Microbiol* **13**: 551–562.
- Kloda, A., and Martinac, B. (2002) Mechanosensitive channels of bacteria and archaea share a common ancestral origin. *Eur Biophys J* **31**: 14–25.
- Kobus, S., Widderich, N., Hoepfner, A., Bremer, E., and Smits, S.H.J. (2015) Overproduction, crystallization and X-ray diffraction data analysis of ectoine synthase from the cold-adapted marine bacterium *Sphingopyxis alaskensis*. *Acta Cryst* **F71**: 1027–1032.
- Kol, S., Merlo, M.E., Scheltema, R.A., de Vries, M., Vonk, R.J., Kikkert, N.A., et al. (2010) Metabolomic characterization of the salt stress response in *Streptomyces coelicolor*. *Appl Environ Microbiol* **76**: 2574–2581.
- Könneke, M., Bernhard, A.E., de la Torre, J.R., Walker, C.B., Waterbury, J.B., and Stahl, D.A. (2005) Isolation of an autotrophic ammonia-oxidizing marine archaeon. *Nature* **437**: 543–546.
- Könneke, M., Schubert, D.M., Brown, P.C., Hugler, M., Standfest, S., Schwander, T., et al. (2014) Ammonia-oxidizing archaea use the most energy-efficient aerobic pathway for CO₂ fixation. *Proc Natl Acad Sci USA* **111**: 8239–8244.
- Kuhlmann, A.U., and Bremer, E. (2002) Osmotically regulated synthesis of the compatible solute ectoine in *Bacillus pasteurii* and related *Bacillus* spp. *Appl Environ Microbiol* **68**: 772–783.
- Kuhlmann, A.U., Bursy, J., Gimpel, S., Hoffmann, T., and Bremer, E. (2008) Synthesis of the compatible solute ectoine in *Virgibacillus pantothenicus* is triggered by high salinity and low growth temperature. *Appl Environ Microbiol* **74**: 4560–4563.
- Kunte, H.J., Galinski, E.A., and Trüper, G.H. (1993) A modified FMOC-method for the detection of amino acid-type osmolytes and tetrahydropyrimidines (ectoines). *J Microbiol Meth* **17**: 129–136.
- Kunte, H.J., Lentzen, G., and Galinski, E. (2014) Industrial production of the cell protectant ectoine: protection, mechanisms, processes, and products. *Curr Biotechnol* **3**: 10–25.
- Kurz, M., Burch, A.Y., Seip, B., Lindow, S.E., and Gross, H. (2010) Genome-driven investigation of compatible solute biosynthesis pathways of *Pseudomonas syringae* pv. *syringae* and their contribution to water stress tolerance. *Appl Environ Microbiol* **76**: 5452–5462.
- Letunic, I., and Bork, P. (2011) Interactive Tree Of Life v2: online annotation and display of phylogenetic trees made easy. *Nucleic Acids Res* **39**: W475–W478.
- Levina, N., Totemeyer, S., Stokes, N.R., Louis, P., Jones, M.A., and Booth, I.R. (1999) Protection of *Escherichia coli* cells against extreme turgor by activation of MscS and MscL mechanosensitive channels: identification of genes required for MscS activity. *EMBO J* **18**: 1730–1737.
- Lippert, K., and Galinski, E.A. (1992) Enzyme stabilization by ectoine-type compatible solutes: protection against heating, freezing and drying. *Appl Microbiol Biotechnol* **37**: 61–65.
- Lo, C.C., Bonner, C.A., Xie, G., D'Souza, M., and Jensen, R.A. (2009) Cohesion group approach for evolutionary analysis of aspartokinase, an enzyme that feeds a branched network of many biochemical pathways. *Microbiol Mol Biol Rev* **73**: 594–651.
- Louis, P., and Galinski, E.A. (1997) Characterization of genes for the biosynthesis of the compatible solute ectoine from *Marinococcus halophilus* and osmoregulated expression in *Escherichia coli*. *Microbiology* **143**: 1141–1149.
- Manzanera, M., Garcia de Castro, A., Tondervik, A., Rayner-Brandes, M., Strom, A.R., and Tunnacliffe, A. (2002) Hydroxyectoine is superior to trehalose for anhydrobiotic engineering of *Pseudomonas putida* KT2440. *Appl Environ Microbiol* **68**: 4328–4333.
- Martens-Habbena, W., Berube, P.M., Urakawa, H., de la Torre, J.R., and Stahl, D.A. (2009) Ammonia oxidation kinetics determine niche separation of nitrifying Archaea and Bacteria. *Nature* **461**: 976–979.
- Miller, J.H. (1972) *Experiments in Molecular Genetics*. Cold Spring Harbor New York: Cold Spring Harbor Laboratory.
- Moritz, K.D., Amendt, B., Witt, E.M.H.J., and Galinski, E.A. (2015) The hydroxyectoine gene cluster of the non-halophilic acidophile *Acidiphilium cryptum*. *Extremophiles* **19**: 87–99.

- Müller, V., Spanheimer, R., and Santos, H. (2005) Stress response by solute accumulation in archaea. *Curr Opin Microbiol* **8**: 729–736.
- Naismith, J.H., and Booth, I.R. (2012) Bacterial mechanosensitive channels – MscS: Evolution's solution to creating sensitivity in function. *Annu Rev Biophys* **41**: 157–177.
- Nakagawa, T., and Stahl, D.A. (2013) Transcriptional response of the archaeal ammonia oxidizer *Nitrosopumilus maritimus* to low and environmentally relevant ammonia concentrations. *Appl Environ Microbiol* **79**: 6911–6916.
- Nakamura, J., Hirano, S., Ito, H., and Wachi, M. (2007) Mutations of the *Corynebacterium glutamicum* NCgl1221 gene, encoding a mechanosensitive channel homolog, induce L-glutamic acid production. *Appl Environ Microbiol* **73**: 4491–4498.
- Nakayama, Y., Yoshimura, K., and Iida, H. (2013) Electrophysiological characterization of the mechanosensitive channel MscCG in *Corynebacterium glutamicum*. *Biophys J* **105**: 1366–1375.
- Nelson-Sathi, S., Sousa, F.L., Roettger, M., Lozada-Chavez, N., Thiergart, T., Janssen, A., *et al.* (2015) Origins of major archaeal clades correspond to gene acquisitions from bacteria. *Nature* **517**: 77–80.
- Nordberg, H., Cantor, M., Dusheyko, S., Hua, S., Poliakov, A., Shabalov, I., *et al.* (2013) The genome portal of the Department of Energy Joint Genome Institute: 2014 updates. *Nucleic Acids Res* **42**: D26–D31.
- Ochman, H., Lawrence, J.G., and Groisman, E.A. (2000) Lateral gene transfer and the nature of bacterial innovation. *Nature* **405**: 299–304.
- Offre, P., Spang, A., and Schleper, C. (2013) Archaea in biogeochemical cycles. *Annu Rev Microbiol* **67**: 437–457.
- Ono, H., Okuda, M., Tongpim, S., Imai, K., Shinmyo, A., Sakuda, S., *et al.* (1998) Accumulation of compatible solutes, ectoine and hydroxyectoine, in a moderate halophile, *Halomonas elongata* KS3, isolated from dry salty land in Thailand. *J Ferment Bioeng* **85**: 362–368.
- Ono, H., Sawada, K., Khunajakr, N., Tao, T., Yamamoto, M., Hiramoto, M., *et al.* (1999a) Characterization of biosynthetic enzymes for ectoine as a compatible solute in a moderately halophilic eubacterium, *Halomonas elongata*. *J Bacteriol* **181**: 91–99.
- Ono, H., Sawada, K., Khunajakr, N., Tao, T., Yamamoto, M., Hiramoto, M., *et al.* (1999b) Characterization of biosynthetic enzymes for ectoine as a compatible solute in a moderately halophilic eubacterium, *Halomonas elongata*. *J Bacteriol* **181**: 91–99.
- Oren, A. (2011) Thermodynamic limits to microbial life at high salt concentrations. *Environ Microbiol* **13**: 1908–1923.
- Oren, A. (2013) Life at high salt concentrations, intracellular KCl concentrations, and acidic proteomes. *Front Microbiol* **4**: 315.
- Pastor, J.M., Salvador, M., Argandona, M., Bernal, V., Reina-Bueno, M., Csonka, L.N., *et al.* (2010) Ectoines in cell stress protection: uses and biotechnological production. *Biotechnol Adv* **28**: 782–801.
- Pester, M., Schleper, C., and Wagner, M. (2011) The Thaumarchaeota: an emerging view of their phylogeny and ecophysiology. *Curr Opin Microbiol* **14**: 300–306.
- Peters, P., Galinski, E.A., and Trüper, H.G. (1990) The biosynthesis of ectoine. *FEMS Microbiol Lett* **71**: 157–162.
- Pivetti, C.D., Yen, M.R., Miller, S., Busch, W., Tseng, Y.H., Booth, I.R., and Saier, M.H., Jr (2003) Two families of mechanosensitive channel proteins. *Microbiol Mol Biol Rev* **67**: 66–85.
- Prabhu, J., Schauwecker, F., Grammel, N., Keller, U., and Bernhard, M. (2004) Functional expression of the ectoine hydroxylase gene (*thpD*) from *Streptomyces chrysomallus* in *Halomonas elongata*. *Appl Environ Microbiol* **70**: 3130–3132.
- Record, M.T., Jr, Courtenay, E.S., Cayley, D.S., and Guttman, H.J. (1998) Responses of *E. coli* to osmotic stress: large changes in amounts of cytoplasmic solutes and water. *Trends Biochem Sci* **23**: 143–148.
- Roberts, M.F. (2004) Osmoadaptation and osmoregulation in archaea: update 2004. *Front Biosci* **9**: 1999–2019.
- Rösser, M., and Müller, V. (2001) Osmoadaptation in bacteria and archaea: common principles and differences. *Environ Microbiol* **3**: 743–754.
- Rowe, I., Anishkin, A., Kamaraju, K., Yoshimura, K., and Sukharev, S. (2014) The cytoplasmic cage domain of the mechanosensitive channel MscS is a sensor of macromolecular crowding. *J Gen Physiol* **143**: 543–557.
- Salvador, M., Argandona, M., Pastor, J.M., Bernal, V., Canovas, M., Csonka, L.N., *et al.* (2015) Contribution of RpoS to metabolic efficiency and ectoines synthesis during the osmo- and heat-stress response in the halophilic bacterium *Chromohalobacter salexigens*. *Environ Microbiol Rep* **7**: 301–311.
- Santoro, A.E., Francis, C.A., de Sieyes, N.R., and Boehm, A.B. (2008) Shifts in the relative abundance of ammonia-oxidizing bacteria and archaea across physicochemical gradients in a subterranean estuary. *Environ Microbiol* **10**: 1068–1079.
- Saum, S.H., and Müller, V. (2008) Growth phase-dependent switch in osmolyte strategy in a moderate halophile: ectoine is a minor osmolyte but major stationary phase solute in *Halobacillus halophilus*. *Environ Microbiol* **10**: 716–726.
- Schwibbert, K., Marin-Sanguino, A., Bagyan, I., Heidrich, G., Lentzen, G., Seitz, H., *et al.* (2011) A blueprint of ectoine metabolism from the genome of the industrial producer *Halomonas elongata* DSM 2581^T. *Environ Microbiol* **13**: 1973–1994.
- Soucy, S.M., Huang, J., and Gogarten, J.P. (2015) Horizontal gene transfer: building the web of life. *Nat Rev Genet* **16**: 472–482.
- Stahl, D.A., and de la Torre, J.R. (2012) Physiology and diversity of ammonia-oxidizing archaea. *Annu Rev Microbiol* **66**: 83–101.
- Stieglmeier, M., Alves, R.J.E., and Schleper, C. (2014) The phylum Thaumarchaeota. In *The Prokaryotes – Other Major Lineages of Bacteria and the Archaea*. Rosenberg, E.I. (ed.). Berlin, Germany: Springer, pp. 347–362.
- Storz, G., and Hengge-Aronis, R. (2000) *Bacterial Stress Responses*. Washington, DC, USA: ASM Press.
- Stöveken, N., Pittelkow, M., Sinner, T., Jensen, R.A., Heider, J., and Bremer, E. (2011) A specialized aspartokinase enhances the biosynthesis of the osmoprotectants ectoine

- and hydroxyectoine in *Pseudomonas stutzeri* A1501. *J Bacteriol* **193**: 4456–4468.
- Strickland, J.D.H., and Parson, T.R. (1972) *A Practical Handbook of Seawater Analysis*. Ottawa, Canada: Fisheries Research Board of Canada.
- Talon, R., Coquelle, N., Madern, D., and Girard, E. (2014) An experimental point of view on hydration/solvation in halophilic proteins. *Front Microbiol* **5**: 66.
- Tanne, C., Golovina, E.A., Hoekstra, F.A., Meffert, A., and Galinski, E.A. (2014) Glass-forming property of hydroxyectoine is the cause of its superior function as a desiccation protectant. *Front Microbiol* **5**: 150.
- Walker, C.B., de la Torre, J.R., Klotz, M.G., Urakawa, H., Pinel, N., Arp, D.J., et al. (2010) *Nitrosopumilus maritimus* genome reveals unique mechanisms for nitrification and autotrophy in globally distributed marine crenarchaea. *Proc Natl Acad Sci USA* **107**: 8818–8823.
- Wang, W., Black, S.S., Edwards, M.D., Miller, S., Morrison, E.L., Bartlett, W., et al. (2008) The structure of an open form of an *E. coli* mechanosensitive channel at 3.45 Å resolution. *Science* **321**: 1179–1183.
- Widderich, N., Höppner, A., Pittelkow, M., Heider, J., Smits, S.H.J., and Bremer, E. (2014a) Biochemical properties of ectoine hydroxylases from extremophiles and their wider taxonomic distribution among microorganisms. *PLoS ONE* **9**: e93809.
- Widderich, N., Pittelkow, M., Höppner, A., Mulnaes, D., Buckel, W., Gohlke, H., et al. (2014b) Molecular dynamics simulations and structure-guided mutagenesis provide insight into the architecture of the catalytic core of the ectoine hydroxylase. *J Mol Biol* **426**: 586–600.
- Wilson, M.E., Maksaev, G., and Haswell, E.S. (2013) MscS-like mechanosensitive channels in plants and microbes. *Biochemistry* **52**: 5708–5722.
- Wood, J.M. (2011) Bacterial osmoregulation: a paradigm for the study of cellular homeostasis. *Annu Rev Microbiol* **65**: 215–238.
- Wood, J.M., Bremer, E., Csonka, L.N., Krämer, R., Poolman, B., van der Heide, T., and Smith, L.T. (2001) Osmosensing and osmoregulatory compatible solute accumulation by bacteria. *Comp Biochem Physiol A Mol Integr Physiol* **130**: 437–460.
- Youssef, N.H., Savage-Ashlock, K.N., McCully, A.L., Luedtke, B., Shaw, E.I., Hoff, W.D., and Elshahed, M.S. (2014) Trehalose/2-sulfotrehalose biosynthesis and glycine-betaine uptake are widely spread mechanisms for osmoadaptation in the *Halobacteriales*. *ISME J* **8**: 636–649.
- Zaparty, M., Hagemann, A., Brasen, C., Hensel, R., Lupas, A.N., Brinkmann, H., and Siebers, B. (2013) The first prokaryotic trehalose synthase complex identified in the hyperthermophilic crenarchaeon *Thermoproteus tenax*. *PLoS ONE* **8**: e61354.
- Zhang, Y., Chen, L., Dai, T., Tian, J., and Wen, D. (2015) The influence of salinity on the abundance, transcriptional activity, and diversity of AOA and AOB in an estuarine sediment: a microcosm study. *Appl Microbiol Biotechnol* **99**: 9825–9833.

Supporting information

Additional Supporting Information may be found in the online version of this article at the publisher's website:

Fig. S1. Phylogenetic tree of EctC-type proteins. Based on an amino acid sequence alignment of 723 EctC-type proteins, a rooted phylogenetic tree was constructed with the ITOL program (Letunic and Bork, 2011). The three regions in the phylogenetic tree populated by archaeal EctC proteins are highlighted by red arrowheads. The position of those 24 EctC-type proteins that originate from bacteria that lack identifiable *ectAB* genes are marked above the phylogenetic tree by a black bar.

Fig. S2. Alignment of the amino acid sequence of the *E. coli* MscS protein with those MscS-type proteins whose corresponding genes are located next to ectoine/hydroxyectoine biosynthetic gene clusters in the genomes of 'Ca. Nitrosopumilus maritimus' SCM 1 and 'Ca. Nitrosopumilus' sp. AR2 (see Fig. 1B in the main text). Red bars indicate the membrane-spanning segments of the *E. coli* MscS protein.

Table S1. Amino acid sequence relatedness of the ectoine biosynthetic proteins from 'Ca. Nitrosopumilus' strains to other ectoine biosynthetic enzymes.

Table S2. Distribution of mechanosensitive channels in potential ectoine-producing *Archaea*.

Czech et al. *Microb Cell Fact* (2016) 15:126
DOI 10.1186/s12934-016-0525-4

Microbial Cell Factories

RESEARCH

Open Access



EctD-mediated biotransformation of the chemical chaperone ectoine into hydroxyectoine and its mechanosensitive channel-independent excretion

Laura Czech¹, Nadine Stöveken^{1,2} and Erhard Bremer^{1,2,3*}

5.2.2. EctD-mediated biotransformation of the chemical chaperone ectoine into hydroxyectoine and its mechanosensitive channel-independent excretion

Czech L, Stöveken N, Bremer E. EctD-mediated biotransformation of the chemical chaperone ectoine into hydroxyectoine and its mechanosensitive channel-independent excretion. *Microb Cell Fact* 2016;15:doi: 10.1186/s12934-016-0525-4.

For the publication "EctD-mediated biotransformation of the chemical chaperone ectoine into hydroxyectoine and its mechanosensitive channel-independent excretion" in *Microbial Cell Factories*, I conducted all experiments, evaluated and analyzed the data, and prepared all figures included in this communication. N. Stöveken was involved during the exploratory phase of the project. Prof. E. Bremer and I discussed the data and wrote the manuscript together.

Supplementary Data can be found at:

<https://microbialcellfactories.biomedcentral.com/articles/10.1186/s12934-016-0525-4>

5.2.2.1. Original publication

Czech et al. *Microb Cell Fact* (2016) 15:126
DOI 10.1186/s12934-016-0525-4

Microbial Cell Factories

RESEARCH

Open Access



EctD-mediated biotransformation of the chemical chaperone ectoine into hydroxyectoine and its mechanosensitive channel-independent excretion

Laura Czech¹, Nadine Stöveken^{1,2} and Erhard Bremer^{1,2,3*}

Abstract

Background: Ectoine and its derivative 5-hydroxyectoine are cytoprotectants widely synthesized by microorganisms as a defense against the detrimental effects of high osmolarity on cellular physiology and growth. Both ectoines possess the ability to preserve the functionality of proteins, macromolecular complexes, and even entire cells, attributes that led to their description as chemical chaperones. As a consequence, there is growing interest in using ectoines for biotechnological purposes, in skin care, and in medical applications. 5-Hydroxyectoine is synthesized from ectoine through a region- and stereo-specific hydroxylation reaction mediated by the EctD enzyme, a member of the non-heme-containing iron(II) and 2-oxoglutarate-dependent dioxygenases. This chemical modification endows the newly formed 5-hydroxyectoine with either superior or different stress-protecting and stabilizing properties. Microorganisms producing 5-hydroxyectoine typically contain a mixture of both ectoines. We aimed to establish a recombinant microbial cell factory where 5-hydroxyectoine is (i) produced in highly purified form, and (ii) secreted into the growth medium.

Results: We used an *Escherichia coli* strain (FF4169) defective in the synthesis of the osmoprotectant trehalose as the chassis for our recombinant cell factory. We expressed in this strain a plasmid-encoded *ectD* gene from *Pseudomonas stutzeri* A1501 under the control of the anhydrotetracycline-inducible *tet* promoter. We chose the ectoine hydroxylase from *P. stutzeri* A1501 for our cell factory after a careful comparison of the in vivo performance of seven different EctD proteins. In the final set-up of the cell factory, ectoine was provided to salt-stressed cultures of strain FF4169 (pMP41; *ectD*⁺). Ectoine was imported into the cells via the osmotically inducible ProP and ProU transport systems, intracellularly converted to 5-hydroxyectoine, which was then almost quantitatively secreted into the growth medium. Experiments with an *E. coli* mutant lacking all currently known mechanosensitive channels (MscL, MscS, MscK, MscM) revealed that the release of 5-hydroxyectoine under osmotic steady-state conditions occurred independently of these microbial safety valves. In shake-flask experiments, 2.13 g l⁻¹ ectoine (15 mM) was completely converted into 5-hydroxyectoine within 24 h.

Conclusions: We describe here a recombinant *E. coli* cell factory for the production and secretion of the chemical chaperone 5-hydroxyectoine free from contaminating ectoine.

Keywords: Osmoprotectants, Compatible solutes, Ectoines, Heterologous production, Dioxygenase, Transporters, Efflux

*Correspondence: bremer@staff.uni-marburg.de

³Laboratory for Microbiology, Department of Biology, Philipps-University at Marburg, Karl-von-Frisch-Str. 8, 35043 Marburg, Germany
Full list of author information is available at the end of the article



© 2016 The Author(s). This article is distributed under the terms of the Creative Commons Attribution 4.0 International License (<http://creativecommons.org/licenses/by/4.0/>), which permits unrestricted use, distribution, and reproduction in any medium, provided you give appropriate credit to the original author(s) and the source, provide a link to the Creative Commons license, and indicate if changes were made. The Creative Commons Public Domain Dedication waiver (<http://creativecommons.org/publicdomain/zero/1.0/>) applies to the data made available in this article, unless otherwise stated.

Background

To balance the osmotic gradient across their cytoplasmic membrane and to maintain turgor, many microorganisms produce large amounts of organic osmolytes when they face high-osmolarity environments [1, 2]. These types of highly water soluble compounds are fully compliant with cellular physiology [3–5] and can therefore be accumulated to exceedingly high intracellular levels; they are generally referred to as compatible solutes [6]. In addition to their well-studied function as water-attracting osmolytes [7–9], compatible solutes also serve as chemical chaperones [10, 11]. They promote the stability and correct folding of proteins and macromolecular assemblies, preserve the integrity of membranes, and positively influence the functionality of nucleic acids [5, 12–16]. They exert these beneficial properties not only in vitro but also in vivo [11, 17, 18].

Ectoine [(S)-2-methyl-1,4,5,6-tetrahydropyrimidine-4-carboxylic acid] and its derivative 5-hydroxyectoine [(4S,5S)-5-hydroxy-2-methyl-1,4,5,6-tetrahydropyrimidine-4-carboxylic acid] are such compatible solutes [19, 20]. Many *Bacteria* and a few *Archaea* synthesize them in response to osmotic stress [21, 22]. Synthesis of ectoine proceeds from L-aspartate- β -semialdehyde [23, 24], and it is catalyzed by the sequential actions of L-2,4-diaminobutyrate transaminase (EctB; EC 2.6.1.76), 2,4-diaminobutyrate acetyltransferase (EctA; EC 2.3.1.178), and ectoine synthase (EctC; EC 4.2.1.108) [23, 25].

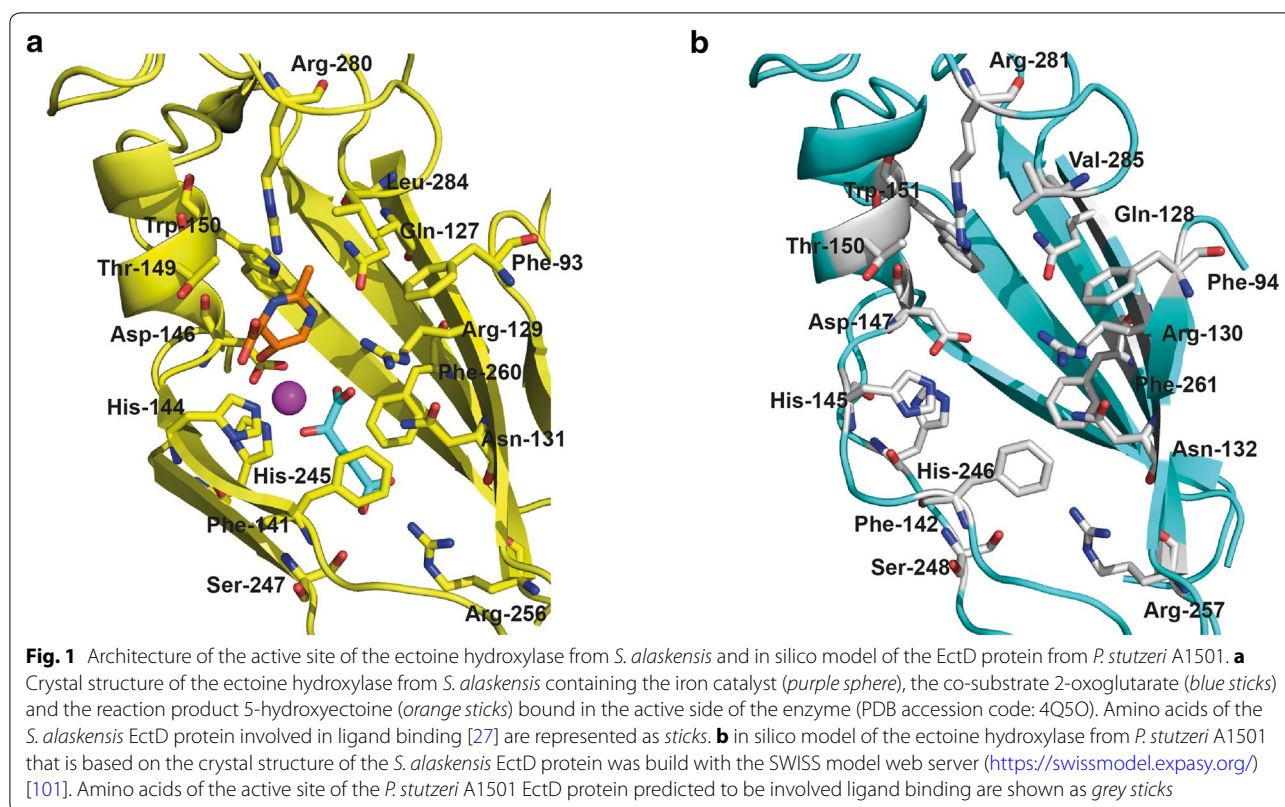
5-Hydroxyectoine is directly formed from ectoine through a position- and stereo-specific modification [20, 26], a reaction carried out by the ectoine hydroxylase (EctD; EC 1.14.11) [26–29]. The hydroxylation reaction catalyzed by EctD proceeds in an O₂-dependent fashion, relies on a mononuclear iron center, uses 2-oxoglutarate as the co-substrate and also yields the side-products CO₂ and succinate [26, 27, 29–31]. The ectoine hydroxylase [21, 22, 26–29] is a member of the non-heme-containing iron(II) and 2-oxoglutarate-dependent dioxygenases [32–35]. Ectoine hydroxylases are closely related in their amino acid sequence and can be distinguished from other members of non-heme-containing iron(II) and 2-oxoglutarate-dependent dioxygenases through the presence of a highly conserved signature sequence [22, 29, 31]. The EctD consensus sequence not only contains residues involved in iron, 2-oxoglutarate, and ectoine/hydroxyectoine binding, but also serves an important architectural role for the structuring of the cupin barrel [27, 29, 31]. A crystal structure of the ectoine hydroxylase from the cold-adapted bacterium *Sphingopyxis alaskensis* in complex with the catalytically important iron, the co-substrate 2-oxoglutarate, and the reaction product 5-hydroxyectoine has been reported [27]. EctD is a homo-dimer both in solution and in the crystal [22,

27, 29], and a view into the active site of this enzyme is shown in Fig. 1a.

5-Hydroxyectoine possesses stress-protective properties that go well beyond its role in osmotic adjustment. Indeed, synthesis of 5-hydroxyectoine often increases in stationary growth phase [26, 36, 37], a condition that confronts microbial cells with considerable physiological challenges [38]. Increased production of 5-hydroxyectoine is also induced in response to increased growth temperature [36, 37, 39], suggesting an in vivo protein stabilizing function at temperatures sub-optimal for growth. The hydroxylation of ectoine endows the newly formed 5-hydroxyectoine with enhanced, or additional, function-preserving properties [28, 36, 40, 41]. For example, 5-hydroxyectoine is a superior desiccation protectant [40, 42], a property that is dependent on its ability to form glasses [41]. Furthermore, 5-hydroxyectoine possesses a superior stabilizing effect on the structural organization of lipid monolayer and bilayer membranes, an attribute that likely stems from the fact that its –OH group partly replaces the water molecules lost from the hydration shell of lipids [16]. Both ectoines have different effects on the melting temperature of DNA; ectoine lowers the melting temperature while 5-hydroxyectoine increases it [43]. As a result, addition of 5-hydroxyectoine to the hybridization solution significantly improves the quality of DNA-microarrays [44]. Most widely noted are the often better protein-stabilizing properties of 5-hydroxyectoine in comparison with its direct biosynthetic precursor ectoine [13, 45–47].

The stabilizing and function-preserving attributes of ectoines led to various practical applications [45, 48, 49] and to the development of an industrial scale production process harnessing the highly salt tolerant bacterium *Halomonas elongata* as a microbial cell factory [50]. In this production process, *H. elongata* is grown in media of elevated salinity to trigger high-level ectoine production. These cells are then subjected to a strong osmotic downshift that leads to the transient opening of mechanosensitive channels [51, 52] and the concomitant release of the newly formed ectoine into the culture supernatant from which it can readily be purified [45, 48]. This ectoine-production scheme has been fashionably coined “bacterial milking” [53].

In addition to the assessment of natural ectoine- and 5-hydroxyectoine-producing microorganisms for practical purposes [45, 48, 49], there have been recently considerable efforts to use recombinant DNA techniques to design synthetic cell factories for these compounds. These efforts include plasmid-based expression systems for the ectoine/5-hydroxyectoine biosynthetic genes (*ectABCD*) placed either under the transcriptional control of the natural osmotically inducible *ect* promoter or of various synthetically inducible



promoters [39, 54–56]. Typically, ectoines produced in this way are retained inside the cells. However, excretion of ectoine or 5-hydroxyectoine has been repeatedly observed when the expression of ectoine/5-hydroxyectoine biosynthetic genes was engineered in non-natural ectoine producers, for instance the Gram-negative bacterium *Escherichia coli*, the Gram-positive bacterium *Corynebacterium glutamicum*, and the yeast *Hansenula polymorpha* [55, 57–59].

With notable exceptions [37, 39], those microorganisms capable of synthesizing 5-hydroxyectoine typically produce naturally a mixture of ectoine and 5-hydroxyectoine, a fact that requires additional purification steps during down-stream processing to obtain pure 5-hydroxyectoine for practical applications [45, 48, 49]. Since 5-hydroxyectoine has a number of interesting attributes, we wondered whether it might be possible to design a synthetic microbial cell factory that could take up ectoine, quantitatively convert it into 5-hydroxyectoine, and secrete almost the entire product into the growth medium. Here we report the implementation of a bacterial cell factory with these desired characteristics.

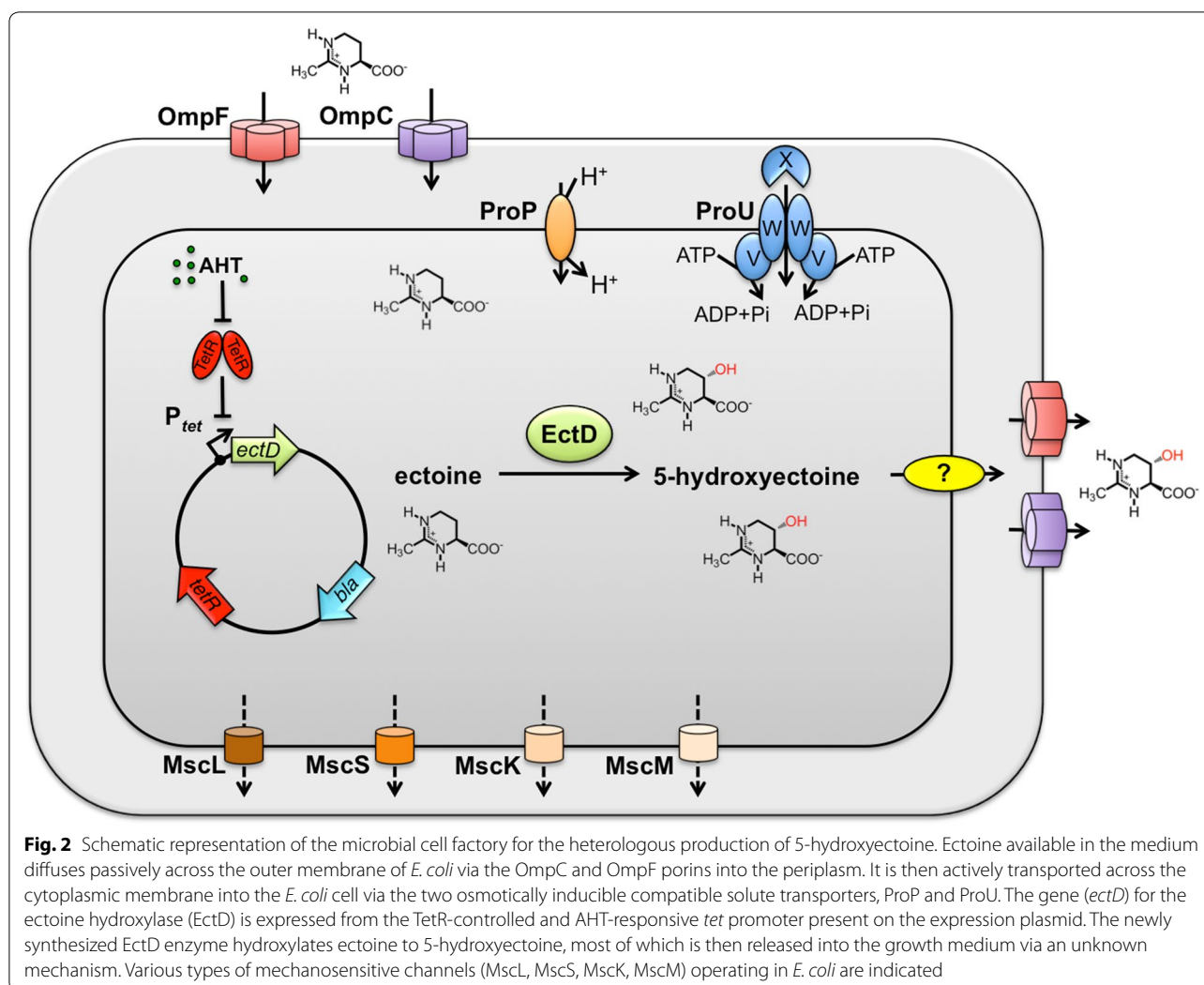
Results

Basic design of the hydroxyectoine cell factory

Escherichia coli cannot synthesize ectoine but it can import it via the osmotically inducible ProP and ProU

osmoprotectant uptake systems [60, 61]. ProP is a proton/solute symporter and a member of the major facilitator (MFS) superfamily [62], whereas ProU belongs to the multi-component ABC-type of transport systems [63, 64]. Ectoine is likely to permeate across the *E. coli* outer membrane by diffusion through the general porins OmpC and OmpF (Fig. 2), as has been shown for the osmoprotectant glycine betaine [65]. We therefore speculated that the heterologous expression of an ectoine hydroxylase gene (*ectD*) [26, 27] in *E. coli* will probably result in the conversion of the imported ectoine into 5-hydroxyectoine and its possible excretion from the recombinant cell factory (Fig. 2). The latter assumption is based on the observation that the synthetic production of ectoine in *E. coli* leads to the excretion of the newly synthesized compound [55, 57].

Trehalose is the only compatible solute that *E. coli* synthesizes de novo as a stress protectant when it is challenged by high osmolarity [66]. To avoid a contamination of the desired 5-hydroxyectoine with trehalose, we used a strain [FF4169; *otsA::Tn10*] [66] which is deficient in trehalose synthesis as our cell factory. For the heterologous production of the ectoine hydroxylase (EctD), we used a set of plasmids in which a particular *ectD* gene is expressed from the strong and tightly regulated *tet* promoter present on the backbone of the used cloning



vectors pASK-IBA3 and pASG-IBA3 (IBA, Göttingen, Germany). The *tet* promoter is negatively controlled by the TetR repressor (Fig. 2) whose DNA-binding activity can be abrogated by adding the synthetic inducer anhydrotetracycline (AHT) to the growth medium.

The *ectD* genes used in our study were derived from various extremophilic microorganisms (*H. elongata*, *S. alaskensis*, *Virgibacillus salexigens*, *Pseudomonas stutzeri*, *Paenibacillus lautus*, *Alkalilimnicola ehrlichii*) [22], and the marine archaeon *Nitrosopumilus maritimus* [21]. Some of these cloned genes were directly derived from chromosomal DNA of the donor microorganisms (*H. elongata*, *S. alaskensis*, *P. stutzeri*, *V. salexigens*), whereas others (*P. lautus*, *A. ehrlichii*, *N. maritimus*) are synthetic, codon-optimized versions of *ectD* genes [21, 22]. The proteins are of similar length and molecular mass, predicted pI and they exhibit a degree of amino acid sequence identity (relative to that of the *P. stutzeri* EctD protein; see below) between about 53 and 41 %

(Additional files 1, 2). The residues involved in iron, co-substrate, and substrate binding by the ectoine hydroxylase [22, 27, 29, 31] are fully conserved in the EctD proteins assessed in our study (Additional file 2).

In vivo benchmarking of ectoine hydroxylases

The kinetic parameters of the seven ectoine hydroxylases employed for our experiments have been obtained with the purified EctD proteins under carefully optimized in vitro conditions for each enzyme. They all possess similar enzyme activities with K_m values ranging from about 6 to 10 mM for the substrate ectoine and V_{max} values ranging between about 1 and 7 U mg⁻¹ of protein [21, 22]. These data are summarized in the Additional file 1. Since in vitro data on the kinetic properties of the EctD enzymes might not necessarily reflect their in vivo performance in a heterologous host bacterium, we benchmarked the ability of the seven enzymes to convert ectoine to 5-hydroxyectoine in the above described

chassis strain to identify the best suited EctD enzyme for its application in the cell factory.

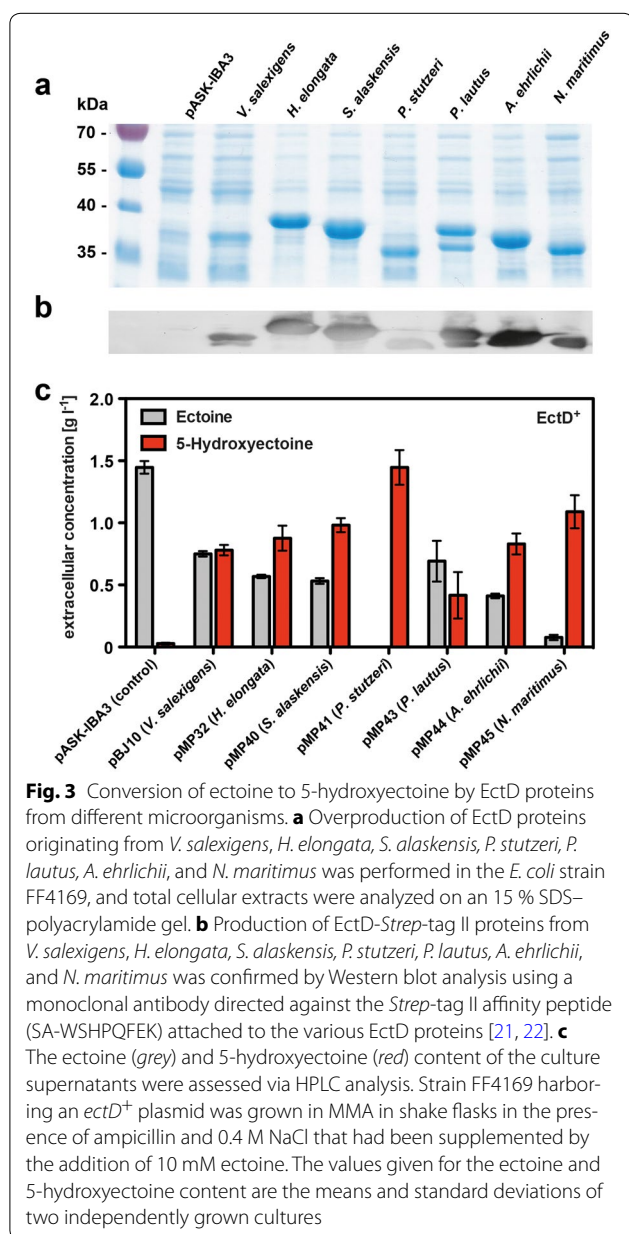
To this end, we expressed seven plasmid-encoded *ectD* genes in the *E. coli* strain FF4169 under high-saline conditions (with 0.4 M NaCl) and in the presence of 10 mM ectoine (this corresponds to 1.42 g l^{-1}) in the growth medium. We then analyzed the amount of the EctD protein by inspecting whole cell extracts applied to SDS polyacrylamide gel electrophoresis (Fig. 3a), and we also measured the ectoine and 5-hydroxyectoine content of the growth medium in cultures that had been propagated for 24 h (Fig. 3c). With the exception of the EctD

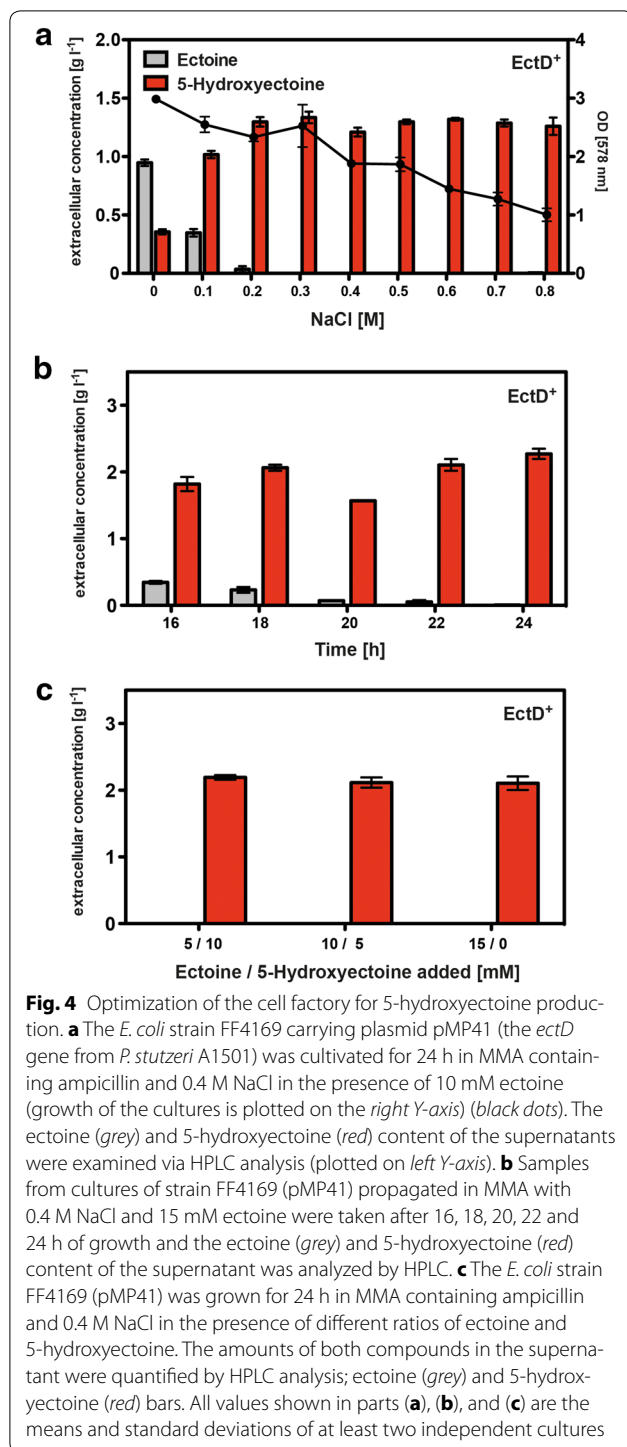
protein from *V. salexigens*, all ectoine hydroxylases were produced in substantial amounts (Fig. 3a) and reacted with an antibody directed against the *Strep*-tag II affinity peptide that had been attached to the corresponding proteins to allow their purification [21, 22] in a Western blot experiment (Fig. 3b). Despite the close match of the various EctD proteins with respect to their calculated molecular mass (Additional file 1), substantial variations in their electrophoretic mobility was observed and signs of proteolysis was noted in two of the EctD proteins (Fig. 3a, b).

There were substantial differences in the ability of the tested ectoine hydroxylases to convert ectoine into 5-hydroxyectoine (Fig. 3c). In most cases a mixture of the added ectoine and the newly produced 5-hydroxyectoine were observed in the culture supernatants. There were two striking exceptions where almost all of the provided ectoine had been converted into 5-hydroxyectoine; these were the ectoine hydroxylases from *P. stutzeri* A1501 [22] and from the archaeon *N. maritimus* [21] (Fig. 3c), leading to the production of 1.57 ± 0.08 and $1.23 \pm 0.05 \text{ g l}^{-1}$ 5-hydroxyectoine, respectively, from the originally 1.42 g l^{-1} ectoine (this corresponds to 10 mM) provided to the cells. Based upon these initial experiments, we chose the ectoine hydroxylase [22] from the plant root-associated bacterium *P. stutzeri* A1501 [67] for the following experiments. A homology model of the *P. stutzeri* EctD enzyme assessed by us showed that this protein adopts in all likelihood a three-dimensional structure matching that of the crystalized EctD protein from *S. alaskensis* (Fig. 1a, b).

Optimization of the parameters for the 5-hydroxyectoine cell factory

The ProP and ProU ectoine uptake systems in *E. coli* are osmotically regulated both at the level of *proP* and *proU* transcription and at the level of their transport activity [60, 62, 68]. As a consequence, increased osmolarity will be a key determinant for the efficient uptake of ectoine by the FF4169 chassis strain. We therefore assessed the influence of increased sustained salinity for the biotransformation of ectoine by growing the cells in media in which the NaCl concentration was increased in a finely tuned manner. In keeping with the osmotic control of the ProP and ProU systems, substantial amounts of ectoine remained in the medium of the cultures that received no additional NaCl (Fig. 4a). Moderate increases in salinity reduced the amount of ectoine remaining in the medium and resulted in an increased 5-hydroxyectoine production (Fig. 4a). When the growth medium contained more than 0.3 M NaCl, there was complete uptake of the provided 10 mM ectoine. It was converted into 5-hydroxyectoine, and the newly formed 5-hydroxyectoine was excreted into the





growth medium (Fig. 4a). Notably, this level of salinity had only a modest effect on the growth yield of the cultures (Fig. 4a), an important parameter that needed to be considered for the final set-up of the cell factory.

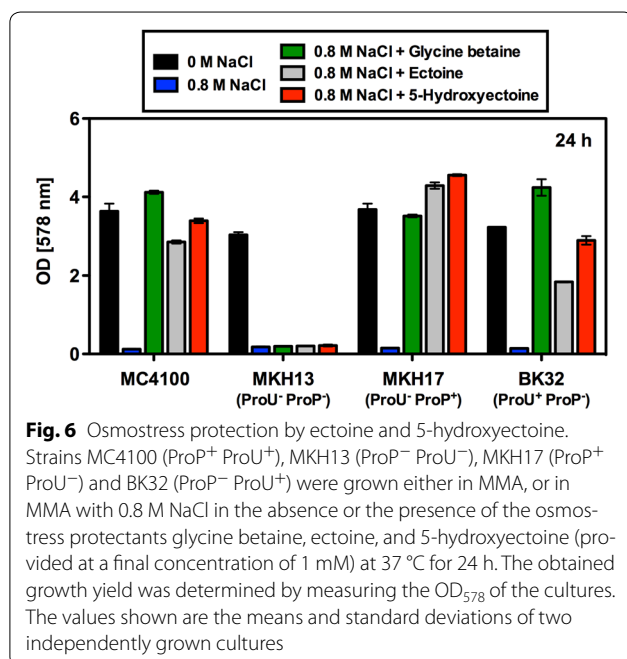
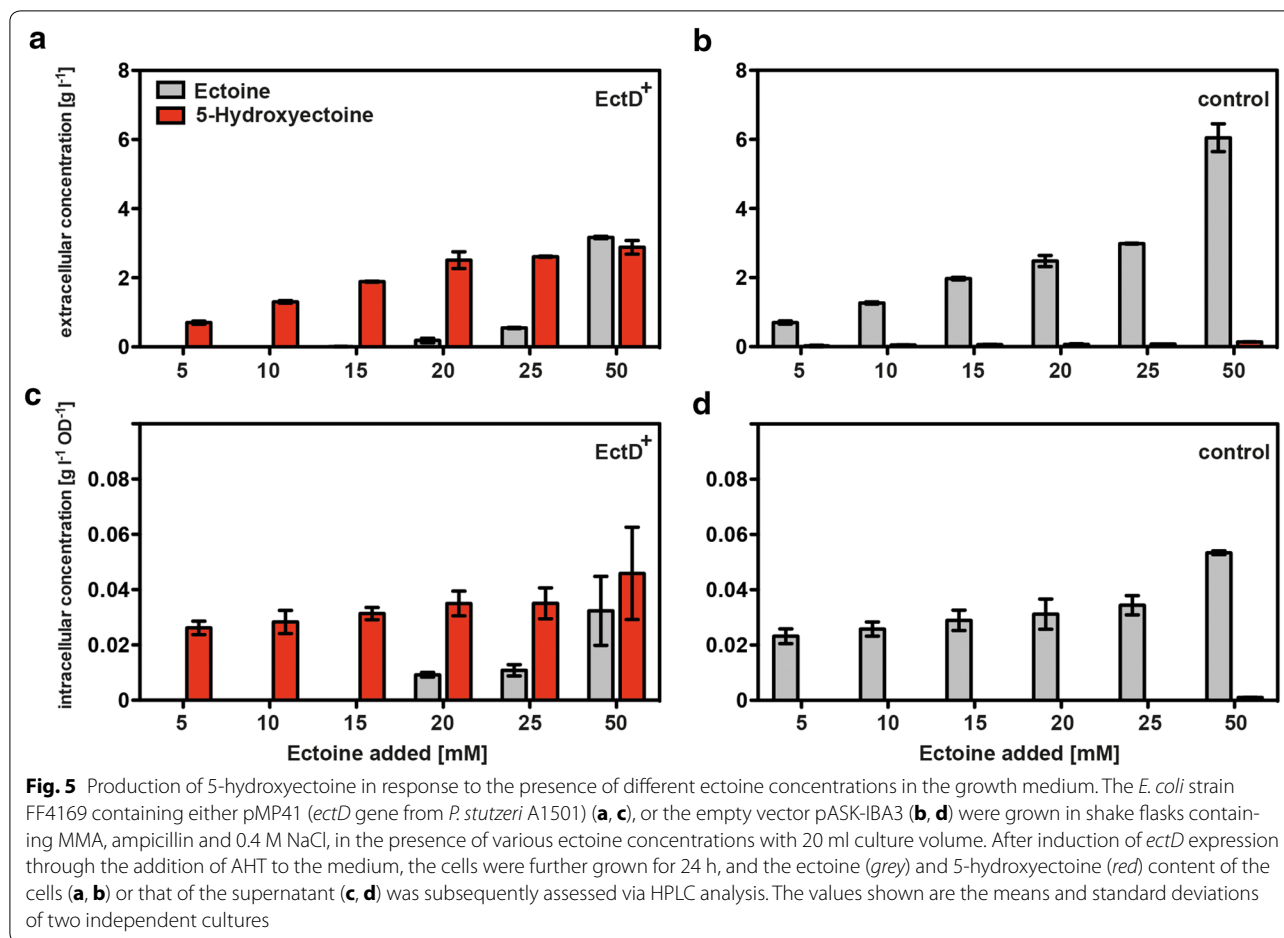
Another parameter that is important for the overall performance of the bioconversion of ectoine into

5-hydroxyectoine is the amount of substrate that can be added to the medium and fully converted into 5-hydroxyectoine. We therefore cultured osmotically stressed cells (with 0.4 M NaCl) in the presence of various ectoine concentrations (from 5 to 50 mM) and determined both the intracellular and extracellular pools of these compounds (Fig. 5). Up to a concentration of 15 mM ectoine (2.13 g l^{-1}) in the growth medium, only 5-hydroxyectoine was found inside and outside of the cells (Fig. 5a, c). Higher concentrations of externally provided ectoine always yielded mixtures of the two ectoines (Fig. 5a, c), a situation that is not desirable for a possible practical application of the 5-hydroxyectoine producing cell factory. Control experiments with a cell factory that contained the expression vector without an insert demonstrated that there was uptake of ectoine but no conversion into 5-hydroxyectoine; hence formation of 5-hydroxyectoine was dependent on the expression of the recombinant *ectD* gene (Fig. 5b, d).

Using the information derived from experiments documented in Figs. 4a and 5a, c, we fed 15 mM ectoine to the cells and monitored its conversion into 5-hydroxyectoine over time. Growth of the cells in shake flasks for 24 h resulted in the production of an essentially ectoine-free 5-hydroxyectoine pool in the supernatant with a maximal yield of $2.3 \pm 0.1 \text{ g l}^{-1}$, a value that corresponds to $14.36 \pm 0.7 \text{ mM}$ of newly formed 5-hydroxyectoine. This conversion rate is close to that theoretically possible given that 15 mM (2.13 g l^{-1}) ectoine was fed to the cells (Fig. 4b). The cell factory was also able to effectively convert different mixtures of ectoine/5-hydroxyectoine into extracellular pools that consisted only of 5-hydroxyectoine (Fig. 4b).

Characteristics of ectoine and 5-hydroxyectoine import via the ProU and ProP transporters

The uptake of ectoine in *E. coli* via the ProP and ProU osmolyte uptake systems [60] is well documented [61]. In contrast, essentially nothing is known about the import of 5-hydroxyectoine, but the ProP and ProU systems are the most likely candidates. To test this, we used an isogenic set of strains in which either only ProP or ProU is functional or in which both osmolyte transporters were defective [69]. These strains were grown in a chemically defined medium (MMA) with 0.8 M NaCl, conditions under which the wild-type strain MC4100 cannot grow in the absence of an osmoprotectant (Fig. 6). The addition of either 1 mM ectoine or 1 mM 5-hydroxyectoine provided osmoprotection of the wild-type strain MC4100 and both compounds were imported via the ProP (strain MKH17) and ProU (strain BK32) systems, whereas there was no osmoprotection of strain MKH13 (Fig. 6) that is deficient in both the



ProP and ProU transporters [69]. Import of ectoine and 5-hydroxyectoine via ProU provided less effective osmotress protection in comparison with a strain where these compounds were taken up via ProP (Fig. 6).

To study the import of 5-hydroxyectoine and ectoine via ProP and ProU further, we conducted competition experiments with radiolabeled [¹⁴C]glycine betaine since this compatible solute is a major substrate for the ProU and ProP transporters and both exhibit high affinity for it [70, 71]. We measured the uptake of [¹⁴C]glycine betaine (provided at a final concentration of 100 μM) in the absence and presence of either ectoine or 5-hydroxyectoine as competitors and used for these experiments strains MKH17 (ProP⁻ ProU⁺) and BK32 (ProP⁺ ProU⁻). Used as a control, the addition of a tenfold excess of unlabeled glycine betaine was able to reduce [¹⁴C]glycine betaine import by about 85 % for both tested strains (Fig. 7).

Inhibition of [¹⁴C]glycine betaine import by ectoine via the ProU ABC transporter was rather weak and even a 1000-fold excess of the competitor was only able

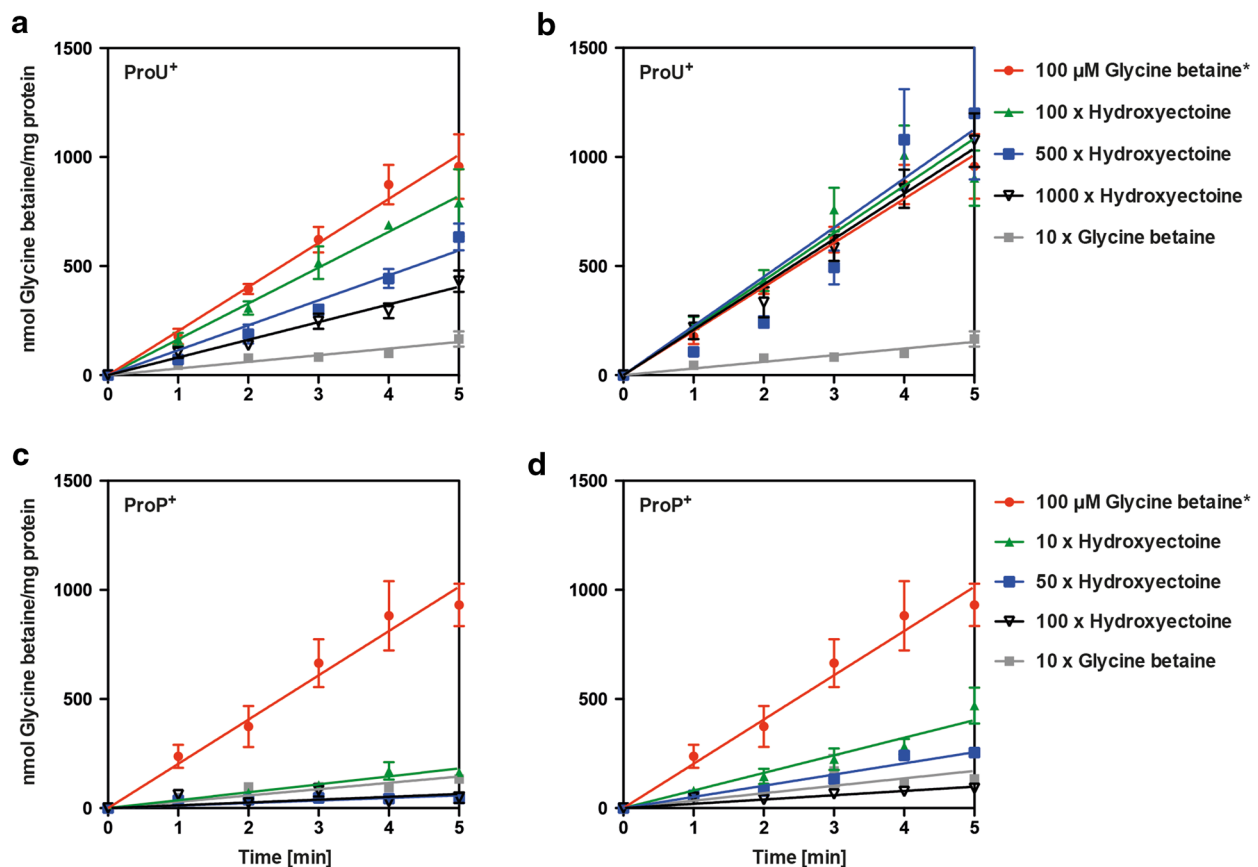


Fig. 7 Inhibition of the uptake of $[1-^{14}\text{C}]$ glycine betaine via the ProU and ProP transporters by an excess of ectoine and 5-hydroxyectoine. The *E. coli* mutant strains BK32 (ProU⁺ ProU⁺) (a, b) and MKH17 (ProP⁺ ProU⁻) (c, d) were cultivated in MMA with 0.4 M NaCl at 37 °C to early exponential phase (OD₅₇₈ 0.3). Two millilitre aliquots were taken and mixed with a solution containing non-labeled glycine betaine and $[1-^{14}\text{C}]$ glycine betaine (the final concentration of glycine betaine in the uptake assay was 100 μM), and the uptake of $[1-^{14}\text{C}]$ glycine betaine by the cells was measured over time (for 5 min). Import of glycine betaine is shown in red. In parallel assays, the inhibition of $[1-^{14}\text{C}]$ glycine betaine uptake was measured with an excesses of either ectoine (a, c) or 5-hydroxyectoine (b, d). For strain BK32 (ProU⁺ ProU⁺), ectoine or 5-hydroxyectoine was provided in 100-, 500-, and 1000-fold excess; for strain MKH17 (ProP⁺ ProU⁻), ectoine or 5-hydroxyectoine was provided in 10-, 50-, and 100-fold excess. As a control, a ten-fold excess of unlabeled glycine betaine was added to the $[1-^{14}\text{C}]$ glycine betaine mixture (grey symbols) to monitor the inhibition of $[1-^{14}\text{C}]$ glycine betaine import by glycine betaine itself. The values shown are the means and standard deviations of four independently tested cultures

to reduce $[^{14}\text{C}]$ glycine betaine import by 45 % (Fig. 7a). Strikingly, there was essentially no competition by 5-hydroxyectoine with the uptake of $[^{14}\text{C}]$ glycine betaine via the ProU system (Fig. 7b). While osmoprotection by both ectoine and 5-hydroxyectoine (provided at a 1 mM concentration) can be observed in the long-term (24 h) growth experiment of the ProU⁺ strain MKH17 (Fig. 6), the transport assays revealed that both ectoines are not favored substrates of the ProU ABC transporter (Fig. 7a, b). This situation is different for the ProP transport system. Both ectoine and 5-hydroxyectoine competed effectively with $[^{14}\text{C}]$ glycine betaine for ProP-mediated import, with ectoine being the somewhat better competitor (Fig. 7c, d). Consequently, ProP is the physiologically more important transport system

for both ectoines when they are provided at low external concentration.

Excretion of 5-hydroxyectoine occurs independent of the MscL, MscS, and MscM mechanosensitive channels

Microbial cells employ safety valves, so called mechanosensitive channels, to prevent lysis when they are subjected to a sudden and severe osmotic down-shock [72, 73]. The opening of these cytoplasmic membrane-embedded channels is triggered by the rapid influx of water under these conditions, which in turn raises turgor and causes increased tension in the lateral plain of the membrane [51, 52, 74, 75]. Typically, microorganisms possess different types of mechanosensitive channels that possess different gating properties and channel

diameters; this offers a graded response to the osmotically challenged cell. Since the structurally and functionally well characterized MscS and MscL mechanosensitive channels from *E. coli* possess large channel diameters in their fully opened forms [76, 77], their gating activity must be tightly controlled [51]. However, it cannot be firmly excluded that these channels sometimes open under osmotic steady-state conditions, and this behavior might thus be responsible for the release of 5-hydroxyectoine from the cell factory (Figs. 3, 4, 5).

We therefore investigated whether the excretion of 5-hydroxyectoine from the *E. coli* cell factory is based on the gating activity of mechanosensitive channels. For these experiments we used a set of isogenic *E. coli* strains that have previously been very carefully studied by physiological and electrophysiological approaches and which carry defects in various channel-forming proteins [72, 78]. Strain MJF465 lacks intact MscL, MscS, and MscK channels, whereas strain MJF641 is defective in all currently known mechanosensitive channels of *E. coli*, including MscM. Strain Frag 1 is the parent of these two mutant strains [79].

We introduced the *ectD*⁺ plasmid pMP41 into strains Frag1, MJF465, and MJF641, and then exposed them to sustained high-salinity growth conditions (by adding 0.4 M NaCl to MMA) in the presence of 10 mM ectoine. After growth for 24 h, we then measured the ectoine and 5-hydroxyectoine pools in the supernatants of the cultures. In all three strains, large amounts of 5-hydroxyectoine were found in the supernatant (Fig. 8a). Since this is also the case in strain MJF641 lacking all currently characterized mechanosensitive channels (MscL, MscS, MscK, MscM), we can firmly conclude that the release of the newly formed 5-hydroxyectoine from the cell factory does not occur via the transient opening of these types of channels under osmotic steady-state conditions.

In direct comparison with the cell factory strain FF4169 (*otsA::Tn10*) carrying the same *ectD*⁺ plasmid pMP41, Frag 1 and its channel-mutant derivatives strains MJF465 and MJF641, the supernatant of the cultures still contained substantial amounts of the precursor ectoine (Fig. 8a). This could potentially be explained by inefficient ectoine import or an ineffective biotransformation of ectoine to 5-hydroxyectoine. The sum of the measured ectoine and 5-hydroxyectoine concentrations in the supernatant of strain MJF641 was $1.31 \pm 0.4 \text{ g l}^{-1}$ compared to the 5-hydroxyectoine content of $1.38 \pm 0.1 \text{ g l}^{-1}$ found in strain FF4169 (Fig. 8a). Hence, like strain FF4169, the channel-deficient strains MJF465 and MJF641 and their parent Frag1 do not permanently accumulate massive amounts of ectoines in their cytoplasm under the growth conditions that we have used for our cell factory (Fig. 8b).

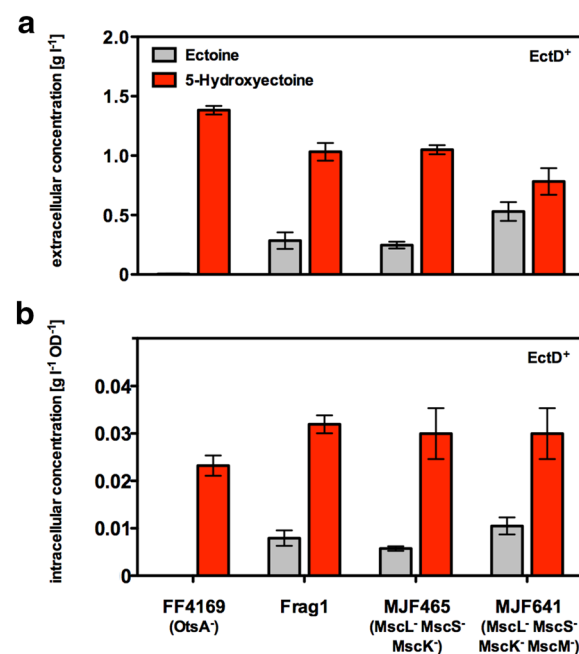


Fig. 8 Excretion of ectoine and 5-hydroxyectoine in *E. coli* strains lacking mechanosensitive channels. The *E. coli* strains FF4169 (*otsA::Tn10*), Frag1 (wild-type), MJF465 (*mscL mscS mscK*), and MJF641 (*mscL mscS mscK mscM*) harboring the plasmid pMP41 (*ectD* gene from *P. stutzeri* A1501) were grown in MMA that contained ampicillin, 0.4 M NaCl, and 10 mM ectoine. Plasmid-based overexpression of the *ectD* gene was induced by the addition of AHT to the growth medium; the cultures were subsequently grown for 24 h. Both the extracellular (a) and the intracellular (b) concentrations of ectoine (grey) and 5-hydroxyectoine (red) were determined via HPLC analysis. The values shown are the means and standard deviations of four independent cultures. The strains with defects in various mechanosensitive channel genes (MJF465, MJF641) are derivatives of Frag1. The values shown are the means and standard deviations of four independently tested cultures

Discussion

Whole cell biocatalysts become increasingly important for environmentally friendly and resource-preserving production of compounds with biotechnological and medical interest. They also provide a suitable chemical space for the regeneration of co-factors and co-substrates required for the functioning of enzymes [80], a process on which the ectoine hydroxylase is dependent [26, 27, 29–31]. As a member of the non-heme-containing iron(II) and 2-oxoglutarate-dependent dioxygenase superfamily [32–35], the ectoine hydroxylase relies on a mononuclear iron center and uses 2-oxoglutarate as its co-substrate [26, 27, 29–31]. The region- and stereo-specific hydroxylation of chemically non-activated carbon atoms is often difficult to achieve through organo-chemical synthesis. However, the ectoine hydroxylase performs such an enzymatic reaction with high precision and

efficiency, both in vitro and in vivo [20, 26, 81]. It converts (4S)-ectoine into (4S,5S)-5-hydroxyectoine in a single step [26, 27, 29, 30].

The function-preserving attributes of ectoines have led to various practical applications and the development of a biotechnological industrial-scale production process [45, 48, 49]. This *bacterial milking* procedure [53] relies on the transient opening of mechanosensitive channels [51, 52] to release the synthesized ectoines from the producer cells in response to a severe osmotic down-shock [48]. Here, we report on the properties of an *E. coli*-based synthetic cell factory that releases almost all of the newly formed 5-hydroxyectoine into the medium under osmotic steady-state growth conditions (Figs. 3c, 4, 5a, 8a). Most interestingly, we found that the excretion of 5-hydroxyectoine from the recombinant cell factory occurs independently of all currently known mechanosensitive channels operating in *E. coli* (MscL, MscS, MscK, MscM) [78].

Excretion of ectoine from recombinant *E. coli* cells expressing the *ectABC* biosynthetic genes has been observed before [55, 57], but the underlying mechanism has remained unclear. Schubert et al. [57] found that the release of ectoine was not accompanied by the accumulation of amino acids in the growth medium, a consequence expected from the transient opening of mechanosensitive channels [51, 52]. These authors therefore argued that ectoine had been released in their experiments via a specific solute efflux system [57]. It is well known that microorganisms possess efflux systems for various types of compounds, in particular for amino acids [82]. One might therefore ask what physiological function and advantage a compatible solute efflux system would offer in comparison with the functioning of mechanosensitive channels. Due to the large diameter of MscS- and MscL-type channels in their open forms (about 13 and 30 Å, respectively) [74–77], these safety valves will indiscriminately release all low-molecular weight compounds from the cell upon a sudden osmotic downshift, a process that negatively impinges on cell growth [51, 52]. An efflux system dedicated to the excretion of compatible solutes would avoid the loss of valuable metabolites. It would also permit the cell to respond more specifically to imbalances in turgor that temporarily might arise during cell elongation and division [83]. A dedicated efflux system could also release compatible solutes under steady-state osmotic conditions when the need arises, whereas the opening of mechanosensitive channels requires an osmotic downshift [51, 52].

Although the molecular identity of such putative compatible solute efflux systems in microorganisms has remained tenuous [84], several observations point to their existence. The release of glycine betaine from

osmotically down-shocked *Lactobacillus plantarum* cells revealed two kinetically distinguishable components; one is related to the operation of mechanosensitive channels, and the other is consistent with a carrier-mediated export process [85]. Furthermore, in different microbial species, substantial accumulation of newly synthesized compatible solutes in the growth medium occurs when the major uptake system for these osmoprotectants is genetically inactivated [83, 86–89]. Particular relevant for our study is the report of Grammann et al. [86], who found considerable amounts of newly synthesized ectoine in the supernatant of an *H. elongata* mutant deficient in the ectoine/5-hydroxyectoine uptake system TeaABC. Furthermore, Jebbar et al. [61] observed a prompt efflux of prior imported radiolabeled ectoine in *E. coli*, when unlabeled ectoine was added to the growth medium. While it is still unclear which system(s) is responsible for the excretion of compatible solutes from the producer cells, this phenomenon worked to our advantage to recover the recombinantly produced 5-hydroxyectoine from our cell factory in the supernatant.

The seven ectoine hydroxylases whose performance we have evaluated in the context of the set-up of our cell factory are closely related in their amino acid sequences (Additional file 1) and those residues that are of functional importance (Fig. 1a) [22, 27] are all strictly conserved (Additional file 2). These EctD-type enzymes exhibit similar kinetic characteristics in vitro (Additional file 1) when they were assayed under conditions optimized for each of them [21, 22]. To our surprise, we observed substantial differences in the efficiency of the biotransformation of ectoine to 5-hydroxyectoine, when we benchmarked the various EctD enzymes in vivo against each other (Fig. 3c). While differences in the expression level of *ectD* or the stability of the produced EctD enzymes in the heterologous *E. coli* host strain might be contributing factors (Fig. 3a, b), other characteristics of these ectoine hydroxylases must come into play to explain their different performances. These differences might be related to the ion pools of the *E. coli* cytoplasm since small but noticeable variations in response to salts have been reported in the course of the biochemical in vitro characterization of various EctD enzymes [21, 22].

When we fed 15 mM ectoine to the *E. coli* cell factory expressing the *P. stutzeri* A1501 *ectD* gene, approximately 98 % of the newly formed 5-hydroxyectoine was found in the supernatant after 24 h of growth. Under these conditions, there is essentially no contaminating ectoine left in the growth medium and the missing 2 % of 5-hydroxyectoine is found inside the cells (Fig. 5a, c). With notable exceptions, most microorganisms that can produce both ectoine and 5-hydroxyectoine contain a varied mixture of

these compounds [21, 24, 26, 36, 37, 39]. Such mixtures of the two ectoines, either extracted or released from the natural producer cells via an osmotic down-shock, can be effectively converted into essentially ectoine-free 5-hydroxyectoine solutions by our synthetic cell factory (Fig. 4c).

The uptake of ectoine through the promiscuous compatible solute importer systems ProP and ProU has previously been assessed [61, 71], but the import characteristics of 5-hydroxyectoine had not been studied in any detail. Our data show that osmoprotection of *E. coli* by either ectoine or 5-hydroxyectoine can be observed in long-term growth experiments with a ProU⁺ ProP[−] strain (Fig. 6). However, competition transport experiments with radiolabel glycine betaine showed that both ectoine and 5-hydroxyectoine are not favorable substrates for ProU (Fig. 7a, b). This can readily be understood in view of the architecture of the ligand-binding site present in the periplasmic solute receptor protein ProX operating in conjunction with the ProU ABC transporter [60, 70]. Its aromatic cage is designed for the efficient capturing of compounds possessing either tri- (e.g. glycine betaine), or di- (e.g. proline betaine)-methylammonium head-groups [69, 90]. As a consequence, the ligand-binding site of ProX is not optimal for the binding of ectoines when one considers the architectural features of the substrate-binding sites of true high-affinity ligand-binding proteins for these types of solutes; e.g., EhuB, UehA, and TeaA [91–93].

In contrast to ProU, the osmotically stimulated ProP transporter [62] exhibits reasonable affinities for both ectoine and 5-hydroxyectoine in competition assays with glycine betaine (Fig. 7c, d). Hence, this member of the MFS superfamily with its broad substrate specificity [71] is certainly the dominant ectoine and 5-hydroxyectoine transporter of *E. coli*. This conclusion is fully consistent with previously reported measurements of ectoine pools built up by osmotically stressed (with 0.7 M NaCl) *E. coli* cells via import, either via the ProP or the ProU systems [61].

Although our cell factory can import 5-hydroxyectoine under osmotic stress conditions, the cells retain only very modest amounts of it when it is newly formed from ectoine via EctD (Fig. 5a, c). These amounts are apparently sufficient to physiologically cope with the sustained but moderate osmotic stress that we imposed onto the *E. coli* cells. Hence in terms of practical application, the re-import of originally excreted 5-hydroxyectoine is apparently of no great concern for the overall performance of our synthetic cell factory.

Synthetic ectoine derivatives with reduced or expanded ring sizes have been reported and shown to possess attributes different from those of ectoine, for instance in

their performance as PCR enhancers [43]. The hydroxylation of such synthetic ectoines (or compounds chemically related to ectoine) might endow them with novel and beneficial characteristics, as has been found in connection with studies assessing 5-hydroxyectoine for its superior desiccation stress and membrane-protecting potential [16, 40–42]. Realizing this, a patent envisioning the import of ectoine-related compounds via osmotically inducible transport systems, their hydroxylation via EctD, and the active or passive release of the newly formed compounds into the growth medium has been granted [94]. However, claims made in this patent have not yet been subjected to scientific scrutiny via a peer-reviewed publication.

The efficiency by which compatible solute transport systems such as ProP and ProU [60, 62] (Figs. 6, 7) might import synthetic ectoine-related substrates will be a key factor in realizing the full potential of cell factories for these compounds. The evaluation of the *in vivo* performance of a considerable number of ectoine hydroxylases for their natural substrate carried out in this study (Fig. 3) strongly hints that not any arbitrary EctD protein will be optimally suited for the hydroxylation of synthetic ectoine derivatives. Of similar importance is the affinity of the chosen EctD protein for synthetic ectoines and for the proper positioning of these non-natural substrates within the active site of the ectoine hydroxylase (Fig. 1a) to allow a position and stereo-specific hydroxylation reaction with high efficiency and precision [27].

Conclusions

We report here the basic design and functional characterization of a synthetic microbial cell factory that can execute the position- and stereo-specific hydroxylation of externally provided ectoine through the activity of the ectoine hydroxylase [26, 27, 29]. An important result of our study is the observation that ectoine hydroxylases possessing similar *in vitro* enzyme characteristics (Additional file 1) can perform quite differently when produced in a heterologous chassis strain. The 5-hydroxyectoine formed in our synthetic cell factory is almost quantitatively excreted into the growth medium from which it can be readily purified [48]. Excretion occurs in a manner that is independent of all currently known mechanosensitive channels of *E. coli* [78], a finding that points to the existence of a compatible solute efflux system in this microorganism. The architecture of the active site of the ectoine hydroxylase, as revealed by crystallographic analysis (Fig. 1a) [27], is probably flexible enough to allow the hydroxylation of already reported synthetic ectoines with slightly reduced or expanded ring sizes [43]. By carefully considering the structural design and spatial constraints of the ectoine hydroxylase catalytic core (Fig. 1a) [27],

it might be possible to rationally devise *in silico* new ectoine derivatives optimized for their chemical modification via EctD. Taken this knowledge together, the cell factory reported here might find biotechnologically interesting applications in chemical biology.

Methods

Chemicals and reagents

Ectoine and 5-hydroxyectoine were kindly provided by the bitop AG (Witten, Germany). Anhydrotetracycline-hydrochloride (AHT) was purchased from IBA GmbH (Göttingen, Germany). Acetonitrile (HPLC-grade) was obtained from VWR International GmbH (Darmstadt, Germany). Ampicillin and all other chemicals were purchased from Serva Electrophoresis GmbH (Heidelberg, Germany) and Carl Roth GmbH (Karlsruhe, Germany). Radiolabeled [$1\text{-}^{14}\text{C}$]glycine betaine (55 mCi mmol^{-1}) was bought from American Radiolabeled Chemicals Inc. (St. Louis, MO; USA).

Bacterial strains and plasmids

The *E. coli* strain FF4169 (*otsA::Tn10*)1 is deficient in the synthesis of trehalose [66]. It is a derivative of strain MC4100 [95]. This latter *E. coli* strain is also the parent of strains BK32 [$\Delta(\textit{proP})2\text{ } \textit{proU}^+$], MKH17 [$\textit{proP}^+ \Delta(\textit{proU}::\textit{spc})608$ (\textit{Spc}^r)], and MKH13 [$\Delta(\textit{proP})2 \Delta(\textit{proU}::\textit{spc})608$] (\textit{Spc}^r) carrying in various combinations defects in the genes encoding the ProP or ProU compatible solute uptake systems [60, 69]. To assess a possible contribution of mechanosensitive channels to the release of 5-hydroxyectoine from the recombinant *E. coli* cell factory, we used strains Frag1, MJF465, and MJF641; these strains have the following genotypes. Frag1: (\textit{F}^- , *rha*, *gal*, *thi*, *lac*); MJF465 (FRAG1, *mscL::Cm*; $\Delta\textit{mscS}$; *mscK::Kan*), and MJF641 (FRAG1, *mscL*, *mscS*, *mscK*, *ybdG*, *ybiO*, *yjeP*, *ynaI*) [72, 78, 79].

The construction of the expression plasmids containing the ectoine hydroxylase structural gene (*ectD*) [26] from various *Bacteria* and *Archaea* has been described [21, 22, 26]. We used the following plasmids: pBJ10 (EctD from *V. salicigena*; accession number: AY935522), pMP32 (EctD from *H. elongata*; accession number: WP_013333764.1), pMP40 (EctD from *S. alaskensis*; accession number: WP_011543221.1), pMP41 (EctD from *P. stutzeri*; accession number: ABP77885.1), pMP43 (EctD from *P. lautus*; accession number: AER00258.1), pMP44 (EctD from *A. ehrlichii*; accession number: AER00257.1), and pMP45 (EctD from *N. maritimus*; accession number: AER00259.1) [21, 22, 26]. The transcription of these various plasmid-encoded *ectD* genes is mediated by the *tet* promoter present on the backbone of the expression vectors pASG-IBA3 and pASK-IBA3 (IBA GmbH, Göttingen) used for the construction of the *ectD* expression

plasmids [21, 22, 26]. The *tet* promoter is controlled by the TetR repressor and its transcriptional activity can be induced by adding AHT to the growth medium.

Growth media for *E. coli* strains

All *E. coli* strains were routinely maintained on Luria Bertani (LB) agar plates and propagated in liquid LB medium [96]. When they contained a recombinant plasmid, ampicillin ($100\text{ }\mu\text{g ml}^{-1}$) was added to the growth medium. For experiments involving the bioconversion of ectoine to 5-hydroxyectoine, *E. coli* strains were grown in minimal medium A (MMA) [96] supplemented with 0.5 % (w/v) glucose as the carbon source, 1 mM MgSO_4 , and 3 mM thiamine. The osmolarity of the growth medium was adjusted by adding various concentrations of NaCl, as specified in the individual experiments. Shake-flask cultures were incubated at $37\text{ }^\circ\text{C}$ in a shaking water bath set to 220 rpm. Osmostress protection assays with *E. coli* strains were conducted in 100-ml Erlenmeyer flasks (culture volume of 20 ml) by growing the cells (at $37\text{ }^\circ\text{C}$) in MMA containing 0.8 M NaCl in absence or presence (1 mM final concentration) of the tested compatible solutes [69]. The growth yield of these cultures was recorded after 24 h by measuring their OD_{578} .

Biotransformation of ectoine into 5-hydroxyectoine in shake flasks

Escherichia coli cells harboring an *ectD*⁺ plasmid, were inoculated into LB medium and incubated for 5 h on a roller at $37\text{ }^\circ\text{C}$. Two hundred microlitre of this culture were then transferred into 20 ml MMA and incubated in a shaking water bath overnight (set to 220 rpm, $37\text{ }^\circ\text{C}$). This pre-culture was used to inoculate fresh media (to an OD_{578} of 0.1) (20 ml MMA) containing various amounts of NaCl and ectoine. When these main cultures contained more than 0.5 M NaCl, cells from the pre-culture were pre-adapted in MMA containing 0.3 M NaCl. All main cultures were grown until they reached an OD_{578} of 0.5. At this time, AHT was added to a final concentration of 0.2 mg l^{-1} to induce the expression of the plasmid-encoded *ectD*⁺ genes; the cells were then grown for additional 24 h. Two times 2-ml samples of each culture were harvested by centrifugation ($16,000g$, for 10 min at room temperature); 1 ml of the supernatant and the cell pellet were stored at $-80\text{ }^\circ\text{C}$ until further use.

The production of recombinant EctD proteins in these cells was analyzed by SDS polyacrylamide gel electrophoresis [97]. For Western blot analysis of these samples, cell pellets were re-suspended to an OD_{578} of ten in TE buffer (10 mM Tris-HCl, pH 7.5, 1 mM EDTA) with lysozyme (final concentration: 1 mg ml^{-1}). Fifty microlitre portions of these samples were incubated for 5 min at $37\text{ }^\circ\text{C}$, mixed with 25 μl SDS-PAGE sample

buffer, and subsequently incubated for 5 min at 95 °C. After centrifugation in an Eppendorf table-top centrifuge (10 min, 16,000g), 10 µl portions of the samples were applied to an 15 % SDS–polyacrylamide gel; the electrophoretically separated proteins were then transferred to a polyvinylidene fluoride (PVDF) membrane via semi-dry blotting. Western blotting of the transferred proteins was performed with a primary mouse monoclonal anti *Strep*-tag II (SA-WSHPQFEK) antibody (purchased from IBA GmbH; Göttingen, Germany), and the formed immune complex was detected with a secondary rabbit anti-mouse alkaline phosphatase-coupled IgG antibody (purchased from Promega, Madison, WI, USA) and the CDP-Star Western blotting detection reagent (Roche Diagnostics GmbH, Mannheim, Germany). Signals were detected by chemiluminescence using an imager system (ChemoCam Imager, Intas Science Imaging Instruments GmbH, Göttingen, Germany).

HPLC analysis of ectoine and 5-hydroxyectoine

Cell pellets of *E. coli* strains were either lyophilized for the determination of the dry weight, or low-molecular-weight compounds were extracted with 70 % ethanol. For this purpose, the cell pellets were re-suspended in 1-ml 70 % ethanol and were shaken for 1 h. After centrifugation at 16,000g (4 °C, 30 min) to remove cell debris, the ethanolic extracts were transferred into fresh Eppendorf tubes, and the ethanol was removed by evaporation (at 55 °C for 20 h). The resulting dried material was suspended in 100 µl of distilled water and insoluble material was removed by centrifugation (16,000g at 4 °C for 30 min). The extracted samples and the cell-free culture supernatant were diluted tenfold with distilled water and acetonitrile (the end concentration of acetonitrile was 50 %) and analyzed for their ectoine/5-hydroxyectoine content by isocratic high-performance liquid chromatography (HPLC) [98]. For these measurements we employed an Agilent 1260 Infinity LC system (Agilent, Waldbronn, Germany) and a GROM-SIL Amino 1PR column (GROM, Rottenburg-Hailfingen, Germany) essentially as described [98] with the exception that a 1260 Infinity Diode Array Detector (DAD) (Agilent) was used, instead of the previously used UV/Vis detector system. The ectoine content of samples was quantified using the OpenLAB software suite (Agilent). Standard curves for the calculation of the ectoine and 5-hydroxyectoine concentrations were determined with commercially available samples (obtained from bitop AG, Witten, Germany).

Transport studies with radiolabeled glycine betaine

To determine glycine betaine uptake and its inhibition by ectoine and 5-hydroxyectoine in cultures of the *E. coli* strain MKH17 (ProP⁺ ProU[−]) and BK32

(ProP[−] ProU⁺), cells were grown in MMA containing 0.4 M NaCl to an OD₅₇₈ of 0.3 at 37 °C. Uptake of [1-¹⁴C]glycine betaine by the cells was assayed at various time points in 2-ml aliquots at 37 °C with a final glycine betaine concentration of 100 µM. The inhibition of [1-¹⁴C]glycine betaine uptake by ectoine and 5-hydroxyectoine was measured by adding 10-, 50- and 100-fold excesses of the ectoine and 5-hydroxyectoine competitors in case of cells from strain MKH17 (ProP⁺ ProU[−]), and 100-, 500- and 1000-fold excesses of the competitors in case of the cells from strain BK32 (ProP[−] ProU⁺). Import of radiolabeled [1-¹⁴C]glycine betaine was followed for 5 min and the amount of [1-¹⁴C]glycine betaine taken up by the *E. coli* cells was determined by scintillation counting. The assay conditions followed a previously described protocol [99].

Alignment of EctD proteins and in silico modeling of the ectoine hydroxylase from *P. stutzeri*

Amino acid sequences of the studied EctD proteins were retrieved from the NCBI database (<http://www.ncbi.nlm.nih.gov/>) and aligned using Clustal Omega (<http://www.ebi.ac.uk/Tools/msa/clustalo/>) [100]. A structural model of the EctD protein from *P. stutzeri* A1501 was built via the SWISS model web server (<https://swissmodel.expasy.org/>) [101] and is based on the crystal structure of the ectoine hydroxylase from *S. alaskensis* (PDB ID: 4Q5O) [27]. This model had an overall Global Model Quality Estimation score of 0.76, a ranking where a score of 1 indicates perfect identity of the experimentally determined crystal structure of the reference protein and the derived in silico model of the target protein [101]. Structures of EctD proteins were visualized and analyzed using the PyMOL Molecular Graphics System suit (<https://www.pymol.org>) [102].

Additional files

Additional file 1: Table S1. Characteristics of the studied ectoine hydroxylases. The data shown were compiled from previous publications [21, 22].

Additional file 2: Fig. S1. Amino acid sequence alignment of selected EctD proteins. The EctD amino acid sequences from *V. salexigens*, *H. elongata*, *S. alaskensis*, *P. lautus*, *A. ehrlichii*, and *N. maritimus* were aligned using the ectoine hydroxylase from *P. stutzeri* A1501 as the query template. The residues of the ectoine hydroxylase coordinating the iron catalyst are highlighted in red, those that bind the co-substrate 2-oxoglutarate are marked in blue, and the residues involved in the binding of ectoine/5-hydroxyectoine are depicted in green [27]. The consensus sequence for ectoine hydroxylases [22, 27, 31] is highlighted in yellow.

Abbreviations

AHT: anhydrotetracycline-hydrochloride; LB: Luria–Bertani medium; MMA: minimal medium A; PCR: polymerase chain reaction; rpm: revolutions per minute; SDS: sodium-dodecylsulfate; Spc^r: spectinomycin resistance.

Authors' contributions

EB designed the study. NS conducted the exploratory phase of the project. LC performed all experiments. LC and EB wrote the manuscript. All authors read and approved the final manuscript.

Author details

¹ Laboratory for Microbiology, Department of Biology, Philipps-University at Marburg, 35043 Marburg, Germany. ² LOEWE Center for Synthetic Microbiology, Philipps-University Marburg at Marburg, 35043 Marburg, Germany.

³ Laboratory for Microbiology, Department of Biology, Philipps-University at Marburg, Karl-von-Frisch-Str. 8, 35043 Marburg, Germany.

Acknowledgements

We thank the bitop AG (Witten; Germany) for the kind gift of ectoine and 5-hydroxyectoine. We are grateful to Samantha Miller and Ian R. Booth (University of Aberdeen, United Kingdom) and Arne R. Strom (University of Trondheim, Norway) for kindly providing various *E. coli* strains. We greatly appreciate the expert help of Vickie Koogle in the language editing of our manuscript.

Competing interests

The authors declare that they have no competing interests.

Availability of data and material

The datasets on which the findings and conclusions of this article is based upon are all included in this manuscript and the Additional files associated with it. The plasmids used for the expression of the various ectoine hydroxylase genes (*ectD*) are all available upon request from E.B. (bremer@staff.uni-marburg.de) at the Department of Biology, Laboratory for Microbiology, Karl-von-Frisch Str. 8, Philipps-University Marburg, 35043 Marburg, Germany.

Funding

Financial support for this study was provided by the Deutsche Forschungsgemeinschaft (DFG) through the framework of the Collaborative Research Centre SFB 987, through the LOEWE Program of the State of Hessen (via the Centre for Synthetic Microbiology; Synmicro; Marburg), and a contribution by the Fonds der Chemischen Industrie. L.C. is a recipient of a Ph. D. fellowship from the International Max-Planck Research School for Environmental, Cellular and Molecular Microbiology (IMPRS-Mic; Marburg). The funders had no influence on the design, the execution of the experiments, or the outcome of this study.

Received: 4 June 2016 Accepted: 12 July 2016

Published online: 20 July 2016

References

- Kempf B, Bremer E. Uptake and synthesis of compatible solutes as microbial stress responses to high osmolality environments. *Arch Microbiol.* 1998;170:319–30.
- Bremer E, Krämer R. Coping with osmotic challenges: osmoregulation through accumulation and release of compatible solutes. In: Storz G, Hengge-Aronis R, editors. *Bacterial stress responses*. Washington DC: ASM Press; 2000. p. 79–97.
- Cayley S, Lewis BA, Record MT Jr. Origins of the osmoprotective properties of betaine and proline in *Escherichia coli* K-12. *J Bacteriol.* 1992;174:1586–95.
- Wood JM. Bacterial osmoregulation: a paradigm for the study of cellular homeostasis. *Annu Rev Microbiol.* 2011;65:215–38.
- Street TO, Bolen DW, Rose GD. A molecular mechanism for osmolyte-induced protein stability. *Proc Natl Acad Sci USA.* 2006;103:13997–4002.
- Brown AD. Microbial water stress. *Bacteriol Rev.* 1976;40:803–46.
- Cayley S, Record MT Jr. Roles of cytoplasmic osmolytes, water, and crowding in the response of *Escherichia coli* to osmotic stress: biophysical basis of osmoprotection by glycine betaine. *Biochemistry.* 2003;42:12596–609.
- Eiberweiser A, Nazet A, Kruchinin SE, Fedotova MV, Buchner R. Hydration and ion binding of the osmolyte ectoine. *J Phys Chem B.* 2015;119:15203–11.
- Hahn MB, Solomun T, Wellhausen R, Hermann S, Seitz H, Meyer S, Kunte HJ, Zeman J, Uhlig F, Smiatek J, Sturm H. Influence of the compatible solute ectoine on the local water structure: implications for the binding of the protein GSP to DNA. *J Phys Chem B.* 2015;119:15212–20.
- Diamant S, Eliahu N, Rosenthal D, Goloubinoff P. Chemical chaperones regulate molecular chaperones in vitro and in cells under combined salt and heat stresses. *J Biol Chem.* 2001;276:39586–91.
- Chattopadhyay MK, Kern R, Mistou MY, Dandekar AM, Uratsu SL, Richarme G. The chemical chaperone proline relieves the thermosensitivity of a *dnaK* deletion mutant at 42 degrees C. *J Bacteriol.* 2004;186:8149–52.
- Kurz M. Compatible solute influence on nucleic acids: many questions but few answers. *Saline Syst.* 2008;4:6.
- Lippert K, Galinski EA. Enzyme stabilization by ectoine-type compatible solutes: protection against heating, freezing and drying. *Appl Microbiol Biotechnol.* 1992;37:61–5.
- Street TO, Krukenberg KA, Rosgen J, Bolen DW, Agard DA. Osmolyte-induced conformational changes in the Hsp90 molecular chaperone. *Protein Sci.* 2010;19:57–65.
- Harishchandra RK, Sachan AK, Kerth A, Lentzen G, Neuhaus T, Galla HJ. Compatible solutes: ectoine and hydroxyectoine improve functional nanostructures in artificial lung surfactants. *Biochim Biophys Acta.* 2011;1808:2830–40.
- Harishchandra RK, Wulff S, Lentzen G, Neuhaus T, Galla HJ. The effect of compatible solute ectoines on the structural organization of lipid monolayer and bilayer membranes. *Biophys Chem.* 2010;150:37–46.
- Ignatova Z, Gierasch LM. Inhibition of protein aggregation in vitro and in vivo by a natural osmoprotectant. *Proc Natl Acad Sci USA.* 2006;103:13357–61.
- Bourot S, Sire O, Trautwetter A, Touze T, Wu LF, Blanco C, Bernard T. Glycine betaine-assisted protein folding in a *lysA* mutant of *Escherichia coli*. *J Biol Chem.* 2000;275:1050–6.
- Galinski EA, Pfeiffer HP, Trüper HG. 1,4,5,6-Tetrahydro-2-methyl-4-pyrimidinecarboxylic acid. A novel cyclic amino acid from halophilic phototrophic bacteria of the genus *Ectothiorhodospira*. *Eur J Biochem.* 1985;149:135–9.
- Inbar L, Lapidot A. The structure and biosynthesis of new tetrahydropyrimidine derivatives in actinomycin D producer *Streptomyces parvulus*. Use of ¹³C- and ¹⁵N-labeled L-glutamate and ¹³C and ¹⁵N NMR spectroscopy. *J Biol Chem.* 1988;263:16014–22.
- Widderich N, Czech L, Elling FJ, Könneke M, Stöveken N, Pittelkow M, Riclea R, Dickschat JS, Heider J, Bremer E. Strangers in the archaeal world: osmoresponsive biosynthesis of ectoine and hydroxyectoine by the marine thaumarchaeon *Nitrosopumilus maritimus*. *Environ Microbiol.* 2016;18:1227–48.
- Widderich N, Höppner A, Pittelkow M, Heider J, Smits SH, Bremer E. Biochemical properties of ectoine hydroxylases from extremophiles and their wider taxonomic distribution among microorganisms. *PLoS One.* 2014;9:e93809.
- Ono H, Sawada K, Khunajakr N, Tao T, Yamamoto M, Hiramoto M, Shinmyo A, Takano M, Murooka Y. Characterization of biosynthetic enzymes for ectoine as a compatible solute in a moderately halophilic eubacterium, *Halomonas elongata*. *J Bacteriol.* 1999;181:91–9.
- Stöveken N, Pittelkow M, Sinner T, Jensen RA, Heider J, Bremer E. A specialized aspartokinase enhances the biosynthesis of the osmoprotectants ectoine and hydroxyectoine in *Pseudomonas stutzeri* A1501. *J Bacteriol.* 2011;193:4456–68.
- Louis P, Galinski EA. Characterization of genes for the biosynthesis of the compatible solute ectoine from *Marinococcus halophilus* and osmoregulated expression in *Escherichia coli*. *Microbiology.* 1997;143:1141–9.
- Bursy J, Pierik AJ, Pica N, Bremer E. Osmotically induced synthesis of the compatible solute hydroxyectoine is mediated by an evolutionarily conserved ectoine hydroxylase. *J Biol Chem.* 2007;282:31147–55.
- Höppner A, Widderich N, Lenders M, Bremer E, Smits SHJ. Crystal structure of the ectoine hydroxylase, a snapshot of the active site. *J Biol Chem.* 2014;289:29570–83.
- García-Estépa R, Argandona M, Reina-Bueno M, Capote N, Iglesias-Guerra F, Nieto JJ, Vargas C. The *ectD* gene, which is involved in the synthesis of the compatible solute hydroxyectoine, is essential for thermoprotection of the halophilic bacterium *Chromohalobacter salexigens*. *J Bacteriol.* 2006;188:3774–84.

29. Widderich N, Bremer E, Smits SHJ. The ectoine hydroxylase: a nonheme-containing iron(II) and 2-oxoglutarate-dependent dioxygenase. *Encycl Inorg Bioinorg Chem*. Online 2016.
30. Widderich N, Pittelkow M, Höppner A, Mulnaes D, Buckel W, Gohlke H, Smits SH, Bremer E. Molecular dynamics simulations and structure-guided mutagenesis provide insight into the architecture of the catalytic core of the ectoine hydroxylase. *J Mol Biol*. 2014;426:586–600.
31. Reuter K, Pittelkow M, Bursy J, Heine A, Craan T, Bremer E. Synthesis of 5-hydroxyectoine from ectoine: crystal structure of the non-heme iron(II) and 2-oxoglutarate-dependent dioxygenase EctD. *PLoS One*. 2010;5:e10647.
32. Aik W, McDonough MA, Thalhammer A, Chowdhury R, Schofield CJ. Role of the jelly-roll fold in substrate binding by 2-oxoglutarate oxygenases. *Curr Opin Struct Biol*. 2012;22:691–700.
33. Hangasky JA, Taabazuing CY, Valliere MA, Knapp MJ. Imposing function down a (cupin)-barrel: secondary structure and metal stereochemistry in the alphaKG-dependent oxygenases. *Metallomics*. 2013;5:287–301.
34. Wojcik A, Radon M, Borowski T. Mechanism of O₂ activation by alpha-ketoglutarate dependent oxygenases revisited. A quantum chemical study. *J Phys Chem A*. 2016;120:1261–74.
35. Prabhu J, Schauwecker F, Grammel N, Keller U, Bernhard M. Functional expression of the ectoine hydroxylase gene (*thpD*) from *Streptomyces chrysomallus* in *Halomonas elongata*. *Appl Environ Microbiol*. 2004;70:3130–2.
36. Bursy J, Kuhlmann AU, Pittelkow M, Hartmann H, Jebbar M, Pierik AJ, Bremer E. Synthesis and uptake of the compatible solutes ectoine and 5-hydroxyectoine by *Streptomyces coelicolor* A3(2) in response to salt and heat stresses. *Appl Environ Microbiol*. 2008;74:7286–96.
37. Schiraldi C, Maresca C, Catapano A, Galinski EA, De Rosa M. High-yield cultivation of *Marinococcus* M52 for production and recovery of hydroxyectoine. *Res Microbiol*. 2006;157:693–9.
38. Weber H, Polen T, Heuveling J, Wendisch VF, Hengge R. Genome-wide analysis of the general stress response network in *Escherichia coli*: sigmaS-dependent genes, promoters, and sigma factor selectivity. *J Bacteriol*. 2005;187:1591–603.
39. Seip B, Galinski EA, Kurz M. Natural and engineered hydroxyectoine production based on the *Pseudomonas stutzeri* ectABCD-ask gene cluster. *Appl Environ Microbiol*. 2011;77:1368–74.
40. Manzanera M, Garcia de Castro A, Tondervik A, Rayner-Brandes M, Strom AR, Tunnacliffe A. Hydroxyectoine is superior to trehalose for anhydrobiotic engineering of *Pseudomonas putida* KT2440. *Appl Environ Microbiol*. 2002;68:4328–33.
41. Tanne C, Golovina EA, Hoekstra FA, Meffert A, Galinski EA. Glass-forming property of hydroxyectoine is the cause of its superior function as a desiccation protectant. *Front Microbiol*. 2014;5:150.
42. Manzanera M, Vilchez S, Tunnacliffe A. High survival and stability rates of *Escherichia coli* dried in hydroxyectoine. *FEMS Microbiol Lett*. 2004;233:347–52.
43. Schnoor M, Voss P, Cullen P, Boking T, Galla HJ, Galinski EA, Lorkowski S. Characterization of the synthetic compatible solute homoectoine as a potent PCR enhancer. *Biochem Biophys Res Commun*. 2004;322:867–72.
44. Mascellani N, Liu X, Rossi S, Marchesini J, Valentini D, Arcelli D, Taccioli C, Helmer Citterich M, Liu CG, Taccioli C, Evangelisti R, et al. Compatible solutes from hyperthermophiles improve the quality of DNA microarrays. *BMC Biotechnol*. 2007;7:82.
45. Pastor JM, Salvador M, Argandona M, Bernal V, Reina-Bueno M, Csonka LN, Iborra JL, Vargas C, Nieto JJ, Canovas M. Ectoines in cell stress protection: uses and biotechnological production. *Biotechnol Adv*. 2010;28:782–801.
46. Knapp S, Ladenstein R, Galinski EA. Extrinsic protein stabilization by the naturally occurring osmolytes beta-hydroxyectoine and betaine. *Extremophiles*. 1999;3:191–8.
47. Andersson MM, Breccia JD, Hatti-Kaul R. Stabilizing effect of chemical additives against oxidation of lactate dehydrogenase. *Biotechnol Appl Biochem*. 2000;32:145–53.
48. Kunte HJ, Lentzen G, Galinski E. Industrial production of the cell protectant ectoine: protection, mechanisms, processes, and products. *Curr Biotechnol*. 2014;3:10–25.
49. Graf R, Anzali S, Buenger J, Pfluecker F, Driller H. The multifunctional role of ectoine as a natural cell protectant. *Clin Dermatol*. 2008;26:326–33.
50. Schwibbert K, Marin-Sanguino A, Bagyan I, Heidrich G, Lentzen G, Seitz H, Rampp M, Schuster SC, Klenk HP, Pfeiffer F, et al. A blueprint of ectoine metabolism from the genome of the industrial producer *Halomonas elongata* DSM 2581^T. *Environ Microbiol*. 2011;13:1973–94.
51. Booth IR. Bacterial mechanosensitive channels: progress towards an understanding of their roles in cell physiology. *Curr Opin Microbiol*. 2014;18:16–22.
52. Booth IR, Blount P. The MscS and MscL families of mechanosensitive channels act as microbial emergency release valves. *J Bacteriol*. 2012;194:4802–9.
53. Sauer T, Galinski EA. Bacterial milking: a novel bioprocess for production of compatible solutes. *Biotechnol Bioeng*. 1998;57:306–13.
54. Rodriguez-Moya J, Argandona M, Iglesias-Guerra F, Nieto JJ, Vargas C. Temperature- and salinity-decoupled overproduction of hydroxyectoine by *Chromohalobacter salexigens*. *Appl Environ Microbiol*. 2013;79:1018–23.
55. He YZ, Gong J, Yu HY, Tao Y, Zhang S, Dong ZY. High production of ectoine from aspartate and glycerol by use of whole-cell biocatalysis in recombinant *Escherichia coli*. *Microb Cell Fact*. 2015;14:55.
56. Ning Y, Wu X, Zhang C, Xu Q, Chen N, Xie X. Pathway construction and metabolic engineering for fermentative production of ectoine in *Escherichia coli*. *Metab Eng*. 2016;36:10–8.
57. Schubert T, Maskow T, Benndorf D, Harms H, Breuer U. Continuous synthesis and excretion of the compatible solute ectoine by a transgenic, nonhalophilic bacterium. *Appl Environ Microbiol*. 2007;73:3343–7.
58. Eilert E, Kranz A, Hollenberg CP, Piontek M, Suckow M. Synthesis and release of the bacterial compatible solute 5-hydroxyectoine in *Hansenula polymorpha*. *J Biotechnol*. 2013;167:85–93.
59. Becker J, Schafer R, Kohlstedt M, Harder BJ, Borchert NS, Stoveken N, Bremer E, Wittmann C. Systems metabolic engineering of *Corynebacterium glutamicum* for production of the chemical chaperone ectoine. *Microb Cell Fact*. 2013;12:110.
60. Lucht JM, Bremer E. Adaptation of *Escherichia coli* to high osmolarity environments: osmoregulation of the high-affinity glycine betaine transport system ProU. *FEMS Microbiol Rev*. 1994;14:3–20.
61. Jebbar M, Talibart R, Gloux K, Bernard T, Blanco C. Osmoprotection of *Escherichia coli* by ectoine: uptake and accumulation characteristics. *J Bacteriol*. 1992;174:5027–35.
62. Culham DE, Shkel IA, Record MT, Wood JM. Contributions of coulombic and Hofmeister effects to the osmotic activation of *Escherichia coli* transporter ProP. *Biochemistry*. 2016;55:1301–13.
63. May G, Faatz E, Lucht JM, Haardt M, Bolliger M, Bremer E. Characterization of the osmoregulated *Escherichia coli* proU promoter and identification of ProV as a membrane-associated protein. *Mol Microbiol*. 1989;3:1521–31.
64. Gowrishankar J. Nucleotide-sequence of the osmoregulatory proU operon of *Escherichia coli*. *J Bacteriol*. 1989;171:1923–31.
65. Faatz E, Middendorf A, Bremer E. Cloned structural genes for the osmotically regulated binding-protein-dependent glycine betaine transport-system (ProU) of *Escherichia coli* K-12. *Mol Microbiol*. 1988;2:265–79.
66. Gjaever HM, Styrvoid OB, Kaasen I, Strom AR. Biochemical and genetic characterization of osmoregulatory trehalose synthesis in *Escherichia coli*. *J Bacteriol*. 1988;170:2841–9.
67. Yan Y, Yang J, Dou Y, Chen M, Ping S, Peng J, Lu W, Zhang W, Yao Z, Li H, et al. Nitrogen fixation island and rhizosphere competence traits in the genome of root-associated *Pseudomonas stutzeri* A1501. *Proc Natl Acad Sci USA*. 2008;105:7564–9.
68. Gul N, Poolman B. Functional reconstitution and osmoregulatory properties of the ProU ABC transporter from *Escherichia coli*. *Mol Membr Biol*. 2013;30:138–48.
69. Haardt M, Kempf B, Faatz E, Bremer E. The osmoprotectant proline betaine is a major substrate for the binding-protein-dependent transport system ProU of *Escherichia coli* K-12. *Mol Gen Genet*. 1995;246:783–6.
70. May G, Faatz E, Villarejo M, Bremer E. Binding protein dependent transport of glycine betaine and its osmotic regulation in *Escherichia coli* K12. *Mol Gen Genet*. 1986;205:225–33.
71. MacMillan SV, Alexander DA, Culham DE, Kunte HJ, Marshall EV, Rochon D, Wood JM. The ion coupling and organic substrate specificities of osmoregulatory transporter ProP in *Escherichia coli*. *Biochim Biophys Acta*. 1999;1420:30–44.

72. Levina N, Totemeyer S, Stokes NR, Louis P, Jones MA, Booth IR. Protection of *Escherichia coli* cells against extreme turgor by activation of MscS and MscL mechanosensitive channels: identification of genes required for MscS activity. *EMBO J*. 1999;18:1730–7.
73. Hoffmann T, Boiangiu C, Moses S, Bremer E. Responses of *Bacillus subtilis* to hypotonic challenges: physiological contributions of mechanosensitive channels to cellular survival. *Appl Environ Microbiol*. 2008;74:2454–60.
74. Naismith JH, Booth IR. Bacterial mechanosensitive channels-MscS: evolution's solution to creating sensitivity in function. *Annu Rev Biophys*. 2012;41:157–77.
75. Haswell ES, Phillips R, Rees DC. Mechanosensitive channels: what can they do and how do they do it? *Structure*. 2011;19:1356–69.
76. Wang W, Black SS, Edwards MD, Miller S, Morrison EL, Bartlett W, Dong C, Naismith JH, Booth IR. The structure of an open form of an *E. coli* mechanosensitive channel at 3.45 Å resolution. *Science*. 2008;321:1179–83.
77. Cruickshank CC, Minchin RF, Le Dain AC, Martinac B. Estimation of the pore size of the large-conductance mechanosensitive ion channel of *Escherichia coli*. *Biophys J*. 1997;73:1925–31.
78. Edwards MD, Black S, Rasmussen T, Rasmussen A, Stokes NR, Stephen TL, Miller S, Booth IR. Characterization of three novel mechanosensitive channel activities in *Escherichia coli*. *Channels (Austin)*. 2012;6:272–81.
79. Epstein W, Kim BS. Potassium transport loci in *Escherichia coli* K-12. *J Bacteriol*. 1971;108:639–44.
80. Carvalho CC. Whole cell biocatalysts: essential workers from Nature to the industry. *Microb Biotechnol*. 2016. doi:10.1111/1751-7915.12363 (in press).
81. Inbar L, Frolow F, Lapidot A. The conformation of new tetrahydropyrimidine derivatives in solution and in the crystal. *Eur J Biochem*. 1993;214:897–906.
82. Eggeling L, Sahm H. New ubiquitous translocators: amino acid export by *Corynebacterium glutamicum* and *Escherichia coli*. *Arch Microbiol*. 2003;180:155–60.
83. Hoffmann T, von Blohn C, Stanek A, Moses S, Barzantny S, Bremer E. Synthesis, release, and recapture of the compatible solute proline by osmotically stressed *Bacillus subtilis* cells. *Appl Environ Microbiol*. 2012;78:5753–62.
84. Bay DC, Turner RJ. Small multidrug resistance protein EmrE reduces host pH and osmotic tolerance to metabolic quaternary cation osmoprotectants. *J Bacteriol*. 2012;194:5941–8.
85. Glaesker E, Konings WN, Poolman B. Glycine betaine fluxes in *Lactobacillus plantarum* during osmotic stress and hyper- and hypo-osmotic shock. *J Biol Chem*. 1996;271:10060–5.
86. Grammann K, Volke A, Kunte HJ. New type of osmoregulated solute transporter identified in halophilic members of the bacteria domain: TRAP transporter TeaABC mediates uptake of ectoine and hydroxyectoine in *Halomonas elongata* DSM 2581^T. *J Bacteriol*. 2002;184:3078–85.
87. Mikkat S, Hagemann M. Molecular analysis of the *ggdBCD* gene cluster of *Synechocystis* sp. strain PCC6803 encoding subunits of an ABC transporter for osmoprotective compounds. *Arch Microbiol*. 2000;174:273–82.
88. Nyyssölä A, Leisola M. *Actinopolyspora halophila* has two separate pathways for betaine synthesis. *Arch Microbiol*. 2001;176:294–300.
89. Lamark T, Styrvoid OB, Strom AR. Efflux of choline and glycine betaine from osmoregulating cells of *Escherichia coli*. *FEMS Microbiol Lett*. 1992;75:149–54.
90. Schiefner A, Breed J, Bösser L, Kneip S, Gade J, Holtmann G, Diederichs K, Welte W, Bremer E. Cation- π interactions as determinants for binding of the compatible solutes glycine betaine and proline betaine by the periplasmic ligand-binding protein ProX from *Escherichia coli*. *J Biol Chem*. 2004;279:5588–96.
91. Hanekop N, Hoing M, Sohn-Bosser L, Jebbar M, Schmitt L, Bremer E. Crystal structure of the ligand-binding protein EhuB from *Sinorhizobium meliloti* reveals substrate recognition of the compatible solutes ectoine and hydroxyectoine. *J Mol Biol*. 2007;374:1237–50.
92. Lecher J, Pittelkow M, Zobel S, Bursy J, Bonig T, Smits SH, Schmitt L, Bremer E. The crystal structure of UehA in complex with ectoine—a comparison with other TRAP-T binding proteins. *J Mol Biol*. 2009;389:58–73.
93. Kuhlmann SI, Terwisscha van Scheltinga AC, Bienert R, Kunte HJ, Ziegler C. 1.55 Å structure of the ectoine binding protein TeaA of the osmoregulated TRAP-transporter TeaABC from *Halomonas elongata*. *Biochemistry*. 2008;47:9475–85.
94. Galinski EA, Stein M, Ures A, Schwarz T. Stereospecific hydroxylation. United States Patent (US 2011/0190498 A1 US 2011/0190498 A). 2011.
95. Casadaban MJ. Transposition and fusion of *lac* genes to selected promoters in *Escherichia coli* using bacteriophage lambda and bacteriophage-Mu. *J Mol Biol*. 1976;104:541–55.
96. Miller JH. Experiments in molecular genetics. Cold Spring Harbor: Cold Spring Harbor Laboratory; 1972.
97. Laemmli UK. Cleavage of structural proteins during assembly of head of bacteriophage-T4. *Nature*. 1970;227:680–5.
98. Kuhlmann AU, Bremer E. Osmotically regulated synthesis of the compatible solute ectoine in *Bacillus pasteurii* and related *Bacillus* spp. *Appl Environ Microbiol*. 2002;68:772–83.
99. Holtmann G, Bremer E. Thermoprotection of *Bacillus subtilis* by exogenously provided glycine betaine and structurally related compatible solutes: involvement of Opu transporters. *J Bacteriol*. 2004;186:1683–93.
100. Sievers F, Wilm A, Dineen D, Gibson TJ, Karplus K, Li W, Lopez R, McWilliam H, Remmert M, Soding J, et al. Fast, scalable generation of high-quality protein multiple sequence alignments using Clustal Omega. *Mol Syst Biol*. 2011;7:539.
101. Biasini M, Bienert S, Waterhouse A, Arnold K, Studer G, Schmidt T, Kiefer F, Cassarino TG, Bertoni M, Bordoli L, Schwede T. SWISS-MODEL: modelling protein tertiary and quaternary structure using evolutionary information. *Nucleic Acids Res*. 2014;42:W252–8.
102. Delano WL. The PyMol molecular graphics system. San Carlos: Delano Scientific; 2002.

Submit your next manuscript to BioMed Central and we will help you at every step:

- We accept pre-submission inquiries
- Our selector tool helps you to find the most relevant journal
- We provide round the clock customer support
- Convenient online submission
- Thorough peer review
- Inclusion in PubMed and all major indexing services
- Maximum visibility for your research

Submit your manuscript at
www.biomedcentral.com/submit



Tinkering with Osmotically Controlled Transcription Allows Enhanced Production and Excretion of Ectoine and Hydroxyectoine from a Microbial Cell Factory

Laura Czech,^a Sebastian Poehl,^a Philipp Hub,^a Nadine Stöveken,^{a,b} Erhard Bremer^{a,b}

^aDepartment of Biology, Laboratory for Microbiology, Philipps University Marburg, Marburg, Germany

^bLOEWE Center for Synthetic Microbiology, Philipps University Marburg, Marburg, Germany

5.2.3. Tinkering with osmotically controlled transcription allows enhanced production and excretion of ectoine and hydroxyectoine from a microbial cell factory

Czech L, Poehl S, Hub P, Stöveken N, Bremer E. Tinkering with osmotically controlled transcription allows enhanced production and excretion of ectoine and hydroxyectoine from a microbial cell factory. *Appl Environ Microbiol* 2018;84:e01772-17. doi: 10.1128/AEM.01772-17.

In the following, the publication with the title "Tinkering with osmotically controlled transcription allows enhanced production and excretion of ectoine and hydroxyectoine from a microbial cell factory" is attached. During this study, Prof. E. Bremer and I designed the experiments and discussed the data. I constructed all strains included in this study, designed the genetic constructs and helped during HPLC analysis. I supervised two bachelor students, P. Hub and B. Poehl, who helped during the construction of plasmids and the insertion of site-directed mutations, performed experiments for the transcriptional analysis, and heterologous expression/production experiments for this publication. N. Stöveken constructed the reporter gene plasmid harboring the *ectA-ectB-lacZ* fusion and its truncated versions. I analyzed all data and prepared the figures for the manuscript. Prof. E. Bremer and I wrote the manuscript.

Supplementary Data can be found at:

<https://aem.asm.org/content/aem/suppl/2017/12/19/AEM.01772-17.DCSupplemental/zam002188252s1.pdf>

5.2.3.1. Original publication

Applied and Environmental
Microbiology®

GENETICS AND MOLECULAR BIOLOGY



Tinkering with Osmotically Controlled Transcription Allows Enhanced Production and Excretion of Ectoine and Hydroxyectoine from a Microbial Cell Factory

Laura Czech,^a Sebastian Poehl,^a Philipp Hub,^a Nadine Stöveken,^{a,b} Erhard Bremer^{a,b}^aDepartment of Biology, Laboratory for Microbiology, Philipps University Marburg, Marburg, Germany^bLOEWE Center for Synthetic Microbiology, Philipps University Marburg, Marburg, Germany

ABSTRACT Ectoine and hydroxyectoine are widely synthesized by members of the *Bacteria* and a few members of the *Archaea* as potent osmoprotectants. We have studied the salient features of the osmoprotectant-responsive promoter directing the transcription of the ectoine/hydroxyectoine biosynthetic gene cluster from the plant-root-associated bacterium *Pseudomonas stutzeri* by transferring it into *Escherichia coli*, an enterobacterium that does not produce ectoines naturally. Using *ect-lacZ* reporter fusions, we found that the heterologous *ect* promoter reacted with exquisite sensitivity in its transcriptional profile to graded increases in sustained high salinity, responded to a true osmotic signal, and required the buildup of an osmotically effective gradient across the cytoplasmic membrane for its induction. The involvement of the -10 , -35 , and spacer regions of the sigma-70-type *ect* promoter in setting promoter strength and response to osmotic stress was assessed through site-directed mutagenesis. Moderate changes in the *ect* promoter sequence that increase its resemblance to housekeeping sigma-70-type promoters of *E. coli* afforded substantially enhanced expression, both in the absence and in the presence of osmotic stress. Building on this set of *ect* promoter mutants, we engineered an *E. coli* chassis strain for the heterologous production of ectoines. This synthetic cell factory lacks the genes for the osmoprotectant-responsive synthesis of trehalose and the compatible solute importers ProP and ProU, and it continuously excretes ectoines into the growth medium. By combining appropriate host strains and different plasmid variants, excretion of ectoine, hydroxyectoine, or a mixture of both compounds was achieved under mild osmotic stress conditions.

IMPORTANCE Ectoines are compatible solutes, organic osmolytes that are used by microorganisms to fend off the negative consequences of high environmental osmolarity on cellular physiology. An understanding of the salient features of osmoprotectant-responsive promoters directing the expression of the ectoine/hydroxyectoine biosynthetic gene clusters is lacking. We exploited the *ect* promoter from an ectoine/hydroxyectoine-producing soil bacterium for such a study by transferring it into a surrogate bacterial host. Despite the fact that *E. coli* does not synthesize ectoines naturally, the *ect* promoter retained its exquisitely sensitive osmotic control, indicating that osmoregulation of *ect* transcription is an inherent feature of the promoter and its flanking sequences. These sequences were narrowed to a 116-bp DNA fragment. Ectoines have interesting commercial applications. Building on data from a site-directed mutagenesis study of the *ect* promoter, we designed a synthetic cell factory that secretes ectoine, hydroxyectoine, or a mixture of both compounds into the growth medium.

KEYWORDS osmoregulation, promoters, compatible solutes, chemical chaperones, excretion

Received 11 August 2017 Accepted 28 October 2017

Accepted manuscript posted online 3 November 2017

Citation Czech L, Poehl S, Hub P, Stöveken N, Bremer E. 2018. Tinkering with osmotically controlled transcription allows enhanced production and excretion of ectoine and hydroxyectoine from a microbial cell factory. *Appl Environ Microbiol* 84:e01772-17. <https://doi.org/10.1128/AEM.01772-17>.

Editor Maia Kivisaar, University of Tartu

Copyright © 2018 American Society for Microbiology. All Rights Reserved.

Address correspondence to Erhard Bremer, bremer@staff.uni-marburg.de.

Ectoine [(5S)-2-methyl-1,4,5,6-tetrahydropyrimidine-4-carboxylic acid] and its derivative 5-hydroxyectoine [(4S,5S)-5-hydroxy-2-methyl-1,4,5,6-tetrahydropyrimidine-4-carboxylic acid] (1) are representatives of a special class of organic osmolytes, the compatible solutes (2). These compounds are widely synthesized as osmoprotectants by members of the *Bacteria* (3) and some members of the *Archaea* (4) and might also be produced by a few obligatory halophilic protists (5). Ectoines are well suited for this physiologically demanding task, since their high water solubility and physicochemical attributes make them compliant with cellular biochemistry and the functionality of macromolecular structures (6–11). The function-preserving characteristics of ectoines allow their high-level cellular accumulation, a process which in turn raises the osmotic potential of the cytoplasm and thereby allows the cell to counteract the high-osmolarity-instigated efflux of water to preserve vital turgor (12, 13). At the same time, the composition and solvent properties of the cytoplasm are optimized for biochemical reactions (13) so that growth of microorganisms can occur under osmotically unfavorable circumstances (2, 14, 15).

The amassing of ectoines by osmotically stressed microbial cells can be accomplished either through uptake from environmental sources via osmotically induced transporters or through *de novo* synthesis. Synthesis of ectoine proceeds from L-aspartate- β -semialdehyde (Fig. 1A), a central hub in bacterial amino acid and cell wall synthesis (16). A considerable number of microbial ectoine producers possess a specialized aspartokinase (Ask_Ect) (Fig. 1A) to ensure a sufficient supply of this precursor when the cellular demand for ectoine synthesis is high (17–19). The EctB protein (L-2,4-diaminobutyrate transaminase) converts L-aspartate- β -semialdehyde into L-2,4-diaminobutyrate, which is then transformed by EctA (L-2,4-diaminobutyrate acetyltransferase) into *N*- γ -acetyl-L-2,4-diaminobutyric acid, a metabolite that is cyclized by ectoine synthase (EctC) to form ectoine (Fig. 1A) (20). In a substantial subgroup of ectoine producers (3), ectoine can be further transformed into 5-hydroxyectoine through a position- and stereospecific enzyme reaction catalyzed by the ectoine hydroxylase (EctD) (21, 22) (Fig. 1A).

The ectoine biosynthetic genes are typically organized as an operon (*ectABC*), which may also comprise the ectoine hydroxylase gene (*ectD*) and the gene (*ask_ect*) for the specialized Ask_Ect aspartokinase (1, 4, 17, 23). Increases in the environmental osmolarity/salinity usually trigger enhanced levels of *ect* expression (21, 23–26). These genes are transcribed in some microorganisms from a single osmotically stimulated promoter (21, 24); however, a more complex arrangement of promoters driving *ect* expression also exists (26–28). The repressor CosR controls *ectABC* transcription in the human pathogen *Vibrio cholerae*, but this MarR-type regulator regulates not only compatible solute synthesis and uptake but also motility and biofilm formation (29). Likewise, *ectABCD* expression in the soil bacterium *Streptomyces coelicolor* is negatively controlled by a regulatory protein (GlnR) which serves as a globally acting transcription factor for nitrogen metabolism in many actinomycetes (30, 31). Since the CosR and GlnR repressors also control cellular processes other than ectoine/hydroxyectoine synthesis, their involvement in the production of ectoines seems to be restricted to the mentioned species and their closest relatives. In contrast, in a substantial subgroup of ectoine/hydroxyectoine producers, a regulatory gene (*ectR*) has been found in close physical association with the corresponding biosynthetic *ect* gene clusters (in 107 out of 440 inspected genome sequences) (3). EctR is a member of the MarR family of transcriptional regulators and was initially discovered in *Methylomicrobium alcaliphilum*, where its operator sequence overlaps with one of the two promoters driving *ectABC-ask_ect* transcription (28). Disruption of the *ectR* gene derepresses *ect* expression but this does not abolish osmotic control of this biosynthetic gene cluster (28); unfortunately, the environmental or cellular cue(s) to which the EctR repressor responds is not known. Despite these interesting findings, osmoregulation of *ect* gene expression is in general not well understood, in particular since many gene clusters for the synthesis of ectoines are not associated with a regulatory gene (3).

In addition to their function as osmoprotectants (1, 32), ectoines also afford

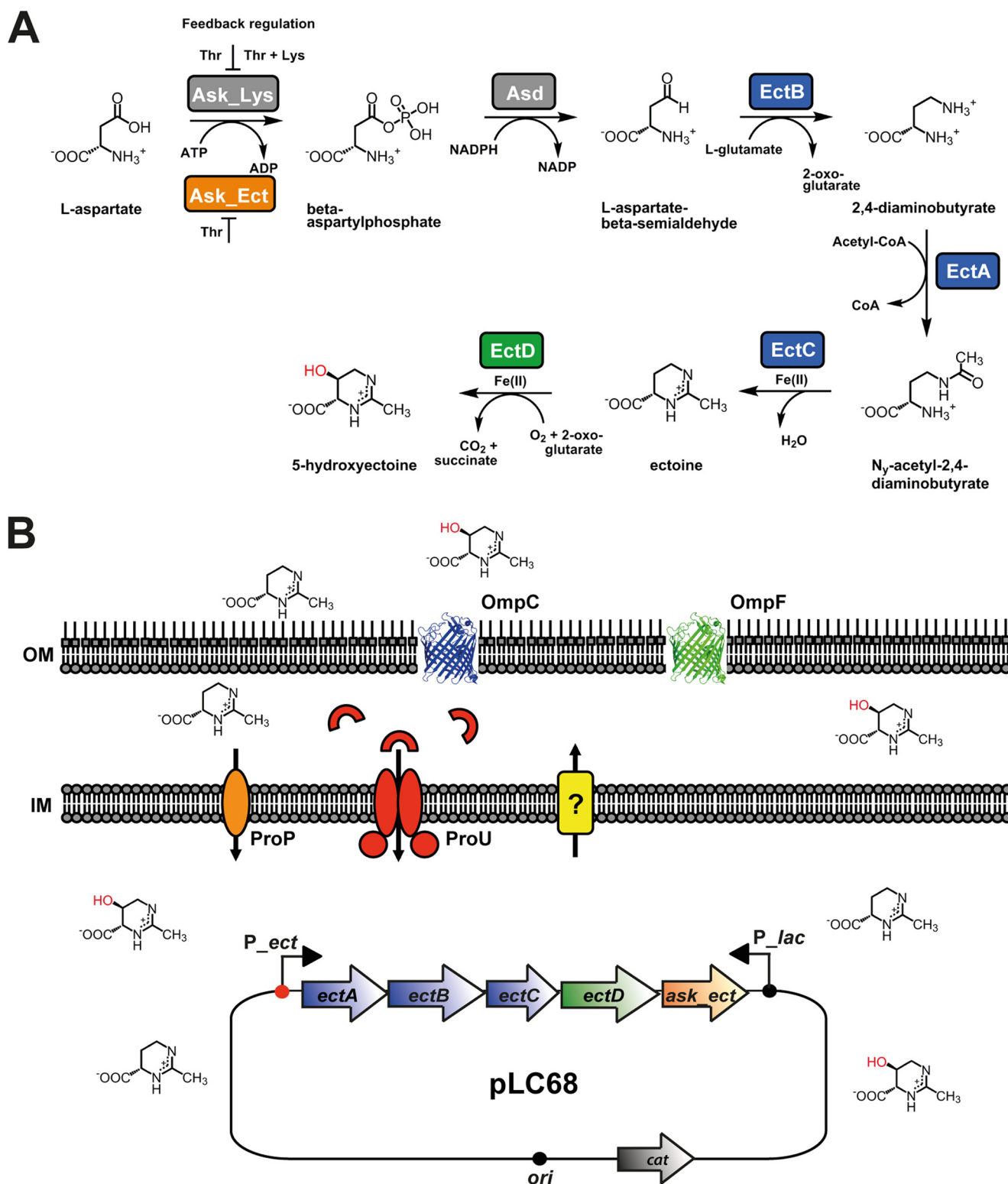


FIG 1 Pathway for the synthesis of ectoine and hydroxyectoine and design of a recombinant cell factory for the production of ectoines. (A) Biosynthetic route for ectoine and its derivative 5-hydroxyectoine from L-aspartate. The relevant data for the enzymes and metabolites involved in this process were compiled from the literature (17, 20, 21, 86). (B) The *E. coli* cell factory carries a low-copy-number plasmid harboring the *ectABCD-ask_ect* gene cluster from *P. stutzeri* A1501 (67) under the control of its authentic and osmotically inducible promoter (P_{ect}) (17). This plasmid (pLC68) is a derivative of the cloning vector pHSG575 (89), which carries a *lac* promoter (P_{lac}) that is constitutively expressed in all the *E. coli* strains used in this study, as they carry a deletion of the entire *lac* operon, including that of the *lacI* regulatory gene. ProP and ProU are osmotically inducible transport systems for osmoprotectants; ProP is a member of the MFS family (88), and ProU is a binding-protein-dependent ABC transporter (80). The presumed ectoine/hydroxyectoine efflux system is shown as a yellow box; its molecular identity is unknown. The trimeric OmpC and OmpF proteins (represented here as monomers) function as general porins that are inserted into the *E. coli* outer membrane. IM, inner membrane; OM, outer membrane.

cytoprotection against extremes in high and low growth temperatures in some bacteria (31, 33–35). The physicochemical characteristics of ectoines (36, 37) bestow them, both *in vivo* and *in vitro*, with excellent function-preserving attributes, e.g., enhancement of protein folding and stability, preservation of membrane structures and membrane proteins, and protection of the integrity of isolated molecules and even of entire cells (38–47). Although the difference between ectoine and 5-hydroxyectoine seems minor from a chemical point of view, hydroxylation of ectoine endows the newly formed 5-hydroxyectoine with substantially enhanced, or additional, stress-protective and function-preserving attributes (e.g., in particular against heat and desiccation stress) (31, 34, 39, 42, 43, 45).

The excellent stress-protective, function-preserving, and anti-inflammatory properties of ectoines attract considerable interest in the biotechnological use of these compounds as protein stabilizers, as well as for skin care and cosmetics, and potential medical applications are also actively pursued (1, 32, 48, 49). The financially rewarding practical applications of ectoines drove the development of an industrial-scale production process which harnesses the highly salt-tolerant ectoine/hydroxyectoine producer *Halomonas elongata* (26) as a natural microbial cell factory (1, 32, 48). In this process, high-level synthesis of ectoines is triggered through the growth of *H. elongata* in high-salinity media. The newly produced ectoines (along with other low-molecular-weight compounds) are then released from the producer cells through the transient opening of mechanosensitive channels (50), an activity that is triggered by a severe osmotic downshock of the cells (1, 32). Since these mechanosensitive safety valves close again once osmotic equilibrium has been achieved (50), the osmotically downshocked *H. elongata* cells survive this harsh treatment. Hence, the already formed biomass can be recycled into the fermentation vessel, while the released ectoines are recovered and purified via downstream processes (1, 32). This bacterial milking procedure (51) was subsequently modified by using a genetically engineered *H. elongata* strain lacking ectoine catabolic genes (26, 52) and in which the osmotically controlled ectoine/hydroxyectoine-specific tripartite ATP-independent periplasmic (TRAP) transport system TeaABC (53) was deleted. Overall, this strain excretes considerable amounts of ectoines into the growth medium and allows their recovery in a highly purified form on the scale of several tons per annum (32).

The very high salinity used to cultivate the ectoine/hydroxyectoine producer organism *H. elongata* in the established industrial production process is harsh on the fermentation and downstream processing equipment (32). Therefore, there has been considerable interest in developing alternative fermentation processes (54, 55), in exploiting additional natural ectoine/hydroxyectoine producers (56, 57) (including a bacterium that secretes them naturally into the medium [58]), and in engineering natural and synthetic microbial production hosts for enhanced recovery of these high-value compounds (1, 32). With respect to the latter approaches, ectoine/hydroxyectoine biosynthetic genes have been cloned into plasmids under the transcriptional control of either natural *ect* or synthetic promoters and transferred to *Escherichia coli* or *Corynebacterium glutamicum* host strains (59–62) or integrated into the chromosomes of biotechnological workhorses such as *C. glutamicum* (63) or the methylotrophic yeast *Hansenula polymorpha* (64). In some cases, advanced pathway engineering approaches were also used to enhance the synthetic production of ectoines in homologous and heterologous hosts (62, 63, 65, 66).

Since most of the ectoine/hydroxyectoine biosynthetic gene clusters are not associated with a dedicated regulatory gene (3), their osmostress-responsive induction might be an intrinsic property of the *ect* promoter elements and their immediate flanking regions. However, the salient features of *ect* type promoters have so far not been genetically analyzed at any level of detail. We focused here on the promoter driving the osmotically induced transcription of the *Pseudomonas stutzeri* A1501 *ectABCD-ask_ect* operon (17) through reporter gene studies and site-directed mutagenesis. Building on the knowledge gained through engineering of the *P. stutzeri* A1501 *ect* promoter, we designed ectoine and/or hydroxyectoine synthetic *E. coli* cell factories

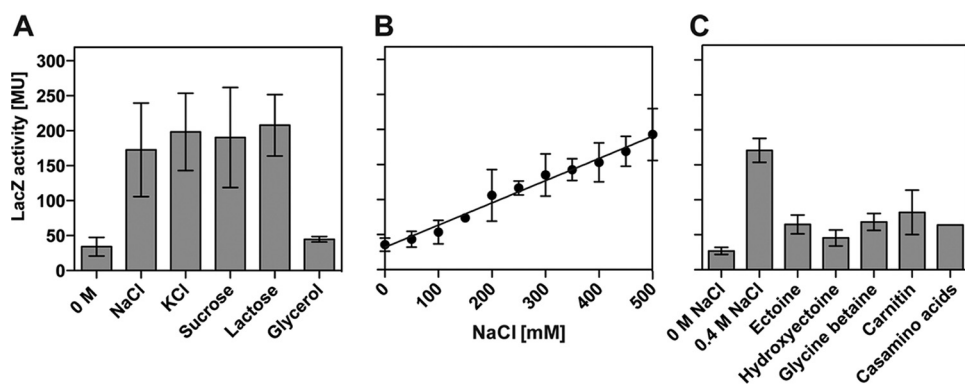


FIG 2 Transcriptional activity of the *ect* promoter in response to increases in osmolarity and presence of compatible solutes. (A) *E. coli* strain MC4100 carrying the *ectB-lacZ* gene fusion plasmid pGJK4 was grown in MMA in the absence or presence of various compounds to increase the osmolarity of the medium. The solute concentration was chosen such that all the media possessed an equivalent osmolarity [$1.000 \text{ mosmol (kg H}_2\text{O)}^{-1}$]. (B) Cultures of strain MC4100(pGJK4) were grown in MMA with increasing NaCl concentrations until they reached approximately the same optical density (OD_{578} of about 1.8), whereupon they were harvested and processed for β -galactosidase reporter enzyme activity assays. (C) Cultures of strain MC4100(pGJK4) were grown in MMA with 0.4 M NaCl in the absence or presence of 1 mM concentrations the indicated compatible solutes or Casamino Acids. When the cultures reached an OD_{578} of about 1.8, the cells were harvested and assayed for β -galactosidase reporter enzyme activity. The data shown were derived from four independently grown cultures, and each enzyme assay was performed at least twice. β -Galactosidase enzyme activity is given in Miller units (MU) (108).

that allow the production and efficient secretion of these compounds into the growth medium.

RESULTS

Osmotic control of the *P. stutzeri* A1501 *ect* promoter in the non-ectoine-producing *E. coli* surrogate host. The activity of the promoter(s) driving transcription of the *ectABCD-ask_ect* gene cluster from the plant-root-associated bacterium *P. stutzeri* A1501 (67) is induced by high salinity of the growth medium (17). However, the molecular identity of this promoter and the details of its transcriptional regulation are not known. We wondered if one could transfer the osmotically inducible pattern of *P. stutzeri* A1501 *ect* gene transcription into *E. coli*, a surrogate host that can import but cannot synthesize ectoines (68). To this end, we constructed an *ect-lacZ* reporter plasmid (pGJK4) that carries 264 bp of genomic DNA upstream of the start codon of *ectA*, the entire *ectA* gene, and a fusion junction to the promoterless *lacZ* gene within codon 87 of *ectB*. We observed a 6.3-fold increase in *lacZ* reporter activity when the MC4100(pGJK4) *E. coli* strain was grown in a chemically defined minimal medium (MMA) in the presence of 0.4 M NaCl in comparison with cells that were grown in MMA (Fig. 2A).

We then asked whether the observed increase in *ect* promoter activity occurred only in response to an increase in the external NaCl concentration or whether its transcriptional activity is responsive to a true osmotic cue. To test this, we grew the MC4100(pGJK4) reporter strain in the presence of both ionic and nonionic osmolytes and with glycerol, a membrane-permeative alcohol that cannot establish an osmotically effective gradient across the cytoplasmic membrane of *E. coli* when provided at high external concentrations. For these experiments, we added the solutes to the growth media in concentrations so that they had about the same osmolarity [$1.000 \text{ mosmol (kg H}_2\text{O)}^{-1}$]. Both ionic (NaCl and KCl) and nonionic (sucrose and lactose) solutes triggered enhanced transcription of the *ect* promoter and activated it to approximately the same degree (Fig. 2A). In contrast, glycerol was unable to stimulate *ect* promoter activity (Fig. 2A).

After we had established that the activity of the *ect* promoter was under true osmotic control, we asked if this was an all-or-none transcriptional response. We therefore monitored *ect-lacZ* promoter activity in cultures of strain MC4100(pGJK4) that were grown in MMA with steadily and sustained increased NaCl concentrations over a wide range of salinities. This experiment revealed an exquisitely sensitive response of

the *ect* promoter to the degree of the osmotic stress imposed onto the *E. coli* cells, since its transcriptional activity increased linearly concomitant with the increase in the NaCl content of the growth medium (Fig. 2B). In this experiment, we tested a substantial concentration range of salinities (from 0 M NaCl to 0.5 M NaCl); salinities higher than 0.5 M NaCl severely impair growth of the *E. coli* cells and were therefore not tested to avoid indirect effects on the transcriptional profile of the *ect* promoter.

Compatible solutes not only are effective osmoprotectants (2, 14, 15) but also frequently downregulate osmotically induced promoters since their accumulation alleviates the degree of osmotic stress perceived by the bacterial cell (18, 69, 70). To test whether the *ect* promoter also responded in its transcriptional activity to an external supply of compatible solutes, we propagated the MC4100(pGJK4) reporter strain at increased salinity (MMA with 0.4 M NaCl) in the absence or the presence (1 mM) of the osmoprotectants ectoine, hydroxyectoine, glycine betaine, and carnitine. Each of these compounds downregulated the activity of the *ect* promoter to approximately the same degree (Fig. 2C). The components of rich media contain compatible solutes or their precursors; e.g., glycine betaine is present in yeast extract, carnitine is present in meat extracts, and proline or proline-containing peptides are present in Casamino Acids. Indeed, the addition of 1 mM Casamino Acids to high-salinity-grown cultures of the MC4100(pGJK4) reporter strain significantly reduced the activity of the *ect-lacZ* reporter fusion (Fig. 2C).

RpoS, H-NS, OmpR, and cAMP/CRP do not participate in osmoregulation of *ect* expression in *E. coli*. A number of regulatory genes have previously been implicated in controlling the transcription of osmoprotectant-responsive genes in *E. coli*. Many osmotically regulated promoters in *E. coli* can be driven by forms of RNA polymerase complexed with the alternative sigma factor RpoS, the master regulator of the general stress response system (71, 72). Likewise, the nucleoid-associated H-NS protein not only affects gene expression on a global scale but also targets various osmotically controlled promoter regions, e.g., that of the *proU* operon encoding a glycine betaine/proline betaine ABC-type transporter (73). The EnvZ/OmpR two-component regulatory system is a key determinant for the reciprocal osmoregulation of the *ompC* and *ompF* porin genes (74). Furthermore, the cAMP/CRP complex has been implicated in osmoregulation (75, 76), e.g., by controlling the induction of the *proP*-P1 promoter (77). Although this promoter (5'-TTGATC-X¹⁷-TAGGGT-3') for the osmolyte importer ProP bears a striking resemblance in its -10 region to the *ect* promoter of *P. stutzeri* A1501 (Fig. 3) (see below), it is transcriptionally active only upon a sudden osmotic upshock (77), while the *ect* promoter operates continuously under sustained high-osmolarity growth conditions (Fig. 2B). We tested an isogenic set of gene disruption mutations for potential effects of the RpoS, H-NS, EnvZ/OmpR, and cAMP/CRP regulatory proteins/complexes on *ect-lacZ* expression under both osmotically noninduced and osmotically induced growth conditions. None of these regulatory proteins had any effect on the *ect* promoter activity (Table 1).

Pinpointing the osmotically regulated *ect* promoter through deletion analysis.

The *ect-lacZ* reporter plasmid (pGJK4) carries 264 bp of genomic DNA upstream of the start codon of *ectA*, a region that will contain the osmotic-stress-responsive *ect* promoter. To delineate its approximate position, we successively shortened the 5' region of this genomic segment while preserving the original *ectB-lacZ* fusion junction in codon 88 of *ectB* (Fig. 3A). The DNA sequences of the various deletion endpoints are summarized in Fig. S1 in the supplemental material and are graphically represented in Fig. 3A. The removal of 47 bp from the 5' end of the original genomic segment preceding the *ectA* start codon (plasmid pGJK4) had only very modest effects on both the noninduced and salt-stress-induced levels of the *lacZ* reporter fusion (up to deletion endpoint K6) (Fig. 3A). By shortening the K6 deletion junction (plasmid pNST29) further by 40 bp (deletion K7; plasmid pNST40), we observed a drastic fall in promoter activity. However, the remaining reporter enzyme activity was still osmotically inducible (Fig. 3A). An additional deletion of 70 bp then abolished the transcriptional activity of the *ect-lacZ* reporter fusion (deletion K8; plasmid pNST41) (Fig. 3A). Since the 5' end of the

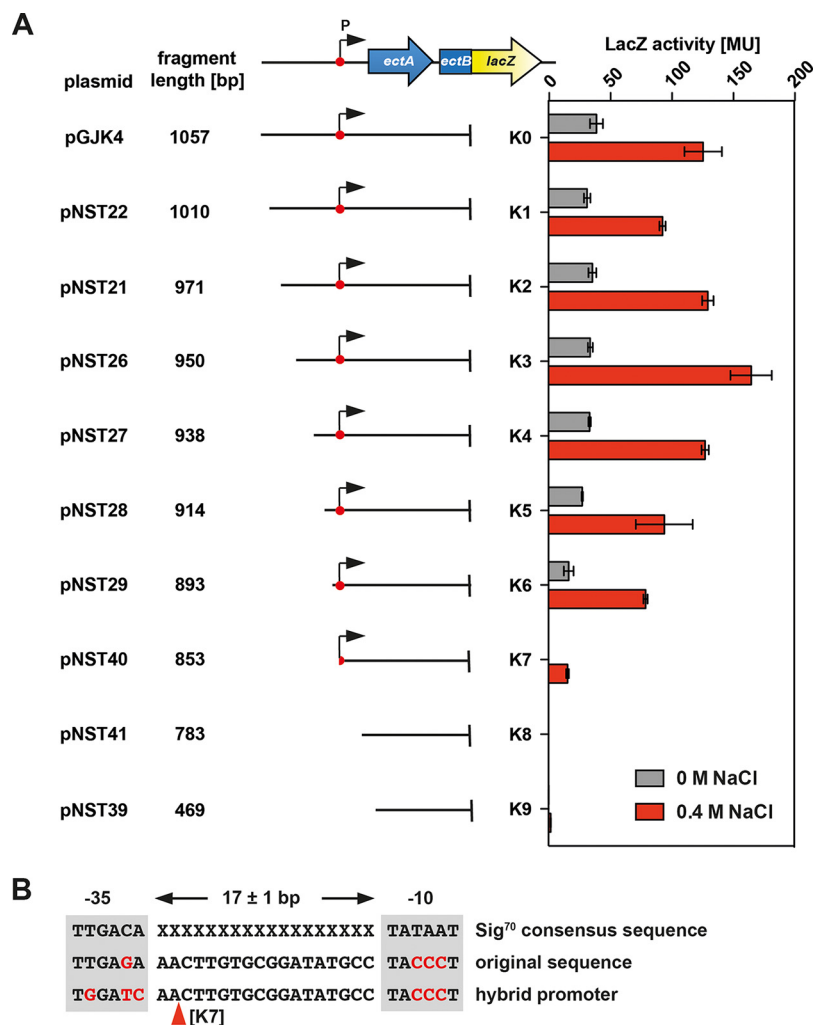


FIG 3 Deletion analysis of the *ect* promoter region. (A) Plasmid pGJK4 carries an *ectB-lacZ* reporter fusion that is expressed from the *ect* promoter present upstream of the *ectA* gene. The *P. stutzeri* A1501 genomic DNA located in front of the *ectA* start codon has a length of 264 bp. This genomic segment was successively shortened from its 5' end, and the resulting *E. coli* reporter strains were assayed for β -galactosidase enzyme activity along with the wild-type plasmid-bearing strain. Cultures were grown in MMA or MMA containing 0.4 M NaCl and were harvested and processed for β -galactosidase enzyme activity when they reached an optical density (OD₅₇₈) of about 1.8. The data shown were derived from four independently grown cultures, and each enzyme assay was performed at least twice. β -Galactosidase enzyme activity is given in Miller units (MU) (108). (B) DNA consensus sequence of Sig⁷⁰-type *E. coli* promoters (78), of the predicted *ect* promoter, and of a hybrid promoter created through deletion analysis of the *ect* regulatory region (deletion junction K7) that generated plasmid pNST40. The -10 and -35 elements are highlighted, and the spacer length typical for Sig⁷⁰-type *E. coli* promoters is indicated.

K8 deletion construct lies in codon four of the *ectA* coding region (Fig. S1), one can infer that no promoter internal to the *ect* gene cluster is present between the K8 deletion endpoint in *ectA* and the fusion junction in codon 88 of *ectB* (Fig. 3A and S1).

We were particularly interested in the striking drop of *ect-lacZ* promoter activity found in strains carrying plasmid pNST40 with the K7 deletion endpoint (Fig. 3A), since it might provide potential clues about the position of either the *ect* promoter or regulatory regions required for its full activity. We therefore inspected the *ect* DNA sequence around the 5' end of the K7 deletion junction more closely and found through sequence gazing potential -10 and -35 elements of sigma-70 (Sig⁷⁰)-type promoters (78) that were separated from each other by 18 bp (Fig. 3B). While the potential -35 region of the *ect* promoter possesses a good fit to the consensus sequence with just a single-base-pair deviation, the putative -10 region diverges very

TABLE 1 Influence on *ect-lacZ* expression of regulatory systems that had previously been implicated in osmotically controlled gene transcription in *E. coli*^a

Strain	Gene disruption	LacZ activity (MU) with:	
		0 M NaCl	0.4 M NaCl
MC4100(pBBR1MCS-2- <i>lacZ</i>)		0.3 ± 0.1	0.3 ± 0.1
MC4100(pGJK4)		29 ± 0.7	141 ± 1.6
PD32(pGJK4)	<i>hns</i>	28 ± 1.6	148 ± 4
RH90(pGJK4)	<i>rpoS</i>	24 ± 0.3	149 ± 3.7
RH76(pGJK4)	<i>cya</i>	29 ± 1.2	143 ± 4.3
LC30(pGJK4)	<i>ompR</i>	24 ± 1.9	140 ± 4.9

^aTranscriptional activity of the *ectB-lacZ* reporter fusion present on plasmid pGJK4 in response to increased salinity. The reporter plasmid was introduced by DNA transformation into an isogenic set of strains harboring different gene disruption mutations: MC4100 (wild type), PD32 (*hns-206::Ap^r*), RH90 (*rpoS359::Tn10*), RH76 (*Δcya-851*), and LC30 (*ompR::Tn10*). These strains are all derivatives of the *ΔlacIZYA* strain MC4100. The vector, pBBR1MCS-2-*lacZ*, used for the construction of the *ect-lacZ* reporter fusion was used as the control. All strains were grown in MMA in the absence or presence of 0.4 M NaCl until they reached an OD₅₇₈ of approximately 1.8; they were then harvested by centrifugation and assayed for β-galactosidase reporter enzyme activity. The data shown (means ± standard deviations) were derived from four independently grown cultures, and each enzyme assay was performed at least twice. β-Galactosidase enzyme activity is given in Miller units (MU).

strongly from the AT-rich consensus sequence (78), since it is very GC rich (Fig. 3B). Furthermore, the spacer length of 18 bp is suboptimal for Sig⁷⁰-type promoters (78). Interestingly, the K7 deletion endpoint removes the −35 region of the putative *ect* promoter and also 2 bp from the spacer region (Fig. 3B). However, DNA sequences derived from the cloning vector with resemblance to a potential −35 region replaced the authentic *ect* −35 DNA sequence while maintaining a spacer length of 18 bp of the hybrid promoter (Fig. 3B). The fortuitously generated −35 region of the K7 deletion junction deviates more strongly from the consensus sequence of −35 regions from Sig⁷⁰-type promoters (78) than the authentic −35 region of the putative *ect* promoter (Fig. 3B). These DNA sequence features of the fortuitously generated hybrid promoter could thus potentially explain the significant drop in *ect-lacZ* reporter activity observed in strain MC4100(pNST40) (Fig. 3A).

Defining a minimal DNA fragment required for osmoregulation of *ect* transcription. Building on the knowledge gained through the deletion analysis of the 5′ segment of the *ect* regulatory region, we constructed an *ect-lacZ* reporter fusion containing a minimal DNA fragment still allowing osmoregulation. To this end, we fused a 116-bp DNA fragment to the *lacZ* reporter gene (Fig. 4A); it contains the −35 and −10 elements of the *ect* promoter, 28 bp upstream of the −35 region, and a fusion junction to *lacZ* within codon seven of *ectA* (Fig. 4B). This *ectA-lacZ* reporter construct (present on plasmid pAST111) provided approximately the same level of gene expression and osmotic inducibility as the parent *ectB-lacZ* reporter fusion (present on plasmid pGJK4) (Fig. 4C). Hence, all elements required in *cis* for osmoregulation of *ect* expression are contained in this 116-bp DNA region. This *ectA-lacZ* reporter construct is a gene fusion that leads to the formation of an EctA-LacZ hybrid protein; as a consequence, its translation depends on the *ectA* ribosome-binding site.

Site-directed mutagenesis of the *ect* promoter reveals major features of its osmotic control. To provide further evidence that the putative −35 and −10 sequences described above (Fig. 3B and 4B) are actually part of the *ect* promoter, we targeted by site-directed mutagenesis base pairs in both the −35 and −10 elements that are highly conserved in Sig⁷⁰-type promoters and crucially contribute to promoter activity and strength (78). To this end, we replaced the highly conserved TTG sequence at the 5′ end of the −35 region with a GGG string of base pairs, and in the −10 region we replaced the so-called invariant T with a GC pair (Fig. 5A). Both promoter variants (Mut 1 and Mut 2) abolished *ect-lacZ* reporter activity down to a basal level (Fig. 5B), thereby providing compelling evidence that the region we deemed to be the *ect* promoter (Fig. 3B and 4B) actually represents this element for the transcriptional control of the ectoine/hydroxyectoine biosynthetic operon from *P. stutzeri* A1501.

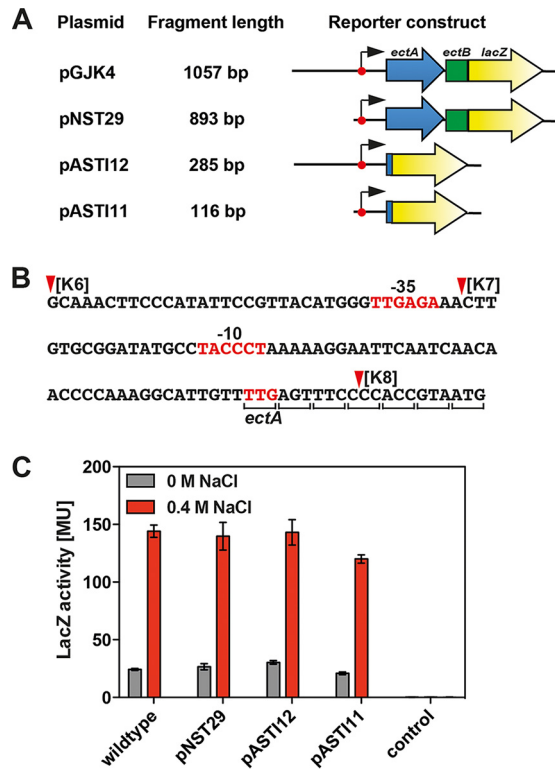


FIG 4 A minimal DNA fragment directing osmoregulated *ect* transcription. (A) Physical structures of *ect-lacZ* reporter constructs. (B) DNA sequence of the DNA fragment present in plasmid pASTI11. The deletion endpoints K6, K7, and K8 defined in the experiments for Fig. 3A are indicated, and the -35 and -10 elements of the *ect* promoter are highlighted. The fusion junction within *ectA* to the *lacZ* reporter gene lies in codon seven. (C) β-Galactosidase reporter enzyme activity in cells of strain MC4100 carrying the plasmids depicted in panel A. Cells of MC4100 carrying the vector (pBBR1MCS-2-*lacZ*) used to construct plasmids pGJK4, pNST29, pASTI12, and pASTI11 were used as the control. Cultures were grown in MMA or MMA containing 0.4 M NaCl and were harvested and processed for β-galactosidase enzyme activity when they reached an optical density (OD₅₇₈) of about 1.8. The data shown were derived from four independently grown cultures, and each enzyme assay was performed at least twice. β-Galactosidase enzyme activity is given in Miller units (MU) (108).

To glean information about the features of the *ect* promoter that contribute to its osmotic control, we first targeted the spacer region. Shortening the spacer to a suboptimal length of 16 bp rendered the promoter constitutive (Mut 3) at an expression level corresponding to that exhibited by the wild-type *ect* promoter in *E. coli* cells grown in minimal medium in the presence of 0.3 M NaCl (Fig. 5B). Conversely, when we extended the spacer sequence of the *ect* promoter to a suboptimal length of 19 bp (Mut 6) for Sig⁷⁰-type promoters (78), *ect-lacZ* reporter activity was abolished (Fig. 5A and B). Interesting effects were seen when we decreased the spacer length of the authentic *ect* promoter from 18 bp to the optimal spacer length of 17 bp for the activity of Sig⁷⁰-type promoters (78) by deleting single base pairs at two different positions in the *ect* promoter sequence. In the corresponding mutants (Mut 4 and Mut 5) (Fig. 5A), the noninduced level of *ect-lacZ* promoter activity rose substantially but both mutant promoters still permitted osmotic induction of transcription (Fig. 5B). Sig⁷⁰/SigA-type promoters from *E. coli* and *Bacillus subtilis* often possess a TG motif at position -16 which contributes to promoter strength (78, 79). We generated through a deletion of one base pair in the *ect* spacer a promoter variant (Mut 18) that generated a TG motif at the -16 position (Fig. 5A). This promoter variant remained osmotically inducible at a level of transcription similar to that observed for the Mut 4 and Mut 5 17-bp spacer variants (Fig. 5B). The properties of the Mut 18 variant indicate that the artificially generated -16 motif is not crucial for either the strength of the *ect* promoter or its response to osmotic stress.

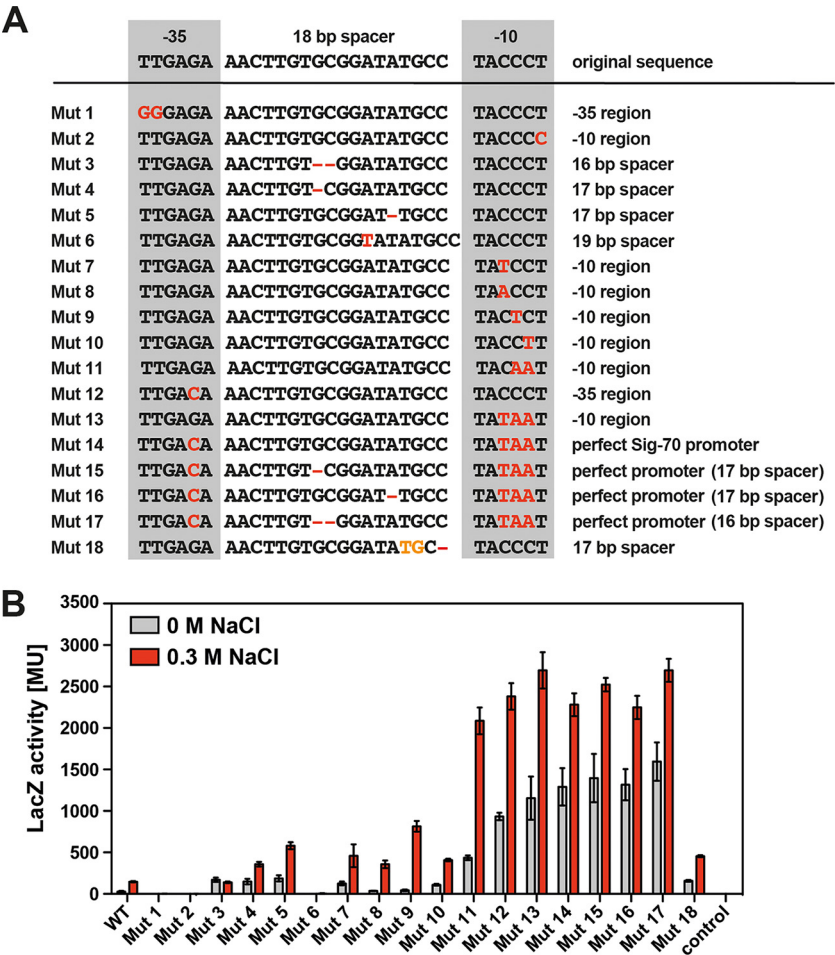


FIG 5 Site-directed mutagenesis of the *ect* promoter and assessment of the transcriptional activities of the promoter variants. (A) DNA sequences of the wild-type *ect* promoter and its mutant derivatives. The base pairs changed through site-directed mutagenesis are highlighted in red. (B) β -Galactosidase reporter enzyme activity of *E. coli* strains (MC4100) harboring the wild-type *ectB-lacZ* fusion or its mutant derivatives. Cultures were grown in MMA or MMA containing 0.3 M NaCl and were harvested and processed for β -galactosidase enzyme activity when they reached an optical density (OD_{578}) of about 1.8. The data shown were derived from four independently grown cultures, and each enzyme assay was performed at least twice. β -Galactosidase enzyme activity is given in Miller units (MU) (108).

We then targeted the unusual GC-rich -10 region of the *ect* promoter by single- and double-base-pair changes that collectively bring the authentic sequence closer to the A/T-rich consensus sequence of Sig⁷⁰-type promoters (78). In all of these mutants, strong osmotic induction occurred (Fig. 5A and B). Particularly notable was the property of the Mut 9 promoter variant, in which one of the three CG base pairs was replaced by a TA base pair (Fig. 5A). It allowed a very strong salt induction, 18.9-fold in the Mut 9 variant versus 5.2-fold for the wild-type promoter (Fig. 5B).

As noted above, the -35 region of the *ect* promoter deviates at just a single position from the consensus Sig⁷⁰-type promoter sequence (Fig. 3B). When we altered the -35 region to a fully consensus-like sequence (Mut 12), a drastic effect on the strength of promoter activity was observed: the basal promoter activity rose by 33.4-fold compared to that of the wild type, and its salt-stress-induced level of activity exceeded that of the wild-type promoter by 16.2-fold (Fig. 5B). Strong increases in transcriptional activity were also seen when we optimized both the -10 and -35 regions and spacer length of the *ect* promoter (Fig. 5A and B). In all these cases, the basal level of *ect* promoter activity was strongly increased in the absence of osmotic stress while still allowing increased promoter activity at high salinity (Fig. 5B). As a result of this profile in

promoter activity, the extent of osmotic induction was reduced. Particularly noteworthy are the properties of the *ect* promoter variants (Mut 15 and Mut 16) that we mutated such that they matched in their -10 and -35 regions, and with their spacer length (17 bp), the features of a perfect consensus sequence of Sig⁷⁰-type promoters (78) (Fig. 5A and B). The transcriptional activities of these mutant promoters occurred at high basal levels but still retained osmotic inducibility, by about 1.8-fold for Mut 15 and 1.7-fold for Mut 16. For a comparison, the osmotic inducibility of the wild-type *ect* promoter under the same experimental conditions was 5.2-fold (Fig. 5A and B).

We noted the presence of an inverted-repeat DNA sequence (5'-CCCAT-N¹⁰-ATGG G-3') just upstream of the *ect* -35 region (see Fig. S2A in the supplemental material). Since this inverted repeat could potentially form the operator sequence for a regulatory protein, we changed the left side of the repeat through site-directed mutagenesis to 5'-GGGTA-3', thereby destroying the dyad symmetry (Fig. S2A). This mutation had no influence on *ect-lacZ* reporter gene expression (Fig. S2B).

As a note of caution, in conducting this comprehensive set of *ect-lacZ* reporter fusion experiments with mutant *ect* promoters, we initially experienced some experimental difficulties. We repeatedly observed that the β -galactosidase reporter enzyme activity varied strongly between parallel-grown cultures of *E. coli* strains carrying the same *ect-lacZ* reporter plasmid when they were grown in MMA with 0.4 M NaCl. Substantial amounts of β -galactosidase protein were present in both cultures (as assessed by Western blotting); however, one culture possessed very high β -galactosidase reporter enzyme activity, while the other culture showed greatly diminished reporter enzyme activity. We therefore took care that the data included in this communication are all derived from experiments where the parallel-grown cultures yielded consistent β -galactosidase reporter enzyme activities. We observed the phenomenon of substantially differing β -galactosidase values only with mutant *ect* promoters exhibiting high transcriptional activity and only when the salinity of the growth medium exceeded that of 0.3 M NaCl. An example of this phenomenon is documented for strain MC4100(pPH11) harboring the perfect Sig⁷⁰-promoter driving *ect-lacZ* expression when it was grown at various salinities (see Fig. S3 and S4 in the supplemental material). We were unable to define the apparently subtle physiological differences in the growth behavior of the cultures incubated in parallel that led to the irregular behavior of the β -galactosidase reporter enzyme. However, it is known from previous studies that high-level expression of hybrid proteins (e.g., ProV-LacZ; ProV is the ATPase of the ProU ABC transporter [80]) can lead to protein aggregation under high-salinity growth conditions and therefore obscure the physiologically correct regulatory pattern of the osmoregulated promoter under study (81). Since the reporter fusion present on plasmid pGJK4 and its derivatives carrying mutant *ect* promoters fuses 88 codons of *ectB* to the *lacZ* reading frame, the resulting EctB-LacZ hybrid protein might be prone to aggregation in a high-osmotic-strength cytoplasm.

Details of the transcriptional responses of selected *ect* promoter variants with high levels of transcriptional activity under sustained osmotic stress. Since we intended to use the wild-type promoter of the *ectABCD-ask_ect* gene cluster from *P. stutzeri* A1501 (67) and some of its promoter up-mutations for the establishment of a heterologous ectoine/hydroxyectoine cell factory (see below), we studied the promoter activities of Mut 12 (with a perfect -35 region) (Fig. 5A) and of Mut 15 (with a consensus Sig⁷⁰-type promoter) (Fig. 5A) in somewhat greater detail. We grew the strains carrying the corresponding *ect-lacZ* reporter plasmids, pPH8 (Mut 12) and pPH11 (Mut 15), under sustained osmotic stress condition in cultures in which we systematically increased the salinity from 0 M NaCl to 0.4 M NaCl (Fig. 6A, B, and C). The β -galactosidase reporter enzyme activities of strains MC4100(pPH8) and MC4100(pPH11) increased in a finely tuned manner in response to corresponding increases in the external salinity. Their pattern of transcriptional activation mirrored that of the wild-type *ect-lacZ* reporter strain MC4100(pGJK4) (Fig. 6). Hence, as noted above (Fig. 5B), the two mutant *ect* promoters had not lost their osmotic control when they were tested in a wider range of salinities. However, the basal activity of the reporter fusion in the absence of

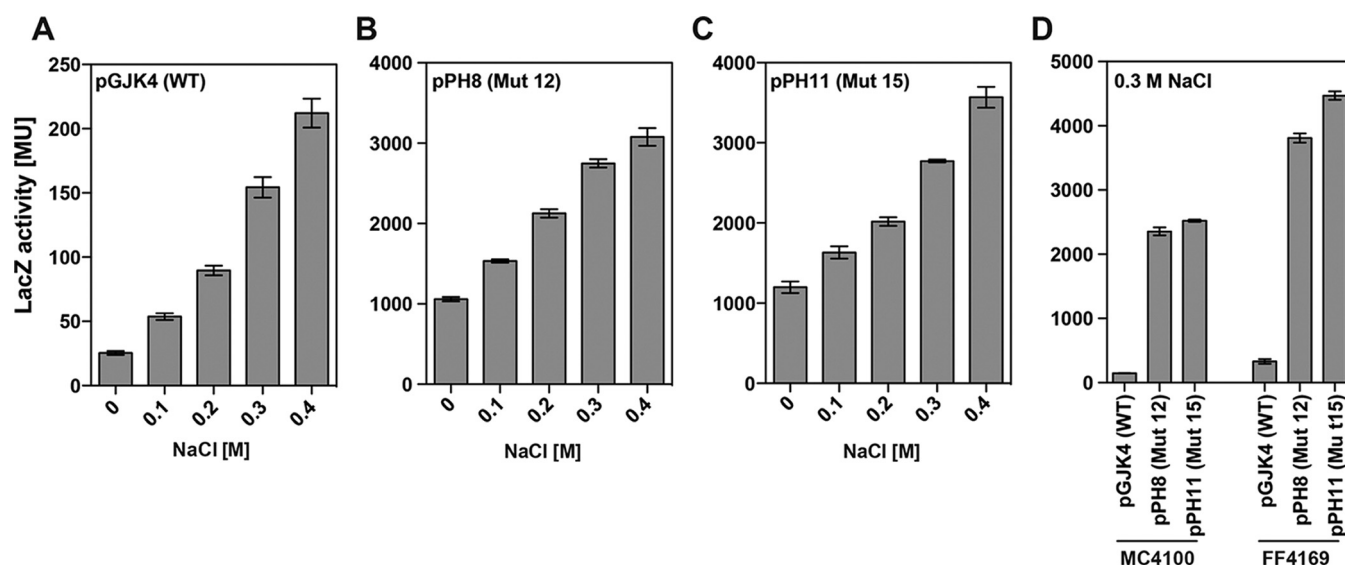


FIG 6 Transcriptional activity of the *ect* wild-type promoter and two of its mutant derivatives in response to sustained osmotic stress. (A to C) *E. coli* strains (MC4100) harboring either the wild-type *ectB-lacZ* reporter fusion plasmid pGJK4 (A), a plasmid (pPH8) carrying a point mutation (Mut 12) (Fig. 4A) in the *ect* -35 region (B), or a plasmid (pPH11) carrying a mutant *ect* promoter (Mut 15) (Fig. 4A) that was changed in its -10 region, -35 region, and spacer length to the consensus sequence of Sig⁷⁰-type *E. coli* promoters (78) (C) were grown at various salinities. (D) Cells of strain MC4100 or FF4169 (*otsA1::Tn10*) carrying the wild-type plasmid pGJK4, pPH8, or pPH11 were grown in MMA with 0.3 M NaCl. Cultures were harvested and processed for β -galactosidase enzyme activity when they reached an optical density (OD_{578}) of about 1.8. The data shown were derived from four independently grown cultures, and each enzyme assay was performed at least twice. β -Galactosidase enzyme activity is given in Miller units (MU) (108).

osmotic stress (cells grown in MMA) was very substantially increased; that of strain MC4100(pPH8) was raised by 42.3-fold (Fig. 6B) and that of strain MC4100(pPH11) (Fig. 6C) by 47.2-fold relative to that with the wild-type plasmid pGJK4 (Fig. 6A). The osmotically induced levels of β -galactosidase reporter enzyme activity in the *ect-lacZ* reporter fusion constructs exceeded greatly the activity of the reporter enzyme in the wild type *ect-lacZ* reporter fusion, by 14.2-fold, and 16.8-fold, respectively (Fig. 6A, B, and C).

Genetic design of a heterologous ectoine/hydroxyectoine cell factory. *E. coli* synthesizes large amounts of the compatible solute trehalose under osmotic stress conditions as a cytoprotectant (82, 83). It partially releases the newly produced trehalose also into the periplasmic space, where this disaccharide is hydrolyzed by an osmotically inducible trehalase (TreA), and the glucose monomers are then recovered again by the *E. coli* cells through a phosphotransferase transport system (PTS) for their use as carbon sources (84). To avoid the contamination of newly produced ectoine/hydroxyectoine by trehalose and to provide an incentive to the osmotically stressed cells to enhance the production of ectoines in response to increased salinity to provide physiologically adequate osmotic stress protection for *E. coli* (2), we used for the setup of the cell factory a strain that is defective in trehalose synthesis (FF4169; *otsA1::Tn10*) (83, 85). The use of such a host strain proved to be beneficial for the expression of the *ect-lacZ* reporter fusions carrying either the wild-type *ect* promoter or its Mut 12 and Mut 15 derivatives in comparison with its *otsBA*⁺ parent strain, MC4100 (Fig. 6D). We therefore constructed derivatives of the wild-type *ectABCD-ask_ect* plasmid pLC68 harboring either the Mut 12 (plasmid pAST11) or Mut 15 (plasmid pAST19) variant in their promoters.

We assessed the production performance of strain MC4100 (*otsAB*⁺) and its *otsA1::Tn10* derivative, strain FF4169, for ectoines when the cells carried plasmid pLC68. In MC4100 cultures, a mixture of ectoine and hydroxyectoine was found intracellularly, while the supernatant contained exclusively hydroxyectoine (Fig. 7A and B). Use of strain FF4169 for such an experiment yielded higher production levels of ectoines, with hydroxyectoine being again exclusively accumulated in the growth medium (Fig. 7A and B). In both strains, the external concentration of hydroxyectoine substantially exceeded that of the internal pool size of ectoines (Fig. 7A and B).

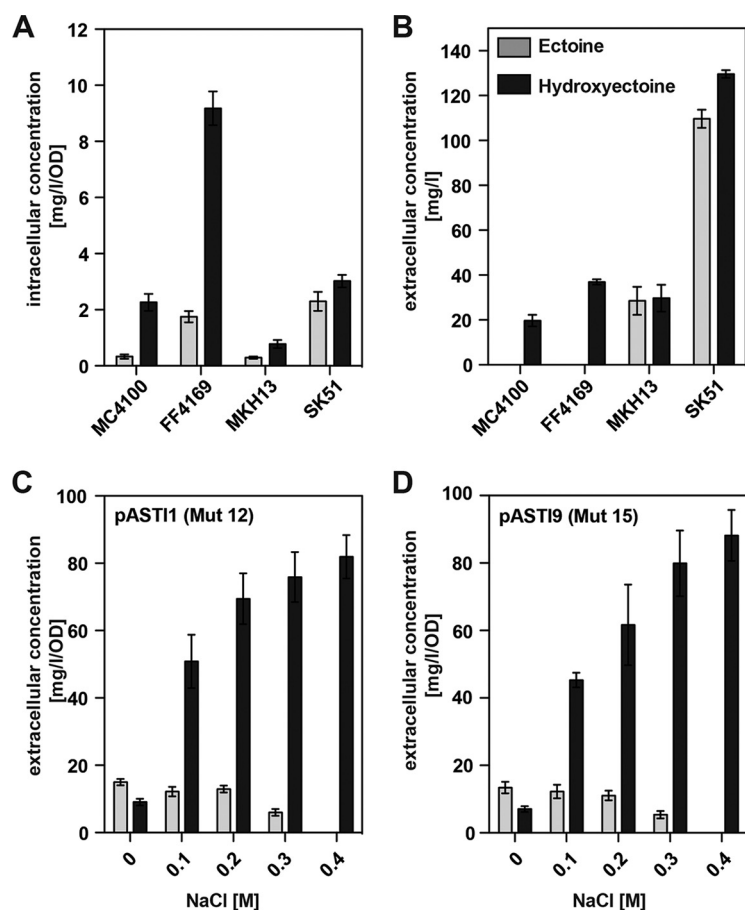


FIG 7 Comparison of ectoine and hydroxyectoine production in different *E. coli* mutant strains. (A and B) Cells of the *E. coli* wild-type strain MC4100 and its mutant derivatives FF4169 (*otsA1::Tn10*), MKH13 [$\Delta(\text{proP})2 \Delta(\text{proU}::\text{spc})608$], and SK51 [$\Delta(\text{proP})2 \Delta(\text{proU}::\text{spc})608 \text{otsA1}::\text{Tn10}$] carrying plasmid pLC68 (with a wild-type *ect* promoter) were cultivated in MMA with 0.4 M NaCl. After incubation for 48 h, cells were harvested and assayed for their intracellular (A) and extracellular (B) concentrations of ectoine (gray bars) and hydroxyectoine (black bars) via HPLC analysis. (C and D) Comparison of ectoine and hydroxyectoine production in strains carrying mutant *ect* promoters in response to graded increases in the external salinity. *E. coli* strain FF4169 (*otsA1::Tn10*) carrying either plasmid pASTI1 (Mut 12; point mutation in the -35 region) (Fig. 3A) (C) or plasmid pASTI9 (Mut 15; consensus Sig⁷⁰-type promoter variant) (Fig. 3A) (D) was cultivated in MMA containing various concentrations of NaCl. The cultures were grown for 24 h, and the extracellular ectoine/hydroxyectoine content was then determined by HPLC analysis. The data shown were derived from four independently grown cultures, and each assessment of their ectoine/hydroxyectoine content was performed at least twice. Since the concentration of NaCl in the medium significantly influences cell growth, the ectoine/hydroxyectoine content of the supernatant was normalized to an OD₅₆₈ of 1 and is reported here as mg/liter/OD unit.

Aspartate is the biosynthetic precursor of ectoine (20, 86) (Fig. 1A), and its addition to the growth medium has already been proven beneficial for the recombinant production of ectoines (87). In exploratory experiments, we observed that the addition of 25 mM aspartate to our *Ots*[−] *E. coli* cell factory harboring plasmid pLC68 substantially enhanced hydroxyectoine production (see Fig. S5A in the supplemental material). However, increases in the aspartate concentration successively reduced the amount of the produced hydroxyectoine, while this phenomenon was not observed in strains harboring the *ectABCD-ask_ect* gene cluster carrying promoter up-mutations (plasmids pASTI1 [Mut 12] and pASTI9 [Mut 15]) (Fig. S5). We did not further investigate the drop in hydroxyectoine production of the *Ots*[−] *E. coli* host strain FF4169(pLC68), but we suspect that it might be related to the notable increase in medium osmolarity caused by the addition of high concentrations of aspartate (see Fig. S6 in the supplemental material). Furthermore, the limited ability of the wild-type *ectABCD-ask_ect* plasmid to

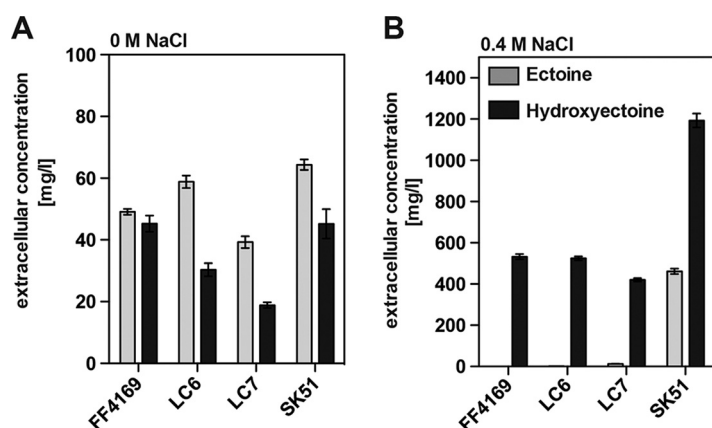


FIG 8 Influence of the ProP and ProU ectoine uptake systems on the extracellular amounts of ectoine and hydroxyectoine. *E. coli* strains FF4169, LC6, LC7, and SK51 carrying plasmid pAST11 (Mut 12; point mutation in the -35 region) (Fig. 3A) were cultivated in MMA containing either 0 M NaCl (A) or 0.4 M NaCl (B) for 48 h, and the extracellular ectoine/hydroxyectoine content was then determined by HPLC analysis. The data shown were derived from four independently grown cultures, and each assessment of their ectoine/hydroxyectoine content was performed at least twice. The relevant genotypes of the *E. coli* strains used are as follows: FF4169, *otsA1::Tn10 proP⁺ proU⁺*; LC6, *otsA1::Tn10 proP⁺ proU⁺*; LC7, *otsA1::Tn10 proP⁺ proU⁺*; and SK51, *otsA1::Tn10 proP⁺ proU⁺*.

provide adequate levels of osmoprotection to the host strain lacking trehalose (82, 83) might also be a contributing factor.

ect promoter mutations increase ectoine/hydroxyectoine production by the *E. coli* cell factory. To further increase ectoine/hydroxyectoine production titers, we separately introduced plasmids pAST11 (Mut 12, a point mutant of the -35 region in the *ect* promoter) (Fig. 5A) and pAST19 (Mut 15, a mutant *ect* promoter altered to the Sig⁷⁰-type consensus sequence) (Fig. 5A) into the *Ots*[−] *E. coli* mutant strain FF4169. Consistent with the *ect-lacZ* reporter fusion assays (Fig. 6D), the presence of either plasmid leads to substantially increased production titers in comparison with those in strain FF4169 carrying the wild-type plasmid pLC68 (Fig. 7A and B) in an osmoprotection-dependent manner, with hydroxyectoine being the predominant compatible solute in the culture supernatant (Fig. 7C and D).

Hypersecretion of ectoine and hydroxyectoine by *E. coli* strains lacking the osmolyte importers ProP and ProU. The osmotically regulated ABC transporter ProU and the major facilitator superfamily (MFS)-type transporter ProP serve as the major uptake systems for compatible solutes in *E. coli* (80, 88) and are also responsible for the uptake of ectoine under osmotic stress conditions (68). We noted that the secretion of both ectoine and hydroxyectoine was particularly pronounced in strain MKH13 (*Ots*⁺ ProP[−] ProU[−]) and in strain SK51, which is simultaneously defective in trehalose synthesis and the ProU and ProP transport systems (Fig. 7A and B). Apparently, *E. coli* continuously secretes substantial amounts of the heterologously produced ectoines into the growth medium that subsequently cannot be recovered again by the cells due to the defects in the ProU and ProP importers (Fig. 7B).

To study this phenomenon in more detail, we constructed an isogenic set of strains that lacked the ability to synthesize trehalose and possessed only either the ProU (strain LC6) or ProP (strain LC7) transporter. As long as one of these ectoine/hydroxyectoine importers was intact, the external pool of hydroxyectoine matched that produced by the ProP⁺ ProU⁺ parent strain FF4169. Notably, ectoine was a very minor component of the supernatant of the osmotically stressed cells (Fig. 8B), while in the supernatant of the non-osmotically challenged cultures ectoine was present (Fig. 8A). This picture changed substantially when we analyzed ectoine/hydroxyectoine excretion in the ProP[−] ProU[−] strain SK51. Supernatants of cultures of the SK51 cell factory contained both ectoine and hydroxyectoine, with hydroxyectoine being the dominant solute again (Fig. 8B).

Deletion of *ectD* results in a recombinant cell factory secreting exclusively ectoine. In strain SK51 (*Ots*[−] ProP[−] ProU[−]) harboring the *ectABCD-ask_ect* wild-type

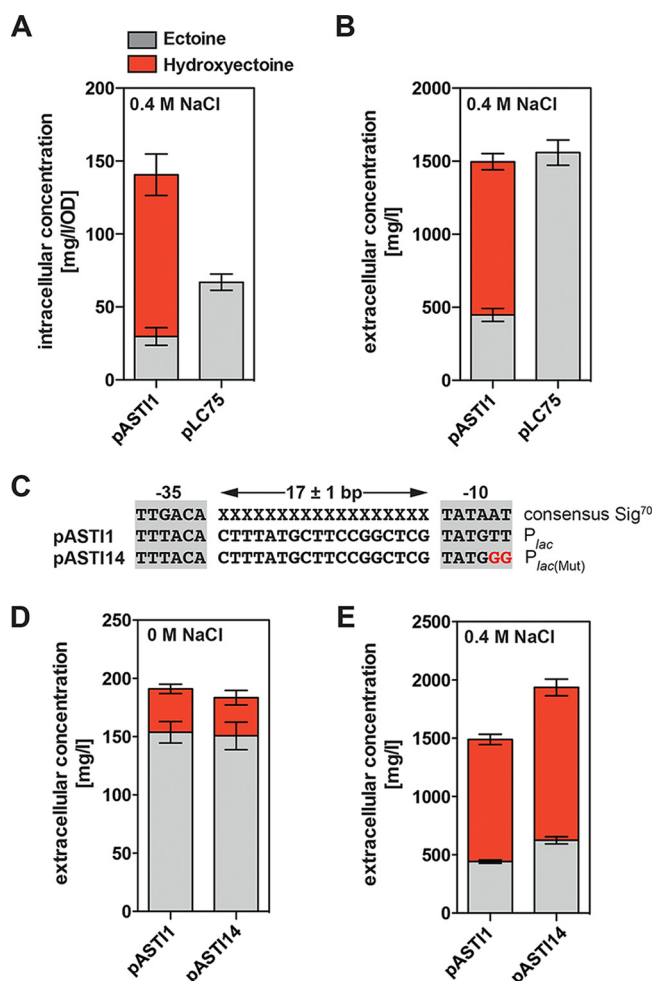


FIG 9 Influence of an *ectD* deletion on ectoine/hydroxyectoine production and secretion. (A and B) *E. coli* strain SK51 (*otsA1::Tn10 proP proU*) harboring either plasmid pAST11 (*ectABCD-ask_ect*) or plasmid pLC75 [*ectABC(Δ*ectD*)-ask_ect*] carrying a point mutation in the -35 region of the *ect* promoter was grown in MMA containing 0.4 M NaCl for 24 h, and the intracellular (A) and extracellular (B) ectoine/hydroxyectoine content was then determined by HPLC analysis. (C) Comparison of the *lac* promoter sequence present in the cloning vector pHS575 (89) and its mutant derivative present in plasmid pAST114 (*ectABCD-ask_ect*). (D and E) Cells of strain SK51 carrying either pAST11 or pAST114 were grown either in MMA (D) or MMA with 0.4 M NaCl (E) for 24 h, and the extracellular ectoine and hydroxyectoine concentrations were then determined by HPLC analysis. The data shown were derived from four independently grown cultures, and each assessment of their ectoine/hydroxyectoine content was performed at least twice.

plasmid pLC68, ectoine and hydroxyectoine are present in an almost a 1:1 mixture (Fig. 7B), while in the supernatant of strain FF4169 (*Ots⁻ ProP⁺ ProU⁺*) carrying the *ect* promoter mutant plasmids pAST11 and pAST19, hydroxyectoine predominates (Fig. 7C and D). To construct a recombinant cell factory producing exclusively high levels of ectoine, we deleted the *ectD* gene from the *ectABCD-ask_ect* gene cluster present on plasmid pAST11. When we introduced the resulting plasmid, pLC75, into strain SK51, only ectoine was found, both intracellularly and extracellularly (Fig. 9A and B). This strain yields an ectoine/hydroxyectoine production titer of 1.5 g liter⁻¹ per 24 h. The strain harboring the corresponding *ectD⁺* plasmid pAST11 had a practically identical productivity but yielded a 2:1 mixture of hydroxyectoine to ectoine in the supernatant (Fig. 9B). Only approximately 8.7% of the ectoines produced were retained by cells of strain SK51(pAST11 [*ectD⁺*]), whereas the corresponding value for cells of strain SK51(pLC75 [*ΔectD*]) was 4.2% (Fig. 9A and B). Hence, these recombinant cell factories secrete the vast majority of the newly produced ectoines into the growth medium. The

TABLE 2 Analysis of glucose, aspartate, and the content of ectoines before and after cultivation of the heterologous *E. coli* cell factory SK51(pASTI1)^a

Compound	Concn (mg/liter) in supernatant			
	Before cultivation		After 24 h of cultivation	
	Without NaCl	With 0.4 M NaCl	Without NaCl	With 0.4 M NaCl
Ectoine	1.5 ± 0.3 ^b	1.4 ± 0.06 ^b	144.1 ± 4.8	371.8 ± 11.6
Hydroxyectoine	ND ^c	ND	18.1 ± 2.4	936.7 ± 48.5
Aspartate	4,246.6 ± 197.6	4,358.8 ± 149.9	2.2 ± 0.4	979.1 ± 94.2
Glucose	4,606.6 ± 200.6	4,627.2 ± 168.4	3.7 ± 0.5	2.2 ± 0.5

^a*E. coli* strain SK51 (*otsA1::Tn10 proP proU*) harboring plasmid pASTI1 (*ectABCD-ask_ect*) was grown in 200 ml MMA (in a 2-liter baffled Erlenmeyer flask) containing either 0 or 0.4 M NaCl. Cells of preculture grown in MMA overnight were used to inoculate the main cultures to an OD₅₇₈ of about 0.15; the cells were then cultivated for 24 h at 37°C on an aerial orbital shaker. Immediately after inoculation and at the end of the experiment after 24 h, 2-ml samples were withdrawn and used to determine the glucose, aspartate, ectoine, and hydroxyectoine contents of the cultures. The data shown (means ± standard deviations) were derived from four independently grown cultures, and each assessment of their ectoine, hydroxyectoine, aspartate, and glucose contents was performed at least twice.

^bThis small amount of ectoine results from carryover from the inoculum.

^cND, not detected.

ca. 1.5 g ectoine produced per liter of culture of strain SK51(pLC75) within 24 h corresponds to a yield of 0.3 g ectoine per g glucose, values that can also be described as 1.3 g ectoine produced per 1.24 g cell dry weight.

Quantitative analysis of the performance of the ectoine/hydroxyectoine synthetic cell factory. To study the salient features of the ectoine/hydroxyectoine synthetic cell factory further, we performed an experiment in which we not only monitored the secretion of ectoines but also quantitated the consumption of glucose and that of the ectoine precursor aspartate under both inducing and noninducing osmotic conditions in baffled shake flask cultures. For these experiments, we used strain SK51(pASTI1) as an example (Table 2). After 24 h of cultivation of this strain in MMA with 0.4 M NaCl, we found ectoine and hydroxyectoine in the growth medium in concentrations similar to that in the experiment for Fig. 9B. Since pASTI1 carries a *ect* promoter up-mutation (in its –35 sequence; Mut 12) (Fig. 5A), we also detected ectoine and hydroxyectoine in the supernatant of the cultures grown in MMA. While the corresponding value for ectoine represented about a third of that detected under osmotic stress conditions, the production of hydroxyectoine was greatly stimulated under high-osmolarity conditions (by about 52-fold) (Table 2). Together, this corresponded to 1.3 g ectoines produced per liter of culture.

By the time the experiment was terminated (after 24 h), both the osmotically nonstressed and the osmotically stressed cells had consumed practically all the glucose that was added to the growth medium (Table 2). In contrast, the cells had consumed essentially all the added aspartate under nonstressed conditions, while substantial amounts of this amino acid were still present in the supernatants of cultures grown under osmotic stress conditions (Table 2). It is thus apparent from this analysis that the SK51(pASTI1) synthetic cell factory is carbon source limited under the studied growth conditions in baffled shake flasks. Furthermore, since both the nonstressed and osmotically stressed cultures reached essentially the same optical density within the 24-h time frame (see Fig. S7 in the supplemental material), it appears that under osmotic nonstressed conditions, the cells funnel aspartate primarily into the formation of biomass, while this route of aspartate consumption is substantially reduced under osmotic stress conditions (Table 2).

By monitoring the growth of the cells, we found the interesting phenomenon that ectoine/hydroxyectoine production was beneficial under osmotic stress conditions, while the growth of the *E. coli* cells was not notably altered under nonstressed conditions (Fig. S7). The improved growth of the ectoine/hydroxyectoine-producing cells at high salinity can readily be understood since the internally amassed ectoines will provide osmoprotection to the otherwise osmotically sensitive host strain SK51, which lacks the ability to synthesize the compatible solute trehalose (82, 83).

A *lac* promoter-directed *ect* antisense transcript limits production of ectoines in plasmid-carrying cells. The low-copy-number vector (pHSG575) used for the cloning of the *ectABCD-ask_ect* operon (plasmid pLC68) carries a *lac* promoter (89) that is constitutively expressed in the $\Delta lacIZYA$ host strain MC4100 and its derivatives that were used in our study. We obtained in our experiments involving cloning of the *ect* gene cluster only pHSG575-derived *ect*⁺ plasmids in which the *lac* promoter will direct an antisense RNA transcript relative to the *ectABCD-ask_ect* mRNA, which is driven by the transcriptional activity of the *ect* promoter (Fig. 1B). This antisense transcript could potentially either destabilize the *ectABCD-ask_ect* mRNA or impair its effective translation. We therefore constructed a derivative of pAST11 in which we inactivated the *lac* promoter through site-directed mutagenesis (Fig. 9C). When we tested the performance of the resulting plasmid, pAST114, for ectoine/hydroxyectoine production in comparison with the parent plasmid pAST11, the extracellular levels of ectoines increased from about 1.5 g liter⁻¹ in strain SK51(pAST11) to about 1.9 g liter⁻¹ in strain SK51(pAST114) under high-salinity growth conditions (Fig. 9E). This corresponded to 1,749 mg ectoines per g (dry weight) of the producing cells. Hence, the *lac* promoter-directed antisense transcript (Fig. 1B) limits the production of ectoines in our cell factory to a notable degree (by approximately 21%).

DISCUSSION

When challenged by high-osmolarity environments, many microorganisms synthesize copious amounts of ectoines as cytoprotectants (1, 3, 4, 32). However, the mechanism(s) through which the cell perceives increases in the environmental osmolarity, how it processes this information, and how it transmits it to the transcriptional apparatus to drive enhanced transcription of ectoine/hydroxyectoine biosynthetic genes are rather incompletely understood. CosR, a regulator of ectoine biosynthetic genes in *V. cholerae*, has been proposed to detect changes in the external osmolarity through the ensuing increases in the ionic strength of the cytoplasm (29). In a recently reported study (3), about a quarter of the 440 inspected ectoine/hydroxyectoine gene clusters were associated with a gene that encodes the MarR-type regulator EctR. However, even in the absence of EctR, osmoregulation of *ect* gene expression persisted in the single microorganism (*M. alcaliphilum*) in which the interaction of this repressor with the *ect* regulatory region has been studied (28). In addition, since the majority of ectoine/hydroxyectoine gene clusters are not associated with a regulatory gene (3), these observations imply that the promoter elements and their flanking region itself probably harbor critical information for osmotic control of *ect* transcription.

Consistent with this concept, we were able to transfer the trait of osmoregulated expression of the *ect* gene cluster from the ectoine/hydroxyectoine producer *P. stutzeri* A1501 (17), an organism that lacks CosR and EctR (3, 67), into the surrogate host *E. coli*, which does not synthesize ectoines naturally (68). While osmoregulation of several heterologous *ect* gene clusters in *E. coli* has already been reported (18, 23, 59), no detailed molecular analysis of this remarkable process has so far been pursued. We were able to show that the *ect* promoter from *P. stutzeri* A1501 responds to a true osmotic signal and requires the buildup of an osmotically effective gradient across the cytoplasmic membrane for enhanced transcriptional activity (Fig. 2A). We ruled out the involvement of the general stress-responsive alternative sigma factor RpoS, of the nucleoid-associated protein H-NS, of the two-component regulatory system EnvZ/OmpR, and of the cAMP/CRP complex, regulatory systems that target various osmotically controlled genes of *E. coli* (71–77), in the osmotic control of the *P. stutzeri* A1501 *ect* expression (Table 1).

Perception of the osmotic stress signal by *E. coli* is finely tuned, because graded increases in sustained high osmolarity led to corresponding linear increases in the lasting transcriptional activity of the *ect* promoter over a wide range of salinities (from 0 M NaCl to 0.5 M NaCl) (Fig. 2B). This finding implies that the *E. coli* host strain can sensitively perceive small increases in sustained high environmental osmolarity and is able to process this information genetically/physiologically such that a precise setting

of the transcriptional activity of the *ect* promoter will ensue (Fig. 2B). We consider it highly unlikely that the non-ectoine/hydroxyectoine-producing enterobacterium *E. coli* possesses specific protein- or RNA-based osmoregulatory circuits that would allow it to control the promoter of a heterologous *ect* biosynthetic gene cluster derived from a plant-root-associated soil bacterium in such a finely tuned fashion. As a working hypothesis, our data therefore suggest that osmoregulation of the *ect* promoter in the heterologous *E. coli* host is an inherent feature of the promoter elements and their flanking regions (Fig. 4). It remains to be determined how RNA polymerase, perhaps with contributions of the intracellular ion and compatible solute pools (Fig. 2C) (90, 91) and increases in global and local DNA supercoiling (92, 93), can afford the exquisitely sensitive transcriptional response to high osmolarity that we observed for the *ect* promoter (Fig. 2B).

It is striking how moderate changes in the *ect* promoter sequence that increase its resemblance to housekeeping Sig⁷⁰-type promoters of *E. coli* (78) cause substantially enhanced expression, both in the absence and in the presence of osmotic stress (Fig. 5A and B and 6A, B, and C). Deviations from the consensus Sig⁷⁰ promoter sequence thus serve to keep *ect* transcription low under osmotic conditions where the cells do not rely on the synthesis of compatible solutes for growth while simultaneously allowing induction of these types of genes when the cell has to physiologically cope with high environmental osmolarity (94). Essentially all of the *ect* promoter variants that we have constructed retained osmotic control, at least to a certain degree (Fig. 5B). Surprisingly, even an *ect* promoter variant in which we adjusted the -35 , and -10 regions, and also the spacer length, to those of corresponding elements present in the consensus Sig⁷⁰-type promoter (78) (e.g., Mut 15) (Fig. 5A) still remains responsive to high salinity (Fig. 6C). It therefore follows from our analysis that DNA sequence determinants for osmotic control of *ect* gene expression reside not only in the canonical promoter elements. Through deletion analysis and the study of reporter fusions, we have delineated all DNA sequences required in *cis* for osmoregulation of the *ect* promoter to a 116-bp DNA fragment. It encompasses the canonical -35 and -10 elements, contains 28 bp upstream of the -35 region, and extends from the beginning of the -10 region 58 bp down to codon seven of *ectA*, the first gene in the *ectABCD-ask_ect* gene cluster (Fig. 4B). DNA sequences relevant for osmotic control of the *ect* operon are certainly not present upstream of the -35 element, since their replacement with a fortuitously fused plasmid-derived DNA sequence somewhat related to canonical Sig⁷⁰-type -35 regions still allows osmotic induction of *ect* transcription (deletion endpoint K7) (Fig. 3A), albeit at a substantially reduced level of promoter activity. Currently, our data cannot exclude the possibility that elements important for osmoregulation are contained in the 5' region of the *ect* transcript or that a small antisense RNA targets the region around the translation initiation site of *ectA* (Fig. 4B). In any event, the identification of a small DNA fragment (116 bp) directing osmoregulated *ect* gene expression should allow the development of genetic screens to search for variants of the *ect* regulatory region that no longer respond to the osmotic cue but that do not simply destroy the promoter.

It is apparent from our mutational analysis of the *P. stutzeri* A1501 *ect* promoter that there is a complex interplay between different promoter elements that allow the cell to respond differently in transcriptional activity to the intracellular cue generated through an increase in the environmental osmolarity (Fig. 5). This proposal is reminiscent of data reported by Borowiec and Gralla (95) on the *lac* promoter from *E. coli*, where point mutations in the -10 , the -35 , or the spacer region alter the transcriptional response to DNA supercoiling in a distinct fashion but where the promoter elements then act as a whole to facilitate unwinding of the DNA during open complex formation and thereby set promoter activity. The strength of the intracellular cue that triggers enhanced *ect* expression is modulated by the accumulation of various types of compatible solutes. Since this also includes ectoine and hydroxyectoine (Fig. 2C), the ectoine/hydroxyectoine producer bacterium is provided with a homeostatic system allowing it to tune down the activity of the *ect* promoter once a physiologically appropriate cellular adjustment to the external osmolarity has been attained.

A particular intriguing feature of the *P. stutzeri* A1501 *ect* promoter is the string of three consecutive CG base pairs in the -10 region, whereas the canonical counterpart of this element in Sig^{70} -type promoters lacks CG pairs altogether (Fig. 3B) (78). Such unusual -10 regions have also been noted in several osmostress-responsive genes in other microorganisms (77, 94). For an understanding of the role possibly played by the three consecutive CG base pairs in the *ect* -10 region (Fig. 3B), we find it useful to consider the properties of the *leu-500* allele of *Salmonella enterica* serovar Typhimurium. In this allele, a single A-to-G point mutation is introduced into the -10 region of the promoter driving expression of the *leu* operon. This mutation renders the already unusual -10 element particularly GC rich (depending on the assumed spacer length of the *leu* promoter, the -10 region is either TGCCAC or GCCACT), strongly impairs *leu* transcription, and thereby causes leucine auxotrophy (96). Suppressors restoring leucine prototrophy map in *topA*, the structural gene for DNA topoisomerase I, a key player in setting the overall level of DNA supercoiling in the cell. Furthermore, local changes in negative superhelicity also stimulate *leu-500* promoter activity strongly (93, 97). It is thus thought that increases in negative DNA superhelicity aid the RNA polymerase in overcoming the increased energy barrier posed by the GC-rich -10 region of the *leu-500* promoter to allow DNA strand separation during open complex formation (78, 93, 97). The degree of DNA supercoiling is an important determinant of bacterial gene expression and growth, and it fluctuates in response to cellular and environmental changes (98, 99). High-osmolarity-instigated increases in negative DNA superhelicity (92) are thus likely to contribute to the unwinding of the CG-rich -10 element of the *ectC* promoter (Fig. 3B and 4B), thereby stimulating its activity under osmotically unfavorable environmental circumstances (2, 12, 14, 15).

There has been a growing interest in ectoines as stabilizers of macromolecules and cellular structures for various practical applications, and both natural and synthetic microbial cell factories for their production have been developed (1, 32, 48, 49, 59, 66). We designed an ectoine/hydroxyectoine-producing synthetic cell factory by combining optimized *ect* promoters with an engineered *E. coli* chassis strain that lacks the ability to synthesize the osmostress protectant trehalose (82, 83) and to import ectoines via the ProP and ProU transport systems (68, 80, 88). By flexibly choosing plasmids with combinations of *ectABCD-ask_ect* or *ectABC(Δ ectD)-ask_ect* gene clusters and different *E. coli* host strains, we were able to achieve production and secretion of either pure ectoine (Fig. 9B) or pure hydroxyectoine (Fig. 7C and D and 8B) or a mixture of both compounds (Fig. 9B, D, and E). Our best-performing cell factory yields a total ectoine/hydroxyectoine production titer of about 1.9 g liter^{-1} within 24 h in baffled shake flask cultures (Fig. 9E). This is probably not the maximal productivity of our synthetic cell factory, since under the evaluated conditions (Table 2), the growth/productivity of the culture is limited by glucose availability but not by the added amount (25 mM) of the ectoine biosynthetic precursor aspartate (Fig. 1A).

Our recombinant cell factory also allows the synthesis of ectoine under nonstressed conditions, but since it is dependent on osmotically stimulated *ect* promoters, its ectoine/hydroxyectoine production yields strongly increase (by about 10-fold) when the cells are osmotically challenged (Table 2; Fig. 7C and D and 9D and E). However, in comparison with natural ectoine/hydroxyectoine-producing microorganisms, which demand very high salinities (between 1 and 2.5 M NaCl) (1) for good production levels, the cell factory that we describe here requires rather moderate salinities (Fig. 2A and 9D and E), conditions that might be more favorable for fermentation vessels and downstream processing equipment (1, 32). Furthermore, recombinant ectoine/hydroxyectoine cell factories that rely on synthetic promoters to drive the expression of the *ect* biosynthetic genes in the absence of osmotic stress often require costly inducers, while the osmotic stimulation of *ect* promoter activity requires only a commodity compound. Another significant advantage of our cell factory is that it does not require osmotic downshifts for the release of the ectoines, and it is designed such that the excreted ectoines cannot be reacquired by the producer cells (Fig. 1B). Others have already described various synthetic ectoine or hydroxyectoine cell factories (for summaries, see

TABLE 3 Comparison of the productivities of different recombinant ectoine/hydroxyectoine cell factories

Compound and host	Origin of ect biosynthetic genes	Titer of ectoines (g liter ⁻¹)	Productivity (g liter ⁻¹ h ⁻¹)	Production yield ^a	Production system	Reference
Ectoine						
<i>C. glutamicum</i> LYS-1	<i>P. stutzeri</i> A1501	6.7	0.28	36.1 μ mol (g DCW ^b) ⁻¹ [5.12 mg (g DCW) ⁻¹]	Fed batch, in a fermentor	63
<i>C. glutamicum</i>	<i>C. salexigens</i>	22	0.32	NR ^c	Fed batch, in a fermentor	62
<i>E. coli</i> DH5 α	<i>C. salexigens</i>	6	0.04	5 mg (g DCW) ⁻¹	Batch, in a fermentor	61
<i>E. coli</i> BW25113	<i>H. elongata</i>	25.1	1.05	4,048 mg (g DCW) ⁻¹	Whole-cell catalysis, in a fermentor	87
<i>E. coli</i> W3110	<i>H. elongata</i>	25.1	0.84	800 mg (g DCW) ⁻¹	Fed batch, in a fermentor	65
<i>E. coli</i> SK51(pASTI14)	<i>P. stutzeri</i> A1501	1.9 ^d	0.08	1,749 mg (g DCW) ⁻¹	Shake flasks	This study
5-Hydroxyectoine						
<i>E. coli</i> DH5 α	<i>P. stutzeri</i> DSM5190	NR	NR	500 μ mol (g DCW) ⁻¹ [79.1 mg (g DCW) ⁻¹]	Shake flasks	59
<i>H. polymorpha</i>	<i>H. elongata</i>	2.8		365 μ mol (g DCW) ⁻¹ [57.7 mg (g DCW) ⁻¹]	Fed batch, in a fermentor	64

^aValues in brackets were recalculated by us on the basis of the molecular mass of ectoine/hydroxyectoine.

^bDCW, dry cell weight.

^cNR, not reported.

^dMixture of ectoine and hydroxyectoine (see Fig. 9E).

references 1, 32, 59, and 66), but we find that the reported performances of these cell factories are rather difficult to compare since the growth and production conditions differ substantially (Table 3).

The recombinant cell factory described here secretes most of the newly synthesized ectoines into the growth medium (Fig. 9B and E). It shares this feature with other synthetic cell factories that rely on microbial chassis strains that do not produce ectoines naturally (61–65, 87). Investigations into the release of hydroxyectoine from a recombinant *E. coli* strain expressing the *ectD* gene from *P. stutzeri* A1501 under the control of the *tet* promoter (85) demonstrated that this process was not mediated, in the absence of an osmotic downshock, by any of the mechanosensitive channels (MscL, MscS, and MscM) operating in *E. coli* (100). In our recombinant cell factory, ectoines were efficiently secreted in strains lacking the ectoine/hydroxyectoine uptake systems ProU and ProP (68, 80, 88) (Fig. 8B), thereby firmly ruling out the possibility that these importers are somehow involved in the release of ectoines as well. Data on the release/excretion of different types of compatible solutes have been reported for cells when the natural producer bacteria lack the corresponding import systems. Examples are the release of glycine betaine synthesized from the precursor choline by *E. coli* (101), glucosylglycerol from *Synechocystis* sp. strain PCC6803 (102), ectoine from *H. elongata* (53), and proline by *Bacillus subtilis* (103). A cycle of synthesis, release, and recapture might thus help osmotically stressed cells to fine-tune the steady-state concentration of compatible solutes, and hence of turgor, in response to cellular and environmentally imposed temporary constraints and cellular imbalances during growth and cell division (103, 104).

Efflux systems for various compounds (105), in particular for amino acids, are well known to exist in microorganisms (106). While passive diffusion of ectoine and hydroxyectoine across the cytoplasmic membrane remains a possibility to explain the accumulation of ectoines in the growth medium of our cell factory (Fig. 9B and E), data reported by Jebbar et al. (68) point to the existence of a yet-unrecognized ectoine efflux system(s) in *E. coli*. Such a system may also be used for the release of types of compatible solutes that *E. coli* actually synthesizes naturally, e.g., glycine betaine from the precursor choline or trehalose (84, 101). Previously published data (53, 103) and our findings on the secretion of substantial amounts of ectoines from an *E. coli* cell factory lacking the ProU and ProP osmolyte importers (Fig. 9B and E) might aid in the setup of a genetic screening procedure to identify potential efflux systems for ectoines.

TABLE 4 *E. coli* strains used in this study

Strain ^a	Genotype	Reference or source
MC4100	F ⁻ $\Delta(\arg F-lac)U169$ <i>araD139 rpsL150 relA1 flbB5301 deoC1 ptsF25 rbsR</i>	116
RH90	F ⁻ MC4100 <i>rpoS359::Tn10</i>	112
PD32	F ⁻ MC4100 <i>hns-206::Ap^r</i>	113
RH76	F ⁻ MC4100 Δ <i>cya-851</i>	111
LC30	F ⁻ MC4100 <i>ompR::Tn10</i>	T. J. Silhavy
FF4169	F ⁻ MC4100 <i>otsA1::Tn10</i>	83
MKH17	F ⁻ MC4100 $\Delta(\textit{proU}::\textit{spc})608$	110
BK32	F ⁻ MC4100 $\Delta(\textit{putPA})101$ $\Delta(\textit{proP})2$	110
MKH13	F ⁻ MC4100 $\Delta(\textit{putPA})101$ $\Delta(\textit{proP})2$ $\Delta(\textit{proU}::\textit{spc})608$	110
SK51	F ⁻ MC4100 $\Delta(\textit{putPA})101$ $\Delta(\textit{proP})2$ $\Delta(\textit{proU}::\textit{spc})608$ <i>otsA1::Tn10</i>	This study
LC6	F ⁻ MC4100 $\Delta(\textit{putPA})101$ $\Delta(\textit{proP})2$ <i>otsA1::Tn10</i>	This study
LC7	F ⁻ MC4100 $\Delta(\textit{putPA})101$ $\Delta(\textit{proU}::\textit{spc})608$ <i>otsA1::Tn10</i>	This study

^aStrains SK51, LC6, and LC7 were constructed by transducing the *otsA1::Tn10* gene disruption mutation with P1vir into strains MKH13, BK32, and MKH17, respectively.

MATERIALS AND METHODS

Chemicals and reagents. Ectoine and 5-hydroxyectoine that were used as standards in high-performance liquid chromatography (HPLC) analysis were kindly provided by bitop AG (Witten, Germany). Acetonitrile (HPLC grade) was obtained from VWR International GmbH (Darmstadt, Germany). All other chemicals were purchased from Serva Electrophoresis GmbH (Heidelberg, Germany), Sigma-Aldrich (St. Louis, MO, USA), and Carl Roth GmbH (Karlsruhe, Germany). All compatible solutes used in this study were from laboratory stocks (107). The colorimetric substrate for β -galactosidase enzyme activity assay, o-nitrophenyl- β -D-galactopyranoside (ONPG), was obtained from Serva Electrophoresis GmbH (Heidelberg, Germany).

Media and growth conditions. All *E. coli* strains and *P. stutzeri* A1501 (67) were routinely maintained on Luria-Bertani (LB) agar plates and propagated in liquid LB medium (108). When the *E. coli* strains used contained a recombinant plasmid, chloramphenicol (30 μ g ml⁻¹) or kanamycin (50 μ g ml⁻¹) was added to the growth medium. For experiments involving the production of ectoine and hydroxyectoine or the measurement of β -galactosidase activity, *E. coli* strains were grown in minimal medium A (MMA) (108) supplemented with 0.5% (wt/vol) glucose as the carbon source, 1 mM MgSO₄, and 3 mM thiamine. When indicated, 25 mM sodium aspartate was added to the modified MMA to provide extra resources of the precursor for the biosynthesis of ectoines (17, 18, 20). The osmolarity of the growth medium was routinely adjusted by adding various concentrations of NaCl from a 5 M stock solution, as specified for the individual experiments. The osmolarity values of these media were determined with a vapor pressure osmometer (Vapor Pressure 5500; Wescor, Inc., UT). Shake flask cultures of *E. coli* strains were incubated at 37°C in a shaking water bath set to 220 rpm. Typically, a 100-ml baffled Erlenmeyer flask filled with 20 ml of growth medium was used to propagate the cultures.

Growth of *E. coli* strain SK51 harboring different plasmids (pAST11 or pAST19) leading to the synthesis of ectoines and the empty cloning vector (pHSG575) used for their construction was monitored within a time frame of 24 h in a microplate reader (Biotek Epoch2, Winooski, VT, USA) using a 48-well microplate. Cultures (500 μ l) were inoculated with a preculture of strain SK51 harboring various plasmids that had been grown in MMA overnight at 37°C to an optical density at 578 nm (OD₅₇₈) of 0.15 and were then incubated in MMA or MMA with 0.4 M NaCl for 24 h with double orbital shaking (800 circles min⁻¹) at 37°C. Optical densities of the cultures were measured once per hour.

To determine the dry weight of the formed biomass, 200-ml cultures of *E. coli* strain SK51(pAST11) (in 2-liter baffled Erlenmeyer flasks) were inoculated with a preculture grown in MMA overnight at 37°C to an OD₅₇₈ of 0.15; the cultures were grown in MMA or in MMA containing 0.4 M NaCl for 24 h in an aerial shaker (set to 200 rpm) at 37°C. Fifty-milliliter samples of the cultures were collected in weighed Falcon tubes, and the cells were then harvested by centrifugation (16,000 \times g for 10 min) in an Eppendorf tabletop centrifuge. The supernatant was discarded, and the cells were washed once with 20 ml distilled water. The cell pellet was dried overnight at 70°C. Falcon tubes with dried cell pellets were weighed and a dry cell weight (DCW) of \sim 0.25 g per OD₅₇₈ unit was calculated.

Bacterial strains and genetic construction of *E. coli* mutants. *P. stutzeri* strain A1501 (67) was kindly provided by C. Elmerich (Institute Pasteur, Paris, France). *E. coli* K-12 strain FF4169 [*otsA::Tn10*] is a derivative of strain MC4100 (109) and is deficient in the synthesis of the stress protectant trehalose (83). MC4100 is also the parent of strains BK32 [$\Delta(\textit{proP})2$ *proU*⁺], MKH17 [*proP*⁺ $\Delta(\textit{proU}::\textit{spc})608$ (Spc^r)], and MKH13 [$\Delta(\textit{proP})2$ $\Delta(\textit{proU}::\textit{spc})608$ (Spc^r)], which carry in various combinations defects in the genes encoding the ProP or ProU compatible solute uptake systems (80, 110). Strains RH76 (Δ *cya-851*) (111), RH90 (*rpoS359::Tn10*) (112), PD32 (*hns-206::Ap^r*) (113), and LC30 (*ompR::Tn10*) (from T. J. Silhavy) are also derivatives of MC4100. The genotypes of these *E. coli* strains are listed in Table 4.

Standard genetic methods such as phage P1vir-mediated transduction were performed as described previously (108). For the construction of *E. coli* strains SK51, LC6, and LC7, a P1vir phage lysate was prepared on cells of strain FF4169 [*otsA::Tn10*] and was then used to transduce the defective trehalose synthesis gene into the *otsBA*⁺ *E. coli* strains MKH13, BK32, and MKH17 (Table 4) by selecting for tetracycline-resistant colonies on LB agar plates containing 15 μ g ml⁻¹ of the antibiotic. Representative

colonies were picked and purified by restreaking several times on tetracycline-containing LB agar plates; the cells were then tested for their inability to produce trehalose in response to osmotic stress (83) using a kit purchased from Megazyme (Wicklow, Ireland).

Construction of recombinant plasmids. To monitor the transcription of the ectoine biosynthetic operon (*ectABCD-ask_ect*) of *P. stutzeri* A1501 (17, 67), a *lacZ* reporter gene fusion was constructed. To this end, a 1,057-bp DNA fragment starting upstream of *ectA* and carrying 396 bp of the *ectB* coding region (Fig. 3A) was amplified from chromosomal DNA of *P. stutzeri* A1501 using the DNA primers EctABC-D_ask_fw(SpeI) and LacZectB_rev(HindIII) (Table 5). Both the PCR fragment and the broad-host-range plasmid pBBR1MCS-2-*lacZ* (114) were digested with SpeI and HindIII prior to ligation. The resulting *ect-lacZ* reporter plasmid was pGJK4 (Table 6). In a similar fashion, a series of *ect-lacZ* reporter plasmids was constructed by systematically shortening the 5' region in front of *ectA* using a set of custom-synthesized DNA primers (Table 5) and the LacZectB_rev(HindIII) DNA primer to provide the same *ectB-lacZ* fusion junction present in plasmid pGJK4; the resulting plasmids are listed in Table 6, and their physical structures are shown in Fig. 3A and 4A. All these plasmids carry the same fusion junction between the *ectB* and *lacZ* genes (in codon 88 of *ectB*), and this leads to the production of a hybrid EctB-LacZ protein whose translation is dependent on the *ectB* ribosome-binding site. The *ectB* and *lacZ* genetic material in this gene fusion is connected by a 48-base-pair DNA region derived from the polylinker of the pBBR1MCS-2-*lacZ* cloning vector that inserts a linker peptide of 16 amino acids between the N-terminal EctB' and C-terminal LacZ proteins in the EctB-LacZ hybrid. To shorten the *ectA* and *ectB* DNA sequences present in the *ectB-lacZ* reporter plasmids, we constructed plasmids pASTI11 and pASTI12 (Fig. 4A), in which we fused codon seven of *ectA* to the *lacZ* coding region, thereby causing the synthesis of a hybrid EctA-LacZ protein. Again, a 48-base-pair region derived from the polylinker of the pBBR1MCS-2-*lacZ* cloning vector inserts a 16-amino-acid peptide between the N-terminal EctA' and C-terminal LacZ proteins in the EctA-LacZ hybrid. The translation of the hybrid *ectA-lacZ* gene fusion is dependent on the *ectA* ribosome-binding site.

A series of *ect* promoter mutants was constructed by site-directed mutagenesis using the *ectB-lacZ* reporter plasmid pGJK4 as the DNA template, custom-synthesized DNA primers (Table 5), and the Q5 site-directed mutagenesis (Q5 Site) kit (New England BioLabs GmbH, Frankfurt, Germany). This resulted in the construction of plasmids pPH1 to pPH17 and plasmids pASTI16 and pASTI17 (Table 6).

For the heterologous production of ectoine and 5-hydroxyectoine in *E. coli*, a 5,065-bp DNA fragment containing the natural *ect* promoter and the complete ectoine gene cluster (*ectABCD-ask_ect*) from *P. stutzeri* A1501 (17, 67) was cloned into the low-copy-number plasmid pHS575 (Cm^r) (89). The corresponding fragment was amplified from genomic DNA of *P. stutzeri* A1501 using the primers Pstutz_Ect-Clu_Blunt_for and Pstutz_EctClu_Blunt_rev (Table 5). The resulting DNA fragment was phosphorylated with the T4 polynucleotide kinase (Thermo Fisher Scientific Inc., Waltham, MA, USA) and was blunt-end-cloned into the linearized (by cutting with SmaI) and dephosphorylated (with FastAP; Thermo Fisher Scientific Inc., Waltham, MA, USA) DNA of pHS575 (89). The resulting plasmid was pLC68 (Fig. 1B; Table 6). After verification of the DNA sequence of the entire cloned *ectABCD-ask_ect* operon (17), selected point mutations were introduced via site-directed mutagenesis (by using the Q5 Site kit) into the -10 and -35 regions of the *ect* promoter and into the spacer region that separates these promoter elements; the resulting plasmids were pASTI1 (with a point mutation in the -35 region) and pASTI9 (with a perfect Sig⁷⁰-type promoter with a 17-bp spacing) (Table 6). Plasmid pASTI1 was used to delete the *ectD* gene from the *ect* operon by using the primers EctD_KO_for and EctD_KO_rev (Table 5); the resulting plasmid was pLC75 (Table 6). The backbone of the pHS575 cloning vector carries a *lac* promoter (89) that will generate an antisense transcript in plasmid pLC68 (Fig. 1B) and its derivatives. To inactivate the *lac* promoter on plasmid pASTI1, a consecutive change of two base pairs (see Fig. 9C) was introduced into the -10 region of the *lac* promoter via site-directed mutagenesis (by using the Q5 Site kit) using the primers plac_kaputt_for and plac_kaputt_rev (Table 5). The resulting plasmid was pASTI14 (Table 6). The correct DNA sequences of the chromosomal inserts in all plasmids constructed in this study (Table 6) were verified by DNA sequence analysis (Eurofins MWG Operon, Ebersberg, Germany); all DNA primers (Table 5) used in this study were custom synthesized by Microsynth AG (Balgach, Switzerland).

Cultivation of recombinant *E. coli* strains for the production of ectoines. For the heterologous production of ectoine and hydroxyectoine in *E. coli*, various strains were transformed with different plasmids carrying either the wild-type *ectABCD-ask_ect* gene cluster or mutant derivatives of it that either carried alterations in the *ect* promoter sequence or lacked the *ectD* gene (Table 6). Twenty-milliliter cultures (in 100-ml baffled Erlenmeyer flasks) of these plasmid-carrying *E. coli* strains were cultivated in MMA with the addition of different concentrations of NaCl and sodium aspartate and with chloramphenicol (30 μ g ml⁻¹) to select for the recombinant plasmids. The cultures were inoculated with a preculture grown in MMA overnight at 37°C to an OD₅₈₇ of 0.15 and incubated for 24 or 48 h (as indicated in the individual experiments) in a shaking water bath (set to 220 rpm and 37°C). Two-milliliter samples were collected from these cultures, and the cells were harvested by centrifugation (16,000 \times *g* for 10 min) in an Eppendorf tabletop centrifuge. The supernatant was separated from the pellet, and both samples were stored at -20°C until further analysis.

Detection and quantification of ectoines. Low-molecular-weight compounds of the *E. coli* cell pellets were extracted with 20% ethanol. For this purpose, the cell pellets were resuspended in 1 ml of 20% ethanol and were shaken for 1 h. After centrifugation at 16,000 \times *g* (4°C for 30 min) to remove cell debris, the ethanolic extracts were transferred into fresh Eppendorf tubes, and the ethanol was removed by evaporation (at 55°C for 20 h). The resulting dried material was resuspended in 100 μ l of distilled water, and insoluble material was removed by centrifugation (16,000 \times *g* at 4°C for 30 min). The extracted samples and the cell-free supernatant derived from the corresponding cell cultures were

TABLE 5 DNA primers used in this study

Plasmid	Primer name	Primer sequence ^a
pGJK4	EctABCD_ask_fw(SpeI) LacZectB_rev(HindIII)	AAAAAAGCTAGTCCGTCAGTCAGAGAACTTCTGACG AAAAAAGCTTGAAGGTTTCGAGGAAACGCTC
pNST22 (K1)	LacZ_ectB_K2(BamHI) LacZectB_rev(HindIII)	AAAAGGATCCCTGAATTCAAATTGCATTTTCGGTG AAAAAAGCTTGAAGGTTTCGAGGAAACGCTC
pNST21 (K2)	LacZ_ectB_K1(BamHI) LacZectB_rev(HindIII)	AAAAGGATCCGGCAAGCTGACCACCGCAATAC AAAAAAGCTTGAAGGTTTCGAGGAAACGCTC
pNST26 (K3)	LacZ_ectB_K6(BamHI) LacZectB_rev(HindIII)	AAAAGGATCCACAGAAACATTCTGCGCGC AAAAAAGCTTGAAGGTTTCGAGGAAACGCTC
pNST27 (K4)	LacZ_ectB_K7(BamHI) LacZectB_rev(HindIII)	AAAAGGATCCCTGCGCGCCAGCATAGTTATC AAAAAAGCTTGAAGGTTTCGAGGAAACGCTC
pNST28 (K5)	LacZ_ectB_K8(BamHI) LacZectB_rev(HindIII)	AAAAGGATCCGCGGGTTTCAGCGGCATATAC AAAAAAGCTTGAAGGTTTCGAGGAAACGCTC
pNST29 (K6)	LacZ_ectB_K9(BamHI) LacZectB_rev(HindIII)	AAAAGGATCCCGCAAACCTCCCATATTCGGTTAC AAAAAAGCTTGAAGGTTTCGAGGAAACGCTC
pNST40 (K7)	LacZ_ectB_K11(BamHI) LacZectB_rev(HindIII)	AAAAGGATCCACTTGTGCGGATATGCCTACCTC AAAAAAGCTTGAAGGTTTCGAGGAAACGCTC
pNST41 (K8)	LacZ_ectB_K13(BamHI) LacZectB_rev(HindIII)	AAAAGGATCCCCACCGTAATGCTCCGTCGC AAAAAAGCTTGAAGGTTTCGAGGAAACGCTC
pNST39 (K9)	LacZ_ectB_K10(BamHI) LacZectB_rev(HindIII)	AAAAGGATCCCGTTACATGGAAACCACTATCTCG AAAAAAGCTTGAAGGTTTCGAGGAAACGCTC
pASTI11	KlacZ-for K11ectAshort-rev	AAGCTTATCGATACCGTCGACCTC CATTACGGTGGGAAACTCAAACAAT
pASTI12	KlacZ-for K11ectAshort-rev	AAGCTTATCGATACCGTCGACCTC CATTACGGTGGGAAACTCAAACAAT
pPH1 (Mut 1)	Mut_35_TTzuGG_for Mut_35_TTzuGG_rev	GTTACATGGGgGAGAAACTTGTGC GGAATATGGGAAGTTTGC
pPH7 (Mut2)	Mut_10_TzuC_for Mut_10_TzuC_rev	ATGCCTACCCcAAAAAGGAATTC ATCCGCACAAGTTTCTCAAC
pPH4 (Mut3)	Mut_Spacer_Del3_for Mut_Spacer_Del3_rev	GGATATGCCTACCCTAAAAAG ACAAGTTTCTCAACCCATG
pPH2 (Mut4)	Mut_Spacer_Del1_for Mut_Spacer_Del1_rev	CGGATATGCCTACCCTAAAAAG ACAAGTTTCTCAACCCATGTAAC
pPH3 (Mut5)	Mut_Spacer_Del2_for Mut_Spacer_Del2_rev	TGCCTACCCTAAAAAGGAATTC ATCCGCACAAGTTTCTCAAC
pPH17 (Mut6)	Mut_Spacer_In1_for Mut_Spacer_In1_rev	tATATGCCTACCCTAAAAAG CCGCACAAGTTTCTCAAC
pPH5 (Mut7)	Mut_10_CzuT_for Mut_10_CzuT_rev	GATATGCCTAtCCTAAAAAGGAATTC CGCACAAGTTTCTCAACC
pPH14 (Mut8)	Mut_10_1. CzuA_for Mut_10_1. CzuA_rev	GATATGCCTAaCCTAAAAAGG CGCACAAGTTTCTCAACC
pPH15 (Mut9)	Mut_10_2. CzuT_for Mut_10_2. CzuT_rev	ATATGCCTACTtCTAAAAAGGAATTC CCGCACAAGTTTCTCAAC
pPH16 (Mut10)	Mut_10_3. CzuT_for Mut_10_3. CzuT_rev	TATGCCTACCtTAAAAAGGAATTC TCCGCACAAGTTTCTCAAC
pPH6 (Mut11)	Mut_10_CCzuAA_for Mut_10_CCzuAA_rev	ATATGCCTACaaTAAAAAGGAATTCATCAAC CCGCACAAGTTTCTCAAC

(Continued on next page)

TABLE 5 (Continued)

Plasmid	Primer name	Primer sequence ^a
pPH8 (Mut12)	Mut_35_perfekt_for Mut_35_perfekt_rev	CATGGGTTGAcAAACTTGTGC TAACGGAATATGGGAAGTTTG
pPH9 (Mut13)	Mut_10_perfekt_for Mut_10_perfekt_rev	GATATGCCTA taa TAAAAAGGAATTCAATCAACAAC CGCACAAAGTTTCTCAACC
pPH10 (Mut14)	Mut_10_perfekt_for Mut_10_perfekt_rev	GATATGCCTA taa TAAAAAGGAATTCAATCAACAAC CGCACAAAGTTTCTCAACC
pPH11 (Mut15)	Mut_Spacer_Del1_for Mut_Spacer_Del1_rev	CGGATATGCCTACCCTAAAAAG ACAAGTTTCTCAACCCATGTAAC
pPH12 (Mut16)	Mut_Spacer_Del2_for Mut_Spacer_Del2_rev	TGCCTACCCTAAAAAGGAATTC ATCCGCACAAGTTTCTCAAC
pPH13 (Mut17)	Mut_Spacer_Del3_for Mut_Spacer_Del3_rev	GGATATGCCTACCCTAAAAAG ACAAGTTTCTCAACCCATG
pASTI16 (Mut18)	Del_TG_for Del_TG_rev	CTACCCTAAAAAGGAATTC CATATCCGCACAAGTTTC
pASTI17 (Mut19)	pGJK4_GGGTA_for pGJK4_GGGTA_rev	ACGCAAACCT gggta ATTCCGTTACATGGGTTGAGAA ACTTGTGCTGTATATGCCGCTGA
pLC68	Pstutz_EctClu_Blunt_for Pstutz_EctClu_Blunt_rev	CCGCAATACACAGAAACATTCTG CTTGCAGCCATGGTCCTC
pASTI1	Mut_35_perfekt_for Mut_35_perfekt_rev	CATGGGTTGAcAAACTTGTGC TAACGGAATATGGGAAGTTTG
pLC75	EctD_KO_for EctD_KO_rev	CAGTATCTCTGAGGCGATGG GTCGGCTTGCATAGGGTTC
pASTI9	Mut_35_perfekt_for Mut_35_perfekt_rev	CATGGGTTGAcAAACTTGTGC TAACGGAATATGGGAAGTTTG
pASTI14	plac_kaputt_for plac_kaputt_rev	AATTCCACAC cc CATACGAGCC GTGAGCGGATAACAATTC

^aMutations are indicated with bold lowercase letters.

diluted 10-fold with distilled water and acetonitrile (the final concentration of acetonitrile was 50%) and analyzed for their ectoine/5-hydroxyectoine content by isocratic high-performance liquid chromatography (HPLC) (24). For these measurements, we employed an Agilent 1260 Infinity LC system (Agilent, Waldbronn, Germany) and a Grom-Sil Amino 1PR column (Grom, Rottenburg-Hailfingen, Germany) essentially as described previously (24) with the exception that a 1260 Infinity diode array detector (DAD) (Agilent) was used instead of the previously used UV/visible detector system (24, 85). The ectoine and 5-hydroxyectoine contents of HPLC-analyzed samples were quantified using the OpenLAB software suite (Agilent). Standard curves for the calculation of the ectoine and 5-hydroxyectoine concentrations were determined with commercially available samples.

Quantification of intracellular trehalose. Cells of *E. coli* strains MC4100, FF4169, SK51, LC6, and LC7 (Table 4) were grown in MMA without and with the addition of 0.4 M NaCl until they reached an OD₅₇₈ of 1. One-milliliter samples of the cultures were harvested by centrifugation, and trehalose was extracted from the cells using the ethanolic extraction protocol used for the recovery of ectoines. The dried pellet was resuspended in 100 μ l distilled water (dH₂O). The trehalose content of the samples was determined with a commercially available kit from Megazyme (Wicklow, Ireland) according to the manufacturer's protocol. The *otsBA*⁺ strain MC4100 accumulated 0.65 μ M trehalose per OD₅₇₈ unit when it was grown in MMA without NaCl and 25.5 μ M trehalose per OD₅₇₈ unit when it was grown in MMA in the presence of 0.4 M NaCl. Strains FF4169, SK51, LC6, and LC7, all of which carry the (*otsA::Tn10*)1 mutation (Table 4), contained between 0.56 μ M and 1.5 μ M trehalose per OD₅₇₈ unit regardless of the absence or presence of 0.4 M NaCl in the growth medium.

Detection and quantification of aspartate. Two-milliliter samples of 200-ml cultures of strain *E. coli* SK51(pASTI1) (grown for 24 h in 2-liter baffled Erlenmeyer flasks) were collected by centrifugation (16,000 \times g for 10 min) in an Eppendorf tabletop centrifuge. The supernatant was separated from the pellet and stored at -20°C until further analysis. For the analysis of the aspartate content, the samples were diluted to an estimated aspartate concentration of 0.5 to 1 mM with distilled water, and 1- μ l aliquots were derivatized using 2 μ l of 10 mM 9-fluorenylmethoxy carbonyl (Fmoc). Excessive Fmoc was removed by adding 3 μ l of 40 mM 1-adamantylamine hydrochloride (ADAM) to the samples. Distilled

TABLE 6 Plasmids used in this study

Plasmid	Description and mutations ^a	Reference or source
pBBR1MCS-2- <i>lacZ</i>	Broad-host-range cloning vector for <i>lacZ</i> reporter gene fusions; Kan ^r	114
pHSG575	Low-copy-number cloning vector; Cat ^r	89
pGJK4	pBBR1MCS-2- <i>lacZ</i> with 1,057-bp fragment starting upstream of <i>ectA</i> and including <i>ectA</i> and 396 bp of <i>ectB</i> ; Kan ^r	This study
pNST22 (K1)	pGJK4 derivative with 1,010-bp fragment starting upstream of <i>ectA</i> and including <i>ectA</i> and 396 bp of <i>ectB</i> ; Kan ^r	This study
pNST21 (K2)	pGJK4 derivative with 970-bp fragment starting upstream of <i>ectA</i> and including <i>ectA</i> and 396 bp of <i>ectB</i> ; Kan ^r	This study
pNST26 (K3)	pGJK4 derivative with 953-bp fragment starting upstream of <i>ectA</i> and including <i>ectA</i> and 396 bp of <i>ectB</i> ; Kan ^r	This study
pNST27 (K4)	pGJK4 derivative with 942-bp fragment starting upstream of <i>ectA</i> and including <i>ectA</i> and 396 bp of <i>ectB</i> ; Kan ^r	This study
pNST28 (K5)	pGJK4 derivative with 918-bp fragment starting upstream of <i>ectA</i> and including <i>ectA</i> and 396 bp of <i>ectB</i> ; Kan ^r	This study
pNST29 (K6)	pGJK4 derivative with 892-bp fragment starting upstream of <i>ectA</i> and including <i>ectA</i> and 396 bp of <i>ectB</i> ; Kan ^r	This study
pNST40 (K7)	pGJK4 derivative with 856-bp fragment starting upstream of <i>ectA</i> and including <i>ectA</i> and 396 bp of <i>ectB</i> ; Kan ^r	This study
pNST41 (K8)	pGJK4 derivative with 786-bp fragment starting upstream of <i>ectA</i> and including <i>ectA</i> and 396 bp of <i>ectB</i> ; Kan ^r	This study
pNST39 (K9)	pGJK4 derivative with 472-bp fragment starting upstream of <i>ectA</i> and including <i>ectA</i> and 396 bp of <i>ectB</i> ; Kan ^r	This study
pASTI11	pNST29 derivative with 116-bp fragment starting upstream of <i>ectA</i> and including 18 bp of <i>ectA</i> ; Kan ^r	This study
pASTI12	pGJK4 derivative with 285-bp fragment starting upstream of <i>ectA</i> and including 18 bp of <i>ectA</i> ; Kan ^r	This study
pPH1 (Mut 1)	pGJK4 derivative with a mutation in the −35 region of the <i>ect</i> promoter; TTGAGA → GGGAGA ; Kan ^r	This study
pPH7 (Mut2)	pGJK4 derivative with a mutation in the −10 region of the <i>ect</i> promoter, TACCT → TACCC ; Kan ^r	This study
pPH4 (Mut3)	pGJK4 derivative with a 2-bp (CG) deletion in the spacer of the <i>ect</i> promoter; Kan ^r	This study
pPH2 (Mut4)	pGJK4 derivative with a 1-bp (G) deletion in the spacer of the <i>ect</i> promoter; Kan ^r	This study
pPH3 (Mut5)	pGJK4 derivative with a 1-bp (A) deletion in the spacer of the <i>ect</i> promoter; Kan ^r	This study
pPH17 (Mut6)	pGJK4 derivative with a 1-bp (T) insertion in the spacer of the <i>ect</i> promoter; Kan ^r	This study
pPH5 (Mut7)	pGJK4 derivative with a mutation in the −10 region of the <i>ect</i> promoter, TACCT → TATCCT ; Kan ^r	This study
pPH14 (Mut8)	pGJK4 derivative with a mutation in the −10 region of the <i>ect</i> promoter, TACCT → TAACCT ; Kan ^r	This study
pPH15 (Mut9)	pGJK4 derivative with a mutation in the −10 region of the <i>ect</i> promoter, TACCT → TACTCT ; Kan ^r	This study
pPH16 (Mut10)	pGJK4 derivative with a mutation in the −10 region of the <i>ect</i> promoter, TACCT → TACCTT ; Kan ^r	This study
pPH6 (Mut11)	pGJK4 derivative with a mutation in the −10 region of the <i>ect</i> promoter, TACCT → TACAAT ; Kan ^r	This study
pPH8 (Mut12)	pGJK4 derivative with a mutation in the −35 region of the <i>ect</i> promoter, TTGAGA → TTGACA ; Kan ^r	This study
pPH9 (Mut13)	pGJK4 derivative with a mutation in the −10 region of the <i>ect</i> promoter, TACCT → TATAAT ; Kan ^r	This study
pPH10 (Mut14)	pPH8 derivative with a mutation in the −10 region of the <i>ect</i> promoter, TACCT → TATAAT ; Kan ^r	This study
pPH11 (Mut15)	pPH10 derivative with a 1-bp deletion (G) in the spacer of the <i>ect</i> promoter leading to a perfect Sig ⁷⁰ -type promoter; Kan ^r	This study
pPH12 (Mut16)	pPH10 derivative with a 1 bp deletion (A) in the spacer of the <i>ect</i> promoter leading to a perfect Sig ⁷⁰ -type promoter; Kan ^r	This study
pPH13 (Mut17)	pPH10 derivative with a 2-bp deletion (GC) in the spacer of the <i>ect</i> promoter leading to a 16-bp spacer; Kan ^r	This study
pASTI16 (Mut18)	pGJK4 derivative with a 1-bp (C) deletion in the spacer of the <i>ect</i> promoter leading to a TG motif at position −16 at the <i>ect</i> promoter; Kan ^r	This study
pASTI17 (Mut19)	pGJK4 derivative with a mutation in the inverted repeat upstream of the <i>ect</i> promoter, CCCAT → GGGTA ; Kan ^r	This study
pLC68	pHSG575 containing a 5,065-bp fragment of the ectoine gene cluster from <i>P. stutzeri</i> A1501; Cat ^r	This study
pASTI1	pLC68 derivative with a mutation in the −35 region of the <i>ect</i> promoter, TTGAGA → TTGACA ; Cat ^r	This study
pLC75	Derivative of plasmid pASTI1 carrying an 885-bp in-frame deletion of <i>ectD</i> ; Cat ^r	This study
pASTI9	Derivative of plasmid pASTI1 carrying a mutant <i>ect</i> promoter changed to the consensus sequence of a Sig ⁷⁰ -type promoter; Cat ^r	This study
pASTI14	a-derivative of plasmid pASTI1 with an inactivated <i>lac</i> promoter, TATGTT → TATGGG ; Cat ^r	This study

^aMutations are indicated with bold letters. Kan^r, the plasmid confers resistance to the antibiotic kanamycin; Cat^r, the plasmid confers resistance to the antibiotic chloramphenicol.

water (494 μ l) was then added to this solution and analyzed for its aspartate content by isocratic high-performance liquid chromatography (HPLC). For these measurements, we employed an Agilent 1260 Infinity LC system (Agilent, Waldbronn, Germany) and a Gemini 5- μ m C₁₈ 110-Å column (Phenomenex, Torrance, CA, USA). Two different solvents (solvent A, 40 mM NaH₂PO₄, pH 7.8; solvent B, 55% HPLC-grade distilled water plus 45% acetonitrile plus 0.1% trifluoroacetic acid [TFA]) were used to create the following gradient: 0 min, 0% solvent B; 2 min, 50% solvent B; 11 min, 70% solvent B; 16 min, 100% solvent B; 24 min, 100% solvent B; 24.5 min, 0% solvent B; and 27 min, 0% solvent B. The flow rate was set to 1 ml min^{−1}, and the temperature for the measurements of the samples was 40°C. The aspartate content of the analyzed samples was quantified using the OpenLAB software suite (Agilent). Standard curves for the calculation of the aspartate concentrations were determined with commercially available samples.

Determination of extracellular glucose concentrations. Two-milliliter samples of various cell cultures were collected by centrifugation (16,000 $\times g$ for 10 min) in an Eppendorf tabletop centrifuge. The supernatants were stored at −20°C until further analysis. The glucose content of these samples was determined with a commercially available kit from Megazyme (Wicklow, Ireland) according to the manufacturer's protocol. Standard curves for the calculation of the glucose concentrations were determined with commercially available reference material.

β -Galactosidase reporter enzyme assays. The *ect-lacZ* reporter gene plasmids (Table 6) were introduced into various *E. coli* strains via routine DNA transformation procedures. Twenty-milliliter cultures (in 100-ml Erlenmeyer flasks) of these plasmid-bearing strains were grown in a shaking water bath at 37°C in MMA with or without the addition of NaCl and in the presence of various types of

compatible solutes until the cultures reached an OD_{587} of between 1.8 and 2. Two-milliliter samples of the cultures were harvested by centrifugation ($16,000 \times g$ for 10 min) and assayed for β -galactosidase activity as described previously (108) using the chromogenic compound ONPG as the substrate. The β -galactosidase enzyme activity is expressed in Miller units (108). Plasmid pBBR1MCS-2-*lacZ* (114), which was used to construct the *ect-lacZ* reporter fusions, was used as a control, and its presence in strains with the entire *lacZYA* operon deleted (Table 4) yielded a background activity of 0 to 2 Miller units.

SDS gels and Western blot analysis. The production of the β -galactosidase protein in *E. coli* strains harboring pBBR1MCS-2 *ect-lacZ* reporter fusions was analyzed by SDS-polyacrylamide gel electrophoresis as described previously (81). For this purpose, the cultures were harvested when they reached late log phase (OD_{587} between 1.8 and 2.2); the volume of the harvested cell culture (2 ml) was adjusted such that the harvested cells of the various cultures possessed the same OD_{587} . For Western blot analysis of these samples, cell pellets were resuspended in 350 μ l of 2 \times loading buffer (0.5 ml β -mercaptoethanol, 0.25 ml 0.1% bromophenol blue, 4 ml 10% SDS, 5.3 ml 2 \times sample buffer [consisting of 21 ml 0.5 M Tris-HCl (pH 6.8), 0.4% SDS, and 34 ml glycerol per liter]) and incubated for 5 min at 95°C. After centrifugation of the disrupted cells in an Eppendorf tabletop centrifuge (5 min, $16,000 \times g$), 30- μ l portions of the supernatants of these samples were applied to a 7% SDS-polyacrylamide gel. The electrophoretically separated proteins from the *E. coli* cell extracts were transferred to a polyvinylidene difluoride (PVDF) membrane (Immobilon-FL; purchased from Merck Millipore Ltd., Darmstadt, Germany) via semidry blotting. Western blotting of the transferred proteins was performed with a primary rabbit antiserum directed against a hybrid ProW-LacZ fusion protein. This antiserum recognizes the inner membrane component (ProW) of the *E. coli* ProU ABC transport system (80) and the β -galactosidase portion of the hybrid protein (115). The immune complex formed on the blotting membrane was detected with a secondary IRDye 800CW fluorescently labeled donkey anti-rabbit IgG antibody (purchased from Li-Cor, Lincoln, NE, USA). Incubation with the ProW-LacZ antibody was performed in Odyssey blocking buffer (purchased from Li-Cor) with 0.2% Tween. For the incubation of the blotting membrane with the second antibody, 0.01% SDS was additionally added to the bathing solution. Signals were detected by fluorescence imaging at 800 nm using an imager system (Odyssey Fc; Li-Cor, Lincoln, NE, USA) by exposing the membrane for 2 min.

SUPPLEMENTAL MATERIAL

Supplemental material for this article may be found at <https://doi.org/10.1128/AEM.01772-17>.

SUPPLEMENTAL FILE 1, PDF file, 2.0 MB.

ACKNOWLEDGMENTS

We thank Oliver Dähn and Florian Kindinger for their participation during the exploratory phase of the project, Susanne Kneip for help with strain constructions, and Alexandra Richter for help with the measurement of the aspartate contents of supernatants of various bacterial cultures by HPLC analysis. We are very grateful to Jutta Gade and Jochen Sohn for their dedicated and expert technical assistance during part of this project. We thank bitop AG (Witten, Germany) for the generous gifts of ectoine and hydroxyectoine reference samples. We appreciate the kind donation of *E. coli* strains by Arne Strom (University of Trondheim, Norway), Regine Hengge (Humboldt University, Berlin, Germany), and Tom Silhavy (Princeton University, USA), of the *P. stutzeri* A1501 strain by Claudine Elmerich (Institute Pasteur, Paris, France), and of the reporter plasmid pBBR1MCS2-*lacZ* by Jürgen Lassak (Ludwig Maximilian University, Munich, Germany). We thank Katrin Ritter for a sample of the ProW-LacZ antiserum. We are grateful to Vickie Koogle for her expert help in the language editing of our manuscript, and we thank our colleague Tamara Hoffmann for insightful discussions.

This work was financially supported by grants from the Deutsche Forschungsgemeinschaft (DFG) through the SFB 987 and by the LOEWE excellence program of the state of Hessen (via the Center for Synthetic Microbiology). L.C. was supported by a Ph.D. fellowship from the International Max Planck Research School for Environmental, Cellular and Molecular Microbiology (IMPRS-Mic, Marburg).

REFERENCES

- Pastor JM, Salvador M, Argandona M, Bernal V, Reina-Bueno M, Csonka LN, Iborra JL, Vargas C, Nieto JJ, Canovas M. 2010. Ectoines in cell stress protection: uses and biotechnological production. *Biotechnol Adv* 28: 782–801. <https://doi.org/10.1016/j.biotechadv.2010.06.005>.
- Kempf B, Bremer E. 1998. Uptake and synthesis of compatible solutes as microbial stress responses to high osmolality environments. *Arch Microbiol* 170:319–330. <https://doi.org/10.1007/s002030050649>.
- Widderich N, Höppner A, Pittelkow M, Heider J, Smits SH, Bremer E. 2014. Biochemical properties of ectoine hydroxylases from extremophiles and their wider taxonomic distribution among microorganisms. *PLoS One* 9:e93809. <https://doi.org/10.1371/journal.pone.0093809>.
- Widderich N, Czech L, Elling FJ, Könneke M, Stöveken N, Pittelkow M, Rieckle R, Dickschat JS, Heider J, Bremer E. 2016. Strangers in the archaeal world: osmopressure-responsive biosynthesis of ectoine and hydroxyectoine by the

- marine thaumarchaeon *Nitrosopumilus maritimus*. *Environ Microbiol* 18: 1227–1248. <https://doi.org/10.1111/1462-2920.13156>.
5. Harding T, Brown MW, Simpson AG, Roger AJ. 2016. Osmoadaptive strategy and its molecular signature in obligately halophilic heterotrophic protists. *Genome Biol Evol* 8:2241–2258. <https://doi.org/10.1093/gbe/evw152>.
 6. Street TO, Bolen DW, Rose GD. 2006. A molecular mechanism for osmolyte-induced protein stability. *Proc Natl Acad Sci U S A* 103: 13997–14002. <https://doi.org/10.1073/pnas.0606236103>.
 7. Street TO, Krukenberg KA, Rosgen J, Bolen DW, Agard DA. 2010. Osmolyte-induced conformational changes in the Hsp90 molecular chaperone. *Protein Sci* 19:57–65. <https://doi.org/10.1002/pro.282>.
 8. Borwankar T, Rothlein C, Zhang G, Techen A, Dosche C, Ignatova Z. 2011. Natural osmolytes remodel the aggregation pathway of mutant huntingtin exon 1. *Biochemistry* 50:2048–2060. <https://doi.org/10.1021/bi1018368>.
 9. Bourot S, Sire O, Trautwetter A, Touze T, Wu LF, Blanco C, Bernard T. 2000. Glycine betaine-assisted protein folding in a *lysA* mutant of *Escherichia coli*. *J Biol Chem* 275:1050–1056. <https://doi.org/10.1074/jbc.275.2.1050>.
 10. Cayley S, Lewis BA, Record MT, Jr. 1992. Origins of the osmoprotective properties of betaine and proline in *Escherichia coli* K-12. *J Bacteriol* 174:1586–1595. <https://doi.org/10.1128/jb.174.5.1586-1595.1992>.
 11. Stadtmiller SS, Gorenske-Benitez AH, Guseman AJ, Pielak GJ. 2017. Osmotic shock induced protein destabilization in living cells and its reversal by glycine betaine. *J Mol Biol* 429:1155–1161. <https://doi.org/10.1016/j.jmb.2017.03.001>.
 12. Bremer E, Krämer R. 2000. Coping with osmotic challenges: osmoregulation through accumulation and release of compatible solutes, p 79–97. In Storz G, Hengge-Aronis R (ed), *Bacterial stress responses*. ASM Press, Washington DC, USA.
 13. Wood JM. 2011. Bacterial osmoregulation: a paradigm for the study of cellular homeostasis. *Annu Rev Microbiol* 65:215–238. <https://doi.org/10.1146/annurev-micro-090110-102815>.
 14. Wood JM, Bremer E, Csonka LN, Krämer R, Poolman B, van der Heide T, Smith LT. 2001. Osmosensing and osmoregulatory compatible solute accumulation by bacteria. *Comp Biochem Physiol A Mol Integr Physiol* 130:437–460. [https://doi.org/10.1016/S1095-6433\(01\)00442-1](https://doi.org/10.1016/S1095-6433(01)00442-1).
 15. Csonka LN. 1989. Physiological and genetic responses of bacteria to osmotic stress. *Microbiol Rev* 53:121–147.
 16. Lo CC, Bonner CA, Xie G, D'Souza M, Jensen RA. 2009. Cohesion group approach for evolutionary analysis of aspartokinase, an enzyme that feeds a branched network of many biochemical pathways. *Microbiol Mol Biol Rev* 73:594–651. <https://doi.org/10.1128/MMBR.00024-09>.
 17. Stöveken N, Pittelkow M, Sinner T, Jensen RA, Heider J, Bremer E. 2011. A specialized aspartokinase enhances the biosynthesis of the osmoprotectants ectoine and hydroxyectoine in *Pseudomonas stutzeri* A1501. *J Bacteriol* 193:4456–4468. <https://doi.org/10.1128/JB.00345-11>.
 18. Bestvater T, Louis P, Galinski EA. 2008. Heterologous ectoine production in *Escherichia coli*: by-passing the metabolic bottle-neck. *Saline Sys* 4:12. <https://doi.org/10.1186/1746-1448-4-12>.
 19. Reshetnikov AS, Khmelenina VN, Trotsenko YA. 2006. Characterization of the ectoine biosynthesis genes of haloalkalotolerant obligate methanotroph "*Methylomicrobium alcaliphilum* 20Z." *Arch Microbiol* 184: 286–297.
 20. Ono H, Sawada K, Khunajakr N, Tao T, Yamamoto M, Hiramoto M, Shinmyo A, Takano M, Murooka Y. 1999. Characterization of biosynthetic enzymes for ectoine as a compatible solute in a moderately halophilic eubacterium, *Halomonas elongata*. *J Bacteriol* 181:91–99.
 21. Bursy J, Pierik AJ, Pica N, Bremer E. 2007. Osmotically induced synthesis of the compatible solute hydroxyectoine is mediated by an evolutionarily conserved ectoine hydroxylase. *J Biol Chem* 282:31147–31155. <https://doi.org/10.1074/jbc.M704023200>.
 22. Höppner A, Widderich N, Lenders M, Bremer E, Smits SHJ. 2014. Crystal structure of the ectoine hydroxylase, a snapshot of the active site. *J Biol Chem* 289:29570–29583. <https://doi.org/10.1074/jbc.M114.576769>.
 23. Louis P, Galinski EA. 1997. Characterization of genes for the biosynthesis of the compatible solute ectoine from *Marinococcus halophilus* and osmoregulated expression in *Escherichia coli*. *Microbiology* 143: 1141–1149. <https://doi.org/10.1099/00221287-143-4-1141>.
 24. Kuhlmann AU, Bremer E. 2002. Osmotically regulated synthesis of the compatible solute ectoine in *Bacillus pasteurii* and related *Bacillus* spp. *Appl Environ Microbiol* 68:772–783. <https://doi.org/10.1128/AEM.68.2.772-783.2002>.
 25. Vargas C, Argandona M, Reina-Bueno M, Rodriguez-Moya J, Fernandez-Aunon C, Nieto JJ. 2008. Unravelling the adaptation responses to osmotic and temperature stress in *Chromohalobacter salexigens*, a bacterium with broad salinity tolerance. *Saline Sys* 4:14. <https://doi.org/10.1186/1746-1448-4-14>.
 26. Schwibbert K, Marin-Sanguino A, Bagyan I, Heidrich G, Lentzen G, Seitz H, Rampp M, Schuster SC, Klenk HP, Pfeiffer F, Oesterheld T, Kunte HJ. 2011. A blueprint of ectoine metabolism from the genome of the industrial producer *Halomonas elongata* DSM 2581^T. *Environ Microbiol* 13:1973–1994. <https://doi.org/10.1111/j.1462-2920.2010.02336.x>.
 27. Calderon MI, Vargas C, Rojo F, Iglesias-Guerra F, Csonka LN, Ventosa A, Nieto JJ. 2004. Complex regulation of the synthesis of the compatible solute ectoine in the halophilic bacterium *Chromohalobacter salexigens* DSM 3043^T. *Microbiology* 150:3051–3063. <https://doi.org/10.1099/mic.0.27122-0>.
 28. Mustakhimov II, Reshetnikov AS, Glukhov AS, Khmelenina VN, Kalyuzhnaya MG, Trotsenko YA. 2010. Identification and characterization of EctR1, a new transcriptional regulator of the ectoine biosynthesis genes in the halotolerant methanotroph *Methylomicrobium alcaliphilum* 20Z. *J Bacteriol* 192:410–417. <https://doi.org/10.1128/JB.00553-09>.
 29. Shikuma NJ, Davis KR, Fong JNC, Yildiz FH. 2013. The transcriptional regulator, CosR, controls compatible solute biosynthesis and transport, motility and biofilm formation in *Vibrio cholerae*. *Environ Microbiol* 15:1387–1399. <https://doi.org/10.1111/j.1462-2920.2012.02805.x>.
 30. Shao Z, Deng W, Li S, He J, Ren S, Huang W, Lu Y, Zhao G, Cai Z, Wang J. 2015. GlnR-mediated regulation of *ectABCD* transcription expands the role of the GlnR regulon to osmotic stress management. *J Bacteriol* 197:3041–3307. <https://doi.org/10.1128/JB.00185-15>.
 31. Bursy J, Kuhlmann AU, Pittelkow M, Hartmann H, Jebbar M, Pierik AJ, Bremer E. 2008. Synthesis and uptake of the compatible solutes ectoine and 5-hydroxyectoine by *Streptomyces coelicolor* A3(2) in response to salt and heat stresses. *Appl Environ Microbiol* 74:7286–7296. <https://doi.org/10.1128/AEM.00768-08>.
 32. Kunte HJ, Lentzen G, Galinski E. 2014. Industrial production of the cell protectant ectoine: protection, mechanisms, processes, and products. *Curr Biotechnol* 3:10–25. <https://doi.org/10.2174/22115501113026660037>.
 33. Kuhlmann AU, Hoffmann T, Bursy J, Jebbar M, Bremer E. 2011. Ectoine and hydroxyectoine as protectants against osmotic and cold stress: uptake through the SigB-controlled betaine-choline-carnitine transporter-type carrier EctT from *Virgibacillus pantothenicus*. *J Bacteriol* 193:4699–4708. <https://doi.org/10.1128/JB.05270-11>.
 34. Garcia-Esteva R, Argandona M, Reina-Bueno M, Capote N, Iglesias-Guerra F, Nieto JJ, Vargas C. 2006. The *ectD* gene, which is involved in the synthesis of the compatible solute hydroxyectoine, is essential for thermoprotection of the halophilic bacterium *Chromohalobacter salexigens*. *J Bacteriol* 188:3774–3784. <https://doi.org/10.1128/JB.00136-06>.
 35. Ma Y, Wang Q, Xu W, Liu X, Gao X, Zhang Y. 2017. Stationary phase-dependent accumulation of ectoine is an efficient adaptation strategy in *Vibrio anguillarum* against cold stress. *Microbiol Res* 205:8–18. <https://doi.org/10.1016/j.micres.2017.08.005>.
 36. Zaccai G, Bagyan I, Combet J, Cuello GJ, Deme B, Fichou Y, Gallat FX, Galvan Josa VM, von Gronau S, Haertlein M, Martel A, Moulin M, Neumann M, Weik M, Oesterheld D. 2016. Neutrons describe ectoine effects on water H-bonding and hydration around a soluble protein and a cell membrane. *Sci Rep* 6:31434. <https://doi.org/10.1038/srep31434>.
 37. Hahn MB, Solomun T, Wellhausen R, Hermann S, Seitz H, Meyer S, Kunte HJ, Zeman J, Uhlig F, Smiatek J, Sturm H. 2015. Influence of the compatible solute ectoine on the local water structure: implications for the binding of the protein GSP to DNA. *J Phys Chem B* 119: 15212–15220. <https://doi.org/10.1021/acs.jpcc.5b09506>.
 38. Knapp S, Ladenstein R, Galinski EA. 1999. Extrinsic protein stabilization by the naturally occurring osmolytes beta-hydroxyectoine and betaine. *Extremophiles* 3:191–198. <https://doi.org/10.1007/s007920050116>.
 39. Tanne C, Golovina EA, Hoekstra FA, Meffert A, Galinski EA. 2014. Glass-forming property of hydroxyectoine is the cause of its superior function as a desiccation protectant. *Front Microbiol* 5:150. <https://doi.org/10.3389/fmicb.2014.00150>.
 40. Schnoor M, Voss P, Cullen P, Boking T, Galla HJ, Galinski EA, Lorkowski S. 2004. Characterization of the synthetic compatible solute homoeoctoine as a potent PCR enhancer. *Biochem Biophys Res Commun* 322:867–872. <https://doi.org/10.1016/j.bbrc.2004.07.200>.
 41. Lippert K, Galinski EA. 1992. Enzyme stabilization by ectoine-type compatible solutes: protection against heating, freezing and drying. *Applied Microbial Biotechnology* 37:61–65. <https://doi.org/10.1007/BF00174204>.

42. Manzanera M, Garcia de Castro A, Tondervik A, Rayner-Brandes M, Strom AR, Tunnacliffe A. 2002. Hydroxyectoine is superior to trehalose for anhydrobiotic engineering of *Pseudomonas putida* KT2440. *Appl Environ Microbiol* 68:4328–4333. <https://doi.org/10.1128/AEM.68.9.4328-4333.2002>.
43. Manzanera M, Vilchez S, Tunnacliffe A. 2004. High survival and stability rates of *Escherichia coli* dried in hydroxyectoine. *FEMS Microbiol Lett* 233:347–352. <https://doi.org/10.1111/j.1574-6968.2004.tb09502.x>.
44. Kolp S, Pietsch M, Galinski EA, Gutschow M. 2006. Compatible solutes as protectants for zymogens against proteolysis. *Biochim Biophys Acta* 1764:1234–1242. <https://doi.org/10.1016/j.bbapap.2006.04.015>.
45. Harishchandra RK, Wulff S, Lentzen G, Neuhaus T, Galla HJ. 2010. The effect of compatible solute ectoines on the structural organization of lipid monolayer and bilayer membranes. *Biophys Chem* 150:37–46. <https://doi.org/10.1016/j.bpc.2010.02.007>.
46. Roychoudhury A, Bieker A, Haussinger D, Oesterhelt F. 2013. Membrane protein stability depends on the concentration of compatible solutes—a single molecule force spectroscopic study. *Biol Chem* 394:1465–1474. <https://doi.org/10.1515/hsz-2013-0173>.
47. Barth S, Huhn M, Matthey B, Klimka A, Galinski EA, Engert A. 2000. Compatible-solute-supported periplasmic expression of functional recombinant proteins under stress conditions. *Appl Environ Microbiol* 66:1572–1579. <https://doi.org/10.1128/AEM.66.4.1572-1579.2000>.
48. Lentzen G, Schwarz T. 2006. Extremolytes: natural compounds from extremophiles for versatile applications. *Appl Microbiol Biotechnol* 72:623–634. <https://doi.org/10.1007/s00253-006-0553-9>.
49. Graf R, Anzani S, Buenger J, Pfluecker F, Driller H. 2008. The multifunctional role of ectoine as a natural cell protectant. *Clin Dermatol* 26:326–333. <https://doi.org/10.1016/j.clindermatol.2008.01.002>.
50. Booth IR. 2014. Bacterial mechanosensitive channels: progress towards an understanding of their roles in cell physiology. *Curr Opin Microbiol* 18:16–22. <https://doi.org/10.1016/j.mib.2014.01.005>.
51. Sauer T, Galinski EA. 1998. Bacterial milking: a novel bioprocess for production of compatible solutes. *Biotechnol Bioeng* 57:306–313. [https://doi.org/10.1002/\(SICI\)1097-0290\(19980205\)57:3<306::AID-BIT7>3.0.CO;2-L](https://doi.org/10.1002/(SICI)1097-0290(19980205)57:3<306::AID-BIT7>3.0.CO;2-L).
52. Schulz A, Stöveken N, Binzen IM, Hoffmann T, Heider J, Bremer E. 2017. Feeding on compatible solutes: a substrate-induced pathway for uptake and catabolism of ectoines and its genetic control by EnuR. *Environ Microbiol* 19:926–946. <https://doi.org/10.1111/1462-2920.13414>.
53. Grammann K, Volke A, Kunte HJ. 2002. New type of osmoregulated solute transporter identified in halophilic members of the bacteria domain: TRAP transporter TeaABC mediates uptake of ectoine and hydroxyectoine in *Halomonas elongata* DSM 2581^T. *J Bacteriol* 184:3078–3085. <https://doi.org/10.1128/JB.184.11.3078-3085.2002>.
54. Fallet C, Rohe P, Franco-Lara E. 2010. Process optimization of the integrated synthesis and secretion of ectoine and hydroxyectoine under hyper/hypo-osmotic stress. *Biotechnol Bioeng* 107:124–133. <https://doi.org/10.1002/bit.22750>.
55. Van-Thuoc D, Hashim SO, Hatti-Kaul R, Mamo G. 2013. Ectoine-mediated protection of enzyme from the effect of pH and temperature stress: a study using *Bacillus halodurans* xylanase as a model. *Appl Microbiol Biotechnol* 97:6271–6278. <https://doi.org/10.1007/s00253-012-4528-8>.
56. Schiraldi C, Maresca C, Catapano A, Galinski EA, De Rosa M. 2006. High-yield cultivation of *Marinococcus* M52 for production and recovery of hydroxyectoine. *Res Microbiol* 157:693–699. <https://doi.org/10.1016/j.resmic.2006.03.004>.
57. Onraedt AE, Walcarus BA, Soetaert WK, Vandamme EJ. 2005. Optimization of ectoine synthesis through fed-batch fermentation of *Brevibacterium epidermis*. *Biotechnol Prog* 21:1206–1212. <https://doi.org/10.1021/bp0500967>.
58. Zhang LH, Lang YJ, Nagata S. 2009. Efficient production of ectoine using ectoine-excreting strain. *Extremophiles* 13:717–724. <https://doi.org/10.1007/s00792-009-0262-2>.
59. Seip B, Galinski EA, Kurz M. 2011. Natural and engineered hydroxyectoine production based on the *Pseudomonas stutzeri* ectABCD-ask gene cluster. *Appl Environ Microbiol* 77:1368–1374. <https://doi.org/10.1128/AEM.02124-10>.
60. Chen W, Zhang S, Jiang PX, Yao J, He YZ, Chen LC, Gui XW, Dong ZY, Tang SY. 2015. Design of an ectoine-responsive AraC mutant and its application in metabolic engineering of ectoine biosynthesis. *Metab Eng* 30:149–155. <https://doi.org/10.1016/j.ymben.2015.05.004>.
61. Schubert T, Maskow T, Benndorf D, Harms H, Breuer U. 2007. Continuous synthesis and excretion of the compatible solute ectoine by a transgenic, nonhalophilic bacterium. *Appl Environ Microbiol* 73:3343–3347. <https://doi.org/10.1128/AEM.02482-06>.
62. Perez-Garcia F, Ziert C, Risse JM, Wendisch VF. 2017. Improved fermentative production of the compatible solute ectoine by *Corynebacterium glutamicum* from glucose and alternative carbon sources. *J Biotechnol* 258:59–69. <https://doi.org/10.1016/j.jbiotec.2017.04.039>.
63. Becker J, Schäfer R, Kohlstedt M, Harder BJ, Borchert NS, Stöveken N, Bremer E, Wittmann C. 2013. Systems metabolic engineering of *Corynebacterium glutamicum* for production of the chemical chaperone ectoine. *Microb Cell Fact* 12:110. <https://doi.org/10.1186/1475-2859-12-110>.
64. Eilert E, Kranz A, Hollenberg CP, Piontek M, Suckow M. 2013. Synthesis and release of the bacterial compatible solute 5-hydroxyectoine in *Hansenula polymorpha*. *J Biotechnol* 167:85–93. <https://doi.org/10.1016/j.jbiotec.2013.02.005>.
65. Ning Y, Wu X, Zhang C, Xu Q, Chen N, Xie X. 2016. Pathway construction and metabolic engineering for fermentative production of ectoine in *Escherichia coli*. *Metab Eng* 36:10–18. <https://doi.org/10.1016/j.ymben.2016.02.013>.
66. Rodriguez-Moya J, Argandona M, Iglesias-Guerra F, Nieto JJ, Vargas C. 2013. Temperature- and salinity-decoupled overproduction of hydroxyectoine by *Chromohalobacter salexigens*. *Appl Environ Microbiol* 79:1018–1023. <https://doi.org/10.1128/AEM.02774-12>.
67. Yan Y, Yang J, Dou Y, Chen M, Ping S, Peng J, Lu W, Zhang W, Yao Z, Li H, Liu W, He S, Geng L, Zhang X, Yang F, Yu H, Zhan Y, Li D, Lin Z, Wang Y, Elmerich C, Lin M, Jin Q. 2008. Nitrogen fixation island and rhizosphere competence traits in the genome of root-associated *Pseudomonas stutzeri* A1501. *Proc Natl Acad Sci U S A* 105:7564–7569. <https://doi.org/10.1073/pnas.0801093105>.
68. Jebbar M, Talibart R, Gloux K, Bernard T, Blanco C. 1992. Osmoprotection of *Escherichia coli* by ectoine: uptake and accumulation characteristics. *J Bacteriol* 174:5027–5035. <https://doi.org/10.1128/jb.174.15.5027-5035.1992>.
69. Hoffmann T, Wensing A, Brosius M, Steil L, Völker U, Bremer E. 2013. Osmotic control of *opuA* expression in *Bacillus subtilis* and its modulation in response to intracellular glycine betaine and proline pools. *J Bacteriol* 195:510–522. <https://doi.org/10.1128/JB.01505-12>.
70. Brill J, Hoffmann T, Bleisteiner M, Bremer E. 2011. Osmotically controlled synthesis of the compatible solute proline is critical for cellular defense of *Bacillus subtilis* against high osmolarity. *J Bacteriol* 193:5335–5346. <https://doi.org/10.1128/JB.05490-11>.
71. Weber H, Polen T, Heuveling J, Wendisch VF, Hengge R. 2005. Genome-wide analysis of the general stress response network in *Escherichia coli*: sigmaS-dependent genes, promoters, and sigma factor selectivity. *J Bacteriol* 187:1591–1603. <https://doi.org/10.1128/JB.187.5.1591-1603.2005>.
72. Weber A, Jung K. 2002. Profiling early osmoresponsive-dependent gene expression in *Escherichia coli* using DNA microarrays. *J Bacteriol* 184:5502–5507. <https://doi.org/10.1128/JB.184.19.5502-5507.2002>.
73. Lucht JM, Dersch P, Kempf B, Bremer E. 1994. Interactions of the nucleoid-associated DNA-binding protein H-NS with the regulatory region of the osmotically controlled *proU* operon of *Escherichia coli*. *J Biol Chem* 269:6578–6578.
74. Pratt LA, Hsing W, Gibson KE, Silhavy TJ. 1996. From acids to *osmZ*: multiple factors influence synthesis of the *OmpF* and *OmpC* porins in *Escherichia coli*. *Mol Microbiol* 20:911–917. <https://doi.org/10.1111/j.1365-2958.1996.tb02532.x>.
75. Balsalobre C, Johansson J, Uhlin BE. 2006. Cyclic AMP-dependent osmoregulation of *crp* gene expression in *Escherichia coli*. *J Bacteriol* 188:5935–5944. <https://doi.org/10.1128/JB.00235-06>.
76. Zhang H, Chong H, Ching CB, Jiang R. 2012. Random mutagenesis of global transcription factor cAMP receptor protein for improved osmotolerance. *Biotechnol Bioeng* 109:1165–1172. <https://doi.org/10.1002/bit.24411>.
77. Landis L, Xu J, Johnson RC. 1999. The cAMP receptor protein CRP can function as an osmoregulator of transcription in *Escherichia coli*. *Genes Dev* 13:3081–3091. <https://doi.org/10.1101/gad.13.23.3081>.
78. Feklistov A, Sharon BD, Darst SA, Gross CA. 2014. Bacterial sigma factors: a historical, structural, and genomic perspective. *Annu Rev Microbiol* 68:357–376. <https://doi.org/10.1146/annurev-micro-092412-155737>.
79. Voskuil MI, Chambliss GH. 1998. The σ^{54} region of *Bacillus subtilis* and other Gram-positive bacterial promoters. *Nucleic Acids Res* 26:3584–3590. <https://doi.org/10.1093/nar/26.15.3584>.
80. Lucht JM, Bremer E. 1994. Adaptation of *Escherichia coli* to high osmolarity environments: osmoregulation of the high-affinity glycine be-

- taine transport system ProU. FEMS Microbiol Rev 14:3–20. <https://doi.org/10.1111/j.1574-6976.1994.tb00067.x>.
81. May G, Faatz E, Lucht JM, Haardt M, Bolliger M, Bremer E. 1989. Characterization of the osmoregulated *Escherichia coli* *proU* promoter and identification of ProV as a membrane-associated protein. Mol Microbiol 3:1521–1531. <https://doi.org/10.1111/j.1365-2958.1989.tb00138.x>.
 82. Hengge-Aronis R, Klein W, Lange R, Rimmel M, Boos W. 1991. Trehalose synthesis genes are controlled by the putative sigma factor encoded by *rpoS* and are involved in stationary-phase thermotolerance in *Escherichia coli*. J Bacteriol 173:7918–7924. <https://doi.org/10.1128/jb.173.24.7918-7924.1991>.
 83. Giaeever HM, Styrvoid OB, Kaasen I, Strom AR. 1988. Biochemical and genetic characterization of osmoregulatory trehalose synthesis in *Escherichia coli*. J Bacteriol 170:2841–2849. <https://doi.org/10.1128/jb.170.6.2841-2849.1988>.
 84. Boos W, Ehmann U, Bremer E, Middendorf A, Postma P. 1987. Trehalase of *Escherichia coli*. Mapping and cloning of its structural gene and identification of the enzyme as a periplasmic protein induced under high osmolarity growth conditions. J Biol Chem 262:13212–13218.
 85. Czech L, Stöveken N, Bremer E. 2016. EctD-mediated biotransformation of the chemical chaperone ectoine into hydroxyectoine and its mechanosensitive channel-independent excretion. Microb Cell Fact 15:126. <https://doi.org/10.1186/s12934-016-0525-4>.
 86. Peters P, Galinski EA, Trüper HG. 1990. The biosynthesis of ectoine. FEMS Microbiol Lett 71:157–162. <https://doi.org/10.1111/j.1574-6968.1990.tb03815.x>.
 87. He YZ, Gong J, Yu HY, Tao Y, Zhang S, Dong ZY. 2015. High production of ectoine from aspartate and glycerol by use of whole-cell biocatalysis in recombinant *Escherichia coli*. Microb Cell Fact 14:55. <https://doi.org/10.1186/s12934-015-0238-0>.
 88. MacMillan SV, Alexander DA, Culham DE, Kunte HJ, Marshall EV, Rochon D, Wood JM. 1999. The ion coupling and organic substrate specificities of osmoregulatory transporter ProP in *Escherichia coli*. Biochim Biophys Acta 1420:30–44. [https://doi.org/10.1016/S0005-2736\(99\)00085-1](https://doi.org/10.1016/S0005-2736(99)00085-1).
 89. Takeshita S, Sato M, Toba M, Masahashi W, Hashimoto-Gotoh T. 1987. High-copy-number and low-copy-number plasmid vectors for *lacZ* alpha-complementation and chloramphenicol- or kanamycin-resistance selection. Gene 61:63–74. [https://doi.org/10.1016/0378-1119\(87\)90365-9](https://doi.org/10.1016/0378-1119(87)90365-9).
 90. Gralla JD, Huo YX. 2008. Remodeling and activation of *Escherichia coli* RNA polymerase by osmolytes. Biochemistry 47:13189–13196. <https://doi.org/10.1021/bi810715x>.
 91. Cayley S, Record MT, Jr. 2003. Roles of cytoplasmic osmolytes, water, and crowding in the response of *Escherichia coli* to osmotic stress: biophysical basis of osmoprotection by glycine betaine. Biochemistry 42:12596–12609. <https://doi.org/10.1021/bi0347297>.
 92. Higgins CF, Dorman CJ, Stirling DA, Waddell L, Booth IR, May G, Bremer E. 1988. A physiological role for DNA supercoiling in the osmotic regulation of gene expression in *S. typhimurium* and *E. coli*. Cell 52:569–584. [https://doi.org/10.1016/0092-8674\(88\)90470-9](https://doi.org/10.1016/0092-8674(88)90470-9).
 93. Lilley DM, Higgins CF. 1991. Local DNA topology and gene expression: the case of the *leu-500* promoter. Mol Microbiol 5:779–783. <https://doi.org/10.1111/j.1365-2958.1991.tb00749.x>.
 94. Hoffmann T, Bremer E. 2016. Management of osmotic stress by *Bacillus subtilis*: genetics and physiology, p 657–676. In de Bruijn FJ (ed), Stress and environmental regulation of gene expression and adaptation in bacteria, vol 1. Wiley-Blackwell Publishers, Hoboken, NJ.
 95. Borowiec JA, Gralla JD. 1987. All three elements of the *lac* ps promoter mediate its transcriptional response to DNA supercoiling. J Mol Biol 195:89–97. [https://doi.org/10.1016/0022-2836\(87\)90329-9](https://doi.org/10.1016/0022-2836(87)90329-9).
 96. Gemmill RM, Tripp M, Friedman SB, Calvo JM. 1984. Promoter mutation causing catabolite repression of the *Salmonella typhimurium* leucine operon. J Bacteriol 158:948–953.
 97. Zhi X, Dages S, Dages K, Liu Y, Hua ZC, Makemson J, Leng F. 2017. Transient and dynamic DNA supercoiling potentially stimulates the *leu-500* promoter in *Escherichia coli*. J Biol Chem 292:14566–14575. <https://doi.org/10.1074/jbc.M117.794628>.
 98. Dorman CJ, Dorman MJ. 2016. DNA supercoiling is a fundamental regulatory principle in the control of bacterial gene expression. Biophys Rev 8:209–220. <https://doi.org/10.1007/s12551-016-0205-y>.
 99. Travers A, Muskhelishvili G. 2005. DNA supercoiling—a global transcriptional regulator for enterobacterial growth? Nat Rev Microbiol 3:157–169. <https://doi.org/10.1038/nrmicro1088>.
 100. Edwards MD, Black S, Rasmussen T, Rasmussen A, Stokes NR, Stephen TL, Miller S, Booth IR. 2012. Characterization of three novel mechanosensitive channel activities in *Escherichia coli*. Channels (Austin) 6:272–281. <https://doi.org/10.4161/chan.20998>.
 101. Lamark T, Styrvoid OB, Strom AR. 1992. Efflux of choline and glycine betaine from osmoregulating cells of *Escherichia coli*. FEMS Microbiol Lett 75:149–154. <https://doi.org/10.1111/j.1574-6968.1992.tb05408.x>.
 102. Mikkat S, Hagemann M. 2000. Molecular analysis of the *ggtBCD* gene cluster of *Synechocystis* sp. strain PCC6803 encoding subunits of an ABC transporter for osmoprotective compounds. Arch Microbiol 174:273–282. <https://doi.org/10.1007/s002030000201>.
 103. Hoffmann T, von Blohn C, Stanek A, Moses S, Barzantny S, Bremer E. 2012. Synthesis, release, and recapture of the compatible solute proline by osmotically stressed *Bacillus subtilis* cells. Appl Environ Microbiol 78:5753–5762. <https://doi.org/10.1128/AEM.01040-12>.
 104. Börngen K, Battle AR, Möker N, Morbach S, Marin K, Martinac B, Krämer R. 2010. The properties and contribution of the *Corynebacterium glutamicum* MscS variant to fine-tuning of osmotic adaptation. Biochim Biophys Acta 1798:2141–2149. <https://doi.org/10.1016/j.bbame.2010.06.022>.
 105. Bay DC, Turner RJ. 2012. Small multidrug resistance protein EmrE reduces host pH and osmotic tolerance to metabolic quaternary cation osmoprotectants. J Bacteriol 194:5941–5948. <https://doi.org/10.1128/JB.00666-12>.
 106. Jones CM, Lozada NJH, Pfleger BF. 2015. Efflux systems in bacteria and their metabolic engineering applications. Appl Microbiol Biotechnol 99:9381–9393. <https://doi.org/10.1007/s00253-015-6963-9>.
 107. Hoffmann T, Bremer E. 2011. Protection of *Bacillus subtilis* against cold stress via compatible-solute acquisition. J Bacteriol 193:1552–1562. <https://doi.org/10.1128/JB.01319-10>.
 108. Miller JH. 1972. Experiments in molecular genetics. Cold Spring Harbor Laboratory, Cold Spring Harbor, NY.
 109. Ferenci T, Zhou Z, Betteridge T, Ren Y, Liu Y, Feng L, Reeves PR, Wang L. 2009. Genomic sequencing reveals regulatory mutations and recombinational events in the widely used MC4100 lineage of *Escherichia coli* K-12. J Bacteriol 191:4025–4029. <https://doi.org/10.1128/JB.00118-09>.
 110. Haardt M, Kempf B, Faatz E, Bremer E. 1995. The osmoprotectant proline betaine is a major substrate for the binding-protein-dependent transport system ProU of *Escherichia coli* K-12. Mol Gen Genet 246:783–786. <https://doi.org/10.1007/BF00290728>.
 111. Hengge-Aronis R, Fischer D. 1992. Identification and molecular analysis of *glgS*, a novel growth-phase-regulated and *rpoS*-dependent gene involved in glycogen synthesis in *Escherichia coli*. Mol Microbiol 6:1877–1886. <https://doi.org/10.1111/j.1365-2958.1992.tb01360.x>.
 112. Lange R, Hengge-Aronis R. 1991. Identification of a central regulator of stationary-phase gene expression in *Escherichia coli*. Mol Microbiol 5:49–59. <https://doi.org/10.1111/j.1365-2958.1991.tb01825.x>.
 113. Dersch P, Schmidt K, Bremer E. 1993. Synthesis of the *Escherichia coli* K-12 nucleoid-associated DNA-binding protein H-NS is subjected to growth-phase control and autoregulation. Mol Microbiol 8:875–889. <https://doi.org/10.1111/j.1365-2958.1993.tb01634.x>.
 114. Kovach ME, Elzer PH, Hill DS, Robertson GT, Farris MA, Roop RM, Peterson KM. 1995. 4 new derivatives of the broad-host-range cloning vector pBRR1MCS, carrying different antibiotic-resistance cassettes. Gene 166:175–176. [https://doi.org/10.1016/0378-1119\(95\)00584-1](https://doi.org/10.1016/0378-1119(95)00584-1).
 115. Ritter K. 1996. Struktur und Funktion der Cytoplasmamembran-Komponente (ProW) des Bindeprotein-abhängigen Glycin-Betain Transportsystems ProU aus *Escherichia coli*. Philipps-Universität Marburg, Marburg, Germany.
 116. Casadaban MJ. 1976. Transposition and fusion of *lac* genes to selected promoters in *Escherichia coli* using bacteriophage lambda and bacteriophage-Mu. J Mol Biol 104:541–555. [https://doi.org/10.1016/0022-2836\(76\)90119-4](https://doi.org/10.1016/0022-2836(76)90119-4).

Illuminating the catalytic core of ectoine synthase through structural and biochemical analysis

Laura Czech¹, Astrid Höppner², Stefanie Kobus², Andreas Seubert³, Ramona Riclea⁴, Jeroen S. Dickschat⁴, Johann Heider^{1,5}, Sander H. J. Smits^{2,6} & Erhard Bremer^{1,5}

5.2.4. Illuminating the catalytic core of ectoine synthase through structural and biochemical analysis

Czech L*, Höppner A*, Kobus S, Seubert A, Riclea R, Dickschat JS, Heider J, Smits SHJ and Bremer E. Illuminating the catalytic core of ectoine synthase through structural and biochemical analysis. *Sci Rep* 2019;9:doi: 10.1038/s41598-018-36247-w.

The next chapter contains the publication "Illuminating the catalytic core of ectoine synthase through structural and biochemical analysis". For this study, I constructed expression plasmids containing side-directed mutations in the EctC enzyme from *P. lantus*, performed overproduction and protein purification. Furthermore, I performed all biochemical experiments. A. Höppner, S. Kobus und S. H. J. Smits, conducted crystallization trials and structure determination. A. Seubert analyzed the metal content of the purified EctC enzymes. R. Riclea and J. S. Dickschat synthesized the substrate (*N*- γ -ADABA) for the ectoine synthase. E. Bremer, H. Heider, J. S. Dickschat, S. H. J. Smits and I discussed the proposal for the EctC reaction mechanism based on the structural and biochemical data. I performed all bioinformatical analysis and prepared the figures. E. Bremer and I wrote the manuscript with input and comments from the co-authors.

Supplementary Data can be found at:

https://static-content.springer.com/esm/art%3A10.1038%2Fs41598-018-36247-w/MediaObjects/41598_2018_36247_MOESM1_ESM.pdf

5.2.4.1. Original publication

www.nature.com/scientificreports

SCIENTIFIC REPORTS

OPEN

Illuminating the catalytic core of ectoine synthase through structural and biochemical analysis

Received: 19 July 2018
Accepted: 16 November 2018
Published online: 23 January 2019

Laura Czech¹, Astrid Höppner², Stefanie Kobus², Andreas Seubert³, Ramona Riclea⁴, Jeroen S. Dickschat⁴, Johann Heider^{1,5}, Sander H. J. Smits^{2,6} & Erhard Bremer^{1,5}

Ectoine synthase (EctC) is the signature enzyme for the production of ectoine, a compatible solute and chemical chaperone widely synthesized by bacteria as a cellular defense against the detrimental effects of osmotic stress. EctC catalyzes the last step in ectoine synthesis through cyclo-condensation of the EctA-formed substrate *N*-gamma-acetyl-L-2,4-diaminobutyric acid via a water elimination reaction. We have biochemically and structurally characterized the EctC enzyme from the thermo-tolerant bacterium *Paenibacillus lautus* (Pl). EctC is a member of the cupin superfamily and forms dimers, both in solution and in crystals. We obtained high-resolution crystal structures of the (Pl)EctC protein in forms that contain (i) the catalytically important iron, (ii) iron and the substrate *N*-gamma-acetyl-L-2,4-diaminobutyric acid, and (iii) iron and the enzyme reaction product ectoine. These crystal structures lay the framework for a proposal for the EctC-mediated water-elimination reaction mechanism. Residues involved in coordinating the metal, the substrate, or the product within the active site of ectoine synthase are highly conserved among a large group of EctC-type proteins. Collectively, the biochemical, mutational, and structural data reported here yielded detailed insight into the structure-function relationship of the (Pl)EctC enzyme and are relevant for a deeper understanding of the ectoine synthase family as a whole.

Ectoine [(S)-2-methyl-1,4,5,6-tetrahydropyrimidine-4-carboxylic acid]¹ (Fig. 1a) and its derivative 5-hydroxyectoine [(4S, 5S)-5-hydroxy-2-methyl-1,4,5,6-tetrahydropyrimidine-4-carboxylic acid]² are representatives of a specialized group of organic osmolytes, the compatible solutes^{3–5}. These types of compounds are widely used by members of each domain of life as effective cytoprotectants⁶, in particular against the detrimental effects caused by high external salinity or osmolarity on cellular hydration, physiology, and growth. Compatible solutes are well suited for this demanding task^{3,7,8} because their physico-chemical attributes make them compliant with cellular biochemistry^{9–11}. The function-preserving properties of these solutes allow their high-level cellular accumulation, a process raising the osmotic potential of the cytoplasm, which then in turn counteracts the high osmolarity-instigated efflux of water from the cell^{3,12}. At the same time, the solvent properties of the crowded cytoplasm are optimized for vital biochemical reactions^{13–15}, so that growth can occur under osmotically unfavorable circumstances^{3,7,16}. Compatible solutes also serve as stabilizers of proteins, macromolecular assemblies, and even entire cells, both *in vitro* and *in vivo*^{11,17–24}, a property that led to their description in the literature as chemical chaperones^{25,26}.

With the notable exception of their recent discovery in a restricted group of obligate halophilic protists^{27–29} and a few *Archaea*³⁰, ectoines are primarily synthesized by members of the *Bacteria*³¹, as judged from the wide occurrence of the ectoine (*ectABC*)³² and 5-hydroxyectoine (*ectD*)³³ biosynthetic genes in microbial genome sequences³. Biosynthesis of ectoine proceeds from L-aspartate-β-semialdehyde, a central hub in bacterial amino acid and cell wall biosynthesis^{34,35} and is catalyzed by the sequential enzyme reactions of L-2,4-diaminobutyrate

¹Department of Biology, Laboratory for Microbiology, Philipps-University Marburg, D-35043, Marburg, Germany. ²Center for Structural Studies, Heinrich-Heine-University Düsseldorf, D-40225, Düsseldorf, Germany. ³Department of Chemistry, Analytical Chemistry, Philipps-University Marburg, D-35043, Marburg, Germany. ⁴Kekulé-Institute for Organic Chemistry and Biochemistry, Friedrich-Wilhelms-University Bonn, D-53121, Bonn, Germany. ⁵LOEWE Center for Synthetic Microbiology, Philipps-University Marburg, D-35043, Marburg, Germany. ⁶Institute of Biochemistry, Heinrich-Heine-University Düsseldorf, D-40225, Düsseldorf, Germany. Laura Czech and Astrid Höppner contributed equally. Correspondence and requests for materials should be addressed to S.H.J.S. (email: sander.smits@hhu.de) or E.B. (email: bremer@staff.uni-marburg.de)

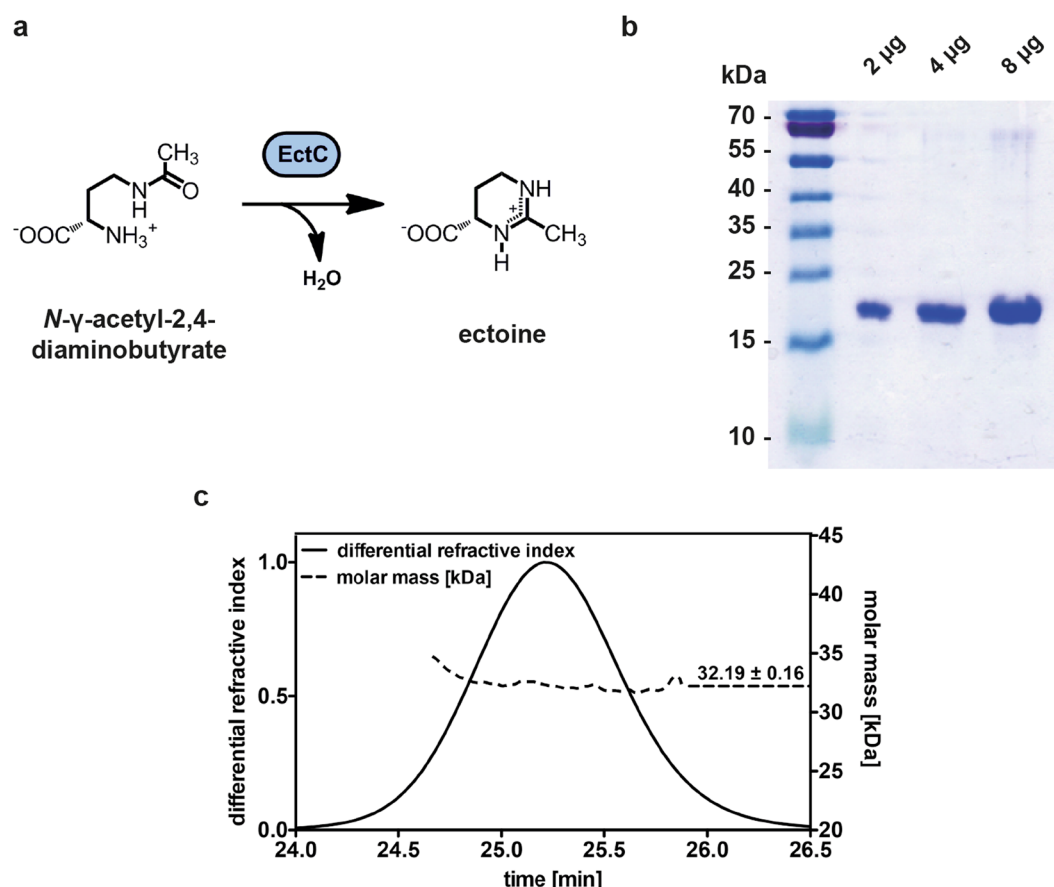


Figure 1. Ectoine synthase-catalyzed enzyme reaction scheme, purification and quaternary assembly of the (PI) EctC protein. (a) Scheme of the ectoine synthase catalyzed cyclo-condensation of the substrate *N*- γ -ADABA to form ectoine. (b) Coomassie brilliant blue stained 15% SDS-polyacrylamide gel with different amounts of the affinity chromatography purified (PI)EctC-Strep-tag II protein. The PageRuler Prestained Protein Ladder (Thermo Scientific) was used as a sizing marker. A picture of the original SDS-gel can be found in Fig. S1. (c) SEC-MALS analysis to determine the quaternary assembly of the purified (PI)EctC-Strep-tag II protein.

transaminase (EctB; EC 2.6.1.76), L-2,4-diaminobutyrate acetyltransferase (EctA; EC 2.3.1.178), and ectoine synthase (EctC; EC 4.2.1.108)^{32,36}. 5-Hydroxyectoine is synthesized from ectoine by the ectoine hydroxylase (EctD; EC 1.14.11.55)^{33,37,38} through a regio- and stereo-specific hydroxylation reaction³³. In comparison with ectoine, this chemical modification endows 5-hydroxyectoine with enhanced, or additional, cellular protection against selected environmental challenges (e.g., heat and desiccation stress)^{21,22,39,40}. High-level expression of the ectoine/5-hydroxyectoine biosynthetic genes is typically triggered by increases in the external osmolarity and sometimes also by extremes in either high or low growth temperatures^{4,41–43}. Disruption of the *ectABC(D)* genes causes sensitivity to such environmental challenges^{39,44}, highlighting the prominent role played by ectoines in the stress management of microbial cells^{4,5,45}.

The macromolecule stabilizing, cytoprotective, and anti-inflammatory effects of ectoines have generated considerable interest in the commercial and medical use of these natural products and led to an industrial scale biotechnological production process that delivers ectoines on the scale of tons. This process relies on the salt-tolerant bacterium *Halomonas elongata* as a natural production host^{4,45–47}. In addition, recombinant cell factories are increasingly developed to offer additional means to produce these valuable compounds biotechnologically^{5,48–56}. Hence, both from the perspective of practical applications and basic science^{4,5,45}, a deeper understanding of the enzymatic and structural properties of the ectoine and 5-hydroxyectoine biosynthetic enzymes is desirable. This has already been achieved to a considerable degree for the ectoine hydroxylase (EctD)^{31,37,38,57}, a member of the non-heme-containing iron(II) and 2-oxoglutarate-dependent dioxygenases enzyme super-family⁵⁸.

In comparison with EctD, the ectoine biosynthetic enzymes (EctABC)^{36,59} are biochemically and structurally far less understood. While the EctA and EctB enzymes have amino acid sequence-related counterparts in various biochemical pathways in microorganisms^{5,32,36}, the ectoine synthase (EctC) is considered the diagnostic enzyme for ectoine production^{30,31,60}. It can be used in database searches of microbial genome sequences to identify potential ectoine producers⁵. EctC catalyzes the final step in the ectoine biosynthetic route and cyclizes the linear, EctA-produced, *N*- γ -acetyl-L-2,4-diaminobutyric acid (*N*- γ -ADABA) to ectoine through a water elimination reaction^{36,60} (Fig. 1a). Basic biochemical characterizations of ectoine synthases from the extremophiles *H.*

elongata, *Methylomicrobium alcaliphilum*, and *Acidiphilium cryptum*^{36,61,62}, the cold-adapted marine bacterium *Sphingopyxis alaskensis*⁶⁰, and the nitrifying archaeon *Nitrosopumilus maritimus*³⁰ have been carried out, but a deeper understanding of this enzyme is lacking.

Crystallographic analysis of the psychrophilic *S. alaskensis* EctC protein [(Sa)EctC] showed that ectoine synthase is a member of the cupin superfamily⁶⁰. This family comprises a large group of pro- and eukaryotic proteins built on a common structural scaffold; its members can perform a variety of both enzymatic and non-enzymatic functions^{63–65}. Most of these proteins contain catalytically important divalent metals (e.g., iron, copper, zinc, manganese, cobalt, or nickel) that allow different types of chemistry to occur within the confines of an evolutionarily conserved tertiary structure^{66,67}. Biochemical studies conducted with the (Sa)EctC protein revealed for the first time that ectoine synthase is also a metal-dependent enzyme, with Fe^{2+} as the physiologically most likely relevant catalyst⁶⁰. This finding has obvious ramifications with respect to the details of the not yet fully understood reaction mechanism catalyzed by the EctC enzyme (Fig. 1a).

One of our major aims is to understand the structure-function relationship of the ectoine synthase through biochemical and crystallographic analysis. In this respect, the structure of the (Sa)EctC protein that we reported recently⁶⁰ provided only restricted functional information because it contained neither the catalytically important metal, nor the substrate or the reaction product. To significantly advance our understanding of the key enzyme for ectoine biosynthesis, we explored the EctC protein from the thermo-tolerant bacterium *Paenibacillus lautus* (Pl)⁶⁸ for biochemical and structural studies. We now report here crystallographic views into the catalytic core of the ectoine synthase prior and subsequent to enzyme catalysis. These crystal structures lay the framework for a proposal for the EctC-mediated cyclo-condensation reaction mechanism. Since the residues participating in metal, substrate, and reaction product binding are highly conserved among a very large collection of EctC-type proteins, the data provided here for the (Pl)EctC enzyme are relevant for a structural and functional understanding of the extended ectoine synthase family as a whole.

Results

Overproduction, purification, and oligomeric state of the (Pl)EctC ectoine synthase. Ectoine biosynthetic genes are present in microorganisms able to colonize ecological niches with rather different physico-chemical attributes^{4,5,30,31}. One of these ectoine-producing microorganisms is *Paenibacillus lautus* (Pl) strain Y4.12MC10, a Gram-positive spore-forming bacterium that was originally isolated from the effluent of the Obsidian hot spring in the Yellowstone Natural Park (USA). It can grow under laboratory conditions up to 50 °C⁶⁸. We therefore explored the EctC protein from *P. lautus* for biochemical and structural studies in the hope that the properties of the ectoine synthase from this thermo-tolerant strain might be more suitable for crystallographic analysis than the psychrophilic EctC protein derived from the cold-adapted bacterium *S. alaskensis* (Sa)⁶⁹ which yielded crystal structures only in its apo-form⁶⁰. The (Pl)EctC protein possesses 130 amino acids, has a calculated molecular mass of 14.7 kDa, and possesses a calculated isoelectric point of 4.7.

We constructed an expression vector carrying a codon-optimized version of the *P. lautus* ectC gene for its heterologous expression in *Escherichia coli* that would lead to a recombinant protein fused at its C-terminus to a Strep-tag II affinity peptide [(Pl)EctC-Strep-tag II] allowing its purification by affinity chromatography (Figs 1b and S1). The quaternary assembly of the purified (Pl)EctC-Strep-tag II protein was assessed by size exclusion chromatography followed by multi-angle light scattering (SEC-MALS); these experiments yielded a value for the molecular mass of 32.2 kDa of the (Pl)EctC-Strep-tag II protein in solution (Fig. 1c). Since the calculated molecular mass for the recombinant (Pl)EctC-Strep-tag II protein is 15.87 kDa, the ectoine synthase from *P. lautus* is a dimer in solution.

Biochemical and kinetic properties of the recombinant (Pl)EctC enzyme. Taking into account that the (Sa)EctC enzyme is an iron-dependent enzyme⁶⁰, we included 0.1 mM $(\text{NH}_4)_2\text{Fe}(\text{SO}_4)_2$ into the buffer solution when we assessed its enzymatic activity. We first determined some basic biochemical properties of the recombinant (Pl)EctC enzyme with respect to its temperature and pH optima and its tolerance towards salt (Fig. 2a–c). In keeping with the thermo-tolerant physiology of the *P. lautus* Y4.12MC10 donor strain⁶⁸, the (Pl)EctC enzyme exhibited a broad window of temperatures in which it could function. Its temperature optimum was about 30 °C but the purified (Pl)EctC enzyme retained 45% and 26% of its activity at 45 °C and 50 °C, respectively, under the tested conditions (Fig. 2a). The (Pl)EctC enzyme had an alkaline pH optimum of 8.5 (Fig. 2b) and was highly NaCl tolerant, allowing the protein to retain even 30% of its activity when the assay buffer contained elevated levels (2 M) of NaCl (Fig. 2c).

Building on these initial biochemical assessments of the (Pl)EctC protein, we formulated an optimized enzyme activity assay [20 mM HEPES buffer (pH 8.5), 50 mM NaCl, 0.1 mM $(\text{NH}_4)_2\text{Fe}(\text{SO}_4)_2$] to determine the kinetic properties of the *P. lautus* ectoine synthase (Fig. 2d). For these assays we used a chemically synthesized and highly purified preparation of *N*- γ -ADABA⁶⁰, the natural substrate of the EctC enzyme^{36,59} (Fig. 1a). The (Pl)EctC protein had the following kinetic parameters: (i) a K_m of 7.8 ± 1.0 mM and (ii) a calculated theoretical V_{\max} of 16.0 ± 1.2 μmol ectoine formed min^{-1} mg protein⁻¹ (Fig. 2d) since the activity of the (Pl)EctC enzyme displayed a substantial substrate (or product) inhibition (calculated K_i of 47 ± 7 mM). The actually measured V_{\max} of the (Pl)EctC enzyme is approximately 9 μmol ectoine formed min^{-1} mg protein⁻¹.

Kinetic characterization of EctC enzyme from five other microorganisms have previously been carried out and the following values for ectoine synthase activity were reported: a K_m of 11 mM and a V_{\max} of 85 μmol min^{-1} mg^{-1} for the *H. elongata* enzyme³⁶ [the parameters for the backward reaction of this enzyme, the hydrolysis of the synthetic ectoine derivative homoeoine, were as follows: a K_m of 28.7 mM and V_{\max} of 4.6 μmol min^{-1} mg^{-1}]⁷⁰; a V_{\max} of 64 μmol min^{-1} mg^{-1} for the *M. alcaliphilum* enzyme⁷¹, a K_m of 5 mM and a V_{\max} of 25 μmol min^{-1} mg^{-1} for the *S. alaskensis* enzyme⁶⁰, and a K_m of 6.4 mM and a V_{\max} of 12.8 μmol min^{-1} mg^{-1} for the *N. maritimus* enzyme³⁰. Preliminary kinetic data were reported for the *A. cryptum* enzyme⁶¹. Hence, the mentioned ectoine synthases

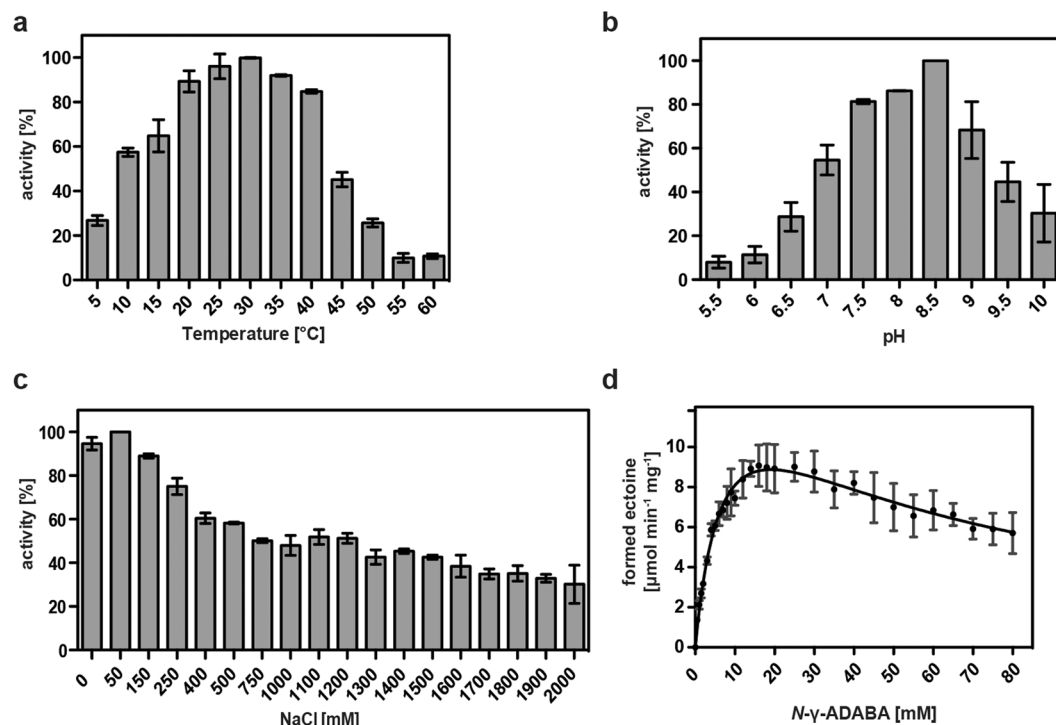


Figure 2. Biochemical properties and kinetic parameters of the *P. lautus* ectoine synthase. The enzyme activity of the affinity-purified (*Pl*)EctC protein was assessed with respect to its temperature (a) and pH optima (b), and its tolerance against NaCl (c). For these enzyme assays 10 mM of the substrate *N*-γ-ADABA and 1 μg of the (*Pl*)EctC protein were used and the assays were run for 5 min at 30 °C. (d) Kinetic parameters of the (*Pl*)EctC enzyme were determined in an optimized buffer solution [20 mM HEPES buffer (pH 8.5), 50 mM NaCl, 0.1 mM (NH₄)₂Fe(SO₄)₂] using 1 μg of the protein and increasing concentrations of the substrate *N*-γ-ADABA. The enzyme assays were conducted at 30 °C and were run for 2.5 min. Formation of ectoine was monitored by HPLC analysis and quantitated as described^{30,41,60}. The data shown represent experiments with three independently purified (*Pl*)EctC protein preparations, and each data-point from the individual protein preparations was assayed twice.

display in some cases notable differences in their kinetic properties but it should be noted that the various EctC enzymes were assessed under rather different buffer, pH, temperature, and salt concentrations (and partially also at different levels of purity). This makes a direct comparison with the kinetic parameters determined in this study for the (*Pl*)EctC enzyme difficult. We also note in this context that the (*Pl*)EctC enzyme is the first ectoine synthase for which a substantial substrate (or product) inhibition was detected (Fig. 2d).

Crystallization of the ectoine synthase in complex with iron, the substrate *N*-γ-ADABA, and the enzyme reaction product ectoine. Crystals of the (*Pl*)EctC protein were obtained using commercial screens and by slightly optimizing the composition of the crystallization solution. Crystals were grown in a solution consisting of 0.2 M ammonium sulfate, 0.1 M phosphate citrate (pH 4.2), 20% (v/v) PEG 300, and 10% (v/v) glycerol. Since the ectoine synthase is an iron dependent enzyme⁶⁰, we added Fe(II)Cl₂ to the crystallization solution of the purified (*Pl*)EctC protein to a final concentration of 4 mM and pre-incubated this mixture for at least 30 minutes prior to crystallization trials. Without this pre-incubation in the presence of iron, no crystals with a quality suitable for X-ray analysis could be grown. This approach yielded crystals which diffracted to a maximum of 1.6 Å for the (*Pl*)EctC::Fe protein complex (Table 1). To obtain crystals of the (*Pl*)EctC enzyme with its substrate *N*-γ-ADABA or its reaction product ectoine, we added these compounds to a final concentration of 40 mM and of 20 mM, respectively, to (*Pl*)EctC preparations pre-incubated with iron. Crystals which diffracted to a maximum of 2.0 Å were obtained for the (*Pl*)EctC::Fe/*N*-γ-ADABA complex and 2.5 Å for the (*Pl*)EctC::Fe/ectoine complex (Table 1).

The high-resolution dataset obtained for the (*Pl*)EctC::Fe crystal complex was phased using molecular replacement with the crystallographic data of the previously solved structure of the (*Sa*)EctC ectoine synthase (PDB entry 5BXX)⁶⁰ as the search model. After several rounds of model building using COOT⁷² and subsequent refinement, the structure of the full-length (*Pl*)EctC protein was solved (Fig. 3a). This was a substantial improvement over the *S. alaskensis* EctC crystal structure⁶⁰ where the spatial orientation of 22 amino acids from the (*Sa*)EctC COOH-terminus could not be localized in the electron density map, probably due to enhanced structural flexibility of this psychrophilic protein^{60,69,73}. The data- and refinement statistics for the (*Pl*)EctC::Fe complex are listed in Table 1.

	(<i>Pl</i>)EctC::Fe (PDB entry: 5ONM)	(<i>Pl</i>)EctC::Fe/ <i>N</i> - γ -ADABA (PDB entry: 5ONN)	(<i>Pl</i>)EctC::Fe/ectoine (PDB entry: 5ONO)
Data collection	P13 DESY Hamburg	P13 DESY Hamburg	P13 DESY Hamburg
Wavelength (Å)	0.953	0.953	0.953
Space group	<i>P</i> 31 2 1	<i>P</i> 31 2 1	<i>P</i> 31 2 1
Cell dimensions			
a, b, c (Å)	71.13; 71.13; 68.66	70.91; 70.91; 68.54	71.41; 71.41; 68.83
α , β , γ (°)	90.0; 90.0; 120.0	90.0; 90.0; 120.0	90.0; 90.0; 120.0
Processing			
Resolution (Å)	35.56–1.6 (1.7–1.6)	31.49–2.0 (2.1–2.0)	46.01–2.5 (2.6–2.5)
R_{merge}	6.5 (45.2)	4.5 (6.89)	8.2 (17.6)
Mean I/sigma (I)	19.14 (1.70)	61.45 (47.39)	8.2 (3.2)
Completeness (%)	99.35 (97.83)	98.05 (97.58)	99.32 (98.33)
Total reflections	586136 (34379)	293346 (29757)	145322 (15326)
Unique reflections	31125 (3015)	13580 (1328)	7282 (706)
Redundancy	18.8 (11.4)	21.6 (22.4)	5.4 (3.0)
Refinement			
Resolution (Å)	35.56–1.6	31.49–2.0	46.01–2.5
No. of reflections	545106	281608	36963
$R_{\text{work}}/R_{\text{free}}$	0.17/0.20	0.17/0.21	0.18/0.24
RMSD			
Bond length (Å)	0.011	0.016	0.014
Bond angles (°)	1.41	1.80	1.48
No. atoms			
Protein	1115	1115	1115
Ligand	6	12	12
Water	133	152	42
B-factors			
Protein (Å)	22.80	21.60	20.70
Ligand (Å)	31.20	35.20	86.10

Table 1. Data collection, phasing and refinement statistics for (*Pl*)EctC::Fe, (*Pl*)EctC::Fe/*N*- γ -ADABA, and (*Pl*)EctC::Fe/ectoine, respectively.

Once the 1.6 Å structure of the (*Pl*)EctC::Fe protein was completely refined, it was used to phase the other two datasets of the (*Pl*)EctC protein containing iron and either the substrate [(*Pl*)EctC::Fe/*N*- γ -ADABA] or the reaction product [(*Pl*)EctC::Fe/ectoine] of the ectoine synthase. A summary of the data collection statistics, refinement details, and model content of these two (*Pl*)EctC crystal structures is given in Table 1 as well. The (*Pl*)EctC-*Strep*-tag II protein carries an affinity tag attached to its carboxy-terminus; this tag consists of an octapeptide with an additional two amino acid linker (SA-WSHPQFEK) sequence. In the (*Pl*)EctC crystal structures the linker region and five amino acids of *Strep*-tag II sequence was visible, while the last three amino acids were disordered and were therefore not visible in the electron density. The crystallographic data of the three (*Pl*)EctC structures reported in this communication have been deposited in the RCSB Protein Data Bank (<https://www.rcsb.org/>) under accession number 5ONM [(*Pl*)EctC::Fe], 5ONN [(*Pl*)EctC::Fe/*N*- γ -ADABA], and 5ONO [(*Pl*)EctC::Fe/ectoine], respectively.

The (*Pl*)EctC::Fe/*N*- γ -ADABA crystals diffracted to very high resolution, but they suffered from severe radiation damage, a process, which lowered the diffraction rapidly during data collection. This phenomenon was encountered for more than 20 examined (*Pl*)EctC::Fe/*N*- γ -ADABA crystals. We therefore designed an experiment with a very low radiation dose and exposure time of the crystals to the X-ray beam. This yielded finally a dataset with a resolution of 2.0 Å in which no evidence for radiation damage was observed when the crystallographic data were processed. After manual rebuilding and several cycles of refinement, the (*Pl*)EctC::Fe/*N*- γ -ADABA crystal structure was finalized with an R -factor of 17.1% and an R_{free} of 21.7%. The Ramachandran plot revealed that 99.3% of the residues are in the allowed region. Already during the first round of refinement of the (*Pl*)EctC::Fe/*N*- γ -ADABA complex, extra density was visible next to the iron atom, large enough to fit the *N*- γ -ADABA molecule (Fig. S2a). This allowed us to pinpoint and trace the spatial position of the *N*- γ -ADABA substrate within the active site of the ectoine synthase.

Crystals of the (*Pl*)EctC protein in complex with ectoine were obtained after the addition of 20 mM ectoine prior to crystallization trials. Within the cupin fold^{63–67} of the (*Pl*)EctC protein (Fig. 3a), clear density was visible for the ectoine molecule (Fig. S2b), that was subsequently manually placed and included during refinement. After manual rebuilding and several cycles of refinement, the structure of the (*Pl*)EctC::Fe/ectoine complex was finalized with an R -factor of 18.2%, an R_{free} of 24%, and a resolution of 2.5 Å. The Ramachandran plot revealed that 99.3% obeyed the rules and fitted into the corresponding plot.

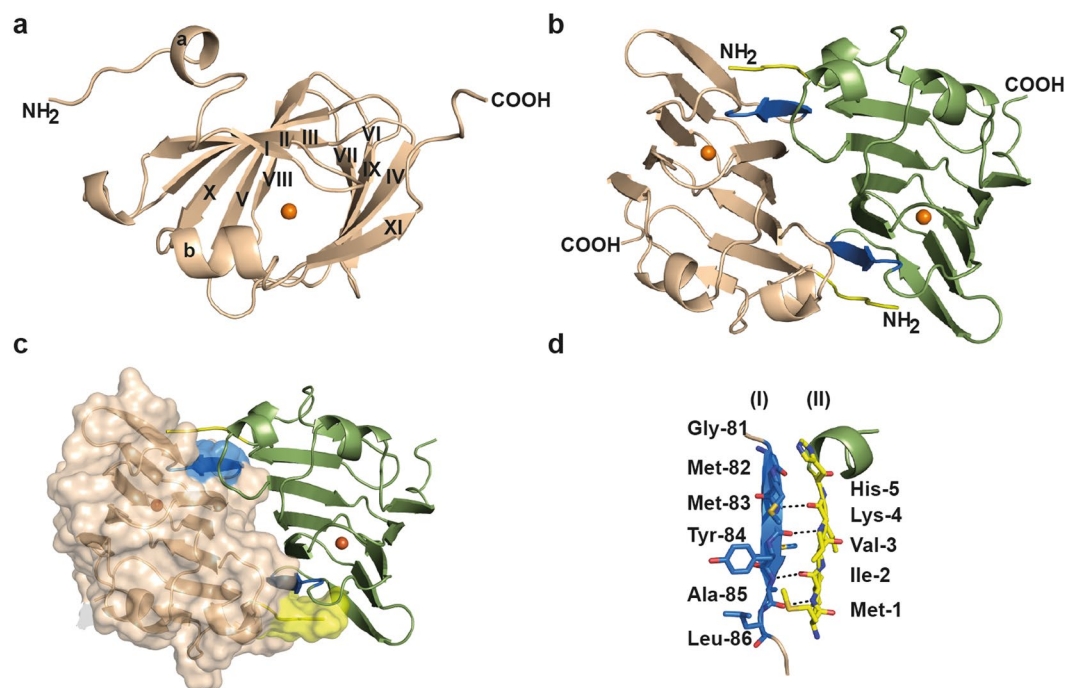


Figure 3. Crystal structure of the (*Pl*)EctC protein and analysis of its dimer interface. The overall fold of the (*Pl*)EctC monomer in its iron-bound state is shown in panel (a), and the head-to-tail dimer of the (*Pl*)EctC protein in panel (b) as a side-view and the position of the iron in each dimer is indicated by an orange sphere. The dimer interface formed by β -strand 6 of one monomer (shown in blue) and the N-terminal region (shown in yellow) of the other monomer is highlighted. These two figures show the (*Pl*)EctC protein in a cartoon representation. Panel (c) represents the interface of the (*Pl*)EctC dimer assembly, where one of the monomers is depicted in a surface representation and the other monomer is shown in a cartoon representation. The areas marked in blue and yellow, respectively, represent the dimer interface, and an orange sphere indicates the position of the iron in each monomer. Panel (d) highlights the structural details of the dimer interface with hydrogen bridges between the backbone functional groups of Met-1 to Lys-4 (N-terminal segment of monomer II) with those of Met-83 to Ala 85 (β -strand 6 from monomer I).

A comparison of the three (*Pl*)EctC crystal structures revealed a root-mean-square deviation (r.m.s.d.) ranging between 0.4 and 0.8 Å over 136 C α atoms. Keeping in mind that crystal structures are snapshots of the three-dimensional space a given protein can potentially adopt, these data indicate that both the binding of the substrate *N*- γ -ADABA to the EctC protein pre-complexed with iron and the binding of the enzyme reaction product ectoine to the protein do not trigger any gross overall structural changes in the thermo-tolerant (*Pl*)EctC enzyme. A high degree of structural identity was also found between the thermo-tolerant (*Pl*)EctC protein and the cold-tolerant (*Sa*)EctC protein^{69,73}; an overall comparison of the three (*Pl*)EctC crystal structures with that of the (*Sa*)EctC protein⁶⁰ revealed r.m.s.d. values ranging between 1.2 and 1.4 Å over 105 C α atoms. These data indicate that the (*Sa*)EctC and the (*Pl*)EctC ectoine synthases display a highly similar three-dimensional structure despite the fact that these proteins were derived from microorganisms living in ecophysiological rather different habitats; the effluent of a hot spring (*P. lautus*) and permanently cold ocean waters (*S. alaskensis*)^{68,69}.

Overall fold of the (*Pl*)EctC protein and analysis of the EctC dimer interface. Since the monomers of the three (*Pl*)EctC crystal structures are nearly identical in overall shape, we only describe in the following section the overall structure for the high-resolution (1.6 Å) (*Pl*)EctC:Fe complex in detail. The structure of the (*Pl*)EctC protein consists of 11 β -strands (β I- β XI) and two α -helices (α -a and α -b) (Fig. 3a). The β -strands form two anti-parallel β -sheet regions consisting of β II, β III, β X, β V, β I, β VI, β IX and β XI. These sets of anti-parallel β -sheets are packed against each other, forming a cup-shaped β -sandwich with a topology characteristic for the widely found cupin-fold of proteins^{63–67}.

The structure of the psychrophilic (*Sa*)EctC protein has previously been solved in two different conformations, which were coined the *open* and *semi-closed* states⁶⁰. In the latter state, only part of the carboxy-terminus of the (*Sa*)EctC protein is visible in the electron density map, and it folds into a small helix (α -b) that closes the active site of the enzyme⁶⁰. The formation of the helix α -b induces a reorientation and shift of a long unstructured loop connecting the beta-sheets β IV and β VI of the (*Sa*)EctC protein, resulting in the formation of the stable β -strand β V. In contrast to the (*Sa*)EctC crystal structure, the COOH-terminus of the thermo-tolerant *P. lautus* EctC protein (Fig. 3a) was completely resolved in the electron density map. The remaining segment of the previously unresolved part of the carboxy-terminus of the ectoine synthase from *S. alaskensis* flanks the cupin fold of the (*Pl*)EctC protein and protrudes out of the protein (Fig. 3a).

The (PI)EctC protein is a dimer in solution as revealed by our SEC-MALS analysis (Fig. 1c). Since the asymmetric unit of the (PI)EctC crystal revealed only a monomer, we inspected the crystal packing and analyzed the respective monomer/monomer interactions to elucidate the functional dimer within the crystal structure. The data resulting from this analysis show that the (PI)EctC dimer in the crystal (Fig. 3b) is composed of two monomers arranged in a head-to-tail orientation; it is stabilized via strong interactions mediated by the N-terminus (sequence ¹MIVKH5) from monomer A and β -strand β VIII from monomer B (sequence ⁸¹GMMYAL⁸⁶) (Fig. 3b–d). The interactions between these two β -strands rely primarily on backbone contacts (Fig. 3b–d). In addition to these interactions, some weaker hydrophobic interactions between the two monomers are also observed in some loop regions connecting the β -strands; these will probably play more subtle roles in dimer formation. Since the (PI)EctC is a head-to-tail dimer, the interaction interface between the monomers occurs twice in the dimer assembly (Fig. 3b,c). As determined by PISA (Proteins, Interfaces, Structures and Assemblies) analysis⁷⁴, the (PI)EctC monomers interact in the dimer assembly through an extensive surface area of 1501 Å² involving 16 hydrogen bonds and 4 salt bridges. The predicted substantial binding energy of $-28.2 \text{ kcal mol}^{-1}$ of the two (PI)EctC monomers indicates that these regions represent the predominant interface within the ectoine synthase dimer (Fig. 3b–d).

To identify the structurally closest homologs of the (PI)EctC protein, we performed a DALI search⁷⁵ which recovered, as expected, a variety of cupin-type proteins, most of which are functionally uncharacterized. Not surprisingly, the apo-form of the (Sa)EctC protein (PDB accession number: 5BXX)⁶⁰ was found as the structurally closest homolog of (PI)EctC; it had a Z-score of 21.1. Among the proteins with the highest Z-scores recovered by the DALI-search that had been biochemically and functionally studied were the KdgF⁷⁶ and DddK⁷⁷ crystal structures with Z-scores of 13.4 and 13.0, respectively. Like the (PI)EctC protein, the cupin-type KdgF and DddK proteins are dimers that possess an overall topology and a dimer interface very similar to that observed for the ectoine synthase.

The KdgF protein from *Halomonas* sp. is an enzyme that catalyzes a step in the microbial metabolism of uronate sugars from two abundant sources of biomass, pectin and alginate. KdgF mediates the conversion of pectin- and alginate-derived 4,5-unsaturated mono-uronates to form linear ketonized forms⁷⁶. Interestingly, KdgF performs an enzyme reaction (hydrolysis of a cyclic molecule) opposite to that performed by EctC (cyclo-condensation of a linear metabolite). We note in this context that the ectoine synthase from *H. elongata* displays a hydrolytic activity towards synthetic ectoine derivatives with either reduced or expanded ring sizes⁷⁰ but the equilibrium for the EctC-catalyzed *N*- γ -ADABA to ectoine biotransformation lies almost completely on the side of the cyclic condensation product ectoine^{36,70}. KdgF exhibits an amino acid sequence identity to (PI)EctC of only 17%, but its crystal structure possesses an r.m.s.d. of 2.1 Å (over 109 C α atoms) to the ectoine synthase. As determined by PISA⁷⁴, the surface area of the dimer interface of KdgF is 1501 Å², and the monomers interact via 16 hydrogen bonds, and 4 salt bridges, yielding an overall predicted binding energy of the two KdgF monomers of about $-30 \text{ kcal mol}^{-1}$ ⁷⁶. The crystal structure of KdgF contains a nickel ion, a metal that might have been acquired during the affinity chromatography of the His-tagged recombinant KdgF enzyme purified from *E. coli* cell extracts⁷⁶. As observed with other cupins^{63,64,66,67}, the KdgF enzyme is promiscuous with respect to the catalytically required metal, with Co²⁺ being the most effective catalyst among the tested divalent metals⁷⁶.

The DddK protein (PDB accession number: 5TFZ) from the marine bacterium *Pelagibacter ubique* HTCC1062 is a dimethylsulfoniopropionate (DMSP) lyase⁷⁷. This enzyme is involved in the catabolism of the organosulfur compound DMSP, an environmentally abundant organic osmolyte produced by marine algae⁷⁸, yielding the reaction products acrylate and the climate-active gas dimethylsulfide (DMS)⁷⁷. The *P. ubique* DddK protein exhibits an amino acid sequence identity to the (PI)EctC protein of 16.3% and its crystal structure possesses an r.m.s.d. of 1.2 Å (over 126 C α atoms) to the ectoine synthase from *P. lautus*. The surface area of the dimer interface of DddK⁷⁷ is 1556.1 Å², and the monomers interact with an overall predicted binding energy of $-28 \text{ kcal mol}^{-1}$. Crystal structures of the DddK protein with either Ni²⁺ or Fe²⁺/Zn²⁺ were recovered⁷⁷, attesting again to the promiscuity of cupins with respect to the metal cofactor used for catalytic activity.

Structural features of the ectoine synthase and functional relevance of the iron-binding site for enzyme activity. Keeping in mind that the (Sa)EctC ectoine synthase is a metal-dependent enzyme, with Fe²⁺ as the physiologically most relevant catalyst⁶⁰, we added Fe(II)Cl₂ to the (PI)EctC protein solution prior to the crystallization at a final concentration of 4 mM. Clear electron density was visible in the 1.6 Å (PI)EctC crystal structure for an atom with a strong electron density, which cannot be accounted for by a water molecule. To identify the probable nature of this ion, we modeled Mg²⁺, Ca²⁺, Fe²⁺, Ni²⁺, Co²⁺, and Zn²⁺ into the electron density and refined the (PI)EctC crystal structure again. Only when we refined the (PI)EctC structure modeled with Fe²⁺, we observed neither negative nor positive differences in electron density, indicating that iron is indeed the most probable element present in the crystallized (PI)EctC protein.

Within the (PI)EctC:Fe crystal structure, the iron atom is tetrahedrally ligated via interactions with the side chains of Glu-57, Tyr-84, and His-92 (Fig. 4a). The distance between the iron atom and the side chains of these three residues are 2.9 Å, 2.8 Å, and 2.9 Å, respectively. A water molecule completes the tetrahedral arrangement of the (PI)EctC iron-binding site in the substrate-free (PI)EctC:Fe crystal structure (Fig. 4a); it is present at a distance of 2.9 Å relative to that of the iron atom. In the previously reported (Sa)EctC crystal structure⁶⁰, no metal atom was visible but a water molecule occupied the same position that we observed here for the iron atom in the (PI)EctC crystal structure (Fig. 4b). An overlay of the three iron-coordinating amino acid residues in the (PI)EctC and (Sa)EctC⁶⁰ structures revealed that they are perfectly superimposable (Fig. 4b), indicating that (i) the iron-binding site in the ectoine synthase is already preformed in the absence of the catalytically important iron co-factor and that (ii) the binding of the iron atom does not seem to trigger substantial structural rearrangements in the overall fold of the enzyme.

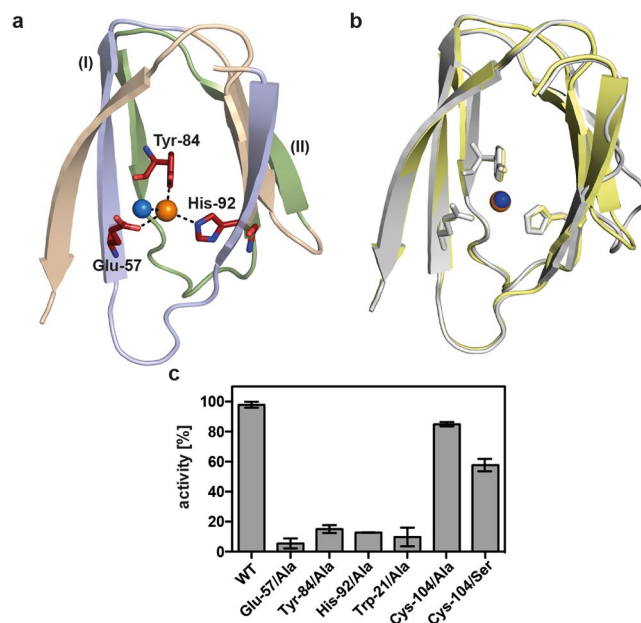


Figure 4. The iron-binding site in the (Pl)EctC protein and enzyme activities of selected (Pl)EctC variants. (a) The iron (represented by an orange sphere) is coordinated by the side-chains of Glu-57, Tyr-84, and His-92 of the (Pl)EctC protein with distances of 2.9 Å, 2.8 Å, and 2.9 Å, respectively. The iron-binding site in the substrate-free (Pl)EctC crystal structure also contains a localized water molecule (blue sphere); it has a distance of 2.9 Å to the iron atom. The two conserved cupin-motifs include those residues that coordinate the metal ion [G(X)₅WY(X)₄E(X)₆G; G(X)₆PG(X)₂Y(X)₃G(X)₃H; letters in bold indicate metal-binding residues] are highlighted as part of the overall protein (Pl)EctC crystal structure. The first cupin motif [G(X)₅WY(X)₄E(X)₆G] is shown in blue, and the second cupin motif [G(X)₆PG(X)₂Y(X)₃G(X)₃H] is represented in green. A number of secondary structure elements of the (Pl)EctC protein were removed in order to highlight the architecture of the iron-binding site and the position of the two cupin motifs. (b) Overlay of the iron-binding site in the (Pl)EctC (shown in yellow) and (Sa)EctC (shown in grey) crystal structures. The three residues involved in the binding of the Fe(II) ion are depicted as sticks. A water molecule (blue sphere) in the (Sa)EctC crystal structure occupies the same location as the Fe(II) ion (orange sphere) in the (Pl)EctC structure. (c) Single amino acid substitution variants of the (Pl)EctC protein were assayed for their enzyme activity. Enzyme activity measurements were conducted under buffer conditions [20 mM HEPES buffer (pH 8.5), 50 mM NaCl, 0.1 mM (NH₄)₂Fe(SO₄)₂] optimized for the wild-type enzyme using 10 µg of protein and 10 mM of the substrate *N*-γ-ADABA. The enzyme assays were conducted at 30 °C and run for 30 min and the formation of ectoine was monitored by HPLC analysis. The enzyme activity of the mutant (Pl)EctC proteins is represented relative to that of the wild-type enzyme (set at 100% activity).

If one considers the architecture of the iron-binding site of (Pl)EctC (Fig. 4a) with respect to the previously established consensus sequence for the amino acid sequences involved in metal coordination in cupin-type proteins^{63,64,66,67,76,77,79}, both common and distinct features are found. The first consensus cupin motif [G(X)₅HXX(X)_{3,4}E(X)₆G] is altered in the (Pl)EctC protein to G(X)₅WY(X)₄E(X)₆G, and the second consensus motif [G(X)₅PXG(X)₂H(X)₃N] is changed in (Pl)EctC to G(X)₆PG(X)₂Y(X)₃G(X)₃H (note: the letters in bold represent those residues that coordinate the metal) (Fig. 5a,b). Thus, in the first consensus cupin motif, none of the two canonical His residues is present in (Pl)EctC; however, the canonical Glu residue (Glu-57) is conserved (Fig. 5a,b). In the second cupin motif of the (Pl)EctC protein, a Tyr residue (Tyr-84) replaces the canonical His residue, and the motif is elongated to include another His residue (His-92) involved in iron binding (Fig. 4a). Variations in the metal-binding motifs of cupins occur frequently^{63,64,66,67,76,77}, but to the best of our knowledge, the one identified here for ectoine synthase is novel (Figs 4a and 5).

In Fig. 4a we have highlighted the positions of the two cupin motifs within the overall (Pl)EctC crystal structure, and we point out their position in EctC protein sequences in Fig. 5. By inspecting a recently reported extended amino acid sequence alignment of 582 EctC-type proteins⁵, we found that minor variations in the amino acid sequences of the overall cupin motifs exist, but none of them affects the residues contacting the iron atom directly (Figs 4a and 5). This is highlighted in an abbreviated alignment of amino acid sequences of 15 randomly picked ectoine synthases from the previously reported dataset of 582 EctC-type proteins⁵ (Fig. 5).

The strict evolutionary conservation of the three iron-contacting residues in ectoine synthases attests to their likely critical role for enzyme function. To assess the individual contributions of the (Pl)EctC iron-binding residues Glu-57, Tyr-84, and His-92 (Fig. 4a) for the functionality of this enzyme, we replaced each of them individually with an Ala residue via site-directed mutagenesis. The three (Pl)EctC variants could be overproduced and purified with the same efficiency as the wild-type (Pl)EctC protein. Each of the individual Ala substitution mutations rendered the mutant (Pl)EctC proteins in essence catalytically inactive with remaining levels of enzyme

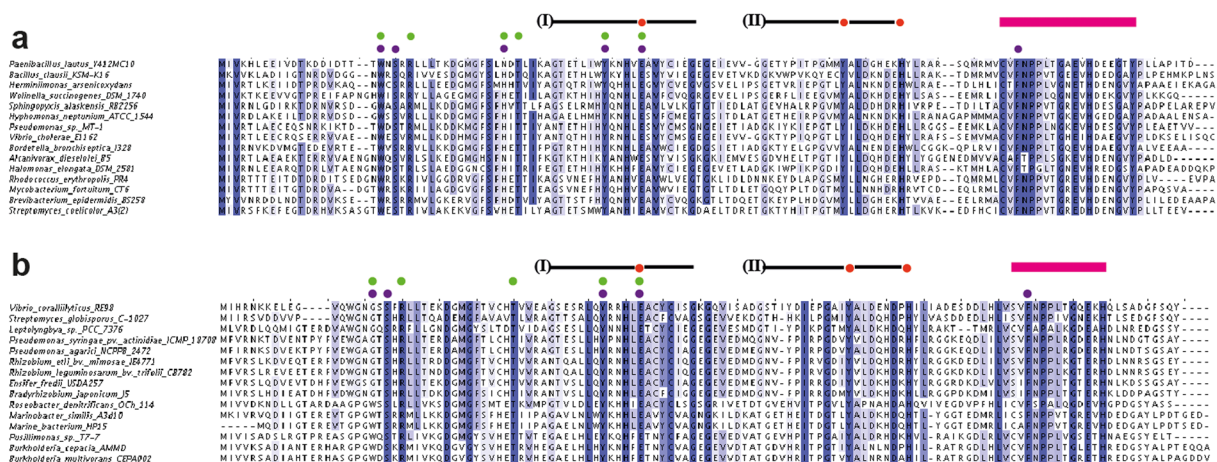


Figure 5. Abbreviated alignment of EctC-type proteins. (a) The amino acid sequences of 15 randomly picked EctC proteins from a dataset of 437 ectoine synthases encoded in ectoine biosynthetic gene clusters (*ect*)⁵ were aligned. Strictly conserved amino acid residues are shaded in dark blue. Dots shown above the (PI)EctC protein sequence indicate residues involved in the binding of the iron atom (red), the *N*- γ -ADABA substrate (green), or the enzyme reaction product ectoine (purple). (b) The amino acid sequence alignment of 15 EctC-type proteins encoded by orphan *ectC* genes⁵. The same color code shown in panel (a) is used to mark those residues that could potentially be involved in iron, substrate, or product binding. The positions of cupin motif-I and cupin motif-II within the EctC amino acid sequence are indicated by a black line. The red box highlights the region in the C-terminal segment of EctC that forms a lid over the entry to the cupin barrel.

activity of 5.4% (Glu-57), 15.1% (Tyr-84), and 12.7% (His-92) (Fig. 4c). Notably, the same conclusion has been reached through mutant analysis of the corresponding putative iron-binding residues present in the (Sa)EctC protein⁶⁰.

Structural features of the binding site for the *N*- γ -ADABA substrate. In the (PI)EctC::Fe/*N*- γ -ADABA crystal structure, the substrate for the ectoine synthase, *N*- γ -ADABA^{36,59}, is positioned in close proximity to the catalytically important iron atom within the cupin barrel (Fig. 6a) and the iron atom is bound in a fashion similar to that observed in the (PI)EctC::Fe complex (Fig. 4a). The substrate *N*- γ -ADABA was added in large excess (40 mM) to the crystallization solution; however, the obtained crystal structure displayed only a partially bound molecule, which resulted in an occupancy of 68% after refinement. The *N*- γ -ADABA molecule is coordinated within the active site of the (PI)EctC enzyme through six direct interactions with residues Trp-21, Arg-25, Asn-38, Thr-40, Tyr-52, and Glu-57. Interactions of *N*- γ -ADABA with the iron atom further stabilize it within the catalytic core of the ectoine synthase (Fig. 6a). In Fig. S3, we provide a numbering scheme for the atoms in the substrate *N*- γ -ADABA and the reaction product ectoine to aid the understanding of the following descriptions.

N- γ -ADABA is coordinated in the active site via two sets of interactions. First, a direct interaction occurs between the O atom of the acetyl group of *N*- γ -ADABA (acetamide oxygen) and the iron co-factor with a distance of 2.6 Å. The N5 atom of the substrate interacts with Glu-57 and with Tyr-52; its α -NH₂ moiety interacts with Thr-40, and one of the carboxylate O atoms interacts with Asn-38. Both of the latter amino acid residues are part of β -sheet β IV. The carboxylate oxygens of *N*- γ -ADABA are also coordinated via interactions with a water molecule, which in turn is held in place via an interaction with the side chain of Arg-25 (Fig. 6a). A second set of interactions is observed for the C3 and C4 atoms of *N*- γ -ADABA, which interact with the side chain of Trp-21 (Fig. 6a). Notably, Trp-21 adopts a dual conformation in the crystal structure of the (PI)EctC::Fe/*N*- γ -ADABA complex, in line with the observed partial occupancy of the crystals with the bound substrate. Only in one of these two conformations of Trp-21, its side chain is oriented towards the *N*- γ -ADABA substrate (52% occupancy) (Fig. 6a). The comparison of the (PI)EctC::Fe and the (PI)EctC::Fe/*N*- γ -ADABA structures therefore suggests that the presence of the *N*- γ -ADABA molecule within the substrate-binding site of the ectoine synthase induces the reorientation of the side-chain of Trp-21 to provide additional stabilizing contacts to the *N*- γ -ADABA molecule. The notion that the side chain of Trp-21 is critically involved in the stable positioning of the substrate in the active site of EctC is supported by data from a site-directed mutagenesis experiment in which we replaced Trp-21 with an Ala residue. This single amino acid substitution yielded a (PI)EctC variant with only 9.7% remaining enzyme activity (Fig. 4c).

A Cys-104/Ala substitution mutation was constructed to assess the importance of this amino acid in enzyme function of the (PI)EctC protein, a residue that is highly conserved in an amino acid sequence alignment of 437 EctC-type proteins encoded by *bona fide ect* gene clusters⁵. Cys-104 is positioned close to the catalytic core, although it appears not to be directly involved in iron binding, or involved in interactions with the substrate *N*- γ -ADABA or the reaction product ectoine within the active site of the ectoine synthase (Fig. 6a,b). Despite the conspicuous spatial arrangement of Cys-104 side-chain (Fig. 6a) and the evolutionary conservation of this residue, the Cys-104/Ala substitution had in essence no effect on the catalytic activity of the (PI)EctC enzyme (Fig. 4c). This result also corroborates the functional relevance of the amino acids whose site-directed change

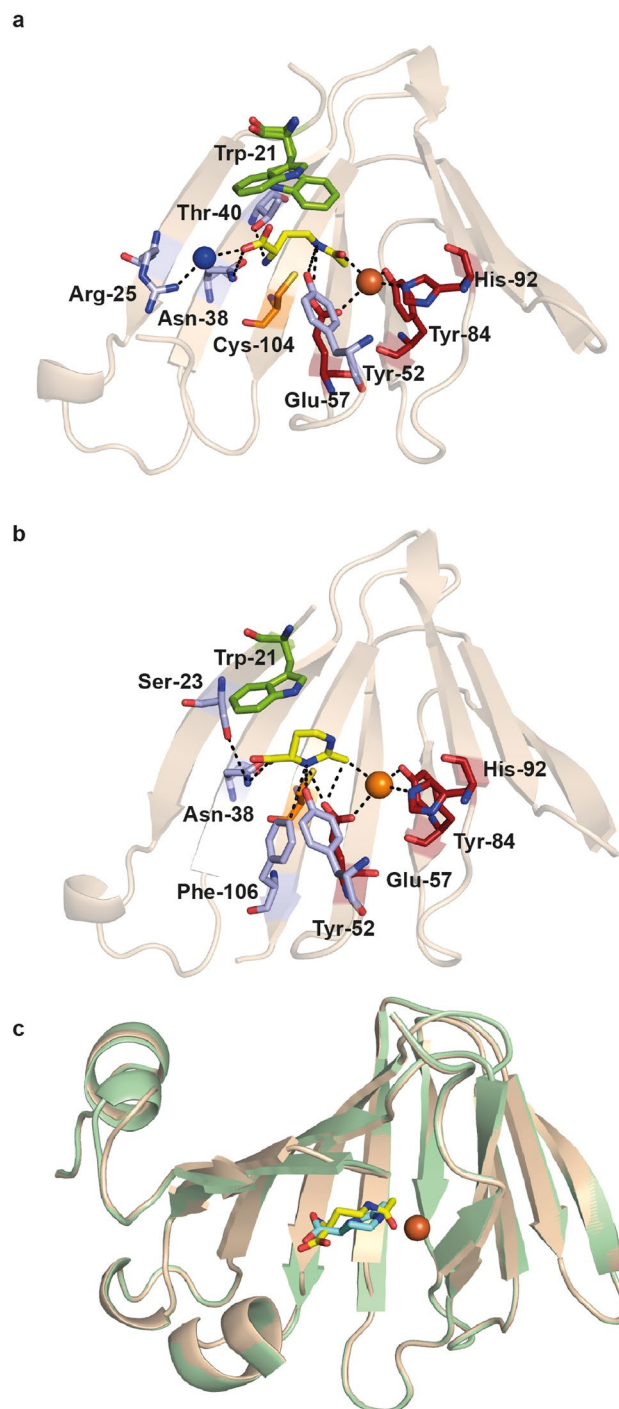


Figure 6. Crystallographic views into the catalytic core of the *P. lautus* ectoine synthase. **(a)** The iron- and substrate-binding network within the catalytic core of the (Pl)EctC protein. The side-chain of Trp-21 that adopts two different conformations in the (Pl)EctC:Fe/*N*- γ -ADABA crystal structure is emphasized in green. The *N*- γ -ADABA molecule is shown as yellow sticks. The iron is represented as an orange sphere and a water molecule (blue sphere) mediating indirect contacts between the *N*- γ -ADABA molecule and the side-chain of Arg-25 is highlighted. In addition, the spatial position of the side-chain of a conserved Cys residue (Cys-104) close to the active site, but not directly involved in enzyme catalysis is shown. **(b)** Details of the iron- and ectoine-bound state of the (Pl)EctC catalytic core are shown. In this structure, the side chain of Trp-21 adopts only a single conformation and provides stabilizing contacts to the ectoine ligand via cation- π interactions. The ectoine molecule is depicted as a yellow stick. **(c)** Cartoon representation of a structural overlay of the (Pl)EctC:Fe/*N*- γ -ADABA (gold) and (Pl)EctC:Fe/ectoine (green) crystal structures. The position of the substrate and reaction product within the confines of the cupin barrel is highlighted and the iron co-factor is shown as an orange sphere. In all panels, parts of the secondary structure elements of the (Pl)EctC protein are omitted in order to provide an unobstructed view into the catalytic core of the ectoine synthase.

impaired the enzyme function of the (PI)EctC protein (Fig. 4c). Unexpectedly, the replacement of Cys-104 of the (PI)EctC protein by a Ser residue, an amino acid often observed in orphan EctC-type proteins^{5,80} in this amino acid position (Fig. 5b) yielded a (PI)EctC variant that retained only approximately 60% of enzyme activity (Fig. 4c). This drop in enzyme activity is currently not understood in functional terms given the frequent occurrence of a Ser residue at position 104 of ectoine synthases^{5,80}.

In the previously reported structural analysis of the *S. alaskensis* EctC protein, it was not possible to obtain (Sa)EctC crystals in complex with the natural substrate of the ectoine synthase, *N*- γ -ADABA. Instead, a chemically not fully defined compound (in all likelihood trapped by the recombinant (Sa)EctC protein either during purification in *E. coli*, or from the crystallization solution) was present⁶⁰. This C-6 molecule was modeled as hexandiol and it was argued by Widderich *et al.*⁶⁰ that its spatial position within the cupin barrel of the (Sa)EctC protein could be used as a proxy for the actual substrate of the ectoine synthase, *N*- γ -ADABA. We now superimposed the (PI)EctC::Fe/*N*- γ -ADABA (PDB accession code: 5ONN) and (Sa)EctC/hexandiol (PDB accession code: 5BXX) crystal structures; this yielded a root-mean-square deviation (r.m.s.d.) of 1.4 Å over 105 C α atoms of the two crystal structures. The overlay showed that the *N*- γ -ADABA and the presumed hexandiol ligand occupy, indeed, a very similar position within the active site of the two studied ectoine synthases (Fig. S4).

Structural features of ectoine binding within the (PI)EctC active site. We were able to obtain a (PI)EctC crystal structure that contained both the iron ion and an ectoine molecule (Fig. 6b). The ectoine molecule is coordinated within the active site of the (PI)EctC enzyme through five direct interactions with the following residues: Ser-23, Asn-38, Tyr-52, Glu-57, and Phe-106 (Fig. 6b). Ectoine exhibits a significantly different conformation to that of the bound *N*- γ -ADABA molecule. In particular, Tyr-52 and Glu-57 are no longer involved in any H-bonding interactions with N1 of ectoine (derived from the amidic N5 of *N*- γ -ADABA), but now both residues form H-bonds to N3 of ectoine, which is derived from the α -amino group of *N*- γ -ADABA. These new H-bonds towards N3 of ectoine also appear to be stronger than those formed originally with *N*- γ -ADABA, as suggested from their shorter distances (3.2 Å to Tyr-52, and 3.7 Å to Glu-57), and are further stabilized by an interaction with Phe-106 (Fig. 6b). In addition, the side-chain of Asn-38 makes a direct contact to the carboxylate of ectoine, and this side chain is in turn held in place through stabilizing interactions with the side-chain of Ser-23 (Fig. 6b). There may also be a direct interaction between the iron and the methyl group of the ectoine molecule (Fig. 6b). The side chain of Trp-21 adopts a single conformation in the (PI)EctC::Fe-ectoine structure and thereby provides additional stabilizing contacts to the ectoine ligand (compare Fig. 6a,b).

A structural comparison of the substrate- and product-bound catalytic core of ectoine synthase.

When the crystal structures of the (PI)EctC::Fe/*N*- γ -ADABA and the (PI)EctC::Fe/ectoine complexes are overlaid, it becomes apparent that the substrate (*N*- γ -ADABA) and the reaction product (ectoine) occupy almost the same position within the (PI)EctC active site (Fig. 6c). The (PI)EctC::Fe/*N*- γ -ADABA structure reveals an extended conformation of the substrate within the catalytic core (Fig. 6a,c). The distance between the carbonyl C-atom and the α -amino group of the bound *N*- γ -ADABA molecule (4.1 Å) is far too large to allow a direct enzymatic attack to initiate ring closure. As a result, the *N*- γ -ADABA molecule needs to bend significantly in order to correctly position the two substituents of the substrate involved in ring closure (Fig. 1a) closely enough to form the intramolecular Schiff-base bond required to generate the enzyme reaction product ectoine. Hence, the observed mode of ectoine binding indicates the requirement of an extensive conformational change of the linear *N*- γ -ADABA molecule during enzyme catalysis to yield the spatial position of the cyclic ectoine molecule (Fig. 6a-c).

Because the *N*- γ -ADABA molecule is bound in an extended, and not in a pre-bent (Fig. 1a), conformation, the main chain region of *N*- γ -ADABA needs to be rearranged to a more bent conformation during the cyclo-condensation reaction. This requires large movements of the carbon atoms (2.0 Å, 1.2 Å, and 1.4 Å of the C-2, C-3 and C-4 of the *N*- γ -ADABA molecule) to yield the positions of the corresponding C-4, C-5, and C-6 atoms of the resulting ectoine molecule. Moreover, the plane described by the acetamide group of *N*- γ -ADABA indicates a required rotation of about 80° for superimposition with the plane of the amidinium group of ectoine captured in the (PI)EctC crystal structure. These changes are associated with an outward spatial extension of the bound *N*- γ -ADABA molecule, which can only occur with an associated flip-over movement of the side chain of Trp-21 from the (partial) position observed in the (PI)EctC::Fe/*N*- γ -ADABA structure (Fig. 6a) to that found in the ectoine-bound structure (Fig. 6b). We note, that the distance between ectoine and the side chain of Trp-21 in the “wrong” conformation (Fig. 6a,b) is only 1.6 Å, a configuration that would likely lead to molecular clashing.

The indole ring of Trp-21 of the (PI)EctC protein stands out as the only amino acid side chain exhibiting a major conformational change between the substrate- and product-bound complexes (Fig. 6a,b). As noted above, this residue is required for enzyme activity (Fig. 4b). Although this residue appears to be present in a mixture of two conformations in the *N*- γ -ADABA bound (PI)EctC structure, we assume that the one deviating from the product-bound state is important for catalysis. In the *N*- γ -ADABA-bound structure, the indole ring of Trp-21 is orientated towards and above the C3 and C4 atoms of the substrate and seems to act as a piston-like element by pushing the *N*- γ -ADABA molecule against the bottom of the active site cavity. This assumption is consistent with the presence of a significant conformational strain in the bound *N*- γ -ADABA molecule, as deduced from large deviations of the bond angles of the C2 and C3 atoms of the diaminobutyrate moiety in the crystal structure from the expected tetrahedral angles (104.9° and 117.5°, respectively, instead of the expected 109.5°). This indicates that Trp-21 might play an important role in exerting conformational constraints on the substrate, which may allow the *N*- γ -ADABA molecule to assume the extended conformation observed in the crystal structure (Fig. 6a). These structural constraints might also move the acetyl group of the substrate close enough towards the iron co-factor to support tautomeric rearrangements of the acetyl substituent.

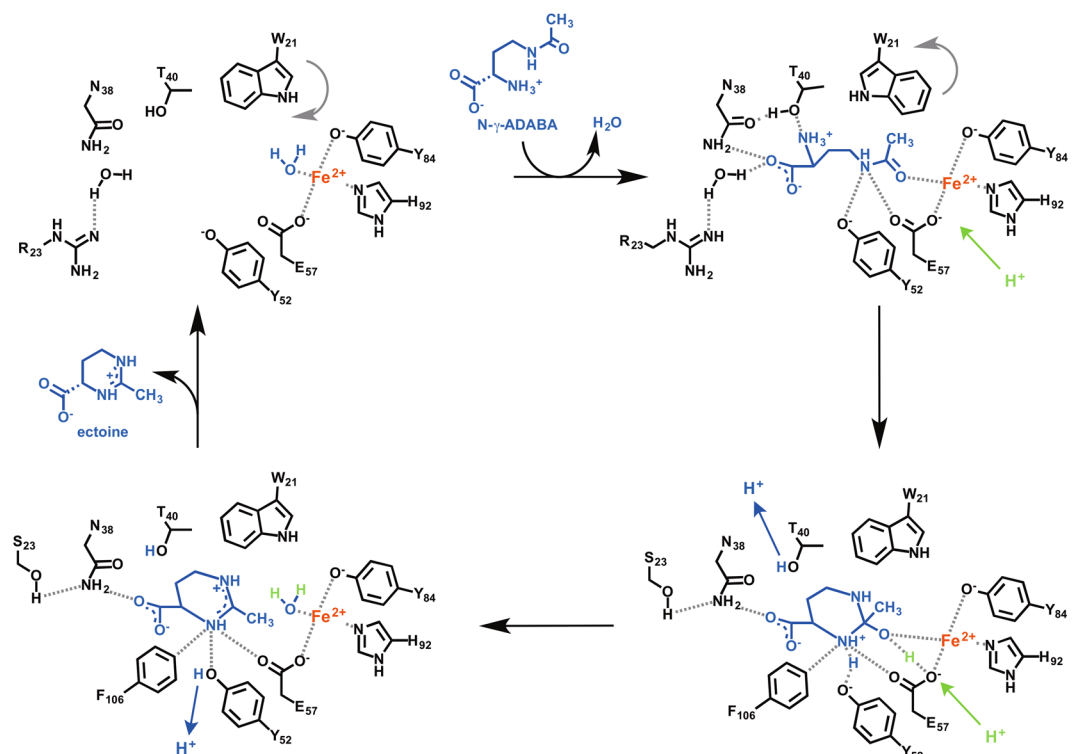


Figure 7. Proposal for the enzyme mechanisms of the ectoine synthase-mediated cyclo-condensation reaction. For a description of the details of the enzyme reaction, see main text.

Apart from the conformational flip of the side-chain of Trp-21 and the reorientation of the bound substrate with respect to the ectoine product, the active site moieties remain remarkably constant in their locations (Fig. 6a,b). Therefore, we assume that the flip-over of Trp-21 triggers the re-orientation of bound substrate during ring formation (or vice versa), and that this coordinated re-organization of the active site is a major driving force for catalysis. Consistent with its predicted critical role in enzyme function (Fig. 4b), we observed that Trp-21 is completely conserved in an amino acid sequence alignment of 437 EctC-type proteins encoded by *ect* gene clusters⁵ (Fig. 5a). The corresponding Trp residue in 145 orphan EctC-type proteins encoded outside canonical *ect* gene clusters⁵ (see below) is conserved as well, but in some cases its position within the EctC protein chain is shifted by two amino acid residues (Fig. 5b).

Proposal for the ectoine synthase-catalyzed reaction mechanism. By comparing the (PI)EctC::Fe to the substrate- and product-bound (PI)EctC structures (Fig. 6a,b), a catalytic cycle for the conversion of the substrate *N*- γ -ADABA into the reaction product ectoine can be suggested (Fig. 7). The (PI)EctC::Fe structure exhibits a tetrahedral coordination of the iron cofactor by the side chains of Glu-57, Tyr-84, His-92 and a water molecule (Fig. 4a). As can be observed in the (PI)EctC::Fe/*N*- γ -ADABA structure, the water is replaced by the amide carbonyl group of *N*- γ -ADABA upon substrate binding (Fig. 6a). This coordination to the Lewis acidic Fe²⁺ cofactor stabilizes the amide functional group of the substrate in its charge-separated mesomeric form with a negative charge at the carbonyl oxygen and a positive charge at the amide nitrogen that is in turn stabilized by cation- π -interactions with the side chain of Trp-21. The resulting increased reactivity of the amide towards nucleophiles triggers the ring closure by attack of the α -amino group of *N*- γ -ADABA that may proceed with a simultaneous proton transfer from the α -amino group or from one of the Fe-coordinating amino acids to the amide carbonyl oxygen. The nucleophilicity of the α -amino group, which is mostly protonated at physiological pH, is increased by the hydrogen bonds to Thr-40 and further to Asn-38 (Fig. 6a,b) thereby allowing a proton transfer during the cyclization of *N*- γ -ADABA to form ectoine. In the next step, the hydroxy group is extruded from the substrate to release the product ectoine (Fig. 7). A simultaneous back-transfer of the proton from Asn-38 via Thr-40 to the expelled hydroxy group may restore the initial binding situation at the central iron with one water ligand (Fig. 7); the product ectoine is finally released from the active site to allow for the initiation of a new catalytic cycle. We note however in this context that the expected water ligand of the Fe²⁺ ion was only confirmed for the substrate-free EctC crystal structure, but not for its ectoine-bound state as this latter crystal structure has a resolution (2.5 Å) that does not allow the positioning of water molecules with confidence.

The residues forming the entire EctC catalytic core are evolutionarily highly conserved. The explosion in the number of available microbial genome sequences allows one to place the salient features of a given protein within an evolutionary context. We have recently conducted an extensive analysis of the phylogenomics of the ectoine synthase protein family⁵ by relying on the Integrated Microbial Genomes & Microbiomes

(IMG/M) database of the DOE's Joint Genome Institute (JGI) (<https://img.jgi.doe.gov/>)⁸¹ for EctC orthologs in members of the *Bacteria* and *Archaea* with deposited complete genome sequences. At the time of the search (13 November 2017), the IMG/M database contained 56 624 bacterial and 1325 archaeal genomes and we identified in this dataset 4493 bacterial and 20 archaeal EctC-type proteins. It should be noted that databases of microbial genome sequences are biased with respect of the type of the represented microorganisms. In our dataset of 4493 bacterial genomes containing *ectC* genes, 1215 *ectC* genes alone were present in the genomes of *Vibrio*-type microorganisms, and 511 *ectC* genes were derived from various *Streptomyces* species and strains⁵. When the phylogenomics of EctC-type proteins was exclusively focused on fully sequenced microbial genomes, 582 predicted EctC-type proteins were retrieved in the search, which were associated with 499 bacterial and 11 archaeal species/strains (Fig. S5)⁵. Hence, in some microbial genomes multiple copies of *ectC*-type genes are present.

Two EctC-type proteins need to be distinguished: (i) those that are encoded in *ect* gene clusters and are thus *bona fide* ectoine synthases, and (ii) those that are encoded by *ectC*-type genes in microorganisms that either lack *ectAB* genes altogether or contain *ectC*-type gene copie(s) in addition to complete *ectABC* operons^{5,60}. A clade analysis of the amino acid sequence of EctC proteins revealed that the EctC proteins encoded by *ect* gene clusters follow, with the notable exceptions of some probable lateral gene transfer events, the taxonomic affiliations of the predicted ectoine-producing microorganisms⁵. However, there is a sub-group of EctC-type proteins that are not part of *ect* biosynthetic gene clusters or that can occur in addition to *bona fide* *ectC* genes (25% in the dataset examined by Czech *et al.*⁵). A microbial strain (*Pseudomonas syringae* pv. *syringae*) with such an exclusive orphan *ectC* gene has been physiologically studied, and seems to be able to produced ectoine when surface sterilized leaves of the host plant of this pathogen were provided to the culture⁸⁰.

Building on the extensive bioinformatic dataset reported by Czech *et al.*⁵ and on the salient features of the crystal structures of the (Pl)EctC protein that we present here (Figs 4 and 6), we now can focus on those ten residues involved in binding iron, the substrate or the product (Fig. 5a,b) in an evolutionary context by inspecting alignments of EctC proteins encoded within complete ectoine biosynthetic gene clusters (437 representatives) and those encoded by orphan *ectC*-type genes (145 representatives). We used the amino acid sequence of the (Pl) EctC protein as query for this search. The degree of amino acid sequence identity of EctC proteins encoded by *ect* biosynthetic genes clusters ranged between 90% (for *Paenibacillus gluconolyticus*) and 49% (for *Streptomyces glaucescens*) when 437 amino acid sequences of *bona fide* EctC proteins were aligned and compared with the amino acid sequence of the crystallized (Pl)EctC protein. Hence, *bona fide* EctC-type proteins are evolutionarily rather well conserved (Fig. 5a). When the (Pl)EctC amino acid sequence was compared with those of 145 orphan EctC-type proteins (Fig. 5b), the degree of amino acid sequence identity decreased and ranged between 42% (*Burkholderia cepacia*) and 37% (*Roseobacter litoralis*).

From an alignment of the 582 EctC-type proteins retrieved through the BLAST search of the IMG/M database⁵ we observed that 20 residues were completely conserved. After we excluded the EctC orphan sequences and only compared the 437 EctC-type proteins encoded by *ect* gene clusters, the number of completely conserved amino acid residues increased to 26 (Fig. 5a,b). Based upon the (Pl)EctC crystal structures (Fig. 6a,b), these conserved residues can be correlated to the following functions: three residues are involved in metal binding (Glu-57, Tyr-84, His-92), six residues are involved in coordinating the substrate *N*- γ -ADABA within the active site (Trp-21, Arg-25, Asn-38, Thr-40, Tyr-52, Glu-57), and five residues coordinate the reaction product ectoine (Ser-23, Asn-38, Tyr-52, Glu-57, Phe-106). The remaining conserved residues (Fig. 5a) might play either structural, or yet not recognized mechanistic roles. Notably, in the carboxy-terminal segment of EctC proteins, there are nine strictly conserved residues but only one of them (Phe-106) is involved in binding a ligand (ectoine) of the ectoine synthase (Fig. 5a). When one views this carboxy-terminal region in the overall EctC structure, it becomes apparent that it forms a lid over the entry to the cupin barrel (Fig. 8a,b). The strong conservation of the participating residues suggests a functionally important role of this presumed lid region. When one removes the 27 amino acid segment *in silico* from the (Pl)EctC::Fe/*N*- γ -ADABA crystal structure, a deep cavity becomes visible that provides a view into the catalytic core of the ectoine synthase with the bound iron, the substrate, and a water molecule (Fig. 8c). These ligands are present at the bottom of a deep tunnel (Fig. 8d).

Discussion

The last step of the biosynthetic route^{36,59} for the potent microbial stress protectant ectoine^{4,5,45} entails an intramolecular condensation reaction in which the EctA-formed linear *N*- γ -ADABA molecule is cyclized by the reaction of the carbonyl group with the α -amino group, whereby a water molecule is eliminated (Figs 1a and 7). The ectoine synthase (EC 4.2.1.108) mediating this cyclo-condensation reaction is classified as a member of the carbon-oxygen hydro-lyases (EC 4.2.1), but the hydrolytic activity (back reaction) of EctC for its own reaction product ectoine is minimal^{36,70}. However, the ectoine synthase from *H. elongata* can hydrolyze, at least to some extent, synthetic ectoine derivatives with either reduced or expanded ring sizes⁷⁰. Judging from the (Pl) EctC::Fe-ectoine crystal structure, the cavity of the ectoine synthase active site would be large enough to accommodate the seven-membered ring of the non-natural homoectoine molecule. The *H. elongata* enzyme is also somewhat promiscuous in its biosynthetic activity as it can form the synthetic compatible solute 5-amino-3, 4-dihydro-2H-pyrrole-2-carboxylate (ADPC) through the cyclic condensation of glutamine in a side reaction⁷⁰. Because the EctC-mediated biotransformation of *N*- γ -ADABA into ectoine is practically an irreversible reaction^{36,70}, one wonders how it was possible in this study to obtain (Pl)EctC::Fe crystals in complex with *N*- γ -ADABA. However, crystallization with this substrate was carried out at pH 4.2, conditions under which the (Pl)EctC protein is practically enzymatically inactive (Fig. 2b).

By using an ectoine synthase from the thermo-tolerant bacterium *P. lautus*⁶⁸, we were able to obtain high-resolution crystal structures of the full-length EctC enzyme in complex with its iron-cofactor, its substrate, and its product (Figs 3 and 6). The information obtained from this structural analysis illuminates for the first time the architecture of the catalytic core of ectoine synthase (Fig. 6a–c). The (Pl)EctC crystal structures presented here

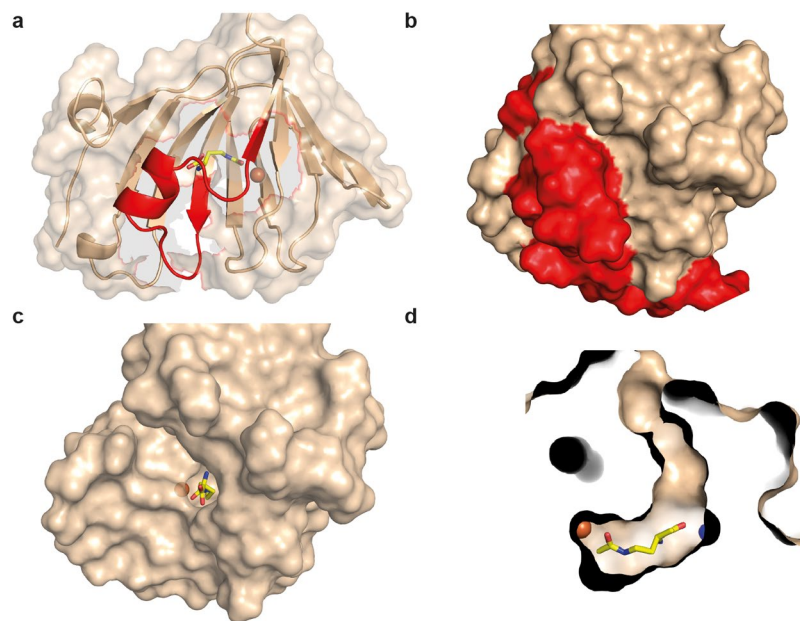


Figure 8. Structural features of the proposed (*Pl*)EctC lid region. (a) Ribbon and surface representation of the (*Pl*)EctC::Fe/*N*- γ -ADABA crystal structure highlighting (in red) the lid-region formed by the carboxy-terminal segment of the ectoine synthase. The spatial position of the *N*- γ -ADABA substrate (shown in yellow sticks) and that of the iron atom (shown as an orange sphere) are highlighted within the EctC active site. (b) Surface representation of the (*Pl*)EctC::Fe/*N*- γ -ADABA crystal structure in which the lid region is highlighted in red. Relative to the representation of the (*Pl*)EctC crystal structure shown in (a), the crystal structure shown in (b) is slightly rotated in order to provide an expanded view onto the lid region. (c) View into the catalytic core of the (*Pl*)EctC::Fe/*N*- γ -ADABA crystal structure after the *in silico* removal of the lid region (amino acids 103 to 130). (d) Cross-section through the catalytic core of the (*Pl*)EctC::Fe/*N*- γ -ADABA crystal structure revealing a plausible entry tunnel for the *N*- γ -ADABA substrate (in yellow sticks) and its spatial positions to the catalytically critical iron atom (orange sphere) and a water molecule (blue sphere) that interacts with the *N*- γ -ADABA molecule.

likely represent catalytic states of the enzyme prior and subsequent to catalysis (Figs 3a,b, and 6), thereby providing the foundation for a proposal for the EctC-catalyzed cyclo-condensation reaction (Figs 1a and 7). The ten residues involved in binding of the iron co-factor, the *N*- γ -ADABA substrate, and the reaction product ectoine are evolutionarily highly conserved among a large group of EctC-type proteins^{5,30,60} (Fig. 5a,b). Our structural and functional studies thus render the (*Pl*)EctC protein as a point of reference for the extended ectoine synthase family as a whole⁵ and thereby provide a blueprint for further biochemical and physiological studies.

A previous bioinformatic analysis has indicated that ectoine synthases form a distinct branch within the cupin protein super-family^{66,67}. The three-dimensional structure of the ectoine synthase⁶⁰ (and this study) follows the basic design principles of proteins belonging to this super-family^{63–67}, and matches closely in its overall fold those of the KdgF and the DddK degradative enzymes. These two cupin-type proteins carry out enzymatic reactions that are different from each other^{76,77} and from that catalyzed by the ectoine synthase (Figs 1a and 7). As expected^{66,67}, all residues important for the catalytic activity of the EctC enzyme protrude into the lumen of the cupin barrel (Fig. 6a,b). The (*Pl*)EctC protein is a head-to-tail dimer where backbone interactions between two β -sheets mediate the contacts between the monomers in the dimer assembly (Fig. 3b–d). A dimeric assembly has previously also been found through biochemical approaches for ectoine synthases from the bacteria *H. elongata*³⁶ and *S. alaskensis*^{60,73} and from the archaeon *N. maritimus*³⁰, suggesting that dimer-formation is probably a general feature of ectoine synthases.

The catalytically critical Fe²⁺ cation (Fig. 4a) is placed somewhat off-center within the central cavity of the (*Pl*)EctC monomer (Fig. 3a) and is part of an intricate network of interactions that position the *N*- γ -ADABA substrate within the active site of the enzyme close to the metal co-factor (Figs 6a and S4). Variations in the metal-binding motifs of cupins occur frequently^{63,64,66,67}, but the one we detected in the ectoine synthase (Figs 4a and 5a,b) is, to the best of our knowledge, novel. Cupins are often promiscuous with respect to the metal used for catalytic activity^{76,77,82–84}. For instance, crystals of the DddK DMSP lyase were found in one form to harbor Ni²⁺ while a second crystal form harbored either Fe²⁺ or Zn²⁺ with different levels of occupancy of the same metal binding site⁷⁷. Likewise, although Ni²⁺ was found in the KdgF crystal structure, reconstitution of the metal-depleted recombinant enzyme with various divalent metals identified Co²⁺ as the most effective catalyst⁷⁷. We obtained crystals of the (*Pl*)EctC protein only after adding substantial Fe²⁺ concentrations to the protein solution prior to crystallization and the previously reported crystal structure of the (*Sa*)EctC enzyme lacks a metal altogether⁶⁰. Despite this difference in metal content, the spatial position of the side chains of the three metal-coordinating residues in the active site of the (*Pl*)EctC and (*Sa*)EctC enzymes are super-imposable in their crystal structures

(Fig. 4a,b). A metal reconstitution experiment with the (Sa)EctC protein has previously revealed that the ectoine synthase can function with various divalent metals (Fe^{2+} , Zn^{2+} , Co^{2+} , Ni^{2+} , Cu^{2+} , Mn^{2+}), albeit with different levels of catalytic activity. Fe^{2+} served as the best-performing co-factor for the (Sa)EctC enzyme⁶⁰. Notwithstanding the apparent constraints in interpreting the specific type(s) of metal present in the enzymatically active (Sa)EctC⁶⁰ and (Pl)EctC proteins, there can be no doubt that the ectoine synthase is metal-dependent. This conclusion is supported by the results of site-directed mutagenesis experiments targeting these residues in both the (Sa)EctC⁶⁰ and (Pl)EctC proteins (Fig. 4c), and the complete conservation of the three metal-binding residues among the inspected 582 members of the extended EctC protein family⁵ (Fig. 5).

The ligand-binding site for ectoine in the (Pl)EctC enzyme differs significantly from those present in ectoine/5-hydroxyectoine-specific extracellular substrate-binding proteins operating in conjunction with either high-affinity ABC- (Ehu)⁸⁵, or TRAP- (Tea and Ueh) type transporters^{86,87}. A complex network of interactions with the ectoine molecule is observed in the corresponding EhuB, TeaA, and UehA substrate-binding proteins. It involves several aromatic side-chains, which contribute strongly to high-affinity binding of ectoine with values for the dissociation constant (K_d) of about 1.6 μM , 0.2 μM , and 1.4 μM , respectively^{85–87}. In contrast, in the (Pl)EctC::Fe-ectoine complex, only the aromatic side chain of Trp-21 contributes to the stabilization of the ectoine molecule in the active site and the carboxylate of ectoine additionally interacts with the side chain of Asn-38 (Fig. 6b).

A key contributor for the co-ordination of the ectoine molecule within the substrate-binding site of the EhuB, TeaA, and UehA ligand-binding proteins is the interaction of the carboxylate of ectoine with the side chain of an Arg residue. Replacement of this Arg residue by Ala abrogates high-affinity ectoine binding^{85,87}. While this interaction plays a central role in capturing ectoine stably by the extracellular substrate-binding proteins, it is not observed in the active site of the (Pl)EctC cytoplasmic enzyme (Fig. 6b). For ecophysiological reasons, a high substrate affinity is needed to scavenge ectoine through transport processes from scarce environmental sources^{88–90} for its use either as an osmoprotectant^{86,91} or as a nutrient^{47,87,92}. On the other hand, a low affinity of the (Pl)EctC enzyme for ectoine will be required to release it from the catalytic core once it has been formed by the cyclization of *N*- γ -ADABA (Figs 1a and 7). Hence, the differences observed in the architecture of the ectoine binding sites present in the EhuB, TeaA, and UehA substrate-binding proteins on one hand^{85–87} and the EctC enzyme on the other hand (Fig. 6a,b), most likely reflect functionally imposed constraints on protein structure.

In the previously reported crystal structures of the ectoine synthase from the cold-adapted marine microorganism *S. alaskensis*⁶⁹, the carboxy-terminal segment of the (Sa)EctC protein appeared to be highly flexible⁶⁰. However, we have no indications to this effect through the crystallographic snapshots of the (Pl)EctC proteins derived from the thermo-tolerant bacterium *P. lautus*⁸⁸. This region (27 amino acids of the 130-amino acids comprising (Pl)EctC protein) contains a surprisingly high number of strictly conserved residues among a large group of *bona fide* ectoine synthases (437 representatives) and orphan (145) EctC-type proteins (Fig. 5a,b)⁵. The crystal structures of the (Sa)EctC⁶⁰ and (Pl)EctC proteins suggest that these conserved carboxy-terminal segments form a lid over the entry to the cupin barrel (Fig. 8a,b). The catalytic core of the ectoine synthase is positioned at a bottom of a deep tunnel (Fig. 8d), and one can therefore readily envision that movement of the lid provides access of the *N*- γ -ADABA substrate to the active site (Figs 3a and 6) and a subsequent exit route for the reaction product ectoine. It therefore seems plausible that the lid region shields the active site of the ectoine synthase from the external solvent and thereby provides a privileged space for the elimination of a water molecule during the cyclo-condensation enzyme reaction (Figs 1a and 7). Moreover, opening and closing of the lid domain may also be required for the incorporation of the catalytically important metal ion into the active site.

When one views the EctC protein family in a phylogenomic context^{30,60}, one finds that the EctC biosynthetic enzyme is taxonomically affiliated with ten bacterial (including five sub-phyla of the *Proteobacteria*) and two archaeal phyla⁵ (Fig. S5). The ability to produce the stress protectant ectoine is thus primarily a trait of the *Bacteria*³⁰, with a dominant representation of ectoine producers among members of the *Proteobacteria* and *Actinobacteria*⁵. The few *Archaea* that possess *ect* biosynthetic genes (Fig. S5) have likely acquired them from bacterial donors via lateral gene transfer³⁰. Such genetic events also seem to be responsible for the introduction of ectoine biosynthetic genes into a few halophilic bacteriophilic protists^{27,28}, as these unicellular *Eukarya* might have gained the *ect* biosynthetic genes from ectoine-producing food bacteria living in the same high-saline habitat²⁹.

A previous study⁶⁰ and our recent comprehensive phylogenomic analysis⁵ revealed the existence of a substantial group of EctC-type proteins that are mostly found in a taxonomically rather heterogeneous group of microorganisms lacking canonical *ect* biosynthetic operons (Fig. S5). The physiological and biochemical function of these orphan EctC-type proteins is not yet clear^{5,60,80}. They may either be remnants of originally functional ectoine biosynthetic gene clusters, or they may possess catalytic activities that might rely on a substrate chemically related to its structure to *N*- γ -ADABA. The orphan EctC proteins often differ notably in their amino acid sequence from that of EctC proteins encoded by genes present in the complete *ectABC* gene cluster (Fig. 5a,b). However, when these proteins are now viewed within the framework of the (Pl)EctC crystal structures, we found that their predicted iron-, *N*- γ -ADABA- and ectoine-binding residues are mostly conserved, as is the spatial relationship of these residues within the main amino acid chain (Fig. 5a,b). Hence, the orphan EctC proteins possess the structural hallmarks of ectoine synthases, as suggested by an exploratory physiological study with the plant pathogen *P. syringae* pv. *syringae*⁸⁰. We do not know, however, of any anabolic or catabolic process in microorganisms that would yield the metabolite *N*- γ -ADABA except in the context of ectoine biosynthesis^{36,59} and, perhaps, also as the result of ectoine degradation^{47,92,93}. Our insights into the structure/function relationship of *bona fide* ectoine synthase reported here and the presented physiological and phylogenomic considerations (Fig. S5) might therefore serve as primers to study the substantial group of orphan EctC-type proteins⁵, both biochemically and structurally in the future to reveal their physiological function.

Methods

Chemicals. Ectoine was a kind gift from the bitop AG (Witten, Germany). Anhydrotetracycline hydrochloride (AHT), desthiobiotin, and Strep-Tactin Superflow chromatography material for the purification of *Strep*-tag II labeled proteins were purchased from IBA GmbH (Göttingen, Germany). The commercially unavailable substrate for the ectoine synthase, *N*- γ -acetyl-L-2,4-diaminobutyric acid (*N*- γ -ADABA), was synthesized through alkaline hydrolysis of ectoine⁹⁴. It was purified from the byproduct *N*- α -acetyl-L-2,4-diaminobutyric acid (*N*- α -ADABA) by repeated chromatography on a silica gel column (Merck silica gel 60) using a gradient of ethanol/25% ammonia/water 50:1:2–10:1:2 as eluent⁶⁰. The identity and purity of the isolated *N*- γ -ADABA was monitored by thin-layer chromatography and nuclear magnetic resonance spectroscopy (¹H-NMR and ¹³C-NMR) on a Bruker AVIII-400 or DRX-500 NMR spectrometer as described^{59,60,94}. All chemicals used to synthesize and purify *N*- γ -ADABA were purchased from either Sigma Aldrich (Steinheim, Germany) or Acros (Geel, Belgium). Numbering of the *N*- γ -ADABA and ectoine follows the IUPAC rules, applying replacement nomenclature for *N*- γ -ADABA as “2-amino-5-aza-6-oxoheptanoic acid” (see Fig. S3).

Recombinant DNA procedures and construction of plasmids. The DNA sequences of the *ectC* genes from the genome sequence of *P. lautus* Y4.12MC10 (accession number: NC_013406)⁶⁸ was used as the template for the synthesis of a codon-optimized version of *ectC* (LifeTechnologies; Darmstadt, Germany) for its heterologous expression in *E. coli*. The DNA sequence of this synthetic *ectC* gene has been deposited in the NCBI database under accession number KR002038. To allow the overproduction of the recombinant (PI)EctC protein in *E. coli* and its purification via affinity chromatography, an overexpression plasmid was constructed, which directs the synthesis of a (PI)EctC-*Strep*-tag II recombinant protein. For this purpose, the *ectC*-containing DNA fragment was retrieved from the plasmid provided by the supplier of the synthetic construct (LifeTechnologies), and inserted into the expression vector pASG-IBA3 (IBA GmbH, Göttingen, Germany). The *ectC* coding sequence was cloned into plasmid pASG-IBA3 in such a way that the resulting EctC protein is fused at its carboxy-terminus to a *Strep*-tag II affinity peptide (SA-WSHPQFEK), thereby allowing the purification of the (PI)EctC-*Strep*-tag II protein by affinity chromatography on a streptavidin affinity matrix (IBA GmbH, Göttingen, Germany). The transcription of the *ectC* gene in the resulting plasmid pWN14 [*P. lautus ectC*⁺; constructed by N. Widderich] is mediated by the *tet* promoter present on the backbone of the expression vector pASG-IBA3 and controlled through the TetR repressor whose DNA-binding activity can be abrogated by adding the synthetic inducer AHT to the growth medium.

Variants of the codon-optimized *ectC* gene from *P. lautus* present on plasmid pWN14 were prepared by site-directed mutagenesis using the Q5 Site-Directed Mutagenesis Kit (New England BioLabs GmbH, Frankfurt a. M., Germany) with custom synthesized DNA primers purchased from Microsynth AG (Lindau, Germany). The DNA sequence of the entire coding region of each mutant *ectC* gene was determined by Eurofins MWG (Ebersberg, Germany) to ensure the presence of the desired mutation and the absence of unwanted alterations. The following variants of the *P. lautus ectC* gene were constructed: pLC55 (Glu-57/Ala; GAA/GCA), pLC56 (Tyr-84/Ala; TAT/GCT), pLC57 (His-92/Ala; CAT/GCT), pLC58 (Cys-104/Ala; TGT/GCT), pLC59 (Cys-104/Ser; TGT/TCT), and pLC67 (Trp-21/Ala; TGG/GCG).

Bacterial strains, media, and growth conditions. The *E. coli* strain TOP10 (Invitrogen, Carlsbad, CA, USA) was used for the propagation of plasmids carrying *ectC* genes. Cultures of the plasmid-carrying *E. coli* strain were grown at 37 °C in Luria-Bertani (LB) liquid medium containing ampicillin (100 μ g ml⁻¹). Heterologous overproduction of the plasmid-encoded *P. lautus* EctC *Strep*-tag II protein [(PI)EctC] was carried out in the *E. coli* B strain BL21 in modified minimal medium A (MMA)⁹⁵ containing 0.5% (w/v) glucose as the carbon source and 0.5% (w/v) casamino acids, 1 mM MgSO₄, and 3 mM thiamine as supplements. Mutant derivatives of the (PI)EctC protein were overproduced and purified as described below for the corresponding wild-type proteins.

Overproduction, purification and analysis of the quaternary assembly of EctC proteins. Cells of the *E. coli* B strain BL21 harboring plasmid pWN14 (*ectC*⁺) were inoculated into modified MMA (1 L medium in a 2-L Erlenmeyer flask) to an OD₅₇₈ of 0.05 from an overnight culture. The cells were grown on an aerial shaker (set to 180 rpm) at 37 °C until the cultures reached an OD₅₇₈ of 0.5. At this time point the synthetic inducer AHT for the TetR repressor was added to a final concentration of 0.2 mg ml⁻¹ to trigger enhanced transcriptional activity of the *tet* promoter and thereby boost the expression of the plasmid-encoded *ectC* gene. After 2 h of further growth of the culture at 37 °C, the *E. coli* BL21 (pWN14) cells were harvested by centrifugation (4 600 \times g) and disrupted by passing them through a French Pressure cell (at 1 000 psi); a cleared cell lysate was prepared from these disrupted cells by ultracentrifugation (100 000 \times g) at 4 °C for 45 min as described⁷³. Cleared cell extracts of the (PI)EctC-*Strep*-tag II overproducing cultures were used to purify the recombinant proteins by affinity chromatography on Strep-Tactin affinity resin as detailed previously^{73,96}. The concentration of the (PI)EctC protein in the individual fractions eluted from the Strep-Tactin Superflow affinity column was measured with the Pierce BCA Protein Assay Kit (Thermo Fisher Scientific, Schwerte, Germany). The purity and apparent molecular mass of the (PI)EctC protein was assessed by SDS-PAGE (15% polyacrylamide), and the PageRuler Prestained Protein Ladder (Thermo Fisher Scientific) was used as a reference to assess the electrophoretic mobility of the (PI)EctC-*Strep*-tag II protein. The recombinant (PI)EctC protein was concentrated to approximately 10 mg ml⁻¹ with Vivaspin 6 columns (Sartorius Stedim Biotech, Göttingen, Germany) with a 10-kDa molecular-weight cutoff value prior to crystallization trials.

To analyze the quaternary assembly of the (PI)EctC protein, we used high-performance liquid chromatography coupled to multi-angle light scattering detection (HPLC-MALS). For these experiments, an Agilent Technologies system connected to a triple-angle light scattering detector (miniDAWN TREOS, Wyatt Technology Europe

GmbH, Dernbach, Germany) followed by a differential refractive index detection system (Wyatt Technology) was used. Typically, 200 μ l of purified (PI)EctC protein (2 mg ml⁻¹) was loaded onto the Bio SEC-5 HPLC column and the obtained data were analyzed with the ASTRA software package (Wyatt Technology).

Ectoine synthase enzyme activity assay. Ectoine synthase activity of the (PI)EctC protein was determined by HPLC-based enzyme assays^{30,60}. The EctC-mediated conversion of *N*- γ -ADABA into ectoine was performed in a 30- μ l reaction volume containing 10 mM *N*- γ -ADABA, 0.1 mM (NH₄)₂Fe(SO₄)₂, 20 mM HEPES (pH 8.5), and 50 mM NaCl at a temperature of 30 °C in a water bath. For these reactions 1 μ g of purified EctC protein was used. Each enzyme assay was run for 2.5 min and was stopped by adding 30 μ l of acetonitrile (100%) to the reaction vessel. The samples were then centrifuged (16 060 \times g, at room temperature for 10 min) to remove the denatured proteins and the supernatant was subsequently analyzed for the formation of ectoine by HPLC analysis. 10- μ l samples were injected into the HPLC system and chromatographed through a GROM-SIL Amino-1PR column (125 \times 4 mm with a particle size of 3 μ m) that was purchased from GROM (Rottenburg-Hailfingen, Germany). The amounts of the EctC-catalyzed enzyme reaction product ectoine in individual samples was monitored using an Infinity 1260 Diode Array Detector (DAD) (Agilent, Waldbronn, Germany) at 210 nm integrated into an Agilent 1260 Infinity LC system (Agilent). The ectoine content of the samples was quantified using the OpenLAB software suite (Agilent) using commercially available ectoine (bitop AG, Witten, Germany) as the standard. For the ectoine synthase enzyme activity assays, three independently isolated (PI)EctC protein preparations were used and each data-point from the individual protein preparations was assayed twice.

When mutant (PI)EctC proteins were assayed for their enzyme activity, the buffer conditions optimized for the wild-type enzyme were used, but 10 μ g of purified (PI)EctC protein were employed and the reaction time was extended to 30 min. During the initial screening for the pH optimum of the (PI)EctC enzyme, a buffer mixture of MES (pH 5.5), PIPES (pH 6.5), TES (pH 7.5), CHES (pH 8), HEPES (pH 8.5), and CAPS (pH 10) (20 mM each) was used. The pH values of these buffer solutions were adjusted with 38% HCl or 5 M NaOH at a temperature (30 °C) that was also used for the ectoine synthase enzyme reaction.

Crystallization of the (PI)EctC protein. Crystal screening was carried out at 285 K using the sitting-drop vapor-diffusion method. Several initial crystallization conditions for the (PI)EctC-*Strep*-tag II protein were obtained using commercial screens from NeXtal (Qiagen, Hilden, Germany) and Molecular Dimensions (Suffolk, England) in Corning 3553 plates. The homogenous (PI)EctC protein solution (8–12 mg ml⁻¹ in 20 mM Tris, pH 7.5, 200 mM NaCl) was premixed first with 100 mM Fe(II)Cl₂ to a final concentration of 4 mM and subsequently with either 1 M ectoine (to a final concentration of 40 mM) or 500 mM *N*- γ -ADABA (to a final concentration of 20 mM). These protein solutions were incubated on ice for one hour prior to crystallization trials. In these crystallization trials, 0.1 μ l (PI)EctC protein solution was mixed with 0.1 μ l reservoir solution and equilibrated against 50 μ l reservoir solution. (PI)EctC crystals were formed under several conditions, and the most promising one consisted of 0.2 M ammonium sulfate, 0.1 M phosphate citrate (pH 4.2), 20% (v/v) PEG 300, 10% (v/v) glycerol from NeXtal Core II suite (Qiagen, Hilden, Germany). The first crystals were obtained after around twelve hours and reached the maximum dimensions of about 120 \times 45 \times 30 μ m³ (with ectoine) and 250 \times 45 \times 35 μ m³ (with *N*- γ -ADABA). The crystallization conditions were optimized by grid screens around the initial condition and by variation of the combination of the added substrates. The drops of (PI)EctC protein composed of 1 μ l protein solution and 1 μ l reservoir solution were equilibrated against 300 μ l reservoir solution in sitting drops. Different premixes were set up (final concentrations): (i) 4 mM Fe(II)Cl₂, (ii) 40 mM ectoine, (iii) 20 mM *N*- γ -ADABA, (iv) 4 mM Fe(II)Cl₂, 40 mM ectoine, or (v) 4 mM Fe(II)Cl₂, 20 mM *N*- γ -ADABA. Large crystals were obtained after twelve hours either without any substrate or with ectoine, *N*- γ -ADABA, iron or alternatively the combination of Fe(II)Cl₂ and ectoine or Fe(II)Cl₂ and *N*- γ -ADABA. The largest crystals reached dimensions of 500 \times 200 \times 100 μ m³. All crystals were cryoprotected by carefully overlaying the crystallization drop with 3- μ l mineral oil before the crystals were harvested and flash-frozen in liquid nitrogen.

Data processing and structure determination. Data sets were collected from a single crystal of either (PI)EctC::Fe, (PI)EctC::Fe/*N*- γ -ADABA, and EctC::Fe/ectoine on beamline P13 at DESY (EMBL, Hamburg, Germany) and/or ID29 at the ESRF, Grenoble, France at 100 K. These data sets were processed using the XDS package⁹⁷ and scaled with XSCALE⁹⁸. Initial phases were obtained by molecular replacement using the program PHASER⁷² with the crystal structure of the *S. alaskensis* EctC protein (PDB entry 5BXX) (without taking its side chains into account) as a template⁶⁰. Model building and refinement were performed using COOT⁹⁹ and REFMAC5¹⁰⁰. Data refinement statistics and model content are summarized in Table 1. The atomic coordinates and structure factors have been deposited in the Worldwide Protein Data Bank (PDB) (<https://www.wwpdb.org/>) under the following accession codes: for the (PI)EctC::Fe complex, 5ONM for the (PI)EctC::Fe/*N*- γ -ADABA complex, and 5ONO for (PI)EctC::Fe/ectoine complex.

Figure preparation of crystal structures. Figures of the crystal structures of the (PI)EctC protein were prepared using the PyMol software suite (www.pymol.org)¹⁰¹.

Database searches and phylogenetic analysis of EctC-type proteins. The amino acid sequence of the *P. lautus* EctC protein (accession number: YP_003245677) was used as the template for BLAST searches¹⁰² (of all finished sequences of the microbial database of the US Department of Energy Joint Genome Institute (<http://jgi.doe.gov/>)⁸¹. EctC-type amino acid sequences⁵ were compared using the MAFFT multiple amino acid sequence alignment server (<http://mafft.cbrc.jp/alignment/server/>)¹⁰³. This data set was then used to construct a rooted phylogenetic tree of EctC-type sequences⁵ by employing the iTOL software suit (<http://itol.embl.de/>)¹⁰⁴. The dimer interface of the (PI)EctC protein was analyzed using PISA⁷⁴ (<http://www.ebi.ac.uk/pdbe/pisa/>). Structural

homologs of (PI)EctC were searched using the DALI-web server (http://ekhidna.biocenter.helsinki.fi/dali_server/start)⁷⁵ using the (PI)EctC:Fe crystal structure as the search query.

Data Availability

All data generated or analyzed during this study are included in this published article (and in its accompanying Supplementary Information). The atomic coordinates and structure factors for the crystal structures of the (PI)EctC protein determined in this study have been deposited in the Protein Data Bank with accession codes 5ONM for the (PI)EctC:Fe complex, 5ONN for the (PI)EctC:Fe/N- γ -ADABA complex, and 5ONO for (PI)EctC:Fe/ectoine complex.

References

- Galinski, E. A., Pfeiffer, H. P. & Trüper, H. G. 1,4,5,6-Tetrahydro-2-methyl-4-pyrimidinecarboxylic acid. A novel cyclic amino acid from halophilic phototrophic bacteria of the genus *Ectothiorhodospira*. *Eur J Biochem* **149**, 135–139 (1985).
- Inbar, L. & Lapidot, A. The structure and biosynthesis of new tetrahydropyrimidine derivatives in actinomycin D producer *Streptomyces parvulus*. Use of ¹³C- and ¹⁵N-labeled L-glutamate and ¹³C and ¹⁵N NMR spectroscopy. *J Biol Chem* **263**, 16014–16022 (1988).
- Kempf, B. & Bremer, E. Uptake and synthesis of compatible solutes as microbial stress responses to high osmolality environments. *Arch Microbiol* **170**, 319–330 (1998).
- Pastor, J. M. *et al.* Ectoines in cell stress protection: uses and biotechnological production. *Biotechnol Advan* **28**, 782–801, <https://doi.org/10.1016/j.biotechadv.2010.06.005> (2010).
- Czech, L. *et al.* Role of the extremolytes ectoine and hydroxyectoine as stress protectants and nutrients: genetics, phylogenomics, biochemistry, and structural analysis. *Genes (Basel)* **9**, 177, <https://doi.org/10.3390/genes9040177> (2018).
- Yancey, P. H. Organic osmolytes as compatible, metabolic and counteracting cytoprotectants in high osmolality and other stresses. *J Exp Biol* **208**, 2819–2830, <https://doi.org/10.1242/jeb.01730> (2005).
- Roeßler, M. & Müller, V. Osmoadaptation in bacteria and archaea: common principles and differences. *Env Microbiol Rep* **3**, 743–754 (2001).
- Wood, J. M. *et al.* Osmosensing and osmoregulatory compatible solute accumulation by bacteria. *Comp Biochem Physiol A Mol Integr Physiol* **130**, 437–460 (2001).
- Street, T. O., Bolen, D. W. & Rose, G. D. A molecular mechanism for osmolyte-induced protein stability. *Proc Natl Acad Sci USA* **103**, 13997–14002, 0606236103 (2006).
- Bolen, D. W. & Baskakov, I. V. The osmophobic effect: natural selection of a thermodynamic force in protein folding. *J Mol Biol* **310**, 955–963, <https://doi.org/10.1006/jmbi.2001.4819> (2001).
- Zaccari, G. *et al.* Neutrons describe ectoine effects on water H-bonding and hydration around a soluble protein and a cell membrane. *Sci Rep* **6**, 31434, <https://doi.org/10.1038/srep31434> (2016).
- Bremer, E. & Krämer, R. In *Bacterial Stress Responses* (eds Storz, G. & Hengge-Aronis, R.) 79–97 (ASM Press, 2000).
- Wood, J. M. Bacterial osmoregulation: a paradigm for the study of cellular homeostasis. *Annu Rev Microbiol* **65**, 215–238, <https://doi.org/10.1146/annurev-micro-090110-102815> (2011).
- Cayley, S., Lewis, B. A. & Record, M. T. Jr. Origins of the osmoprotective properties of betaine and proline in *Escherichia coli* K-12. *J Bacteriol* **174**, 1586–1595 (1992).
- van den Berg, J., Boersma, A. J. & Poolman, B. Microorganisms maintain crowding homeostasis. *Nat Rev Microbiol* **15**, 309–318, <https://doi.org/10.1038/nrmicro.2017.17> (2017).
- Boch, J., Kempf, B. & Bremer, E. Osmoregulation in *Bacillus subtilis*: synthesis of the osmoprotectant glycine betaine from exogenously provided choline. *J Bacteriol* **176**, 5364–5371 (1994).
- Street, T. O., Krukenberg, K. A., Rosgen, J., Bolen, D. W. & Agard, D. A. Osmolyte-induced conformational changes in the Hsp90 molecular chaperone. *Protein Sci* **19**, 57–65, <https://doi.org/10.1002/pro.282> (2010).
- Roychoudhury, A., Bieker, A., Haussinger, D. & Oesterhelt, F. Membrane protein stability depends on the concentration of compatible solutes - a single molecule force spectroscopic study. *Biol Chem* **394**, 1465–1474, <https://doi.org/10.1515/hsz-2013-0173> (2013).
- Bourot, S. *et al.* Glycine betaine-assisted protein folding in a *lysA* mutant of *Escherichia coli*. *J Biol Chem* **275**, 1050–1056 (2000).
- Ignatova, Z. & Gierasch, L. M. Inhibition of protein aggregation *in vitro* and *in vivo* by a natural osmoprotectant. *Proc Natl Acad Sci USA* **103**, 13357–13361, 0603772103 (2006).
- Tanne, C., Golovina, E. A., Hoekstra, F. A., Meffert, A. & Galinski, E. A. Glass-forming property of hydroxyectoine is the cause of its superior function as a desiccation protectant. *Front Microbiol* **5**, 150 (2014).
- Manzanera, M. *et al.* Hydroxyectoine is superior to trehalose for anhydrobiotic engineering of *Pseudomonas putida* KT2440. *Appl Environ Microbiol* **68**, 4328–4333 (2002).
- Lippert, K. & Galinski, E. A. Enzyme stabilization by ectoine-type compatible solutes: protection against heating, freezing and drying. *Appl Microbiol Biotechnol* **37**, 61–65 (1992).
- Stadtmiller, S. S., Gorensek-Benitez, A. H., Guseman, A. J. & Pielak, G. J. Osmotic shock induced protein destabilization in living cells and its reversal by glycine betaine. *J Mol Biol* **429**, 1155–1161, <https://doi.org/10.1016/j.jmb.2017.03.001> (2017).
- Chattopadhyay, M. K. *et al.* The chemical chaperone proline relieves the thermosensitivity of a *dnaK* deletion mutant at 42 degrees C. *J Bacteriol* **186**, 8149–8152, <https://doi.org/10.1128/JB.186.23.8149-8152.2004> (2004).
- Diamant, S., Eliahu, N., Rosenthal, D. & Goloubinoff, P. Chemical chaperones regulate molecular chaperones *in vitro* and in cells under combined salt and heat stresses. *J Biol Chem* **276**, 39586–39591, <https://doi.org/10.1074/jbc.M103081200> (2001).
- Harding, T., Brown, M. W., Simpson, A. G. & Roger, A. J. Osmoadaptive strategy and its molecular signature in obligately halophilic heterotrophic protists. *Genome Biol Evol* **8**, 2241–2258, <https://doi.org/10.1093/gbe/evw152> (2016).
- Weinisch, L. *et al.* Identification of osmoadaptive strategies in the halophile, heterotrophic ciliate *Schmidingerothrix salinarum*. *PLoS Biol* **16**, e2003892, <https://doi.org/10.1371/journal.pbio.2003892> (2018).
- Czech, L. & Bremer, E. With a pinch of extra salt - Did predatory protists steal genes from their food? *PLoS Biol* **16**, e2005163, <https://doi.org/10.1371/journal.pbio.2005163> (2018).
- Widderich, N. *et al.* Strangers in the archaeal world: osmostress-responsive biosynthesis of ectoine and hydroxyectoine by the marine thaumarchaeon *Nitrosopumilus maritimus*. *Env Microbiol* **18**, 1227–1248 (2016).
- Widderich, N. *et al.* Biochemical properties of ectoine hydroxylases from extremophiles and their wider taxonomic distribution among microorganisms. *PLoS One* **9**, e93809, <https://doi.org/10.1371/journal.pone.0093809> (2014).
- Louis, P. & Galinski, E. A. Characterization of genes for the biosynthesis of the compatible solute ectoine from *Marinococcus halophilus* and osmoregulated expression in *Escherichia coli*. *Microbiology* **143**, 1141–1149 (1997).
- Bursy, J., Pierik, A. J., Pica, N. & Bremer, E. Osmotically induced synthesis of the compatible solute hydroxyectoine is mediated by an evolutionarily conserved ectoine hydroxylase. *J Biol Chem* **282**, 31147–31155, <https://doi.org/10.1074/jbc.M704023200> (2007).

34. Lo, C. C., Bonner, C. A., Xie, G., D'Souza, M. & Jensen, R. A. Cohesion group approach for evolutionary analysis of aspartokinase, an enzyme that feeds a branched network of many biochemical pathways. *Microbiol Mol Biol Rev* **73**, 594–651, <https://doi.org/10.1128/MMBR.00024-09> (2009).
35. Stöveken, N. *et al.* A specialized aspartokinase enhances the biosynthesis of the osmoprotectants ectoine and hydroxyectoine in *Pseudomonas stutzeri* A1501. *J Bacteriol* **193**, 4456–4468, <https://doi.org/10.1128/JB.00345-11> (2011).
36. Ono, H. *et al.* Characterization of biosynthetic enzymes for ectoine as a compatible solute in a moderately halophilic eubacterium. *Halomonas elongata*. *J Bacteriol* **181**, 91–99 (1999).
37. Höppner, A., Widderich, N., Lenders, M., Bremer, E. & Smits, S. H. J. Crystal structure of the ectoine hydroxylase, a snapshot of the active site. *J Biol Chem* **289**, 29570–29583, <https://doi.org/10.1074/jbc.M114.576769> (2014).
38. Widderich, N. *et al.* Molecular dynamics simulations and structure-guided mutagenesis provide insight into the architecture of the catalytic core of the ectoine hydroxylase. *J Mol Biol* **426**, 586–600, <https://doi.org/10.1016/j.jmb.2013.10.028> (2014).
39. Garcia-Esteva, R. *et al.* The *ectD* gene, which is involved in the synthesis of the compatible solute hydroxyectoine, is essential for thermoprotection of the halophilic bacterium *Chromohalobacter salexigens*. *J Bacteriol* **188**, 3774–3784, <https://doi.org/10.1128/JB.00136-06> (2006).
40. Bursy, J. *et al.* Synthesis and uptake of the compatible solutes ectoine and 5-hydroxyectoine by *Streptomyces coelicolor* A3(2) in response to salt and heat stresses. *Appl Environ Microbiol* **74**, 7286–7296, <https://doi.org/10.1128/AEM.00768-08> (2008).
41. Kuhlmann, A. U. & Bremer, E. Osmotically regulated synthesis of the compatible solute ectoine in *Bacillus pasteurii* and related *Bacillus* spp. *Appl Environ Microbiol* **68**, 772–783 (2002).
42. Kuhlmann, A. U., Bursy, J., Gimpel, S., Hoffmann, T. & Bremer, E. Synthesis of the compatible solute ectoine in *Virgibacillus pantothenicus* is triggered by high salinity and low growth temperature. *Appl Environ Microbiol* **74**, 4560–4563, <https://doi.org/10.1128/AEM.00492-08> (2008).
43. Vargas, C. *et al.* Unravelling the adaptation responses to osmotic and temperature stress in *Chromohalobacter salexigens*, a bacterium with broad salinity tolerance. *Saline Sys* **4**, 14, <https://doi.org/10.1186/1746-1448-4-14> (2008).
44. Kol, S. *et al.* Metabolomic characterization of the salt stress response in *Streptomyces coelicolor*. *Appl Environ Microbiol* **76**, 2574–2581, <https://doi.org/10.1128/AEM.01992-09> (2010).
45. Kunte, H. J., Lentzen, G. & Galinski, E. Industrial production of the cell protectant ectoine: protection, mechanisms, processes, and products. *Cur Biotechnol* **3**, 10–25 (2014).
46. Graf, R., Anzali, S., Buenger, J., Pfluecker, F. & Driller, H. The multifunctional role of ectoine as a natural cell protectant. *Clinics Dermatol* **26**, 326–333, <https://doi.org/10.1016/j.clindermatol.2008.01.002> (2008).
47. Schwibbert, K. *et al.* A blueprint of ectoine metabolism from the genome of the industrial producer *Halomonas elongata* DSM 2581^T. *Environ Microbiol* **13**, 1973–1994, <https://doi.org/10.1111/j.1462-2920.2010.02336.x> (2011).
48. Schubert, T., Maskow, T., Benndorf, D., Harms, H. & Breuer, U. Continuous synthesis and excretion of the compatible solute ectoine by a transgenic, nonhalophilic bacterium. *Appl Environ Microbiol* **73**, 3343–3347, <https://doi.org/10.1128/AEM.02482-06> (2007).
49. Ning, Y. *et al.* Pathway construction and metabolic engineering for fermentative production of ectoine in *Escherichia coli*. *Metabol Engineering* **36**, 10–18, <https://doi.org/10.1016/j.ymben.2016.02.013> (2016).
50. Becker, J. *et al.* Systems metabolic engineering of *Corynebacterium glutamicum* for production of the chemical chaperone ectoine. *Microb Cell Fact* **12**, 110, <https://doi.org/10.1186/1475-2859-12-110> (2013).
51. He, Y. Z. *et al.* High production of ectoine from aspartate and glycerol by use of whole-cell biocatalysis in recombinant *Escherichia coli*. *Microb Cell Fact* **14**, 55, <https://doi.org/10.1186/s12934-015-0238-0> (2015).
52. Czech, L., Stöveken, N. & Bremer, E. EctD-mediated biotransformation of the chemical chaperone ectoine into hydroxyectoine and its mechanosensitive channel-independent excretion. *Microb Cell Fact* **15**, 126, <https://doi.org/10.1186/s12934-016-0525-4> (2016).
53. Seip, B., Galinski, E. A. & Kurz, M. Natural and engineered hydroxyectoine production based on the *Pseudomonas stutzeri* *ectABCD-ask* gene cluster. *Appl Environ Microbiol* **77**, 1368–1374, <https://doi.org/10.1128/AEM.02124-10> (2011).
54. Rodriguez-Moya, J., Argandona, M., Iglesias-Guerra, F., Nieto, J. J. & Vargas, C. Temperature- and salinity-decoupled overproduction of hydroxyectoine by *Chromohalobacter salexigens*. *Appl Environ Microbiol* **79**, 1018–1023, <https://doi.org/10.1128/AEM.02774-12> (2013).
55. Perez-Garcia, F., Ziert, C., Risse, J. M. & Wendisch, V. F. Improved fermentative production of the compatible solute ectoine by *Corynebacterium glutamicum* from glucose and alternative carbon sources. *J Biotechnol* **258**, 59–69, <https://doi.org/10.1016/j.jbiotec.2017.04.039> (2017).
56. Czech, L., Poehl, S., Hub, P., Stöveken, N. & Bremer, E. Tinkering with osmotically controlled transcription allows enhanced production and excretion of ectoine and hydroxyectoine from a microbial cell factory. *Appl Environ Microbiol* **84**, e01772–01717 (2018).
57. Reuter, K. *et al.* Synthesis of 5-hydroxyectoine from ectoine: crystal structure of the non-heme iron(II) and 2-oxoglutarate-dependent dioxygenase EctD. *PLoS One* **5**, e10647, <https://doi.org/10.1371/journal.pone.0010647> (2010).
58. Islam, M. S., Leissing, T. M., Chowdhury, R., Hopkinson, R. J. & Schofield, C. J. 2-Oxoglutarate-dependent oxygenases. *Annu Rev Biochem* **87**, 585–620, <https://doi.org/10.1146/annurev-biochem-061516-044724> (2018).
59. Peters, P., Galinski, E. A. & Trüper, H. G. The biosynthesis of ectoine. *FEMS Microbiol. Lett.* **71**, 157–162 (1990).
60. Widderich, N. *et al.* Biochemistry and crystal structure of the ectoine synthase: a metal-containing member of the cupin superfamily. *PLoS One* **11**, e0151285 (2016).
61. Moritz, K. D., Amendt, B., Witt, E. M. H. J. & Galinski, E. A. The hydroxyectoine gene cluster of the non-halophilic acidophile *Acidiphilium cryptum*. *Extremophiles* **19**, 87–99, <https://doi.org/10.1007/s00792-014-0687-0> (2015).
62. Reshetnikov, A. S., Khmelina, V. N. & Trotsenko, Y. A. Characterization of the ectoine biosynthesis genes of haloalkalotolerant obligate methanotroph “*Methylobaculum alcaliphilum* 20Z”. *Arch Microbiol* **184**, 286–297, <https://doi.org/10.1007/s00203-005-0042-z> (2006).
63. Agarwal, G., Rajavel, M., Gopal, B. & Srinivasan, N. Structure-based phylogeny as a diagnostic for functional characterization of proteins with a cupin fold. *PLoS One* **4**, e5736, <https://doi.org/10.1371/journal.pone.0005736> (2009).
64. Uberto, R. & Moomaw, E. W. Protein similarity networks reveal relationships among sequence, structure, and function within the Cupin superfamily. *PLoS One* **8**, e74477, <https://doi.org/10.1371/journal.pone.0074477> (2013).
65. Galperin, M. Y. & Koonin, E. V. Divergence and convergence in enzyme evolution. *J Biol Chem* **287**, 21–28, <https://doi.org/10.1074/jbc.R111.241976> (2012).
66. Dunwell, J. M., Culham, A., Carter, C. E., Sosa-Aguirre, C. R. & Goodenough, P. W. Evolution of functional diversity in the cupin superfamily. *Trends Biochem Sci* **26**, 740–746 (2001).
67. Dunwell, J. M., Purvis, A. & Khuri, S. Cupins: the most functionally diverse protein superfamily? *Phytochemistry* **65**, 7–17 (2004).
68. Mead, D. A. *et al.* Complete genome sequence of *Paenibacillus* strain Y4.12MC10, a novel *Paenibacillus lautus* strain isolated from Obsidian Hot Spring in Yellowstone National Park. *Stand Genomic Sci* **6**, 381–400, <https://doi.org/10.4056/sigs.2605792> (2012).
69. Ting, L. *et al.* Cold adaptation in the marine bacterium, *Sphingopyxis alaskensis*, assessed using quantitative proteomics. *Environ Microbiol* **12**, 2658–2676, <https://doi.org/10.1111/j.1462-2920.2010.02235.x> (2010).
70. Witt, E. M., Davies, N. W. & Galinski, E. A. Unexpected property of ectoine synthase and its application for synthesis of the engineered compatible solute ADPC. *Appl Microbiol Biotechnol* **91**, 113–122, <https://doi.org/10.1007/s00253-011-3211-9> (2011).

71. Reshetnikov, A. S., Khmelenina, V. N., Mustakhimov, I. I. & Trotsenko, Y. A. Genes and enzymes of ectoine biosynthesis in halotolerant methanotrophs. *Methods Enzymol* **495**, 15–30, <https://doi.org/10.1016/B978-0-12-386905-0.00002-4> (2011).
72. Emsley, P. & Cowtan, K. Coot: model-building tools for molecular graphics. *Acta Crystallogr D Biol Crystallogr* **60**, 2126–2132, <https://doi.org/10.1107/S0907444904019158> (2004).
73. Kobus, S., Widderich, N., Hoepfner, A., Bremer, E. & Smits, S. H. J. Overproduction, crystallization and X-ray diffraction data analysis of ectoine synthase from the cold-adapted marine bacterium *Sphingopyxis alaskensis*. *Acta Cryst* **F71**, 1027–1032 (2015).
74. Krissinel, E. & Henrick, K. Inference of macromolecular assemblies from crystalline state. *J Mol Biol* **372**, 774–797, <https://doi.org/10.1016/j.jmb.2007.05.022> (2007).
75. Holm, L. & Rosenström, P. Dali server: conservation mapping in 3D. *Nucleic Acids Res* **38**, W545–549, <https://doi.org/10.1093/nar/gkq366> (2010).
76. Hobbs, J. K. *et al.* KdG, the missing link in the microbial metabolism of uronate sugars from pectin and alginate. *Proc Natl Acad Sci USA* **113**, 6188–6193, <https://doi.org/10.1073/pnas.1524214113> (2016).
77. Schnicker, N. J., De Silva, S. M., Todd, J. D. & Dey, M. Structural and biochemical insights into dimethylsulfoniopropionate cleavage by cofactor-bound DddK from the prolific marine bacterium *Pelagibacter*. *Biochemistry* **56**, 2873–2885, <https://doi.org/10.1021/acs.biochem.7b00099> (2017).
78. Broy, S. *et al.* Abiotic stress protection by ecologically abundant dimethylsulfoniopropionate and its natural and synthetic derivatives: insights from *Bacillus subtilis*. *Environ Microbiol* **7**, 2362–2378, <https://doi.org/10.1111/1462-2920.12698> (2015).
79. Widderich, N., Bremer, E. & Smits, S. H. J. The ectoine hydroxylase: a nonheme-containing iron(II) and 2-oxoglutarate-dependent dioxygenase. *Encyclopedia of Inorganic and Bioinorganic Chemistry, Online* (2016).
80. Kurz, M., Burch, A. Y., Seip, B., Lindow, S. E. & Gross, H. Genome-driven investigation of compatible solute biosynthesis pathways of *Pseudomonas syringae* pv. *syringae* and their contribution to water stress tolerance. *Appl Environ Microbiol* **76**, 5452–5462, <https://doi.org/10.1128/AEM.00686-10> (2010).
81. Nordberg, H. *et al.* The genome portal of the Department of Energy Joint Genome Institute: 2014 updates. *Nucleic Acids Res* **42**, D26–D31, <https://doi.org/10.1093/nar/gkt1069> (2013).
82. Silvennoinen, L., Sandalova, T. & Schneider, G. The polyketide cyclase RemF from *Streptomyces resistomycificus* contains an unusual octahedral zinc binding site. *FEBS Lett* **583**, 2917–2921, <https://doi.org/10.1016/j.febslet.2009.07.061> (2009).
83. Hajnal, I. *et al.* Biochemical and structural characterization of a novel bacterial manganese-dependent hydroxynitrile lyase. *FEBS J* **280**, 5815–5828, <https://doi.org/10.1111/febs.12501> (2013).
84. Gopal, B., Madan, L. L., Betz, S. F. & Kossiakoff, A. A. The crystal structure of a quercetin 2,3-dioxygenase from *Bacillus subtilis* suggests modulation of enzyme activity by a change in the metal ion at the active site(s). *Biochemistry* **44**, 193–201, <https://doi.org/10.1021/bi0484421> (2005).
85. Hanekop, N. *et al.* Crystal structure of the ligand-binding protein EhuB from *Sinorhizobium meliloti* reveals substrate recognition of the compatible solutes ectoine and hydroxyectoine. *J Mol Biol* **374**, 1237–1250, <https://doi.org/10.1016/j.jmb.2007.09.071> (2007).
86. Kuhlmann, S. I., Terwisscha van Scheltinga, A. C., Bienert, R., Kunte, H. J. & Ziegler, C. 1.55 Å structure of the ectoine binding protein TeaA of the osmoregulated TRAP-transporter TeaABC from *Halomonas elongata*. *Biochemistry* **47**, 9475–9485, <https://doi.org/10.1021/bi8006719> (2008).
87. Lecher, J. *et al.* The crystal structure of UehA in complex with ectoine-A comparison with other TRAP-T binding proteins. *J Mol Biol* **389**, 58–73, <https://doi.org/10.1016/j.jmb.2009.03.077> (2009).
88. Warren, C. Do microbial osmolytes or extracellular depolymerization products accumulate as soil dries? *Soil Biol & Biochem* **98**, 54–63 (2016).
89. Warren, C. R. Response of osmolytes in soil to drying and rewetting. *Soil Biol & Biochem* **70**, 22–32 (2014).
90. Mosier, A. C. *et al.* Metabolites associated with adaptation of microorganisms to an acidophilic, metal-rich environment identified by stable-isotope-enabled metabolomics. *mBio* **4**, e00484–00412, <https://doi.org/10.1128/mBio.00484-12> (2013).
91. Kuhlmann, A. U., Hoffmann, T., Bursy, J., Jebbar, M. & Bremer, E. Ectoine and hydroxyectoine as protectants against osmotic and cold stress: uptake through the SigB-controlled betaine-choline- carnitine transporter-type carrier EctT from *Virgibacillus pantothenicus*. *J Bacteriol* **193**, 4699–4708, <https://doi.org/10.1128/JB.05270-11> (2011).
92. Schulz, A. *et al.* Feeding on compatible solutes: a substrate-induced pathway for uptake and catabolism of ectoines and its genetic control by EnuR. *Environ Microbiol* **19**, 926–946, <https://doi.org/10.1111/1462-2920.13414> (2017).
93. Schulz, A. *et al.* Transcriptional regulation of ectoine catabolism in response to multiple metabolic and environmental cues. *Env Microbiol* **19**, 4599–4619 (2017).
94. Kunte, H. J., Galinski, E. A. & Trüper, G. H. A modified FMOC-method for the detection of amino acid-type osmolytes and tetrahydropyrimidines (ectoines). *J Microbiol Meth* **17**, 129–136 (1993).
95. Miller, J. H. *Experiments in molecular genetics.*, (Cold Spring Harbor Laboratory, 1972).
96. Hoepfner, A., Widderich, N., Bremer, E. & Smits, S. H. J. Overexpression, crystallization and preliminary X-ray crystallographic analysis of the ectoine hydroxylase from *Sphingopyxis alaskensis*. *Acta Cryst* **F70**, 493–496 (2014).
97. Kabsch, W. XDS. *Acta Crystallogr D Biol Crystallogr* **66**, 125–132, <https://doi.org/10.1107/S0907444909047337> (2010).
98. Kabsch, W. Integration, scaling, space-group assignment and post-refinement. *Acta Crystallogr D Biol Crystallogr* **66**, 133–144, <https://doi.org/10.1107/S0907444909047374> (2010).
99. Emsley, P., Lohkamp, B., Scott, W. G. & Cowtan, K. Features and development of Coot. *Acta Crystallogr D Biol Crystallogr* **66**, 486–501, <https://doi.org/10.1107/S0907444910007493> (2010).
100. Murshudov, G. N. *et al.* REFMAC5 for the refinement of macromolecular crystal structures. *Acta Crystallogr D Biol Crystallogr* **67**, 355–367, <https://doi.org/10.1107/S0907444911001314> (2011).
101. Delano, W. L. *The PyMol molecular graphics system.* (Delano Scientific, 2002).
102. Altschul, S. F., Gish, W., Miller, W., Myers, E. W. & Lipman, D. J. Basic local alignment search tool. *J Mol Biol* **215**, 403–410 (1990).
103. Katoh, K. & Standley, D. M. MAFFT multiple sequence alignment software version 7: improvements in performance and usability. *Mol Biol Evo* **30**, 772–780, <https://doi.org/10.1093/molbev/mst010> (2013).
104. Letunic, I. & Bork, P. Interactive Tree Of Life v2: online annotation and display of phylogenetic trees made easy. *Nucleic Acids Res* **39**, W475–478, <https://doi.org/10.1093/nar/gkr201> (2011).

Acknowledgements

We cordially acknowledge the staff of beamline P13 (DESY, EMBL, Hamburg, Germany) for their kind and helpful support during data collection and are equally thankful to the staff of the ID29 beamline of the European Synchrotron Radiation Facility (Grenoble, France) for expertly providing synchrotron radiation facilities. We greatly appreciate the generous gift of ectoine by the bitop AG (Witten, Germany) for our study and the helpful discussions with Wolfgang Buckel. We thank Jochen Sohn for his excellent technical assistance during EctC protein overproduction and purification, and acknowledge N. Widderich for the construction of the *ectC* overexpression plasmid pWN14. We are grateful to Vickie Koogler for her help in the language editing of our manuscript and to our colleague Lutz Schmitt (Institute of Biochemistry, Heinrich-Heine University Düsseldorf) for his kind support of this project. This work was financially supported in part by grants from

the Deutsche Forschungsgemeinschaft (DFG) through the SFB 987 (Philipps-University Marburg; to E.B.), by the LOEWE program of the state of Hessen (via the Center for Synthetic Microbiology, Marburg; to J.H. and E.B.), by the Institute of Biochemistry (Heinrich-Heine-University Düsseldorf; to S.H.J.S.) and the DFG-funded Transregio research consortium TRR51 (Rheinische Friedrich Wilhelms-Universität Bonn; to J.S.D.). L.C. gratefully acknowledges the receipt of a Ph.D. fellowship from the International Max Planck Research School for Environmental, Cellular and Molecular Microbiology (IMPRS-Mic, Marburg).

Author Contributions

E.B. and S.H.J.S. conceived and coordinated the study and evaluated all data. L.C. performed overexpression, purification, functional characterization of proteins, constructed mutants and analyzed the resulting data. A.H., S.K. and S.H.J.S. designed and performed crystallization experiments, solved the crystal structures and analyzed the data. R.R. and J.S.D. synthesized reagents and analyzed their identity and purity. A.S. performed mass spectrometry. J.H. and J.S.D. made the proposal for the ectoine synthase reaction mechanism. E.B., L.C., S.H.J.S., J.H. and J.S.D. wrote the manuscript with input from other authors.

Additional Information

Supplementary information accompanies this paper at <https://doi.org/10.1038/s41598-018-36247-w>.

Competing Interests: The authors declare no competing interests.

Publisher's note: Springer Nature remains neutral with regard to jurisdictional claims in published maps and institutional affiliations.



Open Access This article is licensed under a Creative Commons Attribution 4.0 International License, which permits use, sharing, adaptation, distribution and reproduction in any medium or format, as long as you give appropriate credit to the original author(s) and the source, provide a link to the Creative Commons license, and indicate if changes were made. The images or other third party material in this article are included in the article's Creative Commons license, unless indicated otherwise in a credit line to the material. If material is not included in the article's Creative Commons license and your intended use is not permitted by statutory regulation or exceeds the permitted use, you will need to obtain permission directly from the copyright holder. To view a copy of this license, visit <http://creativecommons.org/licenses/by/4.0/>.

© The Author(s) 2019

Exploiting substrate promiscuity of ectoine hydroxylase for regio- and stereoselective modification of homoectoine

Laura Czech¹, Sarah Wilcken¹, Oliver Czech¹, Dr. Uwe Linne¹, Jarryd Brauner², Sander H. Smits³, Erwin A. Galinski², Erhard Bremer^{1*}

¹University of Marburg, Germany, ²University of Bonn, Germany, ³Heinrich Heine University of Düsseldorf, Germany

5.2.5. Exploiting substrate promiscuity of ectoine hydroxylase to produce the synthetic osmoprotectant hydroxy-homoectoine

Czech L, Wilcken S, Czech O, Linne U, Brauner J, Smits SHJ, Galinski EA, Bremer E. Exploiting substrate promiscuity of ectoine hydroxylase for regio- and stereoselective modification of homoectoine. *submitted to Front Microbiol.*

The next chapter includes the submitted manuscript to Frontiers in Microbiology "Exploiting substrate promiscuity of ectoine hydroxylase to produce the synthetic osmoprotectant hydroxy-homoectoine". Prof. E. Bremer and I conceived the study and discussed the data. I constructed all strains used in this study and performed enzyme assays, HPLC analysis, biotransformation experiments and osmotic stress protection experiments. I supervised a master student, S. Wilcken, who helped in the exploratory phase of the enzyme assays. She established the improved enzyme assay conditions and the HPLC analysis of homoectoine and hydroxyhomoectoine. Furthermore, S. Wilcken also conducted osmoprotectant growth assays and performed biotransformation experiments. J. Brauner synthesized the substrate homoectoine, U. Linne conducted mass analysis and O. Czech performed NMR studies as well as DFT calculations and analyzed the resulting data. S. H. J. Smits performed modeling and docking analysis. I prepared all figures included in this publication and analyzed the literature together with E. Bremer. E. Bremer, E. A. Galinski and I wrote the manuscript. All other authors commented on the manuscript.

5.2.5.1. Original publication

1

1 **Exploiting substrate promiscuity of ectoine hydroxylase for regio- and**
2 **stereoselective modification of homoectoine**

3

4

5 **Laura Czech¹, Sarah Wilcken¹, Oliver Czech², Uwe Linne², Jarryd Brauner³,**
6 **Sander H.J. Smits^{4,5}, Erwin A. Galinski³, and Erhard Bremer^{1,6*}**

7

8

9 ¹Laboratory for Microbiology, Department of Biology, Philipps-University Marburg,
10 Marburg, Germany

11 ²Department of Chemistry, Philipps-University Marburg, Marburg, Germany

12 ³Institute of Microbiology and Biotechnology, Rheinische Friedrich-Wilhelms-University,
13 Bonn, Germany

14 ⁴Institute of Biochemistry, Heinrich-Heine University Düsseldorf, Düsseldorf, Germany

15 ⁵Center for Structural Studies, Heinrich-Heine University Düsseldorf, Düsseldorf, Germany

16 ⁶SYNMIKRO Research Center, Philipps-University Marburg, Marburg, Germany

17

18

19

20

21

22

23 **Running title:** Chemical biology of homoectoine

24

25 **Word-count:** 256 Abstract/9 024 main text

26 **Number of figures:** eight

27

28

29 **For correspondence during the reviewing and editorial process please contact:**

30 Dr. Erhard Bremer, Philipps-University Marburg, Dept. of Biology, Laboratory for Microbiology, Karl-
31 von-Frisch-Str. 8, D-35032 Marburg, Germany. Phone: (+49)-6421-2821529. Fax: (+49)-6421-
32 2828979. E-Mail: bremer@staff.uni-marburg.de

33

34 *Correspondence:

35 Erhard Bremer: bremer@staff.uni-marburg.de

ABSTRACT

Extant enzymes are not only highly efficient biocatalysts for a single, or a group of chemically closely related substrates but often have retained, as a mark of their evolutionary history, a certain degree of substrate ambiguity. Fashionably addressed as underground metabolism, this substrate ambiguity provides fertile grounds for evolution and can be utilized for protein engineering, developing novel metabolic traits, and custom-designing chemicals with useful attributes. We have exploited the substrate ambiguity of the ectoine hydroxylase (EctD), a member of the non-heme Fe(II)-containing and 2-oxoglutarate-dependent dioxygenase superfamily, for such a task. Naturally, the EctD enzyme performs a precise regio- and stereoselective hydroxylation of the ubiquitous stress protectant and chemical chaperone ectoine to yield *trans*-5-hydroxyectoine. Using a synthetic ectoine derivative, homoectoine, which possess an expanded seven membered ring structure, we were able to selectively generate, both *in vitro* and *in vivo*, *trans*-5-hydroxyhomoectoine. For this transformation, we specifically used the EctD enzyme from *Pseudomonas stutzeri* in a whole cell biocatalyst approach, as this enzyme exhibits high catalytic efficiency not only for its natural substrate ectoine but also for homoectoine. Molecular docking approaches with the crystal structure of the *Sphingopyxis alaskensis* EctD protein predicted the formation of *trans*-5-hydroxyhomoectoine, a stereochemical configuration that we experimentally verified by nuclear-magnetic resonance spectroscopy. An *Escherichia coli* cell factory expressing the *P. stutzeri* *ectD* gene from a synthetic promoter imported homoectoine via the ProU and ProP compatible solute transporters, hydroxylated it, and secreted the formed *trans*-5-hydroxyhomoectoine, independent from mechanosensitive channels, into the growth medium from which it could be purified by high-pressure liquid chromatography.

Keywords: compatible solutes, ectoine, homoectoine, ectoine hydroxylase, biocatalysis, whole cell biotransformation, chemical biology

INTRODUCTION

It is generally assumed that primordial cells had only a restricted number of proteins with different folds and that the enzymes present in these cells exhibited a broad substrate-specificity (Jensen, 1976; Khersonsky and Tawfik, 2010; Michael, 2017). This substrate ambiguity (Jensen, 1976) provided fertile ground for evolution to shape the substrate profiles of enzymes in extant microbial cells towards a higher specificity and catalytic efficiency (Jensen, 1976; Khersonsky and Tawfik, 2010; Pandya et al., 2014; Michael, 2017; Newton et al., 2018). However, it is increasingly recognized that many of the extant enzymes have retained, at least in part, their original substrate ambiguity, thereby creating a metabolic profile of cells that is fashionably addressed as ‘underground metabolism’ (D’Ari and Casadesus, 1998). While imposing a metabolic burden onto the cell, enzyme promiscuity allows the selection of novel metabolic traits when new substrates become available, or relieve constraints in metabolism when bottlenecks arise. Underground metabolism, combined with selective pressures on growth and survival, can thus aid the adaptation of microorganisms to new ecological niches (Barrick and Lenski, 2013; Pandya et al., 2014; Michael, 2017; Newton et al., 2018).

Enzyme promiscuity can also be harnessed in biotechnological applications, long-term evolution experiments for pathway development, shaping of metabolic networks for the production of useful compounds, and the engineering of enzymes with tailor-made functions (Nobeli et al., 2009; Michael, 2017; Guzman et al., 2019; Rosenberg and Commichau, 2019). The substrate ambiguity of enzymes can also be ‘hijacked’ for the biotransformation and production of man-made compounds (D’Ari and Casadesus, 1998). In this study, we have exploited the biochemical properties of the ectoine hydroxylase (EctD) for such a task. Naturally, this enzyme catalyzes the synthesis of the stress protectant and chemical chaperone 5-hydroxyectoine from its precursor ectoine (Bursy et al., 2007; Höppner et al., 2014).

Ectoine [(S)-2-methyl-1,4,5,6-tetrahydropyrimidine-4-carboxylic acid] and its derivative 5-hydroxyectoine [(4S,5S)-5-hydroxy-2-methyl-1,4,5,6-tetrahydropyrimidine-4-carboxylic acid] (**Figure 1**) are members of the so-called compatible solutes, a special class of highly water-soluble organic osmolytes that are compliant with cellular biochemistry and physiology (da Costa et al., 1998; Bolen and Baskakov, 2001; Roberts, 2004). Microorganisms use them widely as osmostress protectants (Galinski and Trüper, 1994; Kempf and Bremer, 1998; Roesser and Müller, 2001; Wood et al., 2001; Gunde-Cimerman et al., 2018). When faced with high osmolarity surroundings, many bacteria accumulate compatible solutes to counteract the outflow of water from the cell, and thereby prevent dehydration of the cytoplasm, increase in molecular crowding, and drop in vital turgor to physiologically unsustainable values (Wood, 2011; van den Berg et al., 2017; Bremer and Krämer, 2019). The amassing of these osmostress protectants can occur either through synthesis or import

(Kempf and Bremer, 1998; Bremer and Krämer, 2000), but their uptake is generally preferred for energetic reasons (Oren, 1999).

In addition to their pure osmopressure adaptive role, compatible solutes protect the functionality of proteins, macromolecular complexes, membranes, and even entire cells, have broad protein anti-aggregating properties, and can influence DNA structure (Lippert and Galinski, 1992; Barth et al., 2000; Bourot et al., 2000; Ignatova and Gierasch, 2006; Harishchandra et al., 2010; Meyer et al., 2017; Stadtmiller et al., 2017). These biological function-preserving attributes have led to their description as chemical chaperones (Diamant et al., 2001; Chattopadhyay et al., 2004). The beneficial effects of compatible solutes on stability and functionality of proteins are generally explained in the framework of the preferential exclusion model (Arakawa and Timasheff, 1985). The unfavorable interactions of compatible solutes with the protein backbone (Liu and Bolen, 1995) and the ensuing uneven distributions of these solutes in the cell water, in conjunction with the modification of the solvation properties of the solvent, leads, for thermodynamic reasons, to well-hydrated and well-folded proteins, a process that has been coined the osmophobic effect (Bolen and Baskakov, 2001). Hence, compatible solutes act against the unfolded state of proteins under intracellular unfavorable osmotic and ionic conditions (Bolen and Baskakov, 2001; Ignatova and Gierasch, 2006; Street et al., 2006; Capp et al., 2009; Zaccai et al., 2016; Stadtmiller et al., 2017). In this respect, the function-preserving and anti-inflammatory attributes of ectoines have attracted particular attention, and ectoines are therefore increasingly exploited for various practical applications (Lentzen and Schwarz, 2006; Graf et al., 2008; Pastor et al., 2010; Kunte et al., 2014).

Ectoine is synthesized from the central microbial metabolite L-aspartate- β -semialdehyde (Lo et al., 2009; Stöveken et al., 2011) in a three-step biosynthetic route involving L-2,4-diaminobutyrate (DAB) transaminase (EctB), L-2,4-diaminobutyrate acetyltransferase (EctA), and ectoine synthase (EctC) (Peters et al., 1990; Ono et al., 1999). In a substantial sub-group of ectoine-producing bacteria (Czech et al., 2018a), ectoine is chemically modified by the ectoine hydroxylase (EctD) to *trans*-5-hydroxyectoine (Prabhu et al., 2004; Garcia-Esteva et al., 2006; Bursy et al., 2007). From a chemical point of view, the regio- and stereoselective modification of ectoine by a hydroxyl group (Inbar and Lapidot, 1988; Bursy et al., 2007) seems to be a rather minor alteration. However, it can have profound consequences with respect to the influence of 5-hydroxyectoine on water structure and its solubility at different temperatures; it often also results in superior function-preserving attributes compared to ectoine (Held et al., 2010; Smiatek et al., 2012; Hahn et al., 2015; Czech et al., 2018a). Examples are superior protective effects against desiccation, the ability to form glasses, and the stabilization of and influence on DNA, proteins, and lipid layers (Lippert and Galinski, 1992; Borges et al., 2002; Manzanera et al., 2004; Harishchandra et al., 2010; Harishchandra et al., 2011; Tanne et al., 2014).

Among all compatible solutes considered for practical uses (Jorge et al., 2016), ectoines have found the widest applications, and numerous products are already commercially available (Graf et al., 2008; Pastor et al., 2010; Kunte et al., 2014). Ectoines have found uses in cosmetics and the stabilization of cells and recombinant proteins; their applications in medicine are actively pursued. Ectoines are currently provided through an industrial-scale biotechnological production process that is able to deliver ectoine on the scale of tons by using *Halomonas elongata* (Schwibbert et al., 2011) as either natural or engineered cell factory (Lentzen and Schwarz, 2006; Pastor et al., 2010; Kunte et al., 2014). Ectoines are commercially high-value products, inspiring not only the development of recombinant microbial cell factories for their production (Giesselmann et al., 2019), but also the design and chemical synthesis of ectoine derivatives. These derivatives possess either reduced or expanded sizes of the six-member ectoine ring structure (**Figure 1**), or were modified with a lipid anchor (lauryl-ectoine) to alter the cellular targeting of the otherwise highly water soluble (up to 7 M) ectoines in eukaryotic cells (Schnoor et al., 2004; Held et al., 2010; Witt et al., 2011; Wedeking et al., 2014).

The synthetic ectoine derivative homoectoine [4,5,6,7-tetrahydro-2-methyl-1H-(1,3)-diazepine-4-carboxylic acid (homoectoine)] (**Figure 1**), the focus of this study, serves as an osmoprotectant for *E. coli*, and functions as a potent PCR-enhancer (Nagata, 2001; Schnoor et al., 2004; Shi and Jarvis, 2006). Notably, it also provides protection against colitis in mice and reduces intestinal inflammation, thereby raising the prospect of medical and other types of practical applications for homoectoine (Castro-Ochoa et al., 2019; Farre and Vicario, 2019). Compared with ectoine, a six-membered ring structure, the synthetic homoectoine molecule possesses a seven-member diazepine ring structure (**Figure 1**).

The fact that the hydroxylation of ectoine often attains superior function-preserving attributes kindled interests to hydroxylate synthetic ectoine derivatives as well (Galinski et al., 2009; 2015). This brings the properties of the ectoine hydroxylase EctD into focus (Prabhu et al., 2004; Garcia-Esteva et al., 2006; Bursy et al., 2007). Biochemical and crystallographic analysis revealed that EctD is a member of the non-heme Fe(II)-containing and 2-oxoglutarate-dependent dioxygenase superfamily (Bursy et al., 2007; Reuter et al., 2010; Höppner et al., 2014; Widderich et al., 2014a; Widderich et al., 2016). Like other dioxygenases (Aik et al., 2012; Hangasky et al., 2013; Herr and Hausinger, 2018), EctD is a cupin and introduces a hydroxyl-group to an inactive carbon on the substrate ectoine through a highly reactive ferryl species that is generated from the Fe(II) catalyst, the α -ketoglutarate co-substrate, and molecular O₂ (Widderich et al., 2014b). EctD forms a dimer in solution and in the crystal (**Figure 2A**). All residues important for substrate/co-substrate binding and enzyme catalysis protrude into the lumen of the cupin barrel that also contains the catalytically critical Fe(II) atom (Höppner et al., 2014; Widderich et al., 2014b) (**Figure 2B**). Hence, the large

barrel-like structure of the EctD monomer might be conducive to accommodating and accurately positioning compounds structurally and chemically related to ectoines and proline (Galinski et al., 2009; 2015; Hara et al., 2019).

The promiscuous activity of biosynthetic enzymes can be exploited in microbial cell factories for the resources-preserving production of valuable synthetic compounds. With a focus on the ectoine hydroxylase, we harnessed the substrate promiscuity of this enzyme for a regio- and stereoselectively hydroxylation of the synthetic ectoine derivative homoectoine in a microbial cell factory that secretes the newly formed *trans*-5-hydroxyhomoectoine into the growth medium.

MATERIALS AND METHODS

Chemicals

Ectoine was a kind gift from bitop AG (Witten, Germany). 5-hydroxyectoine and glycine betaine were purchased from Merck KGaA (Darmstadt, Germany). Homoectoine was synthesized according to previously reported procedures (Koichi et al., 1991; Schnoor et al., 2004). Dithiothreitol (DTT) was purchased from AppliChem (Darmstadt, Germany) and phenylmethylsulfonyl fluoride (PMSF) from Roche (Basel, Switzerland). Desthiobiotin, Strep-TactinSuperflow chromatography material for the purification of proteins fused to a *Strep*-tag II affinity peptide and anhydrotetracycline hydrochloride (AHT) for the induction of the transcriptional activity of the TetR-regulated *tet* promoter present on the *ectD* expression plasmids pMP40 (*ectD* from *Sphingopyxis alaskensis*) and pMP41 (*ectD* from *Pseudomonas stutzeri*) (Widderich et al., 2014a) were purchased from IBA GmbH (Göttingen, Germany). All other chemicals were purchased from Karl Roth GmbH (Karlsruhe, Germany), Merck KGaA (Darmstadt, Germany), and Sigma-Aldrich (Steinheim, Germany).

Bacterial strains, construction of *E. coli* mutants and plasmids

Standard genetic methods such as phage P1*vir*-mediated transduction were performed as described previously (Miller, 1972). For the construction of *E. coli* strain LC11 and LC12, P1*vir* phage lysates were prepared on cells of strains MKH17 [$\Delta(\textit{proU}::\textit{spc})608$] and JW4072-1 [$\Delta(\textit{proP}::\textit{kan})737$], respectively (Haardt et al., 1995; Baba et al., 2006). These were then used to transduce the *E. coli* K-12 wild-type strain MG1655 (Blattner et al., 1997) (**Supplementary Table 1**) by selecting for spectinomycin-resistant or kanamycin-resistant colonies on LB agar plates containing 100 $\mu\text{g ml}^{-1}$ or 50 $\mu\text{g ml}^{-1}$ of the antibiotic, respectively. Representative colonies were picked and purified by re-streaking several times on spectinomycin- or kanamycin-containing LB agar plates. One of the constructed *E. coli* strains, LC11 [$\Delta(\textit{proU}::\textit{spc})608$], was subsequently transduced with a P1*vir* phage lysate prepared on strain JW4072-1 [$\Delta(\textit{proP}::\textit{kan})737$] (Kitagawa et al., 2005) to obtain a double-gene deletion strain defective in the osmoprotectant uptake systems ProP and ProU (Lucht and Bremer,

1994; Haardt et al., 1995). The resulting strain was LC14 [$\Delta(proU::spc)608 \Delta(proP::kan)737$] (**Supplementary Table 1**). To construct the *E. coli* K-12 strain LC15 that is deficient in the synthesis of the osmostress protectant trehalose, a P1vir phage lysate was prepared on cells of strain FF4169 [(*otsA::Tn10*)1] (Giaever et al., 1988) and was then used to transduce the defect in trehalose synthesis into the *otsBA*⁺ *E. coli* strain MG1655 by selecting for tetracycline-resistant colonies on LB agar plates containing 15 $\mu\text{g ml}^{-1}$ of the antibiotic. To test the contribution of mechanosensitive channels in the release of the hydroxylated ectoine derivatives, a pair of isogenic *E. coli* strains Frag1 (parent) and a mutant (MJF641), which lack all known mechanosensitive channels, was used (Edwards et al., 2012). All strains used in this study and their genotypes are listed in **Supplementary Table 1**.

Plasmids carrying the *ectD* gene from *Pseudomonas stutzeri* A1501 (accession number: ABP77885.1) or from *Sphingopyxis alaskensis* (accession number: WP_011543221.1), pMP40 and pMP41, respectively, were used to overproduce the ectoine hydroxylases in the *E. coli* B strain BL21(DE3) (Studier et al., 1990) for their subsequent biochemical characterization (Widderich et al., 2014a). All plasmids used in this study are listed in **Supplementary Table 2**.

Media and growth conditions for osmostress protection assays

The *E. coli* K-12 strain MG1655 and its transporter mutant derivatives LC11, LC12, and LC14 (**Supplementary Table 1**) were routinely maintained on LB agar plates and incubated at 37 °C. For osmostress protection growth assays (Haardt et al., 1995), the strains were inoculated in 5 ml LB medium. After aerobic incubation for 5 hours at 37 °C, 100 μl culture were transferred to 10 ml MMA containing either no additional NaCl or 0.3 M NaCl with the aim to pre-adapt the *E. coli* cells to increased salinity. These cultures were then grown aerobically over night at 37 °C and used to inoculate the main cultures (20 ml in 100-ml Erlenmeyer flasks) in a chemically defined medium (MMA) (Miller, 1972) supplemented with 0.5% glucose, 1mg l⁻¹ thiamine, and 1 mM MgSO₄ to an OD₅₇₈ of 0.1. These cultures contained either no NaCl (control) or 0.8 M NaCl (osmotic stress). Compatible solutes (ectoine, 5-hydroxyectoine, homoectoine, hydroxyhomoectoine, and glycine betaine) were added to high-salinity growth media to a final concentration of 1 mM. The OD₅₇₈ values of the various cultures were measured after 10 h, 24 h, 30 h, 36 h and 48 h in technical duplicates. For the visualization of the growth of cultures, the pre-cultures were grown under the same conditions as mentioned above and the main cultures were incubated in a well-plate reader (Epoch2, BioTek) for 72 hours at 37 °C with constant double-orbital shaking. The culture volume per well was 500 μl with an end-concentration of compatible solutes of 1 mM. The OD₅₇₈ was measured every hour.

***In vivo* biotransformation of ectoine into 5-hydroxyectoine and homoectoine into 5-hydroxyhomoectoine**

Biotransformation assays for various ectoines were conducted as previously described (Czech et al., 2016) in an *E. coli* MG1655 strain background. Strain LC15 (MG1655 *otsA::Tn10*) (**Supplementary Table 1**) harboring the *ectD*⁺ plasmid pMP41 (or pASK-IBA3 as the negative control) (**Supplementary Table 2**) was inoculated in 5 ml LB medium containing 100 µg ml⁻¹ ampicillin and grown aerobically at 37 °C for 5 hours. 100 µl of this pre-culture was used to inoculate 10 ml of MMA without NaCl which was subsequently incubated at 37 °C over night. Main cultures were grown in baffled flasks (100 ml) containing 10 ml of MMA with 0.4 M NaCl and various concentrations of ectoine or homoectoine. Cells were grown to an OD₅₇₈ of 0.5 when 0.2 mg l⁻¹ of the inducer (AHT) of the TetR repressor were added to trigger enhanced activity of the plasmid-based *tet* promoter driving *ectD* transcription; the cultures were further grown for 24 hours at 37 °C. After this time, 2 ml per culture were harvested in duplicates, and supernatants were stored at -20 °C until further use. Extracellular concentrations of ectoine and its derivatives in the supernatant of the cultures were analyzed by high-performance liquid chromatography (HPLC). In order to address the role of mechanosensitive channels (Booth, 2014; Cox et al., 2018) in the release/excretion of hydroxylated derivatives of ectoine or homoectoine, the same types of experiments were conducted with the strains Frag1 and MJF641 (**Supplementary Table 1**).

HPLC-based analysis of ectoines

For the HPLC-based quantification of ectoines an Agilent 1260 Infinity LC system (Agilent, Waldbronn, Germany) was employed. Prior to loading of the samples into the HPLC system, they were diluted 1:2 with acetonitrile and measured as reported previously (Kuhlmann and Bremer, 2002; Czech et al., 2016). For separation and detection of the ectoines, a GROM-SIL Amino-100 PR column (3 µm) (obtained from Dr. Maisch HPLC GmbH, Ammerbuch-Entringen, Germany) with an attached 1260 Infinity Diode Array Detector system was used. Absorbance of the compatible solutes was measured at a wavelength of 210 nm. Commercially available samples of ectoine and 5-hydroxyectoine were used to prepare standard solutions. Separation of homoectoine and hydroxyhomoectoine was achieved by using a gradient of water and acetonitrile as the mobile phase. The portion of water being mixed with acetonitrile during each measurement was increased from 5 % up to 30 % within 17 minutes. Chromatograms of the HPLC runs were analyzed with the OpenLAB software suite (Agilent) and ectoine concentrations in individual samples were determined from measured reference standards and by using the programs Excel (Microsoft) and GraphPad Prism (GraphPad Software, La Jolla California USA, graphpad.com).

Detection of 5-hydroxyhomoectoine in the supernatant of the recombinant cell factory via mass spectrometry

In order to confirm the hydroxylation of homoectoine, the supernatants of two biologically independent *E. coli* cell factory cultures producing ectoine hydroxylases were analyzed by HPLC and subsequent mass-spectrometry. The HPLC conditions were the same as described above. As controls, the supernatants of a cell factory harboring the empty vector pASK-IBA3 (IBA GmbH, Göttingen) and of a cell culture without compatible solutes were measured. HR-ESI mass spectra were acquired with a LTQ-FT Ultra mass spectrometer (Thermo Fisher Scientific). The resolution was set to 100.000. Data was evaluated using Xcalibur (Thermo Fisher Scientific).

HPLC-based preparation of 5-hydroxyhomoectoine from the supernatant of the recombinant cell factory

The supernatants of an *ectD*⁺ *E. coli* cell factory producing 5-hydroxyhomoectoine were used to prepare this compound. For this purpose, the complete supernatant of the culture (10 ml) that had received 5 mM homoectoine and had been grown for 24 h was step-wise loaded on a GROM-SIL Amino-100 PR column (3 µm) and the separation of 5-hydroxyhomoectoine was monitored at 210 nm (Kuhlmann and Bremer, 2002; Czech et al., 2016). The elution peak of 5-hydroxyhomoectoine was automatically collected using a fraction collector (1100 series, Agilent). Because an analytical column was used, only 25 µL of the supernatant could be analyzed in a single run due to observed overloading effects. Combined fractions containing pure 5-hydroxyhomoectoine were subsequently lyophilized and stored at -20 °C. The 5-hydroxyhomoectoine purified from the supernatant of two 10 ml cultures (14 mg dry weight) was dissolved in 780 µl dH₂O resulting in a concentration of 100 mM and was used as a HPLC standard solution, and for osmoprotection assays. Due to the observed instability of 5-hydroxyhomoectoine at neutral pH (**Supplementary Figure 1**), the very first measured standard curve of 5-hydroxyhomoectoine was used to achieve the most reliable quantification of 5-hydroxyhomoectoine in HPLC assays. A second round of 5-hydroxyectoine purification from the supernatants of two *ectD* expressing cultures yielded again approximately 14 mg of 5-hydroxyhomoectoine; they were dissolved in 700 µl water and this solution was employed for NMR analysis.

Stereochemical analysis of hydroxyhomoectoine by NMR

The purified 5-hydroxyhomoectoine was employed to elucidate the stereochemical properties of hydroxyhomoectoine, in particular to reveal the carbon atom at which the hydroxylation takes place and with which selectivity. Broad-band-decoupled ¹H NMR spectra and 2d-NMR spectra were recorded at 300 K on a Bruker AV III HD 500 MHz spectrometer in deuterium oxide (99.9% D)

containing 3-(trimethylsilyl)propionic-2,2,3,3-d₄ acid sodium salt (internal standard) (Sigma-Aldrich Chemie GmbH, München, Germany) at 500.13 MHz or on a Bruker AV II 600 MHz in H₂O using solvent suppression excitation sculpting with gradients at 600.13 MHz. ¹³C NMR spectra were recorded on a Bruker AV II 300 at 75.49 MHz. Chemical shifts are reported in ppm relative to the solvent-residue signal (¹H spectra) or to the internal standard (¹³C spectra), respectively. Multiplicities are given as singlet (s), doublet (d), triplet (t), quartet (q), quintet (quin), multiplet (m) and broad (b) where applicable. The Spectra were processed with Bruker TopSpin® software 4.0.

Density functional theory calculations

Density functional theory (DFT) calculations were performed with Gaussian 2016 Rev. A.03 (<https://gaussian.com/citation/>) employing the Lee Yang Parr hybrid functional B3LYP (Becke, 1993) and the 6-311+G** (Wachters, 1970) split-valence basis set with added polarization and diffuse functions. The RMS force criterion was set to 10⁻⁵. All generated minima were verified to have zero imaginary frequency modes via analytic computation of the Hesse matrix. The computed coordinates of the (4S,5S)-isomer can be found in the supplemental information.

Overproduction and purification of recombinant EctD enzymes

For overproduction of the recombinant EctD enzymes, the *E. coli* strain BL21 (DE3) (Studier et al., 1990) harboring either the plasmid pMP40 (*ectD* gene from *S. alaskensis*) or pMP41 (*ectD* gene from *P. stutzeri* A1501) was used (Widderich et al., 2014a). In these plasmids, expression of the *ectD* genes is under the control of the *tet* promoter which responses to the TetR repressor. Cells harboring one of the plasmids were grown in modified MMA (0.5 % glucose, 1 mg ml⁻¹ thiamine, 1 mM MgSO₄, 0.5% casamino acids) to an OD₅₇₈ of 0.5. AHT was then added to the cultures in a final concentration of 0.2 mg l⁻¹ to induce *ectD* gene expression from the TetR-repressed *tet* promoter, and the cells were then further incubated for 2.5 hours. The cultures were harvested by centrifugation (4 °C, 5063 x g, 20 min) and re-suspended in 20 mM TES (pH 7.5) containing 100 mM KCl; the cells were subsequently pelleted by centrifugation for 10 min. The pelleted cells were stored at -20 °C until further use. To purify the EctD-*Strep*-tag II recombinant proteins by affinity chromatography, the pellets of the overproducing cells were re-suspended in 5 ml 20 mM TES (pH 7.5), containing 100 mM KCl and protease inhibitors (2 mM DTT, 0.5 mM PMSF, 0.5 mM benzamidine). The cells were disrupted by passing them three times through a French Press at 1000 psi; the cell lysate was subsequently centrifuged for 1 h and at 21.000 x g at 4 °C. EctD-*Strep*-tag II recombinant proteins were purified via a Strep-Tactin Superflow column according to a standard protocol (IBA GmbH, Göttingen). Elution of the recombinant EctD-*Strep*-tag II proteins was achieved by adding buffer

[20 mM TES (pH 7.5), containing 100 mM KCl] containing desthiobiotin (2.5 mM) and no protease inhibitors. Enzyme fractions were stored at -80 °C or directly used in EctD enzyme activity assays.

EctD enzyme activity assays

In order to characterize the conversion of ectoine into 5-hydroxyectoine and homoectoine into 5-hydroxyhomoectoine in a quantitative fashion, purified ectoine hydroxylases were used in enzyme activity assays. The assays had a volume of 30 µl and after optimization of the previously used conditions (Höppner et al., 2014; Widderich et al., 2014a), the following conditions were chosen: the reaction mixture contained 100 mM TES (pH 7.5), 1 mM FeSO₄, 10 mM, 2-oxo-glutarate, 100 mM KCl and various amounts of ectoine or homoectoine as substrate. The FeSO₄ solution (dissolved in dH₂O) was always prepared fresh. In case of enzyme assays conducted with the *Sa*EctD protein 1300 U catalase from bovine liver were added to the reaction assay. Before addition of the EctD enzyme, the reaction mixture was pre-incubated for 10 minutes at the optimal assay temperature of 35 °C (for EctD from *P. stutzeri* A1501) or at 15 °C (for EctD from *S. alaskensis*). The enzyme assays were started by adding 1.47 µM of the recombinant ectoine hydroxylase to the pre-mixed assay solution. The enzyme assays were stopped after 5 min by the addition of acetonitrile in a 1:2 ratio. Denatured proteins were removed by centrifugation at 13.000 x g for 10 minutes at room temperature. Ectoines were detected by HPLC analysis as described (Kuhlmann and Bremer, 2002; Czech et al., 2018b). The kinetic parameters were calculated and fitted according to Michaelis Menten kinetics using GraphPad Prism version 5 for MacOSX (GraphPad Software, La Jolla California USA, graphpad.com).

Bioinformatic tools for docking simulations

The crystal structure of the EctD protein from *S. alaskensis* in complex with 5-hydroxyectoine (PDB: 4Q50) (Höppner et al., 2014) was used to dock homoectoine, hydroxyhomoectoine, and hydroxyproline into the active site of the enzyme. The structures of homoectoine, hydroxyhomoectoine, and hydroxyproline were built using the program Phenix (Afonine et al., 2012). With help of the program COOT (Emsley and Cowtan, 2004), the ligands were placed at five different positions in close proximity to the EctD protein structure. To circumvent any bias during the modeling process, the positions of the various ligands were chosen to be either within the active site (two positions) or at the surroundings of the EctD protein (three positions). These positions, together with the monomeric EctD structure in complex with Fe(II) (Höppner et al., 2014), were subjected to the automated software AUTODOCK using standard settings (Trott and Olson, 2010). The results of every docking run were manually inspected. The result showed in every case the binding of homoectoine at the same site as observed for 5-hydroxyectoine in the EctD crystal structure (Höppner et al., 2014). Subsequently, by changing the orientation of the homoectoine molecule

within the EctD active site, a second round of docking was performed. This resulted in a stable conformation of the homoectoine ligand within the EctD active site in close proximity to the catalytically crucial iron (Höppner et al., 2014). The same procedure was performed using hydroxyhomoectoine and hydroxyproline. In all cases the final result was manually inspected using the programs Pymol (Delano, 2002) (www.pymol.org/2/) and COOT (Emsley and Cowtan, 2004).

The volume of the cavity in the active site of (*Sa*)EctD (PDB code: 4MHR) (Höppner et al., 2014) was calculated using the program CastP (Tian et al., 2018) using a monomer of the dimeric EctD protein (Höppner et al., 2014) as the input crystal structure. To verify that the CastP program found the correct substrate-binding pocket of EctD, the calculated pocket was overlaid with the actual crystal structure of the EctD protein in complex with 5-hydroxyectoine (PDB code: 4Q5O). The same procedure was used with the (*Sa*)EctD structure obtain models of EctD in complex with either homoectoine or 5-hydroxyhomoiectoine.

Protein alignments and figure preparation

The protein sequence alignment of the EctD proteins from *S. alaskensis* (WP_011543221.1), *Acidiphilum cryptum* (WP_012040480.1), *Paenibacillus lautus* (WP_015737572.1), *H. elongata* (WP_013333764.1), *Streptomyces coelicolor* (NP_626134.1), *P. stutzeri* (WP_011911424.1), *Halobacillus halophilus* (WP_014643639.1), *Nitrosopumilus maritimus* (WP_012215726.1), *Chromohalobacter salexigens* (WP_011505850.1; WP_011508293.1), *Alkalilimnicola ehrlichii* (WP_011628142.1), *Streptomyces chrysomallus* (WP_030590139.1), and *Virgibacillus salexigens* (AAY29689.1) was performed with SnapGene® software (GSL Biotech; snapgene.com).

All figures were prepared using GraphPad Prism (GraphPad Software, La Jolla California USA, graphpad.com), Adobe Illustrator (www.adobe.com/products/illustrator.html), and Pymol (pymol.org/2/) (Delano, 2002).

RESULTS

Homoectoine is an osmostress protectant for the *E. coli* strain MG1655

E. coli possesses two osmotically regulated uptake systems for a variety of compatible solutes: the proton-solute symporter ProP, a member of the major facilitator superfamily (MFS) and the ABC-type (ATP-binding cassette) transporter ProU (Lucht and Bremer, 1994; Wood et al., 2001). Both transporters can also serve as uptake systems for ectoine and 5-hydroxyectoine (Jebbar et al., 1992; Czech et al., 2016; Culham et al., 2018). For our studies on the osmostress protective properties of homoectoine (Nagata, 2001), we used the well-known *E. coli* K-12 laboratory strain MG1655 (Blattner et al., 1997) and an isogenic set of mutant strains derived from MG1655 with defects in ProP and ProU (**Supplementary Table 1**). We grew the strains in these osmostress protection assays

in a chemically defined medium (MMA) with glucose as the carbon source and 0.8 M NaCl. This degree of osmotic stress prevented the growth of the parent *E. coli* strain MG1655 while the presence of 1 mM ectoine, 5-hydroxyectoine, homoectoine, and, as a control glycine betaine, provided effective osmotic stress protection. Among the tested compatible solutes, homoectoine afforded the weakest level of osmotic stress resistance, while ectoine, 5-hydroxyectoine and glycine betaine rescued growth at high salinity to a similar extent (**Figure 3A**). Cells grown in the presence of homoectoine possessed a substantially longer lag-phase than those cultures that had received glycine betaine, ectoine, or 5-hydroxyectoine. During exponential growth, the cultures had a doubling time of approximately 2.5 h (for glycine betaine), 4 h (for ectoine and 5-hydroxyectoine), and 7.3 h (for homoectoine). The corresponding growth rates (μ) were as follows: $\mu = 0.27 \text{ h}^{-1}$ for glycine betaine, $\mu = 0.17 \text{ h}^{-1}$ for ectoine and 5-hydroxyectoine, and $\mu = 0.09 \text{ h}^{-1}$ for homoectoine (**Figure 3A**).

In a next step of our analysis of the osmotic stress protective potential of homoectoine, we raised the salinity of the growth medium from 0.8 M NaCl to 1 M NaCl and found that it no longer conferred osmotic stress protection (**Figure 3B**). This elevated level of salinity in the growth medium also led to a differentiation of the osmotic stress protective attributes of ectoine, 5-hydroxyectoine, and glycine betaine that is reflected by the growth rates of these cultures: $\mu = 0.16 \text{ h}^{-1}$ for glycine betaine, $\mu = 0.10 \text{ h}^{-1}$ for 5-hydroxyectoine and $\mu = 0.08 \text{ h}^{-1}$ for ectoine. Hence, glycine betaine conferred the strongest level of osmotic stress protection in the *E. coli* strain MG1655, followed by 5-hydroxyectoine and ectoine (**Figure 3B**). Collectively, the data from these osmotic stress protection growth assays show that the synthetic ectoine derivative homoectoine is a moderately effective osmotic stress protectant, a conclusion that has previously also been reached by S. Nagata (Nagata, 2001). However, the *E. coli* W strain ATCC 9637 used by this author can withstand higher levels of salinity than the *E. coli* K-12 strain MG1655, since homoectoine was still osmotic stress protective in a minimal medium containing 1 - 1.2 M NaCl (Nagata, 2001).

The uptake route(s) for homoectoine in *E. coli* are unknown but since ectoine and 5-hydroxyectoine are imported via ProP and ProU (Jebbar et al., 1992), we suspected that these compatible solute importers with a broad substrate-profile would also mediate the uptake of homoectoine. To test this, we constructed an isogenic set of *E. coli* MG1655 derivatives in which either the ProP or the ProU systems were operational, or in which both transport systems were simultaneously not functional. Osmotic stress protection growth assays confirmed that the ProP and ProU transporters were each proficient in homoectoine import, while their simultaneous genetic inactivation prevented its uptake. As expected from previous data, the same pattern was also observed for ectoine, 5-hydroxyectoine and glycine betaine (Jebbar et al., 1992; Lucht and Bremer, 1994; Haardt et al., 1995) (**Figure 3C**).

Docking of homoectoine into the active site of the ectoine hydroxylase EctD

The crystal structure of the ectoine hydroxylase from *S. alaskensis* (*Sa*) in complex with the reaction product 5-hydroxyectoine, the catalytically important iron, and the co-substrate 2-oxoglutarate has recently been determined (PDB number: 4Q5O) (Höppner et al., 2014) (**Figure 2A,B**). This provided us with the opportunity to evaluate the suitability of the EctD active site to potentially accept the seven-membered homoectoine ring as a substrate for a hydroxylation reaction. The overall fold and dimeric assembly of the (*Sa*)EctD protein is shown in **Figure 2A**. The natural reaction product of the ectoine hydroxylase, (4S,5S)-5-hydroxyectoine, is bound within the active site through the coordination by the residues Gln-127, His-144, Thr-149, Trp-150, Arg-280, and Leu-284 (Höppner et al., 2014) (**Figure 2B**). The size of the (*Sa*)EctD enzyme reaction chamber was calculated with the CASTp program (Tian et al., 2018); it has a volume of approximately 77 Å³. Using *in silico* docking analysis with the programs Phenix, COOT and AutoDock (Emsley and Cowtan, 2004; Trott and Olson, 2010; Afonine et al., 2012), we modeled the non-natural substrates for EctD, homoectoine, and its potentially hydroxylated derivative, hydroxyhomoectoine, into the active site of (*Sa*)EctD (**Figure 2C,D**). Both synthetic ectoine derivatives fit into the active site of the ectoine hydroxylase and might be coordinated by the same network of amino acid residues that also coordinate the native reaction product 5-hydroxyectoine (Höppner et al., 2014). As revealed by the docking approach, the spatial positioning of homoectoine and its hydroxylated derivative in the reaction chamber are super-imposable with that of the 5-hydroxyectoine molecule trapped in the (*Sa*)EctD crystal structure (PDB code: 4MHR) (Höppner et al., 2014) (**Supplementary Figure 2A**). Furthermore, our modeling study suggests that homoectoine could be positioned in the active site of the ectoine hydroxylase such that the position C5 of the expanded seven-member diazepine ring would potentially be modified with a hydroxyl group (**Figure 2C,D**).

Enzyme kinetics of ectoine hydroxylases from *P. stutzeri* A1501 and *S. alaskensis* using homoectoine as a synthetic substrate

To biochemically confirm the hypothesis that the EctD enzyme might promiscuously use the synthetic ectoine derivative homoectoine as a substrate, we conducted detailed kinetic analysis of the EctD proteins from *P. stutzeri* A1501 [(*Ps*)EctD] and *S. alaskensis* [(*Sa*)EctD]. These two proteins were chosen for further studies because a crystal structure of (*Sa*)EctD is available (Höppner et al., 2014) and the (*Ps*)EctD enzyme proved to be a highly efficient biocatalyst in an *E. coli* cell factory hydroxylating imported ectoine (Czech et al., 2016). Both recombinant proteins could be readily overproduced in *E. coli* and purified to apparent homogeneity as revealed by SDS-PAGE (**Supplementary Figure S3**). Despite a rather similar number of amino acids, calculated molecular weight [34.14 kDa for (*Sa*)EctD and 34.18 kDa for (*Ps*)EctD], and also pI [(*Sa*) EctD: 5.47, (*Ps*)EctD:

5.5], the electrophoretic mobility of the two proteins were notably different on a 15% SDS-PAGE (**Supplementary Figure S3**). This difference in electrophoretic mobility has previously been observed (Widderich et al., 2014a) but the underlying mechanism(s) remains unclear.

To conduct an analysis of the kinetic parameters of the (*Sa*)EctD and (*Ps*)EctD enzymes, we first optimized the reaction parameters from those of the previously used assay conditions (Höppner et al., 2014; Widderich et al., 2014a). In particular, we now used different temperatures for the two enzymes [15 °C for (*Sa*)EctD and 35 °C for (*Ps*)EctD], shortened the incubation time (5 min) of the assays to ensure linear turn-over during the enzyme reaction, reduced the protein concentration from 15 µM down to 1.47 µM, and substantially increased (four-fold) the concentration of the buffer [100 mM TES (pH 7.5)] but we kept the concentration of FeSO₄ (1 mM), 2-oxoglutarate (10 mM) and KCl (100 mM) in the assay buffers identical to the previously used concentrations.

During the reaction of non-heme-containing iron(II) 2-oxoglutarate dependent enzymes (Aik et al., 2012; Hangasky et al., 2013; Herr and Hausinger, 2018), reactive oxygen species can be produced and catalase is thus frequently used to mitigate their damaging effects. In test assays, the performance of the (*Ps*)EctD enzyme was not enhanced by the addition of catalase (up to 2 500 U), while the performance of (*Sa*)EctD greatly benefitted by the addition of this H₂O₂ detoxifying enzyme. Hence, 1 300 U of bovine liver catalase were added to the enzyme reactions when we assessed the kinetic parameters of the (*Sa*)EctD protein but did not add catalase to enzyme assays conducted with the (*Ps*)EctD protein. The expected reaction products of the ectoine hydroxylase, 5-hydroxyectoine as the authentic product and hydroxyhomoectoine as the predicted synthetic reaction product, were detected and quantified by HPLC analysis using a UV-detector set to 210 nm. Both ectoine and 5-hydroxyectoine (Bursy et al., 2007; Czech et al., 2016), and homoectoine and hydroxyhomoectoine (this study) could be cleanly separated on a GROM-SIL Amino-100 PR column (3 µm) (**Supplementary Figure S4**).

Under the optimized assay conditions and using ectoine as the substrate the (*Sa*)EctD enzyme had a k_m of 0.8 ± 0.1 mM and a V_{max} of 2.9 ± 0.1 µmol formed 5-hydroxyectoine min⁻¹ mg⁻¹ protein, while the (*Ps*)EctD enzyme possessed a k_m of 2.3 ± 0.2 mM and a V_{max} of 23.5 ± 0.5 µmol formed 5-hydroxyectoine min⁻¹ mg⁻¹ protein (**Figure 4A,C**). The V_{max} of the (*Sa*)EctD enzyme for the synthetic substrate homoectoine matched that for its natural substrate, but this protein exhibited an about four-fold lower affinity for homoectoine (**Figure 4D**). While the K_m -values of the (*Ps*)EctD enzyme for ectoine and homoectoine were very similar, the V_{max} for homoectoine substantially exceeded that for its natural substrate ectoine (by about three-fold) (**Figure 4A,B**). Hence, both tested EctD enzymes are able to use the synthetic compound homoectoine as a substrate in a presumed hydroxylation reaction, in which the (*Ps*)EctD enzyme is apparently particularly effective.

***In vivo* hydroxylation of homoectoine using an *E. coli* cell factory**

In vivo biotransformation reactions to specifically hydroxylate chiral compounds using recombinant whole-cell biocatalysis is an environmentally friendly alternative to classical chemical synthetic procedures (Zhao et al., 2017). We have previously used such an approach to hydroxylate exogenously provided, and hence imported, ectoine in an *E. coli* cell factory expressing various plasmid-encoded *ectD* genes. In this cell factory, the newly formed 5-hydroxyectoine is continuously secreted/released into the growth medium (Czech et al., 2016). Building on these data, we fed various concentrations of homoectoine to a derivative of the *E. coli* K-12 strain MG1655 unable to synthesize its main osmostress protectant trehalose due to the presence of a *otsA::Tn10* insertion mutation (Hengge-Aronis et al., 1991; Strom and Kaasen, 1993), but expressing the *P. stutzeri* *ectD* gene under the control of the TetR-responsive *tet* promoter present on the plasmid pMP40 (**Figure 5A**). We grew these cells in MMA with a moderately increased salinity (0.4 M NaCl) to trigger enhanced expression of *proP* and *proU* in order to stimulate the uptake of ectoines via the ProP and ProU transport systems (Jebbar et al., 1992; Lucht and Bremer, 1994). In these experiments, we monitored the disappearance of homoectoine and the appearance of its presumed hydroxylated derivative in the growth medium by HPLC analysis. EctD-mediated biotransformation of ectoine into 5-hydroxyectoine was used as a control (Czech et al., 2016). When the empty expression vector (pASK-IBA3) was present in the *E. coli* MG1655 (*otsA::Tn10*) cell factory, as expected, no hydroxylated derivatives of either ectoine or homoectoine were detectable. The recovered amounts of ectoine and homoectoine closely matched those added to the growth medium at the beginning of experiments (**Figure 5B,C**). In contrast, when the cell factory carried the plasmid with the *P. stutzeri* *ectD* gene, hydroxylated derivatives of either ectoine or homoectoine appeared in the supernatant of the *E. coli* cultures (**Figure 5B,C**). Overall the *E. coli* K-12 strain MG1655 (*otsA::Tn10*) cell factory was only able to fully transform either 5 mM ectoine or 5 mM homoectoine into the corresponding hydroxylated derivatives (**Figure 5B,C**), while in a previous study the *E. coli* K-12 strain MC4100 (*otsA::Tn10*) cell factory fully converted up to 15 mM ectoine into 5-hydroxyectoine (Czech et al., 2016). Hence, differences between even closely related *E. coli* K-12 laboratory strains seem to exist with respect to the efficiency in which they can import ectoines and convert them to the corresponding hydroxylated derivatives.

We observed that at substrate concentrations higher than 5 mM, a mixture of the originally added compound and its hydroxylated derivative was present in the growth medium. By adding up the sum of the substrate and the reaction product in the growth media, we found that the sum of ectoine and 5-hydroxyectoine after 24 h of incubation of the cells equaled the amount of initially added ectoine (**Figure 5B**). The calculated sum of homoectoine and hydroxyhomoectoine was always slightly higher than the initially added homoectoine concentration. We attribute these difficulties in

quantification of hydroxyhomoectoine by HPLC analysis to its instability at neutral pH, complicating the exact calculation of the hydroxyhomoectoine content of samples from standard curves (**Supplementary Figure S1**).

The hydroxylated homoectoine is released from the cell factory independent of mechanosensitive channels

The release of recombinantly produced ectoines for microbial cell factories that do not naturally synthesize these compounds has been repeatedly observed (Schubert et al., 2007; Zhang et al., 2009; Becker et al., 2013; Eilert et al., 2013; Ning et al., 2016). In previous reports, we have shown that newly synthesized ectoine and 5-hydroxyectoine is released from a recombinant *E. coli* cell factory independently of the ectoine importers ProP and ProU (Czech et al., 2018b). Furthermore, 5-hydroxyectoine was released from an EctD-based *E. coli* cell factory in the absence of any known mechanosensitive channels (Edwards et al., 2012; Czech et al., 2016). These types of channels typically function as emergency release valves that allow the rapid and non-specific jettison of low-molecular-weight organic and inorganic solutes from suddenly osmotically down-shocked microbial cells (Booth, 2014; Cox et al., 2018). There is circumstantial evidence for the existence of a compatible solute efflux system in *E. coli* that potentially could also serve for the release of ectoine (Jebbar et al., 1992; Lamark et al., 1992) but its molecular identity and mode of action are unknown.

To assess if mechanosensitive channels were involved in the observed release/excretion of hydroxyhomoectoine (**Figure 5**), we used an *E. coli* mutant that lacks all the so far identified seven mechanosensitive channel genes (Edwards et al., 2012). The amount of hydroxyhomoectoine released from this mutant strain (MJF641) closely matched the amount released by its parental strain FRAG1 in which all mechanosensitive channels are intact (**Supplementary Figure S5A**), as also observed for 5-hydroxyectoine produced from imported ectoine (**Supplementary Figure S5B**). Consequently, these data exclude the involvement of any mechanosensitive channels in the release of synthetically produced hydroxyhomoectoine.

HPLC-MS and NMR analysis reveals regio- and stereoselective hydroxylation of homoectoine by the ectoine hydroxylase

So far, we have assumed that the product that we observe in the EctD-based *in vitro* and *in vivo* hydroxylation assays with homoectoine as the substrate is actually hydroxyhomoectoine (**Figure 4 and 5; Supplementary Figure S4**). To challenge this prediction, we used HPLC-MS (ESI+) to determine the molecular weight of the homoectoine-derived EctD reaction product. We used a supernatant of an *in vivo* biotransformation of an EctD cell factory that had received 5 mM homoectoine, so that the

substrate had been completely imported, converted by the ectoine hydroxylase into the presumed hydroxyhomoectoine, which was then secreted (**Figure 5C**).

The supernatant of *E. coli* LC15 cells harboring the empty expression plasmid pASK-IBA3 (thereby lacking *ectD*) revealed a mass signal at 157.0970 m/z corresponding precisely to homoectoine with the chemical formula $C_7H_{12}N_2O_2$ and a calculated m/z of $[M+H]^+ = 157.0972$ m/z (**Supplementary Figure S6A**). The additionally observed signals at 179.0789 m/z and 195.0529 m/z correspond to homoectoine molecules accompanied by either a Na^+ or K^+ instead of a proton. The supernatant of *E. coli* LC15 cells harboring the expression plasmid pMP41 (*ectD*⁺) revealed, however, a mass signal at 173.0917 m/z that corresponds precisely to hydroxyhomoectoine with the chemical formula $C_7H_{12}N_2O_3$ and a calculated mass of $[M+H]^+ = 173.0921$ m/z (**Supplementary Figure S6B**). Again, the additionally observed signals at 195.0738 m/z and 211.0478 m/z correspond to hydroxyhomoectoine molecules in combination with a Na^+ or K^+ ion, respectively. HPLC-MS (ESI⁺) analysis of the MMA growth medium without cells and added homoectoine did not show any of the corresponding signals. Taken together, the HPLC-MS data thus unambiguously show that the (Ps)EctD enzyme can use the synthetic ectoine derivative homoectoine as a substrate and hydroxylate it.

The ectoine hydroxylase is very precise in its natural enzymatic reaction, both with respect to its regio- and stereoselectivity. It is known to produce, both *in vivo* and *in vitro*, (4*S*,5*S*)-5-hydroxyectoine from its substrate ectoine (Inbar and Lapidot, 1988; Bursy et al., 2007). To assess if the EctD enzyme was also able to selectively hydroxylate the seven-membered ring of homoectoine, we used different types of NMR spectroscopy. For this purpose, we first purified the homoectoine derived hydroxylated compound via preparative HPLC from the supernatant of two 10-ml cultures of strain LC15 (pMP40-*ectD*⁺) that had received 5 mM homoectoine; this finally yielded 14 mg of the dried hydroxylated compound. After a quality check by HPLC-MS that ascertained that the isolated compound was actually hydroxyhomoectoine, the purified hydroxyhomoectoine was dissolved in water and its biosynthetic precursor homoectoine was dissolved in D₂O (each in 700 µl) and were subsequently analyzed via 1d- and 2d-NMR. The comparison of ¹H-, ¹³C, COSY-, HSQC-, and HMBC-spectra revealed exclusive hydroxylation at the C-5 position of the seven-membered homoectoine ring (**Figure 6; Supplementary Figures S7 – S18**). The signals of the NOE-spectrum were assigned to the Density Functional Theory (DFT)-calculated structure of (4*S*,5*S*)-hydroxyhomoectoine, which fits with a *trans*-configuration of the introduced hydroxyl group by the EctD enzyme (**Figure 6C**). The coupling constant between the α-H and the β-H of 5.46 Hz corresponds to a dihedral angle of approximately 38° by the Karplus equation (Karplus, 1959) which fits with a *trans*-configuration of the introduced hydroxyl group by the EctD enzyme (see supplementary data and **Figure 6C**). These data are fully consistent with the stereo-chemical configuration of the hydroxyl-group in 5-

hydroxyectoine isolated from microorganisms and produced in vitro by the ectoine hydroxylase (Inbar and Lapidot, 1988; Bursy et al., 2007) (**Figure 1**). Furthermore, they nicely match the data from the modeling study predicting that EctD would hydroxylate the C-5 atom in the seven-member diazepine ring of homoectoine (**Figure 2C,D**).

5-hydroxyhomoectoine is an osmoprotectant

Having the purified 5-hydroxyhomoectoine in hand, we tested its biological activity in an osmoprotection growth assay in a micro-titer well plate reader. Cells of *E. coli* MG1655 were grown under growth-restricting osmotic conditions (MMA with 0.8 M NaCl) in the absence or presence of various compatible solutes. As observed before (**Figure 3A**), homoectoine was a moderately effective osmoprotection protectant relative to the strong growth promotion afforded by ectoine, 5-hydroxyectoine, and glycine betaine under the osmotically unfavorable conditions (**Figure 7**). 5-hydroxyhomoectoine was also an osmoprotection protectant but its effectiveness was even weaker than that of homoectoine (**Figure 7**). This could potentially be attributed to reduced import, the physico-chemical attributes of the compound itself, or reduced stability of 5-hydroxyhomoectoine in the pH-neutral MMA growth medium. We know that this latter effect plays a role because we observed a decrease in the slope of our standard curves over time when the samples prepared from the same stock solutions were re-measured (**Supplementary Figure S1**).

DISCUSSION

Microbial cells possess an ‘underground metabolism’ originating from the promiscuous use of different substrates in side reactions of enzymes (D’Ari and Casades, 1998). This sloppiness of extant enzymes is an engine for the evolution of novel metabolic traits and can also be exploited for biotechnological purposes. The data that we report here focus on the substrate profile of the ectoine hydroxylase EctD (Bursy et al., 2007; Höppner et al., 2014), an enzyme that performs a precise regio- and stereoselective introduction of a hydroxyl group to an inactivated carbon within the chiral compound ectoine (Bursy et al., 2007; Widderich et al., 2014b). It endows the newly formed 5-hydroxyectoine (Inbar and Lapidot, 1988) with novel stress-protective and function preserving properties (Pastor et al., 2010; Czech et al., 2018a). Hence, the idea arose to exploit possible biosynthetic side-activities of the ectoine hydroxylase as a catalyst in synthetic chemistry (Galinski et al., 2009; Hara et al., 2019). An attractive starting molecule for this approach is the synthetic ectoine derivative homoectoine (Schnoor et al., 2004) (**Figure 1**), as it already has been shown to function as a superior PCR enhancer, and animal experiments suggest it can potentially ameliorate the negative

consequence of colitis better than ectoine by maintaining intestinal mucosal integrity (Schnoor et al., 2004; Shi and Jarvis, 2006; Castro-Ochoa et al., 2019; Farre and Vicario, 2019).

Molecular docking of homoectoine into the cavity of the cupin barrel of the *S. alaskensis* EctD protein, from which a high-resolution crystal structure is available (Höppner et al., 2014) (**Figure 2A,B**), suggested that the expanded seven-membered ring of homoectoine would not only nicely fit into the active site but that the enzyme would also introduce a hydroxyl group into the ring structure of this molecule at position C-5 (**Figure 2C,D**). HPCL-MS and various types of NMR analysis verified our *in silico* prediction when the *P. stutzeri* EctD enzyme was used in an *E. coli* cell factory to produce the hydroxylated derivative of homoectoine (**Figure 5C; Figure 6, and Supplementary Figures S6 – S18**). Collectively, our data show that the synthetic homoectoine molecule is modified in a very precise and regio- and stereoselective fashion to (4S,5S)-5-hydroxy-homoectoine in which the hydroxyl-group is introduced in a *trans* configuration in the seven-member diazepine ring of homoectoine (**Figure 1**).

Some of the kinetic parameters that we measured for the EctD-mediated conversion of homoectoine into 5-hydroxyhomoectoine are rather surprising because the V_{\max} of the (*Ps*)EctD enzyme for its synthetic substrate homoectoine exceeds that for its natural substrate ectoine by about three-fold (**Figure 4**). The (*Ps*)EctD enzyme is also considerably more efficient in converting both ectoine and homoectoine into the corresponding hydroxylated species than the (*Sa*)EctD ortholog (**Figure 4**). The superior performance of the (*Ps*)EctD enzyme was already noted when several EctD enzymes were benchmarked against each other in an *E. coli* cell factory producing 5-hydroxyectoine from imported ectoine (Czech et al., 2016). However, this observation could not be properly explained from the previously determined kinetic parameters obtained under assay conditions somewhat different from those used here (Widderich et al., 2014a).

The ectoine hydroxylase was originally regarded as a highly specific enzyme because the EctD proteins from *Streptomyces coelicolor* and *Salibacillus salexigens* apparently did not hydroxylate L-proline, and the *S. salexigens* enzymes were not active towards the synthetic ectoine derivatives DHMICA, a five-membered ring molecule, and homoectoine, a seven-membered ring molecule (Bursy et al., 2007; Bursy et al., 2008). However, in hindsight, and taking the data from this study into account, these data now need to be viewed with some caution. It is not necessarily clear that these two EctD enzymes cannot perform the hydroxylation reaction using unusual substrates in general but rather additional assay optimization might be required to reveal the complete substrate profiles of the *S. coelicolor* and *S. salexigens* ectoine hydroxylases.

Hydroxylated prolines are interesting building blocks for medical and biotechnological applications as these can be incorporated in cyclic non-ribosomal peptide compounds, such as the antifungal agent echinocandin or the anti-tuberculosis drugs griselimycins (Houwaart et al., 2014;

Lukat et al., 2017; Zhang et al., 2018). In a recent study, the EctD enzymes from *H. elongata* and *Streptomyces cattleya* were utilized to produce hydroxyprolines (Hara et al., 2019). While EctD from *H. elongata* only catalyzed the formation of *trans*-3-hydroxyproline from L-proline, the (Sc)EctD enzyme also accepted 3,4-dehydro-L-proline, 2-methyl-L-proline, and L-pipecolic acid as substrates, highlighting that notable differences in the substrate profiles and kinetic parameters (**Figure 4**) of *bona fide* ectoine hydroxylases exist (Höppner et al., 2014; Widderich et al., 2014a; Czech et al., 2018a).

The (Sa)EctD enzyme reaction chamber has a calculated volume of approximately 77 Å³ (**Figure 8**). This is an important number that should be taken into account when larger non-natural substrates are considered for *in vivo* or *in vitro* EctD-mediated hydroxylation reactions. A model of the (Sa)EctD reaction chamber containing the synthetic substrate homoectoine or the reaction products 5-hydroxyectoine and 5-hydroxyhomoectoine are shown in **Figure 8**. Our data on the docking analysis of homoectoine into the crystal structure of the (Sa)EctD enzyme (**Figure 2C**) suggest that such an *in silico* approach can probably generally serve to predict the hydroxylation site for non-natural substrates of the ectoine hydroxylase. As a proof of principle, the report by Hara *et al.* (2019) that the EctD enzyme from *H. elongata* displays selective *trans*-3-hydroxylation activity towards L-proline (Hara et al., 2019) motivated us to dock L-proline acid into the active site of the (Sa)EctD protein. Notably, this model predicted correctly the position at which the L-proline molecule is actually hydroxylated by the (He)EctD enzyme to form *trans*-3-hydroxyproline (**Supplementary Figure 2B**).

There are three important lessons that can be learned from our studies and the report of Hara *et al.* (2019). First, enzymatic assays with various ectoine hydroxylases might require specific optimization to perform optimally with the natural substrate ectoine and various non-natural substrates. Second, the use of EctD enzymes from different microorganisms can be helpful to benchmark their activities *in vitro* and *in vivo* against each other in order to identify the best suitable candidate for biotransformation reactions. Third, it is clear now that the enzymatic performance of EctD-type enzymes and their promiscuous use of secondary substrates (Galinski et al., 2009; 2015; Hara et al., 2019) (this study) are not *per se* deducible from their amino acid sequences, as these proteins are evolutionarily closely related (**Supplementary Figure S19**) and similar in their structural fold (Reuter et al., 2010; Höppner et al., 2014; Widderich et al., 2014a; Czech et al., 2018a).

Homoectoine and 5-hydroxyhomoectoine are moderately effective osmostress protectants (Nagata, 2001) (**Figure 3A,B and Figure 7**). This could potentially be rooted in their physico-chemical attributes, or more likely, it may be that the *E. coli* ProU and ProP transport systems for ectoines (Jebbar et al., 1992; MacMillan et al., 1999; Czech et al., 2016) are not optimally configured to accommodate the seven-membered rings of these compounds. This points to a potentially serious

limitation when EctD-based microbial cell factories will be used to hydroxylate non-natural substrates of the ectoine hydroxylase (Galinski et al., 2009; 2015). This might be overcome by the use of permeabilized cells (Galinski et al., 2009), as has been demonstrated for the recombinant synthesis of ectoine using the *H. elongata* *ectABC* genes in *E. coli* (He et al., 2015). The ectoine hydroxylase is a strictly oxygen- and 2-oxoglutarate-dependent enzyme (Höppner et al., 2014; Widderich et al., 2014a; Widderich et al., 2014b; Widderich et al., 2016). Hence, insufficient availability of the co-factor 2-oxoglutarate and a limited oxygen supply could severely impede the maximal performance of EctD-based microbial cell factories. In case of the *E. coli* EctD cell factory producing *trans*-3-hydroxyproline, constraints on the supply of 2-oxoglutarate have been averted by deleting the gene for the 2-oxoglutarate-consuming 2-oxoglutarate dehydrogenase, thereby increasing the yield of *trans*-3-hydroxyproline by two-fold (Hara et al., 2019). Limitations in the supply of oxygen were avoided in a synthetic cell factory expressing a proline-4-hydroxylase from *Dactylosporangium* sp. strain RH1 by implanting a hemoglobin gene from *Vitreoscilla* into the *E. coli* chromosome, thereby increasing production of the hydroxylated proline derivative by two-fold (Zhao et al., 2017).

The ability to synthesize ectoine and hydroxylate it via EctD to 5-hydroxyectoine is widely found in members of ten major phyla of the *Bacteria* (Czech et al., 2018a). 5-hydroxyectoine-producing bacteria live in ecophysiologicaly rather varied habitats with respect to salinity, temperature, and pH, and they can also be found both in marine and terrestrial environments. The ectoine hydroxylases from these microorganisms should therefore be a rich source to search for EctD proteins with biotechnologically interesting substrate profiles. Furthermore, the available EctD crystal structures (Reuter et al., 2010; Höppner et al., 2014) can be used as starting templates for targeted or high-throughput mutagenesis approaches to potentially improve the catalytic efficiency of the ectoine hydroxylase for its natural or synthetic substrates, or to broaden its substrate profile (Koketsu et al., 2015; Hara et al., 2019). If appropriate selection conditions can be designed, laboratory evolution experiments (Guzman et al., 2019) could also come into play to shape the catalytic performance and substrate profile of ectoine hydroxylases for uses in commercially interesting biotransformation reactions.

Author contributions

LC and EB conceived and directed this study. LC, SW, OC, UL, JB conducted experiments and evaluated data. SHJS carried out modeling studies. LC, SHJS, EAG and EB wrote the paper. All authors commented on the manuscript.

FUNDING

This project was supported by the Deutsche Forschungsgemeinschaft (DFG) in the framework of the Collaborative Research Center (CRC-987; project number 192445154) (to EB). The Center for Structural Studies at the University of Düsseldorf is funded by the DFG as well (Grant number: 417919780). LC gratefully acknowledges the receipt of a PhD fellowship from the International Max Planck Research School for Environmental, Cellular and Molecular Microbiology (IMPRS-Mic).

ACKNOWLEDGEMENTS

We value the expert technical assistance of Jochen Sohn during part of this study and appreciate our discussions with Tamara Hoffmann. We are grateful to Vickie Koogle for her kind help in the language editing of our manuscript. We thank the Department of Chemistry of the Philipps-University Marburg for access to its core facilities for mass spectrometry and NMR analysis. We are grateful to Ian Booth (University of Aberdeen, United Kingdom) for providing us with bacterial strains.

Data Availability Statement

All data generated in this study, not presented in the manuscript, can be found in the Supplementary Material.

SUPPLEMENTARY MATERIAL

The Supplementary Material for this article can be found online at: <https://www.frontiersin.org/articles/....>

REFERENCES

- Afonine, P.V., Grosse-Kunstleve, R.W., Echols, N., Headd, J.J., Moriarty, N.W., Mustyakimov, M., et al. (2012). Towards automated crystallographic structure refinement with phenix.refine. *Acta Crystallogr D Biol Crystallogr* 68(Pt 4), 352-367. doi: 10.1107/S0907444912001308.
- Aik, W., McDonough, M.A., Thalhammer, A., Chowdhury, R., and Schofield, C.J. (2012). Role of the jelly-roll fold in substrate binding by 2-oxoglutarate oxygenases. *Cur Opin Struct Biol* 22(6), 691-700. doi: 10.1016/j.sbi.2012.10.001.
- Arakawa, T., and Timasheff, S.N. (1985). The stabilization of proteins by osmolytes. *Biophys J* 47(3), 411-414. doi: 10.1016/S0006-3495(85)83932-1.
- Baba, T., Ara, T., Hasegawa, M., Takai, Y., Okumura, Y., Baba, M., et al. (2006). Construction of *Escherichia coli* K-12 in-frame, single-gene knockout mutants: the Keio collection. *Mol Syst Biol* 2, 2006 0008. doi: 10.1038/msb4100050.
- Barrick, J.E., and Lenski, R.E. (2013). Genome dynamics during experimental evolution. *Nat Rev Genet* 14(12), 827-839. doi: 10.1038/nrg3564.
- Barth, S., Huhn, M., Matthey, B., Klimka, A., Galinski, E.A., and Engert, A. (2000). Compatible-solute-supported periplasmic expression of functional recombinant proteins under stress conditions. *Appl Environ Microbiol* 66(4), 1572-1579.
- Becke, A.D. (1993). Density-functional thermochemistry. III The role of exact exchange. *J Chem Phys* 98, 5648-5652.
- Becker, J., Schäfer, R., Kohlstedt, M., Harder, B.J., Borchert, N.S., Stöveken, N., et al. (2013). Systems metabolic engineering of *Corynebacterium glutamicum* for production of the chemical chaperone ectoine. *Microb Cell Fact* 12(1), 110. doi: 10.1186/1475-2859-12-110.
- Blattner, F.R., Plunkett, G., 3rd, Bloch, C.A., Perna, N.T., Burland, V., Riley, M., et al. (1997). The complete genome sequence of *Escherichia coli* K-12. *Science* 277(5331), 1453-1462. doi: 10.1126/science.277.5331.1453.
- Bolen, D.W., and Baskakov, I.V. (2001). The osmophobic effect: natural selection of a thermodynamic force in protein folding. *J Mol Biol* 310, 955-963. doi: 10.1006/jmbi.2001.4819.
- Booth, I.R. (2014). Bacterial mechanosensitive channels: progress towards an understanding of their roles in cell physiology. *Curr Opin Microbiol* 18, 16-22. doi: 10.1016/j.mib.2014.01.005.
- Borges, N., Ramos, A., Raven, N.D., Sharp, R.J., and Santos, H. (2002). Comparative study of the thermostabilizing properties of mannosylglycerate and other compatible solutes on model enzymes. *Extremophiles* 6(3), 209-216. doi: 10.1007/s007920100236.
- Bourot, S., Sire, O., Trautwetter, A., Touze, T., Wu, L.F., Blanco, C., et al. (2000). Glycine betaine-assisted protein folding in a *lysA* mutant of *Escherichia coli*. *J Biol Chem* 275(2), 1050-1056.

- 827 Bremer, E., and Krämer, R. (2000). "Coping with osmotic challenges: osmoregulation through
828 accumulation and release of compatible solutes.," in *Bacterial Stress Responses*, eds. G. Storz
829 & R. Hengge-Aronis. (Washington DC, USA: ASM Press), 79-97.
- 830 Bremer, E., and Krämer, R. (2019). Responses of microorganisms to osmotic stress. *Annual Review*
831 *Microbiology* 73, (in press) (doi: 10.1146/annurev-micro-020518-115504).
- 832 Bursy, J., Kuhlmann, A.U., Pittelkow, M., Hartmann, H., Jebbar, M., Pierik, A.J., et al. (2008). Synthesis
833 and uptake of the compatible solutes ectoine and 5-hydroxyectoine by *Streptomyces*
834 *coelicolor* A3(2) in response to salt and heat stresses. *Appl Environ Microbiol* 74(23), 7286-
835 7296. doi: 10.1128/AEM.00768-08.
- 836 Bursy, J., Pierik, A.J., Pica, N., and Bremer, E. (2007). Osmotically induced synthesis of the compatible
837 solute hydroxyectoine is mediated by an evolutionarily conserved ectoine hydroxylase. *J Biol*
838 *Chem* 282(43), 31147-31155. doi: 10.1074/jbc.M704023200.
- 839 Capp, M.W., Pegram, L.M., Saecker, R.M., Kratz, M., Riccardi, D., Wendorff, T., et al. (2009).
840 Interactions of the osmolyte glycine betaine with molecular surfaces in water:
841 thermodynamics, structural interpretation, and prediction of m-values. *Biochemistry* 48(43),
842 10372-10379. doi: 10.1021/bi901273r.
- 843 Castro-Ochoa, K.F., Vargas-Robles, H., Chanez-Paredes, S., Felipe-Lopez, A., Cabrera-Silva, R.I.,
844 Shibayama, M., et al. (2019). Homoectoine protects against colitis by preventing a claudin
845 switch in epithelial tight junctions. *Dig Dis Sci* 64(2), 409-420. doi: 10.1007/s10620-018-5309-
846 8.
- 847 Chattopadhyay, M.K., Kern, R., Mistou, M.Y., Dandekar, A.M., Uratsu, S.L., and Richarme, G. (2004).
848 The chemical chaperone proline relieves the thermosensitivity of a *dnaK* deletion mutant at
849 42 degrees C. *J Bacteriol* 186(23), 8149-8152. doi: 10.1128/JB.186.23.8149-8152.2004.
- 850 Cox, C.D., Bavi, N., and Martinac, B. (2018). Bacterial mechanosensors. *Annu Rev Physiol* 80, 71-93.
851 doi: 10.1146/annurev-physiol-021317-121351.
- 852 Culham, D.E., Marom, D., Boutin, R., Garner, J., Ozturk, T.N., Sahtout, N., et al. (2018). Dual role of
853 the C-terminal domain in osmosensing by bacterial osmolyte transporter ProP. *Biophys J*
854 115(11), 2152-2166. doi: 10.1016/j.bpj.2018.10.023.
- 855 Czech, L., Hermann, L., Stöveken, N., Richter, A.A., Höppner, A., Smits, S.H.J., et al. (2018a). Role of
856 the extremolytes ectoine and hydroxyectoine as stress protectants and nutrients: genetics,
857 phylogenomics, biochemistry, and structural analysis. *Genes (Basel)* 9(4), 177. doi:
858 10.3390/genes9040177.
- 859 Czech, L., Poehl, S., Hub, P., Stoeveken, N., and Bremer, E. (2018b). Tinkering with osmotically
860 controlled transcription allows enhanced production and excretion of ectoine and
861 hydroxyectoine from a microbial cell factory. *Appl Environ Microbiol* 84(2), e01772-01717.

- 862 Czech, L., Stöveken, N., and Bremer, E. (2016). EctD-mediated biotransformation of the chemical
863 chaperone ectoine into hydroxyectoine and its mechanosensitive channel-independent
864 excretion. *Microb Cell Fact* 15(1), 126. doi: 10.1186/s12934-016-0525-4.
- 865 D'Ari, R., and Casadesus, J. (1998). Underground metabolism. *Bioessays* 20(2), 181-186. doi:
866 10.1002/(SICI)1521-1878(199802).
- 867 da Costa, M.S., Santos, H., and Galinski, E.A. (1998). An overview of the role and diversity of
868 compatible solutes in *Bacteria* and *Archaea*. *Adv Biochem Eng Biotechnol* 61, 117-153.
- 869 Delano, W.L. (2002). *The PyMol molecular graphics system*. San Carlos, CA, USA: Delano Scientific.
- 870 Diamant, S., Eliahu, N., Rosenthal, D., and Goloubinoff, P. (2001). Chemical chaperones regulate
871 molecular chaperones *in vitro* and in cells under combined salt and heat stresses. *J Biol Chem*
872 276(43), 39586-39591. doi: 10.1074/jbc.M103081200.
- 873 Edwards, M.D., Black, S., Rasmussen, T., Rasmussen, A., Stokes, N.R., Stephen, T.L., et al. (2012).
874 Characterization of three novel mechanosensitive channel activities in *Escherichia coli*.
875 *Channels (Austin)* 6(4), 272-281. doi: 10.4161/chan.20998.
- 876 Eilert, E., Kranz, A., Hollenberg, C.P., Piontek, M., and Suckow, M. (2013). Synthesis and release of the
877 bacterial compatible solute 5-hydroxyectoine in *Hansenula polymorpha*. *J Biotechnol* 167(2),
878 85-93. doi: 10.1016/j.jbiotec.2013.02.005.
- 879 Emsley, P., and Cowtan, K. (2004). Coot: model-building tools for molecular graphics. *Acta Crystallogr*
880 *D Biol Crystallogr* 60(Pt 12 Pt 1), 2126-2132. doi: 10.1107/S0907444904019158.
- 881 Farre, R., and Vicario, M. (2019). Maintaining intestinal mucosal integrity by plugging leaks with
882 homoectoine. *Dig Dis Sci* 64(2), 292-293. doi: 10.1007/s10620-018-5383-y.
- 883 Galinski, E.A., Stein, M., Ures, A., and Schwarz, T. (2009). *Stereo-specific hydroxylation*.
- 884 Galinski, E.A., Stein, M., Ures, A., and Schwarz, T. (2015). *Stereo-specific hydroxylation*.
- 885 Galinski, E.A., and Trüper, H.G. (1994). Microbial behaviour in salt-stressed ecosystems. *FEMS*
886 *Microbiol Rev* 15, 95-108.
- 887 Garcia-Esteva, R., Argandona, M., Reina-Bueno, M., Capote, N., Iglesias-Guerra, F., Nieto, J.J., et al.
888 (2006). The *ectD* gene, which is involved in the synthesis of the compatible solute
889 hydroxyectoine, is essential for thermoprotection of the halophilic bacterium
890 *Chromohalobacter salexigens*. *J Bacteriol* 188(11), 3774-3784. doi: 10.1128/JB.00136-06.
- 891 Giaever, H.M., Styrvold, O.B., Kaasen, I., and Strom, A.R. (1988). Biochemical and genetic
892 characterization of osmoregulatory trehalose synthesis in *Escherichia coli*. *J Bacteriol* 170(6),
893 2841-2849.
- 894 Giesselmann, G., Dietrich, D., Jungmann, L., Kohlstedt, M., Jeon, E.J., Yim, S.S., et al. (2019).
895 Metabolic engineering of *Corynebacterium glutamicum* for high-level ectoine production -

design, combinatorial assembly and implementation of a transcriptionally balanced heterologous ectoine pathway. *Biotechnol J*, e201800417. doi: 10.1002/biot.201800417.

Graf, R., Anzali, S., Buenger, J., Pfluecker, F., and Driller, H. (2008). The multifunctional role of ectoine as a natural cell protectant. *Clin Dermatol* 26(4), 326-333. doi: 10.1016/j.clindermatol.2008.01.002.

Gunde-Cimerman, N., Plemenitas, A., and Oren, A. (2018). Strategies of adaptation of microorganisms of the three domains of life to high salt concentrations. *FEMS Microbiol Rev* 42(3), 353-375. doi: 10.1093/femsre/fuy009.

Guzman, G.I., Sandberg, T.E., LaCroix, R.A., Nyerges, A., Papp, H., de Raad, M., et al. (2019). Enzyme promiscuity shapes adaptation to novel growth substrates. *Mol Syst Biol* 15(4), e8462. doi: 10.15252/msb.20188462.

Haardt, M., Kempf, B., Faatz, E., and Bremer, E. (1995). The osmoprotectant proline betaine is a major substrate for the binding-protein-dependent transport system ProU of *Escherichia coli* K-12. *Mol Gen Genet* 246(6), 783-786.

Hahn, M.B., Solomun, T., Wellhausen, R., Hermann, S., Seitz, H., Meyer, S., et al. (2015). Influence of the compatible solute ectoine on the local water structure: implications for the binding of the protein G5P to DNA. *J Phys Chem B* 119(49), 15212-15220. doi: 10.1021/acs.jpcb.5b09506.

Hangasky, J.A., Taabazuing, C.Y., Valliere, M.A., and Knapp, M.J. (2013). Imposing function down a (cupin)-barrel: secondary structure and metal stereochemistry in the alphaKG-dependent oxygenases. *Metallomics* 5, 287-301. doi: 10.1039/c3mt20153h.

Hara, R., Nishikawa, T., Okuhara, T., Koketsu, K., and Kino, K. (2019). Ectoine hydroxylase displays selective trans-3-hydroxylation activity towards L-proline. *Appl Microbiol Biotechnol* 103(14), 5689-5698. doi: 10.1007/s00253-019-09868-y.

Harishchandra, R.K., Sachan, A.K., Kerth, A., Lentzen, G., Neuhaus, T., and Galla, H.J. (2011). Compatible solutes: ectoine and hydroxyectoine improve functional nanostructures in artificial lung surfactants. *Biochim Biophys Acta* 1808(12), 2830-2840. doi: 10.1016/j.bbamem.2011.08.022.

Harishchandra, R.K., Wulff, S., Lentzen, G., Neuhaus, T., and Galla, H.J. (2010). The effect of compatible solute ectoines on the structural organization of lipid monolayer and bilayer membranes. *Biophys Chem* 150(1-3), 37-46. doi: 10.1016/j.bpc.2010.02.007.

He, Y.Z., Gong, J., Yu, H.Y., Tao, Y., Zhang, S., and Dong, Z.Y. (2015). High production of ectoine from aspartate and glycerol by use of whole-cell biocatalysis in recombinant *Escherichia coli*. *Microbial Cell Factories* 14:55. doi: 10.1186/s12934-015-0238-0.

- 930 Held, C., Neuhaus, T., and Sadowski, G. (2010). Compatible solutes: Thermodynamic properties and
 931 biological impact of ectoines and prolines. *Biophys Chem* 152(1-3), 28-39. doi:
 932 10.1016/j.bpc.2010.07.003.
- 933 Hengge-Aronis, R., Klein, W., Lange, R., Rimmele, M., and Boos, W. (1991). Trehalose synthesis genes
 934 are controlled by the putative sigma factor encoded by *rpoS* and are involved in stationary-
 935 phase thermotolerance in *Escherichia coli*. *J Bacteriol* 173(24), 7918-7924.
- 936 Herr, C.Q., and Hausinger, R.P. (2018). Amazing diversity in biochemical roles of Fe(II)/2-oxoglutarate
 937 oxygenases. *Trends Biochem Sci* 43(7), 517-532. doi: 10.1016/j.tibs.2018.04.002.
- 938 Höppner, A., Widderich, N., Lenders, M., Bremer, E., and Smits, S.H.J. (2014). Crystal structure of the
 939 ectoine hydroxylase, a snapshot of the active site. *J Biol Chem* 289(43), 29570-29583. doi: Doi
 940 10.1074/Jbc.M114.576769.
- 941 Houwaart, S., Youssar, L., and Huttel, W. (2014). Pneumocandin biosynthesis: involvement of a trans-
 942 selective proline hydroxylase. *Chembiochem* 15(16), 2365-2369. doi:
 943 10.1002/cbic.201402175.
- 944 Ignatova, Z., and Gierasch, L.M. (2006). Inhibition of protein aggregation *in vitro* and *in vivo* by a
 945 natural osmoprotectant. *Proc Natl Acad Sci USA* 103(36), 13357-13361. doi: 0603772103
 946 10.1073/pnas.0603772103.
- 947 Inbar, L., and Lapidot, A. (1988). The structure and biosynthesis of new tetrahydropyrimidine
 948 derivatives in actinomycin D producer *Streptomyces parvulus*. Use of ¹³C- and ¹⁵N-labeled L-
 949 glutamate and ¹³C and ¹⁵N NMR spectroscopy. *The Journal of biological chemistry* 263(31),
 950 16014-16022.
- 951 Jebbar, M., Talibart, R., Gloux, K., Bernard, T., and Blanco, C. (1992). Osmoprotection of *Escherichia*
 952 *coli* by ectoine: uptake and accumulation characteristics. *J Bacteriol* 174(15), 5027-5035.
- 953 Jensen, R.A. (1976). Enzyme recruitment in evolution of new function. *Annu Rev Microbiol* 30, 409-
 954 425. doi: 10.1146/annurev.mi.30.100176.002205.
- 955 Jorge, C.D., Borges, N., Bagyan, I., Bilstein, A., and Santos, H. (2016). Potential applications of stress
 956 solutes from extremophiles in protein folding diseases and healthcare. *Extremophiles* 20(3),
 957 251-259. doi: 10.1007/s00792-016-0828-8.
- 958 Karplus, M. (1959). Contact electron-spin coupling of nuclear magnetic moments. *J Chem Phys* 30,
 959 11-15.
- 960 Kempf, B., and Bremer, E. (1998). Uptake and synthesis of compatible solutes as microbial stress
 961 responses to high osmolality environments. *Arch Microbiol* 170, 319-330.
- 962 Khersonsky, O., and Tawfik, D.S. (2010). Enzyme promiscuity: a mechanistic and evolutionary
 963 perspective. *Annu Rev Biochem* 79, 471-505. doi: 10.1146/annurev-biochem-030409-143718.

- Kitagawa, M., Ara, T., Arifuzzaman, M., Ioka-Nakamichi, T., Inamoto, E., Toyonaga, H., et al. (2005). Complete set of ORF clones of *Escherichia coli* ASKA library (a complete set of *E. coli* K-12 ORF archive): unique resources for biological research. *DNA Res* 12(5), 291-299. doi: 10.1093/dnares/dsi012.
- Koichi, M., Mitsuhiro, M., Tatsuo, N., and Yoshio, S. (1991). *Production of tetrahydropyrimidine derivatives*. Patent
- Koketsu, K., Shomura, Y., Moriwaki, K., Hayashi, M., Mitsuhashi, S., Hara, R., et al. (2015). Refined regio- and stereoselective hydroxylation of L-pipecolic acid by protein engineering of L-proline cis-4-hydroxylase based on the X-ray crystal structure. *ACS Synth Biol* 4(4), 383-392. doi: 10.1021/sb500247a.
- Kuhlmann, A.U., and Bremer, E. (2002). Osmotically regulated synthesis of the compatible solute ectoine in *Bacillus pasteurii* and related *Bacillus* spp. *Appl Environ Microbiol* 68(2), 772-783.
- Kunte, H.J., Lentzen, G., and Galinski, E. (2014). Industrial production of the cell protectant ectoine: protection, mechanisms, processes, and products. *Current Biotechnology* 3, 10-25.
- Lamark, T., Styrvold, O.B., and Strom, A.R. (1992). Efflux of choline and glycine betaine from osmoregulating cells of *Escherichia coli*. *FEMS Microbiol Lett* 75(2-3), 149-154.
- Lentzen, G., and Schwarz, T. (2006). Extremolytes: Natural compounds from extremophiles for versatile applications. *Appl Microbiol Biotechnol* 72(4), 623-634. doi: 10.1007/s00253-006-0553-9.
- Lippert, K., and Galinski, E.A. (1992). Enzyme stabilization by ectoine-type compatible solutes: protection against heating, freezing and drying. *Applied Microbial Biotechnology* 37, 61-65.
- Liu, Y., and Bolen, D.W. (1995). The peptide backbone plays a dominant role in protein stabilization by naturally occurring osmolytes. *Biochemistry* 34(39), 12884-12891. doi: 10.1021/bi00039a051.
- Lo, C.C., Bonner, C.A., Xie, G., D'Souza, M., and Jensen, R.A. (2009). Cohesion group approach for evolutionary analysis of aspartokinase, an enzyme that feeds a branched network of many biochemical pathways. *Microbiol Mol Biol Rev* 73(4), 594-651. doi: 10.1128/MMBR.00024-09.
- Lucht, J.M., and Bremer, E. (1994). Adaptation of *Escherichia coli* to high osmolarity environments: osmoregulation of the high-affinity glycine betaine transport system ProU. *FEMS Microbiol Rev* 14(1), 3-20.
- Lukat, P., Katsuyama, Y., Wenzel, S., Binz, T., Konig, C., Blankenfeldt, W., et al. (2017). Biosynthesis of methyl-proline containing griselimycins, natural products with anti-tuberculosis activity. *Chem Sci* 8(11), 7521-7527. doi: 10.1039/c7sc02622f.

- 997 MacMillan, S.V., Alexander, D.A., Culham, D.E., Kunte, H.J., Marshall, E.V., Rochon, D., et al. (1999).
 998 The ion coupling and organic substrate specificities of osmoregulatory transporter ProP in
 999 *Escherichia coli*. *Biochim Biophys Acta* 1420(1-2), 30-44.
- 1000 Manzanera, M., Vilchez, S., and Tunnacliffe, A. (2004). High survival and stability rates of *Escherichia*
 1001 *coli* dried in hydroxyectoine. *FEMS Microbiol Lett* 233(2), 347-352. doi:
 1002 10.1016/j.femsle.2004.03.005.
- 1003 Meyer, S., Schröter, M.A., Hahn, M.B., Solomun, T., Sturm, H., and Kunte, H.J. (2017). Ectoine can
 1004 enhance structural changes in DNA in vitro. *Sci Rep* 7(1), 7170. doi: 10.1038/s41598-017-
 1005 07441-z.
- 1006 Michael, A.J. (2017). Evolution of biosynthetic diversity. *Biochem J* 474(14), 2277-2299. doi:
 1007 10.1042/BCJ20160823.
- 1008 Miller, J.H. (1972). *Experiments in molecular genetics*. Cold Spring Harbor New York: Cold Spring
 1009 Harbor Laboratory.
- 1010 Nagata, S. (2001). Growth of *Escherichia coli* ATCC 9637 through the uptake of compatible solutes at
 1011 high osmolarity. *J Biosci Bioeng* 92(4), 324-329.
- 1012 Newton, M.S., Arcus, V.L., Gerth, M.L., and Patrick, W.M. (2018). Enzyme evolution: innovation is
 1013 easy, optimization is complicated. *Curr Opin Struct Biol* 48, 110-116. doi:
 1014 10.1016/j.sbi.2017.11.007.
- 1015 Ning, Y., Wu, X., Zhang, C., Xu, Q., Chen, N., and Xie, X. (2016). Pathway construction and metabolic
 1016 engineering for fermentative production of ectoine in *Escherichia coli*. *Metab Eng* 36, 10-18.
 1017 doi: 10.1016/j.ymben.2016.02.013.
- 1018 Nobeli, I., Favia, A.D., and Thornton, J.M. (2009). Protein promiscuity and its implications for
 1019 biotechnology. *Nat Biotechnol* 27(2), 157-167. doi: 10.1038/nbt1519.
- 1020 Ono, H., Sawada, K., Khunajakr, N., Tao, T., Yamamoto, M., Hiramoto, M., et al. (1999).
 1021 Characterization of biosynthetic enzymes for ectoine as a compatible solute in a moderately
 1022 halophilic eubacterium, *Halomonas elongata*. *J Bacteriol* 181(1), 91-99.
- 1023 Oren, A. (1999). Bioenergetic aspects of halophilism. *Microbiol Mol Biol Rev* 63(2), 334-348.
- 1024 Pandya, C., Farelli, J.D., Dunaway-Mariano, D., and Allen, K.N. (2014). Enzyme promiscuity: engine of
 1025 evolutionary innovation. *J Biol Chem* 289(44), 30229-30236. doi: 10.1074/jbc.R114.572990.
- 1026 Pastor, J.M., Salvador, M., Argandona, M., Bernal, V., Reina-Bueno, M., Csonka, L.N., et al. (2010).
 1027 Ectoines in cell stress protection: uses and biotechnological production. *Biotechnol Adv* 28(6),
 1028 782-801. doi: 10.1016/j.biotechadv.2010.06.005.
- 1029 Peters, P., Galinski, E.A., and Trüper, H.G. (1990). The biosynthesis of ectoine *FEMS Microbiol. Lett.* 71,
 1030 157-162.

- 1031 Prabhu, J., Schauwecker, F., Grammel, N., Keller, U., and Bernhard, M. (2004). Functional expression
1032 of the ectoine hydroxylase gene (*thpD*) from *Streptomyces chrysomallus* in *Halomonas*
1033 *elongata*. *Appl Environ Microbiol* 70(5), 3130-3132.
- 1034 Reuter, K., Pittelkow, M., Bursy, J., Heine, A., Craan, T., and Bremer, E. (2010). Synthesis of 5-
1035 hydroxyectoine from ectoine: crystal structure of the non-heme iron(II) and 2-oxoglutarate-
1036 dependent dioxygenase EctD. *PLoS one* 5(5), e10647. doi: 10.1371/journal.pone.0010647.
- 1037 Roberts, M.F. (2004). Osmoadaptation and osmoregulation in archaea: update 2004. *Front Biosci* 9,
1038 1999-2019.
- 1039 Roesser, M., and Müller, V. (2001). Osmoadaptation in bacteria and archaea: common principles and
1040 differences. *Environmental microbiology* 3(12), 743-754.
- 1041 Rosenberg, J., and Commichau, F.M. (2019). Harnessing underground metabolism for pathway
1042 development. *Trends Biotechnol* 37(1), 29-37. doi: 10.1016/j.tibtech.2018.08.001.
- 1043 Schnoor, M., Voss, P., Cullen, P., Boking, T., Galla, H.J., Galinski, E.A., et al. (2004). Characterization of
1044 the synthetic compatible solute homoectoine as a potent PCR enhancer. *Biochem Biophys*
1045 *Res Commun* 322(3), 867-872. doi: 10.1016/j.bbrc.2004.07.200.
- 1046 Schubert, T., Maskow, T., Benndorf, D., Harms, H., and Breuer, U. (2007). Continuous synthesis and
1047 excretion of the compatible solute ectoine by a transgenic, nonhalophilic bacterium. *Appl*
1048 *Environ Microbiol* 73(10), 3343-3347. doi: 10.1128/AEM.02482-06.
- 1049 Schwibbert, K., Marin-Sanguino, A., Bagyan, I., Heidrich, G., Lentzen, G., Seitz, H., et al. (2011). A
1050 blueprint of ectoine metabolism from the genome of the industrial producer *Halomonas*
1051 *elongata* DSM 2581 T. *Environ Microbiol* 13, 1973-1994. doi: 10.1111/j.1462-
1052 2920.2010.02336.x.
- 1053 Shi, X., and Jarvis, D.L. (2006). A new rapid amplification of cDNA ends method for extremely guanine
1054 plus cytosine-rich genes. *Anal Biochem* 356(2), 222-228. doi: 10.1016/j.ab.2006.06.028.
- 1055 Smiatek, J., Harishchandra, R.K., Rubner, O., Galla, H.J., and Heuer, A. (2012). Properties of
1056 compatible solutes in aqueous solution. *Biophys Chem* 160(1), 62-68. doi:
1057 10.1016/j.bpc.2011.09.007.
- 1058 Stadtmiller, S.S., Gorensek-Benitez, A.H., Guseman, A.J., and Pielak, G.J. (2017). Osmotic shock
1059 induced protein destabilization in living cells and its reversal by glycine betaine. *J Mol Biol*
1060 429(8), 1155-1161. doi: 10.1016/j.jmb.2017.03.001.
- 1061 Stöveken, N., Pittelkow, M., Sinner, T., Jensen, R.A., Heider, J., and Bremer, E. (2011). A specialized
1062 aspartokinase enhances the biosynthesis of the osmoprotectants ectoine and
1063 hydroxyectoine in *Pseudomonas stutzeri* A1501. *J Bacteriol* 193(17), 4456-4468. doi:
1064 10.1128/JB.00345-11.

- Street, T.O., Bolen, D.W., and Rose, G.D. (2006). A molecular mechanism for osmolyte-induced protein stability. *Proceedings of the National Academy of Sciences of the United States of America* 103(38), 13997-14002. doi: 0606236103 10.1073/pnas.0606236103.
- Strom, A.R., and Kaasen, I. (1993). Trehalose metabolism in *Escherichia coli*: stress protection and stress regulation of gene expression. *Mol Microbiol* 8(2), 205-210.
- Studier, F.W., Rosenberg, A.H., Dunn, J.J., and Dubendorff, J.W. (1990). Use of T7 RNA polymerase to direct expression of cloned genes. *Methods Enzymol* 185, 60-89.
- Tanne, C., Golovina, E.A., Hoekstra, F.A., Meffert, A., and Galinski, E.A. (2014). Glass-forming property of hydroxyectoine is the cause of its superior function as a dessication protectant. *Front Microbiol* 5, 150.
- Tian, W., Chen, C., Lei, X., Zhao, J., and Liang, J. (2018). CASTp 3.0: computed atlas of surface topography of proteins. *Nucleic Acids Res* 46(W1), W363-W367. doi: 10.1093/nar/gky473.
- Trott, O., and Olson, A.J. (2010). AutoDock Vina: improving the speed and accuracy of docking with a new scoring function, efficient optimization, and multithreading. *J Comput Chem* 31(2), 455-461. doi: 10.1002/jcc.21334.
- van den Berg, J., Boersma, A.J., and Poolman, B. (2017). Microorganisms maintain crowding homeostasis. *Nat Rev Microbiol* 15(5), 309-318. doi: 10.1038/nrmicro.2017.17.
- Wachters, A.J.H. (1970). Gaussian basis set for molecular wavefunctions containing third-row atoms. *J Chem Phys* 52, 1033-1036.
- Wedeking, A., Hagen-Euteneuer, N., Gurgui, M., Broere, R., Lentzen, G., Tolba, R.H., et al. (2014). A lipid anchor improves the protective effect of ectoine in inflammation. *Curr Med Chem* 21(22), 2565-2572.
- Widderich, N., Czech, L., Elling, F.J., Könneke, M., Stöveken, N., Pittelkow, M., et al. (2016). Strangers in the archaeal world: osmostress-responsive biosynthesis of ectoine and hydroxyectoine by the marine thaumarchaeon *Nitrosopumilus maritimus*. *Env Microbiol* 18, 1227-1248.
- Widderich, N., Höppner, A., Pittelkow, M., Heider, J., Smits, S.H., and Bremer, E. (2014a). Biochemical properties of ectoine hydroxylases from extremophiles and their wider taxonomic distribution among microorganisms. *PLoS One* 9(4), e93809. doi: 10.1371/journal.pone.0093809.
- Widderich, N., Pittelkow, M., Höppner, A., Mulnaes, D., Buckel, W., Gohlke, H., et al. (2014b). Molecular dynamics simulations and structure-guided mutagenesis provide insight into the architecture of the catalytic core of the ectoine hydroxylase. *J Mol Biol* 426, 586-600. doi: 10.1016/j.jmb.2013.10.028.

- 1098 Witt, E.M., Davies, N.W., and Galinski, E.A. (2011). Unexpected property of ectoine synthase and its
1099 application for synthesis of the engineered compatible solute ADPC. *Appl Microbiol*
1100 *Biotechnol* 91(1), 113-122. doi: 10.1007/s00253-011-3211-9.
- 1101 Wood, J.M. (2011). Bacterial osmoregulation: a paradigm for the study of cellular homeostasis.
1102 *Annual Review of Microbiology* 65, 215-238. doi: 10.1146/annurev-micro-090110-102815.
- 1103 Wood, J.M., Bremer, E., Csonka, L.N., Krämer, R., Poolman, B., van der Heide, T., et al. (2001).
1104 Osmosensing and osmoregulatory compatible solute accumulation by bacteria. *Comparative*
1105 *biochemistry and physiology. Part A, Mol & Int Physiol* 130(3), 437-460.
- 1106 Zaccai, G., Bagyan, I., Combet, J., Cuello, G.J., Deme, B., Fichou, Y., et al. (2016). Neutrons describe
1107 ectoine effects on water H-bonding and hydration around a soluble protein and a cell
1108 membrane. *Sci Rep* 6, 31434. doi: 10.1038/srep31434.
- 1109 Zhang, F., Liu, H., Zhang, T., Pijning, T., Yu, L., Zhang, W., et al. (2018). Biochemical and genetic
1110 characterization of fungal proline hydroxylase in echinocandin biosynthesis. *Appl Microbiol*
1111 *Biotechnol* 102(18), 7877-7890. doi: 10.1007/s00253-018-9179-y.
- 1112 Zhang, L.H., Lang, Y.J., and Nagata, S. (2009). Efficient production of ectoine using ectoine-excreting
1113 strain. *Extremophiles* 13(4), 717-724. doi: 10.1007/s00792-009-0262-2.
- 1114 Zhao, T.X., Li, M., Zheng, X., Wang, C.H., Zhao, H.X., Zhang, C., et al. (2017). Improved production of
1115 trans-4-hydroxy-L-proline by chromosomal integration of the *Vitreoscilla* hemoglobin gene
1116 into recombinant *Escherichia coli* with expression of proline-4-hydroxylase. *J Biosci Bioeng*
1117 123(1), 109-115. doi: 10.1016/j.jbiosc.2016.07.018.

1118

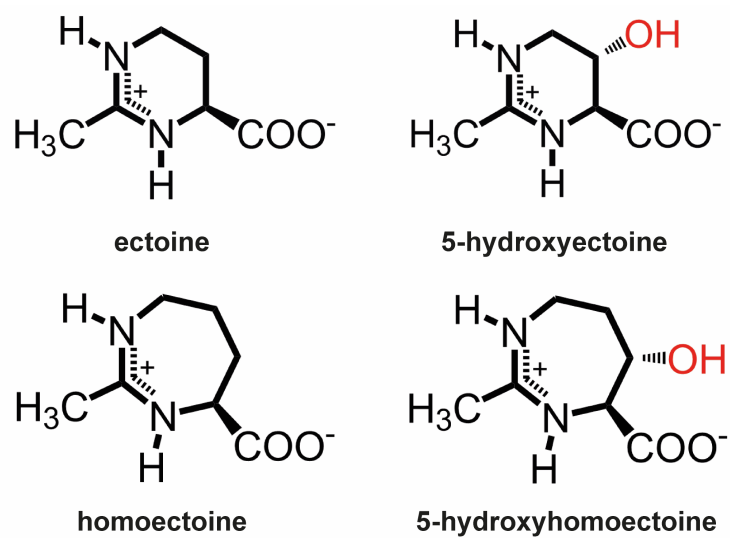


FIGURE 1 | Chemical structures of the compatible solutes **(A)** ectoine, **(B)** 5-hydroxyectoine, **(C)** homoectoine, and **(D)** 5-hydroxyhomoectoine.

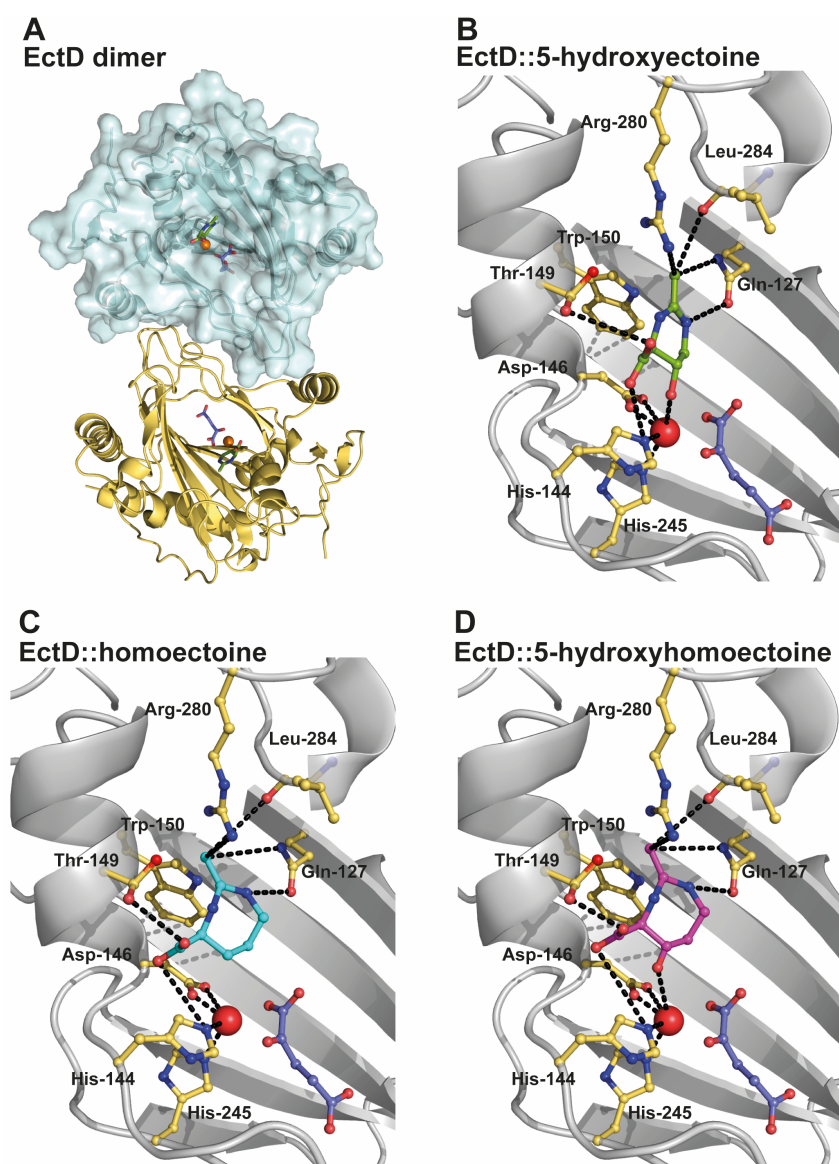


FIGURE 2 | Modeling and docking of different substrates into the crystal structure of the ectoine hydroxylase EctD from *S. alaskensis*. **(A)** The overall fold of the (*Sa*)EctD (PDB: 4Q5O) is shown as a dimer with one monomer presented as the surface structure of the protein and the other monomer in cartoon representation. Each monomer harbors the product, 5-hydroxyectoine (green) of the (*Sa*)EctD-catalyzed enzyme reaction, the co-substrate 2-oxoglutarate (light blue), and the catalytically important ion metal (red ball). **(B, C, D)** Zoom into the active site of (*Sa*)EctD with **(B)** the bound natural reaction product 5-hydroxyectoine (green), **(C)** the modeled synthetic substrate homoectoine (blue), and **(D)** the modeled synthetic reaction product 5-hydroxyhomoectoine (pink). The amino acids involved in substrate binding are shown as yellow sticks and possible interactions are indicated by black dotted lines.

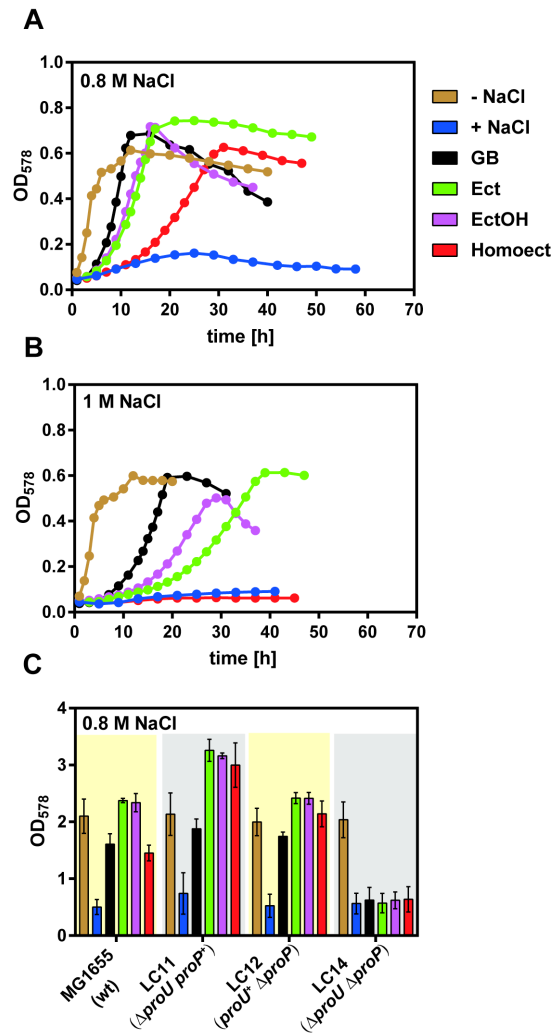


FIGURE 3 | Osmostress protection assay with glycine betaine, ectoine, 5-hydroxyectoine and homoectoine. **(A, B)** Growth of *E. coli* MG1655 ($proU^+ proP^+$) in MMA without NaCl and in MMA containing **(A)** 0.8 M NaCl or **(B)** 1 M NaCl and 1 mM of the indicated osmostress protectants; growth of the cultures was monitored for 60 h. The OD₅₇₈ of the cultures was measured hourly in a plate reader (Epoch2, BioTek). Each osmoprotection assay was conducted with two independently grown cultures. **(C)** *E. coli* strains MG1655 ($proU^+ proP^+$), LC11 ($proU^- proP^+$), LC12 ($proU^+ proP^-$), and LC14 ($proU^- proP^-$) were grown either in MMA or MMA containing 0.8 M NaCl in the absence or presence of the osmostress protectants (1 mM) in shake flasks. The final growth yield was determined by measuring the OD₅₇₈ of the cultures after 30 h. The bars shown are the means and standard deviations of three independently grown cultures.

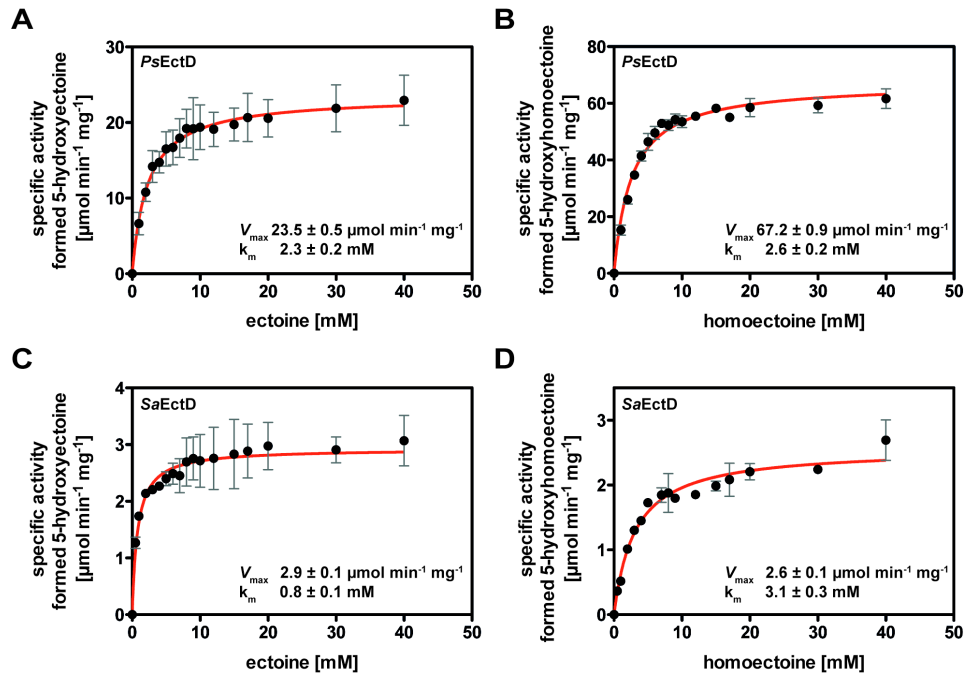


FIGURE 4 | Enzyme kinetics using recombinantly produced and affinity purified EctD proteins from **(A, B)** *P. stutzeri* A1501 [(*Ps*)EctD] and **(C, D)** *S. alaskensis* [(*Sa*)EctD] for the substrates **(A, C)** ectoine, and **(B, D)** homoectoine.

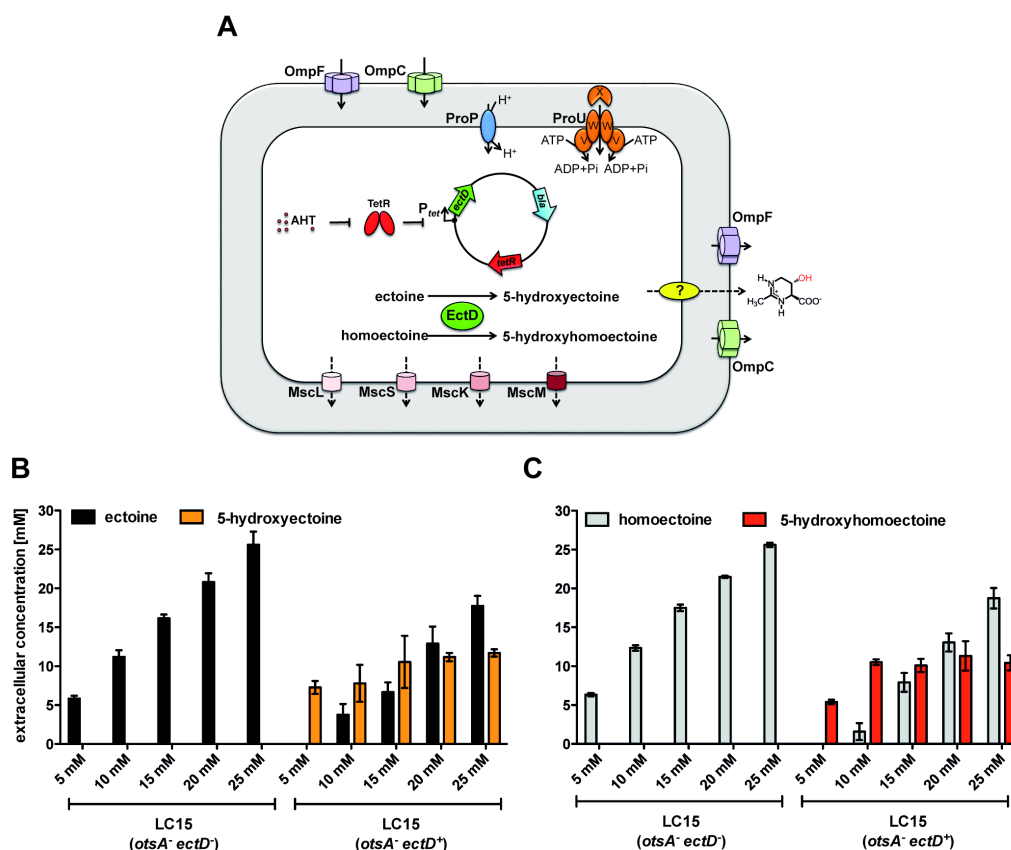


FIGURE 5 | Production of 5-hydroxyectoine or 5-hydroxyhomoectoine from ectoine or homoectoine in an *E. coli* cell factory expressing the (*Ps*)EctD enzyme. **(A)** Schematic overview of the *E. coli* based EctD overproducing cell factory. The *E. coli* strain LC15 (*otsA::Tn10*) contained either the empty vector pASK-IBA3 (control) or the plasmid pMP41 (*ectD* gene from *P. stutzeri* A1501) and was incubated in the presence of various concentrations of **(B)** ectoine or **(C)** homoectoine (ranging from 5 to 25 mM). The cultures were incubated for 24 hours after induction of *ectD* expression with AHT in baffled flasks containing 10 ml of MMA containing 0.4 M NaCl and the concentrations of **(B)** ectoine/5-hydroxyectoine and **(C)** homoectoine/5-hydroxyhomoectoine within the supernatant were determined via HPLC analysis. The data shown represent the means and standard deviations of at least three independently grown cultures (two independently grown cultures for controls).

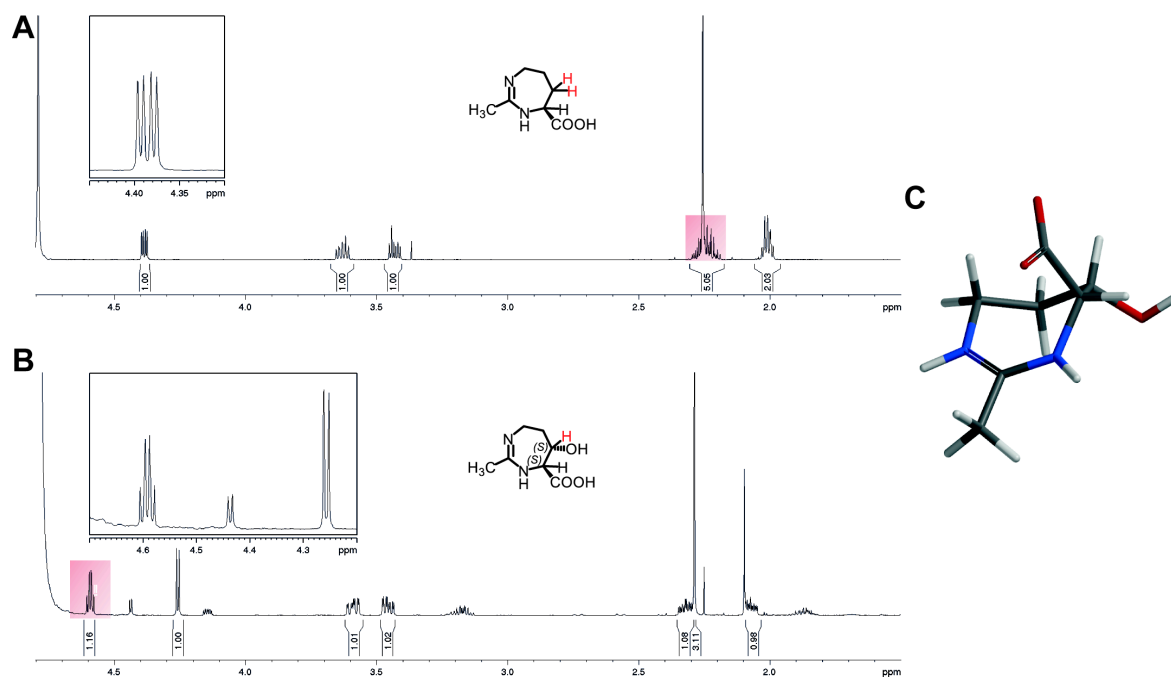


FIGURE 6 | ^1H -NMR spectra of (A) homoectoine and (B) 5-hydroxyhomoectoine. The changing ^1H -signal is highlighted in red. (C) DFT calculated structure of 5-hydroxyhomoectoine. Additional information and the recorded NMR spectra can be found in the Supplementary Material.

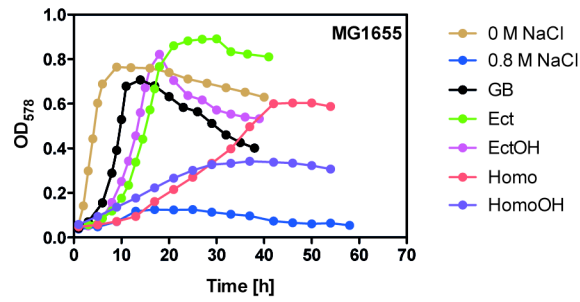


FIGURE 7 | Osmostress protection assay with glycine betaine, ectoine, 5-hydroxyectoine, homoectoine and 5-hydroxyhomoectoine. Growth of *E. coli* MG1655 (*proU*⁺ *proP*⁺) in MMA without NaCl and in MMA containing 0.8 M NaCl without and with the addition of 1 mM of the indicated compatible solutes was monitored for 60 hours. The OD₅₇₈ of the cultures was measured hourly in a plate reader (Epoch2, BioTek). The osmostress protection growth assay was conducted with two independently grown cultures.

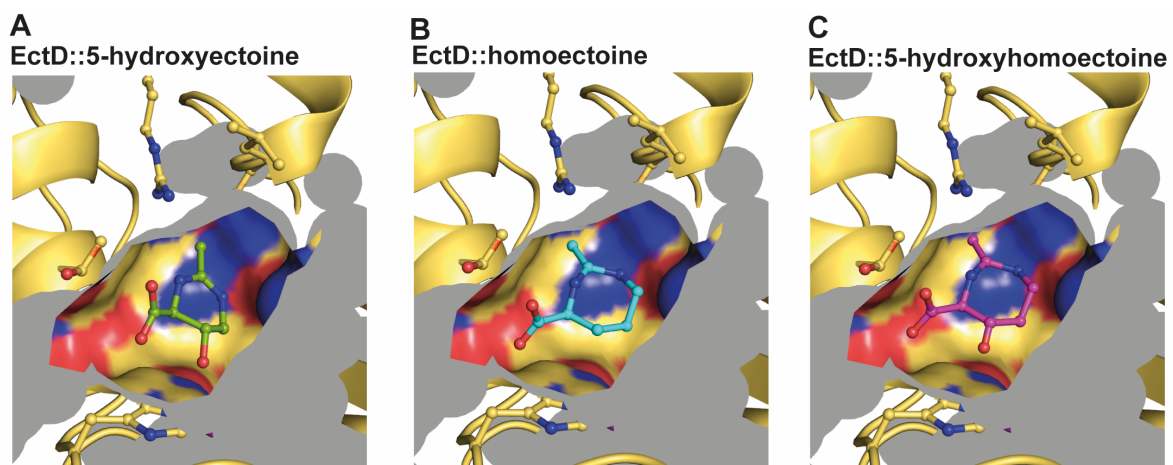


FIGURE 8 I Modeling and docking of different substrates into the crystal structure of the ectoine hydroxylase EctD from *S. alaskensis*. The cavity of the active site of the *Sa*EctD enzyme (PDB: 4Q50) is shown with **(A)** the natural reaction product 5-hydroxyectoine, **(B)** the synthetic substrate homoectoine, and **(C)** the synthetic reaction product 5-hydroxyhomoectoine.

Supplementary material for:

Exploiting substrate promiscuity of ectoine hydroxylase for regio- and stereoselective modification of homoectoine

**Laura Czech¹, Sarah Wilcken¹, Oliver Czech², Uwe Linne², Jarryd Brauner³,
Sander H.J. Smits^{4,5}, Erwin A. Galinski³, and Erhard Bremer^{1,6*}**

¹Laboratory for Microbiology, Department of Biology, Philipps-University Marburg, Marburg, Germany

²Department of Chemistry, Philipps-University Marburg, Marburg, Germany

³Institute of Microbiology and Biotechnology, Rheinische Friedrich-Wilhelms-University, Bonn, Germany

⁴Institute of Biochemistry, Heinrich-Heine University Düsseldorf, Düsseldorf, Germany

⁵Center for Structural Studies, Heinrich-Heine University Düsseldorf, Düsseldorf, Germany

⁶SYNMIKRO Research Center, Philipps-University Marburg, Marburg, Germany

Running title: Chemical biology of ectoines

Number of figures: 19

Number of tables: 2

For correspondence during the reviewing and editorial process please contact:

Dr. Erhard Bremer, Philipps-University Marburg, Dept. of Biology, Laboratory for Microbiology, Karl-von-Frisch-Str. 8, D-35032 Marburg, Germany. Phone: (+49)-6421-2821529. Fax: (+49)-6421-2828979. E-Mail: bremer@staff.uni-marburg.de

*Correspondence:

Erhard Bremer: bremer@staff.uni-marburg.de

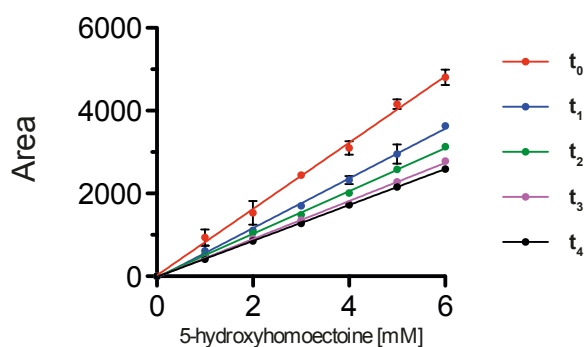
Table S1 Strains used and constructed in this study.

Strain*	Genotype	Reference or source
BL21	<i>E. coli</i> B, F ⁻ <i>ompT gal dcm lon hsdS_B(r_B⁻ m_B⁻) λ(DE3 [<i>lacI</i> <i>lacUV5-T7p07 ind1 sam7 nin5</i>]) [<i>malB</i>⁺]_{K-12}(λ^S)</i>	(Studier et al., 1990)
FRAG1	<i>E. coli</i> K-12, F ⁻ <i>rha thi gal lacZ</i>	(Epstein and Kim, 1971)
MJF641	FRAG1 <i>mscS kefA::kan ybdG::apr ybiO yjeP ynaI ycjM::Tn10 mscL::cml</i>	(Edwards et al., 2012)
MG1655	<i>E. coli</i> K-12, F ⁻ λ ⁻ <i>ilvG rfb-50 rph-1</i>	(Blattner et al., 1997)
LC11	MG1655 (<i>ΔproU::spc</i>)608 [<i>proP</i> ⁺]	This study
LC12	MG1655 (<i>ΔproP::kan</i>)737 [<i>proU</i> ⁺]	This study
LC14	MG1655 (<i>ΔproU::spc</i>)608 (<i>ΔproP::kan</i>)737	This study
LC15	MG1655 <i>otsA1::Tn10</i>	This study

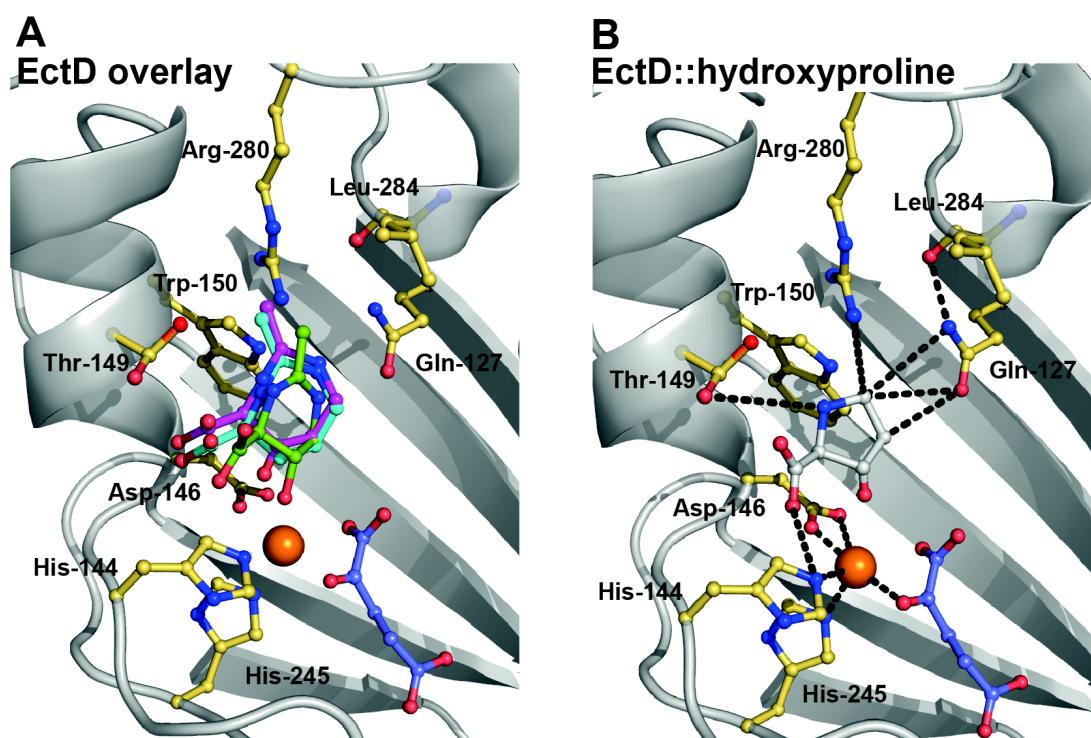
*Strains LC11, LC12, and LC15 were constructed by transducing the *E. coli* strain MG1655 with a P1vir lysates prepared either on strain MKH17 (*ΔproU::spc*)608 (Haardt et al., 1995), on strain JW4072-1 (*ΔproP737::kan*) (Baba et al., 2006), or on strain FF4169 (*otsA1::Tn10*) (Strom and Kaasen, 1993), respectively. Strain LC14 was constructed by transducing strain LC11 with the P1 lysate from strain JW4072-1 (*ΔproP737::kan*). Transductants were selected on LB agar plates containing the appropriate antibiotic.

Table S2 Plasmids used in this study.

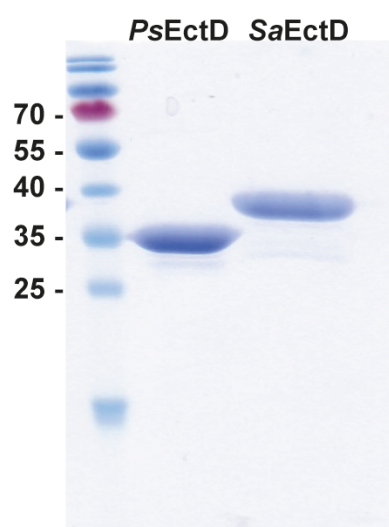
Plasmid	Description	Reference
pASK-IBA3	Expression plasmid, C-terminal Strep-tag, tet _p , Amp ^R	IBA GmbH, Göttingen
pMP40	pASK-IBA3 derivative with <i>ectD</i> from <i>S. alaskensis</i> , Amp ^R	(Widderich et al., 2014)
pMP41	pASG-IBA3 derivative with <i>ectD</i> from <i>P. stutzeri</i> , Amp ^R	(Widderich et al., 2014)



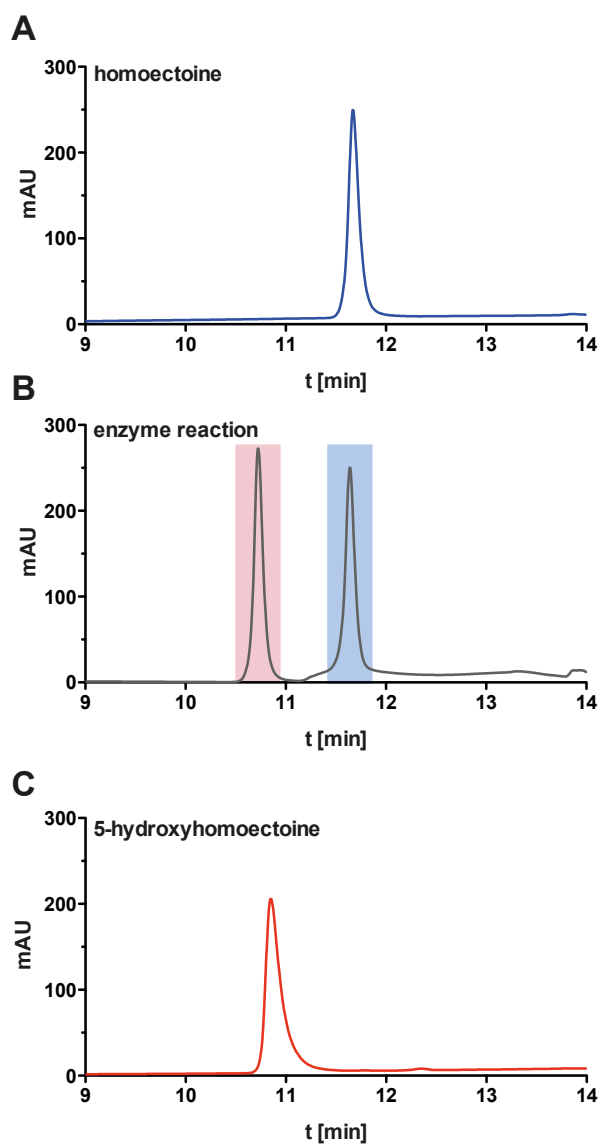
Supplementary Figure 1. Instability of 5-hydroxyhomoectoine standard solutions. Dilutions of purified 5-hydroxyhomoectoine were measured via HPLC to allow the determination of 5-hydroxyhomoectoine concentrations in the supernatants of *E. coli* cell factory expressing the *Pseudomonas stutzeri ectD* gene. The freshly prepared standard dilutions of 5-hydroxyhomoectoine were immediately stored at -20°C. t_0 indicated the fresh standard solution, while t_1 , t_2 , t_3 , t_4 show the standard curves of 5-hydroxyhomoectoine after 2, 12, 13 and 15, weeks of storage at this temperature, respectively.



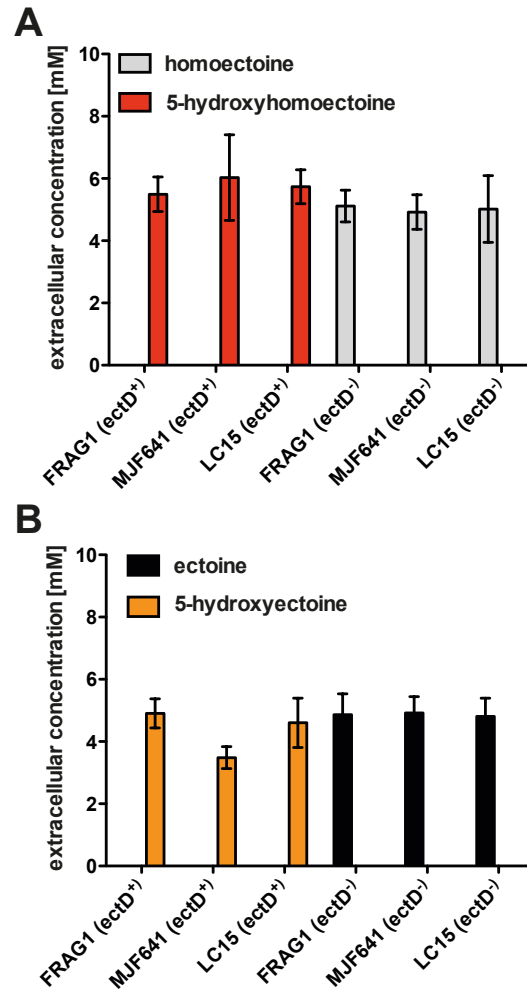
Supplementary Figure 2. Modeling and docking of different substrates into the crystal structure of the ectoine hydroxylase EctD from *S. alaskensis* (PDB: 4Q50). **(A)** Zoom into the active site of one (*Sa*)EctD monomer with an overlay of different substrates. The natural reaction product of the ectoine hydroxylase, 5-hydroxyectoine, is shown in green, the modeled synthetic substrate homoeoctoine in blue, and the modeled reaction product of the EctD-catalyzed hydroxylation of homoeoctoine, 5-hydroxyhomoeoctoine, in pink. The co-substrate of the EctD enzyme, 2-oxoglutarate, is shown in light blue, and the catalytically important iron atom is depicted as an orange ball. **(B)** Zoom into the active site of one (*Sa*)EctD monomer bound to 3-hydroxyproline (grey). This non-natural substrate of the ectoine hydroxylase was modeled into the active side of the EctD enzyme. Amino acids involved in substrate binding are shown as yellow sticks and possible interactions are indicated by black dotted lines.



Supplementary Figure 3. SDS gel of purified ectoine hydroxylases. Shown is a 15 % polyacrylamide SDS gel with the purified recombinant ectoine hydroxylases from *P. stutzeri* A1501 [(*Ps*)EctD] and *S. alaskensis* [(*Sa*)EctD]. The proteins were overexpressed in *E. coli* and purified via an *Strep-Tag-II* affinity chromatography column. 3 µg of both enzymes were applied to the gel, which was run for 1.5 h at 30 mA. The pre-stained PageRuler Protein Ladder (Thermo Scientific) was used as a marker to size the migration of the EctD proteins. The calculated theoretical molecular weight of EctD from *P. stutzeri* A1501 is 34.18 kDa and of EctD from *S. alaskensis* is 34.14 kDa. The unexpected different electrophoretic mobility of the (*Ps*)EctD and (*Sa*)EctD proteins has been noted before (Widderich et al., 2014).



Supplementary Figure 4. HPLC chromatograms of **(A)** the homoectoine standard (blue), **(B)** a (*Ps*)EctD-catalyzed enzyme reaction with a mixture of the substrate homoectoine (blue) and the reaction product 5-hydroxyhomoectoine (red), and **(C)** the 5-hydroxyhomoectoine standard. Ectoines were detected at a wavelength of 210 nm (Kuhlmann and Bremer, 2002).



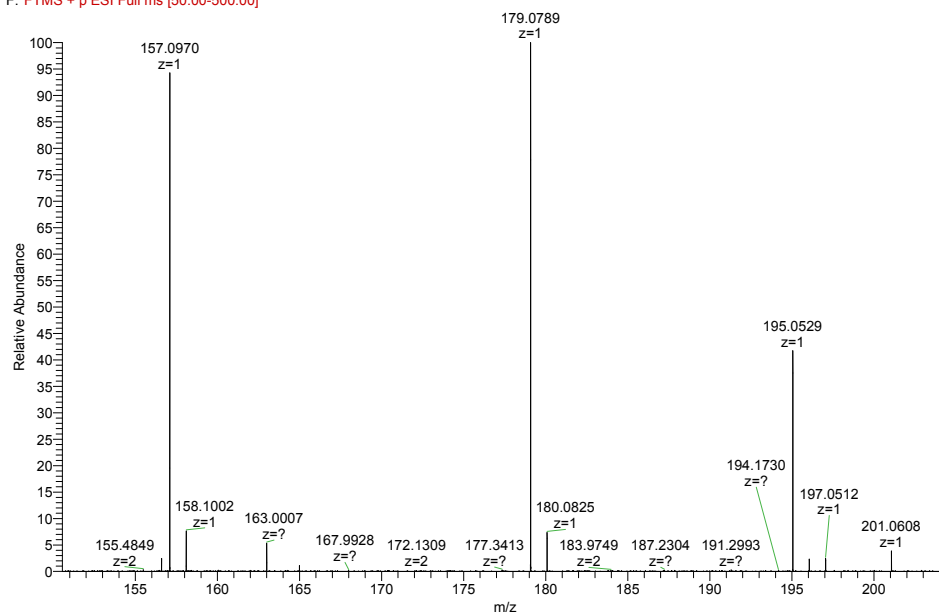
Supplementary Figure 5. Influence of mechanosensitive channels on the release of 5-hydroxyectoine and 5-hydroxyhomoectoine. The *E. coli* strains FRAG1 (wild-type), MJF641 (FRAG1 *mscL mscK mscS mscM*) and LC15 (*otsA1::Tn10*), that contained either the empty vector pASK-IBA3 (control), or the *ectD*-expression plasmid pMP41 (*ectD* gene from *P. stutzeri* A1501), were grown in the presence of **(A)** 5 mM homoectoine or **(B)** 5 mM ectoine. The cultures were grown in baffled flasks containing 10 ml of MMA with 0.4 M NaCl. They were incubated for 24 hours after induction of enhanced *ectD* transcription from the TetR-controlled *tet* promoter with the synthetic inducer AHT. Ectoines were quantified in the supernatants using HPCL analysis. The shown data represent the means and standard deviations of at least four independently grown cultures.

A

181105_LC_007_Sb_181107162223

11/7/2018 4:22:23 PM

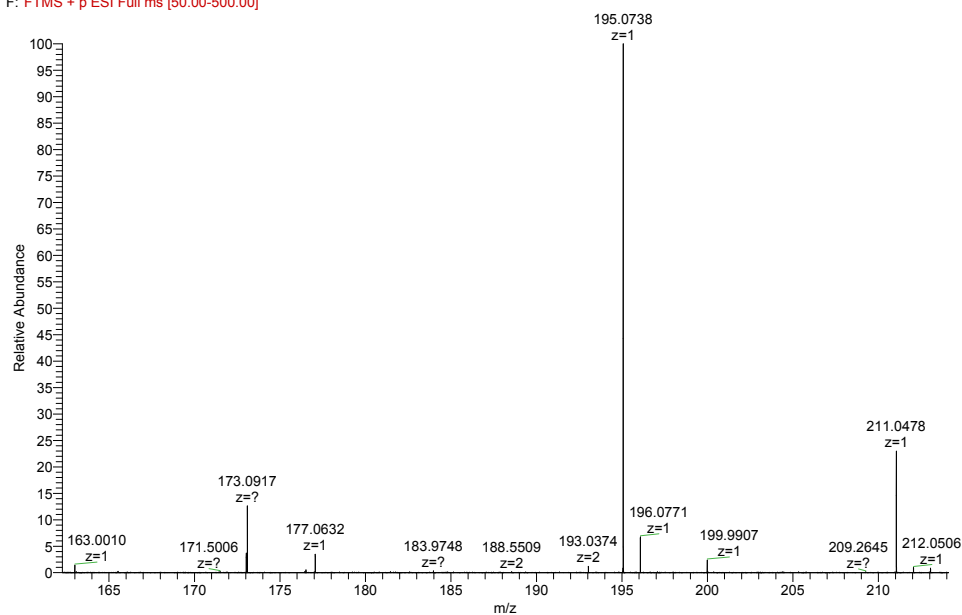
181105_LC_007_Sb_181107162223 #717-742 RT: 5.66-5.84 AV: 13 SM: 7B NL: 1.23E5
 F: FTMS + p ESI Full ms [50.00-500.00]

**B**

O:\2018\...181105_LC_008_Sb_gradient

11/7/2018 8:35:10 PM

181105_LC_008_Sb_gradient #1214-1253 RT: 11.89-12.18 AV: 20 SM: 7B NL: 1.59E5
 F: FTMS + p ESI Full ms [50.00-500.00]



Supplementary Figure 6. Mass spectra of **(A)** homoectoine and **(B)** 5-hydroxyhomoectoine detected in the supernatant of an *E. coli* LC15 (*otsA::Tn10*) cell factory harboring either the empty vector **(A)** pASK-IBA3 or **(B)** expressing the (*Ps*)EctD enzyme from the plasmid pMP41 (*ectD* gene from *P. stutzeri* A1501). The calculated theoretical molecular mass of homoectoine is 157.0972 g/mol and 173.0921 g/mol for 5-hydroxyhomoectoine.

Supplemental information – NMR data

(S)-2-methyl-4,5,6,7-tetrahydro-1H-1,3-diazepine-4-carboxylic acid (homoectoine)

¹H-NMR (D₂O, 500.13 MHz) d = 1.98-2.03 (2H, m, 6-H), 2.21 (1H, ddd, J=6.02, 6.21, 8.85 Hz, 5-H_a), 2.25 (3H, s, 8-H), 2.27 (1H, ddd, J=3.39, 7.53, 14.68 Hz, 5-H_b), 3.43 (1H, ddd, J=5.37, 5.18, 14.81 Hz, 7-H_a), 3.63 (1H, ddd, J=6.37, 7.56, 14.09 Hz, 7-H_b), 4.39 (1H, dd, J=3.90, 8.76 Hz, 4-H).

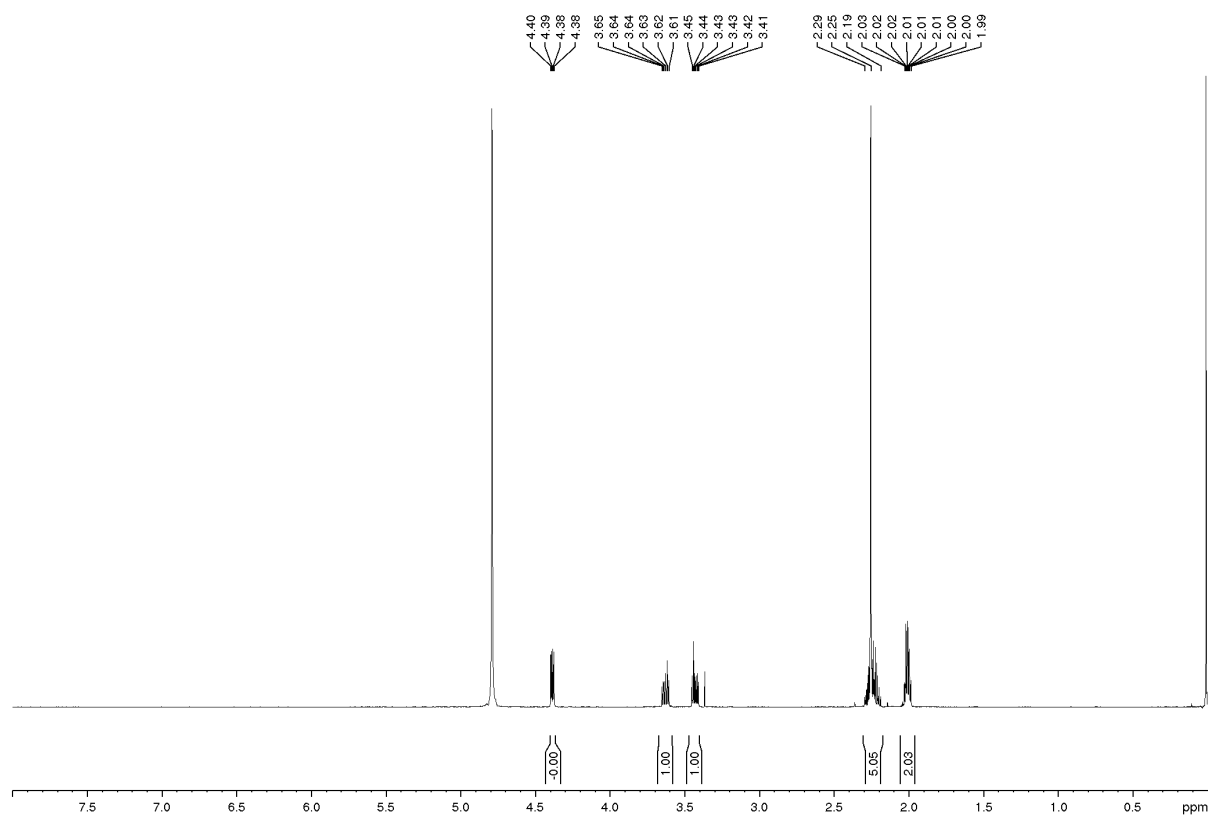
¹³C (75.49 MHz) d = 20.6 (C8), 24.5 (C6), 29.7 (C5), 43.4 (C7), 58.8 (C4), 164.9 (C2), 176.8 (COO⁻).

(4S,5S)-5-hydroxy-2-methyl-4,5,6,7-tetrahydro-1H-1,3-diazepine-4-carboxylic acid (5-hydroxy-homoectoine)

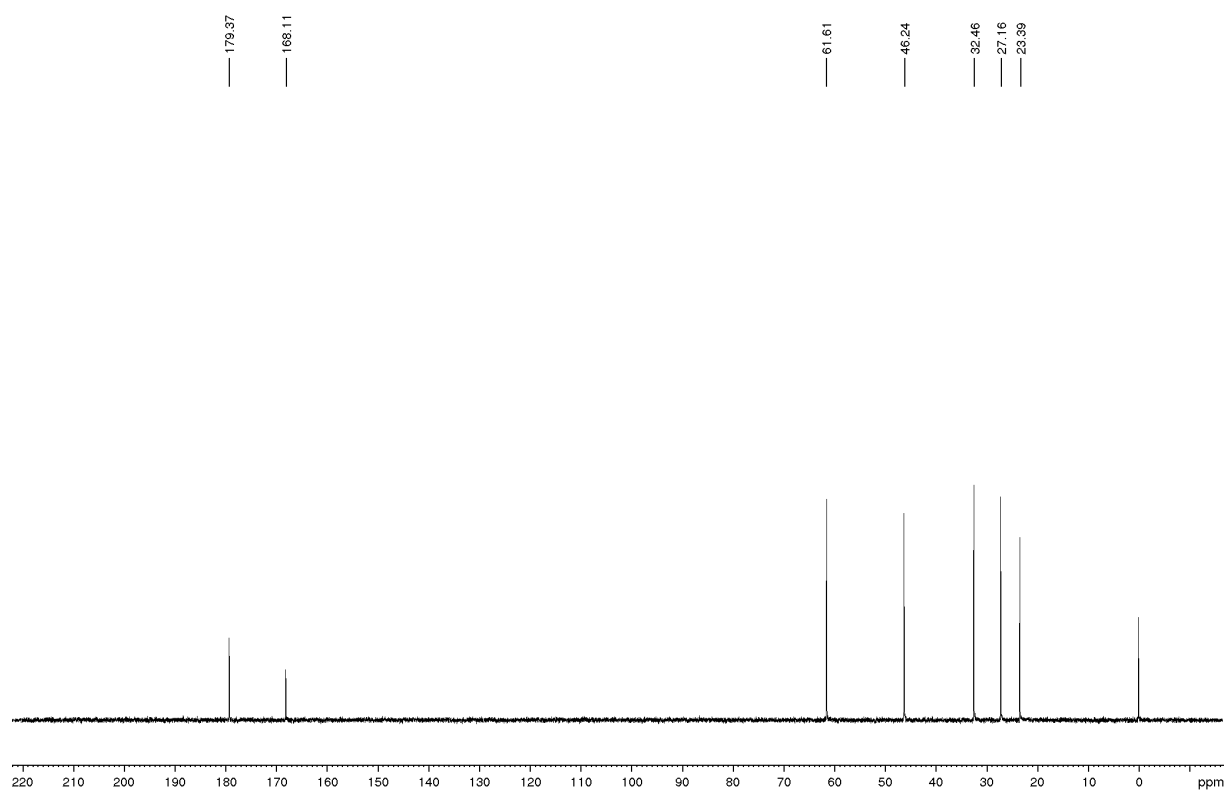
¹H-NMR (H₂O, 600.23 MHz) d = 2.08 (1H, dddd, J=2.85, 4.61, 8.24, 15.80 Hz, 6-H_a), 2.29 (3H, s, 8-H), 2.32 (1H, dddd, J=2.78, 5.83, 9.75, 15.73 Hz, 6-H_b), 3.46 (1H, ddd, J=2.70, 8.46, 15.19 Hz, 7-H_a), 3.59 (1H, ddd, J=2.60, 9.77, 14.99 Hz, 7-H_b), 4.26 (1H, d, J=5.46 Hz, 4-H), 4.51 (1H, dt, J=5.46, 8.24 Hz, 5-H).

¹³C (75.49 MHz) d = 174.4 (COO⁻), 166.0 (C2), 68.7 (C5), 64.1 (C4), 39.0 (C7), 31.9 (C6), 20.3 (C8).

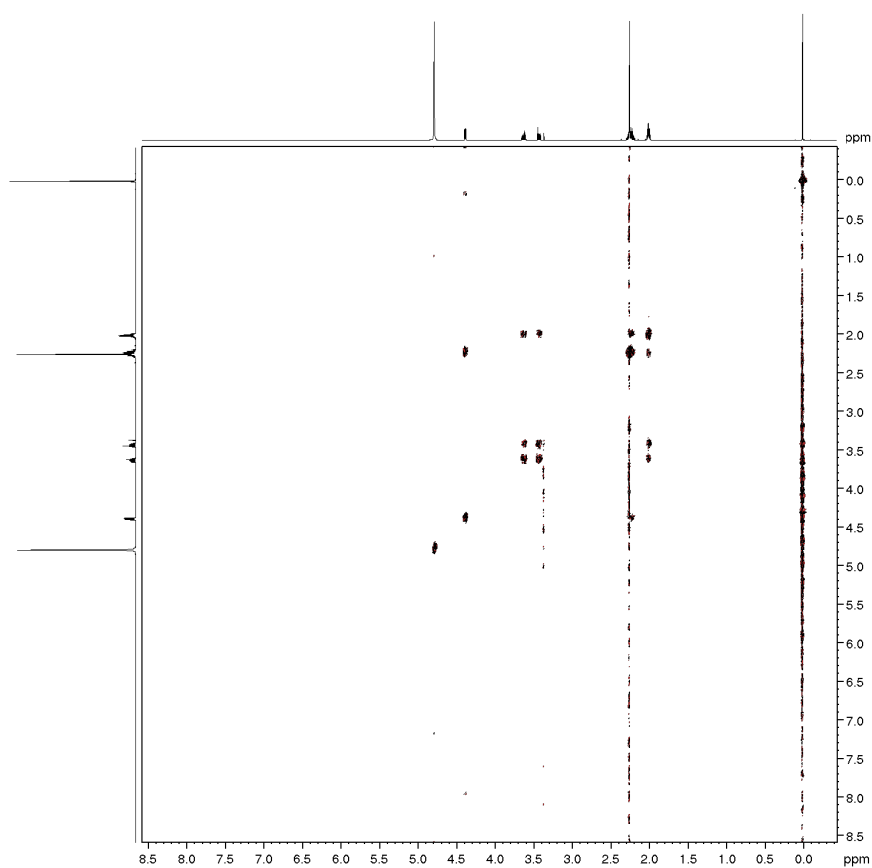
^1H , 500 MHz; Standard homoectoine



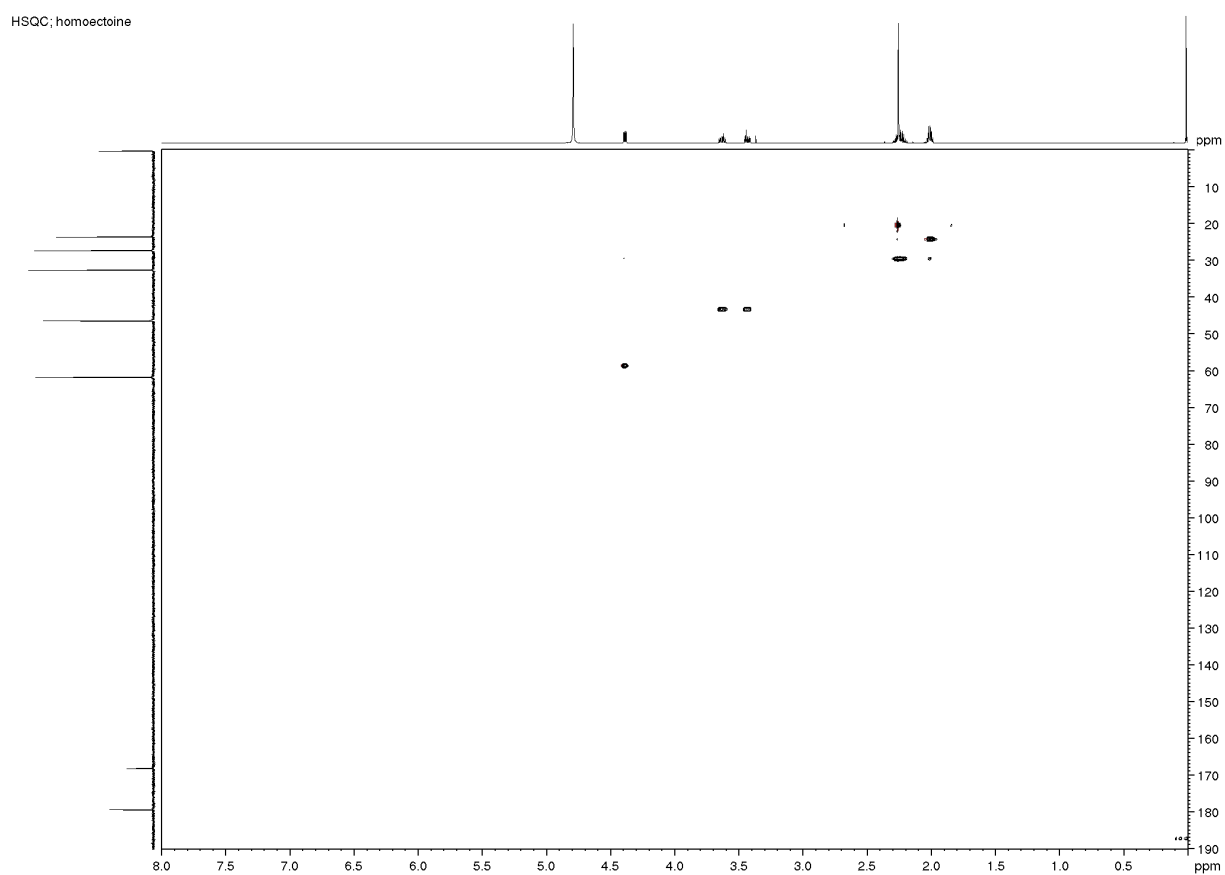
Supplementary Figure 7. ^1H NMR spectrum of homoectoine.



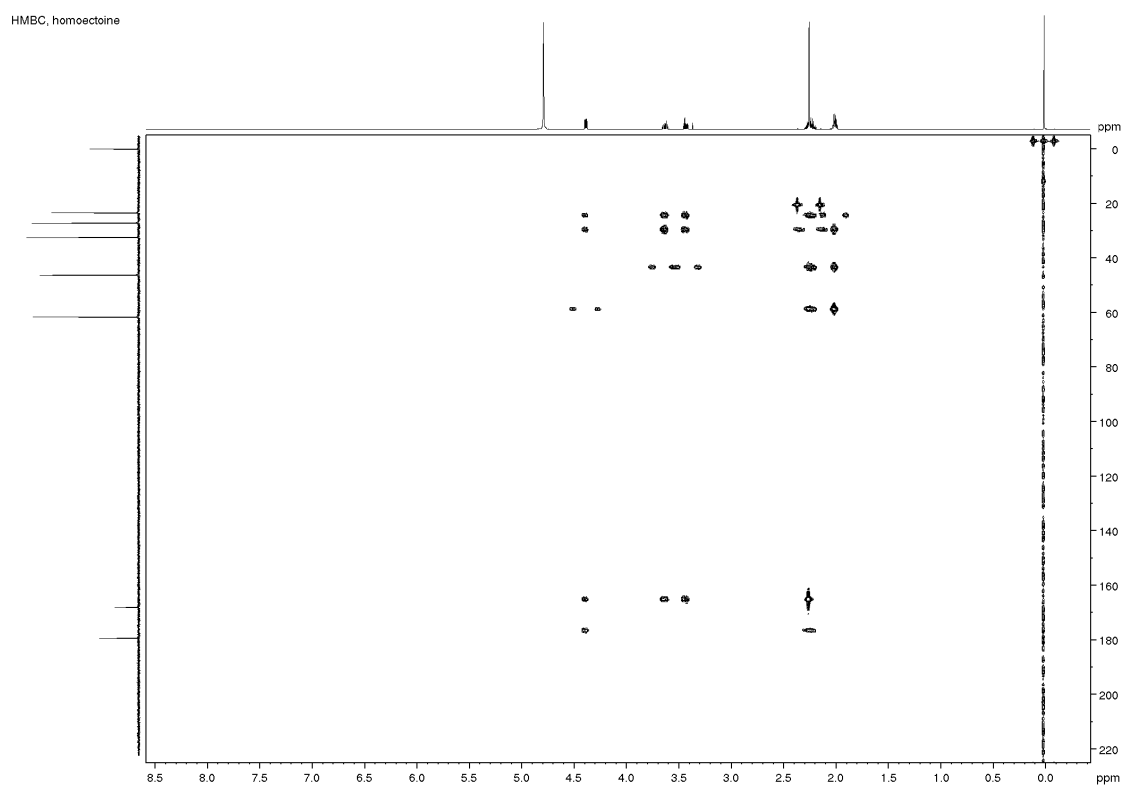
Supplementary Figure 8. ^{13}C NMR spectrum of homoectoine.



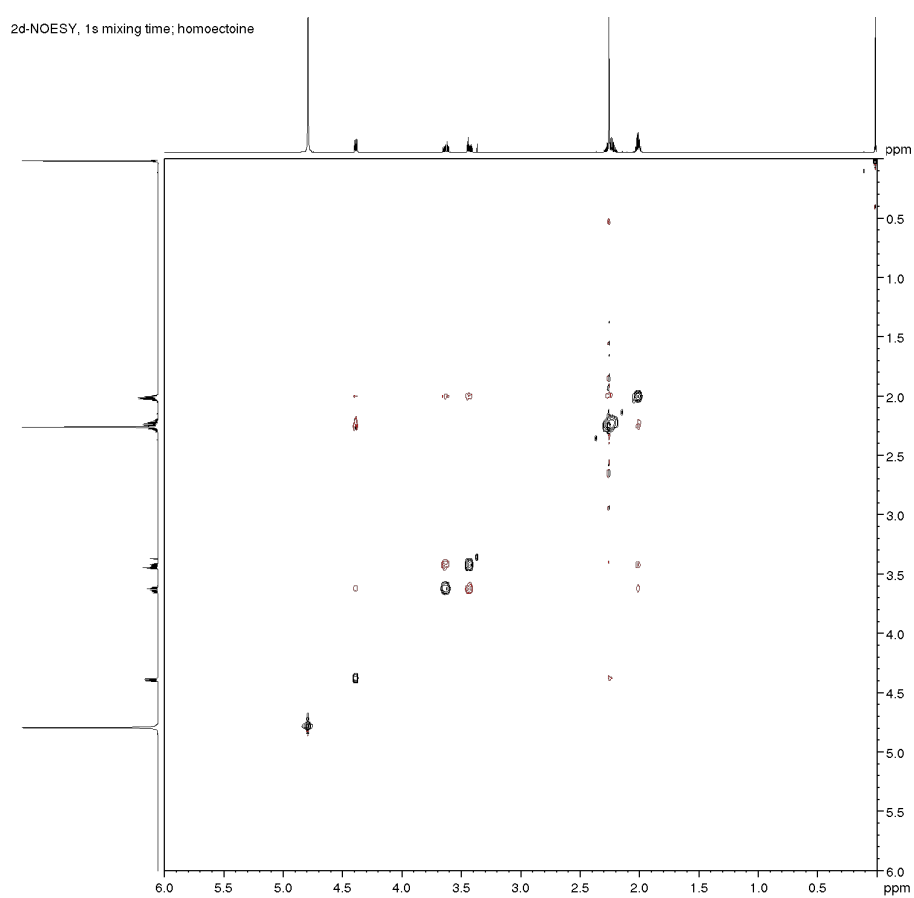
Supplementary Figure 9. COSY spectrum of homoectoine.



Supplementary Figure 10. HSQC spectrum of homoectoine.

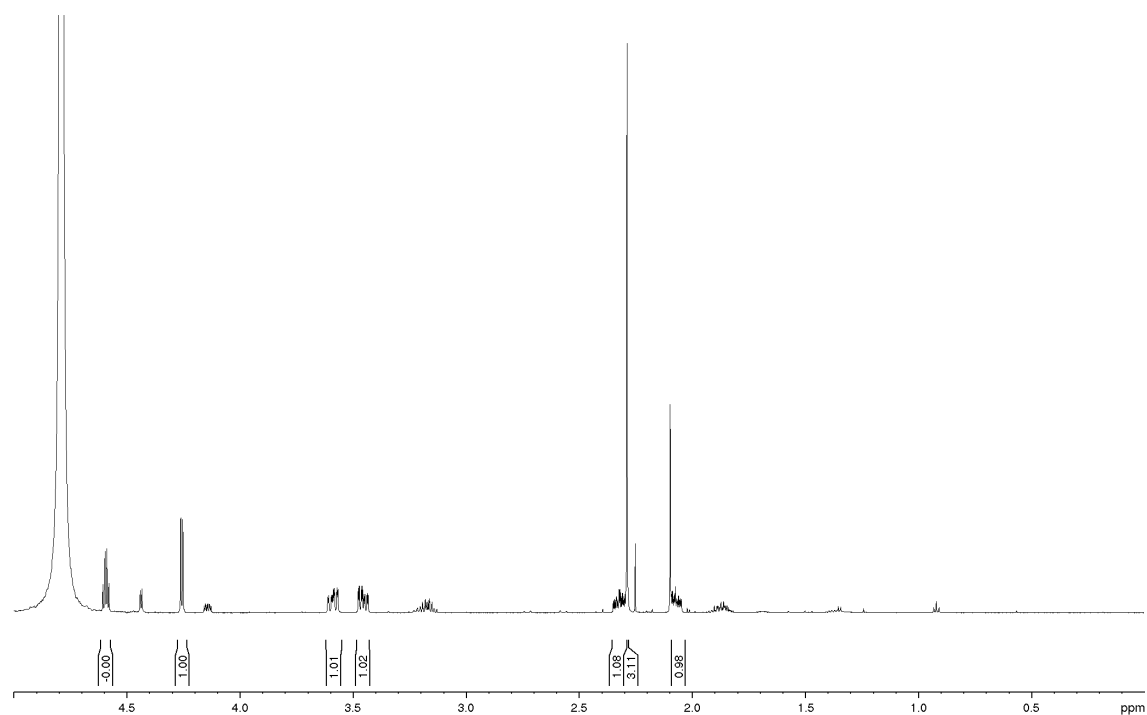


Supplementary Figure 11. HMBC spectrum of homoectoine.



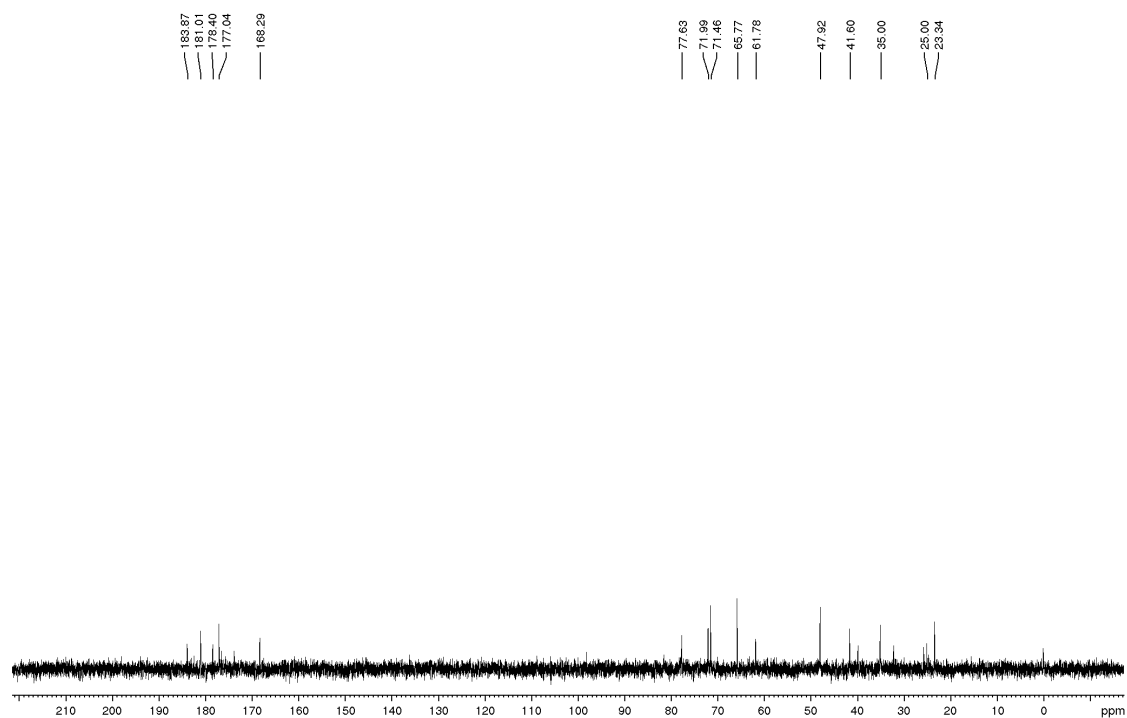
Supplementary Figure 12. NOESY spectrum of homoectoine.

^1H , 600 MHz, H_2O ; 5-hydroxy-homoectoine

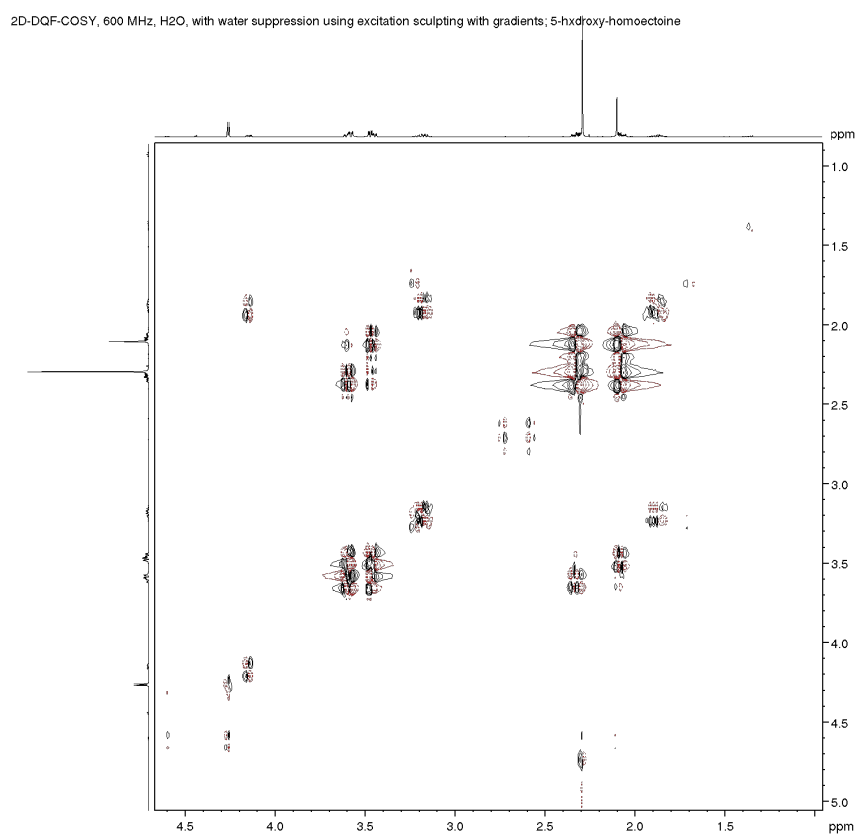


Supplementary Figure 13. ^1H NMR spectrum of 5-hydroxyhomoectoine.

^{13}C , 75.49 MHz, D₂O; 5-hydroxy-homoectoine

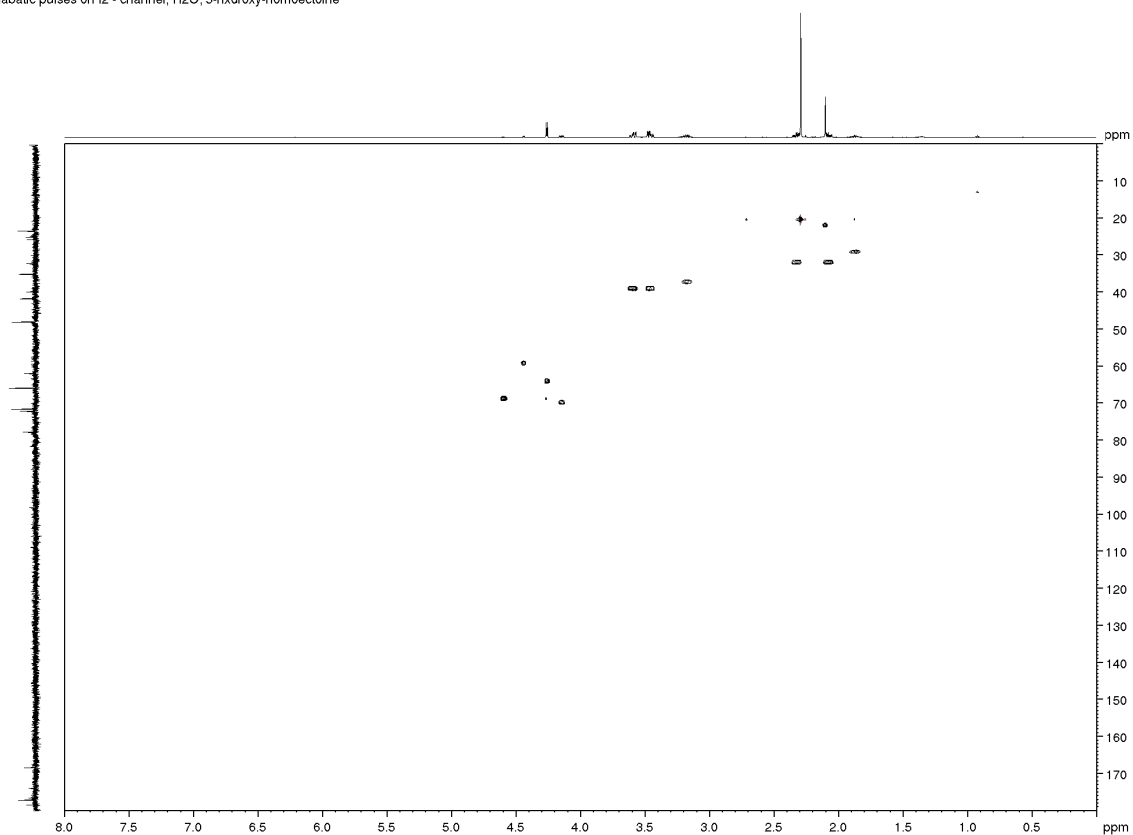


Supplementary Figure 14. ^{13}C NMR spectrum of 5-hydroxyhomoectoine.

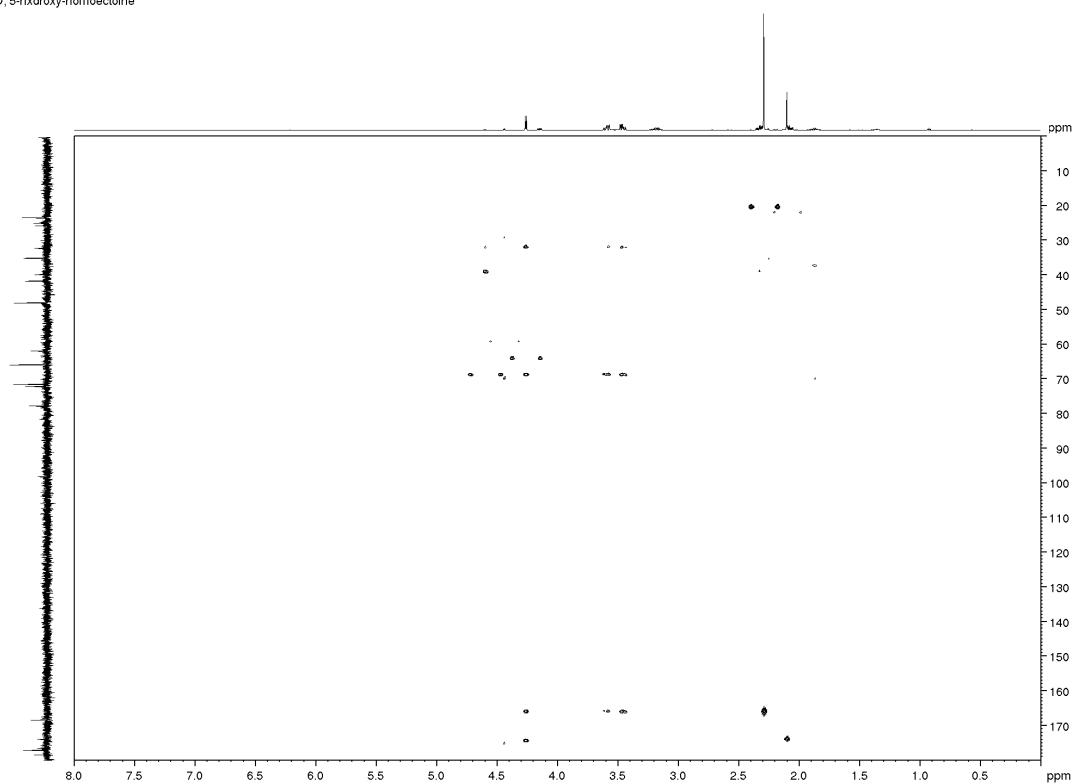


Supplementary Figure 15. COSY spectrum of 5-hydroxyhomoectoine.

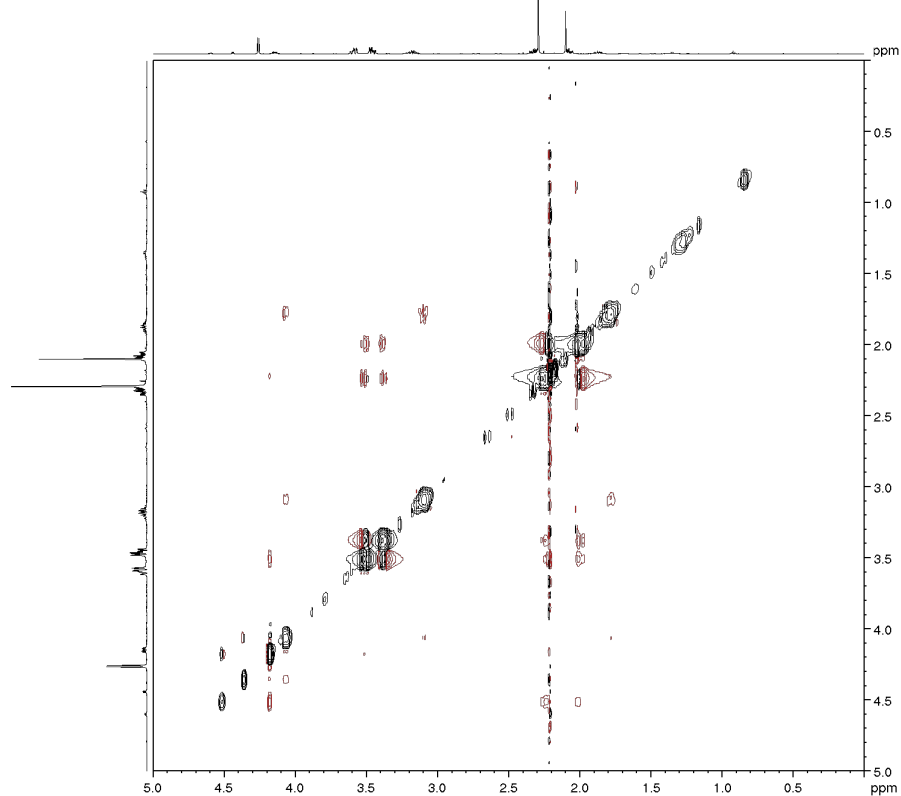
HSQC with adiabatic pulses on f2 - channel, H₂O; 5-hydroxy-homoectoine



Supplementary Figure 16. HSQC spectrum of 5-hydroxyhomoectoine.

HMBC, H₂O; 5-hydroxy-homoectoine**Supplementary Figure 17.** HMBC spectrum of 5-hydroxyhomoectoine.

2D-NOESY, 600 MHz, H₂O, with water suppression using excitation sculpting with gradients, 5-hydroxy-homoectoine
mixing time: 1 s



Supplementary Figure 18. NOESY spectrum of 5-hydroxyhomoectoine.



Supplementary Figure 19. Protein sequence alignment of the EctD proteins from *Sphingopyxis alaskensis* (WP_011543221.1), *Acidiphilum cryptum* (WP_012040480.1), *Paenibacillus lautus* (WP_015737572.1), *Halomonas elongata* (WP_013333764.1), *Streptomyces coelicolor* (NP_626134.1), *Pseudomonas stutzeri* (WP_011911424.1), *Halobacillus halophilus* (WP_014643639.1), *Nitrosopumilus maritimus* (WP_012215726.1), *Chromohalobacter salexigens* (WP_011505850.1; WP_011508293.1), *Alkalilimicola ehrlichii* (WP_011628142.1), *Streptomyces chrysomallus* (WP_030590139.1) and *Virgibacillus salexigens* (AAAY29689.1) was performed with SnapGene® software (GSL Biotech; snapgene.com). The EctD signature sequence and residues involved in the binding of the reaction product (5-hydroxyectoine) (green), the co-factor 2-oxoglutarate (red) or the iron atom (blue) are highlighted (Reuter et al., 2010; Höppner et al., 2014).

References

- Baba, T., Ara, T., Hasegawa, M., Takai, Y., Okumura, Y., Baba, M., et al. (2006). Construction of *Escherichia coli* K-12 in-frame, single-gene knockout mutants: the Keio collection. *Mol Syst Biol* 2, 2006 0008. doi: 10.1038/msb4100050.
- Blattner, F.R., Plunkett, G., 3rd, Bloch, C.A., Perna, N.T., Burland, V., Riley, M., et al. (1997). The complete genome sequence of *Escherichia coli* K-12. *Science* 277(5331), 1453-1462. doi: 10.1126/science.277.5331.1453.
- Edwards, M.D., Black, S., Rasmussen, T., Rasmussen, A., Stokes, N.R., Stephen, T.L., et al. (2012). Characterization of three novel mechanosensitive channel activities in *Escherichia coli*. *Channels (Austin)* 6(4), 272-281. doi: 10.4161/chan.20998.
- Epstein, W., and Kim, B.S. (1971). Potassium transport loci in *Escherichia coli* K-12. *J Bacteriol* 108(2), 639-644.
- Haardt, M., Kempf, B., Faatz, E., and Bremer, E. (1995). The osmoprotectant proline betaine is a major substrate for the binding-protein-dependent transport system ProU of *Escherichia coli* K-12. *Mol Gen Genet* 246(6), 783-786.
- Höppner, A., Widderich, N., Lenders, M., Bremer, E., and Smits, S.H.J. (2014). Crystal structure of the ectoine hydroxylase, a snapshot of the active site. *J Biol Chem* 289(43), 29570-29583. doi: 10.1074/Jbc.M114.576769.
- Kuhlmann, A.U., and Bremer, E. (2002). Osmotically regulated synthesis of the compatible solute ectoine in *Bacillus pasteurii* and related *Bacillus* spp. *Appl Environ Microbiol* 68(2), 772-783.
- Reuter, K., Pittelkow, M., Bursy, J., Heine, A., Craan, T., and Bremer, E. (2010). Synthesis of 5-hydroxyectoine from ectoine: crystal structure of the non-heme iron(II) and 2-oxoglutarate-dependent dioxygenase EctD. *PLoS one* 5(5), e10647. doi: 10.1371/journal.pone.0010647.
- Strom, A.R., and Kaasen, I. (1993). Trehalose metabolism in *Escherichia coli*: stress protection and stress regulation of gene expression. *Mol Microbiol* 8(2), 205-210.
- Studier, F.W., Rosenberg, A.H., Dunn, J.J., and Dubendorff, J.W. (1990). Use of T7 RNA polymerase to direct expression of cloned genes. *Methods Enzymol* 185, 60-89.
- Widderich, N., Höppner, A., Pittelkow, M., Heider, J., Smits, S.H., and Bremer, E. (2014). Biochemical properties of ectoine hydroxylases from extremophiles and their wider taxonomic distribution among microorganisms. *PLoS One* 9(4), e93809. doi: 10.1371/journal.pone.0093809.

5.2.6. *Draft manuscript* In depth analysis of importers, exporters and mechanosensitive channels associated with ectoine biosynthetic gene clusters

Czech L, Smits SHJ, Bremer E. In depth analysis of importers, exporters and mechanosensitive channels associated with ectoine biosynthetic gene clusters. *manuscript in preparation*.

In the following, the draft manuscript with the title “In depth analysis of importers, exporters and mechanosensitive channels associated with ectoine biosynthetic gene clusters” is attached. For this manuscript, I performed all experiments and bioinformatical analysis except of modeling and docking studies, which were conducted by S. H. J. Smits. I analyzed all data, prepared all figures and wrote this draft manuscript.

In depth analysis of importers, exporters and mechanosensitive channels associated with ectoine biosynthetic gene clusters

Laura Czech¹, Sander Smits^{2,3} and Erhard Bremer^{1,4}

¹Laboratory for Microbiology, Department of Biology, Philipps-University Marburg, Marburg, Germany

²Center for Structural Studies, Heinrich-Heine University Düsseldorf, Düsseldorf, Germany

³Institute of Biochemistry, Heinrich-Heine University Düsseldorf, Düsseldorf, Germany

⁴SYNMIKRO Research Center, Philipps-University Marburg, Marburg, Germany

Running title: New insights into import and export of ectoines

Abstract

Osmotic stress is a ubiquitous environmental cue that essentially all free-living microorganisms face. The compatible solutes ectoine and 5-hydroxyectoine can be synthesized or imported by members of all domains of life, to outbalance the osmotic gradient under high salinity conditions. Here, we show through a comprehensive bioinformatical analysis that a substantial number of bacterial and archaeal ectoine producers encode putative transporters in the direct gene neighborhood of the ectoine biosynthetic genes. Using the *ect* gene clusters of two α -proteobacteria, *Hyphomonas neptunium* and *Novosphingobium* sp. LH128, as examples, we analyzed the newly found transporters regarding their physiological function and substrate specificity through osmostress protection assays, modeling and mutant analysis. We identified an MFS-type importer specific for ectoines, a broad substrate-range SSS-type importer and a functional MscS-type mechanosensitive channel within the transcriptional units of the studied *ect* gene clusters. Moreover, our data suggest for the first time that an ectoine-specific MFS-type efflux system is co-transcribed with the *ect* genes.

Keywords: ectoine, transport, import, efflux, export, mechanosensitive channel

Introduction

Presumably, the most important mechanism behind the success of bacteria is their flexibility to adapt to a multitude of different environmental stresses. One of these harsh and ubiquitous stress conditions is the fluctuation of the external water availability and thereby changing osmotic pressure. An increase in the external salinity results in the outflow of water across the cytoplasmic membrane leading to a reduced intracellular turgor [1]. Bacterial cells that employ the *salt-out* mechanism counteract this loss of water by the amassment of so called compatible solutes - low molecular weight, zwitter-ionic compounds, such as sugars, or amino acids and their derivatives [2–5]. Ectoines are among the most important compatible solutes, since they are used by all domains of life [6–11]. A large number of bacteria belonging to ten different phyla were predicted to produce and accumulate ectoines [6]. Beyond that also a few *Archaea* and halophilic *Eukarya* possess the ability to synthesize these compounds and might have acquired the underlying genes through horizontal gene transfer [7–13]. The genes encoding the core enzymes for the production of ectoine (*ectABC*) and its hydroxylated derivative 5-hydroxyectoine (*ectD*) are often genetically organized as one transcriptional unit controlled by an osmotically regulated promoter [7, 14–16]. Within the past years the enzymes required for the production of ectoine [(L-2,4-diaminobutyrate aminotransferase (EctB); L-2,4-diaminobutyrate acetyltransferase (EctA); ectoine synthase (EctC)] and 5-hydroxyectoine [ectoine hydroxylase (EctD)] have been studied on a biochemical and partially also on a structural (in case of EctA, EctC and EctD) level (Richter *et al.*, *submitted manuscript*) [6, 17–22]. Furthermore, many organisms encode the specialized feedback-resistant aspartokinase Ask_{ect}, which is inhibited by L-threonine but not L-lysine [14]. This enzyme secures the sufficient supply of the precursor molecule and central metabolic hub L-aspartate- β -semialdehyde resulting from the ATP-dependent phosphorylation of L-aspartate [14]. Ectoine is not only an effective osmoprotectant for microorganisms, but it also has protective properties for proteins, DNA, membranes and stabilizes whole cells [23–29]. It therefore finds applications in the biotechnological, medical and cosmetic industry and is produced on an industrial scale by a genetically engineered strain of the halophilic microorganism *Halomonas elongata* [30, 31]. For additional information, detailed review articles have been published [6, 30, 31].

The accumulation of compatible solutes cannot only be accomplished through their *de novo* synthesis; they can also be taken up by ectoine producing and non-producing cells via specialized transport systems - a mechanism that is much less cost-intensive compared to their *de novo* synthesis [15, 32–35]. In numbers, the production of one ectoine molecule is assumed to require between 40 and 55 ATP molecules while for instance the uptake through an ATP-fueled transporter only costs two ATP molecules [36]. High affinity transporters and transporters with a broad substrate range enable microorganisms to benefit from compatible solutes that are available in their direct environment. Compatible solutes are present in the natural habitats of microorganisms, since producer cells that can be other bacteria but also higher organisms such as diatoms or flagellates secrete them. They can be released by the transient opening of mechanosensitive channels upon osmotic down-shocks, through their active secretion, by rotting plant material, or lysed bacterial cells attacked by phages or toxins and through the

predatory activity of microorganisms and eukaryotic cells [37–39]. To date, uptake systems for ectoines originating from four different families have been identified: (I) ABC-, (II) BCCT-, (III) MFS- and (IV) TRAP-type transporters [15, 35, 40–43]. First, ABC-type transporters (ATP-Binding Cassette) are dependent on ATP- and a specific substrate binding protein. They have previously been described to transport various compatible solutes in different organisms: the ectoine specific transport system EhuABCD is found in *S. meliloti*, while other broad substrate range ABC-type transporters such as the ProU system from *E. coli*, the OusB system from *E. chrysanthemi*, the OpuC transporter from *B. subtilis* and the ProU system from *V. anguillarum* have also been shown to accept ectoine/5-hydroxyectoine as their substrates [6, 15, 33, 35, 42, 44, 45]. Second, BCCT-type (Betaine-Choline-Carnitine-Transport) transport systems are energized either by proton or sodium gradients and many members of this large family are known to import compatible solutes. Examples are the OpuD transporter from *B. subtilis*, EctT from *V. pantothenicus*, EctM from *M. halophilus*, EctP and LcoP from *C. glutamicum* [33, 46–51]. Third, the broad substrate range transporters ProP from *E. coli* and OusA from *E. chrysanthemi* belonging to the Major Facilitator Superfamily (MFS) of transporters are also able to transport ectoines. This transporter family is dependent on the proton motif force [35, 44, 52]. The last group of ectoine transporters belongs to the periplasmic binding protein-dependent TRAP-transporter family (TRipartite ATP independent Periplasmic transporter), which are energized by proton or sodium gradients. The best characterized ectoine/hydroxyectoine specific transporters of this family are the TeaABC and UehABC system from *H. elongata* and *R. pomeroyi* DSS-3 [15, 43, 53, 54]. While the Ehu system is involved in the uptake of ectoines for their catabolic utilization as nutrients [15, 54], the Tea transporter imports ectoines in response to osmotic stress [43, 53].

Efflux and secretion of ectoines and other intracellular solutes can occur during an osmotic down-shock through the opening of so-called mechanosensitive channels. These channels act as emergency release valves to counteract the increasing turgor in consequence of the massive inflow of water when the internal solute pool is higher than the external salinity [38]. Mechanosensitive channels are grouped according to the pore size of the opened channel. For example, *E. coli* cells possess mini (MscM), small (MscS), and large (MscL) mechanosensitive channels. Beyond that, channels with substrate specificities haven been identified, such as the potassium-dependent MscK channel from *E. coli* and the glutamate-specific channel MscCG from *C. glutamicum* [55–58].

Moreover, the secretion of ectoines under steady state osmotic conditions that is not based on the activity of mechanosensitive channels has been demonstrated in different organisms, such as in *E. coli* when the internal solute pool is chased with another compatible solute, glycine betaine [35], or in *H. elongata*, lacking the genes for the ectoine-specific import system TeaABC [43]. One could speculate about different mechanisms for the continuous secretion of compatible solutes; one rather improbable idea is that they might diffuse across the semipermeable membrane. More likely is the involvement of secondary transporters as it has been demonstrated for the secretion of glycine betaine in *E. coli* and *Lactobacillus plantarum* [59–61]. Nevertheless, the exact mechanism or the transport proteins involved in the release of ectoine under stable osmotic conditions have not been identified yet.

Within this study, we focused on an in-depth bioinformatic analysis of ectoine biosynthesis clusters genetically associated with different transporters and we investigated two newly found *ect* gene clusters present in the two α -proteobacteria *Hyphomonas neptunium* [62, 63] and *Novosphingobium* sp. LH128 [64]. Both ectoine gene clusters harbor an interesting set of different transporters, which are co-transcribed with the ectoine biosynthetic genes and are osmotically induced. Their substrate specificity and physiological importance was studied through osmoprotection experiments, *in silico* modeling and docking analysis, and the introduction of site-directed mutations. For the first time, we describe a highly specific MFS-type importer for ectoines (EctU) and a broad substrate range uptake system of the Sodium Solute Superfamily (SSS) (EctI). Furthermore, we identified a functional MscS-like mechanosensitive channel in the same transcription unit with the *ect* genes from *Novosphingobium* sp. LH128 and our data suggest the presence of an MFS-type efflux protein (EctE) in *Novosphingobium* sp. LH128 that specifically exports ectoines.

Results

Bioinformatic analysis of ectoine biosynthetic gene clusters harboring different sets of transporters. In a previous study we inspected 6688 genomes (6427 *Bacteria*, 261 *Archaea*) of all fully sequenced members of the *Bacteria* and *Archaea* deposited in the database of the Joint Genome Institute (JGI) of the US Department of Energy (<http://jgi.doe.gov/>) for the presence of ectoine biosynthetic genes using the amino acid sequence of the ectoine synthase from *P. laetus* [(P_l)EctC] as the search template [6, 65]. In this report, we found 499 bacterial and 11 archaeal genomes that all together harbored 582 potential *ectC* genes for the production of the compatible solutes ectoine and 5-hydroxyectoine [6]. Through detailed inspection of these putative *ect* genes, we found that 144 genomes encode transporters in close vicinity to the ectoine biosynthetic gene clusters. The genetic context of the different types of ectoine gene clusters that are associated with various transporters are shown and classified in examples in Fig. 1, and in detail in Supplementary Fig. S1, and with BLAST results in Supplementary Table 1.

Mostly transporters belonging to six different families have been found in the vicinity of the bioinformatically studied ectoine biosynthetic gene clusters: ABC-; BCCT-; TRAP-; MFS-; and SSS-type transporters, as well as MscS- or MscM-like mechanosensitive channels (Fig.1, Supplementary Fig. S1). The abundance of these transporters and their sequence identities to known transport proteins is summarized in Table 1. Furthermore, 22 putative ectoine gene clusters possessed other transporter types that are only found in minor numbers (Supplementary Table 1).

In this study we decided to focus on two α -proteobacteria, *H. neptunium* [62] and *Novosphingobium* sp. LH128 [64], that both possess novel genetic contexts in the vicinity of the core genes for ectoine biosynthesis. Besides *ectABC*, they also possess the gene for the ectoine hydroxylase (*ectD*), and for the specialized aspartokinase (*ask_ect*). In addition to these central genes for ectoine/5-hydroxyectoine synthesis, both organisms encode the MarR-type regulator EctR upstream of and divergently transcribed from the *ectA* coding region, and a set of different transporters downstream of the *ask_ect* gene [6, 66] (Fig. 2a, d).

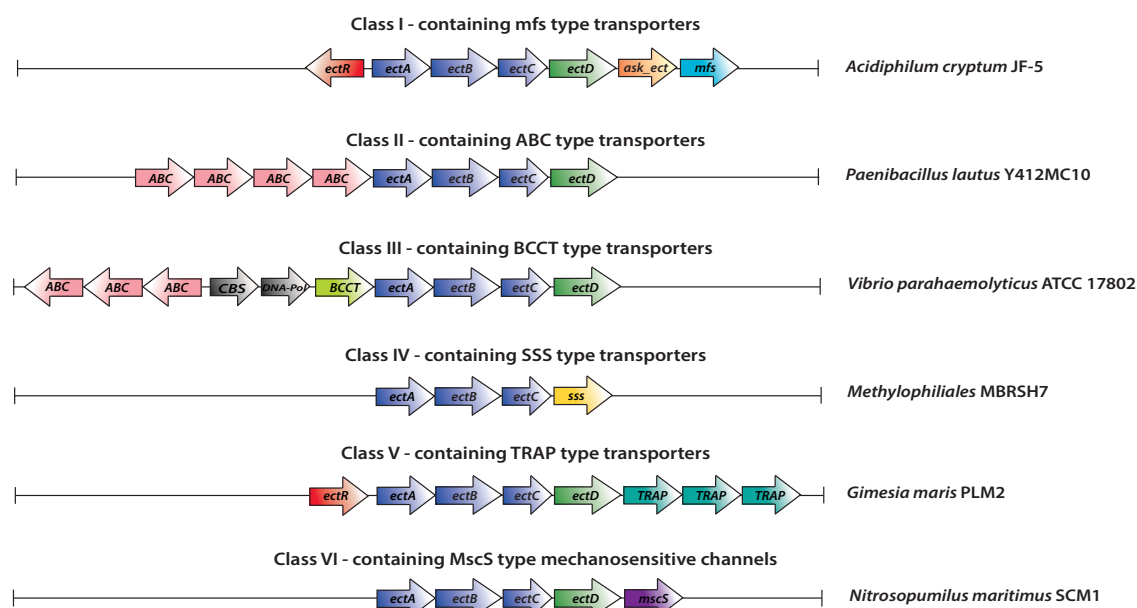


Fig. 1 Overview and classification of ectoine gene clusters associated with different transporters.

Bioinformatic analysis of the two transporter types present downstream of the *ect* genes in *H. neptunium* revealed that the first transporter belongs to the Major Facilitator Superfamily (MFS) and exhibits a sequence similarity of 34.8% to the multidrug exporter MdfA from *E. coli* and 27.6% to the putative exporter YcaD from *E. coli* (Fig. 2d, Supplementary Table 1) [67–69]. We therefor named this putative transporter EctE for ectoine export. The second transporter belongs to the Sodium Solute Superfamily (SSS) of transporters and possesses 24.6% sequence identity to SglT from *Vibrio parahaemolyticus*, and 29% to OpuE from *B. subtilis* hinting that it might serve as an uptake system for compatible solutes (Fig. 2d, Supplementary Table 1) [70–74]. This transporter was named EctI for ectoine import; *ectI* is followed by a 296 bp intergenic region, and by a putative RND family efflux system. In the neighborhood of the ectoine gene cluster of *Novosphingobium* sp. LH128 we also identified an open reading frame encoding a putative MFS-type exporter EctE with a sequence identity of 26.1% to the multidrug exporter MdfA from *E. coli* and 27.2% to the putative exporter YcaD from *E. coli* (Fig. 2a, Supplementary Table 1) [67–69]. In contrast to the SSS-type transport system EctI found in *H. neptunium*, *Novosphingobium* sp. LH128 encodes a second MFS-type transporter with sequence similarities of 42.1% to the osmolyte transporter ProP from *E. coli* and 44.4% to OusA from *Erwinia chrysanthemi* [40, 44, 52, 75]. We named this putative uptake system EctU for ectoine uptake (Fig. 2a, Supplementary Table 1). The next open reading frame is localized 110 bp downstream of the EctU transporter and is annotated as an MscS-like/MscM (mini) mechanosensitive channel with 22.7% sequence identity to MscS from *E. coli* and 54.2% sequence identity to YbdG (MscM) from *E. coli* (Fig. 2a, Supplementary Table 1) [56, 76–79]. A hypothetical protein, an uncharacterized membrane domain-containing protein and a potential citrate transporter with 22.2% sequence similarity to NadC from *Vibrio cholera*, are located downstream of the *mscS* gene (Fig. 2a) [80].

Table 1 Summary, classification and sequence comparison of the different transporters found in the vicinity of ectoine biosynthetic gene clusters.

Class	Transporter family	Abundance	related to	Sequence identity [%]	Reference
I	ABC transporter	49 in total			
		28	EhuB	19-38	[54]
		18	ProX	68	[35, 81]
		1	OpuCC	56	[82, 83]
II	BCCT	21	OpuD; BetP	36-42	[83, 84]
III	TRAP transporter	1	TeaA; UehA	39-42	[42, 53]
IV	MFS transporter	86 in total			
		64	ProP/OusA	39-50	[35, 40]
		22	EmrD/MdfA	20-35	[85, 86]
V	SSS transporter	6	OpuE/PutP	26-30	[72, 74, 87]
VI	MscS/MscM	15	MscS/YbdG	12-52	[79, 88]

H. neptunium and *Novosphingobium* sp. LH128 accumulate hydroxyectoine in response to osmotic stress. To test the functionality of the above described ectoine/5-hydroxyectoine biosynthetic gene clusters and explore the salt tolerance of *H. neptunium* and *Novosphingobium* sp. LH128 the cells were cultivated in medium (MB or SMM, respectively) using increasing NaCl concentrations. After 24 h of incubation we measured the growth (OD₅₇₈), harvested cells and extracted the produced ectoines. *H. neptunium* exhibits tolerance to salt concentrations up to 0.9 M NaCl in addition to the 920 mOsm/kg present in the Marine Broth medium (in total 2860 mOsm/kg = 1.58 M) (Fig. 3a). In contrast, *Novosphingobium* sp. LH128 is only able to grow in a restricted range of salinity from 0 M (377 mOsm/kg) to 0.5 M (1340 mOsm/kg) NaCl (Fig. 3b) in the defined Spizizen minimal medium (SMM). HPLC analysis of the cell extracts showed that both organisms only produced 5-hydroxyectoine in response to increasing osmolarity but no ectoine was present in the cells or the amount was below the detection level of the HPLC analysis (Fig. 3c, b). The intracellular accumulation of 5-hydroxyectoine in *H. neptunium* and *Novosphingobium* sp. LH128 increases linearly in response to small increases in the external salinity (Fig. 3c, d).

The core genes for ectoine biosynthesis are co-transcribed with a set of different transporters. The above described, newly found genetic co-localization of these different transporters with the genes for ectoine production, led us to the question whether these transporters are genetically co-transcribed with the ectoine biosynthetic genes, as this might hint to their functional association with ectoine fluxes across the cytoplasmic membrane. The co-transcription of the core ectoine/5-hydroxyectoine biosynthetic genes (*ectABC* or *ectABCD-ask_ect*) has already been studied in a variety of organisms, such as *P. stutzeri*, *M. alcaliphilum*, *V. pantothenicus*, or ‘*Ca. N. maritimus*’ SCM1 [7, 14, 16, 66]. The distance between the end of the *ask_ect* gene and the start of the gene encoding the first hypothetical transporter EctE is 6 bp in *H. neptunium* and 21 bp in *Novosphingobium* sp. LH128 (Fig. 2a, d), suggesting that the *ectE* genes might be co-transcribed with the *ectABCD-ask_ect* gene clusters as well. Furthermore, the coding regions for the

putative importers *ectI* and *ectU* are in both cases overlapping with the preceding *ectE* gene. Overall, the tight genetic organization of the *ectABCD-ask_ect-ectE-ectI* and *ectABCD-ask_ect-ectE-ectU-mscS* gene clusters [Gene IDs of *ectA*: EJU13512.1 (*Novosphingobium* sp. LH128); WP_011646647.1 (*H. neptunium*)] suggests that these genes might belong to the same transcriptional unit.

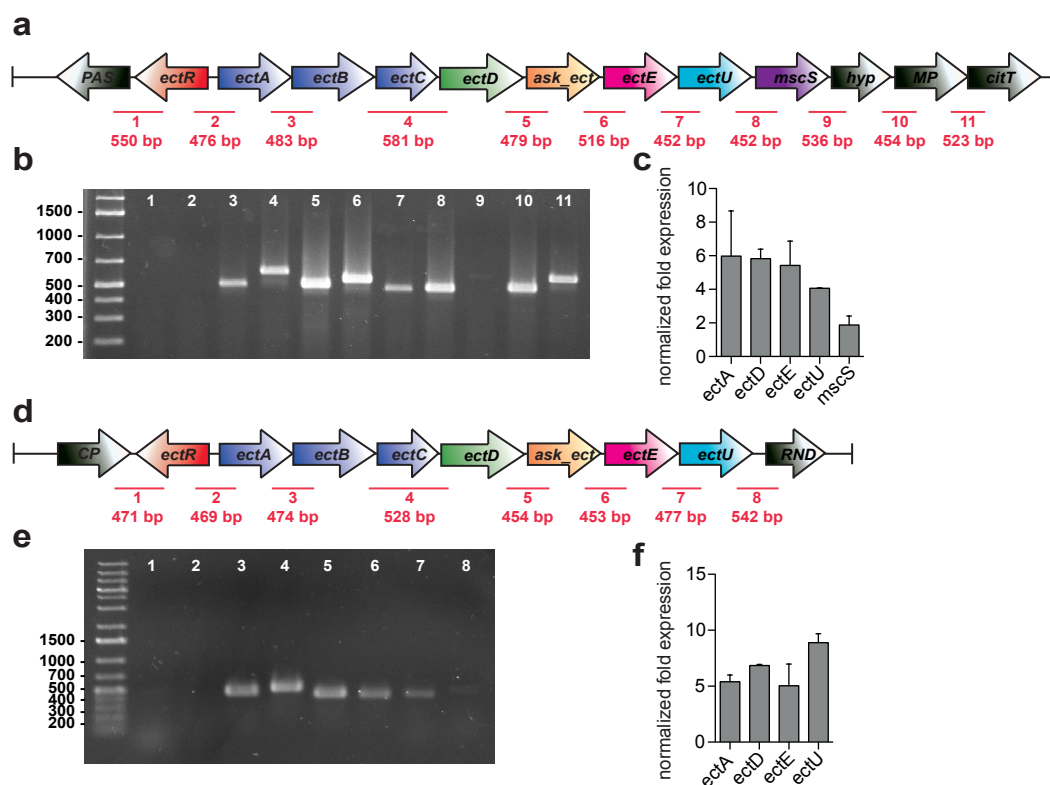


Fig. 2 Transcriptional analysis of the *ect* gene cluster from *Novosphingobium* sp. LH128 and *H. neptunium*. **a, d** Schematic illustration of the *ect* gene clusters from *Novosphingobium* sp. LH128 (**a**) and *H. neptunium* (**d**). The intergenic regions that were amplified during the reverse-transcription PCR (RT-PCR) are indicated in red. **b, e** Agarose gels of the RT-PCR analysing the transcriptional unit of the ectoine gene cluster from *Novosphingobium* sp. LH128 (**b**) and *H. neptunium* (**e**). **c, f** Transcription of the *ectA*, *ectD*, *ectE*, *ectU* and in the case of *Novosphingobium* sp. LH128 *mscS* genes from *Novosphingobium* sp. LH128 (**c**) and *H. neptunium* (**f**) analysed via RT-qPCR. Total RNA was isolated from cells grown in medium without and with the addition of 0.6 M (for *Novosphingobium* sp. LH128) or 0.5 M (for *H. neptunium*) NaCl. The relative expression of each gene under the tested conditions was determined by using the *gyrB* transcript levels in *H. neptunium* and *Novosphingobium* cells grown under optimal or elevated salt concentrations as the standard. Induction values are expressed as the log 2 of the ratio of the value determined for the salt-stressed cells over the value determined for the non-stressed control.

To assess the transcriptional organization of the two reported gene clusters (Fig. 2a, d), we performed a reverse transcription polymerase chain reaction (RT-PCR) analysis using total RNA preparations that were isolated from cells of *H. neptunium* and *Novosphingobium* sp. LH128 grown under increased osmotic stress conditions (0.5 M for *H. neptunium* and 0.3 M NaCl for *Novosphingobium* sp. LH128). The data shown in Fig. 2b and 2e show that the ectoine gene cluster and the genes encoding the different transporters belong to the same transcriptional unit. The co-transcription of a MscS-type mechanosensitive channel with the genes for ectoine biosynthesis has been shown previously for the marine Archaeon ‘*Ca. N. maritimus*’ SCM1 [7]. A genetic co-localization of an putative transport system

together with ectoine biosynthetic genes has until now only been reported in *Paenibacillus lautus*, where an Ehu-type ABC-transporter was found directly upstream of the ectoine biosynthetic genes with an intergenic region of only 23 bp (Richter *et al.*, submitted manuscript). However, a genetic co-localization of ectoine transporters and ectoine degradation genes [6, 15, 42] is already well known.

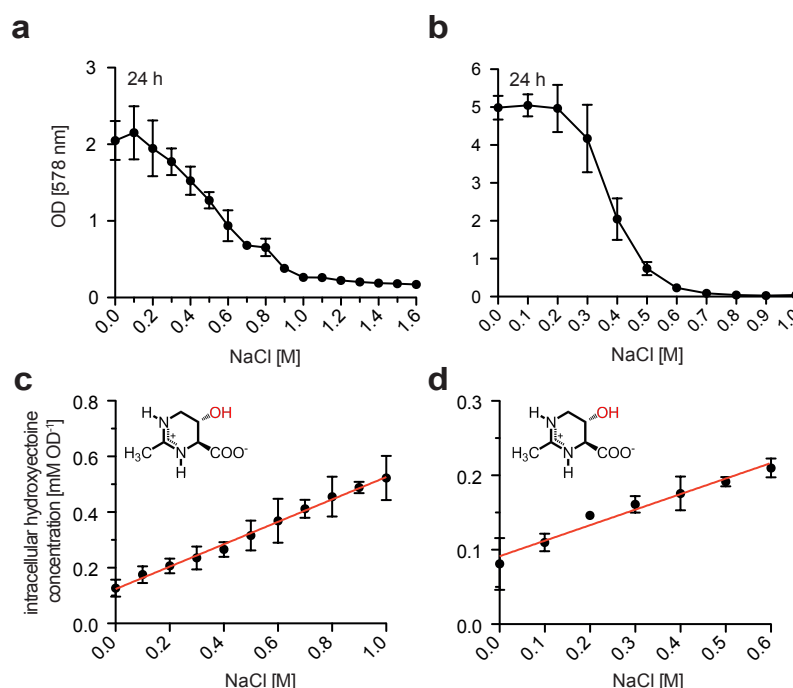


Fig. 3 Ectoine biosynthesis and salt tolerance of *H. neptunium* and *Novosphingobium* sp. LH128. **a, b** Growth yield (OD₅₇₈) of *H. neptunium* (**a**) and *Novosphingobium* sp. LH128 (**b**) cells after 24 h of growth in medium supplemented with increasing NaCl concentrations. **c, d** Intracellular hydroxyectoine content of *H. neptunium* (**c**) and *Novosphingobium* sp. LH128 (**d**) cells grown in medium with increasing NaCl concentrations. Ectoine could not be detected. The data shown represent the mean and standard error mean of at least four biological replicates.

In line with the finely tuned salt-responsive accumulation of ectoines, the expression of the underlying biosynthetic genes is typically up-regulated when cells are confronted with elevated external salt concentrations [6, 7, 34, 89–91]. We performed quantitative real-time PCR to test if the expression of the ectoine biosynthetic genes in *H. neptunium* and *Novosphingobium* sp. LH128 is also increased in response to chronic osmotic stress. *H. neptunium* and *Novosphingobium* sp. LH128 cells were cultivated in medium without and with the addition of 0.5 M and 0.6 M NaCl, respectively, until they reached OD₅₇₈ of 1. Total RNA of these cultures was subsequently isolated and one-step qRT-PCR experiments were conducted in which short fragments in the genes *ectA*, *ectD*, *ectE*, *ectI/ectU* and in case of *Novosphingobium* sp. LH128 also the *mscS* gene were amplified after reverse transcription of the mRNA to cDNA (Fig. 2a, d). Transcripts of the *gyrB* genes of *H. neptunium* (WP_011645581.1) and of *Novosphingobium* (EJU15051.1) were used as a reference to benchmark the *ectA*, *ectD*, *ectE*, *ectI/ectU* and *mscS* transcript amount. The amount of *gyrB* transcripts changed less than two-fold comparing the mRNA levels of salt-stressed cells and non-stressed cells. In contrast, the transcript levels of *ectA*, *ectD*, *ectE* and *ectI* in *H. neptunium* from cells grown with 0.5 M NaCl were 5- to 9.5-fold induced compared to cells grown without additional NaCl (Fig. 2f). This salt-

induction could also be shown for the *ectA*, *ectD*, *ectE* and *ectU* genes from *Novosphingobium* sp. LH128 where the transcript levels changed in average 6-fold, when salt-stressed and non-stressed conditions were compared (Fig. 2c). Surprisingly, the expression level of the gene encoding the MscS-type mechanosensitive channel was only up regulated by 2-fold (Fig. 2c) even though the genes are located on the same mRNA transcript. It is noteworthy that in both cases the transport system showed approximately the same expression levels as the production genes pointing to the importance of these transporters for the physiological adaptation of *Novosphingobium* sp. LH128 and *H. neptunium* to osmotic stress.

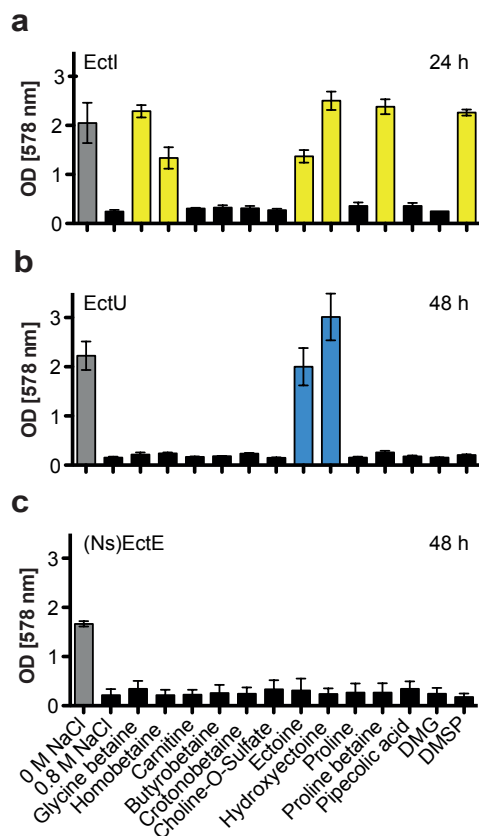


Fig. 4 Heterologous characterization of the substrate specificity of the EctI, EctU, and (Ns)EctE transporters. Growth yield (OD₅₇₈) of *E. coli* MKH13 cells lacking the osmoprotectant uptake systems ProP and ProU and constitutively expressing the EctI importer from *H. neptunium* (a), the EctU transporter from *Novosphingobium* sp. LH128 (b), or the EctE transporter from *Novosphingobium* sp. LH128 (c). The cells were grown for 24 h or 48 h (as indicated) in medium supplemented without or with the addition of 0.8 M NaCl and supplemented with 1 mM of the indicated compatible solute, respectively. The data shown is the mean and standard error mean of at least four biological replicates.

EctI from *H. neptunium* is a broad substrate range transporter for compatible solutes and EctU from *Novosphingobium* sp. LH128 is a specific transporter for ectoines. After the assessment of the salt-responsive expression and the co-translation of the putative transporter genes together with the genes for ectoine/hydroxyectoine biosynthesis, we aimed to identify the substrate specificity of the predicted import systems EctI (*H. neptunium*) and EctU (*Novosphingobium* sp. LH128). Hence, *E. coli* strain MKH13 [92] that is deficient in the broad osmoprotectant uptake systems ProU and ProP was employed in an heterologous osmostress protection experiment, aiming the expression of either EctI (pARO12) or EctU

(pANDA1) from a low-copy number vector (pHSG575) under the control of a constitutive *lac* promoter [93]. *E. coli* MKH13[pARO12] (EctI) or MKH13[pANDA1] (EctU) were propagated in shake flasks and MMA containing 0.8 M NaCl in the absence or presence of different compatible solute (1 mM, respectively) for (in total) 48 h at 37 °C and the OD₅₇₈ was measured after 24, 30 and 48 h of cultivation. The control strain *E. coli* MKH13 harboring the empty vector pHSG575 was not able to grow under any of these conditions, while *E. coli* MKH13 cells expressing EctI (pARO12) were able to grow in presence of the compatible solutes glycine betaine, homobetaine, ectoine, 5-hydroxyectoine, proline betaine and dimethylsulfoniopropionate (DMSP) (Fig. 4a). In contrast, no osmoprotective effect was observed in the presence of carnitine, γ -butyrobetaine, crotonobetaine, choline-*O*-sulfate, proline, pipercolic acid and dimethylglycine (DMG). This observation indicates that the SSS-type transporter EctI from the *ect* gene cluster of *H. neptunium* is a broad substrate range importer for compatible solutes.

The same experiments were conducted with *E. coli* MKH13 cells expressing EctU from *Novosphingobium* sp. LH128 present on plasmid pANDA1. In contrast to the broad substrate range of EctI from *H. neptunium* only the exogenous supply of ectoine and 5-hydroxyectoine exerted an osmoprotective effect on MKH13[pANDA1] (Fig. 4b). This result lead to the conclusion that the MFS-type transporter EctU from *Novosphingobium* sp. LH128 is a specific importer for ectoines.

Table 2 Transport characteristics of EctI and EctU. The determination of the growth rates at different compatible solute concentrations allowed fitting according to the Monod equation, an equation describing the growth of cultures, which is based on the Michaelis-Menten equation [94] (see Supplementary Fig. 2).

transporter	organism	substrate	K_s [μ M]
EctI	<i>Hyphomonas neptunium</i>	glycine betaine	83 \pm 7
		ectoine	16 \pm 3
		hydroxyectoine	25 \pm 3
EctU	<i>Novosphingobium</i> sp. LH128	ectoine	18 \pm 3
		hydroxyectoine	17 \pm 3

In order to determine the apparent kinetic parameters for the substrates glycine betaine, ectoine and 5-hydroxyectoine for EctI and ectoines for EctU, *E. coli* MKH13[pARO12] (EctI) and MKH13[pANDA1] (EctU) was cultivated in 48-well plates in medium with 0.8 M NaCl and increasing concentration of the indicated compatible solutes. The determination of the growth rates at different compatible solute concentrations allowed fitting according to the Monod equation, an equation describing the growth of cultures, which is based on the Michaelis-Menten equation [94]. This revealed the maximum specific growth rate μ_{max} [h^{-1}] and the substrate concentration that supports the half-maximal growth rate K_s [mM compatible solute] of the two studied importers. The mean K_s of EctI was 83 \pm 7 μ M for glycine betaine and 16 \pm 3, and 25 \pm 3 μ M for ectoine and 5-hydroxyectoine, respectively. EctU possessed a K_s of 18 \pm 3 for ectoine and 17 \pm for hydroxyectoine (Table 2, Supplementary Fig. S2).

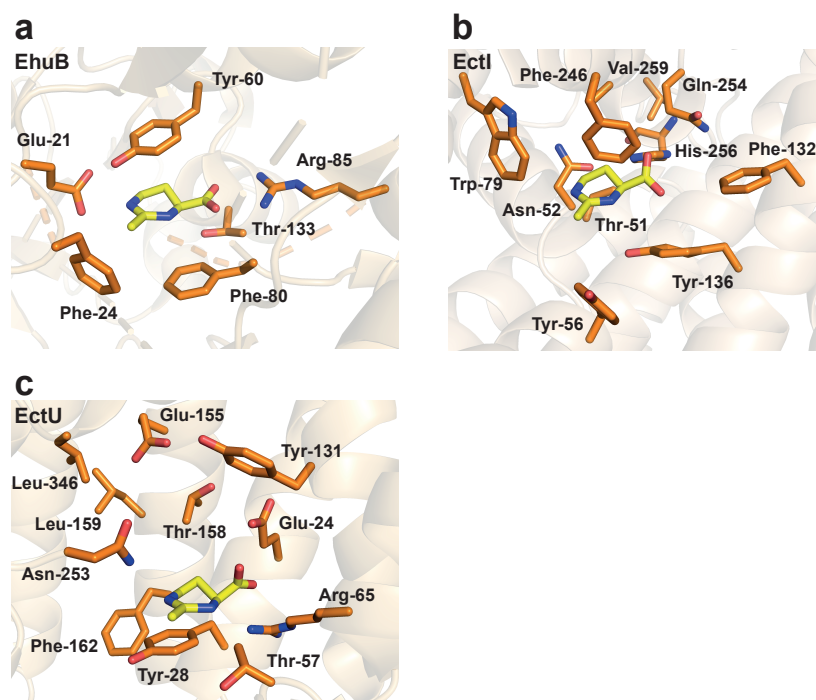


Fig. 5 Comparison of the EhuB substrate binding site to the proposed binding sites of the EctI and EctU transporters. a Zoom into the substrate binding site of the ligand binding protein EhuB of the EhuABCD ABC-type transporter from *S. meliloti* in complex with ectoine (yellow) (PDB: 2Q88) [54]. The residues involved in substrate binding are depicted as orange sticks. b, c Zoom into the potential substrate binding sites of the EctI sss-type transporter from *H. neptunium* (b) and the EcU mfs-type transporter from *Novosphingobium* sp. LH128 (c). The ectoine substrate (yellow) has been docked into the modeled structures. The amino acid residues potentially involved in ligand binding are shown as orange sticks.

When substrate binding sites of compatible solute transporters or their ligand binding proteins are compared, it becomes apparent that these often possess a conserved and highly similar architecture [2]. One example is the identical glycine betaine binding site found in the membrane-bound ligand binding protein (OpuAC) of the *B. subtilis* OpuA transporter [95] and the transmembrane segment of the BCCT'-type transporter BetP from *C. glutamicum* [2, 96, 97]. Moreover both binding sites are highly similar to the binding pocket found in the soluble periplasmic binding ProX from the *E. coli* ProU transporter [81]. The crystal structure of the specific ectoine/5-hydroxyectoine binding protein EhuB of the EhuABCD transporter from *S. meliloti* in complex with both substrates has already been solved and the distinct residues that are involved in the binding of these compounds were identified [PDB: 2Q88 (ectoine); 2Q89 (5-hydroxyectoine)] [54]. We now wondered if this information could be used to search for a putative ectoine binding box in the broad substrate range importer EctI from *H. neptunium* and the specific ectoine importer EctU from *Novosphingobium* sp. LH128. Therefore, models of the EctI and EctU transporters using the Phyre2 [98] web tool were built and *in silico* docking analysis with CLUSPRO [99] and AUTODOCK [100] software for the substrates glycine betaine, ectoine and hydroxyectoine in EctI, and ectoine and hydroxyectoine in EctU was performed (Fig. 5, 6, 7). The ectoine binding motif of EhuB was employed as a blueprint for potential interactions of the substrates with the amino acid residues of the EctI and EctU proteins (Fig. 5). Several residues in close proximity to the ectoine/hydroxyectoine/glycine

betaine substrates within a potential substrate binding pocket were identified, that are similar to those being involved in the binding of the substrates in the EhuB protein (Fig. 5) [54].

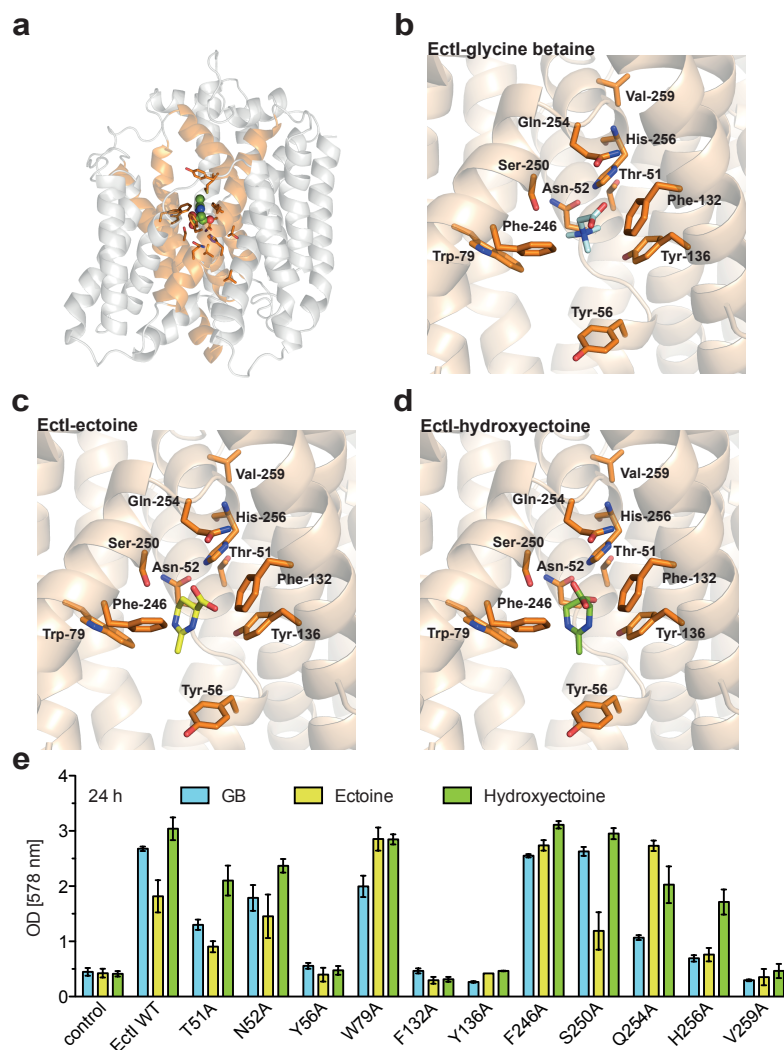


Fig. 6 Modeling, docking and mutational analysis of the EctI transporter. **a** Structural model of the EctI importer from *H. neptunium* based on SglT from *Vibrio parahaemolyticus* (sequence identity of 25%) (PDB: 2XQ2; [70]). The substrate hydroxyectoine is shown as green sticks and has been modeled into the potential binding site. **b**, **c**, **d** Zoom into the potential substrate binding pocket with the ligands glycine betaine (**b**), ectoine (**c**) and hydroxyectoine (**d**). The amino acid residues that are potentially involved in substrate binding are depicted as orange sticks. **e** Growth yield (OD₅₇₈) after 24 h of *E. coli* MKH13 ($\Delta proP \Delta proU$) cells expressing the wild type (WT) or mutant variants of the EctI importer. The cells were incubated in medium supplemented with 0.8 M NaCl and 1 mM of glycine betaine, ectoine or hydroxyectoine, respectively. The data shown is the mean and standard error mean of at least four biological replicates.

Hence, the residues Thr-51, Asn-52, Tyr-56, Trp-79, Phe-132, Tyr-136, Phe-246, Ser-250, Gln-254, His-256 and Val-258, which were predicted to be involved in the trapping of the compatible solute substrates were exchanged by an Ala residue within the protein of the *H. neptunium* EctI importer (Fig. 6 a-d). These mutated EctI transporter proteins were subsequently tested in osmoprotection assays. The uptake of ectoine/5-hydroxyectoine was indirectly tested by measuring the growth of the salt-sensitive *E. coli* strain MKH13 in high salinity medium with exogenous supply of compatible solutes. *E. coli* MKH13 that carried a plasmid encoding either the wild type EctI importer (pARO12), EctI mutant versions (plasmids and amino acid exchanges are listed in Supplementary Table 2) under the control of a

constitutive *lac* promoter [93]. The cells were cultivated at 37 °C in MMA with 0.8 M NaCl and supplemented with either 1 mM glycine betaine, ectoine or 5-hydroxyectoine and the optical density OD₅₇₈ was measured after 24 h of incubation. *E. coli* MKH13 cells harboring the empty vector pHSG575 as a negative control were not able to grow at all tested conditions. MKH13[pARO12] expressing the wild type EctI transporter was able to grow at 0.8 M NaCl when glycine betaine, ectoine and 5-hydroxyectoine were added to the medium (Fig. 4a and Fig. 6e). The tested mutant variants EctI T51A, N52A, W79A, F246A and S250A showed no or only minor defects in growth, when compared to EctI WT growth yield after 24 h. In contrast, EctI mutants Y56A, F132A, H256A and V259A exhibited a drastic decrease in growth yield after 24 h of incubation indicating that these residues are probably crucial for binding or transport of all three tested substrates. Interestingly, EctI variant Q254A seemed to be of importance for the transport of the substrate glycine betaine, while it has only a weak or no effect on the growth in presence of ectoine or 5-hydroxyectoine.

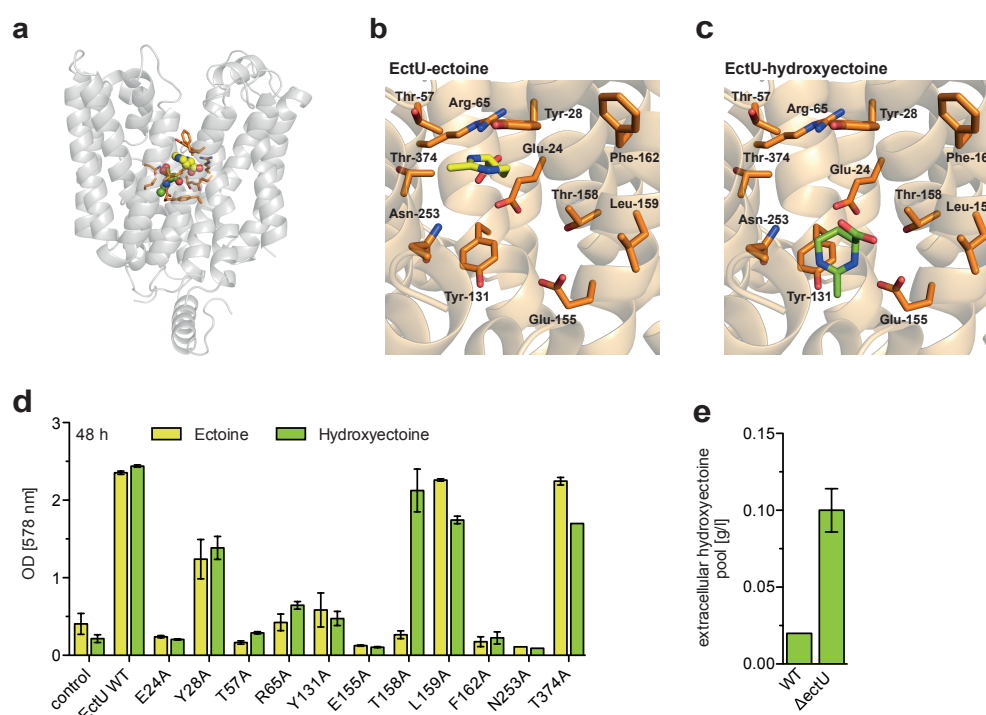


Fig. 7 Modeling, docking and mutational analysis of the EctU transporter **a** Structural model of the EctU importer from *Novosphingobium* sp. LH128 based on XylE from *E. coli* (sequence identity of 18%) (PDB: 4GBY; [101]). The substrates ectoine and hydroxyectoine are shown as yellow and green sticks and have been docked into the potential binding site. **b**, **c** Zoom into the potential substrate binding pocket with the ligands ectoine (**b**) and hydroxyectoine (**c**). The amino acid residues that are potentially involved in substrate binding are depicted as orange sticks. **d** Growth yield (OD₅₇₈) after 24 h of *E. coli* MKH13 ($\Delta proP \Delta proU$) cells expressing the wild type (WT) or mutant variants of the EctU importer. The cells were incubated in medium supplemented with 0.8 M NaCl and 1 mM ectoine or hydroxyectoine, respectively. **e** Quantification of the extracellular hydroxyectoine accumulation in medium of *Novosphingobium* sp. LH128 WT cells or cells of strain LC15 with a chromosomal deletion of the EctU importer ($\Delta ectU$). Cells were grown in medium with 0.3 M NaCl. The data shown is the mean and standard error mean of at least four biological replicates.

In a similar experiment, the amino acid residues Glu-24, Tyr-28, Thr-57, Arg-65, Tyr-131, Glu-155, Thr-158, Lys-159, Phe-162, Asn-253 and Thr-374 (Fig. 7a-c) were exchanged by an Ala residue via site-directed mutagenesis within the EctU protein from *Novosphingobium* sp. LH128. *E. coli* MKH13 carried

a plasmid encoding either the wildtype EctU importer (pANDA1), or the EctU transporter variants (plasmids and amino acid exchanges are listed in Supplementary Table 2) under the control of a constitutive *lac* promoter [93]. The EctU mutant variants E24A, T57A, R65A, Y131A, E155A, F162A and N235A allowed no osmoprotection of the *E. coli* mutant MKH13 in presence of ectoine or 5-hydroxyectoine while mutant Y28A showed a minor degree of osmoprotection by these two compounds (Fig. 7d). The mutations L159A and T374A exhibited no influence on the growth yield after 48 h of incubation. The EctU variant T158A showed an interesting phenotype as it allowed uptake and thereby growth to similar level as the wild type transporter, when hydroxyectoine was present, but allowed no growth in presence of ectoine. This might indicate a slightly different positioning and binding of the two substrates (Fig. 7b, c).

***Novosphingobium* sp. LH128 probably harbors a recycling system for hydroxyectoine.** To further investigate the role of the specific importer EctU, a markerless deletion of the *ectU* gene in the chromosome of *Novosphingobium* sp. LH128 was constructed. When the Δ *ectU* strain LC5 was cultivated in medium with elevated NaCl-concentration (0.3 M NaCl), secretion of the produced hydroxyectoine into the medium supernatant was observed (Fig. 7e). In comparison, the wild type *Novosphingobium* sp. LH128 strain did not accumulate substantial amounts of hydroxyectoine in the culture supernatant (Fig. 7e). Presumably, the produced protectant hydroxyectoine is somehow secreted from the cells and continuously reimported via the specific importer EctU. This phenomenon of production, secretion and reimport has been observed in previous studies e. g. in *H. elongata* when the ectoine specific import system TeaABC was deleted or for the compatible solute proline in *B. subtilis* after deletion of the OpuE importer [43, 72]. However, no specific export system for these solutes has been identified yet. During the bioinformatical analysis of the newly found ectoine gene clusters, that are genetically co-localized with transporters, 21 ectoine gene clusters were found to be associated with potential export systems (Supplementary Fig. S1, Supplementary Table 1). BLAST analysis revealed that these export systems are related to known exporters such as MdfA, EmrD, YajR or MdtM from *E. coli* [67, 85, 86, 102–104]. As stated above such a potential exporter (EctE) is also part of the ectoine biosynthetic gene clusters in *Novosphingobium* sp. LH128 and *H. neptunium*.

In this study we focused on the potential exporter from *Novosphingobium* sp. LH128 [(N_s)EctE]. To exclude that (N_s)EctE functions as an import system for compatible solutes, the same experiment as performed for EctI and EctU in a previous part of this communication was conducted. Hence, (N_s)EctE was cloned into pHSG575 and thereby constitutively expressed from a *lac* promoter. The resulting plasmid pARO11 was transformed into the salt-sensitive *E. coli* strain MKH13 (*proU⁻ proP⁻*) and incubated in MMA without salt (0 M NaCl) and with 0.8 M NaCl and the addition of 1 mM of various compatible solutes, respectively. The growth of these cultures was assessed after 48 h of incubation. While the cells grown without additional NaCl reached an OD of approximately 1.8 after 48 h, none of the cultures containing 0.8 M NaCl and any of the tested compatible solutes was able to grow indicating, that the tested transporter (N_s)EctE might not function as uptake systems for compatible solutes (Fig. 4c, d).

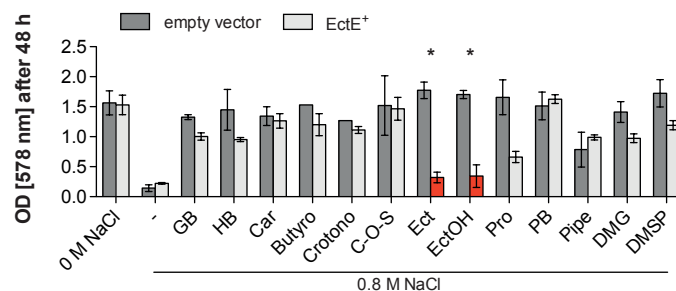


Fig. 8 Heterologous analysis of the putative ectoine exporter EctE from *Novosphingobium* sp. LH128. Growth yield (OD₅₇₈) of *E. coli* MC4100 wild type either harboring the empty expression vector pTrc99a (grey) or plasmid pLC108 where (*Ns*)*ectE* is controlled by an inducible *lac* promoter (EctE⁺, white). The cells were grown for 48 h in MMA medium supplemented without or with the addition of 0.8 M NaCl and supplemented with 1 mM of the indicated compatible solute, respectively. The data shown represent the mean and standard error mean of six biological replicates.

EctE probably functions as a specific exporter for ectoines. Since *in silico* analysis are only predictions, we wondered how to find out if EctE is indeed a specific exporter for ectoines. We used an assay system that has previously been established to assess the role of EmrE in glycine betaine efflux in *E. coli* [59]. The assay is based on the idea, that *E. coli* wild-type cells are able to accumulate compatible solutes, such as glycine betaine or ectoine, through their broad uptake systems ProU and ProP. At the same time the putative exporter is present on a plasmid, and expression and production of the putative exporter might potentially result in the increased release of the tested compatible solutes, which in turn does not allow the cells to build an intracellular compatible solute pool during high external salt stress. As a consequence these cells will not be able to counteract the osmotically instigated outflow of water and are therefore unable to form biomass. To test our hypothesis, the *ectE* coding region from *Novosphingobium* sp. LH128 was cloned under the control of a LacI-regulated *lac* promoter present on the vector pTrc99a [105] resulting in the plasmid pLC108. This plasmid was then introduced into *E. coli* MC4100 wild type cells and the cells were cultivated in MMA without NaCl, with 0.8 M NaCl and the addition of various compatible solutes (1mM), respectively. The expression of the putative exporter EctE was induced by the addition of 0.3 mM IPTG. When OD₅₇₈ was assessed after 48 h, the *E. coli* MC4100 wild type strain carrying the empty vector pTrc99a was able to grow in presence of every tested compatible solutes (Fig. 8). In contrast, MC4100 cells expressing the EctE transporter from *Novosphingobium* sp. LH128 were also able to grow in presence of the compatible solutes glycine betaine, homobetaine, carnithine, γ -butyrobetaine, crotonobetaine, choline-*O*-sulfate, proline betaine, pipercolic acid, DMG and DMSP, while a strongly reduced growth of the cultures containing ectoine, hydroxyectoine or proline was observed (Fig. 8). This observation could be explained by the release of ectoine, hydroxyectoine and proline from the cytoplasm through the heterologously expressed exporter EctE. The *E. coli* cells first import the solutes via the uptake system ProP and ProU, but are not able to build a sufficient pool of ectoine, hydroxyectoine or proline to provide protection towards the applied osmotic stress when the exporter EctE is expressed. Hence, the MFS-type exporter EctE is assumed to be the missing link in the ectoine recycling system of *Novosphingobium* sp. LH128 and that *Novosphingobium* sp. LH128 has evolved an ectoine

biosynthesis cluster with specific import and export systems to finely tune the intracellular hydroxyectoine pools during changes in cell size (growth and division) or small changes in the external osmotic conditions.

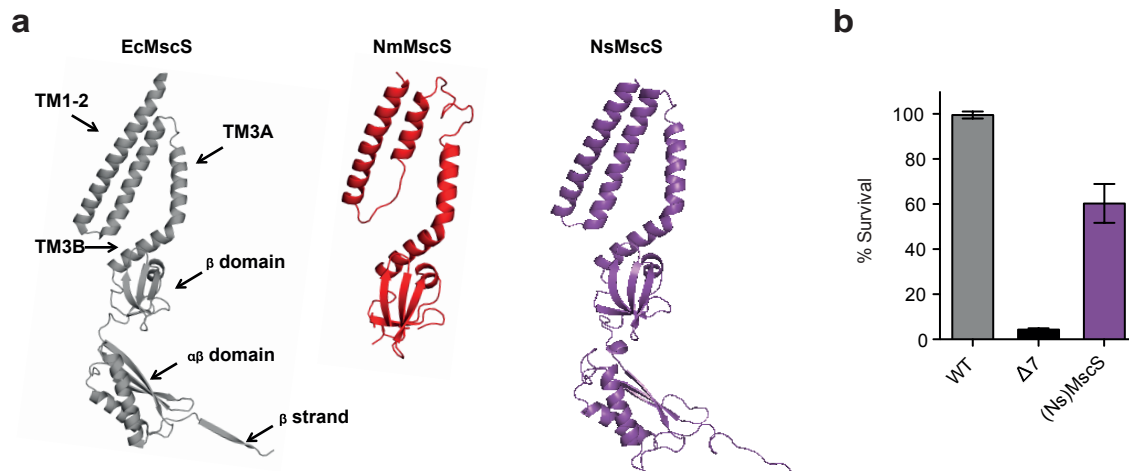


Fig. 9 Bioinformatic and functional assessment of the MscS-like mechanosensitive channel from *Novosphingobium* sp. LH128. **a** Structural model of a monomer of the MscS-like mechanosensitive channel from *N. maritimus*, (Ns)MscS (red) [7] and the (Nm)MscS mechanosensitive channel from *Novosphingobium* sp. LH128 (purple) in comparison to the *E. coli* mechanosensitive channel, (Ec)MscS (grey; PDB: 2VV5; [88]). **b** Survival (%) of *E. coli* WT cells (FRAG1), *E. coli* strain MJF641 ($\Delta 7$; lacking all known mechanosensitive channels) and *E. coli* MJF641 expressing the MscS-like mechanosensitive channel from *Novosphingobium* sp. LH128 after an osmotic downshock from 0.3 M NaCl to 0 M NaCl [56, 76]. The data shown represent the mean and standard error mean of three independent biological replicates.

A co-transcribed MscS-like mechanosensitive channel complements channel-defective *E. coli* cells. In the first report of an MscS-like mechanosensitive channel that is co-transcribed with the *ect* genes in the marine Thaumarchaeon ‘Ca. *N. maritimus*’ SCM1 it has also been demonstrated that the channel functionally protects an *E. coli* mutant lacking all seven known mechanosensitive channels after a severe osmotic down-shock [7]. A comparison of structural models of these mechanosensitive channels shows, that the (Nm)MscS lacks a long intracellular domain [7], which is present in the *E. coli* MscS (PDB: 2VV5) (Fig. 9) [88] and also the mechanosensitive channel of *Novosphingobium* sp. LH128 [(Ns)MscS] that is co-transcribed with the ectoine biosynthesis genes (Fig. 2a and Fig. 9). In the next step, the functionality of the latter mechanosensitive channel was tested. We therefor used a complementation experiment that has been established by Levina and co-workers [76]. A synthetic version of the (Ns)*mscS* codon-optimized for its expression in *E. coli* was cloned into an IPTG-inducible expression plasmid pTrc99a [105]. We employed an *E. coli* $\Delta 7$ mutant-strain (MJF641) that lacks all seven known mechanosensitive channels [56]. In the down-shock experiment, *E. coli* MJF641 carrying the (Ns)MscS expression plasmid pLC19 was grown at 0.3 M NaCl and expression of (Ns)*mscS* was induced with IPTG. The cells were then confronted with a rapid osmotic downshift to 0 M NaCl. The parent (strain FRAG1) of the $\Delta 7$ mutant-strain carrying the empty plasmid pTrc99a survived this osmotic downshift to nearly 100% (99.5% \pm 1.6%) recovery. In contrast only 4.3% \pm 0.7% of the cells of the $\Delta 7$ mutant-strain MJF641 (pTrc99a) survived this treatment. When MJF641 (pLC19; (Ns)*mscS*⁺) was subjected to this osmotic down-shock, the (Ns)MscS protein

rescued cellular survival to a large extent ($60.3\% \pm 8.6\%$ surviving cells) (Fig. 9b). Therefore, we conclude that a physiologically functional mechanosensitive channel is co-transcribed with the ectoine genes in *Novosphingobium* sp. LH128. Hence, the bacterial cells already prepare themselves for an eventually occurring osmotic down-shock at high osmolarity conditions.

Discussion

Since the discovery of the stress protectant ectoine in *Ectothiorhodospira halochloris* in 1985, the underlying genes, biosynthetic enzymes and several transport systems have been studied to detail [6, 17, 106]. Their broad occurrence within the bacterial domain and the establishment of its industrial production, together with the development of different biotechnological, medical and cosmetic applications has promoted ectoine as a highly valuable and widely known compound [6, 30, 31]. Here, we show through the bioinformatical information obtained within a broad phylogenetic analysis, that the core genes for ectoine biosynthesis are often accompanied by genes encoding different types of transporters. We identified (at least) seven different transporter types in close vicinity of the ectoine genes (Fig. 1, Table 1, Supplementary Fig. 1, Supplementary Table 1) and exemplarily studied the novel ectoine biosynthetic gene clusters from the two α -proteobacteria *H. neptunium* and *Novosphingobium* sp. LH128 (Fig. 2a, d). Our findings shed new light on the importance of specialized uptake and probably also the secretion systems for ectoines.

Our data show that both studied organisms only accumulate 5-hydroxyectoine in response to salt stress (Fig. 3a, b), which can either be explained by a more efficient ectoine hydroxylase EctD, or the possibility of substrate channeling between the EctC and EctD enzyme. A mechanism that could be investigated in future studies. Differences in the capacities and performances of ectoine hydroxylases originating from different organisms have already been described in a study that aimed the establishment of a synthetic *E. coli*-based cell factory for the production of 5-hydroxyectoine [107]. The ability to produce pure 5-hydroxyectoine could be an interesting trait for biotechnology since on the one hand most producers accumulate a mixture of both ectoine and 5-hydroxyectoine, which requires difficult and expensive purification steps to separate the two compounds [6, 31], and on the other hand because 5-hydroxyectoine possesses different and often superior functional attributes compared to ectoine [28, 108].

Our experiments show, that the accumulation of 5-hydroxyectoine as an osmotic stress protectant is finely tuned to the externally applied salinities (Fig. 3c, d). This observation has previously been made in other natural and non-natural producers [14, 109]. It implicates that the bacterial cells can sense the exact external salinity even if it changes subtly and as a consequence finely adjust the internal solute pool - a signaling mechanism, which is until now unexplained and needs further investigations.

Through the analysis of the transcriptional units, we were able to show that the identified transporters EctE/EctI and EctE/EctU/MscS are co-transcribed with the ectoine biosynthetic genes in *H. neptunium* and *Novosphingobium* sp. LH128 (Fig. 2b, e). Until now, the co-localization of a putative ectoine transporter has only been described in *P. lautus*, where an Ehu-type ABC-transporter is found upstream of the *ect* gene cluster (Richter *et al*, submitted manuscript). While the co-transcription of ectoine-

specific transporters together with genes encoding enzymes that are involved in the utilization of ectoines as nutrients is well known [15, 42, 43]. Moreover, the co-transcription of a MscS-type mechanosensitive channel has been investigated in the marine Thaumarchaeon *N. maritimus* [7]. The (Nm)MscS channel was highly up-regulated under chronic and acute osmotic stress conditions. Surprisingly, the expression level of the gene encoding the MscS-type mechanosensitive channel in *Novosphingobium* sp. LH128 was only up-regulated 2-fold compared to the ectoine biosynthesis genes that were 6-fold induced even though the genes are located on the same mRNA transcript (Fig. 2c). An explanation for this observation could either be the instability of the long mRNA (8521 bp) or the presence of not yet identified weak terminators upstream of the *mscS* gene. It is noteworthy that the transport system (EctE/EctU and EctE/EctI) showed approximately the same expression levels as the ectoine production genes in both organisms pointing to the importance of these transporters for the accumulation of ectoines and their physiological adaptation to high osmolarity conditions (Fig. 2c, e).

The studied (Ns)MscS mechanosensitive channel possesses a higher sequence identity to the YbdG mechanosensitive channel than to the MscS mechanosensitive channel from *E. coli* (Supplementary Table 1). The physiological role of the YbdG has been studied within the past years and it was characterized as a mechanosensitive channel that plays only minor roles in maintaining cell integrity. It is rather suggested to act as a mini-conductance channel (MscM), that extends the range of hypoosmotic shock that *E. coli* cells can survive, but its expression level was insufficient to protect against severe shocks. Nevertheless, the overexpression of YbdG resulted in the same protection to a hypoosmotic shock as MscS or MscL channels [79]. In a more recent study, YbdG was described to function as a component of a mechanosensing system that transmits signals triggered by external osmotic changes to intracellular factors [110]. It remains to be investigated if the (Ns)MscS channel possesses the same function.

Highly specific ectoine uptake systems have been identified in various organisms [6]. The here identified EctU (*Novosphingobium*) transporter is the first MFS-type transporter that is highly selective for ectoines (Fig. 4b and Fig. 7b), compared to the MFS-transporter ProP from *E. coli* (42% sequence identity) that is able to import at least nine different compatible solutes [40]. The second investigated transporter EctI (*H. neptunium*) belongs to SSS transporters and in contrast to the highly specific proline SSS-type transporters OpuE and PutP from *B. subtilis* [72, 111] it was found to transport six different compatible solutes (Fig. 6a). Taken together, this study revealed new aspects of osmoprotectant uptake system from the MFS or SSS and modeling-based analysis together with site-directed mutations facilitated a detailed understanding of the substrate binding sites within the newly found EctI and EctU transporter.

The secretion of ectoines and other compatible solutes under steady state osmotic conditions has been observed in a variety of organisms. For example, ectoine is secreted continuously by *E. coli* cells during synthetic production [109, 112]. Interestingly, *E. coli* does not naturally possess the ability to synthesize ectoines, but is nevertheless able to excrete it into the medium. Presumably this secretion seems to be an essential feature of *E. coli* or even bacterial cells in general in order to avoid *over*-accumulation of compatible solutes, which will hinder balancing of the osmotic gradient.

Beyond that, *H. elongata* permanently secretes the produced ectoine into the medium and reimports it via specific ectoine uptake system TeaABC. Hence, the a genetic inactivation of the Tea transporter resulted in the accumulation of ectoine in the medium [43] - a feature that has also been observed for proline, when the specialized proline transporter OpuE is deleted in *B. subtilis* [72]. It is therefor long thought that osmoprotectants are not only produced and accumulated by the bacterial cells but are also permanently released via a yet unkown mechanism and recaptured by highly specific import systems. These observations led to the idea that also specialized export systems for osmoprotectants must be present in ectoine-producing organisms. A first hint on the molecular identity of such an exporter was the study by Bay and Turner on the multidrug efflux system EmrE - it was shown to be involved in the release of quarternary cation osmoprotectants in *E. coli* such as glycine betaine and choline, when *emrE* was carried by a plasmid [59]. Furthermore, the co-cultivation of the diatom *Thalassiosira pseudonana* with the ectoine-catabolizing strain *R. pomeroyi* DSS-3 revealed the induction of the ectoine utilization genes which indicates that ectoine is produced and secreted by the diatom and taken up and digested by the bacterial cells [113]. Nevertheless, the secretion mechanism for ectoines in all these cases remained unidentified. In the presented study, we show for the first time that an MFS-type exporter might be involved in the specific secretion of ectoines in *Novosphingobium* sp. LH128 (Fig. 8). Furthermore, our bioinformatic analysis implicates that such transporters can be found in a considerable number of *ect* gene clusters (Table 1, Supplementary Fig.1, Supplementary Table 1), pointing to the importance of this secretion mechanism. We believe that the secretion can be beneficial for the bacterial cells to (I) exactly fine-tune the intracellular osmoprotectant pool, (II) to rapidly react to small changes in the external salinity, (III) to adapt the pool during growth an division, and (IV) to potentially release the protectants when the cells grow in biofilms as there might for example be producer and cheater cells, or ectoines could function as a common good within a microbial community. To underline the importance of ectoine production in biofilms, a previous study by Fida *et al.* identified the ectoine biosynthetic genes and also the transporters as the most highly induced genes upon osmotic shock and chronic stress within biofilms of *Novosphingobium* sp. LH128 [114] (data summarized in Supplementary Table 3). The ability to form biofilms and act as primary colonizers of marine surfaces was also described for various *Hyphomonas* species [115]. The link between biofilm formation and compatible solute uptake or synthesis has also been observed in *B. subtilis* and *V. cholera* [116, 117]. In *B. subtilis* the DNA-binding protein RemA was found to activate the expression of genes required for the biofilm matrix and of genes involved in compatible solute accumulation such as the osmoprotectant uptake system OpuA [117–119]. Furthermore, the regulatory protein CosR in *V. cholera* regulates the genes required for biofilm formation and the genes for the compatible solute uptake system OpuD and the ectoine biosynthetic pathway [116]. These findings open up future research question on the exact role of ectoines and the involved transporters in bacterial biofilms. Taken together our data suggest that the import and also the release of compatibles solutes such as ectoines is of large importance for bacterial cells to react to the ever-changing osmotic concentration in their natural environment. Furthermore, the newly found potential ectoine exporter could be exploited for biotechnological processes to synthetically enhance the release of ectoines from producing cells and

thereby result in higher ectoine concentrations in the medium supernatant and thereby enable easier purification.

Methods

Chemicals

Ectoine and 5-hydroxyectoine were kindly provided by the bitop AG (Witten, Germany). Acetonitrile (HPLC-grade) was obtained from VWR International GmbH (Darmstadt, Germany). Chloramphenicol, ampicillin, kanamycin and streptomycin and all other chemicals were purchased from Sigma-Aldrich (Steinheim, Germany), Serva Electrophoresis GmbH (Heidelberg, Germany) and Carl Roth GmbH (Karlsruhe, Germany). Enzymes and chemicals for DNA manipulations were obtained from Thermo Fisher Scientific GmbH (Dreieich, Germany), Roche Diagnostics GmbH (Mannheim, Germany) and New England BioLabs GmbH (Frankfurt, Germany).

Bacterial strains, media and growth conditions

The *E. coli* wild type strain MC4100 is the parent of the strain MKH13 [$\Delta(\text{proP})2 \Delta(\text{proU}::\text{spo})608$] (Spc^r) carrying defects in the genes encoding the ProP or ProU compatible solute uptake systems [92, 120]; see Supplementary Table 4. All *E. coli* strains were routinely maintained on Luria Bertani (LB) agar plates and propagated in liquid LB medium [121]. When they contained a recombinant plasmid, ampicillin ($100 \mu\text{g ml}^{-1}$), chloramphenicol ($30 \mu\text{g ml}^{-1}$) or kanamycin ($50 \mu\text{g ml}^{-1}$) was added to the growth medium. For heterologous experiments of the *E. coli* strains carrying various plasmids, cells were grown in minimal medium A (MMA) supplemented with 0.2% (w/v) glucose as the carbon source, 1 mM MgSO_4 , and $1.5 \mu\text{M}$ ($= 0.5 \text{ mg l}^{-1}$) thiamine [121]. The osmolarity of the growth medium was adjusted by adding various concentrations of NaCl, as specified in the individual experiments. Shake-flask cultures were incubated at 37°C in a shaking water bath set to 220 rpm.

Osmostress protection assays with *E. coli* strains MC4100 and MKH13 [92] carrying different plasmids were conducted in 100-ml Erlenmeyer flasks (culture volume of 20 ml) by growing the cells (at 37°C) in MMA containing 0.8 M NaCl in absence or presence (1 mM final concentration) of the tested compatible solutes [121]. The cultures were inoculated to an OD_{578} of 0.1 and the growth yield of these cultures was recorded after 24, 30 and 48 h by measuring their OD_{578} . In various cases, such as for the determination of the apparent k_m (in terms of the K_s based on the Monod equation) of the EctI and EctU transporters, cultures were grown in 48-well plates. Each well contained 500 μl of the indicated medium and the well plate was incubated in an Epoch 2 microplate spectrophotometer (Biotek, Bad Friedrichshall, Germany) at 37°C with double orbital vigorous shaking. The growth of the cultured was monitored every hour for 48 or 96 h.

The *Novosphingobium* sp. LH128 [64] strain was kindly provided by Dirk Springael (KU Leuven, Belgium) and cultivated in LB or Spizizen's minimal medium (SMM), with 0.5% (wt/vol) glucose as the carbon source. The medium was supplemented with L-tryptophan (20 mg liter^{-1}), L-phenylalanine (18 mg liter^{-1}), and a trace element solution [122]. This medium possesses a measured osmolarity of 377 mOsm/kg. Cells were routinely grown aerobically at 30°C in 100-ml baffled Erlenmeyer flasks with a culture volume of 10 ml in a shaking water bath set at 220 rpm. The growth of the bacterial cultures was monitored spectrophotometrically at a wavelength of 578 nm (OD_{578}). The salinity of bacterial cultures was raised by adding appropriate volumes of NaCl from a 5 M stock solution. For the growth curves, cells were incubate in a volume of 10-ml medium inoculated to OD_{578} 0.1 in 100-ml baffled Erlenmeyer flasks at 30°C in a shaker set at 220 rpm.

The *H. neptunium* strain LE670 (ATCC15444) [62, 63] was a kind gift from Martin Thanbichler (Philipps University Marburg, Germany) and was cultivated aerobically in Difco marine broth 2216 (MB) (BD Biosciences, Heidelberg, Germany) at 30°C under vigorous shaking (220 rpm) in baffled flasks. This medium possessed a measured osmolarity of 924 mOsm/kg. For the cultivation at increasing salinities, the MB medium was prepared in a 2-fold concentration and then diluted to 1-fold MB with water and if needed appropriate volumes of NaCl from a 5 M stock solution.

The osmolarity of the used media was measured according to the manufacturer's protocol using a Gonotec freezing point osmometer (Osmomat 3000basic, Gonotec, Berlin, Germany).

Recombinant DNA procedures, construction of plasmids and site-directed mutagenesis

Routine manipulations of plasmid DNA, the construction of recombinant plasmids and the isolation of chromosomal DNA from *H. neptunium* and *Novosphingobium* sp. LH128 were carried out using standard techniques [123]. The genes *ectI* (*H. neptunium*) and *ectU* (*Novosphingobium* sp. LH128) were amplified from chromosomal DNA using the synthetic primers Hypho5_EcoRI_for and Hypho3+5_HindIII_rev (for *ectI*) and EctU EcoRI for and EctU HindIII rev (for *ectU*) (Supplementary Table 5). The obtained DNA fragments contained artificial EcoRI and HindIII restriction sites at their 5'-ends and were inserted into a pHSG575 vector (Cm^r) [93] that had been cut with

EcoRI and HindIII. This yielded in the plasmids pARO12 (*ectI* from *H. neptunium*) and pANDA1 (*ectU* from *Novosphingobium*).

For the heterologous expression of the *mscS* and *ectE* genes from *Novosphingobium* sp. LH128 and *H. neptunium* in *E. coli*, the genes were cloned into the expression vector pTrc99a [105]. In case of *mscS*, a codon-optimized synthetic *mscS* gene was amplified from the plasmid obtained from the supplier (GeneArt Gene Synthesis, Thermo Fisher Scientific, Dreieich, Germany) by PCR using the custom synthesized DNA primers MscS_Sphingo EcoRI for and MscS_Sphingo HindIII rev (Supplementary Table 5). The (*Ns*)*ectE* gene was amplified using EctE_pTrc99a NcoI for and EctE_pTrc99a BamHI rev. The resulting short DNA fragments carried NcoI and HindIII restriction sites, respectively, were attached either to the 5' or to the 3' prime ends of the PCR product, thereby enabling its directional insertion into the expression vector pTrc99a [105]. This positioned the transcription of the *mscS* gene under the control of the *lac* promoter carried by the pTrc99a vector and resulted in the isolation of plasmid pLC19. The plasmid pLC108 harbouring the *ectE* gene from *Novosphingobium* sp. LH128 under the control of the *lac* promoter present on pTrc99a were constructed identically, except its amplification from chromosomal DNA from *Novosphingobium* sp. LH128, instead of a codon-optimized synthetic version of this gene (Supplementary Table 2). The nucleotide sequence of the synthetic (*Ns*)*mscS* gene was deposited at the NCBI database under the accession number KT313590.1.

Variants of the *ectU* and *ectI* gene present on the plasmids pANDA1 and pARO12, respectively, were generated by site-directed mutagenesis using the Q5 Site-Directed Mutagenesis Kit (New England BioLabs GmbH, Frankfurt, Germany) with custom synthesized primers that were designed using the NEBaseChanger online tool (<https://nebasechanger.neb.com>) (Supplementary Table 5).

Markerless gene deletion in *Novosphingobium* sp. LH128 of the gene encoding the importer EctU was constructed as reported by Kaczmarczyk *et al.* [124]. Upstream and down-stream regions of approximately 750 bp that flanked the corresponding gene(s) were PCR amplified using the custom synthesized primers 5 Sph 5'Del for, 5 Sph 3'Del for, 5 Sph 5'Del rev, and 5 Sph 3'Del rev (Supplementary Table 5). The 3'- and 5'-fragments were joined by overlap extension PCR, and then ligated into pAK405 using the restriction sites KpnI and HindIII. This resulted in the plasmid pLC61 (Δ *ectU*).

All custom synthesized primers were purchased from Microsynth AG (Lindau, Germany) (Supplementary Table 5). The correct nucleotide sequence of all constructed plasmids was ascertained by DNA sequence analysis, which was carried out by Eurofins MWG Operon (Ebersberg, Germany). All used plasmids are listed in Supplementary Table 2.

Construction of markerless gene deletions in *Novosphingobium* sp. LH128

Novosphingobium sp. LH128 knock-out strain carrying markerless gene deletion of the importer EctU was constructed as reported by Kaczmarczyk *et al.* with minor variations of the protocol [124]. The plasmids pLC61 (Δ *ectU*) was transformed into *Novosphingobium* sp. LH128 by electroporation [124]. Bacteria were subsequently plated on LB supplemented with 50 μ g kanamycin ml⁻¹. Individual colonies were restreaked once on the same medium and then inoculated in LB supplemented with 100 μ g streptomycin ml⁻¹ to enforce the second homologous recombination event. After 40 h of incubation the cultures were transferred to fresh LB supplemented with 100 μ g streptomycin ml⁻¹ (OD₅₇₈ of 0.1) and further incubated at 30 °C in a shaking waterbath set to 220 rpm. After 24 h the cells were adjusted to an OD₅₇₈ of 0.5 and serially diluted. The 10⁻⁶ dilution was plated on LB supplemented with 100 μ g streptomycin ml⁻¹ and incubated for 48 h. Resulting colonies were restreaked on both LB supplemented with 100 μ g streptomycin ml⁻¹ and LB containing 50 μ g kanamycin ml⁻¹, and kanamycin-sensitive clones were analyzed by colony PCR using primers flanking the respective loci. This resulted in the Δ *ectU* strain LC5 (Supplementary Table 4)

Isolation of total RNA and transcription analysis of the 5-hydroxyectoine/ectoine biosynthetic gene cluster

The total RNA from *H. neptunium* and *Novosphingobium* cells cultured under different conditions was isolated as reported previously [114]. In brief - *H. neptunium* and *Novosphingobium* were cultivated at 30 °C in MB or SMM, respectively, with or without the addition of NaCl until they reached an OD₅₇₈ of 1. 1 ml of cell culture was mixed with 2 ml of fresh RNA protect bacterial reagent (QIAGEN, Hilden, Germany), vortexed for 5 s, incubated at RT for 5 min and then harvested at 2415 x g for 10 min at RT. RNA was immediately extracted using Promega SV total RNA extraction kit (Promega, Madison, USA) with minor modifications of the protocol (centrifugation was performed at 15.115 x g instead of at 14,000 x g and 200 μ l of Tris-EDTA containing 0.4 mg ml⁻¹ lysozyme was used instead of 100 μ l). The RNA was eluted with 60 μ l of RNase-free water. Traces of remaining DNA were removed by

using the Turbo DNA-free kit according to the manufacturer's protocol (Ambion, Invitrogen, Thermo Fisher Scientific, USA).

The isolated RNA was further used for one-step RT-PCR assays to assess the transcriptional organization of the *ect* operon from *H. neptunium* and *Novosphingobium*. To analyse whether the *ectR-ectABCD-ask-ectE-ectU-mscS* genes are transcribed in a unit, 11 (*Novosphingobium* sp. LH128) or 8 (*H. neptunium*) intergenic regions of the putative operons were amplified from isolated RNA using the Qiagen One Step RT-PCR Kit (QIAGEN, Hilden, Germany) and custom synthesized DNA primers (MWG, Ebersberg, Germany) (Supplementary Table 5). As controls, we also amplified DNA regions between genes that were divergently transcribed (Fig. 2a). To ensure that the formed PCR products did not result from DNA contaminations of RNA sample used for the RT-PCR reaction, an assay was performed in which total RNA was used as a PCR template. This resulted in no amplification of the potential fragments.

Transcriptional analyses by quantitative RT-PCR

For studying the expression of the ectoine biosynthesis gene cluster in *H. neptunium* and *Novosphingobium* under different osmotic growth conditions, cells that had been cultured either at low (0 mM), or high salt (500 mM NaCl for *H. neptunium* and 600 mM NaCl for *Novosphingobium* sp. LH128) were used. Total RNA was extracted from these cells as described above. The absence of DNA contamination was ascertained by PCR analysis. The relative abundance of the *ectA*, *ectD*, *ectE*, *ectU* and *mscS* mRNA in salt-stressed compared to non-stressed cells was determined by real-time PCR in a CFX96 Touch Real-Time PCR Detection System (Bio-Rad Laboratories GmbH, München, Germany) with the LightCycler RNA Master SYBR green I kit (Roche Diagnostics, Mannheim, Germany). Each reaction of the one-step RT-PCR was conducted in a 20- μ l volume containing 50 ng template RNA, 0.5 μ M of each primer, 3.25 mM Mn(OAc)₂ and 7.5 μ l of LightCycler RNA Master SYBR green I. The PCR primer sets used are shown in Supplementary Table 5. The thereby amplified PCR products range between 120 and 160 bp in length. The PCR cycling conditions were used as described in the manufacturer's instructions with 30 min of reverse transcription to cDNA at 61 °C, followed by an initial denaturation step at 95 °C for 2 min. Then 45 PCR cycles were run with denaturation at 95°C for 5 s, annealing at 56°C for 10 s and extension at 72°C for 10 s. After this qRT-PCR a melting curve for quality control was obtained: 95 °C for 10 s, followed by a temperature ramp from 65 to 95 °C in 0.5 °C steps for 15 s. The relative expression of each gene under the tested conditions was determined by using the *gyrB* transcript level in *H. neptunium* and *Novosphingobium* cells as the standard. Induction values are expressed as the log₂ of the ration of the value determined for the salt-stressed cells over the value determined for the non-stressed control. All of the experiments were conducted in at least two independent replicates, and relative expression levels were measured using the 2^{- Δ Ct} method [125].

Modelling and docking of three-dimensional protein structures and preparation of figures of crystal structures

Amino acid sequences of the studied proteins were retrieved from the IMG database [126]. Structural models of the EctI transporter from *H. neptunium* and the EctU transporter from *Novosphingobium* sp. LH128 were built via a modelling program Phyre2 [98]. The models obtained were manually inspected to avoid clash of site chains. After this glycine betaine (EctI) ectoine and hydroxyectoine (both transporters) were separately modeled into the model using AUTODOCK [100] and the webserver CLUSPRO [127]. As a result ten different docking solution were obtained which were manually inspected using Pymol [128]. The possible binding sites were compared to the known binding sites of ectoine and hydroxyectoine obtained by the structures of several substrate binding proteins [54]. From these two binding position were selected and redocked into the transporter model resulting in one location of the ligand afterwards. This procedure was independently performed for the EctU and EctI protein separately. Modelling of the mechanosensitive channels was conducted using the SWISS Model webserver [129]. Structures of all proteins were visualized and analyzed using the PyMOL Molecular Graphics System suit ([https:// www.pymol.org](https://www.pymol.org)) [128].

HPLC analysis of ectoine and hydroxyectoine content

Cell pellets of *Novosphingobium* sp. LH128 and *H. neptunium* were extracted with 20% ethanol. For this purpose, the cell pellets were resuspended in 1-ml 20% ethanol and were shaken for 1 h. After centrifugation at 16.000 x g (4 °C, 30 min) to remove cell debris, the ethanolic extracts were transferred into fresh Eppendorf tubes, and the ethanol was removed by evaporation (at 65 °C for 20 h). The resulting dried material was suspended in 100 μ l of distilled water and insoluble material was removed by centrifugation (16.000 x g at 4 °C for 30 min). The extracted samples and the cell-free culture supernatants were diluted ten-fold with distilled water and acetonitrile (the end concentration of acetonitrile was 50%) and analyzed for their ectoine/5-hydroxyectoine content by isocratic high-

performance liquid chromatography (HPLC) [89]. For these measurements we employed an Agilent 1260 Infinity LC system (Agilent, Waldbronn, Germany) and a GROM-SIL Amino 1PR column (Dr. Maisch GmbH, Ammerbuch-Entringen, Germany) essentially as described [89] with the exception that a 1260 Infinity Diode Array Detector (DAD) (Agilent) was used, instead of the previously used UV/Vis detector system. The ectoine content of samples was quantified using the OpenLAB software suite (Agilent). Standard curves for the calculation of the ectoine and 5-hydroxyectoine concentrations were determined with commercially available samples (obtained from bitop AG, Witten, Germany).

Functional complementation of the mechanosensitive-channel-defective *E. coli* mutant MJF641 by the *Novosphingobium* sp. LH128 MscS protein

For the analysis of cell viability of strains FRAG1(pTrc99a), MJF641(pTrc99a) and MJF641(pLC19) subsequent to an osmotic down-shock, we used the growth medium and the procedure described by Levina and colleagues [56, 76]. In brief, osmotically unstressed cells were grown at 37°C in a 100-ml Erlenmeyer flask filled with 20 ml of medium in a shaking water bath (set to 220 rpm) using a citrate-phosphate buffered chemically defined, medium (pH 7.0). It contained per litre: 8.58 g Na₂HPO₄, 0.87 g K₂HPO₄, 1.34 g citric acid, 1.0 g (NH₄SO₄), 0.001 g thiamine, 0.1 g MgSO₄ × 7 H₂O and 0.002 g (NH₄)₂SO₄ × FeSO₄ × 6 H₂O, and was supplemented with 0.2% (w/v) glucose as the carbon source [76]. This medium possessed a measured osmolarity of 235 mOsm. For cells that were grown at high salinity, 0.3 M NaCl were added to the basal medium; it had a measured osmolarity of 730 mOsm. The osmolarity of growth media was determined with an osmometer (Vapor Pressure Osmometer 5500, Wesco, USA). The *E. coli* strains FRAG1 and MJF641 [56] harbouring different plasmids were inoculated in 5 ml LB medium containing ampicillin (100 µg ml⁻¹) and were grown for 5 h. Cells were subsequently transferred into the above-described citrate-phosphate medium and incubated over-night at 37 °C. Cells were then diluted to an OD₅₇₈ of 0.05 into 20 ml of the above-described minimal medium, or into 20 ml medium that contained 0.3 M NaCl, and the cultures were subsequently grown to an OD₅₇₈ of 0.15. At this point, IPTG was added to the cultures (final concentration 1 mM) to induce the activity of the *lac* promoter present on the back-bone of the expression plasmid pTrc99a [105], thereby triggering the transcription of the codon-optimized *Novosphingobium* sp. LH128 *mscS* gene. Growth of the cells was subsequently continued until they reached an OD₅₇₈ of about 0.35. These cultures were then diluted 20-fold into pre-warmed medium (37 °C) containing 1 mM IPTG with (no osmotic down-shock) or without (osmotic down-shock) 0.3 M NaCl; the cells were subsequently incubated at 37 °C in a shaking water bath for 30 min. To determine the number of cells that survived the osmotic down-shock, 50-µl samples were taken after 30 min of incubation from these cultures, serially diluted in four independent sets in media with corresponding osmolarities and four 5 µl samples of the osmotically downshifted cells were then spotted onto Luria-Bertani (LB) agar plates [121]. Those from the high osmolarity grown cells were spotted onto LB agar plates with a total NaCl content of 0.3 M NaCl. Colony-forming units were determined after overnight incubation of the LB plates at 37 °C.

Database searches for ectoine biosynthesis-related proteins

Bioinformatical analysis was built on a dataset consisting of 582 EctC-type proteins found in all fully sequenced bacterial and archaeal genomes at the online database of the DOE Joint Genome Institute (<http://www.jgi.doe.gov>), that was obtained by Czech *et al.* in 2017 [6, 65].

The bioinformatics tools available at the DOE Joint Genome Institute website were used to retrieve all putative ectoine gene clusters from this dataset, that harbored different transporters in the direct gene neighborhood. The organization of these genes was visualized using Adobe Illustrator. Protein sequences were aligned and compared using ClustalW [130] or the alignment tool available at the NCBI website (<https://www.ncbi.nlm.nih.gov>) [131].

References

1. Grant WD. Life at low water activity. *Philos Trans R Soc Lond B Biol Sci* 2004;359:1249–1267.
2. Bremer E, Krämer R. Responses of microorganisms to osmotic stress. *Annu Rev Microbiol* 2019;73:313–334.
3. Kempf B, Bremer E. Uptake and synthesis of compatible solutes as microbial stress responses to high-osmolality environments. *Arch Microbiol* 1998;170:319–330.
4. Wood JM. Bacterial osmoregulation: a paradigm for the study of cellular homeostasis. *Annu Rev Microbiol* 2011;65:215–238.
5. Csonka LN. Physiological and genetic responses of bacteria to osmotic stress. *Microbiol Rev* 1989;53:121–147.
6. Czech L, Hermann L, Stöveken N, Richter A, Höppner A, *et al.* Role of the extremolytes ectoine and hydroxyectoine as stress protectants and nutrients: genetics, phylogenomics, biochemistry, and structural analysis. *Genes (Basel)* 2018;9:177. doi: 10.3390/genes9040177.
7. Widderich N, Czech L, Elling FJ, Könneke M, Stöveken N, *et al.* Strangers in the archaeal world: osmotic stress-responsive biosynthesis of ectoine and hydroxyectoine by the marine thaumarchaeon *Nitrosopumilus maritimus*. *Environ Microbiol* 2016;18:1227–1248.
8. Weinisch L, Kühner S, Roth R, Grimm M, Roth T, *et al.* Identification of osmoadaptive strategies in the halophile, heterotrophic ciliate *Schmidingerothrix salinarum*. *PLoS Biol* 2018;16:e2003892. doi: 10.1371/journal.pbio.2003892.
9. Weinisch L, Kirchner I, Grimm M, Kühner S, Pierik AJ, *et al.* Glycine betaine and ectoine are the major compatible solutes used by four different halophilic heterotrophic ciliates. *Microb Ecol* 2019;77:317–331.
10. Harding T, Brown MW, Simpson AGB, Roger AJ. Osmoadaptative strategy and its molecular signature in obligately halophilic heterotrophic protists. *Genome Biol Evol* 2016;8:2241–2258.
11. Czech L, Bremer E. With a pinch of extra salt - Did predatory protists steal genes from their food? *PLOS Biol* 2018;16:e2005163. doi: 10.1371/journal.pbio.2005163.
12. Harding T, Simpson AGB. Recent advances in halophilic protozoa research. *J Eukaryot Microbiol* 2018;65:556–570.
13. Ren M, Feng X, Huang Y, Wang H, Hu Z, *et al.* Phylogenomics suggests oxygen availability as a driving force in *Thaumarchaeota* evolution. *ISME J* 2019;13:2150–2161.
14. Stöveken N, Pittelkow M, Sinner T, Jensen RA, Heider J, *et al.* A specialized aspartokinase enhances the biosynthesis of the osmoprotectants ectoine and hydroxyectoine in *Pseudomonas stutzeri* A1501. *J Bacteriol* 2011;193:4456–4468.
15. Jebbar M, Sohn-Bösser L, Bremer E, Bernard T, Blanco C. Ectoine-induced proteins in *Sinorhizobium meliloti* include an ectoine ABC-type transporter involved in osmoprotection and ectoine catabolism. *J Bacteriol* 2005;187:1293–1304.
16. Kuhlmann A, Bursy J, Gimpel S, Hoffmann T, Bremer E. Synthesis of the compatible solute ectoine in *Virgibacillus pantothenicus* is triggered by high salinity and low growth temperature. *Appl Environ Microbiol* 2008;74:4560–4563.
17. Ono H, Sawada K, Khunajakr N, Tao T, Yamamoto M, *et al.* Characterization of biosynthetic enzymes for ectoine as a compatible solute in a moderately halophilic eubacterium, *Halomonas elongata*. *J Bacteriol* 1999;181:91–99.
18. Reshetnikov AS, Khmelenina VN, Mustakhimov II, Trotsenko YA. Genes and enzymes of ectoine biosynthesis in halotolerant methanotrophs. *Methods Enzymol* 2011;495:15–30.
19. Czech L, Höppner A, Kobus S, Seubert A, Riclea R, *et al.* Illuminating the catalytic core of ectoine synthase through structural and biochemical analysis. *Sci Rep* 2019;9:doi: 10.1038/s41598-018-36247-w.
20. Widderich N, Kobus S, Höppner A, Riclea R, Seubert A, *et al.* Biochemistry and crystal structure of ectoine synthase: a metal-containing member of the cupin superfamily. *PLoS One* 2016;11:e0151285. doi:10.1371/journal.pone.0151285.
21. Höppner A, Widderich N, Lenders M, Bremer E, Smits SHJ. Crystal structure of the ectoine hydroxylase, a snapshot of the active site. *J Biol Chem* 2014;289:29570–29583.
22. Widderich N, Höppner A, Pittelkow M, Heider J, Smits SHJ, *et al.* Biochemical properties of ectoine hydroxylases from extremophiles and their wider taxonomic distribution among microorganisms. *PLoS One* 2014;9:e93809. doi:10.1371/journal.pone.0093809.
23. Harishchandra RK, Wulff S, Lentzen G, Neuhaus T, Galla HJ. The effect of compatible solute ectoines on the structural organization of lipid monolayer and bilayer membranes. *Biophys Chem* 2010;150:37–46.
24. Lentzen G, Schwarz T. Extremolytes: natural compounds from extremophiles for versatile applications. *Appl Microbiol Biotechnol* 2006;72:623–634.
25. Graf R, Anzali S, Buenger J, Pfluecker F, Driller H. The multifunctional role of ectoine as a natural cell protectant. *Clin Dermatol* 2008;26:326–333.
26. Schröter MA, Meyer S, Hahn MB, Solomun T, Sturm H, *et al.* Ectoine protects DNA from damage by ionizing radiation. *Sci Rep* 2017;7:doi: 10.1038/s41598-017-15512-4.
27. Meyer S, Schröter MA, Hahn MB, Solomun T, Sturm H, *et al.* Ectoine can enhance structural changes in DNA in vitro. *Sci Rep* 2017;7:doi: 10.1038/s41598-017-07441-z.
28. Lippert K, Galinski E. Enzyme stabilization by ectoine-type compatible solutes: protection against heating,

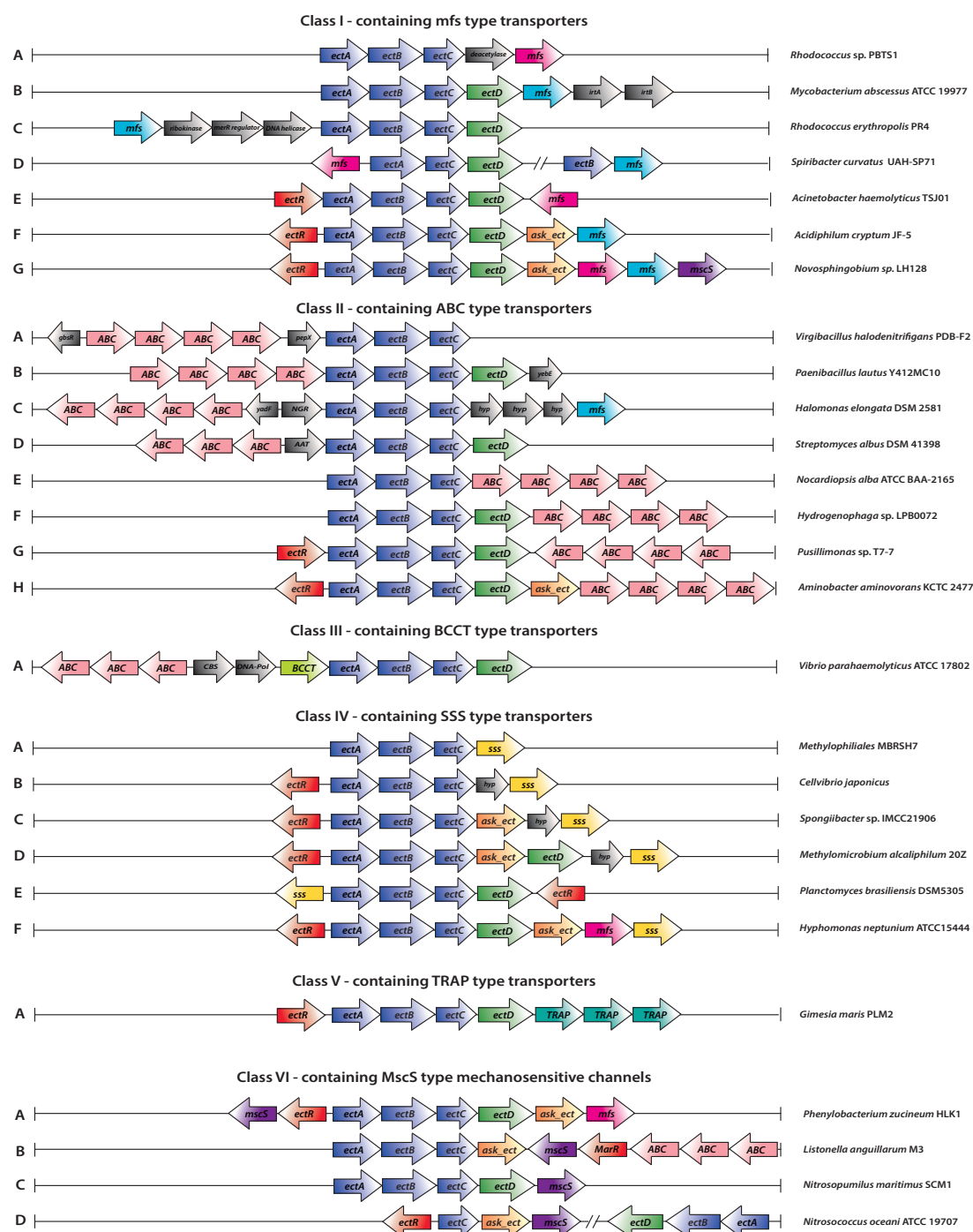
- freezing and drying. *Applied Microbiology and Biotechnology* 1992;37:61–65.
29. Roychoudhury A, Haussinger D, Oesterhelt F. Effect of the compatible solute ectoine on the stability of the membrane proteins. *Protein Pept Lett* 2012;19:791–794.
 30. Kunte H, Lentzen G, Galinski E. Industrial production of the cell protectant ectoine: protection mechanisms, processes, and products. *Curr Biotechnol* 2014;3:10–25.
 31. Pastor JM, Salvador M, Argandoña M, Bernal V, Reina-Bueno M, *et al.* Ectoines in cell stress protection: uses and biotechnological production. *Biotechnol Adv* 2010;28:782–801.
 32. León MJ, Hoffmann T, Sánchez-Porro C, Heider J, Ventosa A, *et al.* Compatible solute synthesis and import by the moderate halophile *Spiribacter salinus*: physiology and genomics. *Front Microbiol* 2018;9:doi: 10.3389/fmicb.2018.00108.
 33. Jebbar M, Von Blohn C, Bremer E. Ectoine functions as an osmoprotectant in *Bacillus subtilis* and is accumulated via the ABC-transport system OpuC. *FEMS Microbiol Lett* 1997;154:325–330.
 34. Bursy J, Kuhlmann AU, Pittelkow M, Hartmann H, Jebbar M, *et al.* Synthesis and uptake of the compatible solutes ectoine and 5-hydroxyectoine by *Streptomyces coelicolor* A3(2) in response to salt and heat stresses. *Appl Environ Microbiol* 2008;74:7286–7296.
 35. Jebbar M, Talibart R, Gloux K, Bernard T, Blanco C. Osmoprotection of *Escherichia coli* by ectoine: uptake and accumulation characteristics. *J Bacteriol* 1992;174:5027–5035.
 36. Oren A. Bioenergetic aspects of halophilism. *Microbiol Mol Biol Rev* 1999;63:334–348.
 37. Welsh DT. Ecological significance of compatible solute accumulation by micro-organisms: from single cells to global climate. *FEMS Microbiol Rev* 2000;24:263–290.
 38. Booth IR. Bacterial mechanosensitive channels: progress towards an understanding of their roles in cell physiology. *Curr Opin Microbiol* 2014;18:16–22.
 39. Booth IR, Blount P. The MscS and MscL families of mechanosensitive channels act as microbial emergency release valves. *J Bacteriol* 2012;194:4802–4809.
 40. MacMillan S V., Alexander DA, Culham DE, Kunte HJ, Marshall E V., *et al.* The ion coupling and organic substrate specificities of osmoregulatory transporter ProP in *Escherichia coli*. *Biochim Biophys Acta - Biomembr* 1999;1420:30–44.
 41. Ongagna-Yhombi SY, McDonald ND, Boyd EF. Deciphering the role of multiple Betaine-Carnitine-Choline Transporters in the halophile *Vibrio parahaemolyticus*. *Appl Environ Microbiol* 2015;81:351–363.
 42. Lecher J, Pittelkow M, Zobel S, Bursy J, Bönig T, *et al.* The crystal structure of UehA in complex with ectoine-A comparison with other TRAP-T binding proteins. *J Mol Biol* 2009;389:58–73.
 43. Grammann K, Volke A, Kunte HJ. New type of osmoregulated solute transporter identified in halophilic members of the *Bacteria* domain: TRAP transporter TeaABC mediates uptake of ectoine and hydroxyectoine in *Halomonas elongata* DSM 2581T. *J Bacteriol* 2002;184:3078–3085.
 44. Gouesbet G, Trautwetter A, Bonnassie S, Wu LF, Blanco C. Characterization of the *Erwinia chrysanthemi* osmoprotectant transporter gene *ousA*. *J Bacteriol* 1996;178:447–455.
 45. Ma Y, Wang Q, Xu W, Liu X, Gao X, *et al.* Stationary phase-dependent accumulation of ectoine is an efficient adaptation strategy in *Vibrio anguillarum* against cold stress. *Microbiol Res* 2017;205:8–18.
 46. Ziegler C, Bremer E, Krämer R. The BCCT family of carriers: from physiology to crystal structure. *Mol Microbiol* 2010;78:13–34.
 47. Kempf B, Bremer E. Stress responses of *Bacillus subtilis* to high osmolarity environments: uptake and synthesis of osmoprotectants. *J Biosci* 1998;23:447–455.
 48. Kuhlmann AU, Hoffmann T, Bursy J, Jebbar M, Bremer E. Ectoine and hydroxyectoine as protectants against osmotic and cold stress: uptake through the SigB-controlled Betaine-Choline-Carnitine Transporter-type carrier EctT from *Virgibacillus pantothenticus*. *J Bacteriol* 2011;193:4699–4708.
 49. Vermeulen V, Kunte HJ. *Marinococcus halophilus* DSM 20408T encodes two transporters for compatible solutes belonging to the Betaine-Carnitine-Choline Transporter family: identification and characterization of ectoine transporter EctM and glycine betaine transporter BetM. *Extremophiles* 2004;8:175–184.
 50. Peter H, Weil B, Burkovski A, Krämer R, Morbach S. *Corynebacterium glutamicum* is equipped with four secondary carriers for compatible solutes: identification, sequencing, and characterization of the proline/ectoine uptake system, ProP, and the ectoine/proline/glycine betaine carrier, EctP. *J Bacteriol* 1998;180:6005–6012.
 51. Weinand M, Krämer R, Morbach S. Characterization of compatible solute transporter multiplicity in *Corynebacterium glutamicum*. *Appl Microbiol Biotechnol* 2007;76:701–708.
 52. Culham DE, Marom D, Boutin R, Garner J, Ozturk TN, *et al.* Dual role of the C-Terminal domain in osmosensing by bacterial osmolyte transporter ProP. *Biophys J* 2018;115:doi: 10.1016/j.bpj.2018.10.023.
 53. Kuhlmann SI, van Schelting ACT, Bienert R, Kunte HJ, Ziegler CM. 1.55 Å structure of the ectoine binding protein TeaA of the osmoregulated TRAP-transporter TeaABC from *Halomonas elongata*. *Biochemistry* 2008;47:9475–9485.
 54. Hanekop N, Höing M, Sohn-Bösser L, Jebbar M, Schmitt L, *et al.* Crystal structure of the ligand-binding protein EhuB from *Sinorhizobium meliloti* reveals substrate recognition of the compatible solutes ectoine and hydroxyectoine. *J Mol Biol* 2007;374:1237–1250.
 55. Becker M, Krämer R. MscCG from *Corynebacterium glutamicum*: functional significance of the C-terminal

- domain. *Eur Biophys J* 2015;44:577–588.
56. **Edwards MD, Black S, Rasmussen T, Rasmussen A, Stokes NR, et al.** Characterization of three novel mechanosensitive channel activities in *Escherichia coli*. *Channels* 2012;6:272–281.
 57. **Miller S, Bartlett W, Chandrasekaran S, Simpson S, Edwards M, et al.** Domain organization of the MscS mechanosensitive channel of *Escherichia coli*. *EMBO J* 2003;22:36–46.
 58. **Martinac B.** Mechanosensitive channels in prokaryotes. *Cell Physiol Biochem* 2001;11:61–76.
 59. **Bay DC, Turner RJ.** Small multidrug resistance protein EmrE reduces host pH and osmotic tolerance to metabolic quaternary cation osmoprotectants. *J Bacteriol* 2012;194:5941–5948.
 60. **Glaasker E, Heuberger EHML, Konings WN, Poolman B.** Mechanism of osmotic activation of the quaternary ammonium compound transporter (QacT) of *Lactobacillus plantarum*. *J Bacteriol* 1998;180:5540–5546.
 61. **Glaasker E, Konings WN, Poolman B.** Glycine betaine fluxes in *Lactobacillus plantarum* during osmostasis and hyper- and hypo-osmotic shock. *J Biol Chem* 1996;271:10060–10065.
 62. **Badger JH, Eisen JA, Ward NL.** Genomic analysis of *Hyphomonas neptunium* contradicts 16S rRNA gene-based phylogenetic analysis: implications for the taxonomy of the orders ‘Rhodobacterales’ and ‘Caulobacterales’. *Int J Syst Evol Microbiol* 2005;55:1021–1026.
 63. **Leifson E.** *Hyphomicrobium neptunium* sp. n. *Antonie Van Leeuwenhoek* 1964;30:249–256.
 64. **Bastiaens, L, Springael D, Wattiau P, Harms H, et al.** Isolation of adherent polycyclic aromatic hydrocarbon (PAH)-degrading bacteria using PAH-sorbing carriers. *Appl Environ Microbiol* 2000;66:1834–1843.
 65. **Nordberg H, Cantor M, Dusheyko S, Hua S, Poliakov A, et al.** The genome portal of the Department of Energy Joint Genome Institute: 2014 updates. *Nucleic Acids Res* 2014;42:26–31.
 66. **Mustakhimov II, Reshetnikov A, Clukhov A, Khmelenina V, Kalyuzhnaya M, et al.** Identification and characterization of EctR1, a new transcriptional regulator of the ectoine biosynthesis genes in the halotolerant methanotroph *Methylobacterium alcaliphilum* 20Z. *J Bacteriol* 2010;192:410–417.
 67. **Edgar R, Bibi E.** MdfA, an *Escherichia coli* multidrug resistance protein with an extraordinarily broad spectrum of drug recognition. *J Bacteriol* 1997;179:2274–2280.
 68. **Nagarathinam K, Jaenecke F, Nakada-Nakura Y, Hotta Y, Liu K, et al.** The multidrug-resistance transporter MdfA from *Escherichia coli*: crystallization and X-ray diffraction analysis. *Acta Crystallogr Sect F Struct Biol Commun* 2017;73:423–430.
 69. **Zhao Y, Heng J, Zhao Y, Liu M, Liu Y, et al.** Substrate-bound structure of the *E. coli* multidrug resistance transporter MdfA. *Cell Res* 2015;25:1060–1073.
 70. **Watanabe A, Choe S, Chaptal V, Rosenberg JM, Wright EM, et al.** The mechanism of sodium and substrate release from the binding pocket of vSGLT. *Nature* 2010;468:988–991.
 71. **Faham S, Watanabe A, Besserer GM, Cascio D, Specht A, et al.** The crystal structure of a sodium galactose transporter reveals mechanistic insights into Na⁺/sugar symport. *Science (80-)* 2008;321:810–814.
 72. **Hoffmann T, von Blohn C, Stanek A, Moses S, Barzantny H, et al.** Synthesis, release, and recapture of compatible solute proline by osmotically stressed *Bacillus subtilis* cells. *Appl Environ Microbiol* 2012;78:5753–5762.
 73. **von Blohn C, Kempf B, Kappes RM, Bremer E.** Osmostress response in *Bacillus subtilis*: characterization of a proline uptake system (OpuE) regulated by high osmolarity and the alternative transcription factor sigma B. *Mol Microbiol* 1997;25:175–187.
 74. **Spiegelhalter F, Bremer E.** Osmoregulation of the *opuE* proline transport gene from *Bacillus subtilis*: contributions of the sigma A- and sigma B-dependent stress-responsive promoters. *Mol Microbiol* 1998;29:285–296.
 75. **Culham DE, Lasby B, Marangoni AG, Milner JL, Steer BA, et al.** Isolation and sequencing of *Escherichia coli* gene *proP* reveals unusual structural features of the osmoregulatory proline/betaine transporter, ProP. *J Mol Biol* 1993;229:268–276.
 76. **Levina N, Totemeyer S, Stokes NR, Louis P, Jones M a, et al.** Protection of *Escherichia coli* cells against extreme turgor by activation of MscS and MscL mechanosensitive channels: identification of genes required for MscS activity. *EMBO J* 1999;18:1730–1737.
 77. **Malcolm HR, Blount P.** Mutations in a conserved domain of *E. coli* MscS to the most conserved superfamily residue leads to kinetic changes. *PLoS One* 2015;10:doi: 10.1371/journal.pone.0136756.
 78. **Wilson ME, Maksaev G, Haswell ES.** MscS-like mechanosensitive channels in plants and microbes. *Biochemistry* 2013;52:5708–5722.
 79. **Schumann U, Edwards MD, Rasmussen T, Bartlett W, van West P, et al.** YbdG in *Escherichia coli* is a threshold-setting mechanosensitive channel with MscM activity. *Proc Natl Acad Sci* 2010;107:12664–12669.
 80. **Nie R, Stark S, Symersky J, Kaplan RS, Lu M.** Structure and function of the divalent anion/Na⁺ symporter from *Vibrio cholerae* and a humanized variant. *Nat Commun* 2017;8:doi: 10.1038/ncomms15009.
 81. **Schiefner A, Breed J, Bösner L, Kneip S, Gade J, et al.** Cation- π interactions as determinants for binding of the compatible solutes glycine betaine and proline betaine by the periplasmic ligand-binding protein ProX from *Escherichia coli*. *J Biol Chem* 2004;279:5588–5596.
 82. **Du Y, Shi WW, He YX, Yang YH, Zhou CZ, et al.** Structures of the substrate-binding protein provide

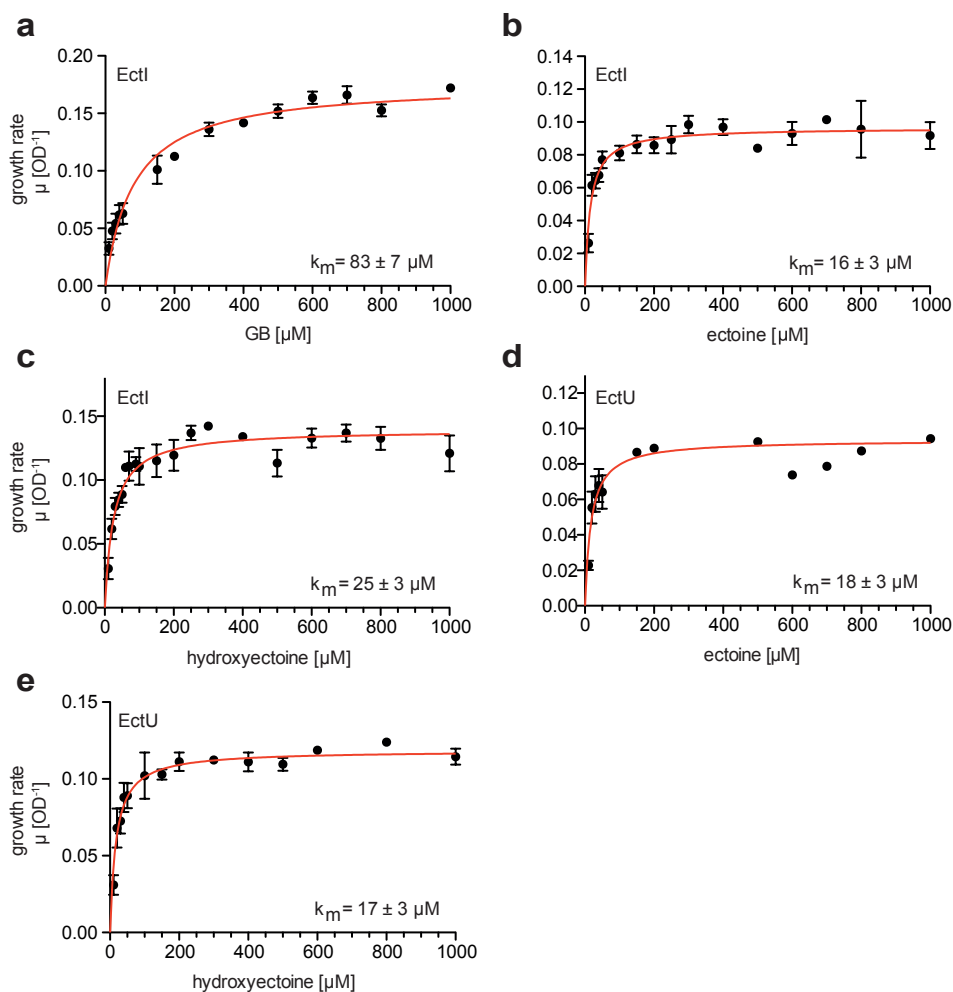
- insights into the multiple compatible solute binding specificities of the *Bacillus subtilis* ABC transporter OpuC. *Biochem J* 2011;436:283–289.
83. **Kappes RM, Kempf B, Bremer E.** Three transport systems for the osmoprotectant glycine betaine operate in *Bacillus subtilis*: characterization of OpuD. *J Bacteriol* 1996;178:5071–5079.
 84. **Krämer R, Morbach S.** BetP of *Corynebacterium glutamicum*, a transporter with three different functions: betaine transport, osmosensing, and osmoregulation. *Biochim Biophys Acta* 2004;1658:31–36.
 85. **Yin Y, He X, Szweczyk P, Nguyen T, Chang G.** Structure of the multidrug transporter EmrD from *Escherichia coli*. *Science* (80-) 2006;312:741–744.
 86. **Nagarathinam K, Nakada-Nakura Y, Parthier C, Terada T, Juge N, et al.** Outward open conformation of a major facilitator superfamily multidrug/H⁺ antiporter provides insights into switching mechanism. *Nat Commun* 2018;9:doi: 10.1038/s41467-018-06306-x.
 87. **Jung H, Hilger D, Raba M.** The Na⁺/L-proline transporter PutP. *Front Biosci* 2012;17:745–759.
 88. **Wang W, Black SS, Edwards MD, Miller S, Morrison EL, et al.** The structure of an open form of an *E. coli* mechanosensitive channel at 3.45 Å resolution. *Science* (80-) 2008;321:1179–1183.
 89. **Kuhlmann AU, Bremer E.** Osmotically regulated synthesis of the compatible solute ectoine in *Bacillus pasteurii* and related *Bacillus* spp. *Appl Environ Microbiol* 2002;68:772–783.
 90. **Bursy J, Pierik AJ, Pica N, Bremer E.** Osmotically induced synthesis of the compatible solute hydroxyectoine is mediated by an evolutionarily conserved ectoine hydroxylase. *J Biol Chem* 2007;282:31147–31155.
 91. **Calderón MI, Vargas C, Rojo F, Iglesias-Guerra F, Csonka LN, et al.** Complex regulation of the synthesis of the compatible solute ectoine in the halophilic bacterium *Chromohalobacter salexigens* DSM 3043T. *Microbiology* 2004;150:3051–3063.
 92. **Haardt M, Kempf B, Faatz E, Bremer E.** The osmoprotectant proline betaine is a major substrate for the binding-protein-dependent transport system ProU of *Escherichia coli* K-12. *Molecular & general genetics*, 1995, pp. 783–786.
 93. **Takeshita S, Sato M, Toba M, Masahashi W, Hashimoto-Gotoh T.** High-copy-number and low-copy-number plasmid vectors for *lacZ* alpha-complementation and chloramphenicol- or kanamycin-resistance selection. *Gene* 1987;61:63–74.
 94. **Monod J.** The growth of bacterial cultures. *Annu Rev Microbiol Microbiol* 1949;3:371–394.
 95. **Horn C, Sohn-Bösser L, Breed J, Welte W, Schmitt L, et al.** Molecular determinants for substrate specificity of the ligand-binding protein OpuAC from *Bacillus subtilis* for the compatible solutes glycine betaine and proline betaine. *J Mol Biol* 2006;357:592–606.
 96. **Perez C, Koshy C, Yildiz Ö, Ziegler C.** Alternating-access mechanism in conformationally asymmetric trimers of the betaine transporter BetP. *Nature* 2012;490:126–130.
 97. **Perez C, Faust B, Mehdipour AR, Francesconi KA, Forrest LR, et al.** Substrate-bound outward-open state of the betaine transporter BetP provides insights into Na⁺ coupling. *Nat Commun* 2014;5:doi: 10.1038/ncomms5231.
 98. **Kelley LA, Mezulis S, Yates CM, Wass MN, Sternberg MJE.** The Phyre2 web portal for protein modeling, prediction and analysis. *Nat Protoc* 2015;10:845–858.
 99. **Kozakov D, Hall DR, Xia B, Porter KA, Padhorny D, et al.** The ClusPro web server for protein-protein docking. *Nat Protoc* 2017;12:255–278.
 100. **Trott O, Olson AJ.** AutoDock Vina: improving the speed and accuracy of docking with a new scoring function, efficient optimization and multithreading. *NIH Pubic Access* 2010;31:455–461.
 101. **Sun L, Zeng X, Yan C, Sun X, Gong X, et al.** Crystal structure of a bacterial homologue of glucose transporters GLUT1-4. *Nature* 2012;490:361–366.
 102. **Koita K, Rao C V.** Identification and analysis of the putative pentose sugar efflux transporters in *Escherichia coli*. *PLoS One* 2012;7:e43700. doi: 10.1371/journal.pone.0043700.
 103. **Law CJ, Alegre KO.** Clamping down on drugs: the *Escherichia coli* multidrug efflux protein MdtM. *Res Microbiol* 2018;169:461–467.
 104. **Jiang D, Zhao Y, Wang X, Fan J, Heng J, et al.** Structure of the YajR transporter suggests a transport mechanism based on the conserved motif A. *Proc Natl Acad Sci* 2013;110:14664–14669.
 105. **Amann E, Ochs B, Abel KJ.** Tightly regulated *tac* promoter vectors useful for the expression of unfused and fused proteins in *Escherichia coli*. *Gene* 1988;69:301–315.
 106. **Galinski EA, Pfeiffer HP, Trüper HG.** 1,4,5,6-Tetrahydro-2-methyl-4-pyrimidinecarboxylic acid. A novel cyclic amino acid from halophilic phototrophic bacteria of the genus *Ectothiorhodospira*. *Eur J Biochem* 1985;149:135–139.
 107. **Czech L, Stöveken N, Bremer E.** EctD-mediated biotransformation of the chemical chaperone ectoine into hydroxyectoine and its mechanosensitive channel-independent excretion. *Microb Cell Fact* 2016;15:doi: 10.1186/s12934-016-0525-4.
 108. **Manzanera M.** High survival and stability rates of *Escherichia coli* dried in hydroxyectoine. *FEMS Microbiol Lett* 2004;233:347–352.
 109. **Czech L, Poehl S, Hub P, Stöveken N, Bremer E.** Tinkering with osmotically controlled transcription allows enhanced production and excretion of ectoine and hydroxyectoine from a microbial cell factory. *Appl*

- Environ Microbiol* 2018;84:e01772-17. doi: 10.1128/AEM.01772-17.
110. **Amemiya S, Toyoda H, Kimura M, Saito H, Kobayashi H, et al.** The mechanosensitive channel YbdG from *Escherichia coli* has a role in adaptation to osmotic up-shock. *J Biol Chem* 2019;294:12281–12292.
 111. **Moses S, Sinner T, Zapras A, Stöveken N, Hoffmann T, et al.** Proline utilization by *Bacillus subtilis*: uptake and catabolism. *J Bacteriol* 2012;194:745–758.
 112. **Schubert T, Maskow T, Benndorf D, Harms H, Breuer U.** Continuous synthesis and excretion of the compatible solute ectoine by a transgenic, nonhalophilic bacterium. *Appl Environ Microbiol* 2007;73:3343–3347.
 113. **Landa M, Burns AS, Roth SJ, Moran MA.** Bacterial transcriptome remodeling during sequential co-culture with a marine dinoflagellate and diatom. *ISME J* 2017;11:2677–2690.
 114. **Fida TT, Breugelmans P, Lavigne R, Coronado E, Johnson DR, et al.** Exposure to solute stress affects genome-wide expression but not the polycyclic aromatic hydrocarbon-degrading activity of *Sphingomonas* sp. strain LH128 in biofilms. *Appl Environ Microbiol* 2012;78:8311–8320.
 115. **Badger JH, Hoover TR, Brun Y V, Weiner RM, Laub MT, et al.** Comparative genomic evidence for a close relationship between the dimorphic prosthecate bacteria *Hyphomonas neptunium* and *Caulobacter crescentus*. *J Bacteriol* 2006;188:6841–6850.
 116. **Shikuma NJ, Davis KR, Fong JNC, Yildiz FH.** The transcriptional regulator, CosR, controls compatible solute biosynthesis and transport, motility and biofilm formation in *Vibrio cholerae*. *Environ Microbiol* 2013;15:1387–1399.
 117. **Winkelman JT, Bree AC, Bate AR, Eichenberger P, Gourse RL, et al.** RemA is a DNA-binding protein that activates biofilm matrix gene expression in *Bacillus subtilis*. *Mol Microbiol* 2013;88:984–997.
 118. **Winkelman JT, Blair KM, Kearns DB.** RemA (Ylza) and RemB (YaaB) regulate extracellular matrix operon expression and biofilm formation in *Bacillus subtilis*. *J Bacteriol* 2009;191:3981–3991.
 119. **Kempf B, Bremer E.** OpuA, an osmotically regulated binding protein-dependent transport system for the osmoprotectant glycine betaine in *Bacillus subtilis*. *J Biol Chem* 1995;270:16701–16713.
 120. **Lucht JM, Bremer E.** Adaptation of *Escherichia coli* to high osmolarity environments: osmoregulation of the high-affinity glycine betaine transport system ProU. *FEMS Microbiol Rev* 1994;14:3–20.
 121. **Miller J.** *Experiments in molecular genetics*. 1972.
 122. **Harwood CR, Archibald AR.** Growth, maintenance and general techniques. In: Harwood CR, Cutting SM (editors). *Molecular biological methods for Bacillus*. Chichester, United Kingdom.: John Wiley & Sons, Inc.; 1990. pp. 1–26.
 123. **Sambrook J, W Russell D.** Molecular Cloning: A Laboratory Manual. *Cold Spring Harb Lab Press Cold Spring Harb NY* 2001;999.
 124. **Kaczmarczyk A, Vorholt JA, Francez-Charlot A.** Markerless gene deletion system for *Sphingomonads*. *Appl Environ Microbiol* 2012;78:3774–3777.
 125. **Livak KJ, Schmittgen TD.** Analysis of relative gene expression data using real-time quantitative PCR and the 2^{-ΔΔC_T} method. *Methods* 2001;25:402–408.
 126. **Chen IA, Chu K, Palaniappan K, Pillay M, Ratner A, et al.** IMG/M v.5.0: an integrated data management and comparative analysis system for microbial genomes and microbiomes. *Nucleic Acids Res* 2018;doi: 10.1093/nar/gky901.
 127. **Kozakov D, Hall DR, Xia B, Porter KA, Padhorny D, et al.** The ClusPro web server for protein–protein docking. *Nat Protoc* 2017;12:255–278.
 128. **DeLano WL.** The PyMOL Molecular Graphics System, Version 1.8 Schrödinger, LLC. *San Carlos Delano Sci.* <http://www.pymol.org> (2002).
 129. **Biasini M, Bienert S, Waterhouse A, Arnold K, Studer G, et al.** SWISS-MODEL: Modelling protein tertiary and quaternary structure using evolutionary information. *Nucleic Acids Res* 2014;42:W252–W258.
 130. **Thompson JD, Plewniak F, Thierry J, Poch O.** DbClustal: rapid and reliable global multiple alignments of protein sequences detected by database searches. *Nucleic Acids Res* 2000;28:2919–2926.
 131. **Johnson M, Zaretskaya I, Raytselis Y, Merezhuk Y, McGinnis S, et al.** NCBI BLAST: a better web interface. *Nucleic Acids Res* 2008;36:5–9.

SUPPLEMENTARY DATA



Suppl. Fig. 1 Schematic illustration of *ect* gene clusters encoding putative transporters in their gene neighborhood.



Suppl. Fig. 2 Transport characteristics of EctI and EctU. *E. coli* MKH13 ($\Delta proP \Delta proU$) cells expressing the either the (a, b, c) EctI importer from *H. neptunium* or the (d, e) EctU importer from *Novosphingobium* sp. LH128 from the plasmid pARO12 or pANDA were incubated in medium supplemented with 0.8 M NaCl and increasing concentrations (from 10 to 1000 μM) of (a) glycine betaine, (b, d) ectoine or (d, e) hydroxyectoine, respectively. The determination of the growth rates at different compatible solute concentrations allowed fitting according to the Monod equation, an equation describing the growth of cultures, which is based on the Michaelis-Menten equation [1]. The data shown is the mean and standard error mean of at least six biological replicates.

Suppl. Table 1 BLAST Results of the transporters found in the gene neighborhood of ectoine biosynthetic gene clusters are listed in Excel document 'Transporter blasts'.

Suppl. Table 2 Plasmids used and constructed in this study.

Plasmid	Description and mutations	Reference or source
pHSG575	low-copy-number plasmid; Cat ^R	[2]
pTrc99a	mid-copy-number plasmid; inducible with IPTG; Amp ^R	[3]
pAK405	plasmid for markerless gene deletions in <i>Sphingomonads</i> ; Kan ^R	[4]
pARO12	pHSG575 containing a 1,529 bp fragment with the coding region for <i>ectI</i> from <i>Hyphomonas neptunium</i> ATCC15444; Cat ^R	this study
pANDA1	pHSG575 containing a 1,343 bp fragment with the ORF of <i>ectU</i> from <i>Novosphingobium</i> sp. LH128; Cat ^R	this study
pLC19	pTrc99a encoding a codon-optimized version of <i>mscS</i> (1227 bp) from <i>Novosphingobium</i> sp. LH128 for the heterologous expression in <i>E. coli</i> (Accession Number: MK761064.1); Amp ^R	this study
pLC61	pAK405 derivative containing 781 bp upstream and 779 bp downstream of <i>ectU</i> for the markerless knock out of <i>ectU</i> in the <i>Novosphingobium</i> sp. LH128 chromosome; Kan ^R	this study
pLC62	pANDA1 derivative with a point mutation in the putative substrate binding site of EctU; E24A (GAA→GCA); Cat ^R	this study
pLC63	pANDA1 derivative with a point mutation in the putative substrate binding site of EctU; Y28A (TAC→GCC); Cat ^R	this study
pLC64	pANDA1 derivative with a point mutation in the putative substrate binding site of EctU; R65A (CGC→GCC); Cat ^R	this study
pLC65	pANDA1 derivative with a point mutation in the putative substrate binding site of EctU; Y131A (TAC→GCC); Cat ^R	this study
pLC85	pANDA1 derivative with a point mutation in the uptake system EctU; T57A (ACG→GCG); Cat ^R	this study
pLC86	pANDA1 derivative with a point mutation in the uptake system EctU; T158A (ACG→GCG); Cat ^R	this study
pLC87	pANDA1 derivative with a point mutation in the uptake system EctU; N253A (AAC→GCC); Cat ^R	this study
pLC88	pANDA1 derivative with a point mutation in the uptake system EctU; T374A (ACT→GCT); Cat ^R	this study
pLC99	pHSG575 containing a 1,294 bp fragment with the coding region for <i>ectE</i> from <i>Novosphingobium</i> sp. LH128; Cat ^R	this study
pLC101	pARO12 derivative with a point mutation in the uptake system EctI; T51A (ACA→GCA); Cat ^R	this study
pLC102	pARO12 derivative with a point mutation in the uptake system EctI; N52A (AAC→GCC); Cat ^R	this study
pLC103	pARO12 derivative with a point mutation in the uptake system EctI; Y56A (TAC→GCC); Cat ^R	this study
pLC104	pARO12 derivative with a point mutation in the uptake system EctI; W79A (TGG→GCG); Cat ^R	this study
pLC105	pARO12 derivative with a point mutation in the uptake system EctI; F246A (TTC→GCC); Cat ^R	this study
pLC106	pARO12 derivative with a point mutation in the uptake system EctI; S250A (TCC→GCC); Cat ^R	this study
pLC107	pARO12 derivative with a point mutation in the uptake system EctI; Q254A (CAG→GCG); Cat ^R	this study
pLC108	pTrc99a harboring the <i>ectE</i> gene (1241 bp) from <i>Novosphingobium</i> sp. LH128 under the inducible <i>lac</i> promoter for	this study

	its heterologous expression in <i>E. coli</i> ; Amp ^R	
pLC109	pARO12 derivative with a point mutation in the uptake system EctI; H256A (CAT → GCT); Cat ^R	this study
pLC110	pARO12 derivative with a point mutation in the uptake system EctI; F132A (TTC → GCC); Cat ^R	this study
pLC111	pARO12 derivative with a point mutation in the uptake system EctI; V259A (GTG → GCG); Cat ^R	this study
pLC112	pANDA1 derivative with a point mutation in the uptake system EctU; F162A (TTC → GCC); Cat ^R	this study
pLC113	pANDA1 derivative with a point mutation in the uptake system EctU; L159A (CTG → GCG); Cat ^R	this study
pLC114	pANDA1 derivative with a point mutation in the uptake system EctU; E155A (GAA → GCA); Cat ^R	this study
pLC126	pARO12 derivative with a point mutation in the uptake system EctI; Y136A (TAT → GCT); Cat ^R	this study

^aMutations are indicated with bold letters

Suppl. Table 3 Modified list of differentially expressed genes in *Novosphingobium* sp. LH128 biofilm in response to chronic and acute solute stress compared to non-stressed control biofilms [5]

Fold change	putative predicted gene product
chronic solute stress	
44.2	ectoine synthase (<i>ectC</i>)
29.6	ectoine hydroxylase (<i>ectD</i>)
16.7	L-2,4-diaminobutyric acid acetyltransferase (<i>ectA</i>)
11.1	small-conductance mechanosensitive channel (outside of the <i>ect</i> cluster)
10.4	4-aminobutyrate aminotransferase and related aminotransferase (<i>ectB</i>)
8.4	amino acid MFS transporter (<i>ectU</i>)
3.4	major facilitator family transporter (<i>ectE</i>)
acute solute stress	
46.8	ectoine synthase (<i>ectC</i>)
37.6	ectoine hydroxylase (<i>ectD</i>)
13.7	amino acid MFS transporter (<i>ectU</i>)
11.8	small-conductance mechanosensitive channel (outside of the cluster)
8.1	L-2,4-diaminobutyric acid acetyltransferase (<i>ectA</i>)
6.3	4-aminobutyrate aminotransferase and related aminotransferase (<i>ectB</i>)
3.9	major facilitator family transporter (<i>ectE</i>)
3.5	small-conductance mechanosensitive channel (<i>mscS</i>)

Suppl. Table 4 Strains used and constructed in this study.

Strain	Genotype	Reference or source
<i>H. neptunium</i> ATCC15444	wild type strain	[6, 7]
<i>Novosphingobium</i> sp. LH128	wild type strain	D. Springael; [5, 8]
LC5	<i>Novosphingobium</i> sp. LH128 Δ <i>ectU</i>	this study
<i>E. coli</i> MC4100	F ⁻ Δ (<i>argF-lac</i>)U169 <i>araD139 rpsL150 relA1 flbB5301 deoC1</i> <i>ptsF25 rbsR</i>	[9]
<i>E. coli</i> MKH13	F ⁻ MC4100 Δ (<i>putPA</i>)101 Δ (<i>proP</i>)2 Δ (<i>proU::spc</i>)608	[10]
<i>E. coli</i> FRAG1	F ⁻ <i>thi rha lac gal</i>	W. Epstein; [11]
<i>E. coli</i> MJF641	FRAG1 Δ (<i>mscL::cm</i>) Δ <i>mscS</i> Δ (<i>mscK::kan</i>) Δ (<i>ybdG::apr</i>) Δ <i>ybiO</i> Δ <i>yjeP</i> Δ <i>ynal</i>	[11]

Suppl. Table 5 Primers used in this study.

Plasmid/experiment	Primer name	Primer sequence ^a
pARO12	Hypho5_EcoRI_for	AAAGAATTCCCCGCAGGAGACTGCCTC
	Hypho3+5_HindIII_rev	AAAAAGCTTCCGTTTGGTCTTGATCATGG
pANDA1	EctU EcoRI for	AAAGAATTCCGCCGACGAAAGCACATC
	EctU HindIII rev	AAAAAGCTTGGCATCGATCGGCAAGAG
pLC19	MscS_Sphingo EcoRI for	AAAGAATTCATGGTCTTGGCAGGTAGCGCATG
	MscS_Sphingo HindIII rev	AAAAAGCTTTTATTATCATTAGGCGTGAACGG
pLC61	5 Sph 5'Del for	AAAGGTACCCAGGCTCGATCCTGATCTCG
	5 Sph 3'Del for	GAAAGTCCCCCAAGGTTGTTGGAAGATGTGCTTCGTCGGC
	5 Sph 5'Del rev	GCCGACGAAAGCACATCTTCCAACAACCTTGGGGGACTTTC
	5 Sph 3'Del rev	AAAGTTAACGCGTGGGTATGGTGGTTATC
pLC62	Mut_EctU_E24A_for	AACGCCACCGcATGGTTCGACTACG
	Mut_EctU_E24A_rev	GCCGATAGCCGAGGCGGC
pLC63	Mut_EctU_Y28A_for	ATGGTTTCGACgcCGGCATCTACGCATATG
	Mut_EctU_Y28A_rev	TCGGTGGCGTTGCCGATA
pLC64	Mut_EctU_R65A_for	GTTCTGATCgcCCCGCTCGGAGG
	Mut_EctU_R65A_rev	GAGATCGCGAACGTCGCC
pLC65	Mut_EctU_Y131A_for	AGGCGGCGAAgcCGGCGCGCG
	Mut_EctU_Y131A_rev	GTCGAGAACCCTTGACCATGC
pLC85	Mut_EctU_T57A_for	TGCGCTGGCGgCGTTCGCGAT
	Mut_EctU_T57A_rev	AACAGCGTCGCCTCCGCC
pLC86	Mut_EctU_T158A_for	CGAAGTCGGCgCGCTGGCGGG
	Mut_EctU_T158A_rev	AGAAAGCTGCCGTAGAAGCCGC
pLC87	Mut_EctU_N253A_for	CAACGTCGTAgcCTATACGCTGCTGAGCTACATG
	Mut_EctU_N253A_rev	AGCGCGATGACAAGGCCG
pLC88	Mut_EctU_T374A_for	CAACCTGTGCGgCTTCGCTGTT
	Mut_EctU_T374A_rev	TAGGCGATTGCAAAGCCC
pLC99	EctE EcoRI for	AAAGAATTCCGCCGACGAAAGCACATC
	EctE HindIII rev	AAAAAGCTTGGCATCGATCGGCAAGAG
pLC101	EctI_T51A_for	GGCGGTGCGCgCAAACAATTC
	EctI_T51A_rev	GAAAGCCCCGCGAGCCAG
pLC102	EctI_N52A_for	GGTCGCCACAgcCAATTCCGGCTACATGTTTCATCGG
	EctI_N52A_rev	GCCGAAAGCCCCGCGAGC
pLC103	EctI_Y56A_for	CAATTCGGCgCATGTTTCATCGGCGTC
	EctI_Y56A_rev	TTTGTGGCGACCGCCGAA

pLC104	EctI_W79A_for	GATGATCGGC gc GATCGTGGGCGACTTCATCG
	EctI_W79A_rev	AGCCACATGGCCGCCAGG
pLC105	EctI_F246A_for	CGGTTGGCTG gc CGCCGGTTTC
	EctI_F246A_rev	ACAATAAAGAGCCCCATGC
pLC106	EctI_S250A_for	CGCCGGTTTC gc CGTGGTCGG
	EctI_S250A_rev	AACAGCCAACCGACAATAAAGAGCC
pLC107	EctI_Q254A_for	CGTGGTCGGC gc GCCCCATGTG
	EctI_Q254A_rev	GAGAAACCGGCGAACAGC
pLC108	EctE_pTrc99a NcoI for	aaaccatggATGCTGAACGCCATCCTTC
	EctE_pTrc99a BamHI rev	aaaggatccGAAGATGTGCTTTTCGTCGG
pLC109	EctI_H256A_for	CGGCCAGCCC gc TGTGATGGTCCG
	EctI_H256A_rev	ACCACGGAGAAACCGGCG
pLC110	EctI_F132A_for	CATGATCGTT gc CCTGATCGCCTATG
	EctI_F132A_rev	ATGACGCCGGCAATCTTC
pLC111	EctI_V259A_for	CCAGCCCCAT gc GATGGTCCGC
	EctI_V259A_rev	CCGACCACGGAGAAACCG
pLC112	EctU_F162A_for	GCTGGCGGGC gc CTGTGCGGGC
	EctU_F162A_rev	GTGCCGACTTCGAGAAAGCTGC
pLC113	EctU_L159A_for	AGTCGGCACG gc GGCGGGCTTC
	EctU_L159A_rev	TCGAGAAAGCTGCCGTAG
pLC114	EctU_E155A_for	CAGCTTTCTC gc AGTCGGCACG
	EctU_E155A_rev	CCGTAGAAGCCGCGCTTC
pLC126	EctI_Y136A_for	CCTGATCGCC gc TGCCGCCGCC
	EctI_Y136A_rev	AAAACGATCATGATGACGCCG

Transcriptional analysis *H. neptunium*

TA_Hypho_1_for	GAGACCATGGATGCCTGGTC
TA_Hypho_1_rev	GATTTGCTGCAGGCCGAG
TA_Hypho_2_for	GTGAGGCTTGATCGCGC
TA_Hypho_2_rev	CGAATTCGTATCCAGTGGCGGAC
TA_Hypho_3_for	GAAACATTCTTGCCCGCCAG
TA_Hypho_3_rev	GTTTCAGCTCGGGATGGTTG
TA_Hypho_4_for	CCTCAAAATTCTTGCGGACGC
TA_Hypho_4_rev	GGGTAAAGGTCTTGTTCTGTTTC
TA_Hypho_5_for	GGTTCGGTTGTGATCTTTGATTGC
TA_Hypho_5_rev	CTCGGTCCAGGCCCATTTG
TA_Hypho_6_for	GTTGCCATCGTCTCGGTCATC
TA_Hypho_6_rev	GAAAGCCCGCCGAATAGG
TA_Hypho_7_for	GATCGCAGGCGCCTTTCTC
TA_Hypho_7_rev	CAGGCCTGTCTGGTAGGTG
TA_Hypho_8_for	CATGAGAGCATCTATGAGGGCC
TA_Hypho_8_rev	CTCGGCGGTCTGGTATTAG

Transcriptional analysis *Novosphingobium* sp. LH128

TA_hyp-EctR for	GCAATTGCGACCTGCAAGG
TA_hyp-EctR rev	GAACGACAAGCGGCAGATCC
TA_EctR-EctA for	GATTTTCCAGATCGGCGGC

TA_EctR-EctA rev	GCGAAATCGCTGCACTGAAG
TA_EctA-EctB for	GATGAACTGGTCTCGCTGC
TA_EctA-EctB rev	CGTCGCTGCCGATGTAATC
TA_EctB-EctC-EctD for	CATTCTGGAAGAGGCCGTCG
TA_EctB-EctC-EctD rev	CGGAAACAGCTGGGGTTC
TA_EctD-Ask_Ect for	GCAACACGATGCATGGTTCC
TA_EctD-Ask_Ect rev	GCGCAAACATCTCGGCATTG
TA_Ask_ect-EctE for	CAAGAGCTCCAACGCCAAC
TA_Ask_ect-EctE rev	GGTGCCGACAAGACCGATC
TA_EctE-EctU for	CTGTTCGTCGCAGTCTGCG
TA_EctE-EctU rev	CGCCATCATCACGATCGTC
TA_EctU-MscS for	GATGCCCGCCTACTTGATG
TA_EctU-MscS rev	CTGACGATGATGATGGCTGC
TA_MScS-hyp for	CAAGGACAAGACCATGCTGG
TA_MScS-hyp rev	GTAAATCAGGGCCTCGGTCTG
TA_hyp-mp for	CAGCGCAAAGCAGGAACAG
TA_hyp-mp rev	CCGTCTCATCTCGCTGAAGTC
TA_mp-cit for	GAATGTGCGTGCTCTCGG
TA_mp-cit rev	CCAGAGCGGCGATATTGTTC
qRT-PCR primers <i>H. neptunium</i>	
Hn_gyrB_for	GACATCAATCCCGAAGCCCC
Hn_gyrB_rev	GTCATCGGTGTCGCCGATG
Hn_ectA_for	GGACAGACATCGTCCCAGACC
Hn_ectCD_for	CCCCAATGATGATGGCCTGTG
Hn_ectE_for	GTTCTGGTGGCCGCACTG
Hn_ectU_for	GGCAACAGGCAAGCGAAAG
qRT-PCR primers <i>Novosphingobium</i> sp. LH128	
Ns_gyrB_for	CTCCTACGGTGCCGATTCCG
Ns_gyrB_rev	CCGAAACCTCGAACACCATG
qRT-PCR ectA Sphingo for	GACTACCTCGCCGGTCC
qRT-PCR ectD Sphingo for	CATGACGAGAACGGTGCC
qRT-PCR ectE Sphingo for	GGTTCCACTTCGTGATGC
Ns_ectU_for	CTTTTCCCCGGGGACACG
qRT-PCR mscS Sphingo for	GTCTCGCGCCTTTTGAAC

^aMutations are indicated with bold lowercase letters

References

1. **Monod J.** The growth of bacterial cultures. *Annu Rev Microbiol Microbiol* 1949;3:371–394.
2. **Takeshita S, Sato M, Toba M, Masahashi W, Hashimoto-Gotoh T.** High-copy-number and low-copy-number plasmid vectors for *lacZ* alpha-complementation and chloramphenicol- or kanamycin-resistance selection. *Gene* 1987;61:63–74.
3. **Amann E, Ochs B, Abel KJ.** Tightly regulated *tac* promoter vectors useful for the expression of unfused and fused proteins in *Escherichia coli*. *Gene* 1988;69:301–315.
4. **Kaczmarczyk A, Vorholt JA, Francez-Charlot A.** Markerless gene deletion system for Sphingomonads. *Appl Environ Microbiol* 2012;78:3774–3777.
5. **Fida TT, Breugelmans P, Lavigne R, Coronado E, Johnson DR, et al.** Exposure to solute stress affects genome-wide expression but not the polycyclic aromatic hydrocarbon-degrading activity of *Sphingomonas* sp. strain LH128 in biofilms. *Appl Environ Microbiol* 2012;78:8311–8320.
6. **Badger JH, Eisen JA, Ward NL.** Genomic analysis of *Hyphomonas neptunium* contradicts 16S rRNA gene-based phylogenetic analysis: implications for the taxonomy of the orders ‘Rhodobacterales’ and ‘Caulobacterales’. *Int J Syst Evol Microbiol* 2005;55:1021–1026.
7. **Leifson E.** *Hyphomicrobium neptunium* sp. n. *Antonie Van Leeuwenhoek* 1964;30:249–256.
8. **Bastiaens, L, Springael D, Wattiau P, Harms H, et al.** Isolation of adherent polycyclic aromatic hydrocarbon (PAH)-degrading bacteria using PAH-sorbing carriers. *Appl Environ Microbiol* 2000;66:1834–1843.
9. **Casadaban MJ.** Transposition and fusion of the *lac* genes to selected promoters in *Escherichia coli* using bacteriophage Lambda and Mu. *J Mol Biol* 1976;104:541–555.
10. **Haardt M, Kempf B, Faatz E, Bremer E.** The osmoprotectant proline betaine is a major substrate for the binding-protein-dependent transport system ProU of *Escherichia coli* K-12. *Molecular & general genetics*, 1995, pp. 783–786.
11. **Edwards MD, Black S, Rasmussen T, Rasmussen A, Stokes NR, et al.** Characterization of three novel mechanosensitive channel activities in *Escherichia coli*. *Channels* 2012;6:272–281.

5.2.7. *Draft manuscript* The MarR-type regulator from *Novosphingobium* sp. LH128

Czech L, Höppner A, Kobus S, Smits SHJ, Bremer E. Crystal structure and *in vitro* analysis of the MarR-type regulator EctR involved in ectoine biosynthesis. *draft manuscript*.

The next chapter includes a draft manuscript with the work on the MarR-type regulator EctR from *Novosphingobium* sp. LH128. During my PhD thesis I constructed the expression plasmid, overproduced and purified the regulator and performed *in vitro* DNA electrophoretic shift mobility assays (EMSA). Furthermore, I constructed and analyzed the genetic disruption of the *ectR* gene in *Novosphingobium* sp. LH128. S. H. J. Smits, S. Kobus and A. Höppner conducted the crystallographic analysis including SAXS analysis and performed HPLC-MALS. E. Bremer designed the study and we discussed the data. I performed all bioinformatical analysis, prepared all figures and wrote this draft manuscript.

Adjusting ectoine biosynthesis: Crystallographic and functional analysis of the EctR regulator

Laura Czech¹, Stefanie Kobus², Astrid Höppner²,
Sander Smits² and Erhard Bremer^{1,3}

¹Laboratory for Microbiology, Department of Biology, Philipps-University Marburg, Marburg, Germany

²Institute of Biochemistry, Heinrich-Heine University Düsseldorf, Düsseldorf, Germany

³Center for Synthetic Microbiology, Philipps-University Marburg, Marburg, Germany

Running title: EctR regulator of ectoine biosynthesis

Abstract

Upon osmotic stress, members of all three domains of life were found to produce the cytoprotectants and chemical chaperones, ectoine and 5-hydroxyectoine, to counteract the osmotically instigated outflow of water. The expression level of the underlying biosynthetic genes [*ectABC(D)*] increases in response to increases in the external salinity and must be tightly controlled to avoid wasteful production of ectoines. Here, we focus on the MarR-type regulator EctR, found in 22% of putative ectoine producing bacteria. Phylogenetic analysis revealed a rather restricted occurrence of *ectR* in the vicinity of ectoine gene clusters of *Proteobacteria*. Using EctR from the *Alphaproteobacterium* *Novosphingobium* sp. LH128, we obtained a crystal structure at 2.2 Å resolution. Structural and biochemical analysis revealed an unusual tetrameric assembly of two head-to-head homodimers positioning the winged-helix-turn-helix DNA-binding domains at the outside of the protein complex. The *ectR* gene of *Novosphingobium* sp. LH128 is located upstream and divergent of the *ect* gene cluster. *In vitro* binding analysis revealed two individual binding regions of EctR upstream of the hypothetical sigma-70-type promoter of *ectR* and downstream of the potential sigma-70-type promoter in front of *ectA*. Inspection of these regions highlight two pseudopalindromic sequences as potential binding sites for the EctR regulator.

Keywords: ectoine, regulation, MarR regulator, structural analysis, compatible solutes, DNA binding protein

Introduction

Many microorganisms prevent the outflow of water resulting from elevated external salt concentrations through the active amassment of small, often zwitterionic compounds, so called compatible solutes [1–4]. Two of the best studied compatible solutes are the chemical chaperones ectoine and its hydroxylated derivative 5-hydroxyectoine [5–7]. These stress protectants can be either taken up via specialized transporters or synthesized *de novo* [8–13]. During biosynthesis, ectoine is formed from the central metabolic hub L-aspartate- β -semialdehyde through a three-step enzymatic route performed by EctABC [14, 15]. The ectoine hydroxylase EctD is further required for the production of 5-hydroxyectoine from ectoine [16–19]. Ectoine producing microorganisms have been detected in ten different bacterial and two archaeal phyla [5, 20]. Even a selected group of halophilic *Eukarya* has recently been identified to produce this osmoprotectant [21–25]. The core genes for ectoine/5-hydroxyectoine biosynthesis are mostly encoded in an operon under the control of an osmotically inducible promoter [5, 11, 26–30]. Detailed bioinformatic analysis of the biosynthetic gene clusters revealed a rather stable organization of these core genes (*ectABC*) that are often accompanied by the gene encoding the ectoine hydroxylase (*ectD*) and a specialized aspartokinase (*ask_ect*) (Fig. 1a) [5, 31, 32]. Moreover, genome-mining studies identified the broad occurrence of genes involved in ectoine transport encoded in close vicinity of the ectoine biosynthetic gene clusters (Czech *et al.*, *manuscript in preparation*) and the presence of a MarR (Multiple antibiotic resistance Regulator)-type regulator [5, 32]. Trotsenko and co-workers studied this MarR-type regulator, called EctR, present in the genetic neighborhood of the *ect* gene cluster in various aerobic, moderately halophilic methylotrophic bacteria [33, 34]. In *Methylobacterium alcaliphilum* 20Z, the gene for EctR [(Ma)EctR] was found to be transcribed upstream and divergently of the *ectABC-ask_ect* operon [34]. Studies on the influence of the (Ma)EctR regulator on the activity of the sigma-70-type *ectAp₁* and *ectAp₂* promoters in wild type *M. alcaliphilum* 20Z and *ectR* deletion strains suggested that EctR functions as a repressor for *ectABC-ask_ect* transcription but is not controlling the osmotic induction of the *ect* biosynthetic genes [34]. Biochemical analysis revealed that EctR forms a homodimer that binds to two pseudopalindromic sequences in front of *ectA* and *ectR*, also suggesting an autoregulatory function [34]. In *Vibrio cholera* another MarR-type regulator, named CosR, has been demonstrated to negatively regulate ectoine biosynthesis, compatible solute uptake and motility, and at the same time activate biofilm formation [35]. Also after deletion of *cosR*, expression of ectoine biosynthetic genes remained osmotically inducible [35]. This phenomenon has also been observed for the OmpR family regulator GlnR in *Streptomyces coelicolor*, which serves a global regulator and regulates mostly nitrogen metabolism-associated genes and in addition represses ectoine gene expression [36].

Transcription factors belonging to the MarR-family typically form homodimers and bind to inverted or palindromic repeats in the DNA sequence with a winged helix-turn-helix motif that regularly consists of two β -strands and two α -helices [37–40]. These types of regulators control the gene expression of various physiological tasks, including adjustment of metabolic pathways, virulence genes, and determinants for multi-drug resistance [38, 41]. Most regulators of this superfamily are encoded upstream and divergently of the controlled gene and also possess an autoregulatory function [39]. The binding of

MarR-family regulators to the intergenic region often controls the expression of both genes by affecting the interaction of RNA polymerase with the gene promoters [39, 40, 42]. They can either act as activators or repressors, and often respond to changes in the protein oxidation or to binding of a small ligand molecule. This in turn modulates the DNA binding properties of the regulator, resulting in altered expression of the divergent genes [38, 39, 43]. Structural and biochemical analyses of ligand binding to numerous MarR homologs are converging to identify a shared ligand-binding *hot-spot* [39]. For many regulatory proteins involved in the control of osmotically responsive genes including the EctR-type regulators, the sensed signal is still unknown [34]. Other regulators, such as the MarR-type regulator GbsR that controls uptake and biosynthesis of the compatible solute glycine betain from its precursor choline in *Bacillus subtilis* [44, 45] or the GntR-type regulator EnuR, involved in the control of the genes required for ectoine utilization as nutrients in *Ruegeria pomeroyi* [46, 47], bind intermediates of the controlled pathway and thereby change the DNA binding properties of the regulator. For the regulators of the MarR-family, CosR from *V. cholera* and BusR from *Lactococcus lactis* (controlling glycine betaine uptake), it is assumed that they respond to changes in the ionic strength of the cytoplasm, when cells are confronted with elevated external salinities [35, 48].

Here we used the MarR-type regulator EctR that is encoded upstream of the ectoine biosynthetic genes in *Novosphingobium* sp. LH128 to elucidate functional and structural features of this transcription factor. We obtained a high-resolution crystal structure that, in conjunction with our biochemical analyses, revealed a tetrameric assembly of the EctR regulator with the typical winged helix-turn-helix DNA-binding motifs exposed at the top and at the bottom of the EctR tetrameric complex. Electrophoretic mobility shift assays showed specific binding of EctR to the intergenic region between *ectR* and *ectA* and systematic truncations of the tested intergenic DNA fragments allowed the localization of potential DNA binding sequences. The data presented raise the hypothesis, that the DNA might bend around the EctR tetramer upon binding of both potential binding sites. Furthermore, a detailed phylogenomic analysis underlines a habitat- and phylum-specific distribution of the EctR regulator among putative ectoine producing bacteria.

Results

Overproduction, purification, and oligomeric state of the EctR regulator from *Novosphingobium* sp. LH128. Bioinformatic analysis on the presence of the MarR-type regulator, EctR, within the neighborhood of ectoine biosynthetic gene clusters in all fully sequenced genomes of the JGI IMG database (DOE Joint Genome Institute) [49], revealed its occurrence in 97 putative ectoine producing organisms in the vicinity of the 437 bacterial *ect* gene clusters found in total in all fully sequenced genomes [5]. One of these organisms is the *Alphaproteobacterium Novosphingobium* sp. LH128 that has been isolated as a polycyclic aromatic hydrocarbon (PAH)-utilizing bacterium from PAH-contaminated soil and sludge samples [50]. Its ectoine/5-hydroxyectoine biosynthetic gene cluster consists of the *ectABCD_ask-ect* genes that are followed by genes for a specific ectoine/5-hydroxyectoine exporter (*ectE*), an importer (*ectI*) and an MscS-like mechanosensitive channel (Fig. 1a) (Czech *et al.*, manuscript in preparation). The gene encoding

the putative regulator, (*N_s*)EctR, is located 300 bp upstream and antilinear of the *ect* gene cluster (Fig. 1a). Herein, we used this MarR-type regulator for biochemical, functional and structural studies.

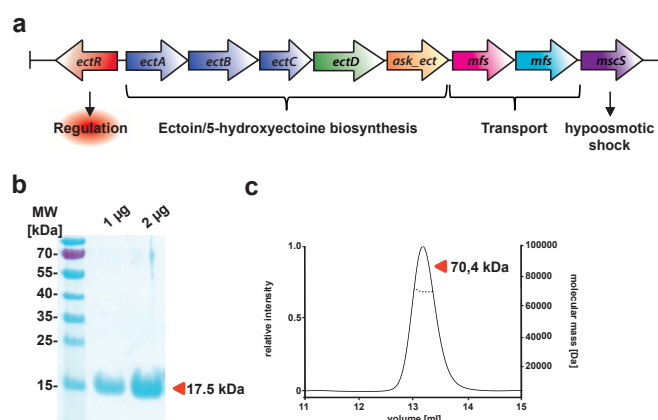


Fig. 1 The EctR regulator from *Novosphingobium* sp. LH128. **a** Schematic illustration of the *ect* gene clusters from *Novosphingobium* sp. LH128. **b** SDS gel of the purified recombinant EctR protein. EctR was overexpressed in *E. coli* and purified by *Strep*-tag II affinity chromatography. After purification, 1 and 2 µg of the regulator protein were applied to a 15% polyacrylamide SDS gel that was run for 1 h at 30 mA. The prestained PageRuler Protein Ladder (Thermo Fisher) served as a marker for protein size. The calculated theoretical molecular weight of *Strep*-tag II-EctR is 18 kDa. **c** HPLC-MALS analysis of the recombinant EctR protein to determine the oligomeric state of the EctR protein. 100 µl of the purified *Strep*-tag II-EctR protein (2 mg ml⁻¹) were applied to the Bio SEC-5 HPLC column and the detected signal corresponds to a mass of 70.4 kDa.

We constructed an expression vector harboring a codon-optimized synthetic version of the (*N_s*)*ectR* gene. The expression plasmid additionally contained a sequence encoding a *Strep*-tag II affinity peptide fused to the (*N_s*)*ectR* gene at the 5' end. This enables the production of a recombinant fusion protein [*Strep*-tag II-(*N_s*)EctR] when it is heterologously expressed in *Escherichia coli* and allows its purification by affinity chromatography (Fig. 1b). The (*N_s*)EctR protein possesses 151 amino acids with a calculated theoretical molecular mass of 16.3 kDa, and 17.5 kDa when it is fused to *Strep*-tag II peptide. The calculated theoretical pI is 8.25. The oligomeric state of the purified fusion protein was assessed using high-performance liquid chromatography coupled to multi-angle light scattering detection (HPLC-MALS). This analysis revealed a molecular mass of 70.4 kDa for the *Strep*-tag II-(*N_s*)EctR protein in solution, which indicated that this regulatory protein forms a tetramer in solution (Fig. 1c).

Crystallization, overall fold and structural features of the (*N_s*)EctR regulator. Crystals of the (*N_s*)EctR protein were obtained using commercial screens and by optimizing the composition of the crystallization solution. Crystallization, structural data acquisition and analysis was performed by our collaboration partners A. Höppner, S. Kobus and S. H. J. Smits at the University of Düsseldorf. The obtained crystals diffracted to 2.2 Å and were phased using crystals that contained the heavy metal mercury.

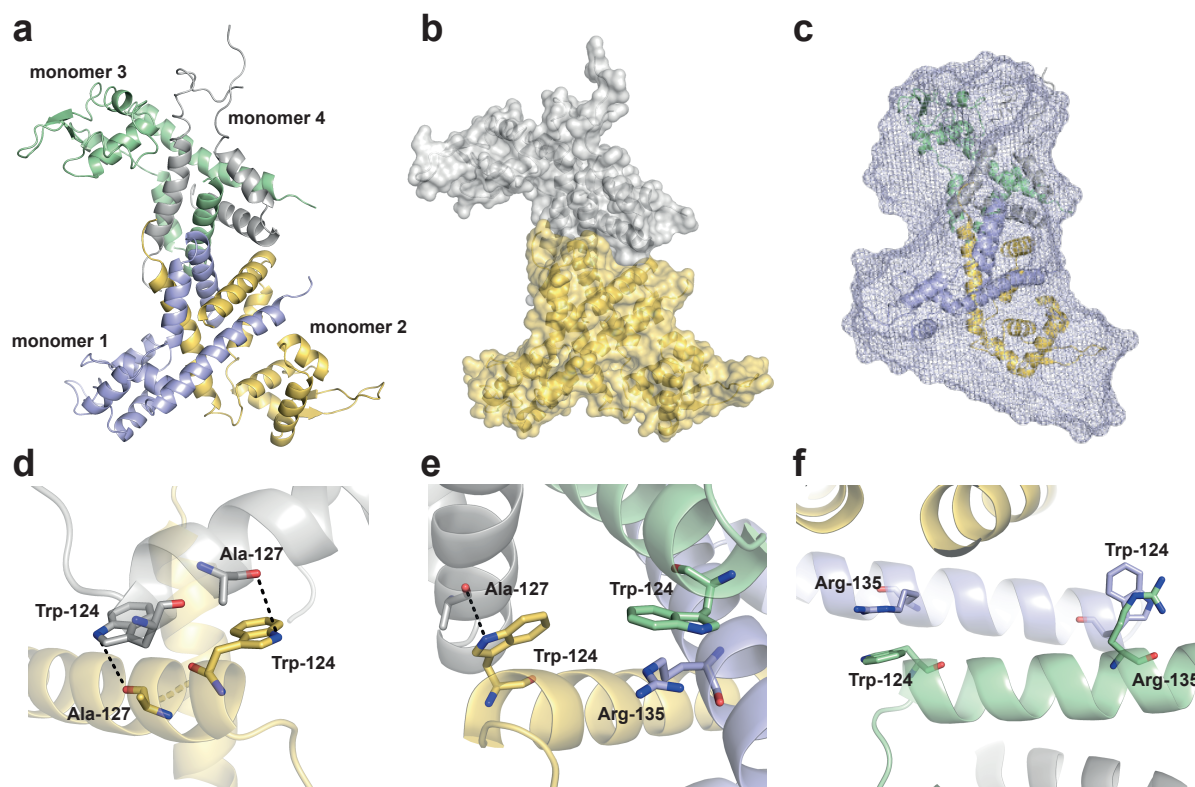


Fig. 2 Crystal structure and tetrameric assembly of the EctR regulator from *Novosphingobium* sp. LH128. **a** Overall assembly of the crystallized EctR tetramer, consisting of two homo-dimers. Each monomer is shown in a different color. **b** Surface representation of the EctR regulator. **c** SAXS structure of the EctR tetramer. **d-f** Residues that are potentially involved in the formation of the EctR tetramer are shown in stick representation. Residue Trp-124 of monomer 2 (yellow) contacts Ala-127 of monomer 4 (grey)(**d**), while Trp-124 and Arg-135 of monomer 1 (blue) and 3 (green), respectively, interact via a cation- π interaction (**e**, **f**).

The (N_3)EctR protein is a tetramer in solution as demonstrated by the HPLC-MALS analysis (Fig. 1c). A. Höppner, S. Kobus and S. H. J. Smits inspected the crystal packing and analyzed the respective interactions to elucidate the functional tetramer within the EctR crystal structure. This analysis showed that the (N_3)EctR tetramer in the crystal consists of two homo-dimers arranged in a head-to-head orientation (Fig. 2a, b). The arrangement of the two dimers is not symmetrical, as the upper dimer (consisting of monomer 3 and 4) is slightly tilted (Fig. 2a, b). Surface representation of the (N_3)EctR tetramer revealed a tight organization of the two dimers (Fig. 2b). To substantiate, that the (N_3)EctR regulator forms a tetrameric complex, A. Höppner, S. Kobus and S. H. J. Smits performed small-angle X-ray scattering (SAXS) analysis. This experiment verified the tetrameric assembly of (N_3)EctR protein in solution (Fig. 2c). The tetramer might be stabilized by interactions between Trp-124/Ala-127 of monomer 2 (yellow) and Trp-124/Ala-127 of monomer 4 (grey), respectively (Fig. 2d, e). However, the corresponding Trp residues in the other monomer subunits, rather position close to an Arg residue (Arg-135) in the opposing monomer, respectively (Fig. 2d, e). These residues might interact through a cation- π interaction between the aromatic, indole ring of the Trp-124 side chain and the positive charge of the guanidino group of Arg-135 (Fig. 2e, f). The distances between the side chains of Trp-124 and Arg-135 vary between 3.5 and 4.1 Å (Fig. 2e, f), which fits nicely to the typical distance required for the formation of cation- π within a peptide chain, as they occur within a distance of 6 Å [51].

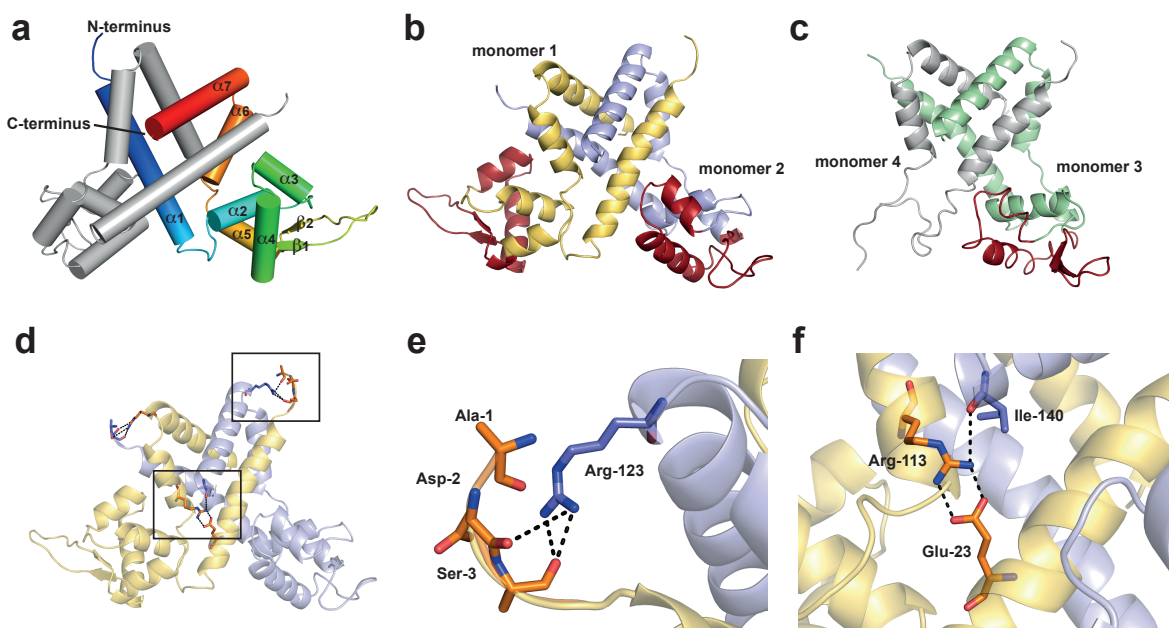


Fig. 3 Structural assembly of the two dimers forming the tetrameric EctR. **a-c** The overall fold of monomer 1 (grey) and 2 (rainbow) is shown and labeled in panel (a), and the DNA binding motifs [winged helix-turn-helix (wHTH)] are highlighted in red for monomer 1 (yellow) and 2 (blue) in (b) and monomer 3 (green) and 4 (grey) in panel (c). The beta sheets $\beta 1$ and $\beta 2$ form the wing, and the helices $\alpha 3$ and $\alpha 4$ contain the HTH motif of the DNA binding domain of EctR. **d-f** Residues that serve as contacts between monomer 1 (yellow) and 2 (blue) are highlighted (d). Ala-1, Asp-2 and Ser-3 of monomer 1 contact Arg-123 of monomer 2 (e). Arg-113 (monomer 1) forms a contact with Glu-23 (monomer 1) and Ile-140 (monomer 2).

The structure of one monomer of the (*N_s*)EctR protein consists of seven α -helices ($\alpha 1$ - $\alpha 7$) and two β -helices ($\beta 1$ and $\beta 2$) (Fig. 3a). The two β -strands form a wing structure that accompanies the helix-turn-helix (HTH) motif formed by the $\alpha 3$ and $\alpha 4$ helices, which jointly function as the DNA binding domains (shown in red) (Fig. 3b, c). This winged HTH arrangement in EctR is typical for DNA binding proteins belonging to the MarR-type family of regulators (Fig. 3a-c) [39]. It must be noted, that only the winged HTH-motif of monomer 2 (yellow) is fully resolved in the crystal structure (Fig. 3b). In all other monomers the wing is either only partially shown as β -sheets (monomer 3) or as loops (monomer 1 and 4) (Fig. 3b, c). Especially monomer 4 (grey) is only resolved in fragments since only helix 1 and the helices 6 and 7 could be solved (Fig. 3c). Several attempts to optimize the resolution of this part of the crystal structure have been made, but resolution of monomer 4 was always weak. Possible interactions within the dimers are shown in Fig. 3d-e. At the N-terminal end of monomer 1 (blue), the positive side chain of Arg-123 might interact with the negatively charged of the amino group of Ser-3 of monomer 2 (yellow) (Fig. 3e). Furthermore, in the core of the dimer Arg-113 of monomer 2 might interact with Glu-23 of the same monomer and Ile-140 of monomer 1 (Fig. 3f).

Functional analysis of (*N_s*)EctR through *in vitro* DNA binding assays. First we aimed to identify potential promoter regions of the *ectR* gene and the *ect* biosynthetic operon. Inspection of the intergenic region led to the hypothesis that in the case of *ectR* a sigma-70-like promoter might be located 60 bp upstream of *ectR* and its -35 region (TTGATG) and -10 region (AATATI) possesses a short 16 bp spacer.

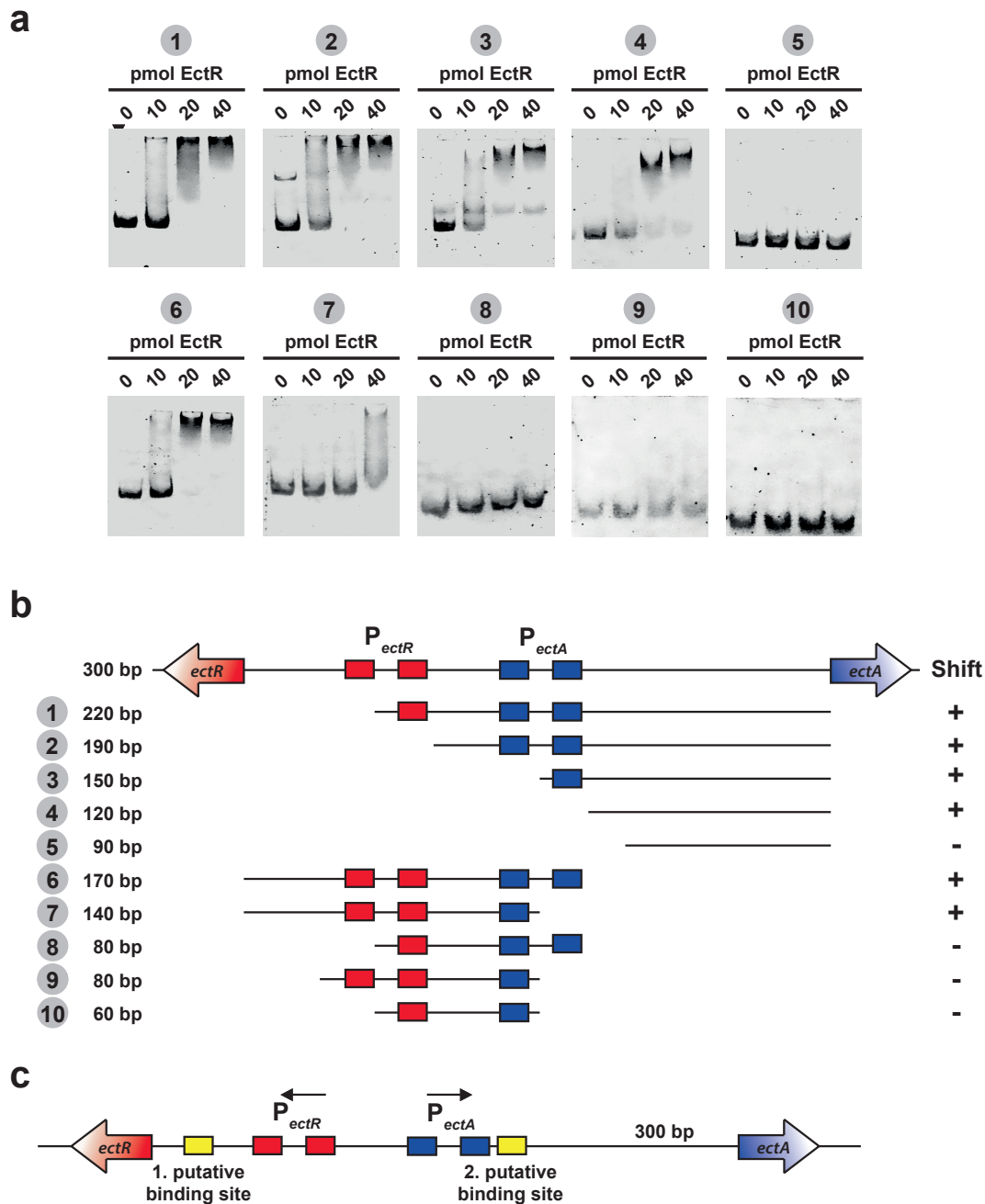


Fig. 4 Binding of recombinant EctR protein to the intergenic region between the *ectR* gene and the *ect* operon. **a** EMSAs of Cy781-fluorescently labeled DNA fragments (2 pmol) ranging between 220 and 60 bp were performed with purified *Strep*-tag II-EctR in the presence of 0.1 μ g herring sperm DNA. In each gel, the leftmost lane represents the labeled DNA probe alone. Increasing amounts of recombinant *Strep*-tag II-EctR protein (10, 20, and 40 pmol) were added to the assay mixture. Samples were applied to a 6% polyacrylamide TBE gel, run for 2 h at 120 V. **b** Schematic illustrations of the DNA fragments used for EMSAs shown in panel (a). The *ectR* gene and its putative promoter is shown in red, the *ectA* gene and the corresponding promoter are depicted in blue. In the right lane a positive EMSA shift is indicated by a plus (+), while no shift of the DNA-EctR complex is shown by a minus (-). **c** Summary of the EMSA assay that led to the identification of potential DNA binding sites (yellow) of EctR.

The potential promoter of the *ect* gene cluster is located 126 bp upstream of *ectA* and consists of a -35 region (T⁺TGCAA) and -10 region (TATGT⁺T) with a 16 bp spacer and thereby also resembles the features of a sigma-70-type promoter. A perfect sigma-70 promoter recognized by the *E. coli* house-keeping sigma factor consists of T⁺TGACA in the -35 region and TATAAT in its -10 box normally linked by a 17 bp

spacer [52]. Both potential promoters in the intergenic region between *ectR* and *ectA* in *Novosphingobium* sp. LH128 were also identified as potential promoter regions by *in silico* promoter prediction analysis using the PromoterHunter online tool (<http://www.phisite.org/>) but still require experimental verification (Supplementary Fig. S1) [53, 54].

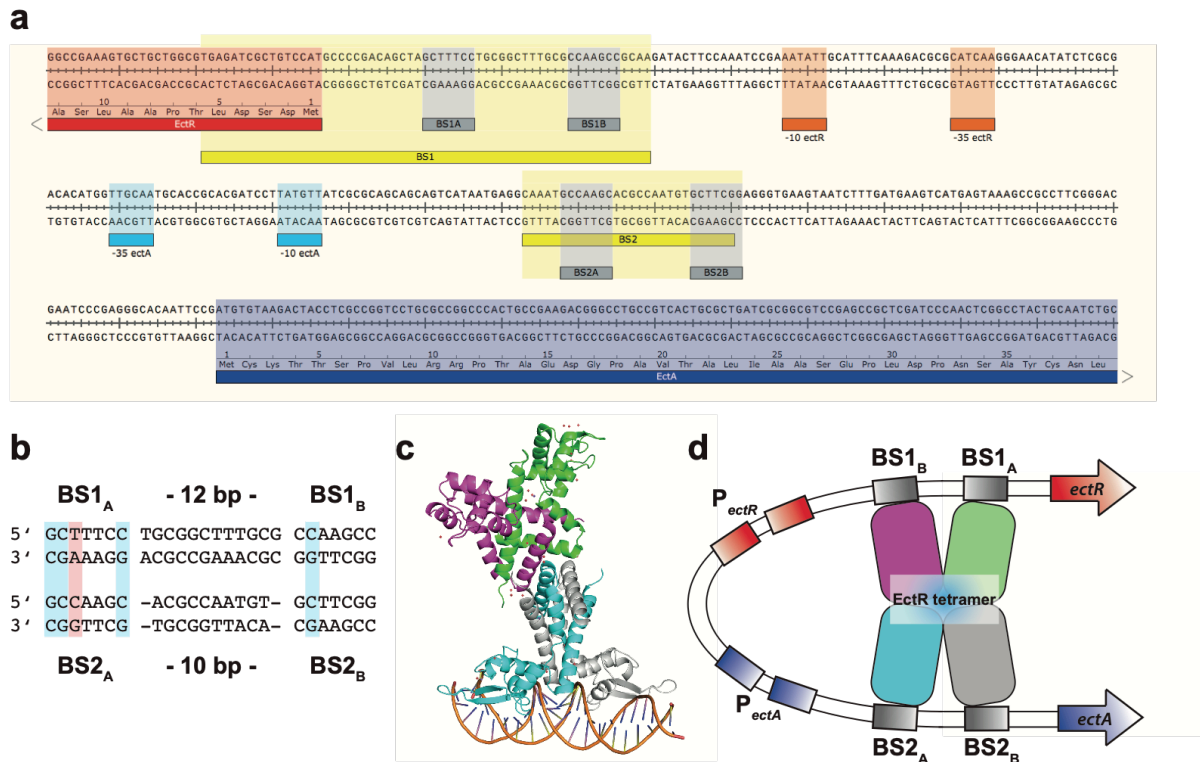


Fig. 5 Intergenic region between *ectR* and *ectA*. **a** Putative promoter regions of *ectR* and *ectA* are highlighted in red and blue, respectively. Regions that might contain DNA elements, to which the EctR regulator binds are shown in yellow. BS1 in front of *ectR* and BS2 upstream of *ectA*. Potential pseudopalindromic sequences are highlighted in grey. **b** DNA sequences of the pseudopalindromes that potentially serve as binding sites for the EctR protein. Minor deviations between BS1 and BS2, where a C/G is exchanged to G/C are highlighted in blue, while major deviations from A/T to C/G are shown in red. **c** Model of the EctR regulator bound to DNA. **d** Schematic illustration of the working hypothesis, how the tetrameric EctR complex might bind the BS1 and BS2 regions at the same time.

The recombinant (*N_s*)EctR protein was further used for *in vitro* analysis to prove the specific binding of (*N_s*)EctR to the DNA of the intergenic region between *ectR* and the *ect* operon (Fig. 1a). Electrophoretic mobility shift assay (EMSA) performed with a fluorescently labeled DNA fragment consisting of 220 bp of the intergenic region between *ectR* and *ectA* (fragment 1) revealed a clear shift upon addition of 20 pmol of the *Strep*-tag II-(*N_s*)EctR protein to the assay mixture (Fig. 4a, b). Incubation of *Strep*-tag II-(*N_s*)EctR with unlabeled specific DNA fragments (at a 5 to 15-fold molar ratio) abolished the retardation of the labeled DNA (Supplementary Fig. S2). These results suggested a specific interaction of the (*N_s*)EctR regulator with the DNA region between the promoter regions of the *ectR* gene and ectoine biosynthetic genes (Supplementary Fig. S2). To narrow the sequence to which (*N_s*)EctR binds, systematic truncations of this DNA fragment were analyzed. Four different truncations (fragment 2-5) positioned upstream of *ectA* were tested ranging from 190 bp to 90 bp DNA fragments. The fragments 2

and 3 with a length of 190 and 150 bp showed a clear retardation of the DNA-protein complex in the EMSA gel, when 20 or 40 pmol of the *Strep*-tag II-(N₃)EctR protein were added (Fig. 4a, b). While the 120 bp fragment (number 4) still shifted when 20 pmol of the *Strep*-tag II-(N₃)EctR protein were applied to the assay mixture, the 90 bp truncation fragment (number 5) showed no shift of the fluorescently labeled DNA fragment in presence of up to 40 pmol *Strep*-tag II-(N₃)EctR (Fig. 4a, b). This indicates that the binding site of the (N₃)EctR regulator might potentially be located within these 30 bp downstream of the potential *ect* promoter and upstream of *ectA* (Fig. 4 c, 5a).

In the next step, we tested DNA fragments upstream of the potential *ectA* promoter to elucidate a potential second binding site of EctR in front of the *ectR* gene. The length of the tested truncations in the DNA region between the start of the *ectR* gene and the potential *ectA* promoter ranged between 170 and 60 bp (fragment 6-10). While fragment 6 and 7 (170 and 140 bp) still revealed a shift in the EMSA when 20 or 40 pmol of *Strep*-tag II-(N₃)EctR were added, the 80 and 60 bp fragments (number 8-10) did not reveal a retardation in the gel of the DNA-regulator assay mixtures (Fig. 4a, b). Again these findings indicate that a potential binding site of the EctR regulatory protein is located in a 60 bp region in between the start of the *ectR* gene and the its putative promoter (Fig. 4c, 5a). The DNA sequence of the intergenic region between *ectR* and *ectA* is presented in Fig. 5a - the putative *ectR* and *ectA* promoters are highlighted in red and blue, respectively, and the DNA sequences, where the potential EctR binding sites are located are marked in yellow. Inspection of these regions led to the assumption that two pseudopalindromic sequences might function as the binding sites for the EctR regulator (Fig. 5b). Binding site 1 (BS1) upstream of *ectR* might be GCTTTCC and CCAAGCC separated by a 12 bp spacer, while binding site 2 (BS2) upstream of *ectA* might be GCCAAGC and GCTTCGG interlinked by a 10 bp spacer (Fig. 5b). Altogether, these findings lead to the hypothesis, that the EctR tetramer might be able to bind two binding sites within the intergenic region of *ectR* and *ectA* which might eventually result in a loop formation of the DNA (Fig. 5 c, d).

Genetic disruption of the *ectR* gene results in a lower production of 5-hydroxyectoine. In order to elucidate the function of EctR with respect to the regulation of the *ect* operon, we constructed a markerless *ectR* gene deletion mutant via homologous recombination in *Novosphingobium* sp. LH128 [55]. Using this strain, we measured the accumulation of produced 5-hydroxyectoine in *Novosphingobium* sp. LH128 wild type cells and cells of the *ectR* deletion mutant, when they were grown in 0 M NaCl and 0.3 M NaCl, respectively. Under both tested salinities, the *ectR* mutant strain accumulated less 5-hydroxyectoine compared to the wild type strain (3-fold at 0 M NaCl and 1.4-fold at 0.3 M NaCl) (Fig. 6a). This pattern was also found, when we determined the external amount of 5-hydroxyectoine in the medium supernatant. The supernatant of the *ectR* deletion strain showed 1.6-fold at 0 M NaCl and 1.4-fold at 0.3 M NaCl less extracellular 5-hydroxyectoine than the wild type strain (Fig. 6b). However, both strains exhibited a salt-induced production of 5-hydroxyectoine. The intracellular production of 5-hydroxyectoin in wild type strain increased by 5.4-fold, compared to 12.5-fold in the *ectR* mutant when 0.3 M NaCl was present in the medium (Fig. 6).

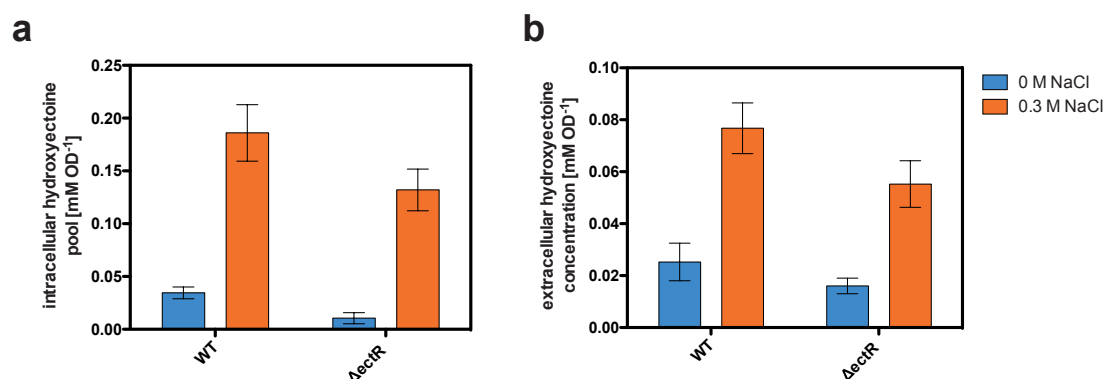


Fig. 6 Analysis of hydroxyectoine production in *ectR* deletion strain. **a, b** Cells of *Novosphingobium* sp. LH128 wild type the *ectR* deletion mutant were grown in SMM without and with 0.3 M NaCl, respectively, and were harvested at OD₅₇₈ of 1.5. The produced hydroxyectoine was extracted from the cells using 20% ethanol. The intracellular hydroxyectoine content (**a**) and the extracellular concentrations in the growth medium (**b**) were analyzed via HPLC. The data shown represent the mean and the standard error of six independently grown cultures.

Surprisingly, these preliminary data indicate that, unlike most MarR-type regulatory proteins, (N₃)EctR might function as a positive transcriptional regulator. A picture, that can yet not be explained and does not agree with the findings that the (N₃)EctR regulator potentially binds downstream of the assumed *ectA* promoter and might thereby hinder the transcription of the *ect* genes. However, it is also apparent that (N₃)EctR is not the only regulatory element involved in the control of ectoine production, since the salt-induction persists in the *ectR* deletion strain (Fig. 6).

Phylogenetic analysis of EctR-type regulators. When we analyzed the presence of the ectoine biosynthetic genes in all fully sequenced genomes deposited at the IMG database of the JGI in a previous study (date of search: November 2017), we found that 437 genomes contained potential ectoine biosynthetic gene clusters [*ectABC(D)*] [5]. Among these, 97 organisms (22%) harbored an EctR-type regulator in the direct gene neighborhood of the *ect* genes [5]. Analysis of the genetic organization of these gene clusters revealed three different types of *ect* operons accompanied by *ectR* (Fig. 7). One group of organisms encodes the EctR regulator upstream and colinear of the *ect* genes (Fig. 7). In a second group the *ectR* gene is located upstream and divergent to the *ect* operon and a third group comprises a rather scrambled organization with the *ectR* gene located downstream of the ectoine biosynthetic gene cluster oriented either co- or antilinear (Fig. 7). Within the three different types of *ectR*-associated *ect* gene cluster, minor variations in the composition of the ectoine biosynthesis gene clusters were observed. While some only possess the core genes for ectoine biosynthesis *ectABC*, such as *Acidihalobacter prosperus* and *Cellvibrio japonicus*, others harbor either additionally the *ectD* gene for the ectoine hydroxylase (e. g. *Achromobacter xylosoxidans*, *Sphingobium* sp. YBL2); the gene for the aspartokinase *ask_ect* (e. g. *M. alcaliphilum*, *Allivibrio fischeri*); or both of these genes such as e. g. *Acidiphilum cryptum* or *Novosphingobium* sp. LH128 (Fig. 7) [34, 56].

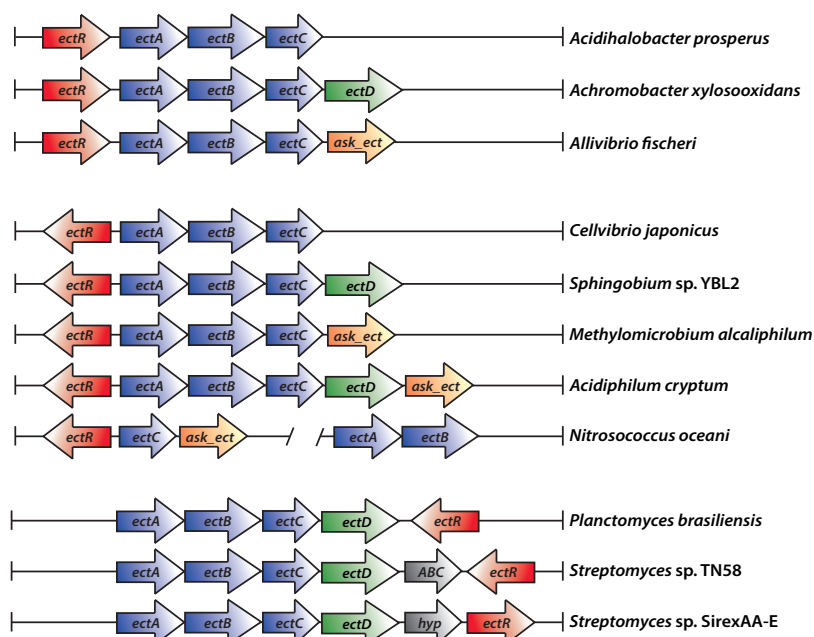


Fig. 7 Genetic organization of *ect* gene clusters containing *ectR* in their genetic neighborhoods. The *ectR* gene is shown in red, the genes involved in the synthesis of ectoine (*ectABC*) are depicted in blue, *ectD* encoding the ectoine hydroxylase for the production of 5-hydroxyectoine is colored in green and the gene for the specialized aspartokinase (*ask-ect*) is shown in orange. Grey arrows show either a hypothetical gene (*hyp*) or summarize four genes of an ABC transporter (ABC).

Phylogenetic analysis of the microorganisms that harbor the gene for an EctR-type regulator in the genetic vicinity of the *ect* gene cluster only occurred in three different bacterial phyla (*Proteobacteria*, *Actinomycetes* and *Planctomycetes*) and three subphyla (Class) (*Alpha*-, *Beta*- and *Gamma*proteobacteria) (Fig. 8). In the next step, we calculated a phylogenetic tree based on a sequence comparison of the various EctR proteins found in our database analysis (Supplementary Fig. 3) [5]. Interestingly, the microorganisms belonging to the same phylum cluster together within this EctR-tree and these groups also exhibit the same genetic organization of the *ectR-ect* gene clusters (Fig. 8). While the group that harbors the *ectR* gene upstream of and colinear with the *ect* gene cluster mainly consists of *Betaproteobacteria*, all *Alphaproteobacteria* encode the *ectR* gene upstream and antilinear to the *ect* genes (Fig. 8). Among the *Gamma*proteobacteria only a small group encodes the *ectR* gene colinear. In the majority of the organisms belonging to this class, it is transcribed antilinear to the ectoine biosynthetic genes (Fig. 8). The EctR proteins of the two Actinomycetes (*Streptomyces* sp. SirexAA-E and *Streptomyces* sp. TN58) and the Planctomycete *Planctomyces brasiliensis* [57] cluster in the middle of the EctR-tree in between the EctR proteins of *Beta*- and *Gamma*proteobacteria that carry the corresponding gene upstream and colinear (Fig. 8).

When we now assigned the habitats or ecosystems of the EctR-containing microorganisms found to the phylogenetic tree, we also observed a habitat-specific clustering of the different genetic organizations (Fig. 8). Most *Betaproteobacteria* are microorganisms that are host-associated or opportunistic pathogens, such as *Achromobacter xylosoxidans* [58] or *Bordetella bronchiseptica* [59] (Fig. 8). The found *Gamma*proteobacteria mainly inhabit aquatic, marine or saline habitats such as *Alcanivorax dieselolei* [60] or *M. alcaliphilum* [61]. Furthermore, the EctR-possessing *Alphaproteobacteria* either live in marine

environments, such as *H. neptunium* [62], or in soil/terrestrial habitats, such as *Acidiphilum cryptum* [63] or *Novosphingobium* sp. LH128 [50] (Fig. 8).

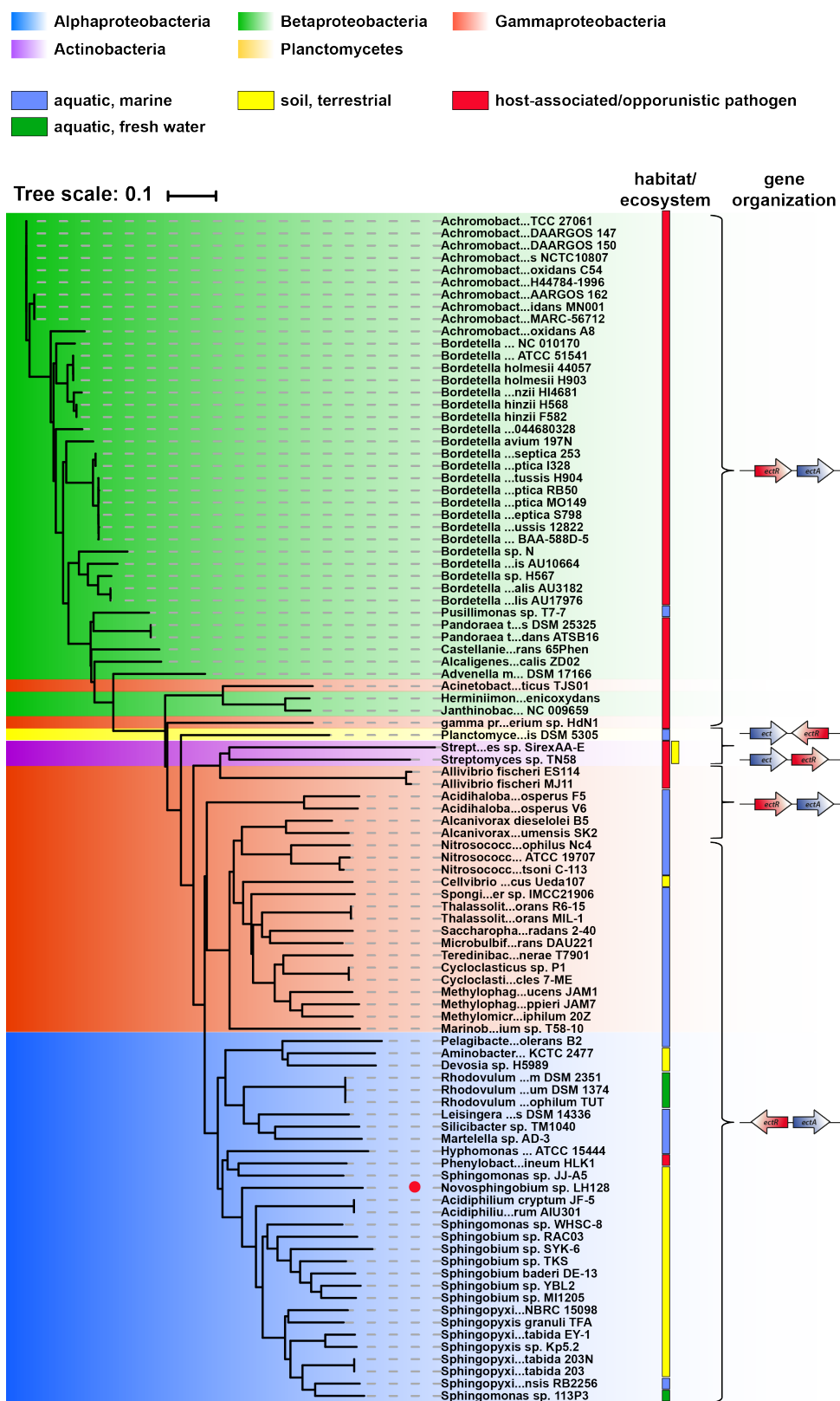


Fig. 8 Phylogenetic analysis of EctR proteins. The amino acid sequences of 97 EctR-type proteins were retrieved from microorganisms with fully sequenced genomes, aligned with SnapGene and then used for a clade analysis using the iTOL software [64]. The phylogenetic and ecosystem/habitat affiliations of the bacteria that possessed the EctR protein are depicted in different colors, and the color code is explained in the figure. EctR of *Novosphingobium* sp. LH128 is marked with a red dot.

Discussion and Perspectives

Since the production of compatible solutes such as ectoine and 5-hydroxyectoine is rather costly for the bacterial cells (40-55 ATP per molecule), the microorganisms aim to tightly control the biosynthesis routes of these stress protective molecules [65]. Although some regulators and mechanisms involved in the control of ectoine biosynthetic gene expression have been described in the past years, only little is known about the mechanisms how bacteria sense the strength of the external osmotic stress and transform this stimulus into a cellular response and transcriptional changes [5, 27, 29, 34–36]. The presented study focused on the MarR-type regulator EctR from *Novosphingobium* sp. LH128 that has previously been studied in methylotrophs, such as *M. alcaliphilum* [33, 34]. Its rather broad occurrence has been further substantiated by a comprehensive bioinformatical analysis, where EctR was shown to be present in the gene neighborhood of the *ect* gene clusters of 22% putative ectoine producers identified in all fully sequenced organisms deposited at the IMG database (date of search: November 2017) [5, 49]. Taking this data as a basis, we calculated a phylogenomic tree based on an amino acid sequence comparison of the found EctR-type regulators (Fig. 8). Interestingly, while the ectoine biosynthetic genes are found in 10 bacterial and two archaeal phyla, the presence of the EctR-type regulator in the vicinity of the *ect* gene clusters seems to be rather restricted to *Proteobacteria* (Fig. 8), with the exceptions of two Actinomycetes and one Planctomycete, that might have acquired the *ect* gene cluster via horizontal gene transfer, as they cluster in the middle of the EctR phylogenetic tree between strains of *Beta*- and *Gammaproteobacteria* (Fig. 8). The acquisition of ectoine biosynthetic genes via horizontal gene transfer might be further underlined by the rather unusual orientation of the gene encoding the EctR regulator in these phyla (Fig. 7). The hypothesis that *ect* genes are interchanged between different species has been substantiated within the past years, when ectoine biosynthetic genes have been found in different *Archaea* and even halophilic unicellular *Eukarya* [20–25, 66]. Furthermore, a recent study discovered for the first time ectoine biosynthetic genes present on plasmid, which is carried by a halophilic *Bacillus* strain making the horizontal exchange of these genes even more likely [67].

When we further assigned the habitat/ecosystem to the strains possessing an EctR-type regulator, we found that there seem to be habitat specific adaptations of the organization of the *ect* gene clusters. All identified *Betaproteobacteria* possessed the same gene organization (*ectR* gene transcribed colinear with the *ect* gene cluster) and were found to be opportunistic pathogens (Fig. 8). On the other site, most organisms, that encoded the *ectR* gene antilinear to the *ect* gene cluster (most *Gamma*- and all *Alphaproteobacteria*), were free living bacteria, that inhabit either marine/saline aquatic environments, or soil, sediment and terrestrial habitats, such as the studied *Alphaproteobacterium* *Novosphingobium* sp. LH128 (Fig. 8). Furthermore, the EctR-based phylogenetic tree indicates, that the *Betaproteobacteria* might have acquired the *ectR-ect* gene cluster from a common ancestor and that the *ectR* containing gene clusters of the *Alpha*- and *Gammaproteobacteria* might have evolved from that. In addition, one can hypothesize, that the genetic orientation of the *ectR* gene in respect to the ectoine biosynthetic genes might have changed from co- to antilinear orientation during this evolutionary step (Fig. 8).

We studied the EctR regulator from *Novosphingobium* sp. LH128 on a biochemical and structural basis. HPLC-MALS, crystallographic and SAXS analysis of the (N₃)EctR regulator revealed a tetrameric assembly of the protein in solution and in the crystal structure (Fig. 1 and 2a-c). The (N₃)EctR tetramer is formed by two homodimers that contact each other in a head-to-head arrangement with the typical DNA binding motifs (winged HTH-motifs) [39] positioned at the top and the bottom of the tetrameric complex (Fig. 2a; 3c, d). A structural arrangement that has not yet been observed for any other regulator belonging to the MarR-type superfamily [39]. Inspection of possible interactions between the homodimers of the (N₃)EctR protein led to the assumption, that the residues Trp-124 and Arg-135 (in three of the four monomers) might form cation- π interactions between the π -electrons of the indole ring of the Trp-124 side chain and the positive charge of the guanidino group of Arg-135 (Fig. 2e, f). Interestingly, the residues Trp-124 and Arg-135 are fully conserved in all organisms, that encode *ectR* upstream and antilinear of *ectA*, while there are deviations in EctR proteins that are positioned upstream and colinear or down-stream of the *ect* gene cluster (Fig. 2, Supplementary Fig. S3, Supplementary Fig. S4, Supplementary Fig. S5). In many cases (50% of the EctR proteins), Trp-124 is exchanged by a Leu residue (37 EctR proteins), which is not able to contribute to a cation- π interaction. In minor cases it also is exchanged by an Ala, Thr, Asp, Asn, Gln, or Glu residue (Supplementary Fig. S3). Arg-135 is also highly conserved (91%) in EctR proteins whose gene is oriented colinear to the *ect* genes, in some organisms it is exchanged by a Lys or a Gln residue, while the cationic side chain of a Lys would still be capable of building a cation- π interaction when it contacts an appropriate amino acid with an aromatic side chain (Supplementary Fig. S3). This observation leads to the hypothesis, that (I) these residues might be important for the assembly of the EctR regulator within organisms where the *ectR* gene is located upstream and divergently of the *ect* gene cluster (such as *Novosphingobium* sp. LH128) and (II) it potentially indicates a different mechanism of EctR assembly in microorganisms, where these residues are substituted by other amino acid within the EctR protein (Fig. 2, Supplementary Fig. S3, Supplementary Fig. S4, Supplementary Fig. S5). Since the finding, that the (N₃)EctR is rather unusual for a member of the MarR-superfamily, it would be interesting, to mutate these residues within the (N₃)EctR protein and test whether this mutant protein still forms a tetrameric complex [39].

One of the best studied MarR-type regulators is OhrR that negatively regulates the genes involved in hydroperoxide resistance in *Bacillus subtilis*, and has been crystallized in complex with the specific DNA region, to which it binds [40, 68]. This crystallographic analysis allowed the understanding of the detailed binding mechanism and the identification of the residues of OhrR that directly contact the DNA. Sequence comparison of OhrR to (N₃)EctR revealed an identity of 19% (Fig. 9). Within the OhrR protein, 13 residues are involved in the direct binding of the DNA. Only five of these residues involved in DNA binding are found at the same position in the sequence of the (N₃)EctR protein (Fig. 9). Some are exchanged by amino acids that might function similarly (e. g. Arg to Lys), while others possess completely different properties (e. g. Tyr to Ala) (Fig. 9). It would be an interesting task in the future to identify the residues within the (N₃)EctR protein involved in DNA binding, and study if the DNA indeed forms a

loop around the protein as indicated by the tetrameric assembly of (N_s)EctR and the presence of two independent binding sites (Fig. 4, 5).

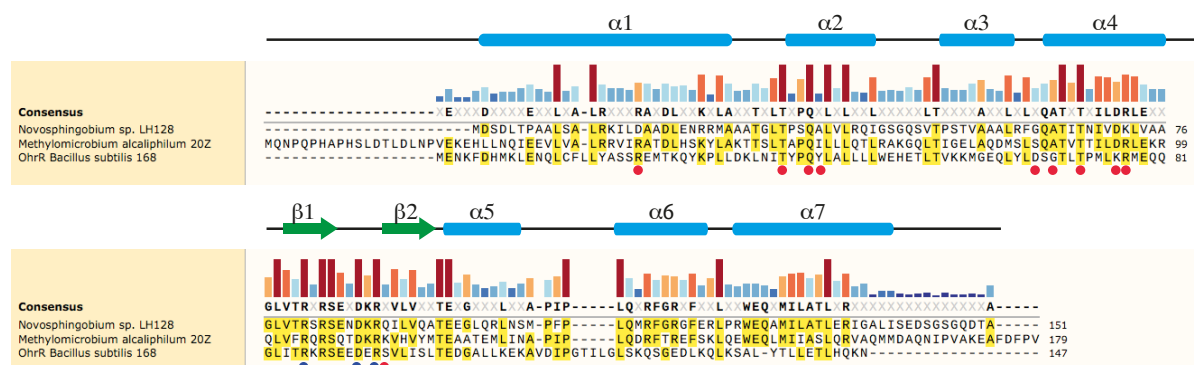


Fig. 9 Alignment of MarR-type regulators. EctR regulators from *Novosphingobium* sp. LH128 and *Methylobacterium alcaliphilum* [34] were compared to the amino acid sequence of the MarR-type regulator OhrR from *B. subtilis*. The residues of OhrR that contact DNA are marked with red and blue dots. The blue dots denote residues that are part of the wing domain of the OhrR regulator [68]. The secondary structure elements of EctR are indicated above the sequence by arrows (β -strands), and rectangles (α -helices).

Studies on the EctR regulator from *M. alcaliphilum* [(*Ma*)EctR] revealed that this regulatory protein functions as a repressor, that binds to an pseudopalindromic sequence (TATT^{*}TAGT-GT-ACTATATA) overlapping the *ectA* promoter and to a second binding site upstream of the *ectR* promoter, thereby additionally serving as an autoregulator of *ectR* gene expression [34]. Unfortunately this binding sequence is not detectable in the intergenic region between *ectR* and *ectA* found in *Novosphingobium* sp. LH128. Compared to the tetrameric state of (N_s)EctR, (*Ma*)EctR was found to form a dimer and two of those dimers might individually bind the two described binding sites [34]. The two proteins possess a sequence identity of 30% and the highest sequence similarities are observed in the β -sheets that form the wing domain and α -helix three, that is also part of the DNA binding motif (Fig. 9). We hypothesize, that like (*Ma*)EctR, the EctR regulator from *Novosphingobium* sp. LH128 might also bind to pseudopalindromes downstream of the *ectR* and *ectA* promoter, respectively (Fig. 4, 5). However, the true DNA binding regions of (N_s)EctR need to be identified for example via DNase footprint assays in the future.

The (*Ma*)EctR regulator reduces ectoine gene expression under low, moderate and high salinities [34]. In contrast to that, on the level of 5-hydroxyectoine production, a (N_s)*ectR* deletion strain accumulated only reduced amounts of 5-hydroxyectoine under low and moderate salinities (Fig. 6). An observation that might indicate a positive regulatory function of (N_s)*ectR*. It is yet unclear and requires further experimental work, to find out what leads to this reduced production levels, since the binding assays indicate, that also (N_s)EctR might rather function as a repressor for ectoine gene expression binding to the DNA in-between the potential promoter and the transcriptional start site of *ectA* (Fig. 4, 5). In the future, the hypothesized sigma-70-type promoters of *ectA* and *ectR* need to be experimentally verified either through mutational analysis or mapping of the transcriptional start sites for example using primer extension experiments. Furthermore, transcriptional analysis, such as reporter gene fusion to *ectA*

and *ectR* or quantitative PCR analysis of *ectA* and *ectR* should be performed in the wild type and *ectR* deletion strain grown under different salinities, to elucidate the true regulatory function of EctR. Moreover, the influence of EctR could be studied by overexpression of *ectR* itself and complementation of the *ectR* deletion strain by a plasmid carrying the *ectR* gene. Beyond that it is unclear, whether additional regulatory proteins or elements co-regulate ectoine gene expression. The fact that the osmotic induction of *ect* gene expression is still preserved when the regulatory proteins functioning as repressor were genetically inactivated (such as GlnR in *S. meliloti*, CosR in *V. cholera* or EctR1 in *M. alcaliphilum*) underlines the presence of unknown regulatory mechanisms [34–36]. Also in the case of *Novosphingobium* sp. LH128, the osmotic induction of 5-hydroxyectoine production is preserved in a (*Ns*)*ectR* mutant compared to the wild type strain (Fig. 6). The finely tuned transcriptional response and linear increase of ectoine production in relation to the externally applied salinity has also been previously observed in various organisms, that lack the EctR-type regulator within the *ect* gene neighborhood [12, 27, 31]. It will be an interesting task in the future to fully understand the regulation of osmo-responsive genes and elucidate the players involved in this life-assuring process when bacterial cells face fluctuations in the external salinities.

Moreover it remains to be studied, to which signal the EctR regulator responds. For the regulators BusR, controlling the glycine betain uptake system in *L. lactis* and CosR, adjusting ectoine biosynthesis, compatible solute transport, biofilm formation and motility in *V. cholera*, it has been suggested (from the results of *in vitro* experiments), that they might sense increased ionic strength within the cells and as a consequence, their DNA binding abilities are modulated [35, 48]. In the future, EMSAs with (*Ns*)EctR in the presence of increasing ionic strength, mimicked by the addition of different salts such as NaCl/KCl or Na/K-glutamate, should be conducted to test this hypothesis. For other osmotically induced genes it has been hypothesized that DNA supercoiling might function as a global regulatory element [69, 70]. Increased or decreased superhelicity might influence the positioning of the -35 and -10 promoter regions to each other and thereby effectuate either optimal or suboptimal distance between the two promoter elements. This in turn enables only the binding of the RNA polymerase, when the -10 and -35 region of the promoter are perfectly positioned [69–71]. One can imagine, that such a global changes might also affect the binding of other DNA binding proteins such as regulators to the DNA, when for example the distances between the bases that are recognized by the regulatory protein change.

Material and Methods

Chemicals and reagents

Ectoine and 5-hydroxyectoine were kindly provided by the bitop AG (Witten, Germany). Anhydrotetracycline-hydrochloride (AHT) was purchased from IBA GmbH (Göttingen, Germany). Acetonitrile (HPLC-grade) was obtained from VWR International GmbH (Darmstadt, Germany). Ampicillin and all other chemicals were purchased from Serva Electrophoresis GmbH (Heidelberg, Germany), Sigma-Aldrich (Munich, Germany) and Carl Roth GmbH (Karlsruhe, Germany).

Strains, media and growth conditions

E. coli strains were routinely maintained on Luria Bertani (LB) agar plates and propagated in liquid LB medium [72]. When they contained a recombinant plasmid, ampicillin (100 µg ml⁻¹) or kanamycin (50 µg ml⁻¹) was added to the growth medium. When appropriate, X-gal (5-bromo-4-chloro-3-indolyl-β-D-galactopyranoside) was included in agar plates to screen for the insertion of the desired DNA fragments into the cloning vectors pENTRY-IBA20 or pASG-IBA5 (IBA, Göttingen, Germany). For the heterologous overproduction of the EctR regulator from *Novosphingobium* sp. LH128 [(N₅)EctR] fused to a Strep-tag-II affinity peptide carried by plasmid pLC29 in *E. coli* strain BL21, minimal medium A (MMA) was supplemented with 0.5 % (w/v) glucose as the carbon source, 1 mM MgSO₄, and 3 mM thiamine and 0.5% (w/v) casamino acids. Shake-flask cultures were incubated at 37 °C in a shaking water bath set to 220 rpm [72].

The *Novosphingobium* sp. LH128 strain was kindly provided by Dirk Springael (KU Leuven, Belgium) and cultivated in LB or Spizizen's minimal medium (SMM), with 0.5% (wt/vol) glucose as the carbon source [50, 73]. The medium was supplemented with L-tryptophan (20 mg liter⁻¹), L-phenylalanine (18 mg liter⁻¹), and a trace element solution [74]. Cells were routinely grown aerobically at 30°C in 100-ml baffled Erlenmeyer flasks with a culture volume of 20 ml in a shaking water bath set at 220 rpm. The growth of the bacterial cultures was monitored spectrophotometrically at a wavelength of 578 nm (OD₅₇₈). The salinity of bacterial cultures was raised by adding appropriate volumes of NaCl from a 5M stock solution.

Construction of plasmids and strains

Routine manipulations of plasmid DNA, the construction of recombinant plasmids and the isolation of chromosomal DNA from *Novosphingobium* sp. LH128 were carried out using standard techniques [75]. The expression plasmid carrying the *Novosphingobium* sp. LH128 *ectR* gene with a N-terminal Strep-tag-II affinity peptide were constructed using the IBA Stargate cloning system (IBA, Göttingen, Germany). The *ectR* gene present on pLC20 was synthetically manufactured and optimized for the expression in *E. coli* by GeneArt (Thermo Fisher Scientific, Waltham, Massachusetts, USA). The *ectR* gene (pLC20) carried a synthetically added LguI DNA restriction site at each end; these restriction sites enabled its cloning into the donor vector pENTRY-IBA20 via LguI restriction and concurrent ligation thereby yielding plasmid pLC21. To clone the *ectR* gene present on pLC21 into the pASG-IBA5 expression vector, Esp3I restriction and concurrent ligation of this plasmid was carried out. In this way, the *ectR* gene was fused to a short DNA fragment encoding the Strep-tag-II affinity peptide at its 5' end. The resulting plasmid was pLC29.

Markerless gene deletion of *ectR* in *Novosphingobium* sp. LH128 was constructed as reported by Kaczmarczyk *et al.* [55]. Upstream and down-stream regions of approximately 750 bp that flanked the corresponding gene(s) were PCR amplified using the custom synthesized primers: 1 Sph 5'Del for (AAAGGTACCCGCCGCTCAAAGGA TCG) and 2 Sph 3'Del for (GCTAGCTGTCGGGGCCGCCTCACACCTCGAAC) for the 3' region; and 2 Sph 5'Del rev (GTTTCGAGGTGTGAGGCGGCCCCGACAGCTAGC) and 2 Sph 3'Del rev (AAAGTTAACGATGGT CGCCTGCCATTC) for the 5' region of *ectR*. The 3'- and 5'-fragments were joined by overlap extension PCR using 1 Sph 5'Del for and 2 Sph 3'Del rev, and then ligated into pAK405 using the restriction sites KpnI and HindIII. This resulted in the plasmid pLC60 (Δ *ectR*). All custom synthesized primers were purchased from Microsynth AG (Lindau, Germany). The correct nucleotide sequence of all constructed plasmids was ascertained by DNA sequence analysis, which was carried out by Eurofins MWG Operon (Ebersberg, Germany).

Novosphingobium sp. LH128 knock-out strain carrying markerless gene deletions of the EctR regulator was constructed as reported by Kaczmarczyk *et al.* with minor variations of the protocol [55]. The plasmid pLC60 (Δ *ectR*) was transformed into *Novosphingobium* sp. LH128 by electroporation [55]. Bacteria were subsequently plated on LB supplemented with 50 µg ml⁻¹ kanamycin. Individual colonies were restreaked once on the same medium and then inoculated in LB supplemented with 100 µg ml⁻¹ streptomycin to enforce the second homologous recombination event. After 40 h of incubation the cultures were transferred to fresh LB supplemented with 100 µg ml⁻¹

streptomycin (OD₅₇₈ of 0.1) and further incubated at 30 °C in a shaking waterbath set to 220 rpm. After 24 h the cells were adjusted to an OD₅₇₈ of 0.5 and serially diluted. The 10⁻⁶ dilution was plated on LB supplemented with 100 µg ml⁻¹ streptomycin and incubated for 48 h. Resulting colonies were restreaked on both LB supplemented with 100 µg ml⁻¹ streptomycin and LB containing 50 µg ml⁻¹ kanamycin, and kanamycin-sensitive clones were analyzed by colony PCR using primers flanking the respective loci. To further analyze the correct construction of the gene deletion, chromosomal DNA was prepared, the region of interest was amplified via PCR and the PCR products were verified by sequencing. The resulting strain was LC6.

Overproduction, purification and determination of the quaternary assembly of the (N₃)EctR regulator

For the overproduction of the Strep-tag II-(N₃)EctR an overnight culture of strain BL21 carrying pLC29 was prepared in MMA and used to inoculate 1 l of MMA (in a 2 l Erlenmeyer flask) to an OD₅₇₈ of 0.05. The cells were grown on an aerial shaker (set to 180 rpm) at 37°C until the culture reached an OD₅₇₈ of 0.5. At this time point, AHT was added to the growth medium at a final concentration of 0.2 mg ml⁻¹ to induce expression of the recombinant *ectR* gene. After 2 h of further incubation of the culture, the *E. coli* cells were harvested by centrifugation and disrupted by passing them four times through a French Pressure cell; a cleared cell lysate was prepared by ultracentrifugation (100 000 g) at 4°C for 45 min. The supernatant of this cleared lysate was then passed through a column filled with 5ml of Strep-Tactin Superflow material (IBA GmbH, Göttingen, Germany); the column had been equilibrated with a buffer containing 150 mM NaCl and 100 mM Tris-HCl (pH 7.5). The Strep-tag II-(N₃)EctR protein was eluted from the affinity matrix with three column volumes of the same buffer containing 2.5 mM desthiobiotin. The recombinant Strep-tag II-(N₃)EctR protein was then concentrated to 10 mg ml⁻¹ for crystallization trials using Vivaspin 6 columns (Satorius Stedim Biotech GmbH, Göttingen, Germany) in the same buffer as described above. Desthiobiotin was not removed by dialysis from these protein preparations.

To determine the oligomeric state of the Strep-tag II-(N₃)EctR protein in solution, we used high-performance liquid chromatography coupled to multi-angle light scattering detection (HPLC-MALS). A Bio SEC-5 HPLC column (Agilent Technologies Deutschland GmbH, Böblingen, Germany) with a pore size of 300 Å was equilibrated with 20 mM Tris-HCl (pH 7.5), 150 mM NaCl for high-performance liquid chromatography analysis. For these experiments, an Agilent Technologies system connected to a triple-angle light scattering detector (miniDAWNTEOS, Wyatt Technology Europe GmbH, Dernbach, Germany) followed by a differential refractive index detection system (Optilab trEX, Wyatt Technology) was used. Typically, 100 µl of the purified Strep-tag II-(N₃)EctR protein (2 mg ml⁻¹) was loaded onto the Bio SEC-5 HPLC column and the obtained data were analyzed with the ASTRA software package (Wyatt Technology).

The purity of the recombinant protein was assessed by SDS-polyacrylamide gel electrophoresis (15%); the electrophoretically separated proteins were stained with Coomassie Brilliant Blue. Page Ruler Prestained Marker was included as a standard on the gel to allow determination of the protein size.

Crystallization of (N₃)EctR protein

Our collaboration partners A. Höppner and S. Smits (Heinrich-Heine University Düsseldorf, Germany) performed crystallization, HPLC-MALS and small-angle X-ray scattering (SAXS) analysis of EctR.

Initial screening was performed at 285 K and the vapor-diffusion method in Corning 3553 sitting drop plates with several commercial screens (Nextal, Qiagen, Hilden, Germany; Molecular Dimensions, Suffolk, UK and Hampton Research, Aliso Viejo, USA). 0.1 µl homogenous (N₃)EctR [100 mM Tris pH 7.5, 150 mM NaCl (increased to 300 mM NaCl before setting up plates), 9 mg ml⁻¹] was mixed with 0.1 µl of the reservoir solution and equilibrated against 50 µl. Several needle clusters and grown together crystals were obtained after 4 days or up to 3-4 month. Initial crystals were optimized with a promising condition from the Nextal Core II suite (Qiagen, Hilden, Germany) via grid screens: 0.4-2 M lithium chloride, 17-26% PEG 6000 and 0.1 M MES pH 5. Crystals are grown in 2 M lithium chloride, 17% PEG 6000, 0.1 M MES pH 5 after 1-3 days at 285 K to their maximum size of approximately 220x100x50 µm. Each drop consists of 1 µl protein solution (18 mg ml⁻¹ (N₃)EctR) and 1 µl reservoir solution and equilibrated against 300 µl reservoir solution. Additionally 0.2 µl mercury (II) chloride (end concentration 10 mM) was added to some of the drops. Crystals with heavy atoms are grown to a maximum size of around 300x120x50 µm. The crystals were harvested after overlaying the drop with 1µl mineral oil and flash frozen with liquid nitrogen. Crystallization information is summarized in Supplementary Table 1. Data sets were collected from a few crystals of the EctR with the heavy metal Hg on beamline ID30A-3 at the ESRF (Grenoble, France) at 100 K using an Eiger_4M detector.

Electrophoretic mobility shift assays (EMSA)

DNA fragments with different lengths ranging from 60 to 220 bp, corresponding to the full length or truncations of the intergenic region between *ectR* and *ectA* were amplified by PCR using different primer sets summarized in Supplementary Table 2. Each of the used reverse primers contained a Cy781 fluorescent dye oligo modification to allow fluorescence detection of the amplified PCR fragments. Two picomoles of the labeled DNA fragments were incubated for 15 min at room temperature in 20 µl of binding buffer [20 mM Tris-HCl (pH 8.3), 10 mM MgCl₂, 200 mM KCl] with increasing amounts of pure Strep-tag II-(N₃)EctR (from 1 to 40 pmol) and 0.1 µg of herring sperm DNA. For the competition assay, labeled DNA was added to the reaction mixture after addition of the unlabeled fragment. Samples were mixed with 5 µl 50% glycerol and analyzed by native gel (6% polyacrylamide) electrophoresis in 1x Tris-borate-EDTA (TBE) buffer [75]. The gel was run for 2 h at 120 V in 0.5x TBE buffer. DNA fragments were detected with a Licor Odyssey Fc scanner (Licor, Lincoln, Nebraska USA) for 2 min using the 700 nm channel.

Database searches and phylogenetic analysis

The bioinformatics tools available at the DOE Joint Genome Institute website (<http://www.jgi.doe.gov>) [76] were used to retrieve EctR-, and EctC-type protein sequences from all microbial genomes (search date: 12/2017) and also DNA sequences of the regions between *ectR* and *ectA*. For these database searches, the amino acid sequence of EctC (accession number: WP_009589551.1) protein from *P. laetus* [77] was used as the query sequence using the BLAST program [78]. The retrieved protein sequences were aligned and compared using ClustalOmega [79] and SnapGene. Based on these alignments, phylogenetic trees were calculated using the iTOL-software package (<http://itol.embl.de/>) [64] to visualize the distribution of EctR proteins among members of the Bacteria and Archaea. The genetic organization of the *ectABC(ectD)* gene cluster and its flanking sequences were analyzed using the online tool available from the DOE Joint Genome Institute website [76].

HPLC analysis of ectoine and hydroxyectoine content

Cell pellets of *Novosphingobium* sp. LH128 WT and *ectR* deletion mutant grown under different salinities were extracted with 70% ethanol. For this purpose, the cell pellets were resuspended in 1-ml 70% ethanol and were shaken for 1 h. After centrifugation at 16.000 x g (4 °C, 30 min) to remove cell debris, the ethanolic extracts were transferred into fresh Eppendorf tubes, and ethanol was removed by evaporation (incubation at 55 °C for 20 h). The resulting dried material was suspended in 100 µl of distilled water and insoluble material was removed by centrifugation (16.000 x g at 4 °C for 30 min). The extracted samples and the cell-free culture supernatant were diluted ten-fold with distilled water and acetonitrile to an end concentration of 50%. Samples were subsequently analyzed for their ectoine/5-hydroxyectoine content by isocratic high-performance liquid chromatography (HPLC) [11]. For these measurements we employed an Agilent 1260 Infinity LC system (Agilent, Waldbronn, Germany) and a GROM-SIL Amino 1PR column (GROM, Rottenburg-Hailfingen, Germany) essentially as described [11] with the exception that a 1260 Infinity Diode Array Detector (DAD) (Agilent) was used, instead of the previously used UV/Vis detector system. The ectoine content of samples was quantified using the OpenLAB software suite (Agilent). Standard curves for the calculation of the ectoine and 5-hydroxyectoine concentrations were determined with commercially available samples (obtained from bitop AG, Witten, Germany).

Preparation of crystal structures and figures

The crystal structure of EctR was visualized and analyzed using the PyMOL Molecular Graphics System suit (<https://www.pymol.org>) (DeLano Scientific LLC, Schrödinger, New York City, New York, USA) [80]. All other data was analyzed and represented using Microsoft Excel (Microsoft Corp., Redmond, Washington, USA), GraphPad Prism (<https://www.graphpad.com>) (GraphPad Software, San Diego, California, USA), SnapGene (<https://www.snapgene.com>) (GSL Biotech LLC, Chicago, Illinois, USA) and Adobe Illustrator (Adobe Inc., San José, California, USA).

References

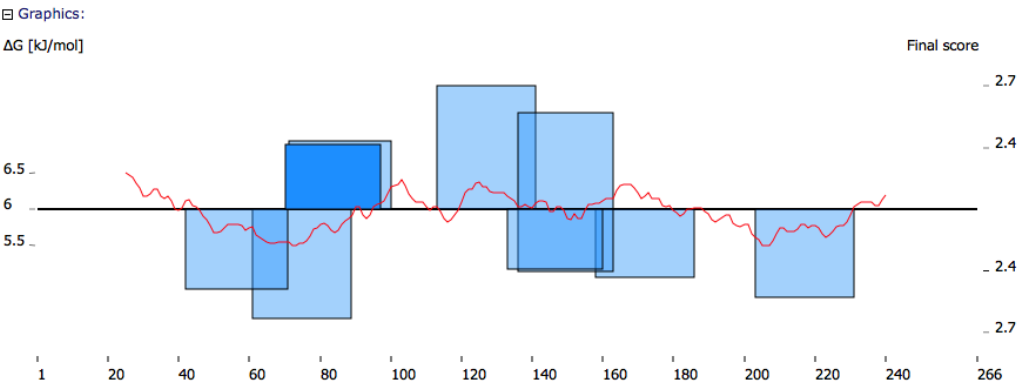
1. Bremer E, Krämer R. Responses of microorganisms to osmotic stress. *Annu Rev Microbiol* 2019;73:313–334.
2. Gunde-Cimerman N, Plemenitaš A, Oren A. Strategies of adaptation of microorganisms of the three domains of life to high salt concentrations. *FEMS Microbiol Rev* 2018;42:353–375.
3. Burg MB, Ferraris JD. Intracellular organic osmolytes: function and regulation. *J Biol Chem* 2008;283:7309–7313.
4. Wood JM. Bacterial osmoregulation: a paradigm for the study of cellular homeostasis. *Annu Rev Microbiol* 2011;65:215–238.
5. Czech L, Hermann L, Stöveken N, Richter A, Höppner A, *et al.* Role of the extremolytes ectoine and hydroxyectoine as stress protectants and nutrients: genetics, phylogenomics, biochemistry, and structural analysis. *Genes (Basel)* 2018;9:177. doi: 10.3390/genes9040177.
6. Pastor JM, Salvador M, Argandoña M, Bernal V, Reina-Bueno M, *et al.* Ectoines in cell stress protection: uses and biotechnological production. *Biotechnol Adv* 2010;28:782–801.
7. Galinski EA, Pfeiffer HP, Trüper HG. 1,4,5,6-Tetrahydro-2-methyl-4-pyrimidinecarboxylic acid. A novel cyclic amino acid from halophilic phototrophic bacteria of the genus *Ectothiorhodospira*. *Eur J Biochem* 1985;149:135–139.
8. Jebbar M, Talibart R, Gloux K, Bernard T, Blanco C. Osmoprotection of *Escherichia coli* by ectoine: uptake and accumulation characteristics. *J Bacteriol* 1992;174:5027–5035.
9. Kuhlmann SI, van Schelting ACT, Bienert R, Kunte HJ, Ziegler CM. 1.55 Å structure of the ectoine binding protein TeaA of the osmoregulated TRAP-transporter TeaABC from *Halomonas elongata*. *Biochemistry* 2008;47:9475–9485.
10. Lecher J, Pittelkow M, Zobel S, Bursy J, Bönig T, *et al.* The crystal structure of UehA in complex with ectoine-A comparison with other TRAP-T binding proteins. *J Mol Biol* 2009;389:58–73.
11. Kuhlmann AU, Bremer E. Osmotically regulated synthesis of the compatible solute ectoine in *Bacillus pasteurii* and related *Bacillus* spp. *Appl Environ Microbiol* 2002;68:772–783.
12. Kuhlmann A, Bursy J, Gimpel S, Hoffmann T, Bremer E. Synthesis of the compatible solute ectoine in *Virgibacillus pantothenticus* is triggered by high salinity and low growth temperature. *Appl Environ Microbiol* 2008;74:4560–4563.
13. Bursy J, Kuhlmann AU, Pittelkow M, Hartmann H, Jebbar M, *et al.* Synthesis and uptake of the compatible solutes ectoine and 5-hydroxyectoine by *Streptomyces coelicolor* A3(2) in response to salt and heat stresses. *Appl Environ Microbiol* 2008;74:7286–7296.
14. Ono H, Sawada K, Khunajakr N, Tao T, Yamamoto M, *et al.* Characterization of biosynthetic enzymes for ectoine as a compatible solute in a moderately halophilic eubacterium, *Halomonas elongata*. *J Bacteriol* 1999;181:91–99.
15. Peters P, Galinski EA, Trüper HG. The biosynthesis of ectoine. *FEMS Microbiol Lett* 1990;71:157–162.
16. Inbar L, Lapido A. The structure and biosynthesis of new tetrahydropyrimidine derivatives in actinomycin D producer *Streptomyces parvulus*. Use of ¹³C- and ¹⁵N-labeled L-glutamate and ¹³C and ¹⁵N NMR spectroscopy. *J Biol Chem* 1988;263:16014–16022.
17. Höppner A, Widderich N, Lenders M, Bremer E, Smits SHJ. Crystal structure of the ectoine hydroxylase, a snapshot of the active site. *J Biol Chem* 2014;289:29570–29583.
18. Bursy J, Pierik AJ, Pica N, Bremer E. Osmotically induced synthesis of the compatible solute hydroxyectoine is mediated by an evolutionarily conserved ectoine hydroxylase. *J Biol Chem* 2007;282:31147–31155.
19. Reuter K, Pittelkow M, Bursy J, Heine A, Craan T, *et al.* Synthesis of 5-hydroxyectoine from ectoine: crystal structure of the non-heme iron(II) and 2-oxoglutarate-dependent dioxygenase EctD. *PLoS One* 2010;5:e10647. doi:10.1371/journal.pone.0010647.
20. Widderich N, Czech L, Elling FJ, Könneke M, Stöveken N, *et al.* Strangers in the archaeal world: osmotic-stress-responsive biosynthesis of ectoine and hydroxyectoine by the marine thaumarchaeon *Nitrosopumilus maritimus*. *Environ Microbiol* 2016;18:1227–1248.
21. Weinisch L, Kirchner I, Grimm M, Kühner S, Pierik AJ, *et al.* Glycine betaine and ectoine are the major compatible solutes used by four different halophilic heterotrophic ciliates. *Microb Ecol* 2019;77:317–331.
22. Weinisch L, Kühner S, Roth R, Grimm M, Roth T, *et al.* Identification of osmoadaptive strategies in the halophile, heterotrophic ciliate *Schmidingerotrix salinarum*. *PLoS Biol* 2018;16:e2003892. doi: 10.1371/journal.pbio.2003892.
23. Harding T, Brown MW, Simpson AGB, Roger AJ. Osmoadaptive strategy and its molecular signature in obligately halophilic heterotrophic protists. *Genome Biol Evol* 2016;8:2241–2258.
24. Harding T, Roger AJ, Simpson AGB. Adaptations to high salt in a halophilic protist: differential expression and gene acquisitions through duplications and gene transfers. *Front Microbiol* 2017;8:doi: 10.3389/fmicb.2017.00944.
25. Czech L, Bremer E. With a pinch of extra salt - Did predatory protists steal genes from their food? *PLoS Biol* 2018;16:e2005163. doi: 10.1371/journal.pbio.2005163.
26. Kuhlmann AU, Hoffmann T, Bursy J, Jebbar M, Bremer E. Ectoine and hydroxyectoine as protectants

- against osmotic and cold stress: uptake through the SigB-controlled Betaine-Choline-Carnitine Transporter-type carrier EctT from *Virgibacillus pantothenticus*. *J Bacteriol* 2011;193:4699–4708.
27. **Czech L, Poehl S, Hub P, Stöveken N, Bremer E.** Tinkering with osmotically controlled transcription allows enhanced production and excretion of ectoine and hydroxyectoine from a microbial cell factory. *Appl Environ Microbiol* 2018;84:e01772-17. doi: 10.1128/AEM.01772-17.
 28. **Bestvater T, Galinski EA.** Investigation into a stress-inducible promoter region from *Marinococcus halophilus* using green fluorescent protein. *Extrem Life under Extrem Cond* 2002;6:15–20.
 29. **Calderón MI, Vargas C, Rojo F, Iglesias-Guerra F, Csonka LN, et al.** Complex regulation of the synthesis of the compatible solute ectoine in the halophilic bacterium *Chromohalobacter salexigens* DSM 3043T. *Microbiology* 2004;150:3051–3063.
 30. **Cánovas D, Vargas C, Calderón MI, Ventosa A, Nieto JJ.** Characterization of the genes for the biosynthesis of the compatible solute ectoine in the moderately halophilic bacterium *Halomonas elongata* DSM 3043. *Syst Appl Microbiol* 1998;21:487–497.
 31. **Stöveken N, Pittelkow M, Sinner T, Jensen RA, Heider J, et al.** A specialized aspartokinase enhances the biosynthesis of the osmoprotectants ectoine and hydroxyectoine in *Pseudomonas stutzeri* A1501. *J Bacteriol* 2011;193:4456–4468.
 32. **Widderich N, Höppner A, Pittelkow M, Heider J, Smits SHJ, et al.** Biochemical properties of ectoine hydroxylases from extremophiles and their wider taxonomic distribution among microorganisms. *PLoS One* 2014;9:e93809. doi:10.1371/journal.pone.0093809.
 33. **Reshetnikov AS, Khmelenina VN, Mustakhimov II, Kalyuzhnaya M, Lidstrom M, et al.** Diversity and phylogeny of the ectoine biosynthesis genes in aerobic, moderately halophilic methylotrophic bacteria. *Extremophiles* 2011;15:653–663.
 34. **Mustakhimov II, Reshetnikov A, Clukhov A, Khmelenina V, Kalyuzhnaya M, et al.** Identification and characterization of EctR1, a new transcriptional regulator of the ectoine biosynthesis genes in the halotolerant methanotroph *Methylobaculum alcaliphilum* 20Z. *J Bacteriol* 2010;192:410–417.
 35. **Shikuma NJ, Davis KR, Fong JNC, Yildiz FH.** The transcriptional regulator, CosR, controls compatible solute biosynthesis and transport, motility and biofilm formation in *Vibrio cholerae*. *Environ Microbiol* 2013;15:1387–1399.
 36. **Shao Z, Deng W, Li S, He J, Ren S, et al.** GlnR-mediated regulation of *ectABCD* transcription expands the role of the GlnR regulon to osmotic stress management. *J Bacteriol* 2015;197:3041–3047.
 37. **Alekshun MN, Levy SB, Mealy TR, Seaton BA, Head JF.** The crystal structure of MarR, a regulator of multiple antibiotic resistance, at 2.3 Å resolution. *Nat Struct Biol* 2001;8:710–714.
 38. **Wilkinson SP, Grove A.** Ligand-responsive transcriptional regulation by members of the MarR family of winged helix proteins. *Curr Issues Mol Biol* 2006;8:51–62.
 39. **Deochand DK, Grove A.** MarR family transcription factors: dynamic variations on a common scaffold. *Crit Rev Biochem Mol Biol* 2017;52:595–613.
 40. **Fuangthong M, Atichartpongkul S, Mongkolsuk S, Helmann JD.** OhrR is a repressor of *obrA*, a key organic hydroperoxide resistance determinant in *Bacillus subtilis*. *J Bacteriol* 2001;183:4134–4141.
 41. **Grove A.** Regulation of metabolic pathways by MarR family transcription factors. *Comput Struct Biotechnol J* 2017;15:366–371.
 42. **Lim D, Poole K, Strynadka NCJ.** Crystal structure of the MexR repressor of the *mexRAB-oprM* multidrug efflux operon of *Pseudomonas aeruginosa*. *J Biol Chem* 2002;277:29253–29259.
 43. **Kim Y, Joachimiak G, Bigelow L, Babnigg G, Joachimiak A.** How aromatic compounds block DNA binding of HcaR catabolite regulator. *J Biol Chem* 2016;291:13243–13256.
 44. **Nau-Wagner G, Oppen D, Rolbetzki A, Boch J, Kempf B, et al.** Genetic control of osmoadaptive glycine betaine synthesis in *Bacillus subtilis* through the choline-sensing and glycine betaine-responsive GbsR repressor. *J Bacteriol* 2012;194:2703–2714.
 45. **Ronzheimer S, Warmbold J, Arnhold C, Bremer E.** The GbsR family of transcriptional regulators: functional characterization of the OpuAR repressor. *Front Microbiol* 2018;9:doi: 10.3389/fmicb.2018.02536.
 46. **Schulz A, Stöveken N, Binzen IM, Hoffmann T, Heider J, et al.** Feeding on compatible solutes: a substrate-induced pathway for uptake and catabolism of ectoines and its genetic control by EnuR. *Environ Microbiol* 2017;19:926–946.
 47. **Schulz A, Hermann L, Freibert S-A, Bönig T, Hoffmann T, et al.** Transcriptional regulation of ectoine catabolism in response to multiple metabolic and environmental cues. *Environ Microbiol* 2017;19:4599–4619.
 48. **Romeo Y, Bouvier J, Gutierrez C.** Osmotic regulation of transcription in *Lactococcus lactis*: Ionic strength-dependent binding of the BusR repressor to the *busA* promoter. *FEBS Lett* 2007;581:3387–3390.
 49. **Chen IA, Chu K, Palaniappan K, Pillay M, Ratner A, et al.** IMG/M v.5.0: an integrated data management and comparative analysis system for microbial genomes and microbiomes. *Nucleic Acids Res* 2018;doi: 10.1093/nar/gky901.
 50. **Bastiaens, L, Springael D, Wattiau P, Harms H, et al.** Isolation of adherent polycyclic aromatic hydrocarbon (PAH)-degrading bacteria using PAH-sorbing carriers. *Appl Environ Microbiol* 2000;66:1834–1843.
 51. **Gallivan JP, Dougherty DA.** Cation- π interactions in structural biology. *Proc Natl Acad Sci* 1999;96:9459–

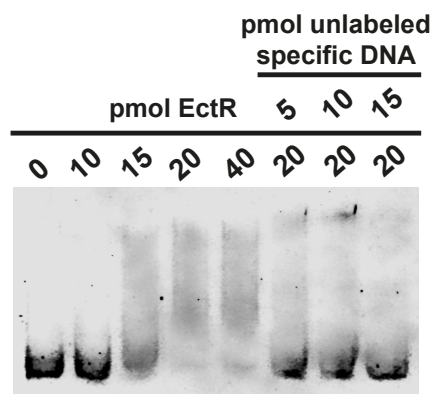
- 9464.
52. **Paget MS.** Bacterial sigma factors and anti-sigma factors: structure, function and distribution. *Biomolecules* 2015;5:1245–1265.
 53. **Stano M, Klucar L.** PhiGENOME: an integrative navigation throughout bacteriophage genomes. *Genomics* 2011;98:376–380.
 54. **Klucar L, Stano M, Hajduk M.** phiSITE: database of gene regulation in bacteriophages. *Nucleic Acids Res* 2010;38:D366–D370.
 55. **Kaczmarczyk A, Vorholt JA, Francez-Charlot A.** Markerless gene deletion system for Sphingomonads. *Appl Environ Microbiol* 2012;78:3774–3777.
 56. **Moritz KD, Amendt B, Witt EMHJ, Galinski EA.** The hydroxyectoine gene cluster of the non-halophilic acidophile *Acidiphilium cryptum*. *Extremophiles* 2014;19:87–99.
 57. **Scheuner C, Tindall BJ, Lu M, Nolan M, Lapidus A, et al.** Complete genome sequence of *Planctomyces brasiliensis* type strain (DSM 5305T), phylogenomic analysis and reclassification of *Planctomycetes* including the descriptions of *Gimesia* gen. nov., *Planctopirus* gen. nov. and *Rubinisphaera*/. *Stand Genomic Sci* 2014;9:10. doi: 10.1186/1944-3277-9–10.
 58. **Igra-Siegmán Y, Chmel H, Cobbs C.** Clinical and laboratory characteristics of *Achromobacter xylosoxidans* infection. *J Clin Microbiol* 1980;11:141–145.
 59. **Gross R, Keidel K, Schmitt K.** Resemblance and divergence: the “new” members of the genus *Bordetella*. *Med Microbiol Immunol* 2010;199:155–163.
 60. **Liu C, Shao Z.** *Alcanivorax dieselolei* sp. nov., a novel alkane-degrading bacterium isolated from sea water and deep-sea sediment. *Int J Syst Evol Microbiol* 2005;55:1181–1186.
 61. **Khmelenina VN, Kalyuzhnaya MG, Starostina NG, Suzina NE, Trotsenko YA.** Isolation and characterization of halotolerant alkaliphilic methanotrophic bacteria from Tuva soda lakes. *Curr Microbiol* 1997;35:257–261.
 62. **Leifson E.** *Hyphomicrobium neptunium* sp. n. *Antonie Van Leeuwenhoek* 1964;30:249–256.
 63. **Küsel K, Dorsch T, Acker G, Stackebrandt E.** Microbial reduction of Fe(III) in acidic sediments: isolation of *Acidiphilium cryptum* JF-5 capable of coupling the reduction of Fe(III) to the oxidation of glucose. *Appl Environ Microbiol* 1999;65:3633–3640.
 64. **Letunic I, Bork P.** Interactive Tree Of Life v2: online annotation and display of phylogenetic trees made easy. *Nucleic Acids Res* 2011;39:W475–W478.
 65. **Oren A.** Bioenergetic aspects of halophilism. *Microbiol Mol Biol Rev* 1999;63:334–348.
 66. **Ren M, Feng X, Huang Y, Wang H, Hu Z, et al.** Phylogenomics suggests oxygen availability as a driving force in *Thaumarchaeota* evolution. *ISME J* 2019;13:2150–2161.
 67. **Mukhtar S, Ahmad S, Bashir A, Mehnaz S, Mirza MS, et al.** Identification of plasmid encoded osmoregulatory genes from halophilic bacteria isolated from the rhizosphere of halophytes. *Microbiol Res* 2019;228:126307.
 68. **Hong M, Fuangthong M, Helmann JD, Brennan RG.** Structure of an OhrR-*ohrA* operator complex reveals the DNA binding mechanism of the MarR family. *Mol Cell* 2005;20:131–141.
 69. **Graeme-Cook KA, May G, Bremer E, Higgins CF.** Osmotic regulation of porin expression: a role for DNA supercoiling. *Mol Microbiol* 1989;3:1287–1294.
 70. **Higgins CF, Dorman CJ, Stirling DA, Waddell L, Booth IR, et al.** A physiological role for DNA supercoiling in the osmotic regulation of gene expression in *S. typhimurium* and *E. coli*. *Cell* 1988;52:569–584.
 71. **Hoffmann T, Bremer E.** Management of osmotic stress by *Bacillus subtilis* genetics and physiology. In: Bruijn FJ de (editor). *Stress and Environmental Regulation of Gene Expression and Adaptation in Bacteria*. Hoboken, NJ, USA: John Wiley & Sons, Inc. pp. 657–676.
 72. **Miller J.** *Experiments in molecular genetics*. 1972.
 73. **Spizizen J.** Transformation of biochemically deficient strains of *Bacillus subtilis* by deoxyribonucleate. *Proc Natl Acad Sci* 1958;44:1072–1078.
 74. **Harwood CR, Archibald AR.** Growth, maintenance and general techniques. In: Harwood CR, Cutting SM (editors). *Molecular biological methods for Bacillus*. Chichester, United Kingdom: John Wiley & Sons, Inc.; 1990. pp. 1–26.
 75. **Sambrook J, W Russell D.** Molecular Cloning: A Laboratory Manual. *Cold Spring Harb Lab Press Cold Spring Harb NY* 2001;999.
 76. **Nordberg H, Cantor M, Dusheyko S, Hua S, Poliakov A, et al.** The genome portal of the Department of Energy Joint Genome Institute: 2014 updates. *Nucleic Acids Res* 2014;42:26–31.
 77. **Czech L, Höppner A, Kobus S, Seubert A, Riclea R, et al.** Illuminating the catalytic core of ectoine synthase through structural and biochemical analysis. *Sci Rep* 2019;9:doi: 10.1038/s41598-018-36247-w.
 78. **Altschul SF, Gish W, Miller W, Myers EW, Lipman DJ.** Basic local alignment search tool. *J Mol Biol* 1990;215:403–410.
 79. **Thompson JD, Plewniak F, Thierry J, Poch O.** DbClustal: rapid and reliable global multiple alignments of protein sequences detected by database searches. *Nucleic Acids Res* 2000;28:2919–2926.
 80. **DeLano WL.** The PyMOL Molecular Graphics System, Version 1.8 Schrödinger, LLC. *San Carlos Delano Sci*. <http://www.pymol.org> (2002).

SUPPLEMENTARY DATA

Strand	Begin 1	Score 1	Begin 2	Score 2	Summary score	Energy score	Final score	Sequence
+	113	4.26	135	4.86	9.12	5.97	2.67 ✓	CGACACATGGTTGCAATGCACCGCACGATCCTTATGTTATCGCGCAGC
-	83	3.97	61	4.27	8.24	5.96	2.63 ✓	ATATGTTCCCCTTGATGCGCGTCTTTGAAATGCAATATTCGGATTGG
+	136	2.65	157	5.61	8.26	6.00	2.59 ✓	CACGATCCTTATGTTATCGCGCAGCAGCAGTCATAATCAGGCAAATG
-	225	4.68	203	2.07	6.75	5.87	2.56 ✓	CGAAGCGGCCTTACTCATGACTTCATCAAGATTACTTCACCCCTCCG
-	65	2.33	42	4.79	7.12	5.98	2.53 ✓	CGTCTTTGAAATGCAATATTTTCGGATTGGAAGTATCTTTCGGCTTGGC
+	71	4.50	94	1.22	5.72	5.96	2.48	AATATTGCATTTCAAAGACGCGCATCAAGGGAACATATCTCGCGACACA
-	180	2.25	158	4.00	6.25	5.96	2.48	CCGAAGCACAATGGCGTGCTTGGCATTTCGCTCATTTGACTGCTGCT
+	70	3.71	91	1.84	5.55	5.95	2.46	AAATATTGCAATTCAAAGACGCGCATCAAGGGAACATATCTCGCGAC
-	157	1.49	136	4.72	6.21	5.98	2.45	CATTTCCTCATTTATGACTGCTGCTGCGCGATTAACATAAGGATCGTG
-	154	3.30	133	2.21	5.51	5.99	2.44	TTGCCTCATTATGACTGCTGCTGCGGATAAACATAAGATCGTGCGG



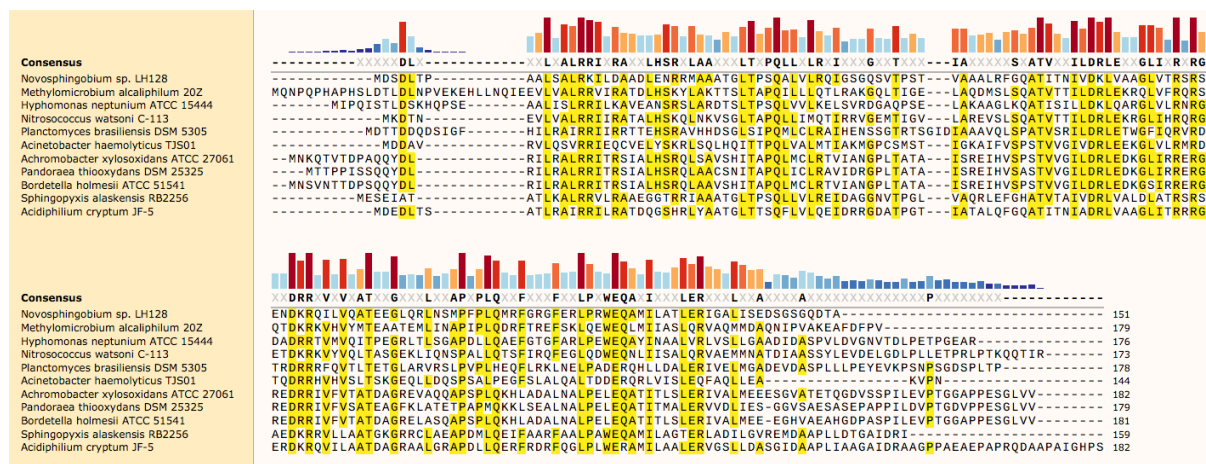
Suppl. Fig. 1 Results of *in silico* promoter mining in the intergenic region between *ectR* and *ectA* in *Novosphingobium* sp. LH128 using PromoterHunter online tool (<http://www.phisite.org/>) [1, 2].



Suppl. Fig. 2 Competition assay to verify specific binding of recombinant EctR protein to the intergenic region between the *ectR* gene and the *ect* operon. EMSAs were performed with a Cy781-fluorescently labeled DNA fragments and the same fragment, which was not fluorescently labeled, was used as a competitor. Samples were incubated without or with increasing amounts of purified *Strep-II-EctR* (0, 10, 15, 20 or 40 pmol) in the presence of 0.1 μ g herring sperm DNA. The leftmost lane represents the labeled DNA probe alone. Unlabeled DNA was added at 5-, 10-, and 15-molar-ratio excesses (three rightmost lanes) to a assay reaction containing 20 pmol of the purified *Strep-II-EctR* protein. Samples were applied to a 6% polyacrylamide TBE gel, run for 2 h at 120 V.







Suppl. Fig. 5 Abbreviated alignment of EctR-type regulators from bacteria belonging to different phyla.

Supplementary Table 1. Crystallization conditions.

Method	Vapor diffusion
Plate type	Sitting drop
Temperature (K)	285
Protein concentration (mg mL⁻¹)	18
Buffer composition of protein solution	100 mM Tris pH 7.5, 150 mM NaCl (freshly increased to 300 mM NaCl before use)
Composition of reservoir solution	2 M lithium chloride, 17% PEG 6000, 0.1 M MES pH 5
Ratio of drop	1:1
Volume of reservoir	300

Supplementary Table 2. Primers used for EMSAs.

Fragment nr.	Fragment size [bp]	Primer name	Primer sequence
1	220	BS_220bp_for	GCATTTCAAAGACGCGC
		Sphingo_EctR_BS_rev	CGAGGTAGTCTTACACATCG
2	190	BS_190bp_for	CATATCTCGCGACACATG
		Sphingo_EctR_BS_rev	CGAGGTAGTCTTACACATCG
3	150	Sphingo_EctR_BS_kurz_for	CTTATGTTATCGCGCAGC
		Sphingo_EctR_BS_rev	CGAGGTAGTCTTACACATCG
4	120	BS_100bpvorEctA_for	CAAATGCCAAGCACGC
		Sphingo_EctR_BS_rev	CGAGGTAGTCTTACACATCG
5	90	BS_75bpvorEctA_for	GAGGGTGAAGTAATCTTTGATG
		Sphingo_EctR_BS_rev	CGAGGTAGTCTTACACATCG
6	170	Sphingo_EctR_BS_lang_for	TGAGATCGCTGTCCATG
		BS_Mitte_rev	GCTGCGCGATAACATAAG
7	140	Sphingo_EctR_BS_lang_for	TGAGATCGCTGTCCATG
		BS_Promotor_rev	GGTGCATTGCAACCATG
8	80	BS_220bp_for	GCATTTCAAAGACGCGC
		BS_Mitte_rev	GCTGCGCGATAACATAAG
9	80	BS_240bp_for	GATACTTCCAAATCCGAAATATTG
		BS_Promotor_rev	GGTGCATTGCAACCATG
10	60	BS_220bp_for	GCATTTCAAAGACGCGC
		BS_Promotor_rev	GGTGCATTGCAACCATG

References

1. **Stano M, Klucar L.** PhiGENOME: an integrative navigation throughout bacteriophage genomes. *Genomics* 2011;98:376–380.
2. **Klucar L, Stano M, Hajduk M.** phiSITE: database of gene regulation in bacteriophages. *Nucleic Acids Res* 2010;38:D366–D370.

6. Discussion and Perspectives

The research field focusing on the chemical chaperones ectoine and 5-hydroxyectoine has been constantly growing since the discovery of these small versatile protective compounds over 30 years ago, the identification of the enzymes required for their biosynthesis and the description of the underlying genes [57, 58, 62, 64, 69, 77, 80]. Within the past decades it became increasingly apparent that ectoines are not only used as effective stress- and cytoprotectants by microorganisms but can also be exploited for various biotechnological and medical applications [57, 60, 61, 152, 165, 180]. Moreover, the broad environmental importance of ectoines is strengthened by their ubiquitous distribution as microbial stress protectants and their utilization as nutrients, which also suggests the involvement of these nitrogen-rich compounds in ecophysiological important food webs [59, 67, 97, 242, 249, 250, 260].

The findings presented in this work, shed new light on various aspects of ectoine-related research topics. Previous phylogenomic analyses have been extended and analyzed on a broader level. Insights into regulatory mechanisms controlling ectoine biosynthetic gene expression have been obtained in different organisms and combinations of structural and functional analysis enabled novel insights into the enzyme reaction mechanism performed by the ectoine synthase (EctC) and the substrate ambiguity of the ectoine hydroxylase (EctD). Moreover, new routes have been opened in the framework of this dissertation: by the analysis of mechanosensitive channels that are co-regulated with ectoine biosynthetic genes; through the discovery and functional studies of novel ectoine transporters involved in import and export of ectoines; and by the first description of the crystal structure and preliminary analysis of the regulatory function of the MarR-type regulator EctR from *Novosphingobium* sp. LH128. In the following sections, the results and new insights obtained in course of the presented dissertation will be discussed and integrated into the common knowledge of the ectoine research field.

6.1. Phylogenomic distribution of ectoine biosynthetic genes and horizontal gene transfer

Within the ectoine biosynthetic pathway, the ectoine synthase (EctC) functions the key enzyme since it catalyzes the ring-closure of the *N*- γ -ADABA precursor resulting in the formation of the stress-relieving compound ectoine [68, 77, 86]. This signature enzyme was used as a marker to identify potential ectoine producing microorganisms through *in silico* genome mining of the ever increasing number of sequenced microbial genomes [59, 67, 72]. The phylogenomic distribution of the ectoine biosynthetic genes within the domain of *Bacteria* and *Archaea* was first studied in the context of analyzing ectoine hydroxylases from different extremophilic bacteria [67]. This first bioinformatical approach by Widderich *et al.* led to the discovery of ectoine biosynthetic genes in organisms belonging to ten different bacterial, and two different archaeal phyla [67]. The *in silico* analysis was extended and analyzed on a broader level within the framework of the presented dissertation: (I) in the publication that verified the functionality of the ectoine/5-hydroxyectoine biosynthetic gene cluster in the marine Thaumarchaeon Cand. *N. maritimus* (see 5.2.1), (II) within our comprehensive review on the *Role of the extremolytes ectoine and hydroxyectoine as stress*

protectants and nutrients (see 5.1.1) and (III) within the structural and biochemical analysis of the ectoine synthase (EctC) from *P. lautus* (see 5.2.4).

Taken together, the bioinformatical analyses underlined a highly conserved organization of the ectoine/5-hydroxyectoine biosynthetic genes [*ectABC(D)*] (Figure 3A) identified in bacterial and archaeal genomes. However it also highlighted the frequency of accessory genes that accompany *ectABC(D)* gene clusters and variations within the composition of *ect* genes in a restricted number of microorganisms. In approximately 30% of the potential ectoine/5-hydroxyectoine producers, the *ectABC(D)* genes are accompanied by the gene for the specialized aspartokinase (Ask_Ect) that has been functionally studied in *P. stutzeri* in a previous report by Stöveken *et al.* (see 4.2.2.5 and 5.1.1) [59, 79]. Ask_Ect, is a feed-back resistant enzyme that allows a higher flux of precursor molecules into the ectoine biosynthetic pathway thereby preventing of a metabolic bottleneck, when the demand for ectoine production in osmotically stressed cells is high [79]. Previous studies in methylotrophic bacteria identified the presence of a MarR-type (Multiple antibiotic resistance Regulator) regulator EctR in the vicinity of their *ect* gene clusters [81, 100, 142]. Our bioinformatical analysis identified the presence of this transcriptional regulator in 22% of the assumed producer organisms but also underlined its rather restricted occurrence in the phylum of *Proteobacteria* (see 4.2.3.1 and 5.2.7) [59, 100, 101, 142]. Furthermore, the genetic co-localization of different types of transporters with *ect* genes was observed in 33% of the putative ectoine producers belonging to six different phyla (see 5.2.6). The majority of these organisms belonged to the phyla *Actinobacteria*, *Firmicutes* and *Proteobacteria*.

While many bacteria possess only one gene cluster for ectoine/5-hydroxyectoine production, others harbor additional copies of either, the complete cluster, or only single *ect* genes [59, 67, 71, 72, 315]. Moreover, some organisms were identified that harbored the ectoine biosynthetic genes distributed over different locations in their genomes [59, 67, 70, 83, 97]. An example for the presence of multiple copies of complete *ect* gene clusters or solitary *ectC*-type genes is *Streptomyces reticuli*, which harbours two *ectABCD* gene clusters and an additional *ectD*-type gene [59]. An explanation for these multiple copies could either be gene duplications or gene transfer (see below). However, the detection of a reasonable number of organisms, that only encode a solitary EctC-type protein or possess this gene in addition to a complete *ect* gene clusters raises the question if these proteins fulfill the same function as canonical ectoine synthases (discussion see 6.2) [67, 72, 86, 315]. This topic remains to be further addressed in future investigations. A studied example for the functionality of re-arranged and separated genes required for ectoine production is the proteobacterium *Spiribacter salinus*, which was isolated from a hypersaline salt pond [316, 317]. *S. salinus* and other related organisms such as various *Marinobacter* strains were shown to possess completely re-arranged *ect* genes that are located separately within their genomes [83]. Nevertheless, the identified *ectAC* / *ectB* genes from *S. salinus* proved to be functional and facilitated ectoine production in response to salt stress [83]. Interestingly, many organisms related to *Spiribacter* also harbored genes encoding putative transporters in the genetic context of the *ect* genes [83]. In conjunction with the knowledge gained from our phylogenomic analysis, these results stress the hypothesis that mostly

members of the *Actino*- and *Proteobacteria* possess highly evolved ectoine/5-hydroxyectoine gene clusters since these exhibit the highest variations and different adaptations.

Besides these rather uncommon variations, the high conservation of the ectoine biosynthetic gene clusters [*ectABC(D)*] is contrary to the diverse genetic organization of the ectoine catabolic genes that has been detected within a bioinformatical analysis of the ectoine degradation gene clusters reported by Schulz *et al.* (Figure 3A and Figure 6A) [249]. Moreover, it is highly interesting, that only bacterial species that belong to the phylum of the *Proteobacteria* were found to possess ectoine catabolic genes. Among the 539 potential ectoine catabolic organisms, 100 bacteria (19%) also harbored the genes for ectoine biosynthesis, including the industrial ectoine producer strain *H. elongata* [97, 242]. This co-occurrence requires a tight genetic regulation of the two contrary biochemical pathways to avoid a futile cycle - another aspect in the field of ectoine production and catabolism that remains to be elucidated in the future.

Despite the fact, that ectoine production is a major trait of members of the *Bacteria*, the detection of ectoine biosynthetic genes in *Archaea* and *Eukarya* indicate the horizontal transfer of ectoine biosynthetic genes [59, 72–76, 279]. Moreover, most compatible solutes used by *Archaea* and *Eukarya* differ from the once used by *Bacteria*, for example many archaeal are a negatively charged [4, 44, 47, 48, 51] and the detection of ectoines in these organisms was therefor even more surprising. However, horizontal transfer of ectoine biosynthetic genes might not only happen between organisms of different phyla, also the presence of different *ect*-type genes within the same bacterial genome may be attributed to mobile genetic elements. Recently, a study on *Bacillus filamentous* HL2HP6 detected, for the first time, the ectoine biosynthesis genes (*ectABC*) encoded on a plasmid - an interesting finding, since plasmids can be easily exchanged (via conjugation) between and taken up by different microorganisms (transformation/competence) [318, 319]. These authors also showed that this plasmid was transferrable to *E. coli* leading to a higher salt-tolerance of the transformed organism; unfortunately ectoine production/accumulation was not tested [318]. Moreover, a phylogenomic study on the phylum of *Thaumarchaeota* suggests a horizontal acquisition of the ectoine biosynthetic genes found in *Archaea* from bacterial donors during their adaptation to specific ecological niches, such as marine, aerobic habitats [279]. Interestingly, our bioinformatical analysis revealed that aerobic and anaerobic *Archaea* possessed ectoine biosynthetic enzymes (see 5.1.1 and 5.2.1) [59, 72]. The identified gene clusters differed in the presence of the gene encoding the ectoine hydroxylase EctD [72]. We found that only aerobic *Archaea* harbored an *ectD* gene, which is not surprising, since the activity of the ectoine hydroxylase is strictly dependent on the presence of oxygen [64, 72, 78]. Also the presence of ectoine biosynthetic genes in bacteriovorous, unicellular protists raise the hypothesis that these organisms might have acquired the genes for the production of the osmoprotective compounds from their microbial prey [73–75, 280, 320]. The presence of spliceosomal introns and a mitochondrial targeting sequence within the ectoine genes found in these eukaryotic microorganisms, indicate a genetic adaptation of the *ect* genes to the common functions of the eukaryotic transcriptional and translational apparatus [73]. Taken together, the findings underline that ectoines are potent stress protectants that can be used by members of all three domains of life and future research within this field might lead to even more surprising discoveries.

6.2. New insights into the key enzymes for ectoine and 5-hydroxyectoine production

The key role of the ectoine synthase (EctC) during ectoine biosynthesis has been pointed out at several places within this thesis [68, 77, 86]. In previous publications, purified EctC proteins from different organisms have been studied on a biochemical basis, including *H. elongata*, *A. cryptum*, *S. alaskensis*, *Cand. N. maritimus*, and *M. alcaliphilum* [72, 77, 81, 86, 91]. The previously reported crystal structures of the apo- and iron-containing form of the ectoine synthase from the cold-adapted organism *S. alaskensis* revealed a dimeric assembly of the protein with a characteristic cupin-fold of each monomer (PDB: 5BXX; 5BY5). Crystals of the iron-bound form and analysis of mutant enzymes enabled the identification of the residues Glu-57, Tyr-85 and His-93 to be critical for iron-binding within cupin barrel of the (*Sa*)EctC protein [86]. The crystal structure of the ectoine synthase from *P. lantus* reported in context of this dissertation resembles those features (see 5.2.4). Both EctC dimers exhibit a head-to-tail arrangement with two dimeric interfaces that are tightly stabilized and formed by two anti-parallel β -sheets at both terminal ends of the proteins (see 5.2.4) [86].

A major contribution to the understanding of the enzymatic reaction performed by the ectoine synthase was reported in this thesis, when the crystal structure of the ectoine synthase from *P. lantus* [(*Pl*)EctC] was solved in three different conformations - in complex with (I) the catalytically critical iron, (II) the precursor *N*- γ -ADABA, and (III) the product ectoine (see 5.2.4). The snapshots of the different (*Pl*)EctC complexes in combination with the biochemical analysis of (*Pl*)EctC variants harboring site-specific mutations allowed a detailed insight into the performed catalysis and laid the foundation for the proposal of the underlying reaction mechanism. In addition the residues of the (*Pl*)EctC protein that are involved in substrate, product and iron binding, we found that especially the highly conserved Trp-21 is essential for the reaction mechanisms. While all other residues remain remarkably constant in their location in all obtained crystal structures, the side-chain of Trp-21 performs a major rotamer conformational change. The observed twist of the Trp-21 side-chain may trigger the re-orientation of the bound *N*- γ -ADABA substrate during ring formation to yield ectoine (or vice versa). We therefore assume that this coordinated re-organization of the active site is a major driving force for catalysis.

Furthermore, within a phylogenetic analysis based on the EctC-type proteins of all fully sequenced genomes the frequent occurrence of solitary *ectCs* (in 25%) was highlighted. Amino acid sequence comparison of *bona fide* and orphan EctC-type proteins revealed that orphan EctCs often differ significantly from each other. However, we observed that the predicted iron-, *N*- γ -ADABA- and ectoine-binding residues are mostly conserved, as well as their spatial relationship within the amino acid chain. It became apparent that orphan EctC proteins possess the structural features of *bona fide* ectoine synthases. In a previous report by Kurz *et al.*, the plant-pathogen *Pseudomonas syringae* *pv.* *syringae* that harbors an exclusive orphan *ectC* gene has been physiologically studied. *P. syringae* *pv.* *syringae* was shown to produce ectoine when surface sterilized leaves of its host plant were added to the culture. However, the physiological and biochemical function of these orphan EctC-type proteins is not fully clear, since the presence of environmental *N*- γ -ADABA has never been reported. The described orphan *ectCs* may either

be remnants of previously functional ectoine biosynthetic gene clusters, or they may catalyze reactions of substrates that are chemically related in its structure to *N*- γ -ADABA. However, the reported insights into the structure/function relationship of the *bona fide* ectoine synthase from *P. laetus* and the ancillary physiological and phylogenomic considerations might serve as a foundation to unravel the functional role of the substantial group of orphan EctC-type proteins.

Various bacterial and also an archaeal representatives of ectoine hydroxylases (EctD) responsible for the synthesis of 5-hydroxyectoine have been extensively studied on a structural, biochemical, bioinformatical and functional basis [64, 67, 69, 70, 72, 77, 78, 81, 85]. In parts of the presented PhD thesis, the ectoine hydroxylase from different organisms was exploited for (I) its implementation in an *E. coli* based 5-hydroxyectoine cell factory (see 5.2.2 and discussion 6.3) and (II) the stereo- and regioselective hydroxylation of the synthetic, seven-membered ring analog of ectoine, called homoectoine (see 5.2.5) [218]. An early patent application already claimed the idea that the EctD enzyme could promiscuously modify other natural and synthetic chiral molecules but no experimental data were provided in this patent that would support such a claim [321, 322]. Several investigations have described that the introduction of the hydroxyl group to ectoine employs the formed product (5-hydroxyectoine) with new attributes. It exhibits differences in water binding [151, 157, 161, 323] and it possesses superior function-preserving properties compared to ectoine in the context of protection against desiccation, the ability to form glasses, as well as the stabilization of and influence on DNA, proteins and lipid layers [38, 153, 155, 175, 212, 217]. These observations motivated the idea to hydroxylate the synthetic compound homoectoine, that possessed beneficial effects on colitis in mice, thereby potentially endowing it with novel or superior attributes [218, 238]. This part of my thesis revealed that homoectoine could be hydroxylated *in vitro* and *in vivo* in a highly precise manner by the EctD enzyme yielding exclusively *trans*-5-hydroxyhomoectoine (see 5.2.5). During our studies we used EctD enzymes originating from two different organisms - *S. alaskensis* and *P. stutzeri* A1501 (see 5.2.2, 5.2.5 and 6.3). Through the investigations in the context of the construction of the EctD-cell factory it became apparent that not all EctD proteins possess the same efficiency *in vivo* (see 5.2.2 and for discussion 6.3). After further optimization of the enzymatic parameters within this study this was also observed *in vitro*. The EctD enzyme from *P. stutzeri* displayed a 10-fold higher V_{\max} for the formation of hydroxyectoine compared to the hydroxylase from *S. alaskensis*. Furthermore, the enzymes displayed notable differences for the synthetic substrate - while (*Sa*)EctD possessed rather the same properties for both substrates, the (*Ps*)EctD displayed an even higher turnover rate for homoectoine compared to the authentic substrate ectoine. In a previous publication by Bursy *et al.* it has been stated that the EctD enzymes from *V. salexigens* and *S. coelicolor* are not able to hydroxylate proline or the synthetic ectoine derivatives DHMICA (smaller ring size) and homoectoine [36, 64]. From the knowledge that we have gained now, it is not necessarily clear that these enzymes cannot perform this reaction using the synthetic substrates but rather additional assay optimization might be required. In accordance to our results, the EctD enzymes from *H. elongata* and *S. cattleya* were recently employed to produce hydroxyproline, since different hydroxylated prolines are interesting building blocks for medical and biotechnological applications [324–

cyclic non-ribosomal peptide compounds, such as the antifungal agent echinocandin or the anti-tuberculosis drugs griselimycins [325, 327, 328]. In the study reported by Hara *et al.*, EctD from *H. elongata* exclusively catalyzed the formation of *trans*-3-hydroxyproline from the non-natural substrate L-proline, while the (*S*)EctD enzyme also accepted 3,4-dehydro-L-proline, 2-methyl-L-proline, and L-pipecolic acid as substrates [324].

Taken together, the reported findings emphasize that it is helpful to benchmark the (*in vitro* and *in vivo*) efficiency of the same enzyme originating from different organisms to identify the best suitable candidate for the desired biocatalysis. The phylogenomic data reported in context of our review article (see 5.1.1) might therefore serve as a guide to screen ectoine biosynthetic enzymes originating from microorganisms living in ecophysiologically varied habitats that are best suited for different biotransformation approaches. Furthermore, genetic engineering of EctD enzymes might also allow the modification of synthetic chiral substrates with larger or different side chains. The enzymatic introduction of a stereo- and regioselective hydroxyl-group to chiral compounds (such as homoectoine or proline) using (*in vivo*) whole cell biocatalysis is an environmentally friendly way to produce chiral building blocks. In the future, this substrate flexibility in combination with enzyme engineering might be exploited for the design of novel molecules with potential medical and biotechnological applications.

6.3. Ectoine biosynthesis - a structural view

Over thirty years after the pioneering discovery of the stress-protectants ectoine in *E. halochloris* by Galinski *et al.* [58] and 5-hydroxyectoine in *S. parvulus* by Inbar and Lapidot [63], we now have a structure-based view of the complete pathway at hand (Figure 9). Within the last years, high-resolution crystal structures of three of the four enzymes required for the synthesis of ectoine (EctABC) and 5-hydroxyectoine (EctD) have been solved. Recently, the first enzyme involved in the synthesis of ectoine (L-2,4-diaminobutyrate aminotransferase EctB) was studied via an *in silico* model based on the crystal structure of an γ -aminobutyrate transaminase from *Arthrobacter aureescens* (PDB: 4ATP) [329] and this PLP-dependent enzyme was further analyzed by site-directed mutagenesis (Figure 9) (Richter *et al.*, *submitted manuscript*). The second enzyme required for ectoine biosynthesis, the L-2,4-diaminobutyrate acetyltransferase (EctA) was recently studied on a structural and functional level leading to a proposal of the performed reaction mechanism (Figure 9) (Richter *et al.*, *submitted manuscript*). In the context of this thesis, the enzymatic reaction mechanism of the ectoine synthase (EctC) was proposed based on crystal structures in complex with the catalytically critical iron, the substrate *N*- γ -ADABA and the reaction product ectoine (Figure 9) (see 5.2.4) [71]. Furthermore, a study by Höppner *et al.* in 2014 reported the crystal structure of the ectoine hydroxylase (EctD) in complex with the iron catalyst, the co-substrate 2-oxoglutarate and the reaction product 5-hydroxyectoine (Figure 9) [78].

These structural and modeling analyses allow a detailed understanding of the enzymes required for the biosynthesis of the versatile stress protectants ectoine and 5-hydroxyectoine. Furthermore, they open up

future research studies for their exploitation as biocatalysts and might serve as blueprints for studies on related enzymes.

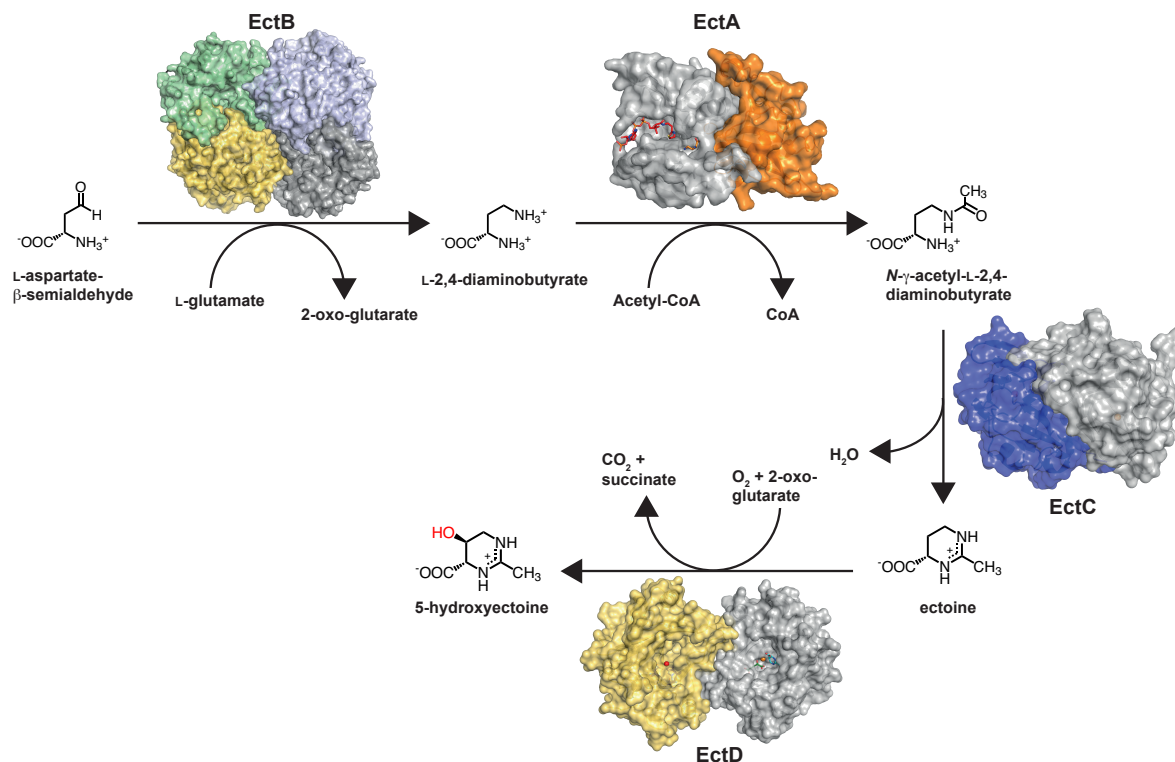


Figure 9 A structural view on the ectoine/5-hydroxyectoine biosynthetic pathway. The L-2,4-diaminobutyrate (DABA) aminotransferase EctB from *P. lautus* has been modeled on the crystal structure of *Arthrobacter aureus* γ-aminobutyrate transaminase (PDB: 4ATP) [329; Richter *et al.*, submitted manuscript). The crystal structure of the L-2,4-diaminobutyrate (DABA) acetyltransferase EctA from *P. lautus* has been solved recently (PDB: 6SLL) (Richter *et al.*, submitted manuscript). The high resolution crystal structure of the ectoine synthase EctC from *P. lautus* has been reported in the context of this PhD thesis (PDB: 5ONM) [71] and the structure of the ectoine hydroxylase EctD from *S. alaskensis* was solved in a previous study (PDB: 4Q5O) [78].

6.4. Production of ectoine and 5-hydroxyectoine in microbial cell factories and their biotechnological use

Despite few exceptions [169, 190], most microorganisms that possess the ectoine hydroxylase EctD produce mixtures of ectoine and 5-hydroxyectoine in response to elevated salinities [36, 37, 82, 91, 170, 183, 185]. For biotechnological uses and practical applications, this combined production might entail further costly and difficult purification steps during down-stream processing to obtain either pure ectoine or 5-hydroxyectoine. Production of pure ectoine can be achieved rather simple, through the genetic inactivation of the *ectD* gene or the use of an ectoine synthesizing organism that naturally lacks the gene encoding the ectoine hydroxylase. For the production of pure 5-hydroxyectoine, we reported the construction of an EctD-mediated *E. coli* whole cell catalysis as part of this PhD thesis (see 5.2.2). The cell factory was able to fully transform up to 15 mM of externally supplied ectoine to 5-hydroxyectoine within 24 h at moderate salt concentrations. Using the EctD enzyme from *P. stutzeri* A1501, an AHT-inducible *tet*

promoter present on the expression plasmid controlled the transcription of the *ectD* gene. Furthermore, the synthetic *E. coli* cell factory secreted the produced 5-hydroxyectoine into the medium supernatant independent of the presence of mechanosensitive channels (see discussion 6.6) [57]. During the evaluation phase of the study, great differences between the *in vivo* performances/efficiencies of ectoine hydroxylase originating from different organisms (various habitats and phyla) were observed. We found that despite rather large sequence identities, similar molecular weight and pI, only the ectoine hydroxylase from *P. stutzeri* A1501 yielded a full conversion of ectoine to 5-hydroxyectoine within our heterologous *E. coli* cell factory *in vivo*. This again indicates that the performance and catalytic efficiency of an EctD enzyme is *per se* not deducible from its protein sequence and that a functional comparison of the same enzyme originating from different organisms might help to identify a suitable catalyst for biotechnological purposes.

A major drawback of many biotechnological ectoine/5-hydroxyectoine production methods is the high amount of salt, required to boost ectoine/5-hydroxyectoine production since the salt effectuates corrosion of the equipment needed for cultivation [57, 60]. It thereby has negative constraints on the investment and operation costs, design, and durability of the reactor systems and downstream processing [93]. Furthermore, it often results in reduced growth rates and maximal cell densities of the bacterial cultures [57, 179]. To overcome these problems various attempts have been made to construct synthetic microbial cell factories that require less or even no salt for ectoine synthesis [57, 179]. Within the framework of this thesis, promoter engineering of the *ect* gene cluster originating from *P. stutzeri* A1501 expressed in *E. coli*, aimed to unravel the molecular determinants within the promoter region required for osmotic control of *ect* gene expression (also see discussion 6.5). Adjustment of the *P. stutzeri* *ect* promoter region, which possessed a GC-rich -10 region and an unusual 18 bp spacer between the -35 and -10 region, to a perfect sigma-70 house-keeping promoter of *E. coli* (-35: TTGACA; -10: TATAAT; 17 bp spacer) resulted in a more than 35-fold increase in the promoter activity under both low (0 M NaCl) and moderate salt (0.4 M NaCl) concentrations. This mutated perfect sigma-70 promoter was in turn introduced into a plasmid that carried the complete *P. stutzeri* A1501 ectoine biosynthetic gene cluster for heterologous ectoine/5-hydroxyectoine production in *E. coli* to obtain higher ectoine/5-hydroxyectoine production levels at moderate salinity (0.4 M NaCl). Unfortunately, the achieved production yields (2 g l⁻¹) lay far behind the achieved ectoine titers of other heterologous cell factories at that time, that employed *E. coli* W3110 and BW25113 expressing the *ect* genes from *H. elongata* (25 g l⁻¹) or a genetically engineered *C. glutamicum* strain carrying the *ect* genes from *C. salexigens* (22 g l⁻¹). To achieve higher yields of our cell factory further optimizations of the host strain, cultivation conditions and media composition would be required [200, 201, 206].

In general, a major disadvantage of plasmid-based cell factories is the continuous need of an antibiotic to maintain the plasmid, the instability of plasmids during long growth or incubation times and - if applicable - the need of rather expensive inducer molecules such as anhydrotetracycline (AHT) or isopropyl- β -D-thiogalactopyranosid (IPTG) to trigger *ect* gene transcription. This problem might be overcome by the chromosomal integration of the biosynthetic genes and the use of different promoters.

An important advantage of these heterologous factories is the permanent secretion of the produced ectoines into the medium supernatant as it has been demonstrated in the three *E. coli* based cell factories that were constructed during this thesis (see 5.2.2, 5.2.3, 5.2.5 for results and 6.6. for discussion).

Finally, a recent study by Wittmann and co-workers set milestones in heterologous ectoine production as they achieved (I) highest yield (65 g l^{-1}) and specific productivity ($120 \text{ mg g}^{-1} \text{ h}^{-1}$), (II) salt-independence, (III) permanent secretion, (IV) no side products, and (V) use of cheap carbon sources [93, 109, 169, 190]. They employed a *C. glutamicum* cell factory that harbors the ectoine biosynthetic genes (*ectABC*) from *P. stutzeri* A1501 encoded on a plasmid [179]. In an elegant procedure, ectoine production in *C. glutamicum* was engineered via flux analysis and transcriptional balancing using libraries of different synthetic promoter for each gene involved in ectoine production (*ectABC*) [179]. Furthermore, *C. glutamicum* was grown on sugar and molasses in a fed-batch system without the need of salt addition to induce ectoine production. Ectoine was secreted into the medium with a high-efficiency since no contaminating side products were detected. The polycistronic design of the ectoine genes yielded an optimal balance in enzymatic capacity for the different steps involved in production. As a result, a high expression of EctB and a well-balanced expression ratio between EctA and EctB (1:1.4) are apparently the key factors to drive the high-flux ectoine pathway [179].

6.5. Regulation of ectoine biosynthesis - a dark spot

A remarkable and yet insufficiently explained feature of osmotically stressed cells is their ability to finely sense the external degree of osmotic stress and transduce this information to unknown cellular signals that in turn control production and accumulation of ectoines in a finely tuned manner [66, 109, 139]. The linear correlation between extracellular stress and the internally accumulated solute pool allows the bacterial cell to maintain their physiological function, cellular hydration and growth under fluctuating osmotic circumstances. This principle is not only existent in the case of ectoine synthesis and accumulation; it rather represents a general feature of microbial cells independent of the employed osmoprotective compound [111, 125, 128, 330]. Even though some studies on the control of ectoine biosynthesis, in respect of the promoters driving *ect* gene transcription or the influence of different transcription factors, have been conducted within the past years, little is still known about the involved regulatory mechanisms [68, 97, 100, 102, 139, 141, 149]. It is in all cases apparent that the transcriptional profile of the ectoine biosynthetic genes is fully compliant with their physiological osmoprotecting task in the studied microorganisms, but no consistent picture can be drawn how genetic and physiological regulatory circuits control *ect* gene expression in response to environmental and cellular cues in various microorganisms.

In conclusion, besides the evolutionary rather stable genetic organization of the ectoine biosynthetic genes [*ectABC(D)*] (see 6.1), major differences seem to exist in the underlying regulatory determinants in most of the studied organisms. Some of the natural ectoine producers were shown to possess different *ect* promoters recognized by different transcription factors besides the housekeeping sigma factor (e.g. RpoS; sigma-B) [37, 68, 97, 139], while others potentially use promoters that function independently of specific

transcription factors [97], such as the *P. stutzeri* *ect* promoter studied herein (see 5.2.3). Furthermore, in some bacteria regulatory proteins such as the MarR-type regulator EctR (mainly found in *Proteobacteria*) (see 5.2.7) [100], CosR studied in *V. cholera* [102] or GlnR identified in *S. coelicolor* [149] seem to be involved in the regulation of the ectoine biosynthetic gene clusters. However, in the case of all these regulatory proteins, osmoregulation of *ect* gene expression persisted even when they were genetically inactivated [100, 102, 149]. In addition, a large group of ectoine/5-hydroxyectoine gene clusters are not directly associated with a regulatory gene encoded within their gene neighborhood (78% of our database analysis), and must thereby rely on other regulatory mechanisms. These findings indicate that the promoter elements and their flanking regions might harbor critical information required for osmotic control of *ect* gene transcription.

In a publication reported in the context of this thesis, the upstream region of the ectoine biosynthetic gene cluster from *P. stutzeri* A1501, together with a short region of the *ectA* gene were fused to the transcriptional regulator *lacZ* and introduced into an *E. coli* (wild type) chassis strain (see 5.2.3). Transcriptional analysis led to four remarkable observations: (I) the finely tuned linear relationship between the external salt concentration and the *ect* promoter activity was fully transferable to the *E. coli* host, that by it self does not possess ectoine biosynthetic genes; (II) *ect* gene expression was reduced to a basal level, when the *E. coli* host accumulated compatible solutes (e. g. glycine betaine) that were supplied in the medium; (III) an imperfect sigma-70 promoter is responsible for low expression levels of the *ect* genes under low osmolarity conditions since its mutation to a perfect sigma-70 promoter led to an 34-fold increase in promoter activity under low salt concentrations and 16-fold at moderate osmotic stress; (IV) nevertheless, even this perfect sigma-70 promoter remained to be osmotically inducible (at least to some extent 1.8-fold compared to 5.2-fold of the wild type promoter). The striking observation that imported compatible solutes reduced the expression levels of the *ect* promoter under high salinity conditions has already been reported for other osmolyte biosynthesis clusters or genes encoding import systems [105, 106, 127]. However, it is noteworthy that the employed *E. coli* wild type cells were also able to synthesize the compatible solute trehalose *de novo* in response to the externally applied osmotic stress. Interestingly, the accumulation of trehalose does not seem to influence the expression levels of the *ect* genes to same extent as externally supplied compatible solutes (such as glycine betaine, ectoine or 5-hydroxyectoine). It is yet not clear how the cells distinguish between externally supplied and internally produced compatible solutes; and why diverse compatible solutes act differently on the activity of one promoter [126]. A comparable observation has been described in *B. subtilis* when the interplay between externally provided and internally produced proline and its influence on the promoter of the *proHJ* operon was investigated. The authors described that expression of the *proHJ* operon responsible for the production of proline as an osmoprotectant was both repressed by the exogenous supply of glycine betaine and proline, but in the case of proline to a much lesser extent [126]. In another study the osmoprotective effect and the catabolism of proline was addressed [331]. Therein, it was highlighted that *B. subtilis* can somehow physiologically distinguish between an externally supplied proline and the intracellular proline pool amassed through *de novo* synthesis under osmotic stress conditions to induce the expression of the proline

catabolic system *putBCP* [331]. This observation was further strengthened in a study, that addressed the osmoprotection of *B. subtilis* through the import and proteolysis of proline-containing peptides [332].

The detailed analyses of the *P. stutzeri ect* promoter now strengthen the hypothesis, that osmoregulation of the *ect* promoter in the heterologous *E. coli* host is an inherent feature of the promoter elements, their spacer and flanking regions. Moreover, it is rather implausible that the non-ectoine producer *E. coli* harbors specific regulatory elements (such as transcription factors or regulatory RNAs) that particularly control the implemented *ect* promoter originating from the plant-root-associated soil bacterium *P. stutzeri*. A potential and yet insufficiently studied fact could be influences of the intracellular ion and compatible solute pool on the RNA polymerase itself [123, 333, 334] or changes in the global or local DNA supercoiling [117, 118, 335].

As stated above, a subset of ectoine producers harbor the MarR-type regulator EctR in the vicinity of the ectoine biosynthetic genes (see 4.2.3.1 and 5.2.7) [100, 101]. In addition to the preliminary studies on EctR from *Novosphingobium* sp. LH128 [(N_s)EctR], this regulatory protein has been investigated in methylophils, such as *M. alcaliphilum*, *M. alcalica*, *M. thalassica* [100, 101, 336]. In these organisms EctR serves as a repressor of *ect* gene expression, but does not seem to be crucial for their osmotic-induction [100, 101, 336]. In the presented dissertation the crystal structure of an EctR regulator was solved in collaboration with Dr. S. Smits (University of Düsseldorf) for the first time (see 5.2.7). Structural and biochemical analysis revealed its tetrameric assembly, that contrasts with the dimeric form of the EctR regulator reported for *M. alcaliphilum* [(Ma)EctR] [100]. In both organisms, the gene encoding the EctR regulator is located divergent and upstream of the *ect* gene cluster. DNA binding studies using purified (N_s)EctR identified two potential DNA binding regions in front of *ectR* and *ectA* that might both function as roadblocks for the RNA polymerase during the binding of the EctR regulator. However, it was not yet studied if EctR binds to both binding sites at the same time, which might hypothetical result in a loop formation of the DNA. In case of (Ma)EctR also two binding sites were detected, one overlaps the sigma-70-type *ectA* promoter and another one is located in front of *ectR*, also emphasizing an autoregulatory function of this protein. In both organisms, the osmotic control of the ectoine biosynthetic genes remained functional, when the *ectR* gene was disrupted. Again this observation highlights the existence of at least two different regulatory mechanisms acting on *ect* gene expression. One potential role of the described regulatory protein could be to keep the gene expression of ectoine biosynthetic genes low under low salt conditions, thereby avoiding unnecessary production of the compatible solute. In sum, it is apparent, that only little is known about the detailed mechanisms responsible for the regulation of ectoine biosynthetic genes, as well as the exact stimuli to which the cells respond and how this signal is then transferred to yet unidentified regulatory elements, different sigma factors or promoter regions.

The environmental or cellular cues that trigger changes in the DNA-binding activity of EctR-type regulators are unknown and hence our understanding of the role of this intriguing regulatory protein in controlling *ect* gene expression is rather incomplete. The preliminary data on the EctR regulator might entail further interesting findings during future investigations. For the MarR-type regulators CosR and BusR involved in regulation of compatible solutes synthesis and acquisition in *V. cholera* and *L. lactis* it has

been hypothesized that they might sense changes in the intracellular ionic strength and as a consequence alter their DNA binding behavior [102, 104]. This observation also represents a possible functional mechanism for the EctR regulator and serves as basis for an experimental investigation.

6.6. Novel insights into ectoine transport

It is well known that import systems for osmoprotectants play a central role during bacterial osmoprotection, since the uptake of compatible solutes from environmental resources is typically cheaper than their *de novo* synthesis [20]. In the context of the bioinformatical analysis of *ect* gene clusters reported in this thesis, a large group of putative ectoine producers (33%) was shown to harbor genes encoding potential transporters in the neighborhood of the ectoine/5-hydroxyectoine biosynthetic gene clusters (see 5.2.6). Grouping of these gene clusters according to the family of the present transporters led to the identification of at least seven major groups, as TRAP-, MFS-, SSS-, ABC-transporters, as well as mechanosensitive channels were found to be co-located with the *ect* genes in various microorganisms. Ectoine biosynthetic gene clusters that contained potential transporters from three different organisms (Cand. *N. maritimus*, *Novosphingobium* sp. LH128 and *H. neptunium*) were studied on a molecular and functional basis within this thesis.

The co-transcription of an MscS-type mechanosensitive channel with ectoine biosynthetic genes was for the first time detected in the marine *Thaumarchaeon* Cand. *N. maritimus* (see 5.2.1) [72]. In a second study, investigating the *ect* gene cluster of the *Alphaproteobacterium* *Novosphingobium* sp. LH128 also revealed the presence of an MscS-type mechanosensitive channel in the same transcriptional unit (see 5.2.6). In both organisms the transcription of the mechanosensitive channel increased under high osmolarity conditions. Sequence alignments and modeling analysis of the MscS-type channel from Cand. *N. maritimus* [(Nm)MscS] in comparison to the MscS channel from *E. coli* indicated that it lacks the soluble C-terminal domain, which forms a central cage in the cytoplasm [288, 293, 314]. It is assumed, that this cytoplasmic cage acts as a strainer allowing the inflow of ions and other small molecules that can then exit the cell via the open pore formed by the mechanosensitive channel [288]. In case of the mechanosensitive channel from *Novosphingobium* sp. LH128 a higher sequence similarity to the YbdG channel from *E. coli* than to the MscS channel was observed. In *E. coli* YbdG alone did not disclose ion channel activity in electrophysiological measurement unless a mutation had been introduced in the β -domain that is part of the C-terminal cage of the MscS channel [312, 313]. Furthermore, its genetic inactivation did not lead to a measurable phenotype - only the genetic disruption of *ybdG* in a strain lacking MscK, MscS, and MscL reduced the threshold of hypoosmotic stress at which death of the *E. coli* mutants occurred [312, 313]. Booth and co-workers therefore hypothesized that YbdG possesses MscM-like (mini conductance) activity and gates at a lower pressure than MscK, MscS, or MscL [312]. A recently published study speculates about the involvement of YbdG in a mechanosensing system that transmits signals triggered by external osmotic changes to intracellular factors [311]. Amemiya *et al.* emphasize that YbdG is not only engaged in the protection against hypoosmotic shocks but also hyperosmotic stress, functioning as a mediator and/or modulator of hyperosmotic stress signaling beyond its possible function as an ion or

solute transport system [311]. If these characteristics are also applicable for the (*Nm*)MscS and (*Ns*)MscS channels, remains to be elucidated. The functionality of the (*Nm*)MscS and (*Ns*)MscS channels as *emergency release valves* during osmotic down-shocks was exclusively verified in heterologous experiments using an *E. coli* mutant strain that lacked all seven known mechanosensitive channels (see 5.2.6) [313]. Overexpression of these channels resulted in an approximately 15-fold higher survival rate compared to the *E. coli* mutant strain, respectively. Taken together, it represents a remarkable finding that functional mechanosensitive channels are co-expressed with genes required for the protection against high osmolarity. It underlines that bacterial cells seemingly already prepare themselves for an eventually occurring osmotic down-shock by precautionary enhancing the production of these safety-valves during high salt conditions.

Several uptake system for free ectoines from natural ecosystems have been studied in the past years, such as e.g. the TeaABC transporter from *H. elongata* or the EctT importer from *V. pantothenticus* [37, 177, 178]. Microorganisms do not only import ectoines from environmental sources via high affinity transport systems for their protection against in salt stress and extremes in temperature, but also for their acquisition as nutrients (e.g., EhuABCD, UehABC) [243, 247, 248]. Furthermore, ectoine importers may function as recycling systems for newly synthesized ectoines that are either leaked or actively excreted from the producer cells [177].

Within this dissertation, the ectoine biosynthetic gene clusters of *Novosphingobium* sp. LH128 and *H. neptunium* have been studied due to the identification of an interesting set of transporters that is co-transcribed with the *ect* genes (see 5.2.6). *H. neptunium* was shown to harbor an osmolyte transporter (EctI) that belongs to the Sodium Solute Superfamily (SSS). EctI represents the first ectoine transporter of this family and it furthermore exhibited a large substrate spectrum for osmostress protectants. Modeling studies and mutational analysis led to the proposal of the potential substrate-binding site. In contrast other transporters of this family, such as the proline transporter PutP, are highly specialized in their substrate profile [331, 337, 338]. The ectoine biosynthetic gene cluster of *Novosphingobium* sp. LH128 is followed by three co-regulated transporter genes: first, a potential exporter (EctE; see below), second, an importer (EctU) and third, the above described MscS-type mechanosensitive channel. Heterologous expression, together with modeling and mutational analysis identified EctU as a high affinity uptake system for ectoine and 5-hydroxyectoine. EctU is part of the Major Facilitator Superfamily (MFS) and displays the first ectoine-specific MFS transporter, since other ectoine-importing members of this family, such as ProP from *E. coli* possess a very broad substrate spectrum [276]. In both, EctI and EctU, the putative ligand binding pockets resembled the key features and characteristics of the specific ectoine-binding protein of the EhuABCD transporter from *S. meliloti*, EhuB [243, 248].

Over the past years, secretion of compatible solutes under stable osmotic conditions (meaning independent of osmotic down-shocks) has been reported in a number of different organisms and it became more and more apparent, that this might represent a general and ubiquitous feature of many microbial cells. Overall, bacteria even aim to balance the in- or outflow of water during the smallest changes in the osmotic potential [1]. These slight changes might for example arise during growth and

division of the cells where a given cell doubles its volume prior to division. Hypothetically, microorganisms might fine-tune the solute concentrations within their cytoplasm through the activity of *export-reimport-cycles* (Figure 10). It has for example been shown in *H. elongata*, that the cells produce ectoine, release it through a yet unknown mechanism and reimport it through the specific uptake system TeaABC [177]. Consequently, a *teaABC* deletion strain accumulated ectoine outside the cells, since they were not able to reimport the osmoprotectant [177]. The same phenomenon was reported for the *de novo* synthesized compatible solute proline in *B. subtilis* [339]. In this case the SSS-type high affinity import system OpuE serves as the recycling system for proline, that is somehow released from the microorganism under steady state osmotic conditions [339]. Deletion mutants of *opuE* exhibited a strong growth defect under high osmolarity conditions and accumulated proline in the medium supernatant. It was demonstrated, that neither the mechanosensitive channels nor the reversal of the proline transporter PutP was involved in this secretion [339, 340]. The molecular mechanism or transporters involved in the secretion of proline were not identified, but the role of OpuE as a proline-specific recycling system was elucidated. In contrast to the *H. elongata* Tea-mutant strain, *B. subtilis* mutant cells lacking the OpuE transporter also overproduced and secreted increased amounts of proline under low external salt concentrations [339].

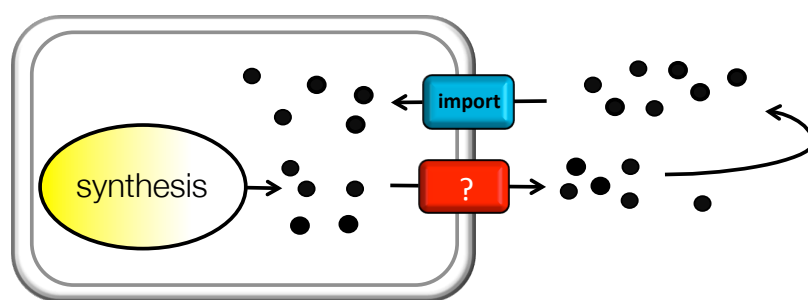


Figure 10 Scheme of the synthesis-export-reimport-cycle of compatible solutes in bacteria.

Besides these two examples, a study by Lamark *et al.* in 1992 already demonstrated that *E. coli* secreted glycine betaine synthesized from the precursor choline into the medium via an unknown mechanism and reimported it through the osmoprotectant uptake systems ProP and ProU [341]. Another example is the secretion of the compatible solute glycosylglycerol from the cyanobacterium *Synechocystis* sp. strain PCC6803 and its reimport via the ABC transporter GgtBC reported by Mikkat & Hagemann [50]. Jebbar *et al.* also reported the release of ectoine from *E. coli* when they preloaded the cells with externally supplied radiolabeled ectoine under moderate osmotic stress conditions and then added unlabeled ectoine or glycine betaine to the cells [268]. An early experiment that demonstrated the constant turnover of the intracellular solute pool [268]. Another important finding in *Lactobacillus plantarum* indicated the existence of compatible solute efflux systems in microorganisms - osmotically down-shocked *L. plantarum* cells depicted two kinetically different components during the release of glycine betaine [342, 343]. While one kinetic signal corresponds to the gating of mechanosensitive channels, another flux is consistent with a

export process mediated by a carrier protein [342]. The secretion of ectoines at constant osmolarity was also demonstrated in heterologous ectoine cell factories using different non-natural ectoine producers, such as various *E. coli* wild type and mutant strains, different *C. glutamicum* strains or the yeast *Hansenula polymorpha* [94, 179, 199, 200, 208].

In two publications that are part of this theses ectoine secretion from non-natural *E. coli* cell factories has been reported (see 5.2.2 and 5.2.3). We employed two different *E. coli* mutant strains to unravel the involvement of the osmoprotectant uptake systems ProU and ProP and its mechanosensitive channels in the observed secretion. In both strains the produced ectoine/5-hydroxyectoine was still secreted into the medium. While the strain lacking the mechanosensitive channels secreted the same amount of ectoines compared to the wild type strain, the *proP* and *proU* mutant contained even higher amounts of ectoines in its supernatant. This observation again underlines the idea that these transporters function as a reimport system for the compatible solutes, which are permanently secreted by the cells during constant osmotic stress. All these studies point to the existence of specific compatible solute exporters, but the overall physiological relevance and molecular details of active compatible solutes secretion from microbial cells required continued investigations.

Bay and Turner reported a first hint on the molecular identity of compatible solutes efflux systems in the study on the multidrug efflux system EmrE. It was shown to be involved in the release of quaternary cation osmoprotectants in *E. coli* such as glycine betaine and choline [344] EmrE belongs to the Small Multidrug Resistance (SMR) family and confers resistance to a wide range of toxic compounds including ethidium bromide, methyl viologen or acriflavine by removing them from the cells [345, 346]. The efflux is coupled to an influx of protons [345, 346]. Most microorganisms including *E. coli* harbor a large variety of different multidrug transporters that can transport similar substrates indicating a functional redundancy of these efflux systems, which often masks phenotypes derived from one single transporter. This may explain why single-gene deletions of *emrE* did not significantly alter hyperosmotic tolerance of the *E. coli* mutant strain [344]. In addition, efflux of the main osmoprotectant glycerol has been observed in the yeast *S. cerevisiae*. Surprisingly, the Major Intrinsic Protein (MIP) family channel Fps1p was described to not only mediate specific uptake of glycerol but also its efflux [51, 347, 348].

We found that a set of transporters was co-transcribed with the ectoine biosynthetic gene cluster of *Novosphingobium* sp. LH128 (see 5.2.6). Among these, we not only identified the ectoine-specific-importer EctI, but also a second MFS-type transporter. Furthermore, genetic inactivation of the specific importer EctI resulted in the same behavior as observed for the *tea* mutant in *H. elongata* [177]: the produced 5-hydroxyectoine accumulated in the medium. Amino acid sequence comparison of the second MFS-type transporter gave the first hints that this transporter might potentially function as an export system and we therefor named this transporter EctE (ectoine export). To exclude that EctE might like EctI function as an importer, we overexpressed EctE in an *E. coli* mutant strain lacking *proU* and *proP* – interestingly, EctE did not allow osmoprotection by any of the tested compatible solutes. The hypothesis that it actually functions as an export system was further strengthened when we found that its overexpression in an *E. coli* wild type strain circumvented osmotic protection by externally supplied ectoines, while all other tested

compatible solutes were still osmoprotective. We concluded that EctE-mediated export of ectoines in *E. coli* is faster than the importer via the uptake systems ProP and ProU, which might result in the disability of the bacterial cells to build an ectoine pool that is high enough to outbalance the outflow of water under osmotic stress conditions. Hence, EctE is most likely the first described specific exporter for ectoines and opens new possibilities to identify other potential ectoine exporters. Our bioinformatical analysis also revealed the existence of at least 22 potential MFS-type exporters in the vicinity of other ectoines biosynthetic gene clusters. The found transporters may represent for the first time the missing link in the *export-reimport-cycle* of ectoines.

Besides fine-tuning of the cytoplasmic solute pool during growth and division, secretion of compatible solutes might also play a role in bacterial communities, quorum sensing and in biofilms. In a co-cultivation experiment of the diatom *Thalassiosira pseudonana* with the ectoine-catabolizing strain *R. pomeroyi* DSS-3, induction of the ectoine utilization genes was reported [260]. An observation which indicates, that ectoine is produced and secreted by the diatom, and taken up and digested by the bacterial cells [260]. Furthermore the importance of glycine betaine in biofilms was reported by Kapfhammer *et al.* in *V. cholera*, where they hypothesize that sharing of compatible solutes might be a mechanism for cooperativity in microbial communities [349]. The idea is that compatible solutes can rapidly disperse after release into aquatic environments, while biofilms are limited in diffusion. Hence, concentrations of released compatible solutes would be sufficient to enhance bacterial growth in high osmolarity environments. These hypothesis were strengthened by the finding that glycine betaine enhanced the formation of biofilms through the transcriptional activation of the *vps* genes, which encode enzymes required for the production of VPS exopolysaccharides important structural components of *V. cholera* biofilms [349]. These findings were supported by a study from Shikuma *et al.* since they demonstrated that *V. cholera* mutants lacking the *ectA* gene and thereby the ability to produce ectoine were unable to form biofilms [102]. Moreover, high transcription levels of the ectoine biosynthetic genes in biofilms was reported in case of the *Alphaproteobacterium* used for soil-bioremediation *Novosphingobium* sp. LH128 when the changes in transcriptional profiles of osmotically stressed biofilms were compared to non-stressed biofilms [350–352]. These observations form the idea that compatible solutes might be exported and reimported by cells living in bacterial communities and thereby might function as public goods [353, 354].

7. References

1. **Bremer E, Krämer R.** Responses of microorganisms to osmotic stress. *Annu Rev Microbiol* 2019;73:313–334.
2. **Csonka LN.** Physiological and genetic responses of bacteria to osmotic stress. *Microbiol Rev* 1989;53:121–147.
3. **Wood JM, Bremer E, Csonka LN, Kraemer R, Poolman B, et al.** Osmosensing and osmoregulatory compatible solute accumulation by bacteria. In: *Comparative Biochemistry and Physiology - A Molecular and Integrative Physiology*. 2001. pp. 437–460.
4. **Roeßler M, Müller V.** Osmoadaptation in bacteria and archaea: common principles and differences. *Environ Microbiol* 2001;3:743–754.
5. **Wood JM.** Osmosensing by bacteria: signals and membrane-based sensors. *Microbiol Mol Biol Rev* 1999;63:230–262.
6. **Booth IR.** Bacterial mechanosensitive channels: progress towards an understanding of their roles in cell physiology. *Curr Opin Microbiol* 2014;18:16–22.
7. **Wood JM.** Bacterial osmoregulation: a paradigm for the study of cellular homeostasis. *Annu Rev Microbiol* 2011;65:215–238.
8. **Van Den Berg J, Boersma AJ, Poolman B.** Microorganisms maintain crowding homeostasis. *Nat Rev Microbiol* 2017;15:309–318.
9. **Scott Cayley D, Guttman HJ, Thomas Record M.** Biophysical characterization of changes in amounts and activity of *Escherichia coli* cell and compartment water and turgor pressure in response to osmotic stress. *Biophys J* 2009;78:1748–1764.
10. **Rojas ER, Huang KC.** Regulation of microbial growth by turgor pressure. *Curr Opin Microbiol* 2018;42:62–70.
11. **Oren A.** Life at high salt concentrations, intracellular KCl concentrations, and acidic proteomes. *Front Microbiol* 2013;4:doi: 10.3389/fmicb.2013.00315.
12. **Galinski EA, Trüper HG.** Microbial behaviour in salt-stressed ecosystems. *FEMS Microbiol Rev* 1994;15:95–108.
13. **Calamita G.** The *Escherichia coli* aquaporin-Z water channel. *Mol Microbiol* 2000;37:254–262.
14. **Kempf B, Bremer E.** Uptake and synthesis of compatible solutes as microbial stress responses to high-osmolality environments. *Arch Microbiol* 1998;170:319–330.
15. **Grant WD.** Life at low water activity. *Philos Trans R Soc Lond B Biol Sci* 2004;359:1249–1267.
16. **Oren A.** Microbial life at high salt concentrations: phylogenetic and metabolic diversity. *Saline Systems* 2008;4:doi:10.1186/1746-1448-4-2.
17. **Galinski EA.** Compatible solutes of halophilic eubacteria: molecular principles, water-solute interaction, stress protection. *Experientia* 1993;49:487–496.
18. **Booth IR, Miller S, Müller A, Lehtovirta-Morley L.** The evolution of bacterial mechanosensitive channels. *Cell Calcium* 2014;57:140–150.
19. **Kung C, Martinac B, Sukharev S.** Mechanosensitive channels in microbes. *Annu Rev Microbiol* 2010;64:313–329.
20. **Oren A.** Bioenergetic aspects of halophilism. *Microbiol Mol Biol Rev* 1999;63:334–348.
21. **Oren A.** Thermodynamic limits to microbial life at high salt concentrations. *Environ Microbiol* 2011;13:1908–1923.
22. **Youssef NH, Savage-Ashlock KN, McCully AL, Luedtke B, Shaw EI, et al.** Trehalose/2-sulfotrehalose biosynthesis and glycine-betaine uptake are widely spread mechanisms for osmoadaptation in the *Halobacteriales*. *ISME J* 2014;8:636–649.
23. **Deole R, Challacombe J, Raiford DW, Hoff WD.** An extremely halophilic proteobacterium combines a highly acidic proteome with a low cytoplasmic potassium content. *J Biol Chem* 2013;288:581–588.
24. **Kokoeva M V., Storch KF, Klein C, Oesterhelt D.** A novel mode of sensory transduction in archaea: binding protein-mediated chemotaxis towards osmoprotectants and amino acids. *EMBO J* 2002;21:2312–2322.
25. **Plemenitaš A, Lenassi M, Konte T, Kejžar A, Zajc J, et al.** Adaptation to high salt concentrations in halotolerant/halophilic fungi: a molecular perspective. *Front Microbiol* 2014;5:doi: 10.3389/fmicb.2014.00199.
26. **Brown AD.** Microbial water stress. *Bacteriol Rev* 1976;40:803–846.
27. **Yancey PH.** Organic osmolytes as compatible, metabolic and counteracting cytoprotectants in high osmolarity and other stresses. *J Exp Biol* 2005;208:2819–2830.
28. **Zhang L, Xue X, Yan J, Yan LY, Jin XH, et al.** L-proline: a highly effective cryoprotectant for mouse oocyte vitrification. *Sci Rep* 2016;6:doi: 10.1038/srep26326.
29. **Cleland D, Krader P, McCree C, Tang J, Emerson D.** Glycine betaine as a cryoprotectant for prokaryotes. *J Microbiol Methods* 2004;58:31–38.
30. **Yancey PH.** Compatible and counteracting solutes: protecting cells from the Dead Sea to the deep sea. *Sci Prog* 2004;87:1–24.
31. **Yancey PH, Blake WR, Conley J.** Unusual organic osmolytes in deep-sea animals: adaptations to

- hydrostatic pressure and other perturbants. *Comp Biochem Physiol - A Mol Integr Physiol* 2002;133:667–676.
32. Sajjad W, Qadir S, Ahmad M, Rafiq M, Hasan F, *et al.* Ectoine: a compatible solute in radio-halophilic *Stenotrophomonas* sp. WMA-LM19 strain to prevent ultraviolet-induced protein damage. *J Appl Microbiol* 2018;125:457–467.
 33. Smiddy M, Sleator RD, Patterson MF, Hill C, Kelly AL. Role for compatible solutes glycine betaine and L-carnitine in listerial barotolerance. *Appl Environ Microbiol* 2004;70:7555–7557.
 34. Hoffmann T, Bremer E. Protection of *Bacillus subtilis* against cold stress via compatible-solute acquisition. *J Bacteriol* 2011;193:1552–1562.
 35. Vargas C, Argandoña M, Reina-Bueno M, Rodríguez-Moya J, Fernández-Aunión C, *et al.* Unravelling the adaptation responses to osmotic and temperature stress in *Chromohalobacter salexigens*, a bacterium with broad salinity tolerance. *Saline Systems* 2008;4:doi: 10.1186/1746-1448-4-14.
 36. Bursy J, Kuhlmann AU, Pittelkow M, Hartmann H, Jebbar M, *et al.* Synthesis and uptake of the compatible solutes ectoine and 5-hydroxyectoine by *Streptomyces coelicolor* A3(2) in response to salt and heat stresses. *Appl Environ Microbiol* 2008;74:7286–7296.
 37. Kuhlmann AU, Hoffmann T, Bursy J, Jebbar M, Bremer E. Ectoine and hydroxyectoine as protectants against osmotic and cold stress: uptake through the SigB-controlled Betaine-Choline-Carnitine Transporter-type carrier EctT from *Virgibacillus pantothenticus*. *J Bacteriol* 2011;193:4699–4708.
 38. Manzanera M. High survival and stability rates of *Escherichia coli* dried in hydroxyectoine. *FEMS Microbiol Lett* 2004;233:347–352.
 39. Louis P, Trüper HG, Galinski EA. Survival of *Escherichia coli* during drying and storage in the presence of compatible solutes. *Appl Microbiol Biotechnol* 1994;41:684–688.
 40. Malin G, Lapidot A. Induction of synthesis of tetrahydropyrimidine derivatives in *Streptomyces* strains and their effect on *Escherichia coli* in response to osmotic and heat stress. *J Bacteriol* 1996;178:385–395.
 41. Bremer E, Krämer R. Coping with osmotic challenges: osmoregulation through accumulation and release of compatible solutes. In: Storz G, Hengge-Aronis R (editors). *Bacterial Stress Responses*. Washington, DC: ASM Press; 2000. pp. 79–97.
 42. Empadinhas N, da Costa MS. Osmoadaptation mechanisms in prokaryotes: distribution of compatible solutes. *Int Microbiol* 2008;11:151–161.
 43. da Costa MS, Santos H, Galinski EA. An overview of the role and diversity of compatible solutes in *Bacteria* and *Archaea*. *Adv Biochem Eng Biotechnol* 1998;61:117–153.
 44. Hagemann M, Pade N. Heterosides - compatible solutes occurring in prokaryotic and eukaryotic phototrophs. *Plant Biol* 2015;17:927–934.
 45. Gunde-Cimerman N, Plemenitaš A, Oren A. Strategies of adaptation of microorganisms of the three domains of life to high salt concentrations. *FEMS Microbiol Rev* 2018;42:353–375.
 46. Welsh DT. Ecological significance of compatible solute accumulation by micro-organisms: from single cells to global climate. *FEMS Microbiol Rev* 2000;24:263–290.
 47. Müller V, Spanheimer R, Santos H. Stress response by solute accumulation in archaea. *Curr Opin Microbiol* 2005;8:729–736.
 48. Klähn S, Hagemann M. Compatible solute biosynthesis in cyanobacteria. *Environ Microbiol* 2011;13:551–562.
 49. Hagemann M. Molecular biology of cyanobacterial salt acclimation. *FEMS Microbiol Rev* 2011;35:87–123.
 50. Mikkat S, Hagemann M. Molecular analysis of the *ggtBCD* gene cluster of *Synechocystis* sp. strain PCC6803 encoding subunits of an ABC transporter for osmoprotective compounds. *Arch Microbiol* 2000;174:273–282.
 51. Burg MB, Ferraris JD. Intracellular organic osmolytes: function and regulation. *J Biol Chem* 2008;283:7309–7313.
 52. Nevoigt E, Stahl U. Osmoregulation and glycerol metabolism in the yeast *Saccharomyces cerevisiae*. *FEMS Microbiology Reviews* 1997;21:231–241.
 53. Bolen DW. Effects of naturally occurring osmolytes on protein stability and solubility: issues important in protein crystallization. *Methods* 2004;34:312–322.
 54. Diamant S, Eliahu N, Rosenthal D, Goloubinoff P. Chemical chaperones regulate molecular chaperones in vitro and in cells under combined salt and heat stresses. *J Biol Chem* 2001;276:39586–39591.
 55. Arakawa T. Protein–solvent interaction. *Biophys Rev* 2018;10:203–208.
 56. Arakawa T, Timasheff SN. The stabilization of proteins by osmolytes. *Biophys J* 1985;46:411–414.
 57. Pastor JM, Salvador M, Argandoña M, Bernal V, Reina-Bueno M, *et al.* Ectoines in cell stress protection: uses and biotechnological production. *Biotechnol Adv* 2010;28:782–801.
 58. Galinski EA, Pfeiffer HP, Trüper HG. 1,4,5,6-Tetrahydro-2-methyl-4-pyrimidinecarboxylic acid. A novel cyclic amino acid from halophilic phototrophic bacteria of the genus *Ectothiorhodospira*. *Eur J Biochem* 1985;149:135–139.
 59. Czech L, Hermann L, Stöveken N, Richter A, Höppner A, *et al.* Role of the extremolytes ectoine and hydroxyectoine as stress protectants and nutrients: genetics, phylogenomics, biochemistry, and structural analysis. *Genes (Basel)* 2018;9:177. doi: 10.3390/genes9040177.
 60. Kunte H, Lentzen G, Galinski EA. Industrial production of the cell protectant ectoine: protection mechanisms, processes, and products. *Curr Biotechnol* 2014;3:10–25.

61. **Lentzen G, Schwarz T.** Extremolytes: natural compounds from extremophiles for versatile applications. *Appl Microbiol Biotechnol* 2006;72:623–634.
62. **Inbar L, Lapido A.** The structure and biosynthesis of new tetrahydropyrimidine derivatives in actinomycin D producer *Streptomyces parvulus*. Use of ¹³C- and ¹⁵N-labeled L-glutamate and ¹³C and ¹⁵N NMR spectroscopy. *J Biol Chem* 1988;263:16014–16022.
63. **Inbar L, Frolow F, Lapidot A.** The conformation of new tetrahydropyrimidine derivatives in solution and in the crystal. *Eur J Biochem* 1993;214:897–906.
64. **Bursy J, Pierik AJ, Pica N, Bremer E.** Osmotically induced synthesis of the compatible solute hydroxyectoine is mediated by an evolutionarily conserved ectoine hydroxylase. *J Biol Chem* 2007;282:31147–31155.
65. **Severin J, Wohlfarth A, Galinski EA.** The predominant role of recently discovered tetrahydropyrimidines for the osmoadaptation of halophilic eubacteria. *J Gen Microbiol* 2009;138:2473–2473.
66. **Kuhlmann AU, Bremer E.** Osmotically regulated synthesis of the compatible solute ectoine in *Bacillus pasteurii* and related *Bacillus* spp. *Appl Environ Microbiol* 2002;68:772–783.
67. **Widderich N, Höppner A, Pittelkow M, Heider J, Smits SHJ, et al.** Biochemical properties of ectoine hydroxylases from extremophiles and their wider taxonomic distribution among microorganisms. *PLoS One* 2014;9:e93809. doi:10.1371/journal.pone.0093809.
68. **Louis P, Galinski EA.** Characterization of genes for the biosynthesis of the compatible solute ectoine from *Marinococcus halophilus* and osmoregulated expression in *Escherichia coli*. *Microbiology* 1997;143:1141–1149.
69. **Prabhu J, Schauwecker F, Grammel N, Keller U, Bernhard M.** Functional expression of the ectoine hydroxylase gene (*thpD*) from *Streptomyces chrysomallus* in *Halomonas elongata*. *Appl Environ Microbiol* 2004;70:3130–3132.
70. **García-Esteva R, Argandoña M, Reina-Bueno M, Capote N, Iglesias-Guerra F, et al.** The *ectD* gene, which is involved in the synthesis of the compatible solute hydroxyectoine, is essential for thermoprotection of the halophilic bacterium *Chromohalobacter salexigens*. *J Bacteriol* 2006;188:3774–3784.
71. **Czech L, Höppner A, Kobus S, Seubert A, Riclea R, et al.** Illuminating the catalytic core of ectoine synthase through structural and biochemical analysis. *Sci Rep* 2019;9:doi: 10.1038/s41598-018-36247-w.
72. **Widderich N, Czech L, Elling FJ, Könneke M, Stöveken N, et al.** Strangers in the archaeal world: osmotic stress-responsive biosynthesis of ectoine and hydroxyectoine by the marine thaumarchaeon *Nitrosopumilus maritimus*. *Environ Microbiol* 2016;18:1227–1248.
73. **Harding T, Brown MW, Simpson AGB, Roger AJ.** Osmoadaptative strategy and its molecular signature in obligately halophilic heterotrophic protists. *Genome Biol Evol* 2016;8:2241–2258.
74. **Weinisch L, Kirchner I, Grimm M, Kühner S, Pierik AJ, et al.** Glycine betaine and ectoine are the major compatible solutes used by four different halophilic heterotrophic ciliates. *Microb Ecol* 2019;77:317–331.
75. **Weinisch L, Kühner S, Roth R, Grimm M, Roth T, et al.** Identification of osmoadaptive strategies in the halophile, heterotrophic ciliate *Schmidingerotrix salinarum*. *PLoS Biol* 2018;16:e2003892. doi: 10.1371/journal.pbio.2003892.
76. **Czech L, Bremer E.** With a pinch of extra salt - Did predatory protists steal genes from their food? *PLoS Biol* 2018;16:e2005163. doi: 10.1371/journal.pbio.2005163.
77. **Ono H, Sawada K, Khunajakr N, Tao T, Yamamoto M, et al.** Characterization of biosynthetic enzymes for ectoine as a compatible solute in a moderately halophilic eubacterium, *Halomonas elongata*. *J Bacteriol* 1999;181:91–99.
78. **Höppner A, Widderich N, Lenders M, Bremer E, Smits SHJ.** Crystal structure of the ectoine hydroxylase, a snapshot of the active site. *J Biol Chem* 2014;289:29570–29583.
79. **Stöveken N, Pittelkow M, Sinner T, Jensen RA, Heider J, et al.** A specialized aspartokinase enhances the biosynthesis of the osmoprotectants ectoine and hydroxyectoine in *Pseudomonas stutzeri* A1501. *J Bacteriol* 2011;193:4456–4468.
80. **Peters P, Galinski EA, Trüper HG.** The biosynthesis of ectoine. *FEMS Microbiol Lett* 1990;71:157–162.
81. **Reshetnikov AS, Khmelenina VN, Mustakhimov II, Trotsenko YA.** Genes and enzymes of ectoine biosynthesis in halotolerant methanotrophs. *Methods Enzymol* 2011;495:15–30.
82. **Tao P, Li H, Yu Y, Gu J, Liu Y.** Ectoine and 5-hydroxyectoine accumulation in the halophile *Virgibacillus halodenitrificans* PDB-F2 in response to salt stress. *Appl Microbiol Biotechnol* 2016;100:6779–6789.
83. **León MJ, Hoffmann T, Sánchez-Porro C, Heider J, Ventosa A, et al.** Compatible solute synthesis and import by the moderate halophile *Spiribacter salinus*: physiology and genomics. *Front Microbiol* 2018;9:doi: 10.3389/fmicb.2018.00108.
84. **Oliveira EF, Cerqueira NMFS, Fernandes PA, Ramos MJ.** Mechanism of formation of the internal aldimine in pyridoxal 5'-phosphate-dependent enzymes. *J Am Chem Soc* 2011;133:15496–15505.
85. **Reuter K, Pittelkow M, Bursy J, Heine A, Craan T, et al.** Synthesis of 5-hydroxyectoine from ectoine: crystal structure of the non-heme iron(II) and 2-oxoglutarate-dependent dioxygenase EctD. *PLoS One* 2010;5:e10647. doi:10.1371/journal.pone.0010647.
86. **Widderich N, Kobus S, Höppner A, Riclea R, Seubert A, et al.** Biochemistry and crystal structure of ectoine synthase: a metal-containing member of the cupin superfamily. *PLoS One* 2016;11:e0151285. doi:10.1371/journal.pone.0151285.

87. Vetting MW, S. de Carvalho LP, Yu M, Hegde SS, Magnet S, *et al.* Structure and functions of the GNAT superfamily of acetyltransferases. *Arch Biochem Biophys* 2005;433:212–226.
88. Dunwell JM, Purvis A, Khuri S. Cupins: The most functionally diverse protein superfamily? *Phytochemistry* 2004;65:7–17.
89. Dunwell JM, Culham A, Carter CE, Sosa-Aguirre CR, Goodenough PW. Evolution of functional diversity in the cupin superfamily. *Trends Biochem Sci* 2001;26:740–746.
90. Khuri S, Bakker FT, Dunwell JM. Phylogeny, function, and evolution of the cupins, a structurally conserved, functionally diverse superfamily of proteins. *Mol Biol Evol* 2001;18:593–605.
91. Moritz KD, Amendt B, Witt EMHJ, Galinski EA. The hydroxyectoine gene cluster of the non-halophilic acidophile *Acidiphilium cryptum*. *Extremophiles* 2014;19:87–99.
92. Widderich N, Pittelkow M, Höppner A, Mulnaes D, Buckel W, *et al.* Molecular dynamics simulations and structure-guided mutagenesis provide insight into the architecture of the catalytic core of the ectoine hydroxylase. *J Mol Biol* 2014;426:586–600.
93. Czech L, Stöveken N, Bremer E. EctD-mediated biotransformation of the chemical chaperone ectoine into hydroxyectoine and its mechanosensitive channel-independent excretion. *Microb Cell Fact* 2016;15:doi: 10.1186/s12934-016-0525-4.
94. Becker J, Schäfer R, Kohlstedt M, Harder BJ, Borchert NS, *et al.* Systems metabolic engineering of *Corynebacterium glutamicum* for production of the chemical chaperone ectoine. *Microb Cell Fact* 2013;12:10.1186/1475-2859-12–110.
95. Lo CC, Bonner CA, Xie G, D'Souza M, Jensen RA. Cohesion group approach for evolutionary analysis of aspartokinase, an enzyme that feeds a branched network of many biochemical pathways. *Microbiol Mol Biol Rev* 2009;73:594–651.
96. Bestvater T, Louis P, Galinski EA. Heterologous ectoine production in *Escherichia coli*: by-passing the metabolic bottle-neck. *Saline Systems* 2008;4:doi:10.1186/1746-1448-4-12.
97. Schwibbert K, Marin-Sanguino A, Bagyan I, Heidrich G, Lentzen G, *et al.* A blueprint of ectoine metabolism from the genome of the industrial producer *Halomonas elongata* DSM 2581^T. *Environ Microbiol* 2011;13:1973–1994.
98. Piubeli F, Salvador M, Argandoña M, Nieto JJ, Bernal V, *et al.* Insights into metabolic osmoadaptation of the ectoines-producer bacterium *Chromohalobacter salexigens* through a high-quality genome scale metabolic model. *Microb Cell Fact* 2018;17:doi: 10.1186/s12934-017-0852-0.
99. Kindzierski V, Raschke S, Knabe N, Siedler F, Scheffer B, *et al.* Osmoregulation in the halophilic bacterium *Halomonas elongata*: a case study for integrative systems biology. *PLoS One* 2017;12:e0168818. doi: 10.1371/journal.pone.0168818.
100. Mustakhimov II, Reshetnikov A, Clukhov A, Khmelenina V, Kalyuzhnaya M, *et al.* Identification and characterization of EctR1, a new transcriptional regulator of the ectoine biosynthesis genes in the halotolerant methanotroph *Methylobacterium alcaliphilum* 20Z. *J Bacteriol* 2010;192:410–417.
101. Mustakhimov II, Reshetnikov AS, Fedorov DN, Khmelenina VN, Trotsenko YA. Role of EctR as transcriptional regulator of ectoine biosynthesis genes in *Methylophaga thalassica*. *Biochemistry (Moscow)* 2012;77:857–863.
102. Shikuma NJ, Davis KR, Fong JNC, Yildiz FH. The transcriptional regulator, CosR, controls compatible solute biosynthesis and transport, motility and biofilm formation in *Vibrio cholerae*. *Environ Microbiol* 2013;15:1387–1399.
103. Romeo Y, Obis D, Bouvier J, Guillot A, Fourçans A, *et al.* Osmoregulation in *Lactococcus lactis*: BusR, a transcriptional repressor of the glycine betaine uptake system BusA. *Mol Microbiol* 2003;47:1135–1147.
104. Romeo Y, Bouvier J, Gutierrez C. Osmotic regulation of transcription in *Lactococcus lactis*: Ionic strength-dependent binding of the BusR repressor to the *busA* promoter. *FEBS Lett* 2007;581:3387–3390.
105. Ronzheimer S, Warmbold J, Arnhold C, Bremer E. The GbsR family of transcriptional regulators: functional characterization of the OpuAR repressor. *Front Microbiol* 2018;9:doi: 10.3389/fmicb.2018.02536.
106. Nau-Wagner G, Oppen D, Rolbetzki A, Boch J, Kempf B, *et al.* Genetic control of osmoadaptive glycine betaine synthesis in *Bacillus subtilis* through the choline-sensing and glycine betaine-responsive GbsR repressor. *J Bacteriol* 2012;194:2703–2714.
107. Winkelman JT, Bree AC, Bate AR, Eichenberger P, Gourse RL, *et al.* RemA is a DNA-binding protein that activates biofilm matrix gene expression in *Bacillus subtilis*. *Mol Microbiol* 2013;88:984–997.
108. Shikuma NJ, Yildiz FH. Identification and characterization of OscR, a transcriptional regulator involved in osmolarity adaptation in *Vibrio cholerae*. *J Bacteriol* 2009;191:4082–4096.
109. Czech L, Poehl S, Hub P, Stöveken N, Bremer E. Tinkering with osmotically controlled transcription allows enhanced production and excretion of ectoine and hydroxyectoine from a microbial cell factory. *Appl Environ Microbiol* 2018;84:e01772-17. doi: 10.1128/AEM.01772-17.
110. Fischer KE, Bremer E. Activity of the osmotically regulated *yqiHIK* promoter from *Bacillus subtilis* is controlled at a distance. *J Bacteriol* 2012;194:5197–5208.
111. Hoffmann T, Bleisteiner M, Sappa PK, Steil L, Mäder U, *et al.* Synthesis of the compatible solute proline by *Bacillus subtilis*: point mutations rendering the osmotically controlled *proHI* promoter hyperactive. *Environ Microbiol* 2017;19:3700–3720.

112. **McLeod SM, Xu J, Johnson RC.** Coactivation of the RpoS-dependent *proP* P2 promoter by Fis and cyclic AMP receptor protein. *J Bacteriol* 2000;182:4180–4187.
113. **Xu J, Johnson RC.** Cyclic AMP receptor protein functions as a repressor of the osmotically inducible promoter *proP* P1 in *Escherichia coli*. *J Bacteriol* 1997;179:2410–2417.
114. **Gundlach J, Krüger L, Herzberg C, Turdiev A, Poehlein A, et al.** Sustained sensing in potassium homeostasis: cyclic di-AMP controls potassium uptake by KimA at the levels of expression and activity. *J Biol Chem* 2019;294:9605–9614.
115. **Schuster CF, Bellows LE, Tosi T, Campeotto I, Corrigan RM, et al.** The second messenger c-di-AMP inhibits the osmolyte uptake system OpuC in *Staphylococcus aureus*. *Sci Signal* 2016;9:doi: 10.1126/scisignal.aaf7279.
116. **Hoffmann T, Bremer E.** Guardians in a stressful world: the Opu family of compatible solute transporters from *Bacillus subtilis*. *Biol Chem* 2017;398:193–214.
117. **Graeme-Cook KA, May G, Bremer E, Higgins CF.** Osmotic regulation of porin expression: a role for DNA supercoiling. *Mol Microbiol* 1989;3:1287–1294.
118. **Higgins CF, Dorman CJ, Stirling DA, Waddell L, Booth IR, et al.** A physiological role for DNA supercoiling in the osmotic regulation of gene expression in *S. typhimurium* and *E. coli*. *Cell* 1988;52:569–584.
119. **Amit R, Oppenheim AB, Stavans J.** Increased bending rigidity of single DNA molecules by H-NS, a temperature and osmolarity sensor. *Biophys J* 2003;84:2467–2473.
120. **Jordi BJAM, Higgins CF.** The downstream regulatory element of the *proU* operon of *Salmonella typhimurium* inhibits open complex formation by RNA polymerase at a distance. *J Biol Chem* 2000;275:12123–12128.
121. **Nagarajavel V, Madhusudan S, Dole S, Rahmouni AR, Schnetz K.** Repression by binding of H-NS within the transcription unit. *J Biol Chem* 2007;282:23622–23630.
122. **Sutherland L, Cairney J, Elmore MJ, Booth IR, Higgins CF.** Osmotic regulation of transcription: induction of the *proU* betaine transport gene is dependent on accumulation of intracellular potassium. *J Bacteriol* 1986;168:805–814.
123. **Gralla JD, Vargas DR.** Potassium glutamate as a transcriptional inhibitor during bacterial osmoregulation. *EMBO J* 2006;25:1515–1521.
124. **Rajkumari K, Kusano S, Ishihama A, Mizuno T, Gowrishankar J.** Effects of H-NS and potassium glutamate on σ^S - and σ^{70} -directed transcription in vitro from osmotically regulated P1 and P2 promoters of *proU* in *Escherichia coli*. *J Bacteriol* 1996;178:4176–4181.
125. **Lucht JM, Bremer E.** Adaptation of *Escherichia coli* to high osmolarity environments: osmoregulation of the high-affinity glycine betaine transport system ProU. *FEMS Microbiol Rev* 1994;14:3–20.
126. **Brill J, Hoffmann T, Bleisteiner M, Bremer E.** Osmotically controlled synthesis of the compatible solute proline is critical for cellular defense of *Bacillus subtilis* against high osmolarity. *J Bacteriol* 2011;193:5335–5346.
127. **Hoffmann T, Wensing A, Brosius M, Steil L, Völker U, et al.** Osmotic control of *opuA* expression in *Bacillus subtilis* and its modulation in response to intracellular glycine betaine and proline pools. *J Bacteriol* 2013;195:510–522.
128. **Hoffmann T, Bremer E.** Management of osmotic stress by *Bacillus subtilis* genetics and physiology. In: Bruijn FJ de (editor). *Stress and Environmental Regulation of Gene Expression and Adaptation in Bacteria*. Hoboken, NJ, USA: John Wiley & Sons, Inc. pp. 657–676.
129. **Hecker M, Pané-Farré J, Uwe V.** SigB-dependent general stress response in *Bacillus subtilis* and related Gram-positive bacteria. *Annu Rev Microbiol* 2007;61:215–236.
130. **Eymann C, Schulz S, Gronau K, Becher D, Hecker M, et al.** In vivo phosphorylation patterns of key stressosome proteins define a second feedback loop that limits activation of *Bacillus subtilis* σ^B . *Mol Microbiol* 2011;80:798–810.
131. **Price CW, Fawcett P, C  r  monie H, Su N, Murphy CK, et al.** Genome-wide analysis of the general stress response in *Bacillus subtilis*. *Mol Microbiol* 2002;41:757–774.
132. **Hecker M, V  lker U.** General stress response of *Bacillus subtilis* and other bacteria. In: *Advances in Microbial Physiology*. pp. 35–91.
133. **Marles-Wright J, Grant T, Delumeau O, van Duinen G, Firbank SJ, et al.** Molecular architecture of the ‘stressosome,’ a signal integration and transduction hub. *Science (80-)* 2008;322:92–96.
134. **C  novas D, Vargas C, Calder  n MI, Ventosa A, Nieto JJ.** Characterization of the genes for the biosynthesis of the compatible solute ectoine in the moderately halophilic bacterium *Halomonas elongata* DSM 3043. *Syst Appl Microbiol* 1998;21:487–497.
135. **Salvador M, Argando  a M, Pastor JM, Bernal V, C  novas M, et al.** Contribution of RpoS to metabolic efficiency and ectoines synthesis during the osmo- and heat-stress response in the halophilic bacterium *Chromohalobacter salexigens*. *Environ Microbiol Rep* 2014;7:301–311.
136. **Rodr  guez-Moya J, Argando  a M, Reina-Bueno M, Nieto JJ, Iglesias-Guerra F, et al.** Involvement of EupR, a response regulator of the NarL/FixJ family, in the control of the uptake of the compatible solutes ectoines by the halophilic bacterium *Chromohalobacter salexigens*. *BMC Microbiol* 2010;10:doi: 10.1186/1471-2180-10-256.
137. **Kuhlmann A, Bursy J, Gimpel S, Hoffmann T, Bremer E.** Synthesis of the compatible solute ectoine in *Virgibacillus pantothenticus* is triggered by high salinity and low growth temperature. *Appl Environ Microbiol*

- 2008;74:4560–4563.
138. **Sadeghi A, Soltani BMB, Nekouei MKM, Jouzani GS, Mirzaei HH, *et al.*** Diversity of the ectoines biosynthesis genes in the salt tolerant *Streptomyces* and evidence for inductive effect of ectoines on their accumulation. *Microbiol Res* 2014;169:699–708.
 139. **Calderón MI, Vargas C, Rojo F, Iglesias-Guerra F, Csonka LN, *et al.*** Complex regulation of the synthesis of the compatible solute ectoine in the halophilic bacterium *Chromohalobacter salexigens* DSM 3043T. *Microbiology* 2004;150:3051–3063.
 140. **Bestvater T, Galinski EA.** Investigation into a stress-inducible promoter region from *Marinococcus halophilus* using green fluorescent protein. *Extrem Life under Extrem Cond* 2002;6:15–20.
 141. **Argandoña M, Nieto JJ, Iglesias-Guerra F, Calderón MI, García-Esteva R, *et al.*** Interplay between iron homeostasis and the osmotic stress response in the halophilic bacterium *Chromohalobacter salexigens*. *Appl Environ Microbiol* 2010;76:3575–3589.
 142. **Reshetnikov AS, Khmelenina VN, Mustakhimov II, Kalyuzhnaya M, Lidstrom M, *et al.*** Diversity and phylogeny of the ectoine biosynthesis genes in aerobic, moderately halophilic methylotrophic bacteria. *Extremophiles* 2011;15:653–663.
 143. **Khmelenina VN, Kalyuzhnaya MG, Starostina NG, Suzina NE, Trotsenko YA.** Isolation and characterization of halotolerant alkaliphilic methanotrophic bacteria from Tuva soda lakes. *Curr Microbiol* 1997;35:257–261.
 144. **Khmelenina VN, Kalyuzhnaya MG, Sakharovsky VG, Suzina NE, Trotsenko Y a., *et al.*** Osmoadaptation in halophilic and alkaliphilic methanotrophs. *Arch Microbiol* 1999;172:321–329.
 145. **Reshetnikov AS, Khmelenina VN, Trotsenko YA.** Characterization of the ectoine biosynthesis genes of haloalkalotolerant obligate methanotroph ‘*Methylobacterium alcaliphilum* 20Z’. *Arch Microbiol* 2006;184:286–297.
 146. **Rigali S, Derouaux A, Giannotta F, Dusart J.** Subdivision of the helix-turn-helix GntR family of bacterial regulators in the FadR, HutC, MocR, and YtrA subfamilies. *J Biol Chem* 2002;277:12507–12515.
 147. **Pham HT, Nhiep NTH, Vu TNM, Huynh TAN, Zhu Y, *et al.*** Enhanced uptake of potassium or glycine betaine or export of cyclic-di-AMP restores osmoresistance in a high cyclic-di-AMP *Lactococcus lactis* mutant. *PLoS Genet* 2018;14:e1007574. doi: 10.1371/ journal.pgen.1007574.
 148. **Tiffert Y, Supra P, Wurm R, Wohlleben W, Wagner R, *et al.*** The *Streptomyces coelicolor* GlnR regulon: identification of new GlnR targets and evidence for a central role of GlnR in nitrogen metabolism in actinomycetes. *Mol Microbiol* 2008;67:861–880.
 149. **Shao Z, Deng W, Li S, He J, Ren S, *et al.*** GlnR-mediated regulation of *ectABCD* transcription expands the role of the GlnR regulon to osmotic stress management. *J Bacteriol* 2015;197:3041–3047.
 150. **Zaccai G, Bagyan I, Combet J, Cuello GJ, Demé B, *et al.*** Neutrons describe ectoine effects on water H-bonding and hydration around a soluble protein and a cell membrane. *Sci Rep* 2016;6:doi: 10.1038/srep31434.
 151. **Smiatek J, Harishchandra RK, Rubner O, Galla HJ, Heuer A.** Properties of compatible solutes in aqueous solution. *Biophys Chem* 2012;160:62–68.
 152. **Ignatova Z, Gierasch LM.** Inhibition of protein aggregation in vitro and in vivo by a natural osmoprotectant. *Proc Natl Acad Sci U S A* 2006;103:13357–13361.
 153. **Harishchandra RK, Wulff S, Lentzen G, Neuhaus T, Galla HJ.** The effect of compatible solute ectoines on the structural organization of lipid monolayer and bilayer membranes. *Biophys Chem* 2010;150:37–46.
 154. **Dwivedi M, Brinkkötter M, Harishchandra RK, Galla HJ.** Biophysical investigations of the structure and function of the tear fluid lipid layers and the effect of ectoine. Part B: Artificial lipid films. *Biochim Biophys Acta - Biomembr* 2014;1838:2716–2727.
 155. **Harishchandra RK, Sachan AK, Kerth A, Lentzen G, Neuhaus T, *et al.*** Compatible solutes: ectoine and hydroxyectoine improve functional nanostructures in artificial lung surfactants. *Biochim Biophys Acta - Biomembr* 2011;1808:2830–2840.
 156. **Eiberweiser A, Nazet A, Kruchinin SE, Fedotova M V., Buchner R.** Hydration and ion binding of the osmolyte ectoine. *J Phys Chem B* 2015;119:15203–15211.
 157. **Hahn MB, Solomun T, Wellhausen R, Hermann S, Seitz H, *et al.*** Influence of the compatible solute ectoine on the local water structure: implications for the binding of the protein G5P to DNA. *J Phys Chem B* 2015;119:15212–15220.
 158. **Meyer S, Schröter MA, Hahn MB, Solomun T, Sturm H, *et al.*** Ectoine can enhance structural changes in DNA in vitro. *Sci Rep* 2017;7:doi: 10.1038/s41598-017-07441-z.
 159. **Schröter MA, Meyer S, Hahn MB, Solomun T, Sturm H, *et al.*** Ectoine protects DNA from damage by ionizing radiation. *Sci Rep* 2017;7:doi: 10.1038/s41598-017-15512-4.
 160. **Malin G, Iakobashvili R, Lapidot A.** Effect of tetrahydropyrimidine derivatives on protein-nucleic acids interaction. *J Biol Chem* 1999;274:6920–6929.
 161. **Sahle CJ, Schroer MA, Jeffries CM, Niskanen J.** Hydration in aqueous solutions of ectoine and hydroxyectoine. *Phys Chem Chem Phys* 2018;20:27917–27923.
 162. **Held C, Neuhaus T, Sadowski G.** Compatible solutes: thermodynamic properties and biological impact of ectoines and prolines. *Biophys Chem* 2010;152:28–39.

163. **Smiatek J, Harishchandra RK, Galla HJ, Heuer A.** Low concentrated hydroxyectoine solutions in presence of DPPC lipid bilayers: a computer simulation study. *Biophys Chem* 2013;180–181:102–109.
164. **Smiatek J.** Osmolyte effects: impact on the aqueous solution around charged and neutral spheres. *J Phys Chem B* 2014;118:771–782.
165. **Graf R, Anzali S, Buenger J, Pfluecker F, Driller H.** The multifunctional role of ectoine as a natural cell protectant. *Clin Dermatol* 2008;26:326–333.
166. **Di Gioacchino M, Bruni F, Sodo A, Imberti S, Ricci MA.** Ectoine hydration, aggregation and influence on water structure. *Mol Phys* 2019;8976:doi: 10.1080/00268976.2019.1649484.
167. **Brands S, Schein P, Castro-Ochoa K, Galinski EA.** Hydroxyl radical scavenging of the compatible solute ectoine generates two N-acetimides. *Arch Biochem Biophys* 2019;doi: 10.1016/j.abb.2019.108097.
168. **Ma Y, Wang Q, Xu W, Liu X, Gao X, et al.** Stationary phase-dependent accumulation of ectoine is an efficient adaptation strategy in *Vibrio anguillarum* against cold stress. *Microbiol Res* 2017;205:8–18.
169. **Schiraldi C, Maresca C, Catapano A, Galinski EA, De Rosa M.** High-yield cultivation of *Marinococcus* M52 for production and recovery of hydroxyectoine. *Res Microbiol* 2006;157:693–699.
170. **Seip B, Galinski EA, Kurz M.** Natural and engineered hydroxyectoine production based on the *Pseudomonas stutzeri* ectABCD-ask gene cluster. *Appl Environ Microbiol* 2011;77:1368–1374.
171. **Saum SH, Müller V.** Growth phase-dependent switch in osmolyte strategy in a moderate halophile: ectoine is a minor osmolyte but major stationary phase solute in *Halobacillus halophilus*. *Environ Microbiol* 2008;10:716–726.
172. **Saum SH, Müller V.** Salinity-dependent switching of osmolyte strategies in a moderately halophilic bacterium: glutamate induces proline biosynthesis in *Halobacillus halophilus*. *J Bacteriol* 2007;189:6968–6975.
173. **Saum SH, Pfeiffer F, Palm P, Rampp M, Schuster SC, et al.** Chloride and organic osmolytes: a hybrid strategy to cope with elevated salinities by the moderately halophilic, chloride-dependent bacterium *Halobacillus halophilus*. *Environ Microbiol* 2013;15:1619–1633.
174. **Saum SH, Müller V.** Regulation of osmoadaptation in the moderate halophile *Halobacillus halophilus*: chloride, glutamate and switching osmolyte strategies. *Saline Systems* 2008;4:doi: 10.1186/1746-1448-4-4.
175. **Tanne C, Golovina EA, Hoekstra FA, Meffert A, Galinski EA.** Glass-forming property of hydroxyectoine is the cause of its superior function as a desiccation protectant. *Front Microbiol* 2014;5:doi: 10.3389/fmicb.2014.00150.
176. **Sauer T, Galinski EA.** Bacterial milking: a novel bioprocess for production of compatible solutes. *Biotechnol Bioeng* 1998;57:306–313.
177. **Grammann K, Volke A, Kunte HJ.** New type of osmoregulated solute transporter identified in halophilic members of the Bacteria domain: TRAP transporter TeaABC mediates uptake of ectoine and hydroxyectoine in *Halomonas elongata* DSM 2581T. *J Bacteriol* 2002;184:3078–3085.
178. **Kuhlmann SI, van Schelting ACT, Bienert R, Kunte HJ, Ziegler CM.** 1.55 Å structure of the ectoine binding protein TeaA of the osmoregulated TRAP-transporter TeaABC from *Halomonas elongata*. *Biochemistry* 2008;47:9475–9485.
179. **Gießelmann G, Dietrich D, Jungmann L, Kohlstedt M, Jeon EJ, et al.** Metabolic engineering of *Corynebacterium glutamicum* for high-level ectoine production – design, combinatorial assembly and implementation of a transcriptionally balanced heterologous ectoine pathway. *Biotechnol J* 2019;1800417:doi: 10.1002/biot.201800417.
180. **Oren A.** Industrial and environmental applications of halophilic microorganisms. *Environ Technol* 2010;31:825–834.
181. **Onraedt AE, Walcarius BA, Soetaert WK, Vandamme EJ.** Optimization of ectoine synthesis through fed-batch fermentation of *Brevibacterium epidermis*. *Biotechnol Prog* 2005;21:1206–1212.
182. **Nagata S, Wang Y, Oshima A, Zhang L, Miyake H, et al.** Efficient cyclic system to yield ectoine using *Brevibacterium* sp. JCM 6894 subjected to osmotic downshock. *Biotechnol Bioeng* 2007;99:941–948.
183. **Frings E, Sauer T, Galinski EA.** Production of hydroxyectoine: high cell-density cultivation and osmotic downshock of *Marinococcus* strain M52. *J Biotechnol* 1995;43:53–61.
184. **Fallet C, Rohe P, Franco-Lara E.** Process optimization of the integrated synthesis and secretion of ectoine and hydroxyectoine under hyper/hypo-osmotic stress. *Biotechnol Bioeng* 2010;107:124–133.
185. **Van-Thuoc D, Guzmán H, Quillaguamán J, Hatti-Kaul R.** High productivity of ectoines by *Halomonas boliviensis* using a combined two-step fed-batch culture and milking process. *J Biotechnol* 2010;147:46–51.
186. **Zhang LH, Lang YJ, Nagata S.** Efficient production of ectoine using ectoine-excreting strain. *Extremophiles* 2009;13:717–724.
187. **Wei YH, Yuan FW, Chen WC, Chen SY.** Production and characterization of ectoine by *Marinococcus* sp. ECT1 isolated from a high-salinity environment. *J Biosci Bioeng* 2011;111:336–342.
188. **Chen WC, Hsu CC, Lan JCW, Chang YK, Wang LF, et al.** Production and characterization of ectoine using a moderately halophilic strain *Halomonas salina* BCRC17875. *J Biosci Bioeng* 2018;125:578–584.
189. **Chen WC, Hsu CC, Wang LF, Lan JCW, Chang YK, et al.** Exploring useful fermentation strategies for the production of hydroxyectoine with a halophilic strain, *Halomonas salina* BCRC 17875. *J Biosci Bioeng* 2019;128:332–336.
190. **Zhao Q, Meng Y, Li S, Lv P, Xu P, et al.** Genome sequence of *Halomonas hydrothermalis* Y2, an efficient

- ectoine-producer isolated from pulp mill wastewater. *J Biotechnol* 2018;285:38–41.
191. **Lang Y, Bai L, Ren Y, Zhang L, Nagata S.** Production of ectoine through a combined process that uses both growing and resting cells of *Halomonas salina* DSM 5928T. *Extremophiles* 2011;15:303–310.
192. **Tanimura K, Nakayama H, Tanaka T, Kondo A.** Ectoine production from lignocellulosic biomass-derived sugars by engineered *Halomonas elongata*. *Bioresour Technol* 2013;142:523–529.
193. **Cantera S, Muñoz R, Lebrero R, López JC, Rodríguez Y, et al.** Technologies for the bioconversion of methane into more valuable products. *Curr Opin Biotechnol* 2018;50:128–135.
194. **Cantera S, Lebrero R, Sadornil L, García-Encina PA, Muñoz R.** Valorization of CH₄ emissions into high-added-value products: assessing the production of ectoine coupled with CH₄ abatement. *J Environ Manage* 2016;182:160–165.
195. **Cantera S, Lebrero R, Rodríguez S, García-Encina PA, Muñoz R.** Ectoine bio-milking in methanotrophs: a step further towards methane-based bio-refineries into high added-value products. *Chem Eng J* 2017;328:44–48.
196. **Cantera S, Sánchez-Andrea I, Lebrero R, García-Encina PA, Stams AJM, et al.** Multi-production of high added market value metabolites from diluted methane emissions via methanotrophic extremophiles. *Bioresour Technol* 2018;267:401–407.
197. **Tanimura K, Matsumoto T, Nakayama H, Tanaka T, Kondo A.** Improvement of ectoine productivity by using sugar transporter-overexpressing *Halomonas elongata*. *Enzyme Microb Technol* 2016;89:63–68.
198. **Sariyar Akbulut B ÖH, Poli A AB, Utkan G DA.** Moderately halophilic bacterium *Halomonas* sp. AAD12: a promising candidate as a hydroxyectoine producer. *J Microb Biochem Technol* 2015;7:262–268.
199. **Schubert T, Maskow T, Benndorf D, Harms H, Breuer U.** Continuous synthesis and excretion of the compatible solute ectoine by a transgenic, nonhalophilic bacterium. *Appl Environ Microbiol* 2007;73:3343–3347.
200. **Ning Y, Wu X, Zhang C, Xu Q, Chen N, et al.** Pathway construction and metabolic engineering for fermentative production of ectoine in *Escherichia coli*. *Metab Eng* 2016;36:10–18.
201. **He Y-Z, Gong J, Yu H-Y, Tao Y, Zhang S, et al.** High production of ectoine from aspartate and glycerol by use of whole-cell biocatalysis in recombinant *Escherichia coli*. *Microb Cell Fact* 2015;14:doi: 10.1186/s12934-015-0238-0.
202. **Zhu D, Liu J, Han R, Shen G, Long Q, et al.** Identification and characterization of ectoine biosynthesis genes and heterologous expression of the *ectABC* gene cluster from *Halomonas* sp. QHL1, a moderately halophilic bacterium isolated from Qinghai Lake. *J Microbiol* 2014;52:139–147.
203. **Stiller LM, Galinski EA, Witt EMHJ.** Engineering the salt-inducible ectoine promoter region of *Halomonas elongata* for protein expression in a unique stabilizing environment. *Genes (Basel)* 2018;9:doi:10.3390/genes9040184.
204. **Parwata IP, Wahyuningrum D, Suhandono S, Hertadi R.** Heterologous ectoine production in *Escherichia coli*: optimization using response surface methodology. *Int J Microbiol* 2019;2019:doi: 10.1155/2019/5475361.
205. **Anbu Rajan L, Joseph TC, Thampuran N, James R, Ashok Kumar K, et al.** Cloning and heterologous expression of ectoine biosynthesis genes from *Bacillus halodurans* in *Escherichia coli*. *Biotechnol Lett* 2008;30:1403–1407.
206. **Pérez-García F, Ziert C, Risse JM, Wendisch VF.** Improved fermentative production of the compatible solute ectoine by *Corynebacterium glutamicum* from glucose and alternative carbon sources. *J Biotechnol* 2017;258:59–68.
207. **Rai M, Pal M, Sumesh K V, Jain V, Sankaranarayanan A.** Engineering for biosynthesis of ectoine (2-methyl 4-carboxy tetrahydro pyrimidine) in tobacco chloroplasts leads to accumulation of ectoine and enhanced salinity tolerance. *Plant Sci* 2006;170:291–306.
208. **Eilert E, Kranz A, Hollenberg CP, Piontek M, Suckow M.** Synthesis and release of the bacterial compatible solute 5-hydroxyectoine in *Hansenula polymorpha*. *J Biotechnol* 2013;167:85–93.
209. **Strong PJ, Kalyuzhnaya M, Silverman J, Clarke WP.** A methanotroph-based biorefinery: potential scenarios for generating multiple products from a single fermentation. *Bioresour Technol* 2016;215:314–323.
210. **Jorge CD, Borges N, Bagyan I, Bilstein A, Santos H.** Potential applications of stress solutes from extremophiles in protein folding diseases and healthcare. *Extremophiles* 2016;20:251–259.
211. **Barth S, Huhn M, Matthey B, Klimka A, Galinski EA, et al.** Compatible-solute-supported periplasmic expression of functional recombinant proteins under stress conditions. *Appl Environ Microbiol* 2000;66:1572–1579.
212. **Lippert K, Galinski E.** Enzyme stabilization by ectoine-type compatible solutes: protection against heating, freezing and drying. *Applied Microbiology and Biotechnology* 1992;37:61–65.
213. **Van-Thuoc D, Hashim SO, Hatti-Kaul R, Mamo G.** Ectoine-mediated protection of enzyme from the effect of pH and temperature stress: a study using *Bacillus halodurans* xylanase as a model. *Appl Microbiol Biotechnol* 2013;97:6271–6278.
214. **Salmannejad F, Nafissi-Varcheh N.** Ectoine and hydroxyectoine inhibit thermal-induced aggregation and increase thermostability of recombinant human interferon Alfa2b. *Eur J Pharm Sci* 2017;97:200–207.
215. **Kolp S, Pietsch M, Galinski EA, Gütschow M.** Compatible solutes as protectants for zymogens against proteolysis. *Biochim Biophys Acta - Proteins Proteomics* 2006;1764:1234–1242.

216. Pul Ü, Wurm R, Wagner R. The role of LRP and H-NS in transcription regulation: involvement of synergism, allostery and macromolecular crowding. *J Mol Biol* 2007;366:900–915.
217. Smiatek J, Kunte H-J, Meyer S, Roloff A, Oprzeska-Zingrebe EA. Influence of compatible solute ectoine on distinct DNA structures: thermodynamic insights into molecular binding mechanisms and destabilization effects. *Phys Chem Chem Phys* 2018;20:25861–25874.
218. Schnoor M, Voß P, Cullen P, Böking T, Galla HJ, *et al.* Characterization of the synthetic compatible solute homoectoine as a potent PCR enhancer. *Biochem Biophys Res Commun* 2004;322:867–872.
219. Mascellani N, Liu X, Rossi S, Marchesini J, Valentini D, *et al.* Compatible solutes from hyperthermophiles improve the quality of DNA microarrays. *BMC Biotechnol* 2007;7:doi: 10.1186/1472-6750-7-82.
220. Unfried K, Krämer U, Sydlik U, Autengruber A, Bilstein A, *et al.* Reduction of neutrophilic lung inflammation by inhalation of the compatible solute ectoine: a randomized trial with elderly individuals. *Int J COPD* 2016;11:2573–2583.
221. Marini A, Reinelt K, Krutmann J, Bilstein a. Ectoine-containing cream in the treatment of mild to moderate atopic dermatitis: a randomised, comparator-controlled, intra-individual double-blind, multi-center trial. *Skin Pharmacol Physiol* 2014;27:57–65.
222. Abdel-Aziz H, Wadie W, Scherner O, Efferth T, Khayyal MT. Bacteria-derived compatible solutes ectoine and 5-hydroxyectoine act as intestinal barrier stabilizers to ameliorate experimental inflammatory bowel disease. *J Nat Prod* 2015;78:1309–1315.
223. Abdel-Aziz H, Wadie W, Abdallah DM, Lentzen G, Khayyal MT. Novel effects of ectoine, a bacteria-derived natural tetrahydropyrimidine, in experimental colitis. *Phytomedicine* 2013;20:585–591.
224. Pech T, Ohsawa I, Praktikno M, Overhaus M, Wehner S, *et al.* A natural tetrahydropyrimidine, ectoine, ameliorates ischemia reperfusion injury after intestinal transplantation in rats. *Pathobiology* 2012;80:102–110.
225. Sydlik U, Gallitz I, Albrecht C, Abel J, Krutmann J, *et al.* The compatible solute ectoine protects against nanoparticle-induced neutrophilic lung inflammation. *Am J Respir Crit Care Med* 2009;180:29–35.
226. Sydlik U, Peuschel H, Paunel-Gorgulu A, Keymel S, Kramer U, *et al.* Recovery of neutrophil apoptosis by ectoine: a new strategy against lung inflammation. *Eur Respir J* 2013;41:433–442.
227. Bazazzadegan N, Shasaltaneh MD, Saliminejad K, Kamali K, Banan M, *et al.* Effects of ectoine on behavior and candidate genes expression in ICV-STZ rat model of sporadic Alzheimer's disease. *Adv Pharm Bull* 2017;7:629–636.
228. Kanapathipillai M, Lentzen G, Sierks M, Park CB. Ectoine and hydroxyectoine inhibit aggregation and neurotoxicity of Alzheimer's β -amyloid. *FEBS Lett* 2005;579:4775–4780.
229. Srinivasan PK, Fet N, Bleilevens C, Afify M, Doorschodt B, *et al.* Hydroxyectoine ameliorates preservation injury in deceased after cardiac death donors in experimental liver grafts. *Ann Transplant* 2014;19:165–173.
230. Manzanera M, Garcia de Castro A, Tondervik A, Rayner-Brandes M, Strom AR, *et al.* Hydroxyectoine is superior to trehalose for anhydrobiotic engineering of *Pseudomonas putida* KT2440. *Appl Environ Microbiol* 2002;68:4328–4333.
231. Nagata S, Maekawa Y, Ikeuchi T, Wang YB, Ishida A. Effect of compatible solutes on the respiratory activity and growth of *Escherichia coli* K-12 under NaCl stress. *J Biosci Bioeng* 2002;94:384–389.
232. Zhang L, Lang Y, Wang C, Nagata S. Promoting effect of compatible solute ectoine on the ethanol fermentation by *Zymomonas mobilis* CICC10232. *Process Biochem* 2008;43:642–646.
233. Maskow T, Kleinsteuber S. Carbon and energy fluxes during haloadaptation of *Halomonas* sp. EF11 growing on phenol. *Extremophiles* 2004;8:133–141.
234. Moghaieb REA, Tanaka N, Saneoka H, Murooka Y, Ono H, *et al.* Characterization of salt tolerance in ectoine-transformed tobacco plants (*Nicotiana tabacum*): photosynthesis, osmotic adjustment, and nitrogen partitioning. *Plant, Cell Environ* 2006;29:173–182.
235. Moghaieb REA, Nakamura A, Saneoka H, Fujita K. Evaluation of salt tolerance in ectoine-transgenic tomato plants (*Lycopersicon esculentum*) in terms of photosynthesis, osmotic adjustment, and carbon partitioning. *GM Crops* 2011;2:58–65.
236. Heinrich U, Garbe B, Tronnier H. In vivo assessment of ectoin: a randomized, vehicle-controlled clinical trial. *Skin Pharmacol Physiol* 2007;20:211–218.
237. Thamm OC, Theodorou P, Stuermer E, Zinser MJ, Neugebauer EA, *et al.* Adipose-derived stem cells and keratinocytes in a chronic wound cell culture model: the role of hydroxyectoine. *Int Wound J* 2015;12:387–396.
238. Castro-Ochoa KF, Vargas-Robles H, Cháñez-Paredes S, Felipe-López A, Cabrera-Silva RI, *et al.* Homoectoine protects against colitis by preventing a claudin switch in epithelial tight junctions. *Dig Dis Sci* 2019;64:409–420.
239. Buenger J, Driller H. Ectoin: an effective natural substance to prevent UVA-induced premature photoaging. *Skin Pharmacol Physiol* 2004;17:232–237.
240. Iizuka H, Ishida-Yamamoto A, Kajita S, Tsutsui M, Ohkuma N. Effects of UVB irradiation on epidermal adenylate cyclase responses in vitro: its relation to sunburn cell formation. *Arch Dermatol Res*

- 1988;280:163–167.
241. **Buommino E, Schiraldi C, Baroni A, Paoletti I, Lamberti M, et al.** Ectoine from halophilic microorganisms induces the expression of *hsp70* and *hsp70B'* in human keratinocytes modulating the proinflammatory response. *Cell Stress Chaperones* 2005;10:197.
242. **Schulz A, Stöveken N, Binzen IM, Hoffmann T, Heider J, et al.** Feeding on compatible solutes: a substrate-induced pathway for uptake and catabolism of ectoines and its genetic control by EnuR. *Environ Microbiol* 2017;19:926–946.
243. **Jebbar M, Sohn-Böscher L, Bremer E, Bernard T, Blanco C.** Ectoine-induced proteins in *Sinorhizobium meliloti* include an ectoine ABC-type transporter involved in osmoprotection and ectoine catabolism. *J Bacteriol* 2005;187:1293–1304.
244. **Galinski EA, Herzog RM.** The role of trehalose as a substitute for nitrogen-containing compatible solutes (*Ectothiorhodospira halochloris*). *Arch Microbiol* 1990;153:607–613.
245. **Vargas C, Jebbar M, Carrasco R, Blanco C, Calderon MI, et al.** Ectoines as compatible solutes and carbon and energy sources for the halophilic bacterium *Chromohalobacter salexigens*. *J Appl Microbiol* 2006;100:98–107.
246. **Salar-García MJ, Bernal V, Pastor JM, Salvador M, Argandoña M, et al.** Understanding the interplay of carbon and nitrogen supply for ectoines production and metabolic overflow in high density cultures of *Chromohalobacter salexigens*. *Microb Cell Fact* 2017;16:doi: 10.1186/s12934-017-0643-7.
247. **Lecher J, Pittelkow M, Zobel S, Bursy J, Bönig T, et al.** The crystal structure of UehA in complex with ectoine-A comparison with other TRAP-T binding proteins. *J Mol Biol* 2009;389:58–73.
248. **Hanekop N, Höing M, Sohn-Böscher L, Jebbar M, Schmitt L, et al.** Crystal structure of the ligand-binding protein EhuB from *Sinorhizobium meliloti* reveals substrate recognition of the compatible solutes ectoine and hydroxyectoine. *J Mol Biol* 2007;374:1237–1250.
249. **Schulz A, Hermann L, Freibert S-A, Bönig T, Hoffmann T, et al.** Transcriptional regulation of ectoine catabolism in response to multiple metabolic and environmental cues. *Environ Microbiol* 2017;19:4599–4619.
250. **Yu Q, Cai H, Zhang Y, He Y, Chen L, et al.** Negative regulation of ectoine uptake and catabolism in *Sinorhizobium meliloti*: characterization of the EhuR gene. *J Bacteriol* 2017;199:e00119-16. doi: 10.1128/JB.00119-16.
251. **Chen IA, Chu K, Palaniappan K, Pillay M, Ratner A, et al.** IMG/M v.5.0: an integrated data management and comparative analysis system for microbial genomes and microbiomes. *Nucleic Acids Res* 2018;doi: 10.1093/nar/gky901.
252. **Bramucci E, Milano T, Pascarella S.** Genomic distribution and heterogeneity of MocR-like transcriptional factors containing a domain belonging to the superfamily of the pyridoxal-5'-phosphate dependent enzymes of fold type I. *Biochem Biophys Res Commun* 2011;415:88–93.
253. **Suvorova IA, Rodionov DA.** Comparative genomics of pyridoxal 5'-phosphate-dependent transcription factor regulons in *Bacteria*. *Microb Genomics* 2016;2:doi: 10.1099/mgen.0.000047.
254. **Belitsky BR.** *Bacillus subtilis* GabR, a protein with DNA-binding and aminotransferase domains, is a PLP-dependent transcriptional regulator. *J Mol Biol* 2004;340:655–664.
255. **Warren CR.** Response of osmolytes in soil to drying and rewetting. *Soil Biol Biochem* 2014;70:22–32.
256. **Warren CR.** Do microbial osmolytes or extracellular depolymerisation products accumulate as soil dries? *Soil Biol Biochem* 2016;98:54–63.
257. **Warren CR.** Quaternary ammonium compounds can be abundant in some soils and are taken up as intact molecules by plants. *New Phytol* 2013;198:476–485.
258. **Bouskill NJ, Wood TE, Baran R, Hao Z, Ye Z, et al.** Belowground response to drought in a tropical forest soil. II. Change in microbial function impacts carbon composition. *Front Microbiol* 2016;7:doi: 10.3389/fmicb.2016.00323.
259. **Bouskill NJ, Wood TE, Baran R, Ye Z, Bowen BP, et al.** Belowground response to drought in a tropical forest soil. I. Changes in microbial functional potential and metabolism. *Front Microbiol* 2016;7:doi: 10.3389/fmicb.2016.00525.
260. **Landa M, Burns AS, Roth SJ, Moran MA.** Bacterial transcriptome remodeling during sequential co-culture with a marine dinoflagellate and diatom. *ISME J* 2017;11:2677–2690.
261. **Ziegler C, Bremer E, Krämer R.** The BCCT family of carriers: from physiology to crystal structure. *Mol Microbiol* 2010;78:13–34.
262. **Culham DE, Marom D, Boutin R, Garner J, Ozturk TN, et al.** Dual role of the C-Terminal domain in osmosensing by bacterial osmolyte transporter ProP. *Biophys J* 2018;115:doi: 10.1016/j.bpj.2018.10.023.
263. **Culham DE, Shkel IA, Record MT, Wood JM.** Contributions of Coulombic and Hofmeister effects to the osmotic activation of *Escherichia coli* transporter ProP. *Biochemistry* 2016;55:1301–1313.
264. **Perez C, Khafizov K, Forrest LR, Krämer R, Ziegler C.** The role of trimerization in the osmoregulated betaine transporter BetP. *EMBO Rep* 2011;12:804–810.
265. **Kappes RM, Kempf B, Kneip S, Boch J, Gade J, et al.** Two evolutionarily closely related ABC transporters mediate the uptake of choline for synthesis of the osmoprotectant glycine betaine in *Bacillus subtilis*. *Mol Microbiol* 1999;32:203–216.
266. **Weinand M, Krämer R, Morbach S.** Characterization of compatible solute transporter multiplicity in

- Corynebacterium glutamicum*. *Appl Microbiol Biotechnol* 2007;76:701–708.
267. **Ongagna-Yhombi SY, McDonald ND, Boyd EF.** Deciphering the role of multiple Betaine-Carnitine-Choline Transporters in the halophile *Vibrio parahaemolyticus*. *Appl Environ Microbiol* 2015;81:351–363.
 268. **Jebbar M, Talibart R, Gloux K, Bernard T, Blanco C.** Osmoprotection of *Escherichia coli* by ectoine: uptake and accumulation characteristics. *J Bacteriol* 1992;174:5027–5035.
 269. **Jebbar M, Von Blohn C, Bremer E.** Ectoine functions as an osmoprotectant in *Bacillus subtilis* and is accumulated via the ABC-transport system OpuC. *FEMS Microbiol Lett* 1997;154:325–330.
 270. **Choquet G, Jehan N, Pissavin C, Blanco C, Jebbar M.** OusB, a broad-specificity ABC-type transporter from *Erwinia chrysanthemi*, mediates uptake of glycine betaine and choline with a high affinity. *Appl Environ Microbiol* 2005;71:3389–3398.
 271. **Gouesbet G, Trautwetter A, Bonnassie S, Wu LF, Blanco C.** Characterization of the *Erwinia chrysanthemi* osmoprotectant transporter gene *ousA*. *J Bacteriol* 1996;178:447–455.
 272. **Vermeulen V, Kunte HJ.** *Marinococcus halophilus* DSM 20408T encodes two transporters for compatible solutes belonging to the Betaine-Carnitine-Choline Transporter family: identification and characterization of ectoine transporter EctM and glycine betaine transporter BetM. *Extremophiles* 2004;8:175–184.
 273. **Peter H, Weil B, Burkovski A, Krämer R, Morbach S.** *Corynebacterium glutamicum* is equipped with four secondary carriers for compatible solutes: identification, sequencing, and characterization of the proline/ectoine uptake system, ProP, and the ectoine/proline/glycine betaine carrier, EctP. *J Bacteriol* 1998;180:6005–6012.
 274. **Kappes RM, Kempf B, Bremer E.** Three transport systems for the osmoprotectant glycine betaine operate in *Bacillus subtilis*: characterization of OpuD. *J Bacteriol* 1996;178:5071–5079.
 275. **Steger R, Weinand M, Krämer R, Morbach S.** LcoP, an osmoregulated betaine/ectoine uptake system from *Corynebacterium glutamicum*. *FEBS Lett* 2004;573:155–160.
 276. **MacMillan S V., Alexander DA, Culham DE, Kunte HJ, Marshall E V., et al.** The ion coupling and organic substrate specificities of osmoregulatory transporter ProP in *Escherichia coli*. *Biochim Biophys Acta - Biomembr* 1999;1420:30–44.
 277. **Du Y, Shi WW, He YX, Yang YH, Zhou CZ, et al.** Structures of the substrate-binding protein provide insights into the multiple compatible solute binding specificities of the *Bacillus subtilis* ABC transporter OpuC. *Biochem J* 2011;436:283–289.
 278. **Mosier AC, Justice NB, Bowen BP, Baran R, Thomas BC, et al.** Metabolites associated with adaptation of microorganisms to an acidophilic, metal-rich environment identified by stable-isotope-enabled metabolomics. *MBio* 2013;4:e00484-12. doi:10.1128/mBio.00484-12.
 279. **Ren M, Feng X, Huang Y, Wang H, Hu Z, et al.** Phylogenomics suggests oxygen availability as a driving force in *Thaumarchaeota* evolution. *ISME J* 2019;13:2150–2161.
 280. **Harding T, Roger AJ, Simpson AGBB.** Adaptations to high salt in a halophilic protist: differential expression and gene acquisitions through duplications and gene transfers. *Front Microbiol* 2017;8:doi: 10.3389/fmicb.2017.00944.
 281. **Harding T, Simpson AGB.** Recent advances in halophilic protozoa research. *J Eukaryot Microbiol* 2018;65:556–570.
 282. **Park JS, Cho BC, Simpson AGB.** *Halocafeteria seosinensis* gen. et sp. nov. (Bicosoecida), a halophilic bacterivorous nanoflagellate isolated from a solar saltern. *Extremophiles* 2006;10:493–504.
 283. **Foissner W, Filker S, Stoeck T.** *Schmidingerothrix salinarum* nov. spec. is the molecular sister of the large Oxytrichid clade (Ciliophora, Hypotricha). *J Eukaryot Microbiol* 2014;61:61–74.
 284. **Ventosa A, de la Haba RR, Sánchez-Porro C, Papke RT.** Microbial diversity of hypersaline environments: a metagenomic approach. *Curr Opin Microbiol* 2015;25:80–87.
 285. **Sukharev S, Sachs F.** Molecular force transduction by ion channels - diversity and unifying principles. *J Cell Sci* 2012;125:3075–3083.
 286. **Martinac B.** Mechanosensitive channels in prokaryotes. *Cell Physiol Biochem* 2001;11:61–76.
 287. **Booth IR, Blount P.** The MscS and MscL families of mechanosensitive channels act as microbial emergency release valves. *J Bacteriol* 2012;194:4802–4809.
 288. **Naismith JH, Booth IR.** Bacterial mechanosensitive channels - MscS: evolution's solution to creating sensitivity in function. *Annu Rev Biophys* 2012;41:157–177.
 289. **Maksaev G, Haswell ES.** Recent characterizations of MscS and its homologs provide insight into the basis of ion selectivity in mechanosensitive channels. *Channels (Austin)* 2013;7:215–220.
 290. **Booth IR, Edwards MD, Black S, Schumann U, Miller S.** Mechanosensitive channels in bacteria: signs of closure? *Nat Rev Microbiol* 2007;5:431–440.
 291. **Perozo E, Rees DC.** Structure and mechanism in prokaryotic mechanosensitive channels. *Curr Opin Struct Biol* 2003;13:432–442.
 292. **Steinbacher S, Bass R, Strop P, Rees DC.** Structures of the prokaryotic mechanosensitive channels MscL and MscS. In: *Current Topics in Membranes*. Elsevier Inc. pp. 1–24.
 293. **Wang W, Black SS, Edwards MD, Miller S, Morrison EL, et al.** The structure of an open form of an *E. coli* mechanosensitive channel at 3.45 Å resolution. *Science (80-)* 2008;321:1179–1183.
 294. **Britten RJ, McClure FT.** The amino acid pool in *Escherichia coli*. *Bacteriol Rev* 1962;26:292–335.

295. **Martinac B, Buechner M, Delcour AH, Adler J, Kung C.** Pressure-sensitive ion channel in *Escherichia coli*. *Proc Natl Acad Sci U S A* 1987;84:2297–2301.
296. **Wilson ME, Maksaev G, Haswell ES.** MscS-like mechanosensitive channels in plants and microbes. *Biochemistry* 2013;52:5708–5722.
297. **Kloda A, Martinac B.** Mechanosensitive channels of bacteria and archaea share a common ancestral origin. *Eur Biophys J* 2002;31:14–25.
298. **Pivetti CD, Yen M-R, Miller S, Busch W, Tseng Y-H, et al.** Two families of mechanosensitive channel proteins. *Microbiol Mol Biol Rev* 2003;67:66–85.
299. **Sukharev SI, Blount P, Martinac B, Blattner FR, Kung C.** A large-conductance mechanosensitive channel in *E. coli* encoded by *mscL* alone. *Nature* 1994;368:265–268.
300. **Nakayama Y, Komazawa K, Bavi N, Hashimoto K ichi, Kawasaki H, et al.** Evolutionary specialization of MscCG, an MscS-like mechanosensitive channel, in amino acid transport in *Corynebacterium glutamicum*. *Sci Rep* 2018;8:doi: 10.1038/s41598-018-31219-6.
301. **Wang Y, Cao G, Xu D, Fan L, Wu X, et al.** A novel *Corynebacterium glutamicum* L-glutamate exporter. *Appl Environ Microbiol* 2018;84:e02691-17. doi: 10.1128/AEM.02691-17.
302. **Becker M, Krämer R.** MscCG from *Corynebacterium glutamicum*: functional significance of the C-terminal domain. *Eur Biophys J* 2015;44:577–588.
303. **Nakayama Y, Hashimoto K ichi, Sawada Y, Sokabe M, Kawasaki H, et al.** *Corynebacterium glutamicum* mechanosensitive channels: towards unpuzzling “glutamate efflux” for amino acid production. *Biophys Rev* 2018;10:1359–1369.
304. **Reuter M, Hayward NJ, Black SS, Miller S, Dryden DTF, et al.** Mechanosensitive channels and bacterial cell wall integrity: does life end with a bang or a whimper? *J R Soc Interface* 2014;11:doi: 10.1098/rsif.2013.0850.
305. **Bass RB, Strop P, Barclay M, Rees DC.** Crystal structure of *Escherichia coli* MscS, a voltage-modulated and mechanosensitive channel. *Science (80-)* 2002;298:1582–1587.
306. **Cruickshank CCC, Minchin RFF, Le Dain ACC, Martinac B.** Estimation of the pore size of the large-conductance mechanosensitive ion channel of *Escherichia coli*. *Biophys J* 1997;73:1925–1931.
307. **Levina N, Totemeyer S, Stokes NR, Louis P, Jones M a, et al.** Protection of *Escherichia coli* cells against extreme turgor by activation of MscS and MscL mechanosensitive channels: identification of genes required for MscS activity. *EMBO J* 1999;18:1730–1737.
308. **Sukharev S.** Purification of the small mechanosensitive channel of *Escherichia coli* (MscS): the subunit structure, conduction, and gating characteristics in liposomes. *Biophys J* 2002;83:290–298.
309. **Walton TA, Idigo CA, Herrera N, Rees DC.** MscL: channeling membrane tension. *Pflügers Arch - Eur J Physiol* 2015;467:15–25.
310. **Kojima S, Nikaido H.** High salt concentrations increase permeability through OmpC channels of *Escherichia coli*. *J Biol Chem* 2014;289:26464–26473.
311. **Amemiya S, Toyoda H, Kimura M, Saito H, Kobayashi H, et al.** The mechanosensitive channel YbdG from *Escherichia coli* has a role in adaptation to osmotic up-shock. *J Biol Chem* 2019;294:12281–12292.
312. **Schumann U, Edwards MD, Rasmussen T, Bartlett W, van West P, et al.** YbdG in *Escherichia coli* is a threshold-setting mechanosensitive channel with MscM activity. *Proc Natl Acad Sci* 2010;107:12664–12669.
313. **Edwards MD, Black S, Rasmussen T, Rasmussen A, Stokes NR, et al.** Characterization of three novel mechanosensitive channel activities in *Escherichia coli*. *Channels* 2012;6:272–281.
314. **Miller S, Bartlett W, Chandrasekaran S, Simpson S, Edwards M, et al.** Domain organization of the MscS mechanosensitive channel of *Escherichia coli*. *EMBO J* 2003;22:36–46.
315. **Kurz M, Buren AY, Seip B, Lindow SE, Gross H.** Genome-driven investigation of compatible solute biosynthesis pathways of *Pseudomonas syringae* pv. *syringae* and their contribution to water stress tolerance. *Appl Environ Microbiol* 2010;76:5452–5462.
316. **León MJ, Ghai R, Fernandez AB, Sanchez-Porro C, Rodriguez-Valera F, et al.** Draft genome of *Spiribacter salinus* M19-40, an abundant Gammaproteobacterium in quatic hypersaline environments. *Genome Announc* 2013;1:e00179-12.
317. **León MJ, Fernández AB, Ghai R, Sánchez-Porro C, Rodríguez-Valera F, et al.** From metagenomics to pure culture: isolation and characterization of the moderately halophilic bacterium *Spiribacter salinus* gen. nov., sp. nov. *Appl Environ Microbiol* 2014;80:3850–3857.
318. **Mukhtar S, Ahmad S, Bashir A, Mehnaz S, Mirza MS, et al.** Identification of plasmid encoded osmoregulatory genes from halophilic bacteria isolated from the rhizosphere of halophytes. *Microbiol Res* 2019;228:126307.
319. **Soucy SM, Huang J, Gogarten JP.** Horizontal gene transfer: building the web of life. *Nat Rev Genet* 2015;16:472–482.
320. **Czech L, Bremer E.** With a pinch of extra salt—Did predatory protists steal genes from their food? *PLoS Biol* 2018;16:e2005163.
321. **Galinski EA, Stein M, Ures A, Schwarz T.** Stereo-specific hydroxylation.
322. **Galinski EA, Stein M, Ures A, Schwarz T.** Stereo-spezifische Hydroxylierung.
323. **Roychoudhury A, Bieker A, Häussinger D, Oesterheld F.** Membrane protein stability depends on the

- concentration of compatible solutes - a single molecule force spectroscopic study. *Biol Chem* 2013;394:1465–1474.
324. Hara R, Nishikawa T, Okuhara T, Koketsu K, Kino K. Ectoine hydroxylase displays selective *trans*-3-hydroxylation activity towards L-proline. *Appl Microbiol Biotechnol* 2019;103:5689–5698.
 325. Zhang F, Liu H, Zhang T, Pijning T, Yu L, *et al.* Biochemical and genetic characterization of fungal proline hydroxylase in echinocandin biosynthesis. *Appl Microbiol Biotechnol* 2018;102:7877–7890.
 326. Zhao TX, Li M, Zheng X, Wang CH, Zhao HX, *et al.* Improved production of *trans*-4-hydroxy-L-proline by chromosomal integration of the *Vitreoscilla* hemoglobin gene into recombinant *Escherichia coli* with expression of proline-4-hydroxylase. *J Biosci Bioeng* 2017;123:109–115.
 327. Houwaart S, Youssar L, Hüttel W. Pneumocandin biosynthesis: involvement of a *trans*-selective proline hydroxylase. *ChemBioChem* 2014;15:2365–2369.
 328. Lukat P, Katsuyama Y, Wenzel S, Binz T, König C, *et al.* Biosynthesis of methyl-proline containing griselimycins, natural products with anti-tuberculosis activity. *Chem Sci* 2017;8:7521–7527.
 329. Bruce H, Nguyen Tuan A, Mangas Sánchez J, Leese C, Hopwood J, *et al.* Structures of a γ -aminobutyrate (GABA) transaminase from the s-triazine-degrading organism *Arthrobacter aureus* TC1 in complex with PLP and with its external aldimine PLP–GABA adduct. *Acta Crystallogr Sect F Struct Biol Cryst Commun* 2012;68:1175–1180.
 330. Giaever HM, Styrvold OB, Kaasen I, Strøm AR. Biochemical and genetic characterization of osmoregulatory trehalose synthesis in *Escherichia coli*. *J Bacteriol* 1988;170:2841–2849.
 331. Moses S, Sinner T, Zapras A, Stöveken N, Hoffmann T, *et al.* Proline utilization by *Bacillus subtilis*: uptake and catabolism. *J Bacteriol* 2012;194:745–758.
 332. Zapras A, Brill J, Thüning M, Wünsche G, Heun M, *et al.* Osmoprotection of *Bacillus subtilis* through import and proteolysis of proline-containing peptides. *Appl Environ Microbiol* 2013;79:576–587.
 333. Gralla JD, Huo Y-X. Remodeling and activation of *Escherichia coli* RNA polymerase by osmolytes. *Biochemistry* 2008;47:13189–13196.
 334. Cayley S, Record MT. Roles of cytoplasmic osmolytes, water, and crowding in the response of *Escherichia coli* to osmotic stress: biophysical basis of osmoprotection by glycine betaine. *Biochemistry* 2003;42:12596–12609.
 335. Lilley DMJ, Higgins CF. Local DNA topology and gene expression: the case of the *leu-500* promoter. *Mol Microbiol* 1991;5:779–783.
 336. Mustakhimov II, Reshetnikov AS, Khmelenina VN, Trotsenko YA. EctR - a novel transcriptional regulator of ectoine biosynthesis genes in the haloalkaliphilic methylotrophic bacterium *Methylophaga alcalica*. *Dokl Biochem Biophys* 2009;429:305–308.
 337. Jung H. Towards the molecular mechanism of Na⁺/solute symport in prokaryotes. *Biochim Biophys Acta - Bioenerg* 2001;1505:131–143.
 338. Peter H, Bader A, Burkovski A, Lambert C, Krämer R. Isolation of the *putP* gene of *Corynebacterium glutamicum* and characterization of a low-affinity uptake system for compatible solutes. *Arch Microbiol* 1997;168:143–151.
 339. Hoffmann T, von Blohn C, Stanek A, Moses S, Barzantny H, *et al.* Synthesis, release, and recapture of compatible solute proline by osmotically stressed *Bacillus subtilis* cells. *Appl Environ Microbiol* 2012;78:5753–5762.
 340. Jung H, Hilger D, Raba M. The Na⁺/L-proline transporter PutP. *Front Biosci* 2012;17:745–759.
 341. Lamark T, Styrvold OB, Strøm AR. Efflux of choline and glycine betaine from osmoregulating cells of *Escherichia coli*. *FEMS Microbiol Lett* 1992;75:149–154.
 342. Glaasker E, Konings WN, Poolman B. Glycine betaine fluxes in *Lactobacillus plantarum* during osmostasis and hyper- and hypo-osmotic shock. *J Biol Chem* 1996;271:10060–10065.
 343. Glaasker E, Heuberger EHML, Konings WN, Poolman B. Mechanism of osmotic activation of the quaternary ammonium compound transporter (QacT) of *Lactobacillus plantarum*. *J Bacteriol* 1998;180:5540–5546.
 344. Bay DC, Turner RJ. Small multidrug resistance protein EmrE reduces host pH and osmotic tolerance to metabolic quaternary cation osmoprotectants. *J Bacteriol* 2012;194:5941–5948.
 345. Saleh M, Bay DC, Turner RJ. Few conserved amino acids in the small multidrug resistance transporter EmrE influence drug polyselectivity. *Antimicrob Agents Chemother* 2018;62:e00461-18. doi: 10.1128/AAC.00461-18.
 346. Bay DC, Rommens KL, Turner RJ. Small multidrug resistance proteins: a multidrug transporter family that continues to grow. *Biochim Biophys Acta - Biomembr* 2008;1778:1814–1838.
 347. Hohmann S. Osmotic stress signaling and osmoadaptation in yeasts. *Microbiol Mol Biol Rev* 2002;66:300–372.
 348. Tamás MJ, Luyten K, Sutherland FCW, Hernandez A, Albertyn J, *et al.* Fps1p controls the accumulation and release of the compatible solute glycerol in yeast osmoregulation. *Mol Microbiol* 1999;31:1087–1104.
 349. Kapfhammer D, Karatan E, Pflughoeft KJ, Watnick PI. Role for glycine betaine transport in *Vibrio cholerae* osmoadaptation and biofilm formation within microbial communities. *Appl Environ Microbiol* 2005;71:3840–3847.

350. **Fida TT, Breugelmans P, Lavigne R, Coronado E, Johnson DR, *et al.*** Exposure to solute stress affects genome-wide expression but not the polycyclic aromatic hydrocarbon-degrading activity of *Sphingomonas* sp. strain LH128 in biofilms. *Appl Environ Microbiol* 2012;78:8311–8320.
351. **Fida TT, Moreno-Forero SK, Heipieper HJ, Springael D.** Physiology and transcriptome of the polycyclic aromatic hydrocarbon-degrading *Sphingomonas* sp. LH128 after long-term starvation. *Microbiology* 2013;159:1807–1817.
352. **Bastiaens, L, Springael D, Wattiau P, Harms H, *et al.*** Isolation of adherent polycyclic aromatic hydrocarbon (PAH)-degrading bacteria using PAH-sorbing carriers. *Appl Environ Microbiol* 2000;66:1834–1843.
353. **Drescher K, Nadell CD, Stone HA, Wingreen NS, Bassler BL.** Solutions to the public goods dilemma in bacterial biofilms. *Curr Biol* 2014;24:50–55.
354. **Yan J, Nadell CD, Stone HA, Wingreen NS, Bassler BL.** Extracellular-matrix-mediated osmotic pressure drives *Vibrio cholerae* biofilm expansion and cheater exclusion. *Nat Commun* 2017;8:doi: 10.1038/s41467-017-00401-1.

8. Scientific CV

Personal data

Name	Laura Czech
Date of birth	4th May 1990
Place of birth	Weilburg/Germany
Marital status	Married, 1 child (Moritz; 17th July 2017)
Nationality	German

Education and academic career

10/2014 - today	Ph. D. in 'Molecular Microbiology' at Philipps-University of Marburg (Germany), funded by a Max Planck fellowship Supervisor: Prof. Dr. Erhard Bremer Thesis: "Synthesis, import and excretion of ectoines in <i>Bacteria</i> and <i>Archaea</i> "
10/2012 - 07/2014	Master degree in 'Molecular and Cellular Biology' at Philipps-University of Marburg (Germany) - grade: very good, 1.2 Supervisor: Prof. Dr. Erhard Bremer Thesis: "Synthesis, import and export of ectoines in the marine Alphaproteo-bacterium <i>Hyphomonas neptunium</i> "
10/2009 - 06/2012	Bachelor degree in 'Biology' at Philipps-University of Marburg (Germany) - grade: very good, 1.8 Supervisor: Prof. Dr. Erhard Bremer Thesis: "Salt-stress induced modifications of the <i>Bacillus subtilis</i> cell wall - analysis of the glycine betaine mediated repression of the salt-induced <i>yqiH</i> operon of <i>Bacillus subtilis</i> "
08/2007 - 06/2009	Secondary School Gymnasium Philippinum Weilburg (Germany) Advanced courses: English, German Graduation with University entrance diploma - grade: very good, 1.7

Fellowships

10/2018	Selected for a fellowship of the Marburg Research Academy (MARA) (Abschlussstipendium Promotion); declined.
10/2014 - current	Fellowship from the International Max Planck Research School for Environmental, Cellular and Molecular Microbiology (IMPRS) funding 2.5 years of my Ph. D. period.
04/2010 - 09/2014	Fellowship from the "Nassauische Zentralstudienfonds" funding of my Bachelor and Master studies.

Commitment & memberships

- **Speaker of the International Max Planck Research School** (Invitation of international guests, organization of retreats with scientific program)
- **Graduate school of the CRC 987** (Collaborative Research Centre SFB 987) funded by the German Research Council (Deutsche Forschungsgemeinschaft (DFG))
- **Selected and active member of 'Scimento-hessenweit'** (Mentoring program for women in science)
- **Member of the VAAM** (German Association for General and Applied Microbiology)
- **Member of MARA** (Marburg Research Academy)

Selected conferences, Talks and Grants

2015	New Approaches and Concepts in Microbiology , EMBL Heidelberg (Germany) - VAAM Travel Grant
2016	BACELL meeting, Paris (France) - VAAM Travel Grant
2019	Annual Meeting of the German Association for General and Applied Microbiology (VAAM) , Mainz (Germany) - Selected for a short talk
2019	Halophiles 2019 , Cluj Napoca (Romania) - Selected for a talk & FEMS Young Scientists Meeting Grant

9. Danksagung

Mein größter Dank gilt meinem Doktorvater und Betreuer dieser Arbeit, Erhard Bremer - nicht nur für die wissenschaftlichen Herausforderungen und Diskussionen, sondern auch für das stets offene Ohr, tiefe Vertrauen und die immerwährende Unterstützung, auch in Zeiten, in denen ich nicht mehr weiter wusste. Vielen Dank für *die gute Schule* und dass ich mit so viel erlerntem Wissen zu neuen Ufern aufbrechen kann.

Des Weiteren möchte ich den Gutachtern Prof. Gert Bange, Prof. Uwe Maier und Prof. Ulrich Mösch für die Beurteilung dieser Arbeit danken. Zusätzlich danke ich Prof. Martin Thanbichler und Prof. Tobias Erb für die Unterstützung im Rahmen meines Thesis Komitees. Außerdem danke ich unserem langjährigen Kollaborationspartner Sander Smits für die gute Zusammenarbeit und netten Gespräche.

Der IMPRS des Max-Planck Instituts für terrestrische Mikrobiologie Marburg bin ich dankbar für zweieinhalb Jahre Finanzierung, sowie den regen Austausch und das hervorragende Netzwerk an motivierten, jungen Wissenschaftlern, dass ich mir innerhalb dieser *research school* aufbauen konnte.

Ein besonderer Dank gilt allen ehemaligen und aktuellen Mitgliedern der Arbeitsgruppe Bremer, vor allen meinen Bachelor und Master Studenten Philipp, Basti und Sarah. Von ganzem Herzen danke ich Annina, Bianca, Daniela, Jochen, Jutta, Laura, Lucas, Steffi und Tamara - ich wüsste nicht, was ich in den letzten Jahren ohne Eure Unterstützung in wissenschaftlichen und oft auch privaten Fragen getan hätte. Besonders hervorzuheben sind Laura, Bianca, Tamara und Jutta, die mich so häufig beim grübeln unterstützt haben! Und vielen Dank Nelli, dass du auch *gefühlt* das Unmögliche möglich machst und immer mit Rat und Tat zur Seite stehst.

Zu guter Letzt ein riesiges *Danke* an meine Familie und Freunde! Ich danke euch für Eure Unterstützung, Eure guten Worte, offenen Ohren und vor allen Dingen dafür, dass Ihr IMMER da seid. Besonders hervorheben möchte ich Opa Rudi und Oma Inge, meine Eltern und meine Schwiegereltern, meine Schwester Anni, Tina und Folko, Basti, Elisa, Marieke und Mathilda - ihr habt einen festen Platz in meinem Herzen!

Mein größter Respekt und meine tiefste Liebe gebührt Oliver und Moritz, dafür dass Ihr mich jeden Tag begleitet, so fest an mich glaubt und meine Träume zu *unseren* werden.

